

This item is held in Loughborough University's Institutional Repository (<https://dspace.lboro.ac.uk/>) and was harvested from the British Library's EThOS service (<http://www.ethos.bl.uk/>). It is made available under the following Creative Commons Licence conditions.



For the full text of this licence, please go to:
<http://creativecommons.org/licenses/by-nc-nd/2.5/>

LOAD TRANSFER ACROSS CRACKS AND JOINTS IN CONCRETE SLABS ON GRADE

By

Stuart John Arnold

**A Doctoral Thesis Submitted in partial fulfilment of the requirements for the
award of
Doctor of Philosophy of Loughborough University**

20th February 2004

© Stuart John Arnold (2004)

ABSTRACT

This research has investigated the behaviour of joints and cracks under single and multiple cycles of load. This provides an increased understanding of concrete slab on grade performance, enabling more effective design and monitoring procedures.

Examination of the geometry of cracks and joints within concrete slabs on grade has demonstrated that the commonly assumed parallel formation is erroneous. Measurements using embedded strain gauges, coring and surface profile levelling have uncovered that a high percentage of joints will contain larger crack widths at the surface than at the base, caused by differential shrinkage. The opening itself is relatively linear; however, the top 50mm of the slab is prone to a higher gradient of movement due to the increased drying effect towards the surface.

A series of deflection tests using a Falling Weight Deflectometer and Prima dynamic plate enabled slab response under load to be evaluated. Four sites were examined in total and correlations found between: load transfer, load step, edge cantilever and crack geometry. This produced valuable information regarding the influence of load transfer and crack width on the overall slab behaviour. Foundation voiding and crack face free slip was also shown to influence deflection magnitude.

A small-scale test facility was developed for the assessment of deterioration in various 'V' shaped and parallel crack widths under high cycle loading. The data demonstrated that joint/crack failure contains four distinct phases of deterioration, each of which is controlled by a different mechanism. 'V' shaped cracks produced a much greater load transfer than that of a parallel crack with the incorporation of A142 mesh and steel fibres reducing differential displacement. Load magnitude and aggregate size were also shown to have significant effects. The value of reinforcement was found to assist with serviceability requirements, keeping displacement within acceptable levels and preventing the onset of serious degradation

A finite element model was developed to enable the load transfer mechanism results from the laboratory test to be used in the assessment of full slab response. Simulations of field-testing produced a series of lower bounds in respect to deflections and the associated response calculations. Theoretical behaviour of a typical slab was assessed with subbase

support, joint stiffness, slab thickness and the incorporation of a subbase, found to be highly influential in reducing slab deflections.

The three main sections of work comprising site data collection, laboratory testing and Finite Element modelling have been used together to provide a much greater understanding of the influence of cracks and joints. This has included the deterioration of cracks over time and an examination of how this and other site-based factors affect overall slab behaviour.

Keywords: *Concrete slabs on grade, Joint behaviour, Load transfer, Deflection testing, Steel fibres, Concrete degradation, Finite Element modelling.*

ACKNOWLEDGEMENTS

Many people have provided me with assistance, guidance and support over the last three years, without whom it would not have been possible to complete this thesis.

Firstly, I would like to thank Professor Simon Austin, Dr. Paul Fleming and Dr. Peter Robins, who have complemented each other perfectly to generate the model supervisory team. Their knowledge, advice and carefully worded constructive criticism have enhanced both my academic and personal development.

I would also like to thank many other staff members in the department of Civil and Building Engineering, most notably the expertise of the laboratory technicians Mark Harrod, Dave Spendlove and David Houghton. Together they have shown that with the inclusion of experience and wisdom, practical research can be both highly rewarding and remarkably pain free.

My thanks go to the ACIFC and all of the steering group members whose input has enabled a project to be developed which will hopefully offer valuable information to the wider construction community.

There are many friends and family who deserve praise for their input; however, two in particular stand out, Adrian Holland and Karan Jalota. Both have been there academically and emotionally through the good and the bad, and amazingly are still here today, proving that they are very special friends.

Heartfelt thanks go to my parents Maureen and David Arnold whose faith in me has been a source of continual strength. They have supported and encouraged me endlessly and for that I love them dearly.

To complete this PhD was not a solitary undertaking, there was always one other who went through every emotion and has probably read and re-read every word as many times as I have. To show my total appreciation towards my partner Chrissie Pepper, I dedicate this thesis to her.

CONTENTS OF THESIS

ABSTRACT..... i

ACKNOWLEDGEMENTS iii

CONTENTS OF THESIS iv

LIST OF TABLES..... ix

LIST OF FIGURESx

NOTATION..... xviii

1. INTRODUCTION.....1

1.1 Background1

1.2 Aims and Objectives2

1.3 Outline of Research Methodology2

1.4 Thesis Structure4

2. CONCRETE SLABS/PAVEMENTS ON GRADE.....8

2.1 Preface.....8

2.2 Concrete Slabs/Pavements on Grade9

2.2.1 Internal Floor Slabs.....9

2.2.2 External Hardstandings12

2.2.3 Concrete Pavements.....14

2.2.3.1 *Jointed*.....15

2.2.3.2 *Continuously Reinforced*.....15

2.2.4 Structure Comparison15

2.3 Typical Actions for Concrete Slabs on Grade16

2.3.1 Moisture17

2.3.1.1 *Drying Shrinkage*17

2.3.1.2 *Plastic Shrinkage*18

2.3.2 Thermal18

2.3.3 Static Load19

2.3.4 Cyclic Dynamic Load20

2.4 Serviceability Problems21

2.4.1 Cracking.....21

2.4.2 Curling23

2.4.3 Pumping26

2.4.4 Faulting/Dynamic Load Step26

2.4.5 Punch-Out27

2.4.6	Spalling	28
2.5	Concrete Slab Design.....	29
2.5.1	Concrete properties	29
2.5.2	Slab Reinforcement.....	29
2.5.2.1	<i>General</i>	29
2.5.2.2	<i>Fabric</i>	30
2.5.2.3	<i>Fibres</i>	32
2.5.2.4	<i>Structural Reinforcing steel</i>	33
2.5.3	Structural Design	33
2.5.3.1	<i>Elastic method</i>	34
2.5.3.2	<i>Plastic Method</i>	35
2.5.4	Detail Design	37
2.5.4.1	<i>Crack Control</i>	37
2.5.4.2	<i>Joint Types</i>	39
2.5.4.3	<i>Joint Layout</i>	41
2.6	Slab/Pavement Foundation	43
2.6.1	Subbase	43
2.6.2	Subgrade	44
2.6.3	Slip Membrane.....	45
2.7	Structural Modelling	46
2.7.1	Modelling of Concrete materials.....	46
2.7.2	Modelling of Foundation materials.....	47
2.7.3	Analysis of Slabs on Grade.....	49
2.7.4	Modelling Limitations	51
2.8	Conclusions.....	52
3.	LOAD TRANSFER ACROSS CRACKS/JOINTS	59
3.1	Introduction.....	59
3.2	Influence on Design.....	59
3.3	Crack Geometry.....	60
3.4	Load Transfer Mechanisms	62
3.4.1	Aggregate Interlock	62
3.4.2	Dowel Bars.....	65
3.4.3	Steel Fabric	66
3.4.4	Steel Fibres.....	67
3.4.5	Proprietary Systems	68
3.5	Degradation of Load Transfer.....	69
3.6	Slab Condition Testing	71

3.6.1	Equipment.....	71
3.6.2	Investigation Techniques	72
3.7	Joint Effectiveness Analysis	75
3.8	Summary.....	80
4.	SLAB CONDITION	90
4.1	Introduction.....	90
4.2	Crack Measurement	91
4.2.1	Surface Measurements	92
4.2.2	Embedded Strain Gauges.....	93
4.2.3	Coring	93
4.3	Curling/Warping.....	94
4.3.1	Introduction.....	94
4.3.2	Precise Levelling.....	95
4.3.3	Builder's Level.....	95
4.3.4	Profilometer	96
4.4	Deflection Measurement.....	96
4.5	Slab Analysis.....	98
4.5.1	Load Transfer.....	99
4.5.2	Load Step	99
4.5.3	Edge Cantilever.....	100
4.5.4	Deflection Basins	100
4.5.5	Void Intercepts.....	101
4.6	Site Information	101
4.6.1	Daventry.....	101
4.6.2	Lutterworth	102
4.6.3	Ballymena	103
4.6.4	Skelmersdale.....	104
5.	JOINT DETERIORATION.....	113
5.1	Introduction.....	113
5.2	Test Variables.....	114
5.2.1	Surface Crack Widths	114
5.2.2	Steel Fibre Types	114
5.2.3	Steel Fibre Quantities.....	115
5.2.4	Non Reinforced.....	115
5.2.5	Mortar	115
5.2.6	Parallel Cracks	115
5.2.7	Fabric	115

5.2.8	Loads.....	115
5.2.9	Summary of Test Variables.....	116
5.3	Load Test Development.....	116
5.3.1	Simulation Method.....	116
5.3.2	Specimen Geometry.....	118
5.3.3	Crack Geometry	118
5.3.4	Subgrade Support.....	119
5.3.5	Load Magnitude	119
5.3.6	Loading repetition.....	120
5.3.7	Load rate	121
5.4	Specimen Production.....	121
5.4.1	Introduction.....	121
5.4.2	Mix Design.....	122
5.4.3	Reinforcement.....	123
5.4.4	Casting	124
5.5	Beam Preparation	125
5.5.1	Crack Timing	125
5.5.2	Crack Technique	125
5.5.3	Crack Width Control.....	127
5.6	Test procedure.....	127
5.6.1	Overview.....	127
5.6.2	Beam Orientation	128
5.6.3	Rig Configuration	128
5.6.4	LVDT Positioning.....	129
5.6.5	Safety Precautions.....	130
5.7	Data Logging	130
6.	RESULTS, ANALYSIS & DISCUSSION	146
6.1	General Introduction.....	146
6.2	Crack Geometry.....	146
6.2.1	Core Samples	146
6.2.2	Strain Gauge Monitoring	151
6.2.3	Levelling Profiles and Crack Measurements	154
6.2.4	Summary	156
6.3	Slab Condition.....	157
6.3.1	Introduction.....	157
6.3.2	Load Transfer Evaluation.....	158
6.3.3	Load Step Evaluation.....	162

6.3.4	Slab Cantilever.....	165
6.3.5	Deflected Shape	166
6.3.6	Voiding	166
6.3.8	Summary	167
6.4	Joint Deterioration.....	168
6.4.1	Specimen Production	169
6.4.2	Specimen Quantities	171
6.4.3	Deterioration Phenomena.....	173
6.4.4	Influence of Initial Crack Angle	175
6.4.5	Volume of Fibre Reinforcement	177
6.4.6	Fibre Aspect Ratio	178
6.4.7	Load Magnitude	180
6.4.8	Parallel Cracks	180
6.4.9	Reinforcement Type.....	181
6.4.10	Serviceability Limitations.....	182
6.4.11	Summary of Laboratory Investigation	184
6.5	Summary of Field and Experimental Work	185
7.	NUMERICAL MODELLING	232
7.1	Introduction.....	232
7.2	Model Set-up.....	232
7.3	Model Verification	233
7.4	Comparison to Laboratory testing	234
7.5	Relationship with Site Data.....	236
7.6	Comparison of Laboratory Obtained Joint Stiffness	238
7.7	Effect of Constituent Material Parameters	240
7.8	Summary.....	243
8.	CONCLUSIONS AND RECOMMENDATIONS FOR FURTHER WORK.....	264
8.1	Overview	264
8.2	Site Testing	264
8.3	Laboratory Testing	265
8.4	Analytical Modelling.....	266
8.5	Final Comments	267
8.6	Recommendations for Further Work	267
9.	REFERENCES.....	269

LIST OF TABLES

Table 2.1 – Typical Industrial Warehouse Loading Values (Knapton 1999b)	10
Table 2.2 – Typical Hardstanding Loading Values (Knapton 1999a)	13
Table 2.3 – Structure Comparison	16
Table 2.4 - Stock Fabric Sizes (Knapton 1999a)	30
Table 2.5 – Problems Associated with Joints and Cracks (Simpson 2001a).	38
Table 2.6 - Recommended Joint Spacing (Knapton 1999b)	42
Table 3.1 - Load Transfer Comparison (Gulden and Brown 1985).....	79
Table 4.1 – Site Testing Matrix	91
Table 5.1 - Testing Schedule	116
Table 5.2a – Typical Site Mixes	122
Table 5.2b – Actual Concrete Mix Specification Used for Laboratory Testing	122
Table 5.2c - Material Information.....	123
Table 5.3 - Steel Fibre Data	124
Table 6.1 – CMT Core Information (Visit 1).....	147
Table 6.2 – CMT Core Information (Visit 2).....	147
Table 6.3 – Comparison Between Actual and Predicted Surface Crack Widths	151
Table 6.4a – Strain Gauge Readings Converted to Crack Width.....	152
Table 6.4b - Strain Gauge Placement.....	152
Table 6.5 – Measured and Projected Surface Measurements	153
Table 6.6 – Effect of Free Slip on Load Transfer	160
Table 6.7 – Load Step Variation (Lutterworth)	163
Table 6.8 – Concrete Compressive Strengths	169
Table 6.9 – Beam Specimens Tested	172
Table 6.10 – Typical Fibre Count across Crack Face	179
Table 6.11 – Differential Deflection at Phase III.....	182
Table 6.12 – Allowable Crack Widths Preventing Serviceability Problems	183
Table 7.1 – Standard Slab Basic Parameters.....	241

LIST OF FIGURES

Figure 1.1 – Data transfer between site data collection, laboratory data collection and Finite Element modelling.....	7
Figure 1.2 – Interaction between thesis Chapters	7
Figure 2.1 – Typical construction of an internal floor slab.....	54
Figure 2.2 – Concrete slab construction methods (Knapton 1999b).....	54
Figure 2.3 – Rigid pavement slip form construction (Wirtgen 2001).....	54
Figure 2.4 – Shrinkage restraint of a concrete slab.....	55
Figure 2.5 – Peeling action caused by fabric reinforcement (Savage 1985).....	55
Figure 2.6 – Temperature induced slab curling (Ytterberg 1987)	55
Figure 2.7 – Rotation of joint faces (Poblette <i>et al.</i> 1988).....	56
Figure 2.8 – Curling profiles of a concrete slab caused by differential shrinkage (Rollings 1993)	56
Figure 2.9 – Faulting (top) and dynamic load step (bottom) across a discontinuity.....	57
Figure 2.10 – Punch out accumulation.....	57
Figure 2.11 – Spalling of a crack edge.....	57
Figure 2.12 – Steel fibre types (Balaguru and Shah 1992)	58
Figure 2.13 – Load/deflection relationship for steel fibre ground supported slab (Concrete Society 2000)	58
Figure 2.14 – Relationship between CBR and modulus of subgrade reaction (Croney and Croney 1997)	58
Figure 3.1 – Effect of crack verticality	82
Figure 3.2 – Global (macro) and local (micro) roughness	82
Figure 3.3 – Aggregate interlock model (Walraven 1981)	82
Figure 3.4 – Effect of crack opening on aggregate contact (Walraven 1981)	83
Figure 3.5 – Effect of crack width on net shear slip (Thompson 2001).....	83
Figure 3.6 – Load/shear slip plot for non-reinforced specimen (Thompson 2001)	84
Figure 3.7 – Load/shear slip plot for fibre reinforced specimen (Thompson 2001).....	84
Figure 3.8 – Joint deterioration of a 175mm slab (Colley and Humprey 1967)	85
Figure 3.9 – Joint deterioration of a 225mm slab (Colley and Humprey 1967)	85
Figure 3.10 – load transfer values from laboratory and field testing (Colley and Humprey 1967)	85
Figure 3.11 – Effect of load on joint deterioration (Colley and Humprey 1967)	86
Figure 3.12 – FWD (Top - graphical representation, Bottom - Plate)	86
Figure 3.13 – Prima dynamic loading plate	87

Figure 3.14 – FWD deflection basin analysis.....	87
Figure 3.15 – Void closure under load.....	88
Figure 3.17 – Geophone locations (Ricci <i>et al.</i> 1985)	89
Figure 3.18 – LT versus TLE (Ioannides and Korovesis 1990).....	89
Figure 3.19 – LT Vs AGG (Ioannides and Korovesis 1990).....	89
Figure 4.1 – Crack width prediction from saw-cut joints	106
Figure 4.2 – Crack microscope measuring a saw-cut joint.....	106
Figure 4.3 – Set of callipers measuring a saw-cut joint.....	106
Figure 4.4 – Set of crack comparators	107
Figure 4.5 – Extrapolation of embedded strain gauges to calculate surface and base crack widths.....	107
Figure 4.6 – Overestimation of base crack width caused by differential shrinkage	108
Figure 4.7 – Estimation of slab curl using builders level and graduated wedge.....	108
Figure 4.8 – Estimation of slab curl using Profilometer	109
Figure 4.9 – FWD and Prima geophone placement for measurement of slab behaviour across cracks and joints.....	109
Figure 4.10 – FWD geophone locations for Daventry (Top) and Lutterworth (Bottom)	110
Figure 4.11 – Load transfer comparison when loaded each side of a joint.....	110
Figure 4.12 – Plan of S.W. corner of Daventry site.....	111
Figure 4.13 – Plan of Lutterworth site	111
Figure 4.14 – Plan of Skelmersdale site.....	112
Figure 5.1 – Cyclic loading test set-up (Schematic)	132
Figure 5.2 – Cyclic loading test set-up (Plate).....	132
Figure 5.3 – Steel fabric and reinforcing bar layout and positioning.....	133
Figure 5.4 – Typical single crack test specimen (Valle and Buyukozturk 1993)	133
Figure 5.5 – Single cycle load test set-up (Millard and Johnson 1984).....	134
Figure 5.6 – Large-scale slab laboratory set-up for cyclic load testing (Colley and Humphrey 1967)	134
Figure 5.7 – Double crack test set-up for cyclic loading (Thompson 2001).....	135
Figure 5.8 – Representation of in service slab loading using positive and negative laboratory loading	136
Figure 5.9 – Reduction in shear displacement gradient over increasing load cycles (Abdel-Maksoud 2000)	137
Figure 5.10 – Reduction in peak and trough deflection gradient with increasing load cycles (Thompson 2001).....	137
Figure 5.11 – Trial testing differential displacement plot, 0 – 250,000 cycles (Top), 250,000 – 500,000 cycles (Bottom).....	138

Figure 5.12 – Measured load cycle of a vehicle crossing a discontinuity at 30mph (Colley and Humphrey 1967)	139
Figure 5.13 – Sinusoidal load application from the Dartec cyclic load test machine	139
Figure 5.14 – Bekaert Dramix® Steel fibres used within the experimentation (from left: RC-65/60-BN, RC-80/60-BN, RL-45/50-BN).....	139
Figure 5.15 – Method of inducing cracks into test specimens.....	140
Figure 5.16 – Extrapolation of demec pip measurements to obtain surface and base crack width measurements.....	141
Figure 5.17 – Comparison of predicted and actual surface crack measurements	141
Figure 5.18 – Measurement of crack opening throughout specimen depth	142
Figure 5.19 – Graphical representation of data logging process.....	142
Figure 5.20 – LVDT positioning (original set-up).....	143
Figure 5.21 – LVDT positioning (updated set-up)	143
Figure 5.22 – Effect of undertaking a discontinuous cyclic load test	144
Figure 5.23 – Maximum and minimum displacement positions.....	144
Figure 5.24 – Positive and negative displacement deterioration plot	145
Figure 5.25 – Differential displacement deterioration plot.....	145
Figure 6.1 – Lutterworth Core Locations (Top – visit 1, Bottom - visit 2).....	187
Figure 6.2 – Core taken during visit 1 (Clockwise from top left, Core 7, Core 17, Core 24, Core 21)	188
Figure 6.3 – Crack profiles from cores taken in visit 1.....	188
Figure 6.4 – Crack profiles from cores taken in visit 2.....	189
Figure 6.5 – Crack offsets from cores taken in visit 1	190
Figure 6.6a – Strain Gauge Positions (Leeds).....	190
Figure 6.6b – Strain Gauge Positions (Northampton).....	191
Figure 6.6c – Strain Gauge Positions (Marston).....	191
Figure 6.7a – Crack width extrapolation (Leeds)	192
Figure 6.7b – Crack width extrapolation (Marston)	192
Figure 6.8 – Actual crack profile using embedded stain gauges and surface measurements (Leeds)	193
Figure 6.9 – Differential shrinkage of concrete open to the environment on one side (Neville 1995).....	194
Figure 6.10 – Erroneous strain gauge reading from Bishop (2001).....	194
Figure 6.11 – Area of floor level surveyed with a precise level (Daventry).....	195
Figure 6.12 – Floor surface profiles (Daventry)	195
Figure 6.13 – Measured edge curl using a builders level (Ballymena).....	196
Figure 6.14 – Predicted crack profile using slab levels and surface width (Daventry)....	196

Figure 6.15 – Predicted crack profiles using edge curl (Ballymena).....	197
Figure 6.16 – Load transfer comparison between FWD and Prima (Daventry)	197
Figure 6.17 – Load transfer comparison between FWD loads (Lutterworth).....	198
Figure 6.18 – Load transfer comparison between FWD and Prima (Lutterworth)	198
Figure 6.19 – Effect of free-slip on load transfer.....	199
Figure 6.20 – Comparison of load transfer equations	199
Figure 6.21a – Comparison of load transfer and crack width (Daventry).....	200
Figure 6.21b – Comparison of load transfer and crack width (Lutterworth)	200
Figure 6.22 - Comparison of load transfer with surface and base slab crack widths (Lutterworth).....	201
Figure 6.23 – Load step comparison between FWD and Prima (Daventry).....	202
Figure 6.24 – Load step comparison between FWD load magnitudes (Lutterworth).....	202
Figure 6.25 – Load step comparison between FWD and Prima (Lutterworth).....	203
Figure 6.26 – Effect of voiding on load magnitude / load step gradients	203
Figure 6.27 – Effect of load on absolute deflection.....	204
Figure 6.28 – Comparison of load transfer and load step (Daventry/Lutterworth/Ballymena/Skelmersdale).....	204
Figure 6.29a – Comparison of load step and crack width (Daventry)	205
Figure 6.29b – Comparison of load step and crack width (Lutterworth).....	205
Figure 6.29c – Comparison of load step and crack width (Skelmersdale).....	206
Figure 6.30 – Comparison of load step and crack width taking into account pre-load (Daventry).....	206
Figure 6.31a – Comparison of load transfer and edge cantilever (Daventry)	207
Figure 6.31b – Comparison of load transfer and edge cantilever (Lutterworth).....	207
Figure 6.31c – Comparison of load transfer and edge cantilever (Ballymena).....	208
Figure 6.31d – Comparison of load transfer and edge cantilever (Skelmersdale).....	208
Figure 6.32a – Comparison of load step and edge cantilever (Daventry).....	209
Figure 6.32b – Comparison of load step and edge cantilever (Lutterworth)	209
Figure 6.32c – Comparison of load step and edge cantilever (Ballymena)	210
Figure 6.32d – Comparison of load step and edge cantilever (Skelmersdale).....	210
Figure 6.33 – Typical deflection bowls (Daventry).....	211
Figure 6.34 – Typical deflection bowls (Lutterworth).....	211
Figure 6.35 – Effect of casting date on cube compressive strength.....	212
Figure 6.36 – Deterioration phases of a concrete crack.....	212
Figure 6.37 – Early deterioration in a concrete test specimen	213
Figure 6.38 – Unequal displacement	213
Figure 6.39 – Influence of aggregate on displacement	214

Figure 6.40 – Negative deterioration caused by small material accumulation	214
Figure 6.41 – Effect of aggregate and steel fibres on differential displacement.....	215
Figure 6.42a – Effect of deterioration on displacement resistance (30kg/m ³ steel fibre with 1.98mm crack width)	215
Figure 6.42b – Effect of deterioration on displacement resistance (30kg/m ³ steel fibre with 5.94mm crack width)	216
Figure 6.43a – Effect of deterioration on displacement resistance (non-reinforced with 0.66mm crack width)	216
Figure 6.43b – Effect of deterioration on displacement resistance (non-reinforced with 1.98mm crack width)	217
Figure 6.44 – Effect of deterioration on displacement resistance (mortar with 0.66mm crack width)	217
Figure 6.45 – Effect of steel fibre quantity on differential displacement	218
Figure 6.46 – Effectiveness of fibre quantity in resistance to displacement.....	218
Figure 6.47a – Effect of deterioration on displacement resistance (20kg/m ³ steel fibre with 0.66mm crack width)	219
Figure 6.47b – Effect of deterioration on displacement resistance (20kg/m ³ steel fibre with 4.62mm crack width)	219
Figure 6.48a – Effect of deterioration on displacement resistance (40kg/m ³ steel fibre with 1.98mm crack width)	220
Figure 6.48b – Effect of deterioration on displacement resistance (40kg/m ³ steel fibre with 5.94mm crack width)	220
Figure 6.49 – Effect of steel fibre aspect ratio on differential displacement	221
Figure 6.50 – Comparison between steel fibre aspect ratios and steel fibre quantities....	221
Figure 6.51 – Effect of crack face fibre count on resistance to deflection.....	222
Figure 6.52 – Effectiveness of aspect ratio in resistance to displacement.....	222
Figure 6.53a – Effect of deterioration on displacement resistance (steel fibre of aspect ratio 80 with 1.98mm crack width).....	223
Figure 6.53b – Effect of deterioration on displacement resistance (steel fibre of aspect ratio 80 with 4.62mm crack width).....	223
Figure 6.54a – Effect of deterioration on displacement resistance (steel fibre of aspect ratio 48 with 1.98mm crack width).....	224
Figure 6.54b – Effect of deterioration on displacement resistance (steel fibre of aspect ratio 48 with 4.62mm crack width).....	224
Figure 6.55 – Effect of load magnitude on differential displacement.....	225
Figure 6.56a – Effect of deterioration on displacement resistance (load magnitude of 2kN with 1.98mm crack width)	225

Figure 6.56b – Effect of deterioration on displacement resistance (load magnitude of 2kN with 4.62mm crack width)226

Figure 6.57a – Effect of deterioration on displacement resistance (load magnitude of 6kN with 0.66mm crack width)226

Figure 6.57b – Effect of deterioration on displacement resistance (load magnitude of 6kN with 1.98mm crack width)227

Figure 6.58 – Effect of load magnitude on displacement227

Figure 6.59 – Effect of crack profile on differential displacement228

Figure 6.60a – Effect of deterioration on displacement resistance (Parallel crack of 0.66mm width).....228

Figure 6.60b – Effect of deterioration on displacement resistance (Parallel crack of 1.98mm width).....229

Figure 6.61 – Effect of steel fabric and reinforcing bar on displacement.....229

Figure 6.62a – Effect of deterioration on displacement resistance (steel fabric with 1.98mm crack width)230

Figure 6.62b – Effect of deterioration on displacement resistance (steel fabric with 4.62mm crack width)230

Figure 6.63 – Serviceability thresholds for crack degradation231

Figure 7.1 – Finite Element model of a concrete slab on grade with a discontinuity245

Figure 7.2a – Comparison of DIANA with Westergaard (1926) for a 100mm slab loaded internally245

Figure 7.2b – Comparison of DIANA with Westergaard (1926) for a 200mm slab loaded internally246

Figure 7.2c – Comparison of DIANA with Westergaard (1926) for a 300mm slab loaded internally246

Figure 7.2d – Comparison of DIANA with Westergaard (1926 and 1947) for a 100mm slab loaded at the edge247

Figure 7.2e – Comparison of DIANA with Westergaard (1926 and 1947) for a 200mm slab loaded at the edge247

Figure 7.2f – Comparison of DIANA with Westergaard (1926 and 1947) for a 300mm slab loaded at the edge248

Figure 7.3 – Comparison of DIANA with Westergaard (1926 and 1947) for a 200mm slab loaded at the edge with lengths of 6, 10 and 15m.....248

Figure 7.4 – Schematic of the Finite Element model of crack behaviour within the laboratory test rig249

Figure 7.5 – Comparison of the laboratory Finite Element model with the standard spring equation.....249

Figure 7.6 – Effect of foundation material under the crack in the laboratory Finite Element model.	250
Figure 7.7a – Comparison of load transfer and load step between the Daventry Finite Element model and in-service slab response	250
Figure 7.7b – Comparison of loaded edge deflection and load transfer between the Daventry Finite Element model and in-service slab response	251
Figure 7.7c – Comparison of unloaded edge deflection and load step between the Daventry Finite Element model and in-service slab response	251
Figure 7.8a – Comparison of load transfer and load step between the Lutterworth Finite Element model and in-service slab response	252
Figure 7.8b – Comparison of loaded edge deflection and load transfer between the Lutterworth Finite Element model and in-service slab response	252
Figure 7.8c – Comparison of unloaded edge deflection and load step between the Lutterworth Finite Element model and in-service slab response	253
Figure 7.9a – Comparison of load transfer and load step between the Ballymena Finite Element model and in-service slab response	253
Figure 7.9b – Comparison of loaded edge deflection and load transfer between the Lutterworth Finite Element model and in-service slab response	254
Figure 7.9c – Comparison of unloaded edge deflection and load step between the Ballymena Finite Element model and in-service slab response	254
Figure 7.10a – Comparison of load transfer and load step between the Skelmersdale Finite Element model and in-service slab response	255
Figure 7.10b – Comparison of loaded edge deflection and load transfer between the Skelmersdale Finite Element model and in-service slab response	255
Figure 7.10c – Comparison of unloaded edge deflection and load step between the Skelmersdale Finite Element model and in-service slab response	256
Figure 7.11a – Comparison of deflection bowls between the Daventry Finite Element model and in-service slab response	256
Figure 7.11b – Comparison of deflection bowls between the Lutterworth Finite Element model and in-service slab response	257
Figure 7.12 – Process diagram for establishing slab response using laboratory cyclic load testing and the Finite Element model	258
Figure 7.13 – Comparison of predicted and actual surface crack width/load transfer behaviour for Daventry	259
Figure 7.14 – Comparison of predicted and actual surface crack width/load step behaviour for Daventry	259

Figure 7.15 – Comparison of predicted and actual surface crack width/load transfer behaviour for Lutterworth.....260

Figure 7.16 – Comparison of predicted and actual surface crack width/load step behaviour for Lutterworth.....260

Figure 7.17 – Effect of modulus of subgrade reaction on the loaded slab edge deflection for a typical in service slab261

Figure 7.18 – Effect of concrete modulus of elasticity on the loaded slab edge deflection for a typical in service slab261

Figure 7.19 – Effect of joint spring stiffness on slab edge deflections for a typical in service slab.....262

Figure 7.20 – Effect of slab depth on the loaded slab edge deflection for a typical in service slab.....262

Figure 7.21 – Effect of subgrade modulus of elasticity on the loaded slab edge deflection for a typical in service slab263

Figure 7.22 – Effect load position on load transfer for a typical in service slab.....263

NOTATION

a	Contact radius of a load
a_l	Distance from corner to load centre
AD	Actual deflection
AGG	Aggregate stiffness
AL	Actual load
$ASDR$	Approach slab deflection ratio
B	Slab bending correction factor
$CRCP$	Continuously reinforced
d	Specimen depth
$d1/2_c$	Deflections at slab centre (305mm apart)
dl	Deflection of loaded slab
do	Deflection directly under load
du	Deflection of unloaded slab
E_c	Youngs modulus of concrete
f	Load factor (assumed 1 under self weight)
f_b	Flexural strength of concrete
f_c	Characteristic strength
f_m	Target mean strength
F_f	Critical stress for load at free edge
F_i	Critical stress for load at joint edge
F_j	Critical stress for load at interior
F_l	Front left LVDT
F_r	Front right LVDT
FWD	Falling Weight Deflectometer
g	Acceleration due to gravity
h	Slab depth
H	Horizontal distance between levelling points
k	Modulus of subgrade reaction
ks	Defectives margin
K	Spring stiffness
l	Radius of relative stiffness
L	Slab length
L_{cr}	Critical slab length
$LSDR$	Leave slab deflection ratio

LT	Load transfer
LTE_{asd}	Load transfer efficiency approach slab deflection
LTE_{lsd}	Load transfer efficiency leave slab deflection
LTE_{stress}	Stress related load transfer efficiency
LVDT	Linear variable differential transducer
MHE	Materials handling equipment
Mo	Maximum yield moment for plain concrete slabs
ND	Normalised deflection
NL	Normalised load
P	Applied load
Po	Slab collapse load
Pt	Total load transferred
R_l	Rear left LVDT
R_r	Rear right LVDT
TLE	Transfer load efficiency
V	Difference in slab surface level
VNA	Very narrow aisle
w	Crack width
W_b	Base crack width
W_s	Surface crack width
x	Specimen width
Zc	Deflection at a corner with no capacity for load transfer
Ze	Deflection at the edge or at a joint that has no capacity for load transfer
Zi	Deflection at the panel interior at a considerable distance from the edge
α_c	Thermal coefficient of expansion for concrete
α_t	Vertical movement caused by slab curling
ΔT	Temperature difference between opposite faces of a member
δt	Temperature induced movement
Δ	Displacement
$\Delta \varepsilon_{sh}$	Differential movement between upper and lower faces of the slab
γ	Eulers constant
μ	Poissons ratio for concrete
ρ_c	Concrete density
ϕ	Diameter
τ	Contact stress

1. INTRODUCTION

1.1 Background

There is a growing demand for in-situ concrete industrial floor slabs and hardstandings throughout the United Kingdom and the world. The increase of internal floor space required for warehousing and manufacturing processes, along with the need for additional external storage areas such as ports, harbours and retail outlets have led to the majority of this growth. The continued use of rigid pavement construction in many countries ensures the quantity of concrete required for this type of infrastructure has also remained high. This demand has been coupled with client requirements for extended life expectancies and tighter tolerances in level and flatness. This necessitates that the design of the structure be extremely thorough to ensure all specifications are met.

Whilst new machinery such as laser screeding plant has helped in providing quicker and more accurate concrete placement, the greater size of the pour creates an increased risk of thermal and hygral movement. All concrete slabs must consequently accommodate significant shrinkage throughout their lifespan, because if restricted, additional stresses and cracking will occur. Some form of control to prevent premature degradation is therefore required within the structure. This is commonly achieved with the use of joints or controlled cracks to enable the concrete to move at designated locations, leaving the remainder of the slab relatively free of restraint induced stress. Unfortunately, these areas often become the main cause of failure if incorrectly designed or constructed (Hulett 2001).

The load transfer mechanism across any crack or joint is essential to the structural capacity of the slab. If this deteriorates for any reason then there is a much greater risk of failure or serviceability problems, such as faulting (change in level across the crack), excessive deformation or further cracking.

Many methods are employed for load transfer. Some utilise the intrinsic properties of the concrete mix such as aggregate interlock, but others such as dowel bar insertion can be used to enhance the mechanism. Steel fabric will reduce movement of the joint or crack faces due to the external climate, and will also have some load transfer potential of its own. Similarly, with steel fibres becoming increasingly popular, it is important that their

impact is incorporated within design. The behaviour assessment of each joint type with respect to load magnitude, crack orientation and long-term fatigue is therefore essential to enable designers to accurately predict slab response.

1.2 Aims and Objectives

The project aims were developed in collaboration with a steering group committee who provided technical and practical knowledge throughout the duration of the research period. These discussions along with a comprehensive review of literature identified the need to ‘develop a more fundamental understanding of the load transfer mechanisms across cracks and joints in concrete floor slabs, hardstandings and rigid pavements’.

In order to achieve this overall aim the following objectives were identified:

- Determine joint and crack profiles, as a result of the interaction of concrete properties and the slab environment (climate).
- Devise and validate experimental procedures to simulate the load transfer behaviour of a slab joint/crack.
- Determine the effect of a selected range of joint/crack openings on the load transfer behaviour of plain, mesh and fibre reinforced specimens.
- Investigate the influence of subgrade support on the load transfer behaviour of plain, mesh and fibre reinforced specimens.
- Develop a structural finite element model to simulate the interaction of joint/crack opening, reinforcement type and subgrade, on load transfer behaviour.

1.3 Outline of Research Methodology

To achieve full understanding of site conditions and for development of the laboratory test methods it was essential that data was collected on typical crack and joint profiles. Unlike previous surveys, this required measurements throughout the depth of the slab and therefore invasive methods were employed. The first of these required the analysis of previous records of crack opening obtained during the research of Bishop (2001). This work utilised embedded strain gauges to calculate slab movements during the early ages of concrete life. Extrapolation from several gauges and demec pips placed above one another at joint positions facilitated the production of overall crack profiles.

Coring was also used to obtain information on crack width variations. This enabled the opening and inclination to be directly measured along the full slab depth using a number of different methods and devices. Surface crack widths alone were obtained at dynamic load test locations to enable its comparison with deflection response.

In addition to direct width measurement, plots of the slab surface profile and slab edge curling enabled the interpretation of crack geometry. Several methods were trialled to obtain accurate measurement at a conveniently fast rate, necessitated by the limited time availability of site access. Initially a precise level was utilised, which although providing high accuracy, was found to be relatively slow and cumbersome. A builders level held at the slab edge and a graduated wedge enabled sufficient approximations of the level of curl. The use of a small profilometer enabled an increased amount of detail to be obtained, with greater accuracy due to the incorporation of a graduated measurement scale.

To enable the effect of crack opening and load transfer on slab response to be determined, deflection testing was undertaken on a number of joints at four different in service sites using a Falling Weight Deflectometer or (Prima) portable dynamic plate test. These devices impart a transient vertical load and monitor deflections on either side of the crack. The measured deflections were then used to derive load transfer, load step and edge cantilever, whilst providing estimates of voiding, thereby providing a greater understanding of the slab behaviour in respect to applied load.

A small-scale laboratory testing facility was developed to enable fatigue of cracks to be investigated under controlled conditions. This incorporated a double cracked specimen loaded across both shear planes with a force of between 2 and 6kN to represent contact loads found on site. A selection of typical slab reinforcements was tested, including steel fibres at quantities between 20 and 40kg/m³ and A142 steel fabric. Crack geometries used were similar to those found from the measurements at in-service site slabs. This consisted of 'V' shaped cracking with surface widths between 0.66 and 4.62mm and several parallel cracks, all of which were below 2mm in width. Each test comprised a minimum of 250,000 cycles with measurements of deflection taken every 600 cycles. The displacements at the relevant load and cycle number were then used to produce a comparison between specimens and produce calculation of joint stiffness. The deterioration of the crack face was also monitored enabling the contributory effects to be determined.

Finite element modelling enabled the effects of load transfer on slab response to be established, with the results obtained from laboratory testing correlated to those found from field testing. The Finite Element model utilised a single joint stiffness only and therefore the deterioration effect could not be incorporated directly; however, the selection of a residual value enabled a characteristic in-service slab response to be obtained. A standard model was developed to be representative of a typical internal slab construction and was compared to the analytical representations proposed by Westergaard (1926 and 1947), and Ioannides *et al.* (1985) to validate the results. A numerical model of the laboratory test beam was also constructed to establish whether the standard spring equation could be used in developing joint stiffness. From these results it was possible to construct a series of models, each representing as closely as possible the conditions found in the field. Comparisons could then be made to the deflection measured responses found on site to assess the accuracy of the numerical representation. This was undertaken for the full range of load transfer values and, using a trial and error approach, enabled the value of foundation support to be determined. After obtaining the correct foundation stiffness comparisons were made between the laboratory fatigue tests and the field data. For two of the sites tested a full range of crack widths were identified along with their associated deflection responses. The finite element model was then used to incorporate the spring stiffness load transfer model obtained from the laboratory, with representative data taken for both reinforcement type and crack width. Once this procedure confirmed reasonable approximation between site and laboratory information, several parameters controlling slab response were altered to enable their influence to be further understood.

Interaction between each section of work was required to enable methodologies to be developed and provide a greater understanding of slab behaviour. Figure 1.1 represents this process, whereby each of the three main sections of work (site data collection, laboratory data collection and finite element analysis) link directly into one another, and into overall analysis.

1.4 Thesis Structure

Each chapter of the thesis is interlinked, and requires cross-referencing of data to enhance its full comprehension. The flow diagram produced in Figure 1.2 is provided to aid the reader's understanding of how this was accomplished.

Chapter 1 provides an introduction to the thesis comprising an overview of the research topic and the importance of the findings to industry. This also encompasses the aims and objectives with a brief description of how each was achieved.

Chapter 2 presents a thorough review of the literature covering concrete slabs on grade and their common failure mechanisms. This includes many of the actions placed onto the structure and how these are controlled through adequate design. Analytical modelling is also introduced with a discussion of some of the difficulties known to exist.

Chapter 3 provides a more detailed account of current knowledge into load transfer across cracks and joints, describing many of the mechanisms alongside their long-term effectiveness. Analysis equations are established for both single and multiple cycle behaviour, with the effect of geometrical and material properties considered. Site testing methods and the analysis procedures are discussed.

Chapter 4 contains the methodology used for the determination of site obtained information, incorporating equipment specifications and the implementation techniques used to obtain information relevant for analysing joint and crack behaviour.

Chapter 5 provides detailed information on the design of a small scale testing facility for examining load transfer deterioration. Information on the test specimens is described, along with the procedures used for translating the data, enabling further analysis and comparison.

Chapter 6 presents the findings from both the site and laboratory testing, highlighting the influence of crack geometries and reinforcement type on load transfer. Evaluation of slab condition is made through analysis of deflection testing which then enables correlation between the various responses. Laboratory simulation results are used to produce a series of degradation curves, providing comparison of joint stiffness and load restraint for a variety of material and load conditions.

Chapter 7 illustrates the development and validation of the finite element model against other well respected analyses. Numerical results are compared to field data for the full range of spring stiffness to enable the accuracy of the model to be determined. Values obtained from laboratory testing are incorporated within the model providing predictions of slab response, which are then compared to site measurements. Finally, the effects of changing structural criterion are investigated to evaluate their effect on behaviour.

Chapter 8 draws from the results of chapters 6 and 7 presenting conclusions on the research undertaken, and offers recommendations for further work.

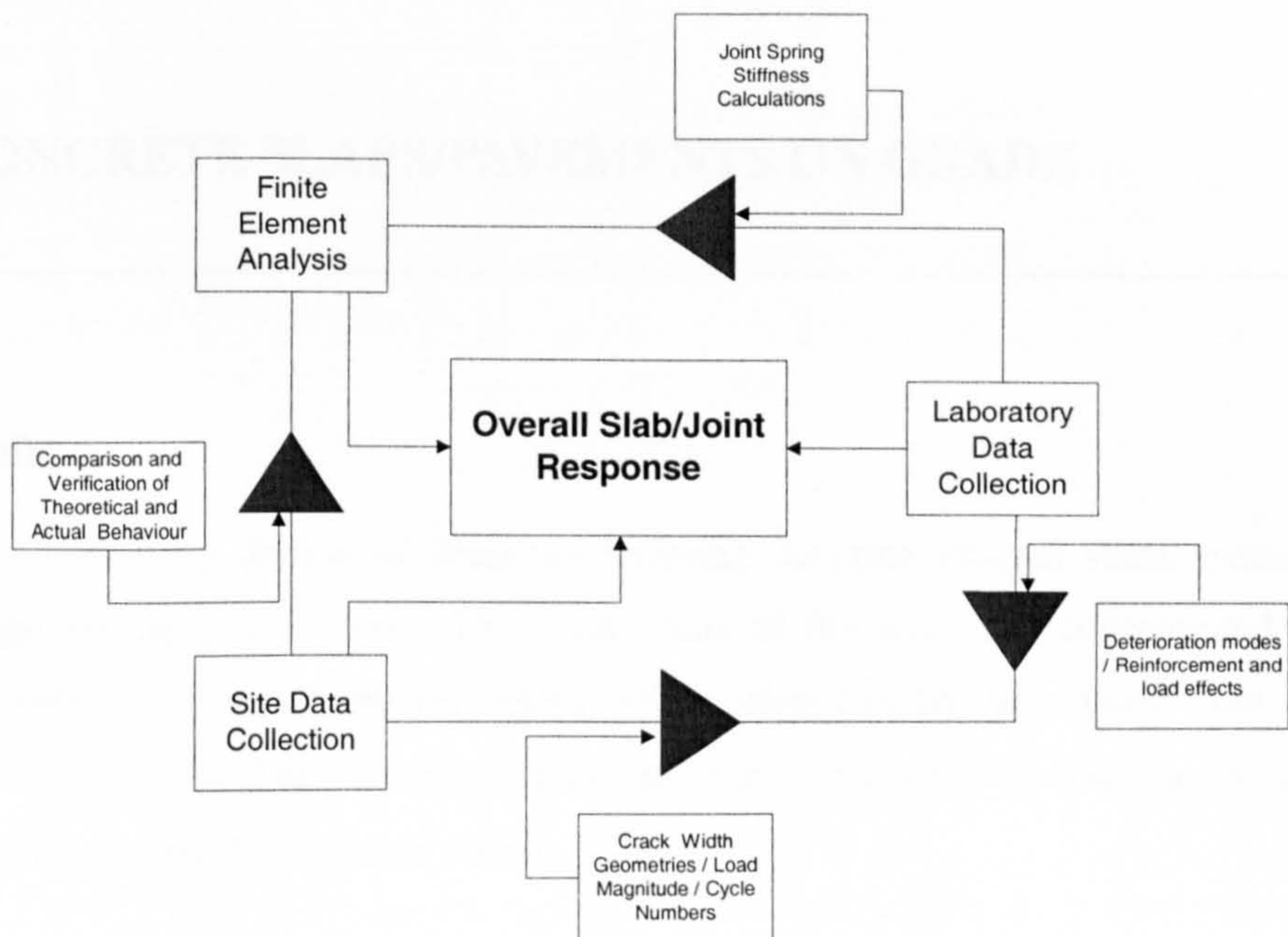


Figure 1.1 – Data transfer between site data collection, laboratory data collection and Finite Element modelling

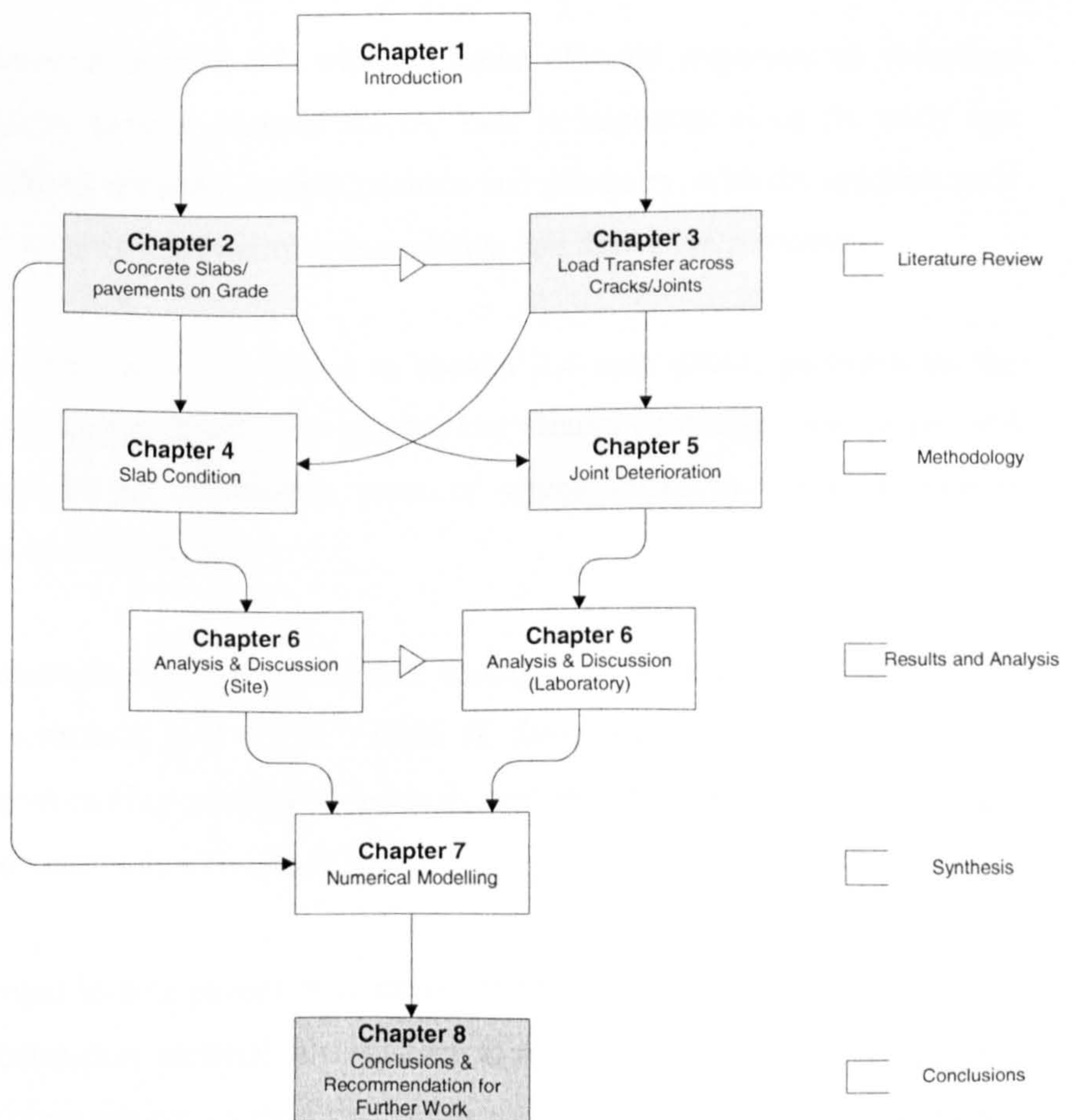


Figure 1.2 – Interaction between thesis Chapters

2. CONCRETE SLABS/PAVEMENTS ON GRADE

2.1 Preface

This chapter presents a review of literature covering concrete internal slabs, external hardstandings and rigid pavements. The main focus of the work has concentrated on industrial warehouse floors. However, useful information can be determined from the other types of ground-bearing structure as there are many similarities in construction and loading. This is explained in detail in section 2.2.4.

The literature review has been arranged so that section 2.2 leads the reader through the basic construction types and methods, discussing the conditions found in each structure whilst demonstrating how they are inter-related.

Actions are introduced in section 2.3, with the initial climatic responses on shrinkage examined, followed by typical imposed forces. This is important since the early age environmental conditions control the crack position and geometry, with the application of load magnitude and repetition influencing degradation and deflection response.

Typical failure mechanisms are discussed in section 2.4 with details provided on the factors which initiate each method. This enables key factors controlling the degree and rate of deterioration to be established, most of which relate to the load transfer effectiveness across cracks and joints.

To indicate how management of these failure mechanisms is undertaken, section 2.5 reviews both the structural and detail design of floor slabs and pavements. This incorporates the serviceability prediction methods and the standard elastic and plastic equations used for determining ultimate strength.

The response of a rigid slab or pavement is influenced heavily by the support conditions provided by the foundation material. In addition to section 2.2, section 2.6 has been dedicated to describing current methods of construction and the reasoning behind the incorporation of each layer.

Finally, in section 2.7 the methods and techniques employed in structural modelling of concrete slabs using finite element packages have been considered in light of their limitations. This enables any future model to be developed to the highest accuracy, whilst retaining computational efficiency.

2.2 Concrete Slabs/Pavements on Grade

Concrete is a universal construction material due to its versatility and cheap constituents. In internal floor slabs and hard-standings it is used almost exclusively as it utilises many of the positive characteristics of concrete. However, there is an ongoing debate regarding the advantages of rigid over flexible pavement construction and as such its use in this situation is limited within the United Kingdom.

In this section each structure is described with respect to its constituent layers, construction method and applied loading. Section 2.2.4 combines this information enabling the reader to cross-reference the key data from each structure.

2.2.1 Internal Floor Slabs

The internal floor slab of a warehouse is often the most important factor in the success or failure of such a construction project. If the floor does not fulfil the required specification and allow the client to utilise the building to its full potential then its capital value is at risk.

The current market for industrial flooring is approximately 6 million square metres of floor per year (Cudworth 2003). The majority of this is used in warehouses and factories, both of which require the floor to satisfy certain criteria if they are to fulfil their potential. The floor itself may be subject to a variety of conditions due to differing load configurations and climate changes, all of which must be correctly managed to prevent failure.

In many factory and warehousing areas there is a requirement to store a vast quantity of goods within a comparatively small floor area. The most common and efficient way to accommodate this is with a racking system. This enables materials to be stacked above each other, whilst still allowing vehicular access and manoeuvrability. The load from this racking is transferred to the slab via small base plates, resulting in high contact stresses and an increased risk of punching shear failure. High uniformly distributed loads (UDL's)

are also commonly found where a number of heavy items are stacked on a pallet or flat bed.

Materials handling equipment (MHE) cause the main dynamic loads on an industrial slab. This can be anything from a pallet truck to a forklift, or 10m high very narrow aisle (VNA) stacker. Many of these MHE's incorporate hard, rigid wheels which create high-localised stresses within the slab. These can create severe problems when the vehicle passes a discontinuity as the impact of the load intensifies the stress on an already weakened edge section. Channelling of vehicles increases this effect as the high number of load repetitions produces a greater risk of concrete fatigue and subgrade damage.

Table 2.1 shows typical load types for industrial floor slabs, alongside their appropriate load classification and magnitude.

Table 2.1 – Typical Industrial Warehouse Loading Values (Knapton 1999b)

Load Type	Load Classification	Typical Load
Pallet Racking	Light – Very heavy	42 – 114 kN
Mezzanine Floor	Light – Very heavy	42 – 114 kN
Shelving	Light – Medium	42 – 60 kN
Fork Lift	Light – Medium	42 – 60 kN

In any large concrete pour some degree of shrinkage or thermal cracking is inevitable. The location of the cracking can be defined by designing in joints which provide planes of weakness. These joints allow movement to be confined to appropriate positions leaving the remainder of the slab intact (see section 2.5.4). In the case of internal floor slabs the concrete can either be plain and jointed, or reinforced, in which case it can either be jointed or jointless. The main difference between the types is the number of designed joints required. Plain concrete jointed slabs necessitate a joint at approximately 6m intervals, whereas reinforcement such as traditional steel bars or mesh enables spacings to be increased to 8-10m (Knapton 1999b). In certain situations where either heavy reinforcement or steel fibres are used, the slab can be constructed using the jointless method. With this technique the slab will tend to crack randomly but within close proximity, ensuring good load transfer.

As described above, joints allow shrinkage cracking to be confined to defined locations. These often become structural weak points due to the continuous movement from moisture and thermal changes and impact from moving vehicles and pallet trucks (Simpson 2001a). As the joint degrades over time, any flaws in design will be accentuated and costly remedial action will almost certainly be required. The types of damage most likely to occur are spalling of the joint surfaces, and faulting due to a difference in level across the joint. Details of the various types of failure are described in section 2.3.

The make up of a typical internal floor slab is shown in Figure 2.1. The concrete slab is approximately 150-300mm in thickness, and may be reinforced with either steel fabric or fibres. This is placed on a subbase which is usually of a similar depth, but limited to 225mm to ensure that it can be placed and compacted in one layer. A slip membrane is sited between the two to reduce any frictional stresses that may increase restraint to movement. This is all placed on the subgrade which may or may not have been treated to increase its strength.

There are a number of ways to construct internal floor slabs; from the more traditional techniques used by contractors for many years, to the more modern practices with technically advanced machinery. The more traditional methods include long strip and wide strip construction which, as the names suggest, are methods of placing the concrete in confined areas. The relatively slow nature of this form of construction, along with the increased number of vulnerable joints created, has led to other methods becoming increasingly popular (Barnbrook 2000). Large bay construction is a more modern approach where high slump concrete is placed by pump or truck directly onto the floor area. Here, it is compacted and levelled off using timber or vibrating screed rails depending on the required tolerance. In this situation the slab may have joint formers inserted into the concrete, or have joints sawn onto the surface of the slab, to provide a control system for any thermal or drying shrinkage movement.

The most modern construction approach of laser screeding is becoming more common due its potential to create large floor areas at high speed. Laser screeds are items of plant which place, compact and level the concrete in one pass. The elevation is monitored with lasers and can produce floors that adhere to much tighter tolerances than can be expected with a manual process. The greater placing accuracy with an increased construction speed means that a more economical floor is produced. This type of construction may require joints to be formed with inserts or by sawing to allow for movement of the concrete. However, it is possible to produce floors containing no joints, especially when steel fibres

are used as reinforcement within the concrete. These floors are more prone to cracking, although the reinforcement prevents the cracks from opening to a level where load transfer will be reduced significantly (The Concrete Society 2003). The different methods of construction available are shown in Figure 2.2.

The concrete used in the construction of a floor slab must be specified correctly to ensure a suitably strong and resistant slab is produced. In circumstances where a highly resistant slab is required due to the presence of chemicals or abrasive materials, the concrete may incorporate an increased concrete or mortar strength in the top section, or a resistant paint on its surface. A dry shake topping can also be introduced to the wearing course layer which can increase abrasion resistance, change the slab colouring and alter the surface texture of the concrete.

2.2.2 External Hardstandings

Industrial external hardstandings are used in a variety of situations and have to provide support for a range of loading. Many are sited around ports and harbours where large container ships deposit cargo directly onto the concrete hardstanding. The majority of the cargo will be in the form of large containers, which can be stacked several high. Each container has small casting feet on the corners through which the majority of the load will be passed. These high bearing pressures increase the risk of punching shear and damage to the slab surface.

The container handling equipment and the smaller forklift and pallet trucks form other loading types on the hardstanding. The handling equipment straddles the containers and enables them to be transported to various positions around the site. To aid in the logistics of movement, lanes are often painted onto the hardstanding to create roadways for the traffic. This can create channels of dynamic loading increasing fatigue damage and therefore the risk of failure. Other forms of loading such as forklifts and pallet trucks will not cause the same amount of stress as the larger containers and their transporters; however, they may cause more localised damage due to their rigid wheels and speed of movement. This will become especially prevalent in areas such as joints and cracks.

Other applications of external hardstandings include storage depots, distribution centres and retail outlets. Many carry delivery vehicles, pallet trucks and forklifts, as well as the temporary storage of items prior to transportation. All of these load conditions must be

accounted for, and designed against, if the hardstanding is to have a long life span. Typical values for these loads are given below in Table 2.2.

Table 2.2 – Typical Hardstanding Loading Values (Knapton 1999a)

Load Source	Load Type	Typical Load
Highway Trailer	Axle	110 kN
Straddle Carrier	Wheel	200 kN
Fork Lift	Axle	980 kN
Container (Full)	Total	210 kN

The structural components of the hardstanding are very similar to that of an internal industrial floor slab. The basic construction consists of the concrete slab (usually reinforced), a slip membrane and a subbase material, which are supported by the subgrade. The slab is between 150 and 300mm in thickness with the subbase being between 150 and 225mm depending on the type of subgrade material beneath. The main difference between an internal and external slab is the wearing surface of the concrete. This will be relatively smooth in an internal condition where movement of vehicles is slow, but will be grooved or textured in an external situation where the increased speed and the weather conditions may require additional slip resistance.

As with internal floor slabs there is a necessity to control the movement occurring due to thermal and drying shrinkage of the concrete. This is often achieved by placing joints at specified locations throughout the slab enabling sections to move relative to each other. In plain concrete the joint spacing is in the region of 6m but where reinforcement such as traditional steel bars, mesh or fibres are used the spacing can be increased up to a value of 12m (Knapton 1999a). In certain situations where heavily reinforced sections are used it is possible to produce jointless floors where natural cracking is allowed to develop. The reinforcement holds these cracks together and prevents much of the load transfer loss that would normally occur.

Construction of an external hardstanding can be accomplished by a variety of methods of standard practice in internal floor slabs. Long strip, large bay, or more commonly nowadays the use of laser screeds, can all provide the necessary quality and finish required to produce a suitably long lasting slab. Figure 2.2 shows pictorially the different construction processes available.

2.2.3 Concrete Pavements

For decades there has been a debate about the advantages and disadvantages of rigid and flexible road pavements. In the UK only a small number of concrete roads have been constructed in recent times as flexible pavements remain the preferred option (Croney and Croney 1997). This is the reverse to the USA where the majority of pavements are of rigid construction. The advantages of rigid pavements have been discussed in a number of texts such as Croney and Croney (1997), and include: 5-11% better fuel economy, increased life expectancy, reduced maintenance costs from a decrease in rutting, and better light reflection. Some disadvantages do exist and these include higher initial construction cost, increased traffic noise and reduced ride quality.

The load applied to a concrete pavement is different to that found in either an internal slab or external hardstanding. The number of load cycles is much higher due to the amount of vehicular traffic using the highway. Generally only the commercial and heavy goods vehicles are used in the calculation of loading for a pavement, as these cause most damage. These are defined as having a standard axle load of 80kN (Croney and Croney 1997). The design loading is expressed in millions of standard axles and calculated from the projected number of commercial vehicles (equated to standard axle passes using equivalence factors) expected to use the pavement in a designated period.

There are two main techniques for constructing pavements, fixed form and slip forming. Fixed form construction requires a concrete train to be mounted on rails to provide the position and levels for concrete placement. The train itself usually includes plant that spreads, compacts, finishes and textures in a single or double pass. Some of the more developed machines also allow for dowel bar insertion and joint construction. Slipform paving works in a similar manner but in this situation the train is electronically guided with wires. As with the fixed form paver, the concrete is placed, compacted and finished, although this is more commonly done in a single pass only. Figure 2.3 shows an example of the slip-forming method.

Movement control is managed with either the introduction of joints, or with the use of continuous reinforcement to hold cracks together. The two methods are described in sections 2.2.3.1 and 2.2.3.2.

2.2.3.1 Jointed

Jointed concrete pavements can be either plain, or reinforced with steel bars, mesh or fibres. In all cases the structure relies on the incorporation of joints to enable movement and stress relief to take place and prevent random cracking (Deen *et al.* 1980). In plain concrete pavements the joints are normally placed every 5m, but this can be increased to 35m if heavily reinforced. As in all slabs and pavements the stresses relieved by the joints are generally those caused by temperature and moisture movements.

The joints may contain load transfer devices such as those described in section 3.4. These help to transfer the loading between adjacent slabs reducing the stress in the concrete and supporting the vulnerable edge sections of the slab.

2.2.3.2 Continuously Reinforced

Continuously Reinforced Concrete Pavements (CRCP) are long sections of un-jointed concrete slab. They are reinforced in both the longitudinal and transverse direction with either traditional steel bars or prefabricated steel mats. The structural integrity of the CRCP is provided by the reinforcement which, although not preventing the concrete from cracking, will hold the sections together.

Design manuals such as American Association of State Highway and Transportation Officials (1986) and Portland Cement Association (1951) agree that the main function of reinforcement is to provide a pavement that cracks at regular and reasonably close spacing, combined with crack widths that provide good load transfer. The amount of reinforcement required is selected from one of the variety of tables produced by the design authorities, which have been shown to provide suitable restraint.

Some states in America have decided that the use of the transverse reinforcement is unnecessary, and is only of use as a construction aid for the placement and maintainment of position for the longitudinal steel (Gregory 1984). However, this has not been verified and it is commented that in construction widths over 3.65m the transverse steel helps to hold the concrete together in cases where longitudinal cracking occurs.

2.2.4 Structure Comparison

Table 2.3 compares the significant parameters common in the design and construction of internal slabs, external hardstandings and rigid pavements. The main variation between the structures is caused by the magnitude and type of loading, with that of the rigid

pavement being smaller but more frequent. Construction layer thicknesses, shrinkage control and the concrete specifications are all similar, with the method of construction changing due to the size and shape of the pour.

Table 2.3 – Structure Comparison

Item	Internal Slab	Ext. Hardstanding	Rigid Pavement
Loading	42 – 114 kN Predominantly Static	100 – 1000 kN Predominantly Static	80 kN Standard Axle Predominantly Dynamic
Component Dimensions	150 – 300mm (Slab) < 225mm Subbase	150 – 300mm (slab) < 225mm Subbase	125 – 300 (Slab) < 225mm Subbase
Movement Control	Plain Jointed Reinforced Jointed Jointless	Plain Jointed Reinforced Jointed Jointless	Plain Jointed Jointed Reinforced CRCP
Construction Techniques	Long Strip Wide Strip Large Bay Laser Screeding	Long Strip Wide Strip Large Bay Laser Screeding	Fixed Form Slip Form
Concrete Specification			
Strength	30 – 50 N/mm ²	30 – 50 N/mm ²	40 N/mm ²
W/C Ratio	< 0.55	< 0.55	< 0.55
Cement Content	325 kg/m ³	325 kg/m ³	325 kg/m ³
Replacement Materials	< 35% PFA < 50% GGBS	< 35% PFA < 50% GGBS	< 35% PFA < 50% GGBS
Max Agg.	20 – 40mm	20 – 40mm	20 – 40mm
Admixtures	Super-Plasticisor	Super-Plasticisor Air Entrainment	Super-Plasticisor Air Entrainment
Drying Shrinkage	< 0.065%	< 0.065%	-----

2.3 Typical Actions for Concrete Slabs on Grade

During the life span of a concrete slab or pavement a number of actions will need to be withstood if failure is to be prevented. These actions can be created from external forces such a racking system or vehicle, or internal strains instigated by the movement of

concrete over time. Each mechanism must be fully understood and designed for if the structure is to behave consistently throughout its life. This section provides an overview of the actions found in slabs and pavements including: moisture movement, thermal movement, static loading, impact loading and cyclic dynamic loading, briefly outlining the effect that each has on the structure.

2.3.1 Moisture

2.3.1.1 Drying Shrinkage

Drying shrinkage is caused by the loss of moisture from concrete resulting in a net decrease in volume. There is however, no relationship between the quantity of moisture removed and the magnitude of volume reduction (Neville 1995).

The principle mechanisms of concrete shrinkage are capillary tension, surface tension, disjoining pressures and movement of interlayer water (Illston 1994). It is thought that early drying shrinkage is caused mainly by the surface tension in the capillary pores, whereas longer-term shrinkage is formed through the loss of water adsorbed on the surfaces of hydrated cement paste (Perenchio 1997). Illston (1994) states that the effect each mechanism has on total shrinkage is unclear, with authors showing large differences of opinion.

Cracking of a slab or pavement due to drying shrinkage occurs when the tensile stress from movement restraint exceeds the tensile strength of the concrete (Sprigg Little Partnership 2000). During the early life of the slab, the tensile strength is poor and therefore the potential for shrinkage cracking is high. Effective curing with the use of a sealant or moist covering can significantly reduce the amount of cracking occurring during this early period. Suprenant (2002) highlights this fact stating good curing has no effect on whether or not the concrete will shrink or to what degree, however it does delay it until a later stage, enabling an increase in strength.

The introduction of joints into concrete slabs aids in the dispersion of shrinkage strains and can prevent related cracking. The joints are weakened planes of concrete whereby the concentration of stress is high enough to induce a crack. With careful planning in the positioning of these joints, random cracking in highly trafficked or loaded areas can be prevented. Details on the various types of joint used in concrete slabs and pavements are described in section 2.5.4.

2.3.1.2 Plastic Shrinkage

Plastic shrinkage is the reduction in volume of concrete caused by the loss of moisture into the atmosphere prior to initial set. The moisture loss may be caused by evaporation from the concrete surface, or suction from the subbase material below. The magnitude of plastic shrinkage is approximately one percent of the volume of dry cement (Neville 1995). Plastic cracking is formed when the removal of water from the surface is greater than the amount of bleed water being transferred to the surface.

Plastic shrinkage cracks are generally not a problem in a structural sense, although they may affect the durability of the surface and lead to crazing and scaling. Power trowelling of the surface often smoothes over these cracks, leaving the appearance of an acceptable slab; however, the crack may have permeated much deeper than this top layer leaving the potential for deterioration at a later stage (Neville 1995).

2.3.2 Thermal

Temperature changes in concrete slabs and pavements can occur from two main sources. Firstly, during its early life, the cement will create heat as it hydrates and sets. This increase in temperature will cause the concrete to expand, the magnitude of which is dependent upon the coefficient of thermal expansion and the extent of temperature increase. Over time the slab will begin to harden, the heat from the hydration process will reduce, and a drop in internal temperature ensues. Studies carried out by Bishop (2001) have recorded the changes in slab dimensions caused by the various hydration processes and discovered that the initial thermal movement instigates crack formation under sawn joints, and creates much of the early age cracking in slabs.

The second cause of thermal movement in slabs and pavements is a variation in temperature due to environmental conditions after the concrete has matured. Some structures such as external hardstandings and pavements will be required to withstand greater fluctuations in temperature than internal floor slabs, but even internally a degree of temperature differential between top and bottom is probable (Suprenant 2002). As the concrete heats up expansion of the slab will occur, as it cools down contraction takes place. There will generally be a differential temperature gradient between the top and bottom of the slab caused by the underlying subbase material. In this situation there is a possibility of curling or warping of the slab, which is further described in 2.4.2.

To accommodate thermal movement it is common for joints to be constructed within the slab. The temperature range will control the size of these joints to some degree, with changes in crack width measurable over different seasons, or to a lesser extent, throughout the day (Gulden and Brown 1985). Minkarah *et al.* (1982) concluded that the commonly used temperature expression given in equation 2.1 resulted in poor comparison of temperature induced movement (δt) when measured against early age field data. However, Bodocsi *et al.* (1994) re-examined a number of these joints after twenty years to establish whether the equation was correct for older concrete, with the results showing good correlation when temperature at mid-slab was used. The effect of subbase support and joint type was also analysed with their effects shown to be negligible.

$$\delta t = \alpha_c \Delta T L \quad \text{equation 2.1}$$

Where:

α_c = Thermal coefficient of expansion for concrete

ΔT = Temperature difference between opposite faces of a member

L = Slab length

The constituents making up the concrete mix determine the exact magnitude of thermal expansion and contraction occurring within the slab. Each element that is placed into the concrete will have its own coefficient of thermal expansion and as such will have an influence on the overall movement. In most concrete the aggregate content will make up 70-80% of the total volume and will therefore have the most impact. Ideally aggregates with a low coefficient of thermal expansion should be used to resist the potential for shrinkage; however, each aggregate type within the mix should be of a similar value to prevent differential movement and matrix cracking.

2.3.3 Static Load

Static loads are found mainly in external hardstandings and internal floor slabs, with the magnitude varying greatly depending on the materials being stored. Typical values for a racking base-plate can differ from 35-100kN, with 200kN quoted for high lifting areas (Knapton 1999b). The layout of the racking often requires base plates to be placed back to back, essentially doubling the force applied. Line loads from mobile racking systems are approximately 150kN/m, with mezzanine floor leg loads of around 200kN. In pavements there is very little static load and this is therefore disregarded during design.

External hardstandings often contain some form of racking system, although it is usually the stacking of large containers used for the transportation of goods on lorries or in ships that creates the highest loads. The small feet on which the container rests create high contact stresses acting directly onto the concrete surface and increasing the risk of damage. Rogers (2000) has postulated that high point loading can also clamp concrete slabs to the foundation. This prevents moisture and thermal movement, resulting in the formation of a restraint crack.

2.3.4 Cyclic Dynamic Load

Cyclic dynamic loading is caused by the movement of vehicular traffic on the slab's surface. For this reason pavements are at greater risk from this type of loading than both industrial floor slabs and external hardstandings due to the higher number of cycles they encounter. The repetitive nature of the load causes fatigue within the concrete, which eventually manifests itself as a crack. The magnitude of the load applied depends upon the vehicle under consideration and its speed of movement. Road Research Laboratory (1955) state that the stress in a road slab due to a moderately fast moving load is similar to that of a stationary vehicle. This is because the deflection magnitude that would occur under a static load is prevented by the elasticity of the road structure, thereby reducing the effective weight, counteracted by the increase in stress from the impact effect. Work completed by Helwany *et al.* (1998) examined the effect of vehicle speed on the deflections in flexible pavements. It was found that the slower vehicle speed (8km/h) caused a higher stress in the pavement than that of a high-speed vehicle (72km/h). Papagiannakis *et al.* (1991) argued that the frequency of loading should be considered in all analysis, as the high-speed repetitive loading of a slab does not allow full recovery to take place, increasing the risk of damage. In warehouses and external hardstandings the majority of the vehicles will be slow moving, thereby negating some of these effects; however, the actions of cornering, accelerating and braking can require increases relative to static loads. The design guides incorporate this phenomenon using a percentage increase of the static load, tables of which are readily available.

There are a number of other forms of dynamic loading found in industrial floor slabs such as: live storage systems that provide continuous movement of goods from one area to another, mobile racking which can be moved to allow for additional floor space, and assembly plant. They all produce similar loads to that found in pavements but at a reduced cycle frequency, and therefore the design philosophies are developed accordingly.

As mentioned previously it is often the joints and cracks in a slab or pavement structure which are prone to the most damage. This is especially prevalent in industrial floor slabs where much of the MHE have small rigid wheels. The high contact stresses on the edge of a discontinuity can result in spalling and deterioration of this material. The design guides suggest that only the heaviest vehicles contribute to fatigue damage of the concrete (Croney and Croney 1997). Cyclic shear testing on cement bound materials conducted by Thompson (2001) shows this not to be the case. Plots of joint net shear slip against load indicated that 80% of shear slip movement took place under only 12.5% of the applied load in non-reinforced specimens. This suggests that more local distress will occur at low load than is currently assumed, thereby shortening the structure's life. More details on the deterioration processes are given in section 2.4.

2.4 Serviceability Problems

A number of serviceability problems can occur in floor slabs and pavements, some of which will develop only in one type of structure, with others common to all. The latter is often the case with failure in and around the joint and crack area which, by its nature, is a structural weak point. This weakness means its degradation will be far quicker than that of any other part of the concrete, and may lead to other serviceability problems. This section provides information on the main causes of failure and how they are formed.

2.4.1 Cracking

As mentioned in sections 2.3.1 and 2.3.2 some degree of concrete cracking will occur during the life of the structure, caused by the thermal and drying shrinkage of the concrete. In general the slab will tend to contract around its central core, with movement increasing with distance from this area (Illston 1994). The slab itself is placed either directly onto a subbase or, more commonly in the UK, on a slip membrane. This provides a low-friction boundary layer between the concrete and sub-base enabling much of the movement to be confined to the joints. There is some dispute as to the effectiveness of the slip membrane layer and whether it should be utilised (Hulett 2001), with further information on this subject discussed in section 2.6.3. In practice the membrane may not provide the required slippage, thus a high level of friction will be retained. This may be caused by the roughness of the subbase, clamping by racking, high loading, or imperfections in the slip membrane. In this situation locking takes place, preventing movement of the slab relative to the subbase. This creates tensile stresses in the concrete which, if high enough, will lead to crack development (Critchell 1958).

A similar slab-locking phenomenon occurs when dowel bars or similar are used as load transfer devices. These should be debonded on one side to allow horizontal movement between the slabs, and release of the shrinkage stress. If these dowels become locked due to misalignment or high friction, movement is prevented and tensile stresses will be set-up in the slab. If these reach critical levels a stress-relieving crack will be produced. Due to the load transfer requirements of the joint it may be necessary to provide dowels around the full perimeter of the slab. In this situation the dowel must allow some degree of lateral, as well as horizontal movement to enable two way shrinkage to take place. Figure 2.4 shows typical examples of restrained movement cracking.

Problems can occur when a high number of fine cracks develop in close proximity to each other (Verhoeven 1993). When these cross, small, unsupported areas of slab are created which are unable to fully withstand the applied loading. These cracks are often caused by poorly designed reinforcement. In areas of slab with high quantities of steel, or other resistance to shrinkage, the stress will be well distributed. However, if the movement is still too great for the tensile strength of the concrete, regularly spaced cracks will be produced. This may occur in one direction only, or may transpire in both directions. In the case where only transverse cracks are produced, bridging may instigate cracking in the opposing direction. According to Verhoeven (1993), 1 - 1.5m is the ideal spacing of cracks in pavements as this ensures tight fitting cracks without excessive concrete break-up.

Poor construction of the slab can create many problems resulting in random cracking (Moody and McCullough 1993). One of these defects is caused by the inadequate compaction of concrete underneath the longitudinal and transverse reinforcing bars, creating localised weak points with reduced resistance to load. Work undertaken by Savage (1985) has also indicated a problem with the insertion of reinforcement. When placed up to the transverse joint it acts as a stress raiser, which when subjected to a high number of load repetitions, causes a peeling action of the upper and lower sections of concrete. If detritus enters between these layers a cantilever action is introduced instigating vertical cracking. This type of failure is found mainly in concrete pavements due to the construction and environmental factors they encounter. The formation of these cracks is shown in Figure 2.5.

Mid slab cracking often occurs when the joints inserted into the concrete fail to open up as expected. This is often caused by saw cutting too late after the concrete has been poured. The Concrete Society (2003) recommend that this is undertaken between 12 and

24 hours after casting as this is when much of the shrinkage and thermal movement takes place. A similar effect occurs if the saw cut is not deep enough as the concentration of stresses may not converge under the joint leading to cracking elsewhere. Careful detailing is therefore essential to make sure movement is confined to the prescribed areas.

The excessive width of a joint or crack within a floor slab or pavement can create severe problems with respect to ride quality, vehicular damage, and increased slab deterioration. The cause of the crack, and its size, can be attributed to inadequate design, poor construction and/or extraordinary climatic conditions (American Association of State Highway and Transportation Officials 1986). Excessive widths (often over 5mm) can also be attributed to the dominant/dormant joint phenomenon whereby some joints remain closed, transferring movement to the next available joint. This increases its size leaving it more susceptible to deterioration.

Structural cracking is a more serious occurrence as it indicates a problem with either the design, or the construction of the slab. This occurs when loads placed onto the element are higher than the structural capacity of the concrete, creating significant tensile stress and full depth cracking. Chou (1989) stated that the failure criterion for rigid pavements is when more than 50% of the slabs have produced this initial first crack due to structural damage, and advised that significant remedial work is then needed.

2.4.2 Curling

Curling in a concrete slab, hardstanding or pavement is caused by a combination of drying shrinkage and temperature movement (Croney and Croney 1997). As described in Section 2.3.1 the majority of drying shrinkage will take place at the surface of the concrete as the base is protected against the atmosphere by the subbase and slip membrane. This sets-up a shrinkage gradient across depth resulting in the slab edges becoming raised above the foundation, and a condition of zero support. Cantilevered sections are thus created, increasing the risk of cracking, pumping and faulting.

Figure 2.6 shows how a similar condition occurs with temperature variations throughout slab depth as in hot conditions concrete will expand and in cold conditions it will contract. The top section of the structure will change in size dependant on the external conditions, with the base temperature stabilised by the subsoil. In conditions where the top surface temperature is colder than the bottom the slab edges will tend to rise above the level of the subbase, whereas when the slab surface is warmer than the bottom the slab

sags at its edges (Armaghani 1993). The subsoil in the latter case (if rigid enough) will prevent the slab edge from deforming into the ground and lift the central section of the slab above the subsoil.

In either of these cases the lack of support created when the slab has been raised above the level of the subsoil can result in increased stresses and severe cracking (Nishizawa *et al.* 1993). Barenberg and Zollinger (1990) concluded that for pavements, the strains created from curling and warping can be larger than those caused by applied loading. Since concrete is relatively weak in tension, applying an additional load, or even the self-weight of the concrete, can result in the formation of a crack. This is extremely prevalent in corner sections of slabs where the support through load transfer from other slabs may be limited anyway. Once these cracks have formed, deterioration can increase extremely quickly and compromise the quality of the slab. According to Walker and Holland (1999) shrinkage stresses are commonly in the region of 0.1-0.4 MPa compared to a curling stress of 1.4-2.8MPa and as a result 'curling crack' would be a far more appropriate term than shrinkage crack in respect to floor slabs.

Frabizzio and Buch (1999) state that transverse cracking of the slab relieves the accumulation of curling stresses and therefore the joints incorporated within the slab can moderate the magnitude of the curl, and reduce stress. Ioannides *et al.* (1990) argue that dowelled joints can have the opposite effect and actually increase stresses due to slab bending. Ytterberg (1987) indicated that a smaller spacing would produce an increased number of curling sites which could prove detrimental, and thus, the spacing of joints is an important consideration in controlling surface profiles and preventing cracking.

The degree of curling and the shape of the slab surface will have an impact on the orientation of the crack face between slabs. Poblete *et al.* (1988) stated that in conditions of negative temperature gradient (top cooler than bottom) the joint faces will be free to rotate upwards so that contact will be limited to the lower transverse edges (see Figure 2.7). This can affect the load transfer potential of the crack, thereby influencing slab behaviour.

Walker and Holland (1999) highlighted the dangers of using high concrete compressive strengths due to the increased risk of shrinkage. This enhanced strength can also reduce creep preventing the relaxation of stresses which, to some degree, would enable the slab to return to its original level position. Similarly, the smaller section thickness used in steel fibre concrete slabs can result in greater curl due to the reduced self-weight (Schrader

1985). The amount of curling, and therefore the size of cantilevered section depends on the properties of concrete, amount of load transfer and degree of subbase support (Al-Nasra and Wang 1994).

Suprenant (2002) examined the results from various authors experimental work and concluded that an increase in Young's modulus of as little as 6.9 MPa can increase curling deflection by approximately 10%. Similarly, an increase in modulus of subgrade reaction from 0.014 to 0.216 N/mm³ increases the curling deflection by 30% (Al-Nasra and Wang 1994). Suprenant (2002) examined the dimensions of a curled pavement to determine at what degree it became unsupported. It was found that the length not in contact with the subbase was approximately 10% of the total length when load transfer was present. Where there was a loss of load transfer this increased to 20%. The magnitude of the curl in pavements is commonly around 6mm, but can be as high as 25mm in extreme circumstances (Suprenant 2002).

Several equations have been produced which enable an estimate of slab curling due to both thermal and hygral effects. It is beyond the scope of this thesis to evaluate these methods and therefore the reader is directed to the work of Bishop (2001) for further information. Robins *et al.* (2002) concluded that the models utilised by Petterson and Alemo (2000) and Rollings (1993) gave very good agreement with a finite element model examining slab movement and restraint stresses. Petterson and Alemo (2000) provided an equation for the critical length of a slab that will develop warping as shown in equation 2.2. The critical length (L_{cr}) is such that at this value the warping stresses are equal to that of the self-weight of the concrete, resulting in zero curl, as shown in Figure 2.8. Equation 2.3 developed by Rollings (1993) enabled determination of the vertical edge movement caused by slab curling (αt).

$$L_{cr} = \sqrt{\frac{4\alpha_c.E_c.\Delta T.h}{5.\rho_c.g.f}} \quad \text{equation 2.2}$$

$$\alpha t = \frac{\Delta \epsilon_{sh}.L^2}{8.h} \quad \text{equation 2.3}$$

Where:

α_c = Thermal coefficient of expansion for concrete

E_c = Youngs modulus of concrete

ΔT = Temperature difference between opposite faces of a member

h = Slab depth

ρ_c = Concrete Density

g = Acceleration due to gravity

f = Load factor (assumed 1 under self-weight)

$\Delta \varepsilon_{sh}$ = Differential movement between upper and lower faces of the slab

L = Slab length

2.4.3 Pumping

Pumping is caused by the ingress of water into the slab/pavement system. Once this occurs a solution is formed between the liquid and the subbase material and on application of load near to the affected zone, deflection takes place forcing the solution out under pressure. This water invariably takes some of the sub-soil material with it leading to a loss of fines underneath the affected zone and thus a greater void is created (Van-Wijk *et al.* 1989). Eventually this routine generates a complete lack of support and an increased risk of failure. Rollings (1993) examined this effect when looking at curled slabs and found that in pavements throughout the United States curling in the region of 3-16mm was associated with signs of pumping from both vehicular and foot traffic. This clearly shows how one method of deterioration (pumping) can easily manifest itself into other causes of failure (cracking).

A number of factors influence pumping and the degree to which it effects the slab. These include, water ingress, drainage, quality of subbase, slab deflection and traffic loading (Van-Wijk *et al.* 1989). Adequate sub-drainage was stated as having the greatest influence on the pumping condition, almost eliminating the risk.

2.4.4 Faulting/Dynamic Load Step

Faulting is the permanent variation in level between each side of a slab or crack as shown in Figure 2.9. The difference in level affects the deterioration rate and life span of vehicles, whilst reducing ride quality. A generally agreed differential of 3.2mm or greater causes very poor ride quality in road pavements, and is therefore classed as a severe problem (Stock 1988). In the case of floor slabs the amount of acceptable level change is dependent upon the use of the floor. Very narrow aisle trucks, which have high reach, may require much tighter floor tolerances compared to smaller, rubber wheeled forklifts.

Dynamic load step is similar to faulting; however, this is a measure of slab edge level variation when placed under load, as shown in Figure 2.9. Walker and Holland (1999) have suggested that a differential vertical movement below 0.5mm should be retained, although it is not stated to which floor class this is directed. A value of 0.1mm is proposed by Pearson (1999), who also suggests a maximum total deflection of 0.15mm in a single slab edge. The Concrete Society (2003) does not provide a value for unacceptable amounts of step as they state that it has not been adequately researched. However, they do indicate that the relevant floor flatness limit (varying between a 2.5 and 7.5mm elevation difference over a 300mm length) should be adhered to as a minimum.

The change in level can be caused by build quality problems in the case of a construction joint, but is more usually due to the lack of load transfer at the joint or crack (Frabizzio and Buch 1999). Poor load transfer causes each slab to work as an individual unit, without distributing load onto adjacent elements. This intensifies the stress within the subbase, increasing the risk of permanent deformation and pumping. In pavements where traffic runs in one direction only the effect is enhanced due to the gradual accumulation of load on the approach slab compared to the sudden impact load on the leave (asymmetric dynamic loading). This difference in load rate creates greater settlement in one section of subbase compared to the other and leads to a dynamic step in the surface level (Cudworth 2001).

Another cause for the variation in subbase settlement has been attributed to trapped water beneath the slab joints (Armaghani 1993). He stated that the movement of fine materials underneath the jointed section causes one area to rise above the other. This is again caused by the approach/leave slab mechanism where a higher stress is produced under one slab section.

2.4.5 Punch-Out

Punch-out failure has been described briefly in section 2.4.1 in relation to excessive cracking. The formation of a punch-out begins with transverse cracking of the concrete caused by shrinkage, temperature movements, or loading. As these cracks open further and deteriorate over time the potential for load transfer is reduced and the stiffness of the structure decreases. These cracks, if positioned near each other, may intersect with longitudinal cracks created by the transverse bridging of the slab and form small localised areas that are no longer integrated with the rest of the concrete structure (Stock 1988). With the lack of load transfer and restraint from the remainder of the slab, the small area

of concrete may be forced from the element under the influence of further dynamic loading and traffic. The progression of punch-out is shown in Figure 2.10.

The cause of the increase in cracking is detailed in section 2.4.1 with the main reason being incorrect reinforcement selection. This leads to poor crack spacing with either too few cracks with large widths, or many cracks with a small width. Compromise between the two is essential and therefore correct sizing and spacing are essential. Darter *et al.* (1979) state that punch-out occurs most often in cracks 300 to 600mm apart, and rarely occurs where spacing is over 1200mm. Gregory (1984) provided some guidance for CRCP with values of ideal crack spacing between 1.5 and 2.5m suggested.

2.4.6 Spalling

Spalling is defined as the degradation of the concrete at the slab surface and occurs next to a crack or joint. This will usually involve a diagonal crack that passes from the top surface of the structure through to the vertical face (Figure 2.11). An area of weakness is created that can easily break off, leading to reduced ride quality and a need for greater vehicle maintenance. The reduced section thickness caused by the spall also cuts the amount of load transfer available from aggregate interlock, which in turn increases the possibility of further deterioration. The cause of the spall is instigated by the delaminations created from early age differential shrinkage (Zollinger and Senadheera 1994). The action of rolling wheels, temperature changes and moisture penetration then enhances this stress until an edge spall is produced. Poor finishing of the structure, ingress of detritus or incorrect selection of mix constituents can accentuate this effect even further (Zollinger and Senadheera 1994).

Stock (1988) has distinguished between the two main types of spall found regularly in continuously reinforced concrete pavements; these being minor and severe. It is noted that severe spalling is not formed from minor spalling with different causes for each. Minor spalling is created by high deflections due to poor support conditions, whereas severe spalling is a function of poor concrete tensile strength from incorrect curing and construction practice. The size of a spall is generally categorised as deep when it is greater than 25mm in depth.

2.5 Concrete Slab Design

The structural and detail design of a concrete slab requires all actions and loads to be thoroughly examined. These must then be controlled with the correct selection of concrete, reinforcement and layout. The design aims to make the structure as economic as possible without compromising the structural capacity, or its serviceability.

2.5.1 Concrete properties

Concrete is the main material controlling the success or failure of the slab element. If it is incorrectly designed then deterioration can occur leading to lifelong problems and the requirement for remediation.

In most design guides the thickness of slab required to withstand the applied loading is controlled by the characteristic flexural strength. Concrete is usually selected dependant on its compressive strength properties and therefore equations and tables to provide comparisons between the two have been developed.

The equations used for design are frequently only appropriate for plain concrete, with the advantages of using mesh or fibres excluded. When reinforcement is to be incorporated The Concrete Society (2003) advise that the value of flexural strength should be determined experimentally using third point loading.

The selection of the concrete constituents controls the properties of the finished slab. Knapton (1999a), Ringo and Anderson (1996) and The Concrete Society (2003) all detail the effects on the slab response enabling the designer to select appropriate mix designs. This can include, surface finish, curing times, characteristic strength and wearing resistance along with many others. It is beyond the scope of this thesis to discuss how each of these can be controlled with mix design, and the reader is directed to the aforementioned literature if further information is required.

2.5.2 Slab Reinforcement

2.5.2.1 General

Concrete is essentially very strong in compression and weak in tension. For this reason it is common to reinforce the concrete with steel bars, mesh or fibres. The reinforcement enables the tensile stresses created by shrinkage and contraction to be redistributed, leaving the concrete relatively undamaged and capable of resisting applied load. In

concrete slabs on grade it is unusual for the structural tensile force to exceed the limitations of the concrete. However, high internal stresses and strains caused by the inherent shrinkage of concrete are often enough to induce a crack. The larger the crack, the more liable it is to deteriorate and lead to failure. The introduction of reinforcement redistributes the tensile stresses throughout the slab, resulting in smaller, more frequent cracks that are less likely to cause a problem at a later stage.

2.5.2.2 Fabric

Steel fabric comes in a variety of diameters and spacing for use in different circumstances. The stronger the fabric required, the greater the wire diameter, and smaller the spacing. Details on standard, stock fabrics are shown in table 2.4.

Table 2.4 - Stock Fabric Sizes (Knapton 1999a)

Fabric Reference	Longitudinal Wires			Cross Wires			
	Nominal size: mm	Pitch: mm	Area: mm ² /m	Nominal Size: mm	Pitch: mm	Area: mm ² /m	Mass: kg/m ²
Square mesh							
A393	10	200	393	10	200	393	6.16
A252	8	200	252	8	200	252	3.95
A193	7	200	193	7	200	193	3.02
A142	6	200	142	6	200	142	2.22
A98	5	200	98	5	200	98	1.54
Structural Mesh							
B1131	12	100	1131	8	200	252	10.9
B785	10	100	785	8	200	252	8.14
B503	8	100	503	8	200	252	5.93
B385	7	100	385	7	200	193	4.53
B283	6	100	283	7	200	193	3.73
B196	5	100	196	7	200	193	3.05
Long mesh							
C785	10	100	785	6	400	70.8	6.72
C636	9	100	636	6	400	70.8	5.55
C503	8	100	503	5	400	49	4.34
C385	7	100	385	5	400	49	3.41
C283	6	100	283	5	400	49	2.61
Wrapping mesh							
D98	5	200	98	5	200	98	1.54
D49	2.5	100	49	2.5	100	49	0.77
Stock sheet size	Longitudinal wires			Cross wires			Sheet area
	Length 4.8 m			Width 2.4 m			11.52m ²

Fabric used in internal slabs is generally of a low strength and in most situations will either be A142 or A193. The A142 fabric is made of 6mm steel wire, spaced at 200mm centres in both the transverse and longitudinal directions. The A193 fabric uses a larger 7mm wire to give it a slightly higher tensile capacity. In external situations the size of

fabric may be larger due to the increased temperature differentials, and therefore greater tensile stresses, under which it will be placed. If the reinforcement is required to serve a structural purpose then similarly a stronger fabric will be required. In rigid pavements a long fabric is generally used, the size of which is selected dependant upon the cumulative number of million standard axles that the pavement is required to withstand (Croney and Croney 1997).

Where light steel meshes, such as the A142 are used the entirety of the slab can be covered. This can continue through any induced joints as its low strength will enable yielding and unrestricted crack formation. Heavier steel should be avoided as it may lead to cracking at areas other than where designed (Concrete Society 2003).

The most suitable depth for fabric is unclear with various authors suggesting different values. Each has its own advantages but as yet no clear preference has emerged. From a constructability standpoint it is advantageous to place the fabric in the base of the slab as this prevents any concerns about cutting through the steel when joints, or wire guidance systems are used.

The Concrete Society (2003) state that the position of the fabric reinforcement matters little as it is of such a small percentage that it contributes insignificantly to the width and spacing of cracks. However, they do acknowledge that the fabric prevents induced, or shrinkage cracks from exceeding 1 to 2mm, except in extreme circumstances. ACI Committee 302 (1996) conflicts with this and provides guidance recommending temperature and shrinkage reinforcement is placed in the upper third of the slab as this is where it provides most restraint. Gregory (1984) reports on studies showing firstly that an optimum depth of 20mm below mid-depth is preferable, with another suggesting mid-depth reinforcement had better cracking performance than slabs with reinforcement in the upper half. Bishop (2001) has concluded that reinforcement in the upper level is the ideal location, with the Belgian standards lowering their recommendations from 70mm below the top surface to mid-depth, in the attempt to improve crack distribution.

The Concrete Society (2003) note that although fabric is not assumed to be structurally active, it can have some effect on load carrying capacity. In this case the positioning is crucial as ground supported slabs are prevented from having load induced cracks at their surface, thereby making only bottom slab reinforcement useful in design.

2.5.2.3 *Fibres*

Fibres have been increasingly used as a method of reinforcing elements such as floor slabs, hardstandings and pavements since the 1970's (ACIFC and the Concrete Society 1999). Various materials have been used to construct the fibre but the two types employed most often are steel and polypropylene. Steel fibres can transmit stresses across micro-cracks and prevent them from increasing in the hardened concrete, whereas polypropylene fibres are used for their ability to prevent shrinkage and reduce cracking during the early life of the concrete. Dosages of steel and polypropylene fibres used in concrete slabs are 20-45 kg/m³ and 0.9 kg/m³ respectively (Concrete Society 2003).

Steel fibres are made of short thin sections of steel that are moulded into a variety of shapes, examples of which are shown in Figure 2.12. These can be anything from a hooked end to a melt extract with each having different properties and making a singular design practice for 'a fibre reinforced element' very difficult. However, these problems need to be overcome, as the advantages that can be achieved are considerable (Hannant 1994).

The fibres can either be inserted into the concrete during mixing at the plant or just prior to the pour commencing. Each method enables the slab to be constructed without some of the build problems commonly found when using traditional reinforcement. Once the fibres are incorporated within the mix it is then possible for the concrete to be placed directly into a slip form paver or screeder, which vibrates, compacts and finishes in one pass.

The introduction of steel fibres into a concrete mix can help with the crack control in a number of ways. Researchers such as Abdul-Wahab and Ahmad (1992) and Knapton (1999a) comment that fibres reduce the concrete shrinkage, which in turn lessens the stresses in the slab and therefore limits the number of cracks. Fibres will also help to prevent any micro-cracks developing into macro cracks, which are less likely to cause deterioration and are therefore highly preferential (Ibrahim and Luxmoore 1987). According to Grzybowski and Shah (1989) the addition of 0.25% of fibres into a concrete mix reduces the size of an un-reinforced crack width by a third. Since the width of a crack greatly affects the load transfer efficiency, any resistance to separation is extremely valuable. Hannant (1994) also concluded that 25kg/m³ of steel fibre restrains forces that cause crack opening to a level comparable with that obtained from using traditional mesh.

2.5.2.4 Structural Reinforcing steel

Bischoff *et al.* (1997) postulated that the amount of reinforcement should be high enough to have a post crack strength exceeding the un-cracked capacity of plain concrete, ensuring the slab is still serviceable after cracking has commenced. Reinforcement quantities as little as 0.13% were found to increase the post-crack strength, although the load to initial first crack did not change. When the quantity was increased to 0.38% a higher residual and first crack level was found. For these increases to be accounted for in design, allowing a decrease in slab thickness, the guidance needs to be changed to advise an ultimate limit state value be used in lieu of the current elastic methods.

Losberg (1978) suggested that structural reinforcement should always be used in slabs and pavements on grade. He stated that the flexural strength of the concrete alone should be disregarded, as in other structural members. This requires bottom reinforcement throughout the slab with top steel also included in high-risk areas such as edges and corners. The Concrete Society (2003) gives values for this reinforcement as 0.25-0.35%.

2.5.3 Structural Design

The structural design of slabs on grade deals with the ability to withstand imposed load. There are two main design methods for analysing a slab, these being the Westergaard (1926), or elastic method, and the Meyerhof (1962) and Losberg (1978) plastic approach. Care should be taken regardless of which method is used as the theory assumes the slab is in good contact with the subbase at all times. Where the slab has curled increased deflections and stresses will be created by the lack of supporting conditions.

The methods of Westergaard (1926) and Meyerhof (1962) have been compared to laboratory formed slabs tested by Beckett (1999). His work examined central, corner and edge conditions using a jointed, 150mm steel fibre reinforced slab with a 150mm subbase. The findings show that the first crack loads are considerably closer to the Meyerhof (1962) equation than to Westergaard (1926) for both edge and central loading; however, the load to first crack for the corner condition provided very close agreement to both. In regard to deflection the corner condition showed close agreement with the Westergaard (1926) equation up to first crack load. For the edge and central conditions the test values were considerably greater than the Westergaard (1926) values.

2.5.3.1 Elastic method

Much of Westergaard's (1926) work, and that continued from it, has examined the internal, edge and corner stress conditions occurring in a slab caused by imposed loading. The maximum stress locations have been identified, and thus the areas most at risk of cracking. In internal conditions and at the slab edge this will transpire at the bottom of the slab; however, corner loading generates most stress at the surface. Chandler and Neal (1988) stated that in conditions where the slab remains in contact with its foundation support, it is the edge loading which creates the greatest overall stress, whereas in slabs that have some degree of curl the stress in the corner will increase significantly leaving it at most risk.

Many of the stress and deflection equations pioneered by Westergaard (1926 and 1947) have been evaluated and modified by several authors to produce more accurate designs which allow for the incorporation of partially supported joints and warped slabs (Portland Cement Association 1951). Regardless of these changes, most of the new design theories are still based on his early work (Beckett 2000).

Ioannides *et al.* (1985) suggested that there have been several situations in which Westergaard's (1926) equations have been misapplied or incorrectly written. Moreover, they conclude that the original edge loading equation is incorrect and the 'amended' equation in his 1947 paper (Westergaard 1947) is preferable. Each of Westergaard's equations were compared to results obtained from the ILLI-SLAB finite element computer program by Ioannides *et al.* (1985). The results show that deflection in the edge situation is in close agreement to the 'amended' 1947 equations although the values are dependent on slab size. Hence, it is important that the 1947 equations are used in any direct use for the design of concrete slabs.

Relevant simplified deflection equations for each area of design as stated by Ioannides *et al.* (1985) and Westergaard (1947) are listed below.

- (Zi) The interior of the panel at a considerable distance from the edges (equation 2.4)
- (Ze) At an edge or at a joint that has no capacity for load transfer (equation 2.5)
- (Zc) At a corner with no capacity for load transfer (equation 2.7)

$$Z_i = (P/8kl^2) \{1 + (1/2\pi) [\ln(a/2l) + \gamma - 5/4] (a/l)^2\} \quad \text{equation 2.4}$$

$$Z_e = (\{P[(2 + 1.2\mu)^{1/2}]\} / [(E_c h^3 k)^{1/2}]) [1 - (0.76 + 0.4\mu) (a/l)] \quad \text{equation 2.5}$$

$$Z_c = (P/kl^2) [1.1 - 0.88 (a_l/l)] \quad \text{equation 2.6}$$

Where:

P = Applied load

k = Modulus of subgrade reaction

l = radius of relative stiffness (see section 3.4.2)

a = Contact radius of a load

γ = Eulers constant

μ = Poissons ratio for concrete

E_c = Young's modulus for concrete

h = Slab depth

a_l = Distance from corner to load centre

When utilising the elastic method of analysis the values of stress and deflection obtained are only accurate until first crack, at which point the behaviour changes. If reinforced, the slab will retain some residual strength after this period, which can only be utilised by using amendments to the original equations. The ACI Committee 360 (2000) have recommended lowering safety factors, or adjusting the load contact areas to suit these particular applications.

2.5.3.2 Plastic Method

Meyerhof (1962) produced equations to allow the ultimate load to be obtained from plastic theory. His deflections were based on applied loading only, and it is thus noted that the theory needs to be adapted to incorporate curling effects. As with the Westergaard (1926) equations, three load positions were used to define the loading regime, these being internal, edge and corner.

When loaded in the central condition radial tension cracks are formed on the underside of the concrete slab. As the load is increased a circumferential crack transpires on the surface of the slab and it is this which creates a mechanism and failure. Similarly, in the edge condition it is the formation of the circumferential crack on the top surface which, when joining the edge position, creates the ultimate failure condition. With load applied at the corner the surface crack will occur first and failure will therefore be instigated much earlier.

From Meyerhof's (1962) calculations the ultimate failure load is approximately twice the first crack load in the case of interior and edge positions (equations 2.8 and 2.9 respectively). However, at the corner the first crack signifies ultimate failure (equation 2.10).

The maximum yield moment per unit length of the slab (M_o) for plain concrete is:

$$M_o = \frac{f_b \cdot h^2}{6} \quad \text{equation 2.7}$$

Collapse loads (P_o) are as shown assuming a/L ratios are greater than 0.2

$$P_o = \frac{4 \cdot \Pi \cdot M_o}{1 - (a/3L)} \quad \text{equation 2.8}$$

$$P_o = \frac{(\Pi + 4) \cdot M_o}{1 - (2a/3L)} \quad \text{equation 2.9}$$

$$P_o = \frac{4 \cdot M_o}{1 - (a/L)} \quad \text{equation 2.10}$$

Where:

f_b = Flexural strength of concrete

h = Slab depth

a = Contact radius of a load

L = Slab length

The magnitude of maximum load for edge conditions is dependent on its distance from the unsupported edge. For a true edge condition to be attained a distance greater than 2-3 times the radius of relative stiffness from the centre is required. The ultimate load will then vary linearly between the two conditions. The effect of load transfer at the edges of the slab will also have a significant influence on the ultimate load, as extremely high values increase the magnitude to that of the central condition. As the capacity of a central load is approximately twice that of an edge load and four times that of a corner load, this increase from load transfer can be highly advantageous.

Meyerhof (1962) compared his work to that of Losberg (1978) and found good agreement. He concluded that his method gave slightly higher collapse loads for central and edge conditions, but similar results for corner loading. As a result, Meyerhof (1962) produced simplified equations giving slightly smaller collapse loads. These new equations have been used in a number of guidance documents (Concrete Society 2003).

ACI Committee 360 (2000) recommend using the Meyerhof (1962) method for the design of slabs utilising steel fibres as it accounts for stress redistribution and therefore does not require any modification in the design procedure. Bischoff *et al.* (1997) agreed with this and stated that when the residual load is greater than that of the first crack, it is more appropriate to use an ultimate limit state analysis. This enables a reduction in thickness and provides a more economic section.

Designers should remember that the serviceability of the slab is as important, if not more so than the ultimate failure. Simpson (2001a) states that failure under static load is extremely rare and almost always occurs at corners and edges due to the effect of dynamic load. Many of the so-called economic design procedures may give satisfactory ultimate limit state results, but will fail due to excessive deflection at the slab edges. The Concrete Society (2003) incorporate this by advising a load deflection relationship is examined, with the results staying within the linear limit (Figure 2.13).

2.5.4 Detail Design

2.5.4.1 Crack Control

Joints are used in concrete slabs and pavements to control cracking caused by movement of the concrete. In slabs on grade the majority of this movement will be shrinkage and contraction from moisture loss and thermal changes as described in section 2.3. In rigid pavements it may be necessary to incorporate expansion joints if the concrete will be subjected to high temperatures, although this is rarely required in the United Kingdom.

There is some debate regarding the benefits of inserting joints into a concrete slab, as in essence it is simply a controlled crack at a known location. Simpson (2001a) has created a chart showing the pros and cons of both cracks and joints, reproduced in Table 2.5. Hulett (2001) states that joints demonstrably create more problems than cracks, but cracks create just as much concern in the industry.

Table 2.5 – Problems Associated with Joints and Cracks (Simpson 2001a).

	Disadvantages	Advantages
Planned Cracks, i.e. Joints	<ul style="list-style-type: none"> • Risk of curling • Reduction of load transfer • Edge damage (particularly at formed joints) • Cost of production • Effect on flatness 	<ul style="list-style-type: none"> • Straight alignment on plan • No ragged edges • Locations planned • Easier to seal if required • Cracks tend to be vertical
Random Cracks	<ul style="list-style-type: none"> • Ragged edges • Irregular alignment • Risk of edge damage • Locations unplanned • Difficult to seal if required • Cracks may be inclined 	<ul style="list-style-type: none"> • No cost of production • Good load transfer (if tied by reinforcement) • Little effect on flatness • Lower risk of curling • Total length of cracking may be less than planned cracks • Reduction in the number of wide free joints

The two main methods of producing joints are formed and induced. Formed joints are created by installing stops at the edges of a concrete pour. When set, a second batch can then be placed up to the concrete face which by its nature will create a plane of weakness. Induced joints utilise a concentration of stress, caused by a reduction in slab thickness, to produce a controlled crack.

Formed joints are constructed using timber or steel formwork although it is becoming more common to use one of the many proprietary systems that are available. These can combine formwork, arris protection and load transfer devices, making for quick, accurate installation. Care should be taken when using formed joints, as the risk of poorly compacted concrete or differential levels is much higher than with the induced method (Concrete Society 2003).

There are several methods of inducing a joint into a slab or pavement. The simplest and most common way is to cut into the concrete with a saw, normally completed between 24 and 48 hours after the slab has reached its initial set. If staged too early then the concrete will tend to break away at its surface leaving a ragged and poor quality joint. If left too late the risk of random shrinkage and contraction cracking increases greatly. Other methods such as soff-cutting (cutting the concrete before initial set) and inserting plastic crack inducers can also be used to good effect; however, increased precision is required when using these methods as there is a greater risk of surface problems when working with wet concrete.

When using the saw cut method to induce the crack at the joint it is recommended that the depth be between 1/4 to 1/3 of the slab thickness. If too shallow then there is a risk that the joint will not open at the required location, and if too deep low load transfer will be reduced. The Concrete Society (2003) advise that the depth required is dependent on the age of the slab, as an increased strength will require deeper cutting. Howell (1982) suggests that the increased tensile strength of a steel fibre reinforced slab may require a saw cut in the range of 50% of the slab depth. This will reduce the load transfer available through aggregate interlock immensely and may necessitate the use of further mechanisms.

As mentioned in section 2.5.2.3 the introduction of steel fibre reinforcement into the concrete mix can increase the cracking resistance and reduce shrinkage. In essence the fibres prevent singular cracks from opening up, instead producing a number of much finer cracks. This has led to the development of jointless construction, whereby movement does not need to be managed with induced joints. However, it has been found that at locations where movement can take place it is much more than would occur with a standard design. In some cases these joint widths can be in excess of 20mm with joint spacing of 40-50m (Concrete Society 2003).

2.5.4.2 Joint Types

There are many terms for the variety of joints used in concrete floor slabs and pavements. Confusion can arise with the joint specification if there is no clear identification as to each joint. The Concrete Society (2003) has realised this problem and produced a simple way of defining the different joint types. These being:

- Free movement joint
 - Sawn
 - Formed
- Restrained movement joints
 - Sawn
 - Formed
- Tied joints
- Isolation details

Other methods such as those described by Ringo and Anderson (1996) utilise a primary and secondary classification, with the primary describing the function and the secondary

the construction method. Knapton (1999a) also uses the construction method and its usage, but has different names for each joint. The method of the Concrete Society (2003) will be used here due to its simple nature.

Rigid pavements generally use the same joints as are found in internal and external slabs, although they may be called different names. A warping joint is used to enable uplift of the slab edges and is formed in the same way as a tied joint. An expansion joint however is rarely used in an internal situation but may be required in certain pavement conditions. Descriptions of the various joint types are given below.

Free movement joints

As the name suggests free movement joints contain no reinforcement across the joint and allow horizontal movement from thermal contraction and drying shrinkage to take place unrestricted. Some form of load transfer system such as a de-bonded dowel bar is often used in this situation to reduce vertical movement from applied loading. The joint can either be constructed using formwork to divide the slabs, or by inducing a crack at a specified location. The Concrete Society (2003) recommends that free movement joints are used in situations where the slab meets an adjoining structure, and is also part of the floor structure loaded by MHE. In general these will open to a greater extent than a restrained movement joint.

Restrained movement joints

These joints utilise reinforcement to reduce shrinkage and thermal movements to an acceptable amount. In sawn joints the steel fabric will be continuous throughout the slab, with reinforcement bars inserted for formed joints.

The Concrete Society (2003) states that shrinkage and contraction movement is expected to be in the region of 1-2mm with joint spacing of approximately 6m, causing yielding of the reinforcement. Load transfer will be provided by aggregate interlock and any support the reinforcement provides. An increase in reinforcement size can reduce movement and increase the load transfer effect but may lead to mid span cracking.

Tied Joints

Tied joints are used in situations where a break in construction is required, but movement is not permitted. Reinforcement is sized to resist all of the tensile force and prevent the joint from opening.

Isolation Details

Isolation details are used to prevent any horizontal movement from damaging adjoining structures. Compressible filler is placed between the two surfaces allowing any differential movement to be accommodated. If some form of interaction is required between the two structures then a free movement joint should be used in lieu.

Expansion Joints

These are rarely used in internal situations where the slab is relatively protected from severe changes in climatic conditions; however, in pavements where there is a risk of thermal expansion they are occasionally inserted. The joints are of the formed types with dowel bars used to transfer load between slabs. The slab and dowel bar will contain compressible filler between its end and the adjoining concrete to enable expansion to take place unimpeded. These joints need to be well sealed to prevent detritus entering the joint preventing movement.

2.5.4.3 Joint Layout

Joints should be positioned carefully to prevent their width from opening up excessively. In cases where the load transfer mechanism is aggregate interlock alone this becomes even more important as it is extremely sensitive to crack width. The Concrete Society (2003) recommends that the maximum distance between internal slab joints is 6m. They mention that in certain situations it may be possible to increase this distance but only limited guidance is given for when this is appropriate. Ringo and Anderson (1996) propose that the Portland Cement Association (1951) method of slab spacing is used as it is the most thorough. This gives values for plain concrete in feet of 2-3 times the slab thickness in inches, for example a 200mm slab should have a joint spacing of 4.9 to 6.1m depending on concrete aggregate size and slump. Knapton (1999a) provides the most comprehensive information on recommended joint spacing, the values changing depending on the concrete strength and quantity of steel fibre included. A section of this is shown in table 2.6 below.

Table 2.6 - Recommended Joint Spacing (Knapton 1999b)

Concrete Type	Joint Spacing: m
Plain C30 concrete	6
Micro-silica C30 concrete	6
20kg/m3 ZC 60/1.00 steel fibre reinforcement C30 concrete	6
30kg/m3 ZC 60/1.00 steel fibre reinforcement C30 concrete	8
40kg/m3 ZC 60/1.00 steel fibre reinforcement C30 concrete	10
Plain C40 concrete	6
Micro-silica concrete	6
20kg/m3 ZC 60/1.00 steel fibre reinforcement C40 concrete	6
30kg/m3 ZC 60/1.00 steel fibre reinforcement C40 concrete	10
40kg/m3 ZC 60/1.00 steel fibre reinforcement C40 concrete	12

In the case of concrete pavements the American Association of State Highway and Transportation Officials (1986) state that the joint spacing is highly dependent on the materials used and the environment. They recommend using local service records of past performance to provide the relevant spacing for an individual area. As a rough guide they provide a formula similar to that used by Ringo and Anderson (1996), whereby the slab spacing in feet equals twice the slab depth in inches. Atkins (1997) recommends contraction joints every 4-7m in non-reinforced concrete with this being extended to 12-30m for lightly reinforced, and none for heavily reinforced sections. Watson (1994) gives more through information for different steel percentages but they generally agree with the conservative values of Atkins (1997).

All authors agree that it will rarely be the case that the idealised spacing can be used due to column spacing and warehouse layouts. It is therefore the responsibility of the designer to ensure joints do not open up to any considerable degree, or that random cracking does not occur. A requirement of this is the control of aspect ratio, with Ringo and Anderson (1996) and The Concrete Society (2003) both recommending a length to width ratio of less than 1.5 for floor slabs, with American Association of State Highway and Transportation Officials (1986) stating a value of below 1.25 for concrete pavements.

Many slabs constructed in South Africa use skewed joints and the action of aggregate interlock to control cracking and enhance load transfer (Prozzi *et al.* 1993). These are said to reduce deflections since only one side of the axle wheel is crossing the joint at a particular time. There is also increased ride quality as the impact is reduced when a vehicle crosses the joint (American Association of State Highway and Transportation Officials 1986). The formation of a skewed joint requires acute angles within the slab, leading to higher stresses and a greater risk of cracking in corner sections. Armaghani

(1993) states that since skewed joints have not provided increased quality, and it is difficult to align any dowels that may be incorporated, their inclusion should not be considered.

2.6 Slab/Pavement Foundation

The foundation of the slab or pavement comprises the subgrade (normally the soil found at formation level on site) and subbase material. Together they resist load and control deformation, whilst providing a working layer on which the concrete slab may be poured. Management of these materials is therefore essential to ensure structural and serviceability requirements are met.

If the foundation of a concrete slab or pavement is designed incorrectly or contains constructional defects then failure is likely to occur regardless of the quality of concrete above (York 2001). The subbase can have a significant effect on the longevity of the structure and this becomes even more important as slab depths become shallower.

The foundation materials used in a concrete pavement, internal slab or hardstanding are very similar. The slab itself will commonly be placed onto a plastic slip membrane which sits on top of a graded subbase material. The base for the entire construction, is the subgrade. This is often the material found at formation level but occasionally it may be replaced by a layer of fill, or modified by mixing in stabilisation materials.

2.6.1 Subbase

Subbase design is critical to CRCP performance since a reduction in support, leading to a loss of load transfer, has been identified as being the primary cause of punch-out distress (Zollinger and Barenberg 1990).

The subbase is the material placed directly above the subgrade material and below the concrete structure. It is the main foundation material for the concrete component and its primary requirement is to disperse any loading passed down from the slab to a level that can be satisfactorily withstood by the subgrade. This loading may be a continuous static load or a short term repetitive dynamic load, both of which should be adequately designed for with the selection of a suitable material. This is commonly a well-graded inert granular fill made from crushed concrete, rock or a general aggregate. In addition to reducing the stresses passing into the subgrade, the subbase must prevent load

deformation which leads to voiding below the concrete slab. Construction traffic running on the foundation prior to concrete placement can also create surface rutting which must be controlled to prevent shrinkage restraint cracking of the slab. These are all requirements relating to the material's strength and stiffness properties and therefore much of the subbase selection is based on these characteristics.

The subbase can be used in floor design to improve the load response of the foundation layer. This can be incorporated directly by increasing the stiffness of the subgrade material or by assuming a deeper structural slab, both of which will reduce any induced deflections. There are some situations when a weak concrete mix may be used as the subbase material due to high granular material costs or very poor subgrade material. Again this can be incorporated into the design by assuming an increased slab thickness to add any beneficial qualities.

The selection of a subbase material is a very important factor in the longevity of the slab. One of the most commonly found and serious problems that can occur in pavements is that of pumping. This is described in detail in section 2.4.3, and is caused when the subbase mixes with ingressing water and a solution is formed. This is then pumped through the crack or joint due to the vertical movement of the slab edges when a load passes over the surface. Ideally a sealant is placed in the crack or joint preventing moisture from reaching the subbase. However, if this does not occur, a correctly sized material can be used to prevent water from entering the system, or avert the formation of a solution, thereby reducing the possibility of voids. The ideal subbase is a well compacted coarse material with a fines content of less than 10% passing a 200-micron sieve (Colley and Nowlen 1958). Care must be taken however to ensure that the subbase material is not of such a coarse grading that the subgrade material can pass into, and mix with, the subbase.

2.6.2 Subgrade

The subgrade is usually the naturally occurring soil at formation level, although it may be imported from off-site to replace areas of poor quality. The material should be of uniform strength without localised hard or soft spots that could affect settlement and bearing characteristics. When fill is imported, it should be of a suitable strength, stiffness, water content and grading to enable good compaction throughout depth, and provide a stable foundation for the slab. In circumstances where a very good subgrade condition exists with high strength and low compressibility, the slab may be constructed directly onto this layer. However, care should be taken to ensure that degradation of the soil due to water

infiltration will not occur if it is a fine grained material, sensitive to moisture increases (Knapton 1999a).

The subgrade must be tested to find its strength and suitability for use in the design of the structure. This can be found using the California Bearing Ratio (CBR) test, which quantifies the force required to cause a specific displacement of a 50mm diameter plate (Atkins 1997). Another method used for evaluating the soil is the plate-bearing test. With this approach a 760mm plate, is forced into the subgrade to a depth of 1.25mm, and from this a modulus of subgrade reaction, or 'k' value, can be determined in N/mm^3 . Many of the design calculations for concrete slabs and pavements use this 'k' value directly to determine the load/deflection behaviour of the soil. An approximate relationship between CBR and modulus of subgrade reaction has been found when the soil is uniform with depth, as shown in Figure 2.14.

2.6.3 Slip Membrane

The main principle behind the use of a slip membrane is to reduce friction between the underside of the concrete and the subbase. If a slip membrane is incorporated into the design then frictional restraint will be minimised, stresses in the slab reduced, and all movement will take place at the slab edges and designed joints. The coefficient of friction can be reduced from 0.7 to 0.2 under ideal conditions (Knapton 1999b), with more comprehensive data provided in Bishop (2001). However, in practice this rarely works as well as expected due to a number of constructional defects.

The reasons for poor slip membrane effectiveness are various, but all create similar problems in respect to slab restraint. One of the most common faults is due to the construction traffic that regularly passes directly over the subgrade (York 2001). Even in well specified, placed and compacted materials some plastic deformation will occur when large vehicles run over its surface, producing localised low spots and rutting from wheel channels. These imperfections act as keys which lock the slab in position when the concrete has cured sufficiently, resulting in cracking if any strains develop later on in the slab life. This is also true in situations where the slip membrane has wrinkled or folded up over itself. The reduction in depth acts as an inducer, causing the slab to crack in the wrong location and leaving the designed joints unable to serve their purpose.

Hulett (2001) suggests that instead of designed cracks or joints situated at large distances, it is preferable to have many cracks distributed throughout the slab. Tight cracks are well

known to transfer load more efficiently regardless of the load transfer system in use, and therefore lead to fewer problems and a more integrated structure (Stock 1988). With a slip membrane all movement is transferred to the designated areas (i.e. the joints) creating larger movements where load transfer will become negligible, the need for strengthening of the joint essential, and the overall stability of the edges reduced. Omission of the slip membrane would cause frictional restraint throughout the concrete and any cracks would be created over the entire area of the slab. These cracks would be narrow, with the load transfer high, creating a system which is well integrated and does not require special construction techniques. This could save on both time and money in the construction of the joints and reduce the risk of failure.

There are other problems associated with the use of a slip membrane. Section 2.4.2 introduced curling which was shown to be a significant fault found in slabs, pavements and hardstandings due to differential shrinkage. If the membrane was removed, and the subbase suitably selected, moisture would be able to drain away from the base of the concrete slab. Although this level of moisture removal may not be the same as that occurring at the top surface of the slab, it could create a much reduced differential. In the United States this problem has been assessed and some of the design procedures call for the use of a thin sand blinding layer between the underside of the concrete slab and the subbase layer. This allows for much greater removal of water from the underside of the slab (although care should be taken as too much could affect curing) and, in theory at least, a reduced amount of curling within the slab.

2.7 Structural Modelling

There are a number of finite element programs available that can model the slab or pavement system; however, the accuracy of these models is highly dependant on the parameters placed within the constitutive model. If accurate results are to be obtained, careful consideration is required for each element with both the values and method of modelling being highly influential.

2.7.1 Modelling of Concrete materials

The effective modelling of concrete is highly important if accurate and computationally efficient results are to be produced. The amount of detail required varies with the type of analysis to be completed. Early age movement, creep or structural deflections all require different degrees of input to produce acceptable results. In analyses of matured concrete it may be acceptable to use only one elastic modulus; however, when early age properties

are required the variation in strength may need to be changed frequently. Bishop (2001) produced a model to examine the early age behaviour of concrete slabs which required thermal properties and concrete strength changes to be continuously updated. Similarly, in models that predict creep, the reduction of stress over time requires changing material behaviour.

Bhatti *et al.* (1998) state that for structural modelling of slabs the concrete material should enable yielding and crushing for compression, and cracking and fatigue for tension. They also recommend dividing the slab into layers, with each having different properties to account for crack propagation throughout depth. Fatigue for concrete compression is not included as "the compressive stresses in typical pavements are so low that no significant fatigue affects are anticipated" (Bhatti *et al.* 1998, pp 50).

Cracking in concrete can be modelled in two distinct ways, these being smeared and discrete. When the smeared approach is used a physical crack is not formed, instead the overall element stiffness is reduced. In the case of the discrete method a crack will develop in the calculated location and the remainder of the structure will remain intact. Al-Nasra and Wang (1994) give guidance on the methods, stating that discrete cracking should be used when local behaviour is required, with smeared cracking used when examining overall load deflection behaviour.

2.7.2 Modelling of Foundation materials

There are two main methods which can be employed to model the subgrade of a concrete slab or pavement system (Channakeshava *et al.* 1993). The first is a Winkler spring, or dense liquid system, and the second is an elastic foundation. Several variations and modifications have been made to each of these to enhance accuracy and make them more computationally effective. The Winkler or dense liquid method utilises springs placed at nodes on the underside of the slab or pavement system, which resist deflections to an amount specified by the stiffness. The method assumes there is no shear effect between each spring and therefore the deflection is solely dependent on the support directly below it.

The elastic foundation uses standard finite element methods to model the subbase. Information such as density, Poissons ratio and elasticity can then be given through the constitutive model which may require variation at different levels. Elastic foundations require the user to provide a boundary layer at some predetermined depth, the position of which can have a large impact on results. This is more computationally expensive than

the Winkler foundation but enables greater control in determining layer properties. Channakeshava *et al.* (1993) comment that a combination of Winkler and elastic methods can represent the real conditions most accurately.

Krauthammer and Western (1988) examined the depth of 2D elastic elements required to simulate the subgrade using wave velocities. Calculation showed that the model would need to be approximately 20m deep to fully represent the site information. This was thought to be too time intensive and therefore linear springs were introduced with a stiffness proportional to the equivalent elastic nature of the soil.

Harichandrian *et al.* (1990) analysed pavement slabs using the MICH-PAVE finite element program. The model was split into three layers, these being the surfacing material, the granular roadbed and the roadbed soil. From work conducted by Duncan *et al.* (1968), Harichandrian *et al.* (1990) recommended that the bottom boundary should be fixed at a depth 50 times the radius of the loaded area, with the side boundary at 12 times the radii. This compared well to a Bousinesq solution with a bottom boundary of 18 times the radius of the loaded area. Harichandrian *et al.* (1990) used a reduced boundary depth of 10 times the radii but made it flexible to allow for further vertical deflection. This boundary was made linear elastic, which was thought acceptable due to the minimal amount of stress that would be caused at this level from the applied surface load. However, it was mentioned that if the boundary position was set too close to the surface, the displacements would be accurate but the stresses would not. In the reverse case where the boundary is too deep, the advantages of the method are lost altogether. This analysis was only completed for central slab loading and comparisons against edge conditions were not undertaken.

For the analysis of slabs tested by Armaghani *et al.* (1986) the values for the modulus of subgrade reaction were back calculated from deflection basins obtained during FWD testing. The actual bowl shape was compared with that obtained from numerical models and the 'k' value altered until a good match was found. This method was also employed for the load transfer spring system with a trial and error approach deemed satisfactory. This method of analysis does not directly compare the analytical model against the results obtained on site, and ideally an independent check should be made, whereby known parameters are used.

Fwa *et al.* (1996) compared the results of numerical models using the traditional Winkler foundation and a Pasternak foundation. The Pasternak foundation uses the modulus of subgrade reaction with a foundation shear modulus to better simulate the effect of the

subgrade. The two models were compared to experimental test slabs loaded at centre, edge and corner positions. The Pasternak foundation showed reduced deflections at all load positions and better predicted the actual results from lab tests. There was however a difficulty in selecting the correct shear modulus as there is no easy test to calculate its magnitude. A value was chosen which gave the closest results to actual measurements, thereby making the predicted deflections open to error.

Bhatti *et al.* (1996) incorporated a pumping effect into the foundation to further enhance accuracy. The general set-up required the Winkler foundation but the Larralde and Chen (1987) model was incorporated within this to allow for a reduction in support over time. At the end of a series of load steps the subgrade reaction was amended due to the pumping effect. Bhatti *et al.* (1996) stated that it is acceptable to change these values after 25,000 to 50,000 cycles, reducing the computational time required whilst still producing acceptable results.

2.7.3 Analysis of Slabs on Grade

The analysis of slabs on grade using numerical computer software has been undertaken for many years. Several packages are available which represent the pavement or slab in a number of different ways. The increase in speed of personal computers has enabled more complex structures to be analysed, many of which involve the use of three-dimensional systems enabling corner situations and the slab formation as a whole to be analysed.

Ioannides *et al.* (1985) used the ILLI-SLAB finite element package to examine the Westergaard (1926 and 1947) equations currently in use. The model utilised plate-bending elements resting on an equivalent mass formation to simulate the Winkler type foundation. Comparisons were made for interior, edge and corner loading conditions and they examined both the stresses and deflections obtained by loading in such a manner. It was found that the Westergaard (1947) equations gave very similar results for most situations, although the radius of relative stiffness and length of slab did affect the accuracy.

Ozbeki *et al.* (1985) argued that the most desirable model for concrete pavement analysis is a three dimensional system. They mention that two-dimensional systems are simplistic and are therefore not ideally suited to looking at a complete slab on grade system. The JSLAB 3-dimensional package used for the analysis compared well to Westergaard (1926) solutions for internal, edge and corner conditions.

Kuo (1995) compared the stress and deflection results of both 2D and 3D models to that obtained from Westergaard (1926) and ILLISLAB analyses. This was undertaken for both the internal and edge loading condition using different load magnitudes. The research concluded that there is good agreement between 2D and 3D results when the slab is a thin plate (length to thickness ratio more than 20). There is however a limited number of problems that the 2D system can model due to the nature of the slab on grade analysis. Typical problems that cannot be modelled include corner loading, slab warping and thickened edges. Work completed by Krauthammer and Western (1988), looking at shear transfer across joints, used a plain strain 2D model to simulate pavement behaviour as the results required were only for edge loading a large distance away from the slab corners.

Most load transfer systems can be modelled using the relevant elements in a software package. For simple mechanisms such as aggregate interlock it is acceptable to incorporate a spring between the two crack faces (Tabatabaie and Barenberg 1980), although more detailed models can be incorporated which utilise the Walraven (1981) two-phase system (Davids *et al.* 1998). This model allows the effects of crack opening to be directly incorporated into the results, reducing the load transfer value as it opens. Where dowel bars are to be incorporated, embedded reinforcement can be employed which allows slippage and looseness in the bond, producing more accurate results.

Few models can take account of warping. Hammons (1998) compared the results of site measured load transfer values at Denver International Airport against those obtained from an ABAQUS finite element model. Although the results were reasonable, some discrepancies were found to exist. It was suggested that the reason for this was some degree of slab curling creating complex support conditions which can vary from full, partial, or none. Where this type of modelling is required a hygral and thermal analysis is required to form the initial condition. Following this a structural analysis needs to be carried out to examine the effect of load on the warped slab. Al-Nasra and Wang (1994) examined this behaviour using a non-linear foundation spring. This is similar to the standard Winkler foundation but contains zero tensile strength so the slab is free to move in an upward direction due to the temperature gradient. This model was compared to limited site data and found to produce good approximation. Bishop (2001) constructed a complex model examining the early age behaviour of concrete slabs. This enabled stresses and deflections of slabs to be ascertained during the early life of the concrete, where both the temperature and concrete strength are constantly changing. In this model a

membrane was utilised between the slab and the subbase allowing a controlled tensile strength between the two. This was found to correlate well with data gathered from site.

There is a requirement in structural models to enable the interface between slab and subbase to be controlled. Kuo (1995) has achieved this with interface elements which allow the non-linear behaviour of the shear slip to be introduced. Kim, Won et al. (1998) achieved the same results using springs in the horizontal direction.

2.7.4 Modelling Limitations

Many models utilise either the Winkler spring or a dense liquid foundation to simulate the effect of the subbase and/or subgrade (Road Research Laboratory 1955). Deflection is resisted only by the spring placed directly under it, and therefore cannot incorporate the effect of the surrounding area. This fails to fully represent a real situation whereby deflection of a single point is dependant upon the adjacent element stress state as well as its own. Similarly, the soil restraint on the opposite side of a loaded slab will be reduced due the shear transfer capabilities of the soil. The soil adjacent to that being loaded may then be compressed, creating a void between foundation and underside of slab. In some cases modifications have been made which improve the simulation, but these need to be enhanced further before they can be used with confidence.

To model the subgrade as a Winkler foundation, the modulus of subgrade reaction first needs to be determined. Tang (1993) postulated that this value is not a constant and is in fact smaller under the slab edge. As most of the tests available for obtaining this value can only be used at the centre of a slab, the results should be used cautiously if selected for the entire length. This issue becomes more important when examining edge deflections as they are much more sensitive to modulus of subgrade reaction values.

Many of the models using standard elements as a foundation assume that the soil is in full contact with the underside of the slab. In most situations, such as that occurring in a slab on grade, the soil in and around the edge of the slab tends to deteriorate over time from compaction, or by being pumped out through the crack or joint (see section 2.4.3). This creates voids underneath the slab edge which lowers the resistance to deflection. By ignoring this phenomenon there is a risk that the calculated deflections will be smaller than those found on site.

Road Research Laboratory (1955) state that some of the main assumptions used when modelling slabs on grade are inconsistent with the realities of site. The first of these is that

the slab is in perfect contact with the foundation. Due to the curling effect caused by the shrinkage gradient this is often not the case. Gap interface elements must therefore be incorporated into the model to allow for uplift caused by warping. If this is not undertaken resistance will be provided, and the slab will not be able to detach itself from the underlying layer. This will affect the friction coefficient between slab and subbase, as in a warped slab it will reduce to a zero value.

One of the main drawbacks of many finite element programs is their ability to adequately model the interface between the concrete slab and the underlying layer. Many of the existing finite element programs for pavement analysis assume either zero or full bond for the interface condition, whereas in reality the amount of layer slippage under a heavy wheel load is somewhere between these two extremes. Having a capability to model and specify the varying levels of slippage between the slab and an underlying layer would greatly improve the ability to fine tune concrete pavement design.

2.8 Conclusions

This Chapter has reviewed literature relating to concrete slabs on grade. Clear similarities between internal floor slabs, external hardstandings and rigid pavements are evident in respect to their relevant constructions. The loads applied to the slab are slightly different in magnitude and the number of cycles they are likely to encounter; however, all are required to withstand many dynamic load applications throughout their working life.

Concrete by its nature will crack to some degree due to restraint against moisture and thermal movement. These cracks have been shown to create problems in respect to strength and serviceability due to the weakened slab sections they produce. Control of these cracks is provided by the insertion of reinforcement, which prevents them opening up excessively and increases the load transfer effect. Joints have also been introduced; however, these only define the location of the crack rather than preventing it occurring. Much of the design guidance has reviewed the effect of static load within the slab; however, it is the cyclic loading across the weakened crack and joint areas which tends to create the greatest risk of failure. The incorporation of a suitable foundation within the slab can resist deflections and rutting which could lead to further restraint cracking. Voiding underneath the slab is also a common occurrence caused by compaction of the soil under repetitive load, pumping and slab edge curling. This results in a reduced resistance to deflection, increasing stresses and the rate of crack or joint deterioration.

The underlying theme of crack and joint behaviour, which has been found to control slab response and resistance to failure, is noted throughout each section. Understanding the load transfer effect of these cracks is therefore essential in improving the design and maintenance strategy of these structures and has therefore become the main focus for this thesis. Chapter 3 addresses load transfer in more detail in relation to its basic mechanisms, calculation and evaluation techniques.

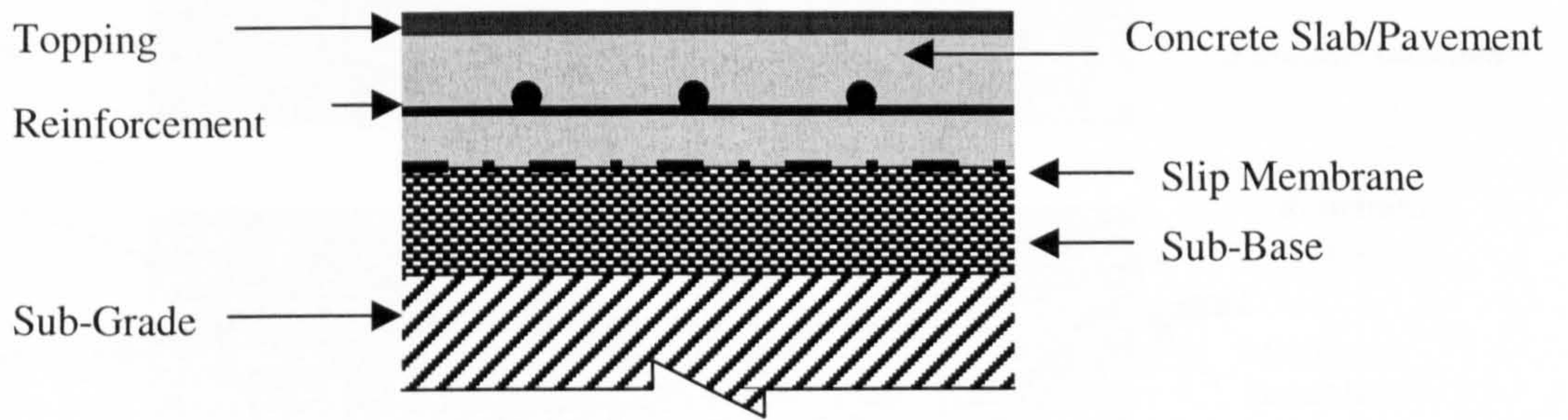
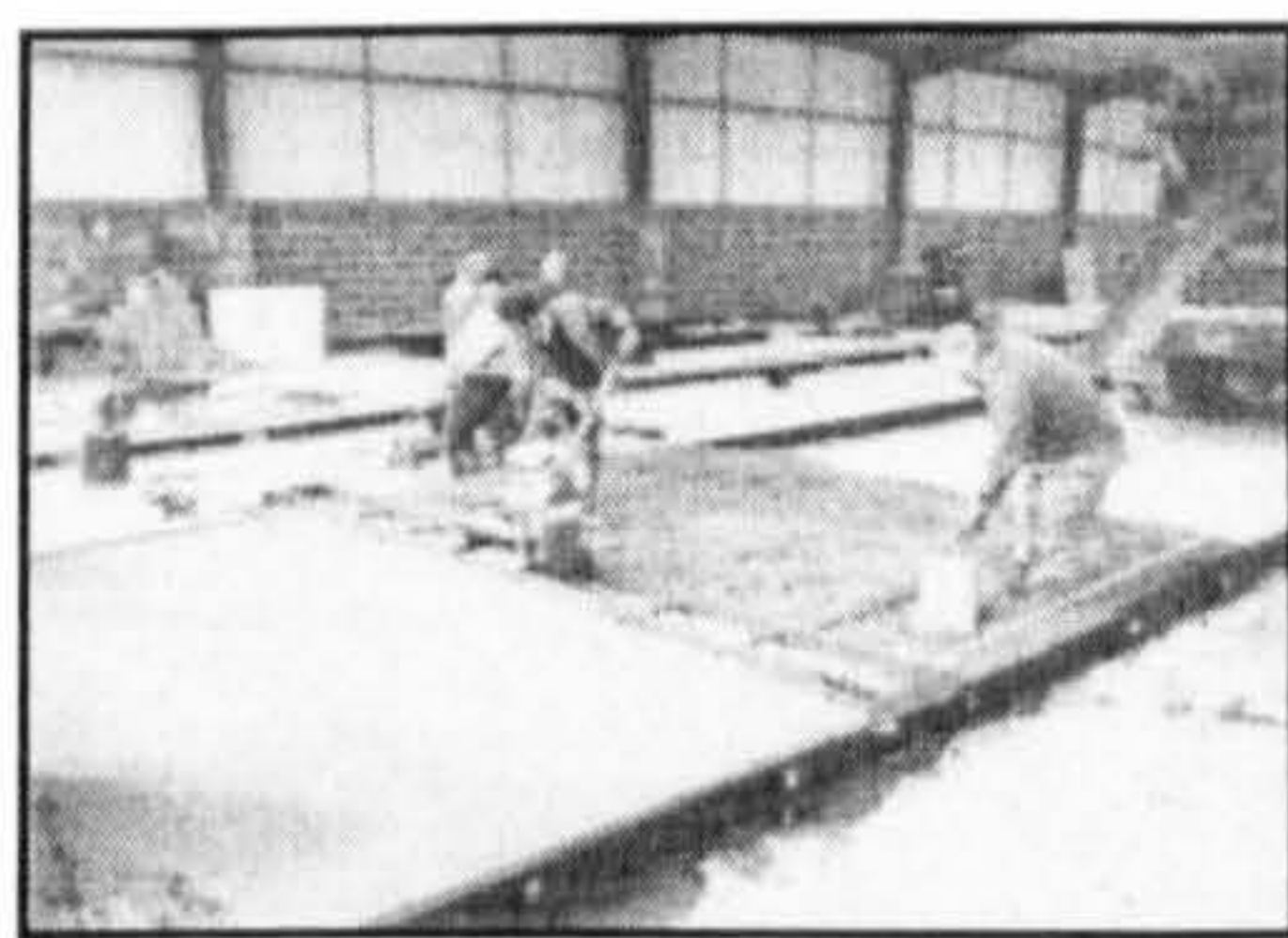
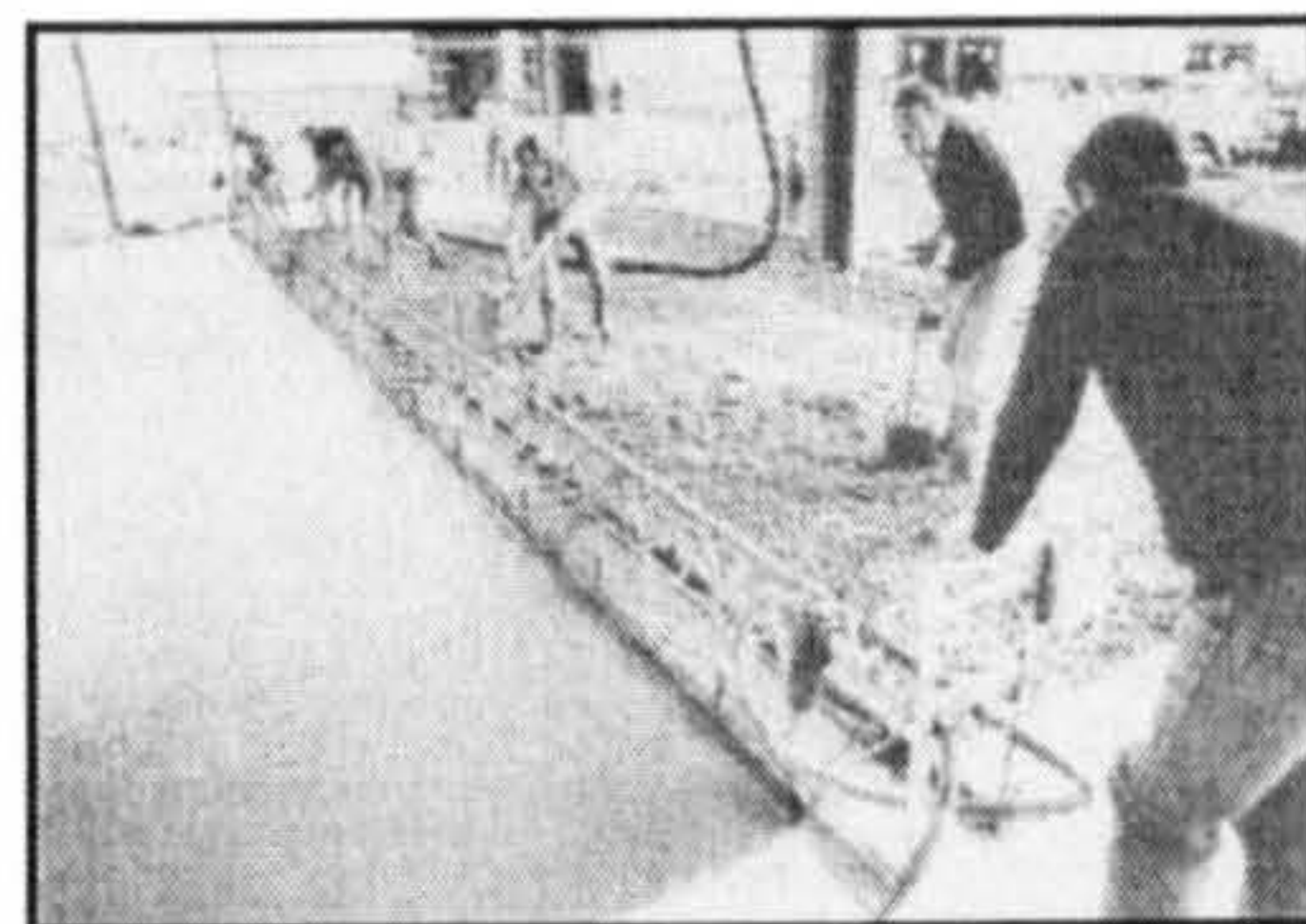


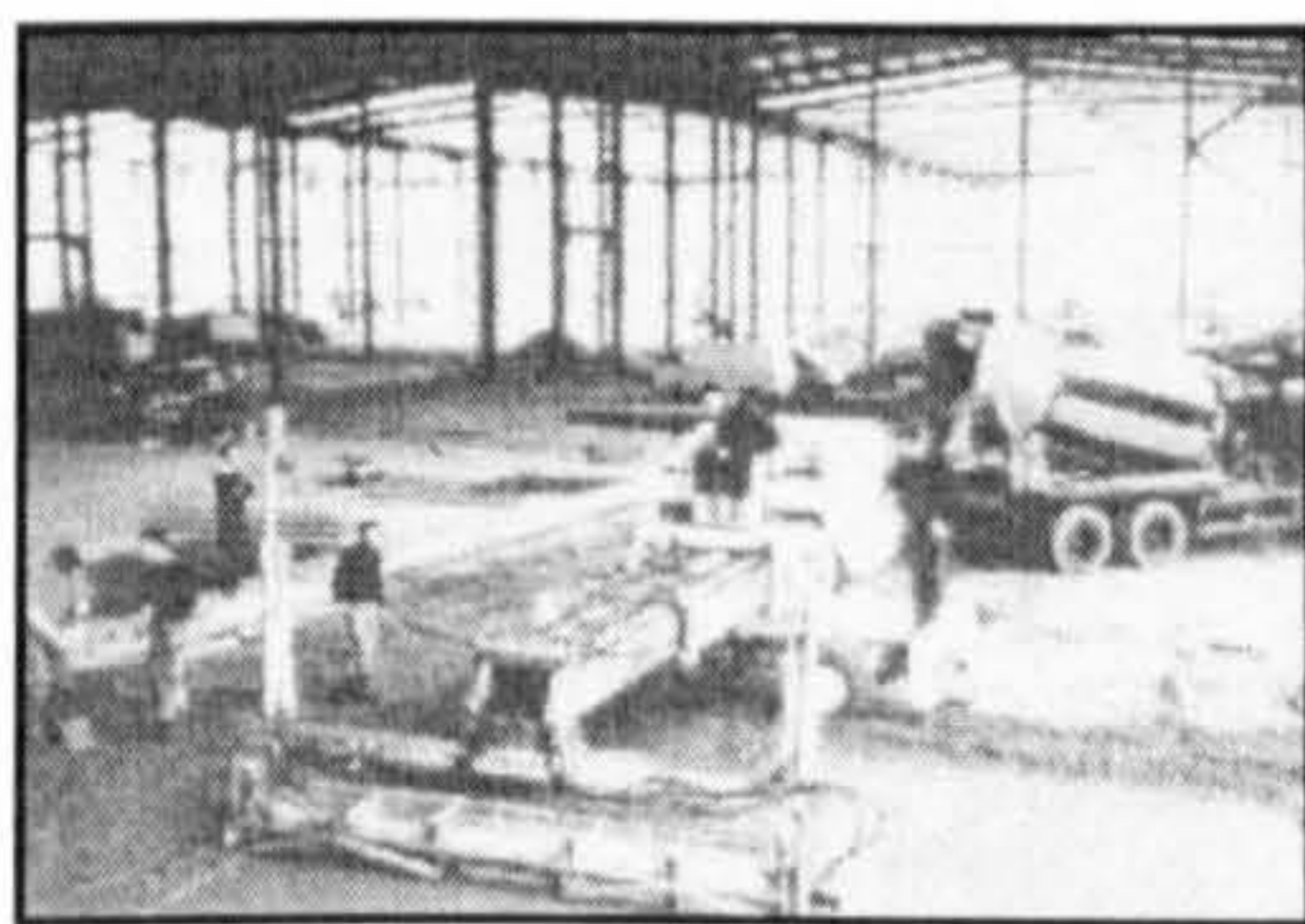
Figure 2.1 – Typical construction of an internal floor slab



Long-strip



Wide-strip



Laser Screeding



Large Bay

Figure 2.2 – Concrete slab construction methods (Knapton 1999b)

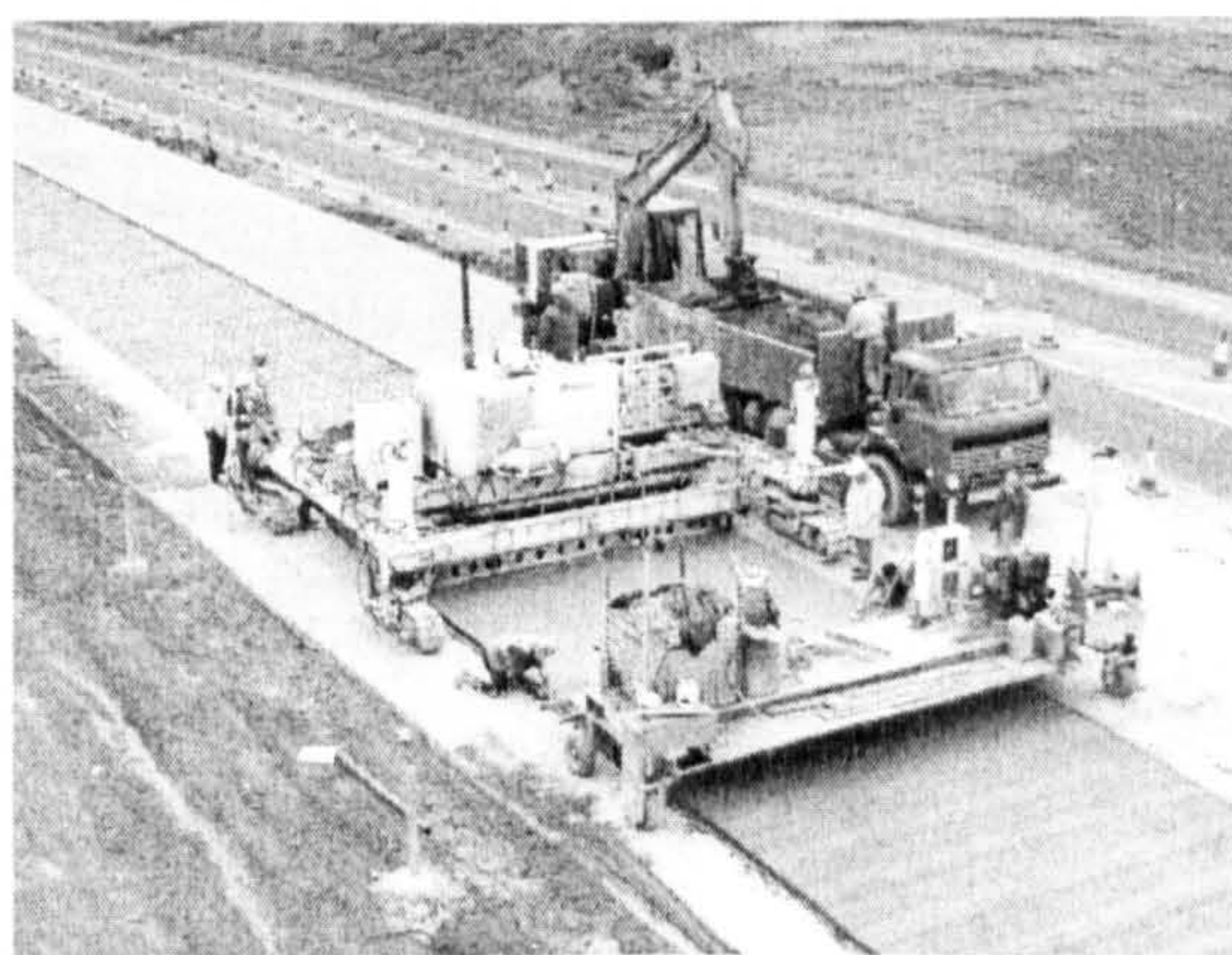


Figure 2.3 – Rigid pavement slip form construction (Wirtgen 2001)

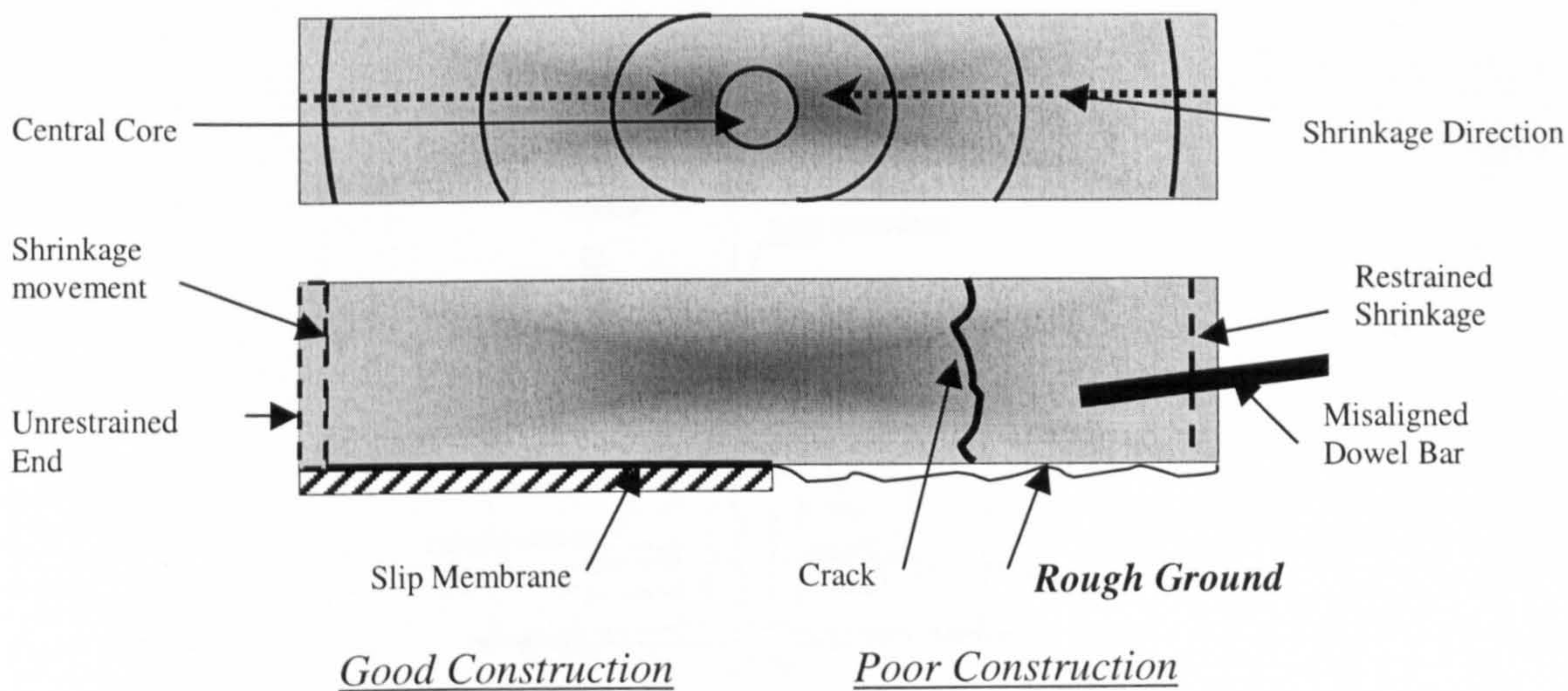


Figure 2.4 – Shrinkage restraint of a concrete slab

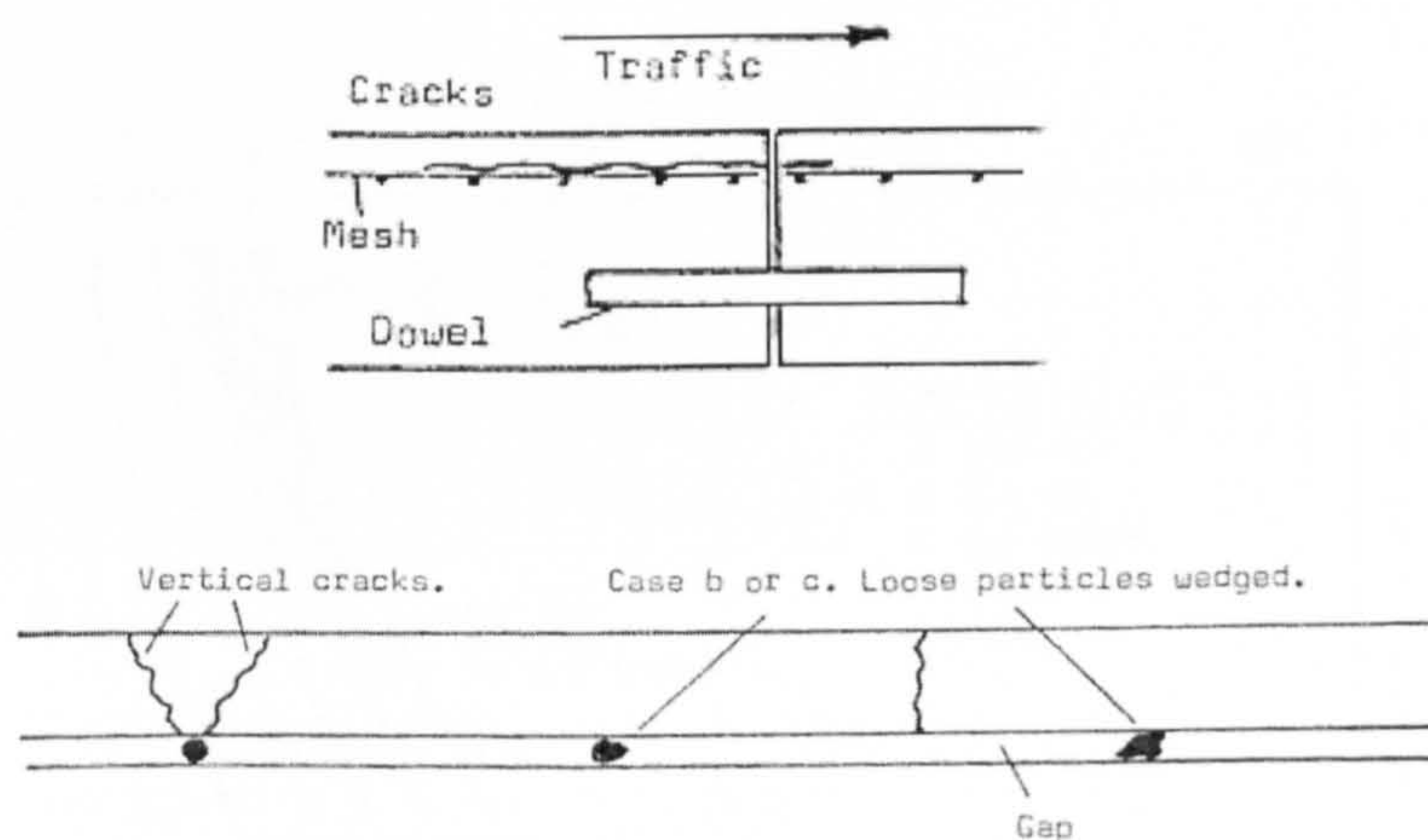


Figure 2.5 – Peeling action caused by fabric reinforcement (Savage 1985)

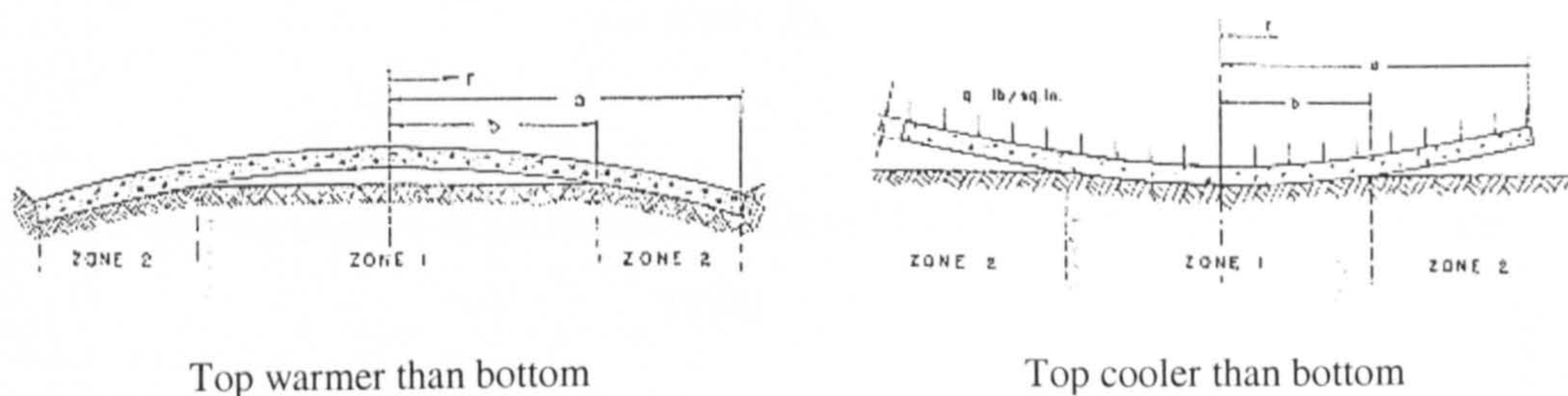


Figure 2.6 – Temperature induced slab curling (Ytterberg 1987)

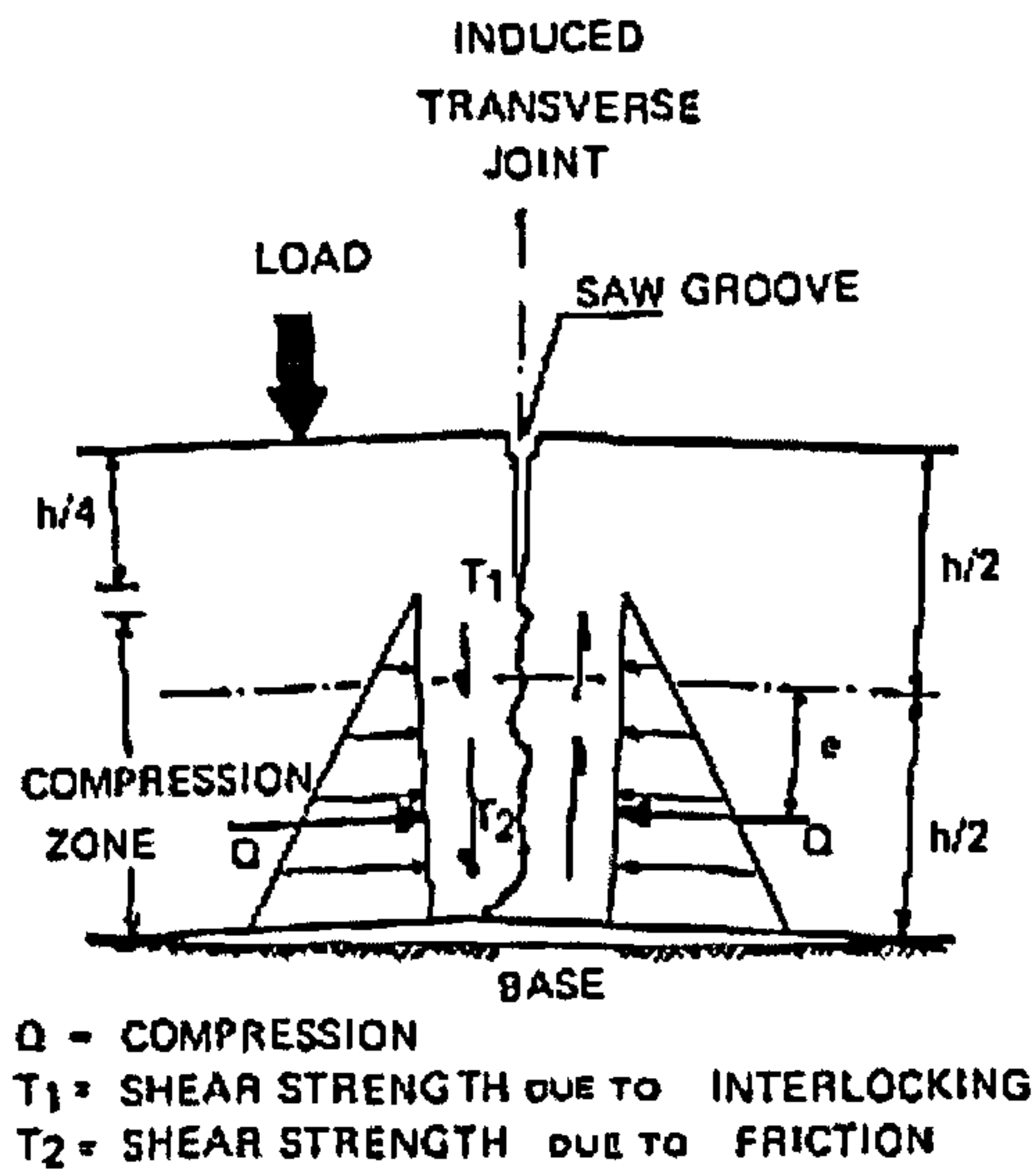


Figure 2.7 – Rotation of joint faces (Poblette *et al.* 1988)

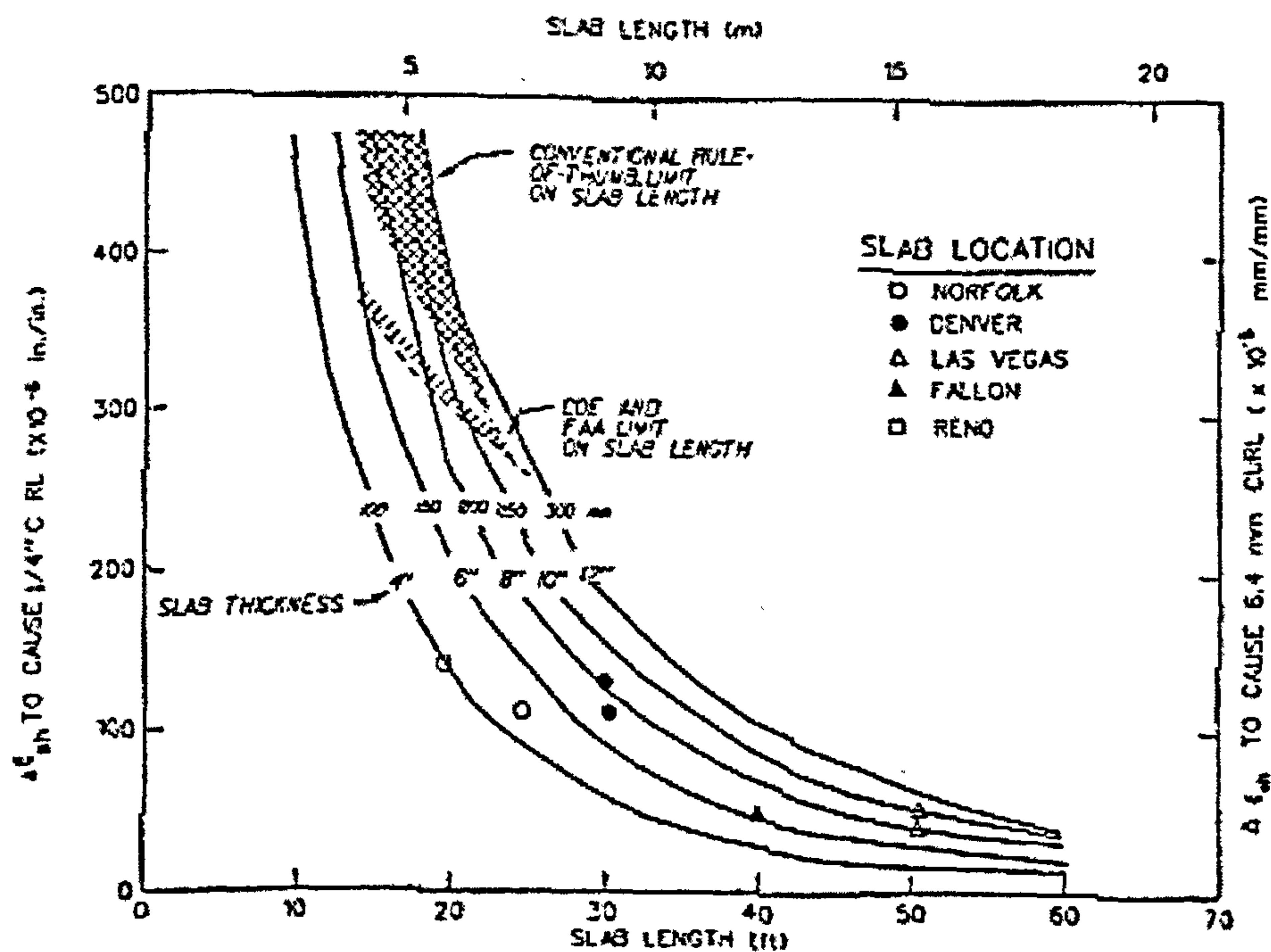


Figure 2.8 – Curling profiles of a concrete slab caused by differential shrinkage (Rollings 1993)

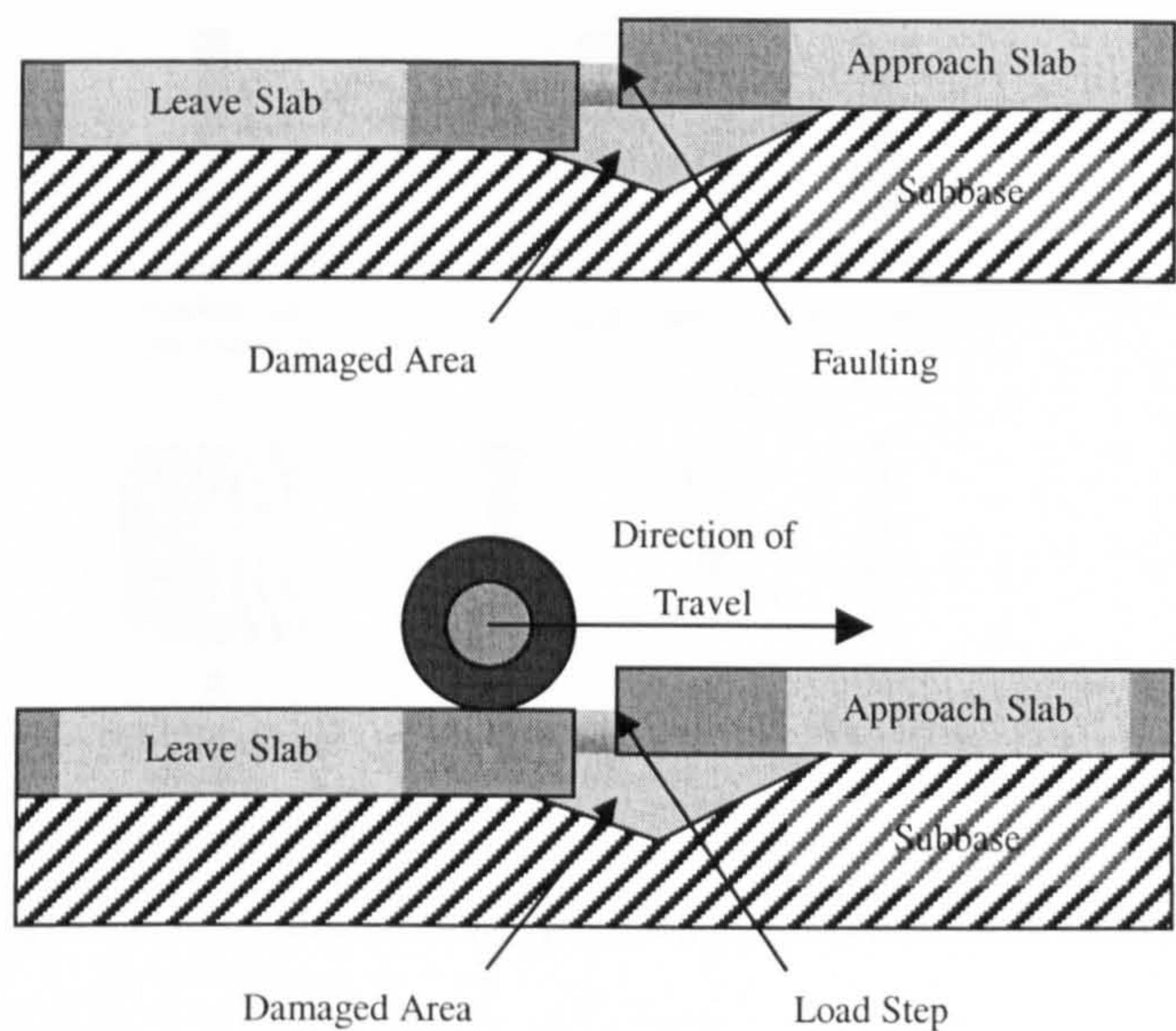


Figure 2.9 – Faulting (top) and dynamic load step (bottom) across a discontinuity

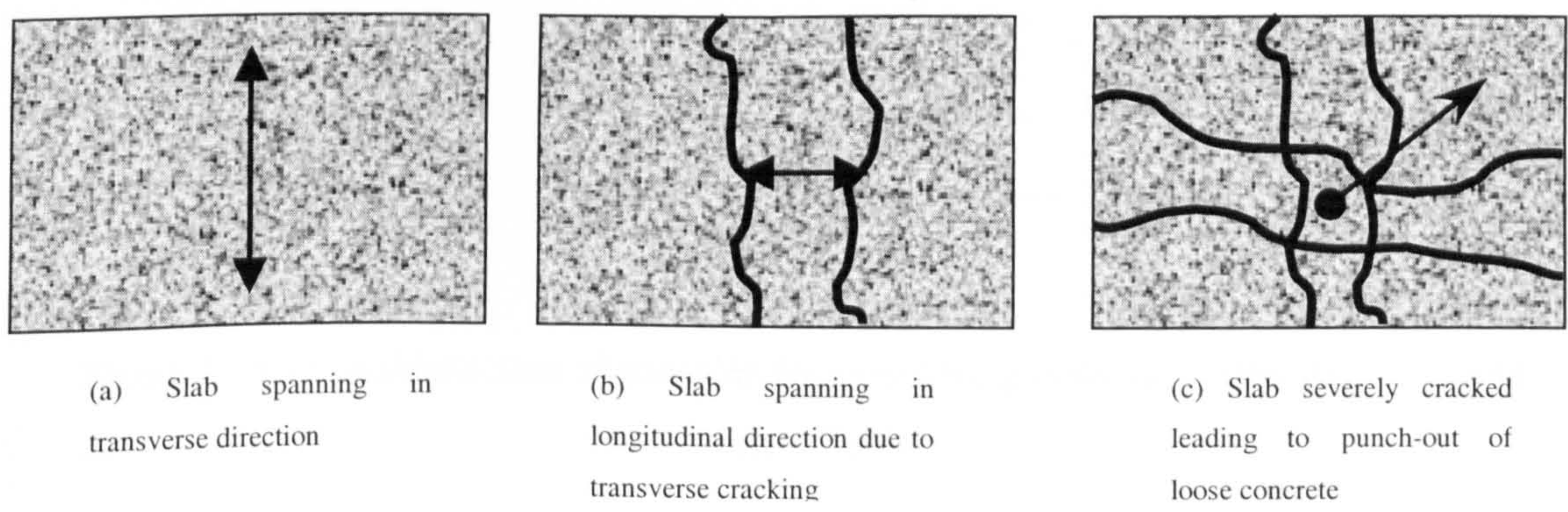


Figure 2.10 – Punch out accumulation

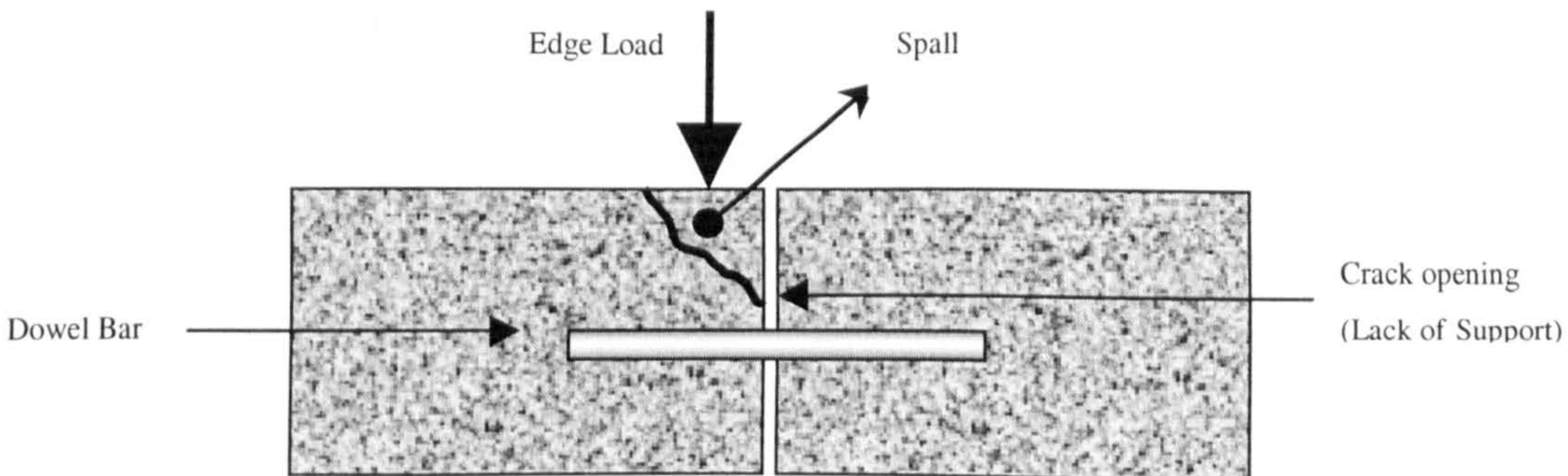


Figure 2.11 – Spalling of a crack edge

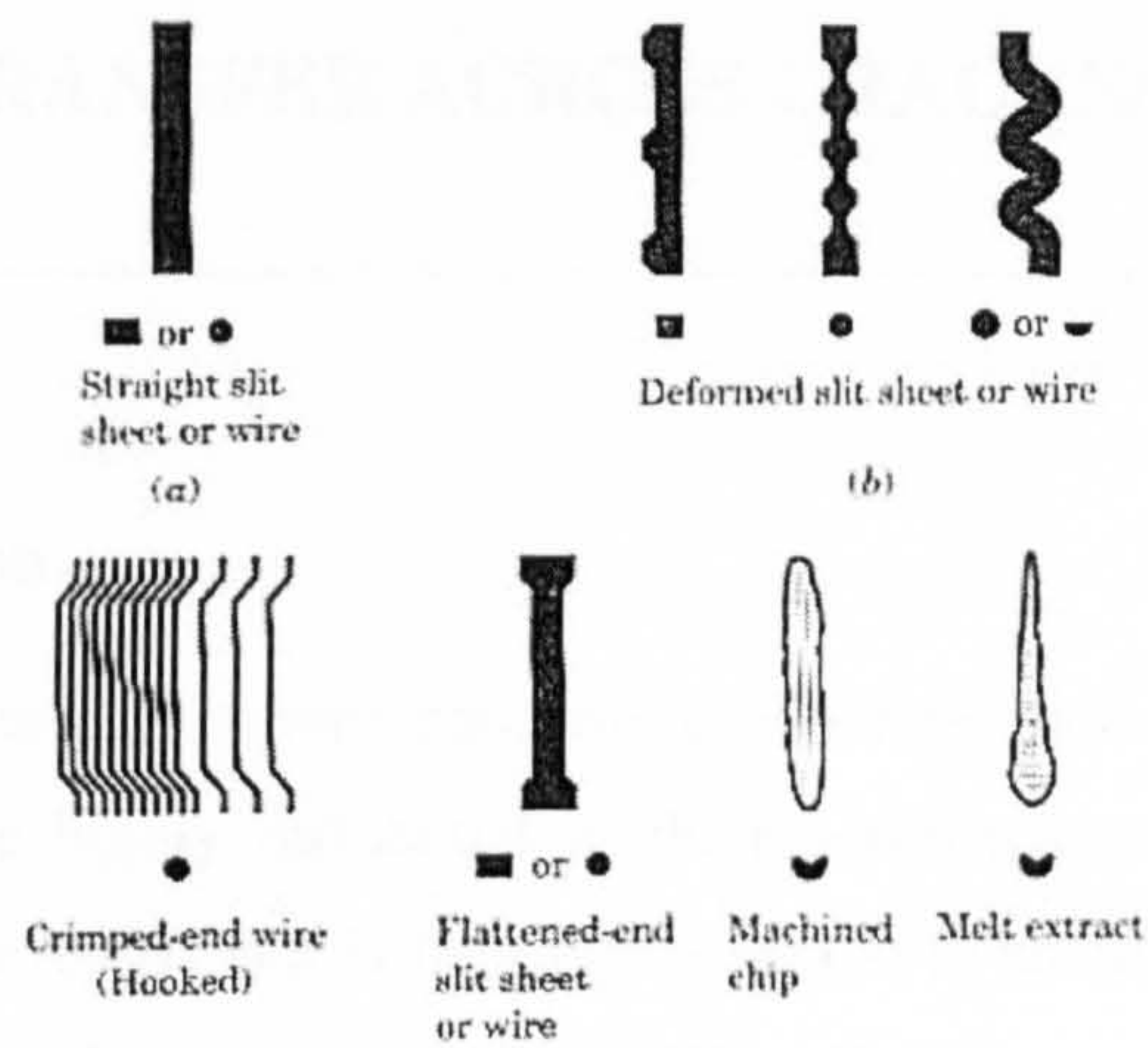


Figure 2.12 – Steel fibre types (Balaguru and Shah 1992)

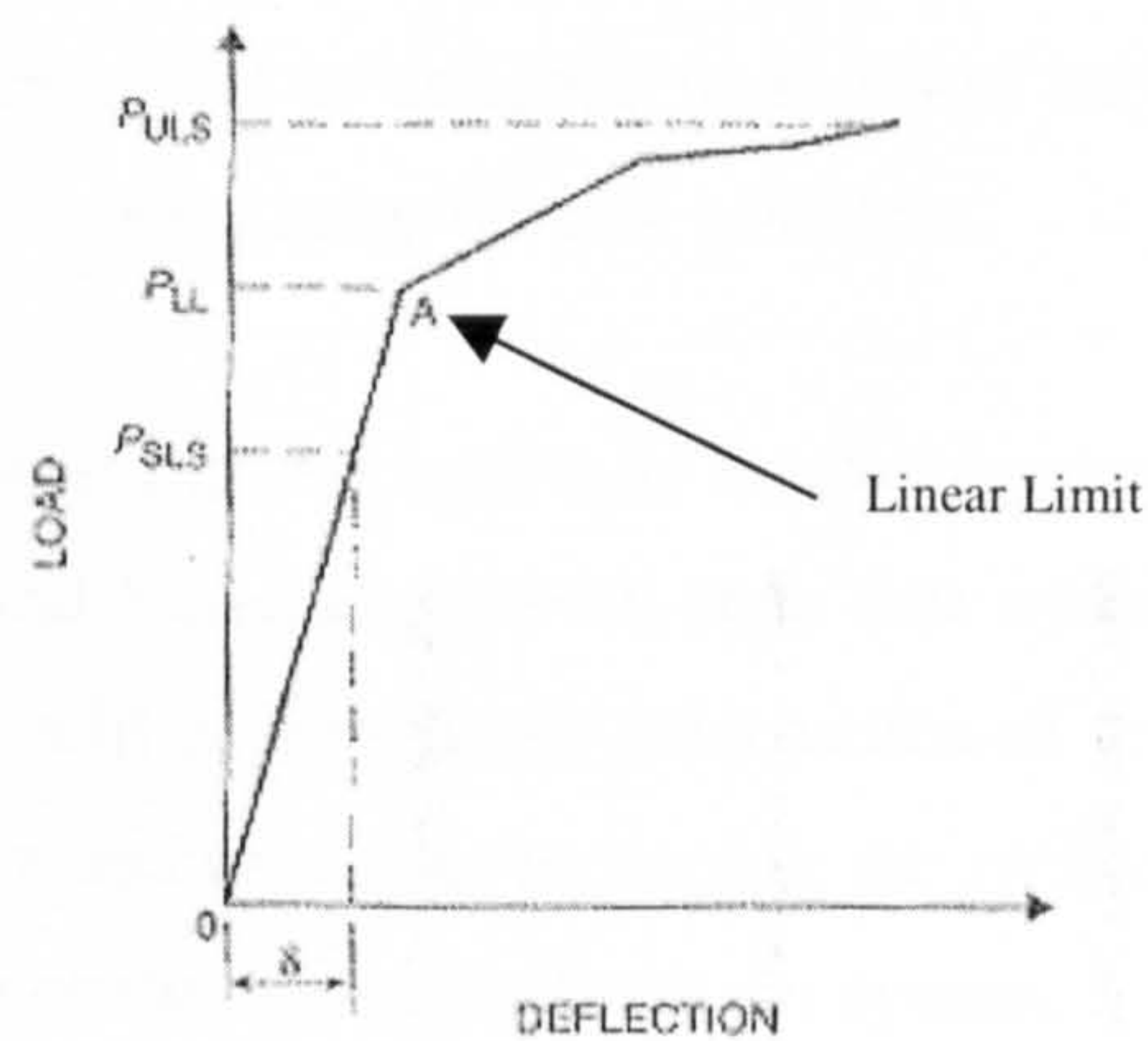


Figure 2.13 – Load/deflection relationship for steel fibre ground supported slab (Concrete Society 2000)

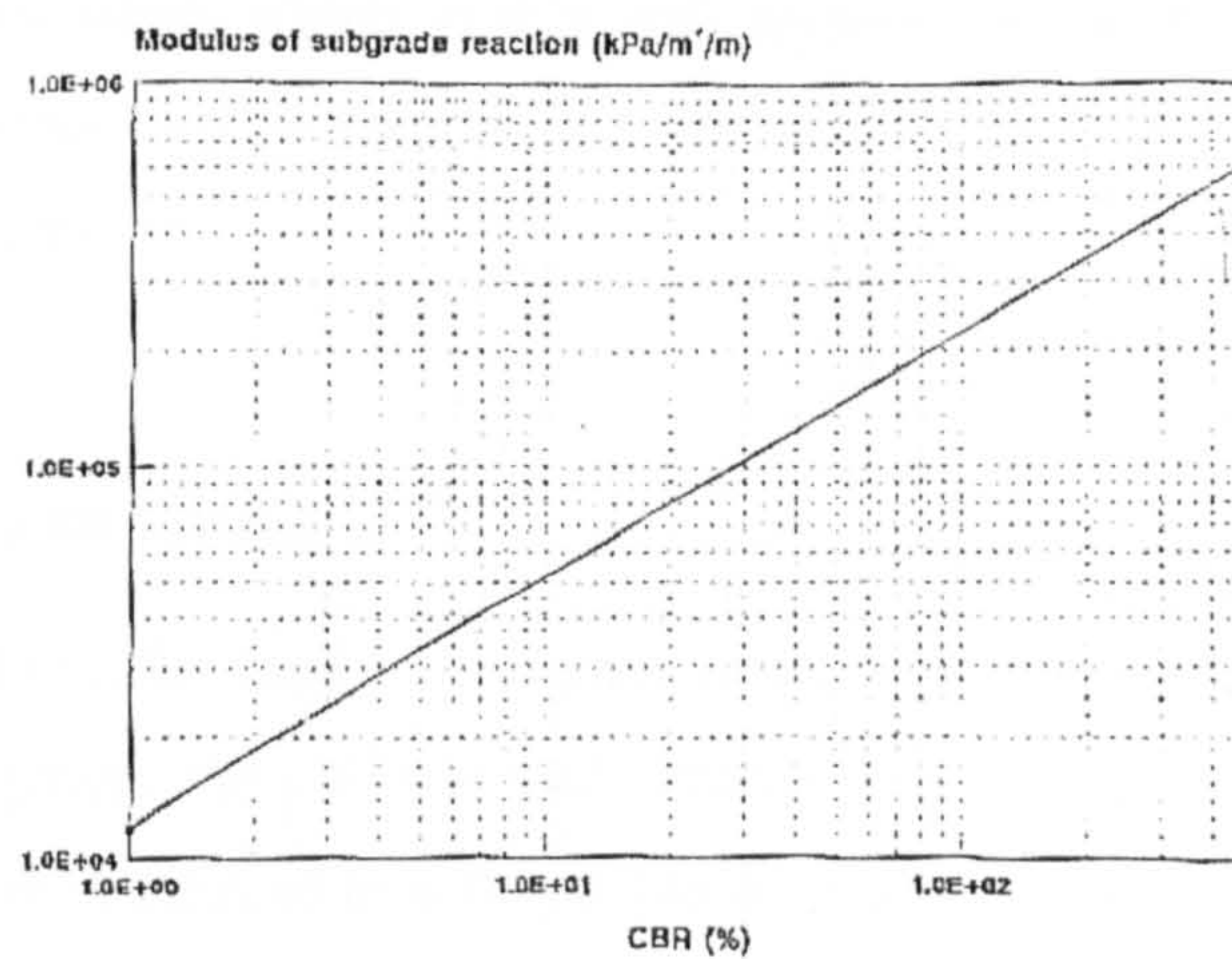


Figure 2.14 – Relationship between CBR and modulus of subgrade reaction (Croney and Croney 1997)

3. LOAD TRANSFER ACROSS CRACKS/JOINTS

3.1 Introduction

Chapter 2 has reviewed literature concerning concrete slabs on grade and found that cracks and joints are highly influential in their performance and deterioration. A full understanding of their behaviour is therefore essential to enable accurate slab design and increase the longevity of the structure's life. The effectiveness of a crack or joint can be determined through a calculation of load transfer. This is the phenomenon whereby a force directed onto one element is passed across a discontinuity into another through a natural (e.g. aggregate protrusion) or designed (e.g. dowel bar) mechanism. This lowers both stress and deflection, thus reducing the risk of failure.

The effectiveness of the load transfer system is vitally important to the longevity of the slab system. Tabatabaie and Barenberg (1980) state that without it both theoretical and field results indicate there will be permanent deformation of the subbase near to the slab corners, leading to faulting and cracking. Increasing the subbase or the slab thickness is reportedly ineffective in substituting the load transfer system.

This Chapter examines current knowledge in respect to load transfer for the design and operation of concrete slabs. The different mechanisms available for increasing load transfer are introduced alongside their benefits and drawbacks. Field investigation techniques are discussed, which enable slab response to be determined. Finally, the mathematical models used to portray load transfer are described for both singular and numerous load cycles.

3.2 Influence on Design

The value of load transfer used for design is often open to interpretation. The higher the level chosen, the greater the ultimate load capacity will be, resulting in a reduced section thickness. However, if the load transfer on site does not match that used in the design then there is an increased risk of failure. This can be anything from faulting to slab cracking, with details of each described in section 2.4. Similarly, if the designed load transfer is

chosen conservatively then an overly thick slab will be selected resulting in an uneconomic structure.

Much of the deterioration encountered during the life span of a concrete pavement, slab or hardstanding can be attributed to the lack of load transfer between the crack faces (Krauthammer and Western 1988). Work completed by Prozzi *et al.* (1993) showed that a reduction in joint efficiency (i.e. load transfer) to 35% would cause a doubling of stresses in the base of the slab under load when compared to full load transfer. Frabizzio and Buch (1999) state that a value of 70% is an acceptable threshold value, above which failures such as faulting will be avoided. A number of different systems can be employed to increase the required load transfer across the joint. These can vary from aggregate interlock, through to the use of dowel bars and keys.

Many of the design guides require load transfer values in their calculations to evaluate the slab's structural capacity. Chou (1983) argued that the load transfer efficiency of a joint would have negligible effect on stresses and deflection when the load is placed in a central position, although when near to the edge or corner it will become a major contributor. Indeed, Westergaard (1926) and Meyerhof (1962) equations (section 2.5.3) both require an estimation of load transfer to enable correct design specification. Chandler and Neal (1988) and Neal (1996) both recommend multiplying the stresses calculated for a free corner or edge by 0.7 and 0.85 respectively if load transfer is present; however, no guidance is given as to what constitutes acceptable load transfer. The U.S. Department of Transportation (1990) suggest that load transfer should only be considered on roads that carry low loading. Again no definition is provided as to what level of load transfer is applicable, and what reduction in stress should be used. The American Association of State Highway and Transportation Officials (1986) provide the most information, producing stress reduction ratios for different slab construction types and climatic conditions.

3.3 Crack Geometry

When examining the geometry of a crack it is common to think only in terms of a single width. This is generally measured at the surface as it is the only visible area; however, the crack often varies with depth, as well as along its length and is therefore 3-dimensional.

Authors have widely agreed that the slab or pavement will curl to some degree, the amount dependant on the materials used, construction methods and climatic conditions

(Poblete *et al.* 1988). As mentioned in section 2.4.2, the direction of curl is determined by the temperature and moisture gradients in the concrete. In both internal and external situations it is common for the edges of the slab to rise above the level of the subbase at either a joint location, or a newly formed crack. Due to the curling effect, the opening at the top surface will be in excess of that found at the bottom, with Poblete *et al.* (1988) concluding that for negative temperature gradients (top cooler than the bottom) the transverse joints and cracks will be relatively open and free to rotate, resulting in contact with the opposing crack face being limited to the lower edges. Similarly, ACI Committee 302 (1996) state that the crack width will be at its widest at the surface and will narrow with depth due to the shrinkage gradient. Bishop (2001) monitored both free movement and restrained joints at several warehouses in the UK. Gauges were placed at different depths throughout the slab and measurements taken at both early ages and long term. The results indicated greater movement at the top of the crack than at the bottom, with some joints showing a 1mm difference between surface and mid-depth readings. Bishop (2001) concluded that the cause of this was slab warping, which was confirmed with a precise level survey of the slab surface.

Cracks in slabs and pavements occasionally propagate towards one side leaving a sub-vertical orientation (Poblete *et al.* 1988). This can produce anomalies in joint effectiveness depending on which side is loaded. In one position the slab will bear directly onto the opposing face, whereas in the other, support will be limited and any resistance to deflection will come solely from the subsoil (Figure 3.1). Highways Department (1999) guidance suggests that where applicable, deflection testing should be undertaken in both directions to detect these variations. If unachievable they recommend that testing be carried out on the downstream as it generally produces the worst case. This indicates that the variation between load positions is caused by factors other than the orientation of the crack. The review of literature shows that little information has been produced on the deviation of the crack from vertical, and is therefore not perceived as a common problem.

The methods of design for joint spacing in floor slabs assume that each joint will open a similar amount. Bishop (2001) concluded that the behaviour of sawn restrained joints varied considerably, with some remaining closed (dormant) and others opening up excessively (dominant), dependant on the behaviour of those surrounding them. This occurrence has been recorded in several investigations (Minkerah *et al.* 1982, Bodocsi *et al.* 1993) and led to the dormant and dominant joint categorisation. Poblete *et al.* (1988) examined the opening of joints through their early ages, and noted that in the initial hours

of concrete placement only one in three would open up. At a later stage all joints were activated, although the joints which opened up first could still be identified due to their larger width. The Concrete Society (2003) reason that the dominant joints are caused by: inadequate timing of the saw-cut, locking up of joints, subbase friction against the slab and early loading restraint. Rogers (2000) concluded that further research needs to be undertaken if the dormant and dominant joint phenomenon is to be avoided.

3.4 Load Transfer Mechanisms

There are many mechanisms available which provide load transfer across joints and cracks. Some of these can be classed as natural i.e. the shape of the crack face caused by the phenomenon of crack initiation, or designed i.e. the insertion of a device across the crack. Ioannides and Koreveis (1990) suggest that a pure shear load transfer mechanism is preferable to one that transmits bending because of the warping effect inducing further stress when movement is prevented. Kelley (1939) agrees, stating that dowels that are too stiff can result in restraint to longitudinal warping, leading to distress. However, in situations where the joint width opens up considerably, or crack face degradation occurs, it will be necessary to incorporate some additional mechanism to prevent failure.

3.4.1 Aggregate Interlock

Aggregate interlock is the most fundamental mechanism of load transfer in concrete slabs and pavements. In instances where the cracking pattern is unknown, and slab reinforcement is not present, it becomes the only means of load transfer. Even in situations where additional mechanisms are provided, aggregate interlock still makes a significant contribution (Abdel-Maksoud 2000). Jimenez *et al.* (1982) estimated that its effect is approximately 75-90% of the total load transfer in crack widths between 0.25 and 0.76mm containing dowel bars. Houde and Mirza (1974) gave the load transfer value to be around 50%, although Swamy and Andriopoulos (1974) propose that the percentage of load transferred by the aggregate interlock effect is dependent on the steel quantity. They gave values of 90% for beams containing 1.97% steel and 50% for beams containing 3.95%. Walraven (1981) and Bazant and Gambarova (1980) both highlight the importance of aggregate interlock in reducing the risk of steel yielding.

When a load is placed on one side of a crack the protruding material will come into contact with recessions on the opposing side. If prevented from moving in the horizontal direction a bearing or shearing stress will be applied across the crack, thus transferring the

load. This mechanism of load transfer is a true shear action, without the bending effect that is found when using dowel bars.

Various authors have divided the mechanism of aggregate interlock into the 'local' and 'global' condition, which are made up of micro and macro roughness respectively (Figure 3.2). The literature shows ambiguity in the definition of micro and macro roughness with different authors using different models. Raja and Snyder (1991) and Laible *et al.* (1977) state that the micro roughness is the interlocking of fine aggregate particles and macro roughness is that of the larger pieces of aggregate. They continue by saying micro roughness creates a crushing and bearing action compared to the sliding and overriding behaviour of the macro roughness. Contrary to this, Walraven (1981) proposed a different model whereby micro-roughness is caused by all aggregate protrusion, and that macro roughness is due to the overall undulations of the crack face. Furthermore, micro roughness will be the dominant of the two systems thus, in modelling terms, the crack plane can be assumed flat. Authors agree that the local roughness is most significant during early load cycles when the crack width is less than 0.25mm. When cracks exceed this width, or after many cycles, attrition of the micro or local roughness takes place and global roughness, or macro-texture, becomes the dominant method of load transfer. Millard and Johnson (1984) tested this theory using several specimens and concluded that shear is resisted by a combination of crushing and sliding and that no distinct point exists whereby the two mechanisms change.

A further model developed by Walraven (1981) simulates the crack face with a system of spheres embedded into a matrix (Figure 3.3). Each sphere and its embedment depth can be statistically calculated to develop a good interpretation of the real situation. The contact areas for each particle can then be calculated and the stresses ascertained. As the sliding action develops, plastic deformation occurs and high contact stresses are produced. This leads to further deformation, until such a stage that an equilibrium of forces is obtained.

The different theories were compared to laboratory testing and the most accurate representation was found to be the rigid sphere model, whereby load transfer is achieved with a combination of crushing and sliding (Walraven 1981). Millard and Johnson (1984) also confirmed that this method provided a more accurate representation of the behaviour found in a number of test specimens.

The type and quality of aggregate, and its bond with the cement matrix, are very important factors in the aggregate interlock effect. If the aggregate is weak and allows cracking to propagate through it, then a smooth face will occur and interlock will be limited (Frabizzio and Buch 1999). When stronger aggregates are used the bond between the aggregate and the cement mortar is found to be the weakest point, resulting in aggregate protrusion and higher amounts of load transfer. The timing of formation will also have some influence over which of the two types of crack will take place. As the bond improves due to the maturing concrete, the risk of aggregate splitting becomes much greater. The majority of slabs crack in the first 24-48 hours due to the thermal contraction and drying shrinkage and therefore a pullout failure rather than an aggregate fracture will define the overall shape (Abdel-Maksoud 2000). Nowlen (1968) examined the effect of crack timing and its associated crack face by comparing the load transfer of test slabs cracked at three time periods. The slab cracked at 1 day showed a 25% increase in one million cycle load transfer effectiveness when compared to a slab cracked at 7 days.

The size of the aggregate is highly influential in the effectiveness of load transfer. A larger sized particle can bridge any crack better than a smaller particle, and tends to have a reduced risk of becoming loose in the cement matrix (Nowlen 1968). Walraven (1981) states that particle sizes less than two times the crack width can be considered as being inactive and having no contribution to load transfer. Nowlen (1968) also found a rise in load transfer of 11% by increasing the aggregate size from 20mm to 40mm, and suggested the cause was a decrease in initial looseness between the aggregate and its socket. The theory assumes a spherical particle, whereby horizontal movement (an increase in crack width) creates greater free movement (Figure 3.4). In general, larger angular particles are more beneficial for load transfer; however, they hinder finishing of the concrete surface and therefore a compromise must be made (Colley and Humphrey 1967).

Aggregate interlock is reduced as crack width is increased in size, with different authors providing information on the associated values. Tables given by Pearson (1999) demonstrate that almost full aggregate interlock is achieved at a crack width of less than 0.5mm. Between 0.5-1mm only partial aggregate interlock is retained, and widths over 1.5mm maintain no interlock at all. Buch (1999) states that the opening of a crack by as little as 0.8mm can reduce the load transfer by up to 50%, and ACI Committee 360 (2000) recommend that load transfer cannot be relied upon if the crack width is greater than 0.9mm. No mention of the effect of aggregate size is provided, although it is expected to be influential.

In a concrete slab the crack width changes dependant on climate, varying between daily and seasonal cycles. Since aggregate interlock load transfer is highly influenced by the crack width it will also change frequently depending on when the calculation is made. Deterioration of the crack face caused by high cycles of loading must also be taken into account, as this will diminish the interlock effect over time, thereby reducing load transfer.

3.4.2 Dowel Bars

Dowel bars are one of the most traditional methods of creating a load transfer system across a predetermined joint; however, they can only be employed when the location of the crack is known, otherwise the system becomes redundant (Critchell 1958). Ringo and Anderson (1996) comment that if well constructed dowels can provide a similar slab strength to that found internally.

According to Millard and Johnson (1984) the mechanism of load transfer for a dowel bar is split into three main areas, these being direct shear, kinking and flexure. They also discovered that flexure of the bar is the main method of transfer due to the significant deformation which occurs within the concrete. Yoder (1959) and Friberg (1938) both suggested that the effective distance at which dowel bars have some proportion of load transfer capacity is $1.8l$ from the load centre, where l is the effective length (equation 3.1). Ioannides *et al.* (1990) argued with this, stating that the effective distance was only $1.0l$, with finite element simulations and site data comparisons confirming their position. All authors agreed that the amount of load each dowel bar transfers reduces linearly with distance from the application position. The Concrete Society (2003) have used the recommendations made by Yoder (1959) and assumed that dowel bars can contribute fully if a distance half the effective length is used ($0.9l$). Once the dowel is selected it should be checked against shear, bearing, bending, punch-out and a combination of shear and bending (Concrete Society 2003). Formulas for calculating each are provided in the relevant guidance documents, and provide a maximum dowel load transfer capacity in kN.

$$l = [E_c h^3 / 12(1 - \mu^2)k]^{0.25} \quad \text{equation 3.1}$$

Where:

E_c = Youngs modulus of concrete

h = Slab depth

μ = Poissons ratio for concrete

k = Modulus of subgrade reaction

The dowel bar itself is commonly 12-25mm in diameter positioned at approximately 300mm spacings across the length of the joint. Due to this spacing it is accepted that only the two to four dowels nearest the load can be considered active. The length is based on the second point of contraflexure, but design manuals and texts have standardised this suggesting values of 400-600mm (Neal 1996). Generally the dowel is required at the mid-section of the slab, with a deviation of no more than 20mm overall, and 3mm between each bar. Other standards have slightly different specifications but they predominantly comply with those written above (Ringo and Anderson 1996).

This type of load transfer system is less affected by the movement of the slab and the width of the crack than non-doweled joints, as any movement will only be a minor proportion of the bar's full length. However, there is a reduction in load transfer that occurs because of the looseness of the dowel from repeated loading cycles. This occurs because the concrete directly above and below the dowel bar begins to erode under load and leads to an ovaling effect (Porter *et al.* 1996).

The construction of the dowel bar system is vitally important as it can create increased stresses within the concrete if not correctly installed. The dowel should be designed to enable independent movement of one slab away from the other, and prevent locking of the joints. This is achieved by placing a sleeve onto the dowel, or by painting on a suitable de-bonding agent, both of which enable the bars to slip on one side. The overall design of the slab must also be examined in detail as the insertion of dowel bars around the perimeter of the slab can restrain movement. Proprietary systems have been developed that contain polystyrene filler at the edges of the dowel bar to overcome this problem. Different shapes of dowel bars varying from square or rectangular to more advanced semi-circular sections have also been developed to allow for some horizontal movement when required (Walker and Holland 2001).

3.4.3 Steel Fabric

The use of reinforcement and fabric is not provided as a load transfer mechanism, and is generally used to control suitable crack spacing and prevent excessive opening (American Association of State Highway and Transportation Officials 1986). Section 3.4.1 describes how the load transfer mechanism of aggregate interlock is reduced when the crack begins

to widen. The ideal situation is therefore one in which there are many narrow cracks instead of a few larger ones. The reinforcement provides this by distributing stresses over the entire slab and restraining any crack opening.

Tests undertaken by Benkelman (1933) indicated that the use of fabric reinforcement significantly reduces crack opening when compared to those with no reinforcement. Joints in similar locations were examined and the non-reinforced cracks showed increased loaded slab deflections of between 54 and 146 percent when compared to those that were reinforced with steel fabric. The variation in crack width changed dependant on the seasonal temperature.

Reinforcement has similar properties to that of a dowel bar in respect to the transference of load between one slab and another. The Concrete Society (2003) has provided tabular information on maximum load transfer capacities for commonly used internal meshes. These are calculated for yielded steel as the shrinkage movement in the concrete will reduce the section diameter and therefore lower its load transfer effectiveness. The Concrete Society (2003) also remark that the choice of mesh should not be based entirely on its load transfer efficiency, as the selection of denser fabric to increase its strength can raise the risk of the joint not opening at all, resulting in mid-slab cracking.

3.4.4 Steel Fibres

Steel fibres are commonly used as a stress distribution material and reduce the overall shrinkage movement found in a slab (Balaguru and Shah 1992). The fibre, in resisting this movement, creates a system of many fine cracks (often micro-cracks) whereby the crack faces are close together. This effect is similar to steel fabric whereby aggregate interlock is increased, resulting in good load transfer (Raja and Snyder 1991).

Although not well researched, the steel fibre itself also provides a contribution to load transfer (Swamy *et al.* 1979 and Schrader 1985). ACI Committee 360 (2000) state that steel fibres offer additional shear load transfer across contraction joints in slabs on ground, but offer no further information on the subject. The mechanism of shear transfer is similar to that of a dowel bar, although instead of one singular element there will be many finer 'dowels' crossing the crack. The pullout resistance of the fibre from the concrete will have a great influence on the load transfer value. This resistance is a factor of the fibre embedment, the orientation and the steel strength, and may thus be increased or decreased depending on the fibre used and the construction process. Little guidance is

available on the load transfer effect of steel fibres and this requires further research and investigation if it is to be utilised in the future.

Thompson (2001) examined the effect of steel fibres in granular cement bound road bases. Cyclic testing was employed on small samples containing fibre quantities of 0, 0.25, 0.5 and 1.0% by volume, with parallel crack widths up to 1mm. The results indicated that an increase in load transfer stiffness, and therefore a reduction in net shear slip, occurs in steel fibre reinforced concrete at high crack widths when compared to that of non-reinforced sections (Figure 3.5). However, there was little indication that the higher stiffness was proportional to the increase in fibre content. The load/shear-slip relationship also altered when fibres were used as reinforcement within the specimen. In non-reinforced tests the shear slip versus load relationship was non-linear with only 12% of the maximum load producing 80% of the maximum slip (Figure 3.6). When fibres were introduced this became much smoother with a near linear increase in slip with load (Figure 3.7). This resulted in a more efficient crack as proportionally more load is required to move the specimen. Thompson (2001) suggested this was caused by the increased frictional restraint as the fibre bent around the aggregate and held the beam together in tension.

3.4.5 Proprietary Systems

A formed joint at the slab edge can provide a satisfactory load transfer condition if correctly designed. The mechanism must contain some kind of interlocking member and usually involves a dowel or plate device to transfer the load into an adjacent slab. The load transfer efficiency of these joints varies between suppliers and as such it is not possible for a singular value to be ascertained (Concrete Society 2003).

The construction is usually formed with a pre-cast panel made of steel which is left in the concrete, helping to strengthen the joint. There are many different types of former available from various companies, each comprising a number of benefits. However, problems can occur, with the main concern being inadequate compaction or under vibration of the concrete around the former. This can create air voids and pockets of loosened material which can crumble and crack under low loading (Concrete Society 2003). Neal (1996) also comments on the possible changes in surface level and excess cement paste around the joint arris, both of which can lead to increased spalling of the slab edge.

3.5 Degradation of Load Transfer

Due to the vast number of vehicles passing over a joint or crack some degree of joint degradation over time is to be expected. Many authors refer to the work of Colley and Humphrey (1967) to determine the amount of deterioration likely to occur. In this work test slabs 1220 by 5500mm in plan, with a non-doweled joint at mid-span, were placed on a subgrade material and repeatedly loaded to a maximum of 53kN for up to 1 million cycles. Measurements of deflection were taken either side of the joint at 50,000 cycle intervals for various joint openings, slab thickness and subbase/subgrade types. A selection of their results are reproduced in Figures 3.8 - 3.11, where effectiveness is calculated using the Teller and Sutherland (1943) method of load transfer (section 3.8.1, equation 3.8).

Figures 3.8 and 3.9 indicate that the majority of degradation occurs during the early stages of the test, with Colley and Humphrey (1967) calculating that 90% of the 1 million load cycle deterioration will have occurred during the first 500,000 cycles.

The greatest influence on joint effectiveness for all load repetitions and construction methods is caused by crack width. For a 175mm (7") slab at 120,000 cycles the width of 1.65mm (0.065") fails completely, whereas the 0.38mm (0.025") crack is still running at over 90% efficiency (Figure 3.8). Using a greater slab thickness of 225mm increases the effectiveness to some degree (Figure 3.9), with a 1.65mm (0.065") crack retaining 20% load transfer at 1 million cycles, but even here small increases in crack width lower the effectiveness greatly.

The results of laboratory testing were compared to data collected from a working site constructed with similar materials and crack width properties. The laboratory data shows increased rates of deterioration, the magnitude of difference increasing with larger crack widths (Figure 3.10). Colley and Humphrey (1967) suggest the cause of this to be higher loading in the laboratory test, and changing of crack widths due to seasonal and daily temperature changes. The evidence for this is limited and its cause is more likely to be from incorrect crack width orientation measurements.

Tests by Colley and Humphrey (1967) examined the effect of load and showed that high magnitudes degrade the joint face at a much faster rate (Figure 3.11). When tests were carried out at 40kN (9 kips) the load transfer fell continuously throughout 1 million cycles due to aggregate attrition; however, when reduced to 31kN (7 kips) the load transfer

dropped up to 300,000 cycles, at which point it levelled off for the remainder of the test. When a 22kN (5 kips) load was used the load transfer showed limited change throughout the test, suggesting that light loads cause little wear of the interface material. Ioannides and Koreveisis (1990) similarly concluded that there is a critical value of load whereby deterioration takes place at a much greater rate, and therefore loads below this value do not generally need to be considered in design.

Nowlen (1968) examined the effect of different aggregate properties on load transfer under a 50,000 cycle 40kN load for crack widths of 0.9 and 1.65mm. Using similar apparatus to that of Colley and Humphrey (1967), maximum aggregate sizes of 19, 38 and 64mm were tested under a 40kN load for one million cycles. The results showed that an increase in aggregate hardness produced better effective endurance throughout the test. Nowlen (1968) also concluded a crushed aggregate in which any natural weakness has been removed, showed better durability than a rounded aggregate even though they were made of the same material. For both crack widths an increase in aggregate size improved the effectiveness; however, the difference was far more noticeable between the 38 and 64mm aggregate than 19 and 38mm.

Other than the direct degradation of the concrete face, it is common for the subbase material to compact under repeated loading. Testing undertaken by Colley and Nowlen (1958) comprised granular or cement treated clay subbases resting on a clay subgrade soil. A 50mm thick concrete slab was placed on top and repeatedly loaded for 500,000 cycles under a 40kN load. Throughout the test measurements were taken of deflection and under slab pressure, with visual observations of pumping also recorded periodically. Increasing the subbase thickness, using well graded material and poor preparation were all found to increase the amount of compaction over time; however, using a soil cement subbase reduced these effects and prevented the risk of pumping. Colley and Nowlen (1958) undertook similar tests and concluded that an increase in foundation support stiffness resulted in a much reduced change in effectiveness. For a crack opening of 0.9mm the one million-cycle effectiveness increased from 27 to 78% when the modulus of subgrade reaction was increased from 0.025 to 0.125N/mm³.

Thompson (2001) investigated deterioration for fibre reinforced cement bound granular road bases and reported that the rate of degradation was significantly reduced when incorporating fibres into the mix (Figure 3.5). In specimens containing fibre fractions of 0.5% or more the magnitude of deterioration was negligible. This reduction in shear slip

and deterioration was thought to be caused by the fibres holding the crack face together, increasing the aggregate interlock, rather than the load transfer potential of the fibre itself.

3.6 Slab Condition Testing

The use of pavement technology for the assessment of floor slab condition is a relatively new concept. As has been shown in section 2.2 the construction and loading conditions between the structures are extremely similar and therefore the techniques of standard practice in highway testing are beginning to be used for internal slabs. The method generally involves measuring deflections on the structure's surface either side of a joint or crack created by a controlled transient load, thereby enabling calculations of slab response.

3.6.1 Equipment

Falling Weight Deflectometer

The falling weight deflectometer (FWD) is commonly used in the non-destructive testing of both flexible and rigid road pavements. The impact of a load on the surface of the structure creates a deflection bowl which is recorded with a series of offset velocity transducers (geophones). Examination of the slab profile then makes it possible to back-calculate the stiffness of each construction layer or determine joint effectiveness.

The FWD operates by enabling a large mass to fall onto a system of springs, which in turn generates a load pulse (Figure 3.12). The magnitude of force is determined by the load applied and the drop height, both of which can be adjusted to obtain a transient contact pressure equal to that of a moving vehicle (Scott Wilson Pavement Engineering 2002). The load pulse rises from start to peak in approximately 30-40 milliseconds, the exact value being dependent on the machine used (Fleming 2000). The peak vertical deflections are measured at several locations radiating out to a maximum of 2.25m from the source of load, with each geophone recording to a resolution of 1 micron over a 2mm maximum range. The positions of the geophones are manoeuvrable depending on the information required by the operator.

The FWD is mounted on a trailer bed to enable ease of movement, and is often hooked onto the back of a vehicle to enable quick progression between test locations. The power required is obtained either directly from the vehicle or from a stand alone battery. A camera and laptop are often mounted within the cab allowing the driver to manoeuvre and

control the FWD without having to leave the vehicle. This configuration enables testing to be undertaken safely and at speed as the operator does not need direct access to the road pavement.

Prima Portable Dynamic Plate

The Prima is a small portable version of the FWD and is commonly used for measuring the bearing capacity of base layers in pavements and other forms of construction (Fleming 2000). The equipment consists of a load dropped onto a series of buffers, which creates a controlled force on the slab surface with a pulse duration of 15-20 milliseconds (Figure 3.13). The weight of the load can be varied between 10 and 20kg, with the drop height further refining the impact. The loading plate can be changed to either 100, 200 or 300mm in diameter, enabling the contact pressure to simulate that of typical wheel loads applied on the structure.

To measure the force and slab deflection a load cell is situated within the Prima's main housing along with a geophone directly underneath the base plate. Two further geophones are attached via a communications lead and are positioned with the aid of a rigid T-beam. This set-up enables deflections to be taken anywhere on the slab, limited only by the length of the lead. The geophones are accurate to +/- 2% and can measure vertical movement to 1 micron, with a maximum range of 2.2mm.

3.6.2 Investigation Techniques

The deflections recorded with either piece of test equipment can be used to develop a number of slab performance parameters. Each is determined with the careful positioning of the geophones and load plate in relation to the joint, or with increasing load magnitudes.

Load Transfer

As described in section 3.2, load transfer is required to transfer force across a discontinuity between slabs. This reduces stress and deflection, and ensures serviceability and structural failures do not ensue.

Section 3.7 provides examples of load transfer equations used in the assessment of floor slabs and pavements, based on either deflection, stress or engineering judgement. Colley and Humphrey (1967) recommend that stress equations should not be used due to

variations of load type in either slab. Similarly, 'engineering judgement' is a subjective perception of joint effectiveness and is therefore difficult to accurately measure.

Deflection testing is therefore commonly used for the determination of load transfer. This is generally calculated by relating the deflection of one slab edge to the other, providing a ratio expressed as a percentage. Further information on calculation methods is described in section 3.7.

Load Step

Load step is the absolute value of differential vertical deflection between the edges of a crack or joint when under dynamic load. The step itself can affect the ride quality for any vehicle crossing the joints and induce spalling of the crack edges. The magnitude of this movement is dependent on the load applied, load transfer and foundation support conditions. The calculation of load step can be achieved with the data obtained from either piece of equipment, it simply being one edge deflection subtracted from the other. Further information is provided in section 3.7.

Edge Cantilever

Edge cantilever determines the rate of bending of the slab edge and is achieved by subtracting the deflection directly under the load from that of the slab edge on the same side. Depending on the degree of joint stiffness the value of cantilever may be negative or positive. A positive result indicates a discontinuity, with a negative value showing good load transfer and a slab that is working as an integrated unit. Highways Agency (1999) comment that this cantilever effect is also of assistance in assessing the quality of slab foundation. Where it is deemed poor the cantilever will be positive with a negative value showing good support. As mentioned in section 1.1, there is an increased demand for tighter tolerances in slab level and flatness. This must be assessed when under dynamic load to ensure vehicle specifications are adhered to (Concrete Society 2003). Calculations of slab edge cantilever enable the relevant standards to be checked, preventing excessive lean or damage to vehicles. The level of allowable floor variation varies depending on the categorisation, with the reader directed to the individual guidance documents if further information is required.

Deflection Basin

Deflection basins enable a profile of the slab to be determined when under dynamic load. This can be used for calculating structural properties or examining the overall response of

the slab. To determine a deflection basin several geophones are placed on the slab surface. Each is positioned in a line at increasing radial intervals from the load, one of which will be on the opposing side of the joint or crack, with the remainder across the same slab. Plotting the deflections of these different geophones against distance enables determination of an extended deflected shape of the slab surface when impacted by load.

When an FWD is used to calculate soil properties, standard practice dictates that it is positioned at the slab centre as any interpretation assumes a semi-infinite length. Each section of the deflection bowl will then provide information into the different layer properties as shown in Figure 3.14. This analysis is often undertaken using a trial and error approach and therefore computer software has been developed to speed up the process significantly. In situations where the FWD is set at the edge of the slab in order to determine load transfer, it is not possible to use this method of analysis. However, the deflection bowl can still provide information into the structural performance and effect of the joint, with a peak deflection occurring directly under the load indicative of good load transfer (Highways Department 1999).

Void intercepts

Void intercepts are used to assist in the detection of voiding underneath the slab edge. Croveti and Darter (1985) found that they could be determined from deflection measurements under three different load magnitudes when taken at a slab edge. As the load increases the void begins to close until such a stage that full contact with the foundation is produced (Figure 3.15). At this point resistance to deflection will be increased and the magnitude of deflection caused by a unit load reduced. If several values are recorded, a plot can be made of deflection against its associated load magnitude. A comparison can then be undertaken of the best-fit line and that produced if each point was simply joined together. Any significant deviation signifies a strong possibility of voiding under the slab edge.

The best fit line can also be extrapolated until it bisects the zero load vertical axis, with the point at which it crosses used to determine the existence of a void (Figure 3.16). Croveti and Darter (1985) propose that a vertical axis value of 50 microns or higher is an accurate guide for detecting voided areas, although Wade *et al.* (1997) suggest 75 microns. Work undertaken by Frabizzio and Buch (1999) examined both of these assumptions and suggested that the intercept magnitude could enable the degree of support to be established. In both cases the values coincided with site data of known

faulted slabs, indicating the correct range had been found. White Young Green (2002) undertook similar testing on sites in the United Kingdom and found that this value could be reduced to 25 microns to enable smaller voids to be detected.

Crovetti and Darter (1985) have stated that the value of void intercept is of direct relationship to the size of void under the slab edge. The accuracy of this analysis has been called into question by Tang (1993) who demonstrated that there is little correlation between the two. This discrepancy was thought to be caused by the varying nature of void, with the depth, length and width of the area all having an effect on the value obtained.

A more complex method to determine the magnitude of the void has been developed by Crovetti and Darter (1985). In this approach deflections are recorded at central, edge and corner positions at different locations across the site. These values are then run through a series of equations enabling a lower bound of zero voiding to be developed. Comparisons of the individual test points can then be made to determine whether neither, one, or both sides of the slab are affected.

Another approach to void detection was developed by Ricci *et al.* (1985). This method compares the slope of the line obtained when joining up the deflection values of selected FWD geophones (W). Equations 3.2 and 3.3 used in the analysis are shown below, with the locations of the geophones given in Figure 3.17.

$$M = \text{Arc tan } [6/(W1-W2)] \quad \text{equation 3.2}$$

$$Q = \text{Arc tan } [(W2-W7)/24] \quad \text{equation 3.3}$$

The results of these calculations are analysed with the following:

If Q is greater than 18, a loss of support is indicated

If Q is greater than 18, the smaller M is the larger the loss of support

If Q is less than 10 and M is greater than 70, then full load transfer can be assumed.

3.7 Joint Effectiveness Analysis

A number of methods have been used to calculate the effectiveness of load transfer. Many of these are based on deflections either side of a known joint or crack from an imposed

load, with a percentage mark given to illustrate the deflection being transferred from one slab to another. Other methods utilise the variation in stress under the slab edge or finite element modelling to predict the load transfer.

Many terms such as ‘load transfer’, ‘joint efficiency’, ‘load transfer efficiency’ and ‘joint transfer efficiency’ have been used to describe the load transfer mechanism, with different authors using the various terms to depict specific calculation methods. In this thesis the terms are all interrelated, with the separate equations described by the author who first used it during analysis of cracks and joints. Where possible ‘load transfer’ has been used to provide clarity to the reader.

Equation 3.4 (Crovetti and Darter 1985) produces a load transfer value (LT) created from the deflection of the loaded (dl) and the unloaded (du) slabs. In the case of a fully transferred load the result will be 100%. In a free edge situation where the load transfer is negligible then the LT will be zero. Cracks are deemed to have adequate load transfer when the LT is in the region of 65-70% or above (Frabizzio and Buch 1999).

$$LT = (du/dl) \times 100\% \quad \text{equation 3.4}$$

Equation 3.5 (Ioannides and Korevesis 1990) yields a slightly different result as it takes into account the amount of load transferred across the crack rather than the deflection. The term P_t is derived from the total load transferred from one side of the joint to the other throughout its entire length. The term P is the total externally applied load, and therefore, in most situations, the value of transfer load efficiency (TLE) will be below 50 %. (Buch *et al.* 2000, pp 329) advise that the P_t value should be used alone as “it has a more physical meaning than its counterpart” and can be back calculated from the transferred load efficiency (TLE), as shown in equation 3.6. Ioannides and Korevesis (1990) have provided graphical relationships between TLE and the LT calculation in equation 3.4 for various a/l ratios, as shown in Figure 3.18, where LT is expressed as LTE_s . Buch *et al.* (2000) used the faulting data obtained from site testing to develop a threshold parameter for P_t , the value depending on the structural design and applied load.

$$TLE = (P_t/P) \cdot 100 \quad \text{equation 3.5}$$

$$P_t = (TLE/100) \cdot P \quad \text{equation 3.6}$$

Aggregate stiffness (AGG) is another factor which is used by Buch *et al.* (2000) to provide an indication of joint effectiveness, and produces a stiffness value per unit length of crack. Buch *et al.* (2000) state that by determining the load transfer (where LT is expressed as LTE_{δ}), and obtaining values for the radius of relative stiffness (l) and modulus of subgrade reaction (k) the AGG value can be derived from the graphical relationship developed by Ioannides and Koreveis (1990) (Figure 3.19).

Other researchers have adopted different methods of analysis, most of which are a direct comparison of loaded and unloaded slab deflections. Pradhan (2002) compared five of the different equations available commenting that most of the methods gave similar results. He argued that his new method of analysis (equation 3.7) was more accurate as it incorporated support from the foundation resulting in higher values. This theory was tested against a visual survey indicating that all of the tested joints were satisfactory as indicated by a plus fifty percent load transfer value. In essence, his method is the same as Croveti and Darter's (1985) with the unloaded and loaded deflections presented in such a way that in almost all situations the load transfer value will be above 50%. This therefore provides very little extra indication as to the effectiveness of the joint.

$$LT = (du + dl)/(2dl) \cdot 100 \quad \text{equation 3.7}$$

Other methods typically used in the determination of joint efficiency from unloaded and loaded deflections are provided in equations 3.8 to 3.11. Several of the equations compare the results of the approach and leave slabs, this being a change in the loaded slab edge.

(Teller and Sutherland 1943)

$$LT = [(2 \cdot du)/(dl + dl)] \cdot 100 \quad \text{equation 3.8}$$

(Jackson *et al.* 1994)

$$LT = \text{Smallest of } LT_{asd} \text{ and } LT_{dsd} \quad \text{equation 3.9}$$

$$LT_{asd} = (dl/du)/100$$

$$LT_{dsd} = (dl/du)/100$$

(Ricci *et al.* 1985)

$$LT = (ASDR + LSDR)/2 \quad \text{equation 3.10}$$

$$ASDR = (du/dl)_{asd}$$

$$LSDR = (du/dl)_{lsd}$$

(American Association of State Highway and Transportation Officials 1986)

$$LT = (du/dl) \cdot B \cdot 100 \quad \text{equation 3.11}$$

$$B = dl_c/d2_c$$

Where:

LT = Load transfer

du = Deflection of unloaded slab

dl = Deflection of loaded slab

$dl/2_c$ = Deflections at slab centre (305mm apart)

LT_{asd} = Load transfer of approach slab

LT_{dsd} = Load transfer of leave slab

$ASDR$ = Approach slab deflection ratio

$LSDR$ = Leave slab deflection ratio

The American Association of State Highway and Transportation Officials (1986) use a J-factor to incorporate the joint efficiency into the design of pavements. The J-factor has a significant influence on slab response, and as such must be chosen with care. The guidance provided in the document for the selection of this value is limited, with the general statement "higher J's should be used with low 'k' values, high thermal coefficients, and large variations in temperature" (American Association of State Highway and Transportation Officials 1986, pp II-27). If 'J' values are to be used confidently more information needs to be supplied to assist the selection of specific values for different conditions. Kuo (1998) has researched the effect of J-factor on the outcome of the design and concluded that there is no significant relationship between the J-value and load transfer efficiency.

Other methods such as that of Sutherland and Cashell (1945) have been developed which compare the stresses under each slab rather than the deflections (equation 3.12). Colley and Humphrey (1967) argue that this method is not strictly reliable because of the different types of loading on either side of the crack. The slab under the load is undertaking direct bearing, whereas the adjacent load is created purely from shear.

$$LT_{\text{stress}} = (F_f - F_j) / (F_f - F_i)$$

equation 3.12

Where:

- LT_{stress} = Stress related load transfer efficiency
- F_f = Critical stress for load at a free edge
- F_j = Critical stress for load at interior
- F_i =Critical stress for load at a joint edge

Gulden and Brown (1985) suggest caution when using load transfer values alone to assess a joint or crack within a slab. Due to the nature of determining load transfer the overall deflection will have a large impact on the value obtained. An example of this is shown below in Table 3.1, where joint efficiency is calculated using equation 3.4 and load transfer with equation 3.8.

Table 3.1 - Load Transfer Comparison (Gulden and Brown 1985)

Test location	Loaded Deflection	Unloaded Deflection	Load Transfer (%)
1	6	1	29
2	10	5	87
3	35	30	92

Clearly test location 1 has the most favourable joint condition despite having the lowest load transfer. Thus, Gulden and Brown (1985) recommend using the overall and differential deflections between slabs, rather than a load transfer value in the assessment of joints. Unfortunately, very little data is available giving guidance on recommended levels for these two values and as such the load transfer value will invariably be used. Informed by the work of Pearson (1999), Cudworth (2000) has produced a criterion table to which it is recommended slabs adhere if they are to show satisfactory behaviour. The work states that differential deflection should be limited to 100 microns, with the overall deflection on one side of the joint no greater than 150 microns. A value of 65% load transfer is provided for completeness, although the method of calculation is not provided. Cudworth (from Arnold 2002) has suggested that a Falling Weight Deflectometer (FWD) load step of 300 microns, created from a 50kN impulse load, is indicative of a serviceability problem within the slab. This value was stated to be relevant only for the test equipment and not as an absolute value of site dynamic faulting. However, the FWD is supposed to simulate the impact of a vehicle on the slab’s surface, with a 49kN load

given by White Young Green (2002), and therefore it can be assumed that this 300-micron value (although site specific) should be representative of general serviceability problems.

Nishizawa *et al.* (1989) developed equation 3.14 relating load transfer (*LT*) to crack width (*w*), with Ioannides *et al.* (1990) proposing that this was a best-fit straight line through the laboratory data collected by Colley and Humphrey (1967). Ioannides *et al.* (1990) suggested that the values obtained could be cross referenced with their graphs enabling the effect of crack width on other slab response parameters to be determined. They did comment that this approach would be hazardous as it combines an empirical relationship with a mathematical function.

$$LT = 100 - (25 \cdot w) \quad \text{equation 3.14}$$

The equation developed by Nishizawa *et al.* (1989) is a generalisation and neglects many of the important factors which determine load transfer effectiveness. According to the equation a 3mm crack would still contain 25% load transfer, whereas Buch (1999) discovered a parallel crack with a width exceeding 1.5mm would provide no load transfer at all.

Buch (1999) examined the effect of pavement properties using an analytical model. The results demonstrated that an increase in slab thickness from 150 to 400mm, or raising the subgrade resilience from 0.027 to 0.135 N/mm³, produced lower load transfer efficiencies despite the joint being of the same stiffness. However, the deflections of the slab edges were reduced leading to lower stresses and a stronger pavement system. Gulden and Brown (1985) also state that load transfer and load efficiency values increase with higher deflections. In analysing the data from field tests they utilised the differential deflections between slabs (i.e. the load step) as it gave a better indication of performance.

3.8 Summary

Load transfer across cracks and joints is vital to the long-term serviceability requirements of concrete floor slabs and pavements. Much of the research undertaken has shown that its effectiveness must remain high throughout the duration of slab life if maintenance is to be kept low, and failure prevented.

The selection of an adequate load transfer value for the structural design of a concrete slab is essential if deflections and stress are to be kept within acceptable levels. This is

generally undertaken assuming crack widths will open equally throughout the site, neglecting the fact of the dormant and dominant joint behaviour. Deterioration of the crack is also often overlooked with a single value assumed throughout the structure's life. The correct equation for calculating load transfer must be stated for analysis, as each will produce different values.

The crack opening itself is well documented as being larger at the surface than at the base, caused by differential shrinkage and slab curling; however, the gradient of this variation is unknown. Many tests have been undertaken comparing crack width to load transfer, although only surface measurements were used.

The load transfer phenomenon is known to be controlled mainly by the aggregate interlock effect regardless any extra mechanisms inserted across the crack or joint. This has been broken down into the local (micro) and global (macro) roughness, with macro roughness only being utilised once cracks become large or crack face deterioration occurs. The role of fibres as a load mechanism is still relatively unknown, although it is thought to aid in load transfer across the crack.

There are many methods of analysing slabs using non-destructive deflection testing techniques. Many of these are commonplace in the examination of external pavements; however, they are relatively new in the assessment of internal floor slabs. Methods to determine load transfer, load step, edge cantilever and void intercepts can all enable actual site behaviour to be quantified.

The purpose of this study is to address the lack of understanding in load transfer across joints and cracks in concrete slabs on grade. This will involve the examination of typical geometries of cracks and joints from in service sites and the determination of slab load transfer and deflection related responses. The longer-term load transfer effects will also be examined in respect to the deterioration of the crack over time. This will incorporate the relatively unknown mechanism of steel fibres.

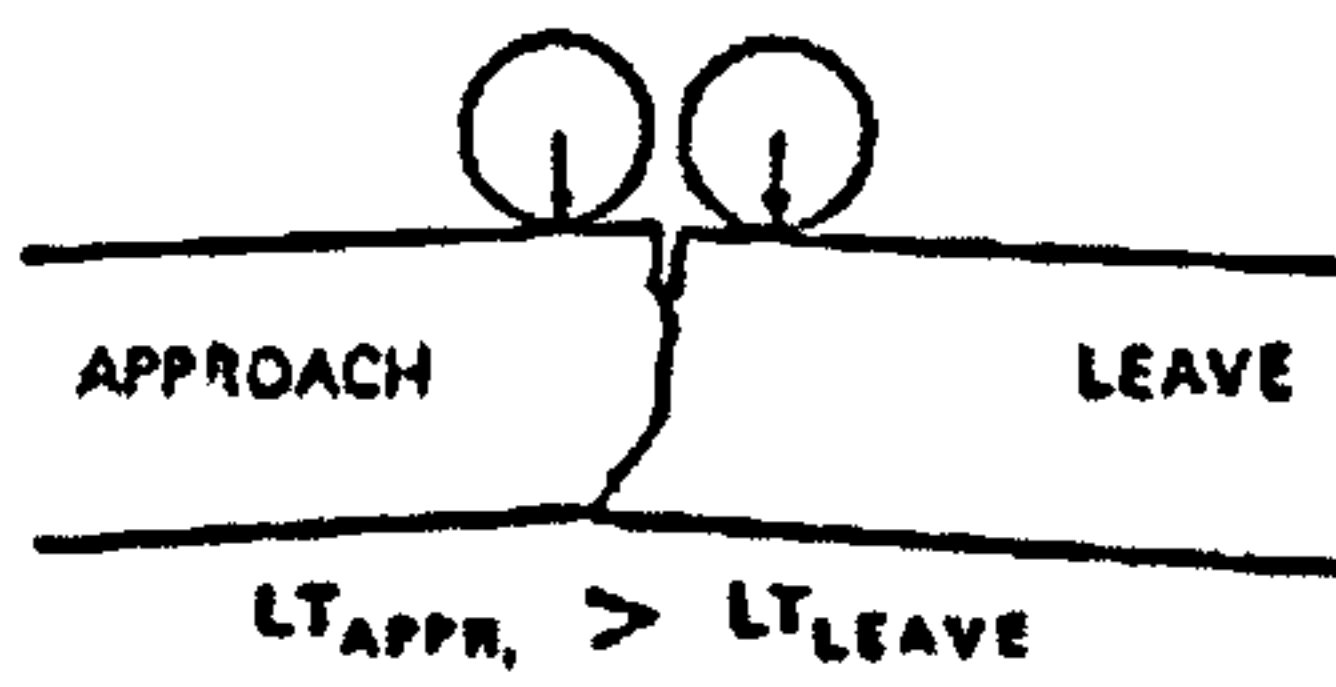
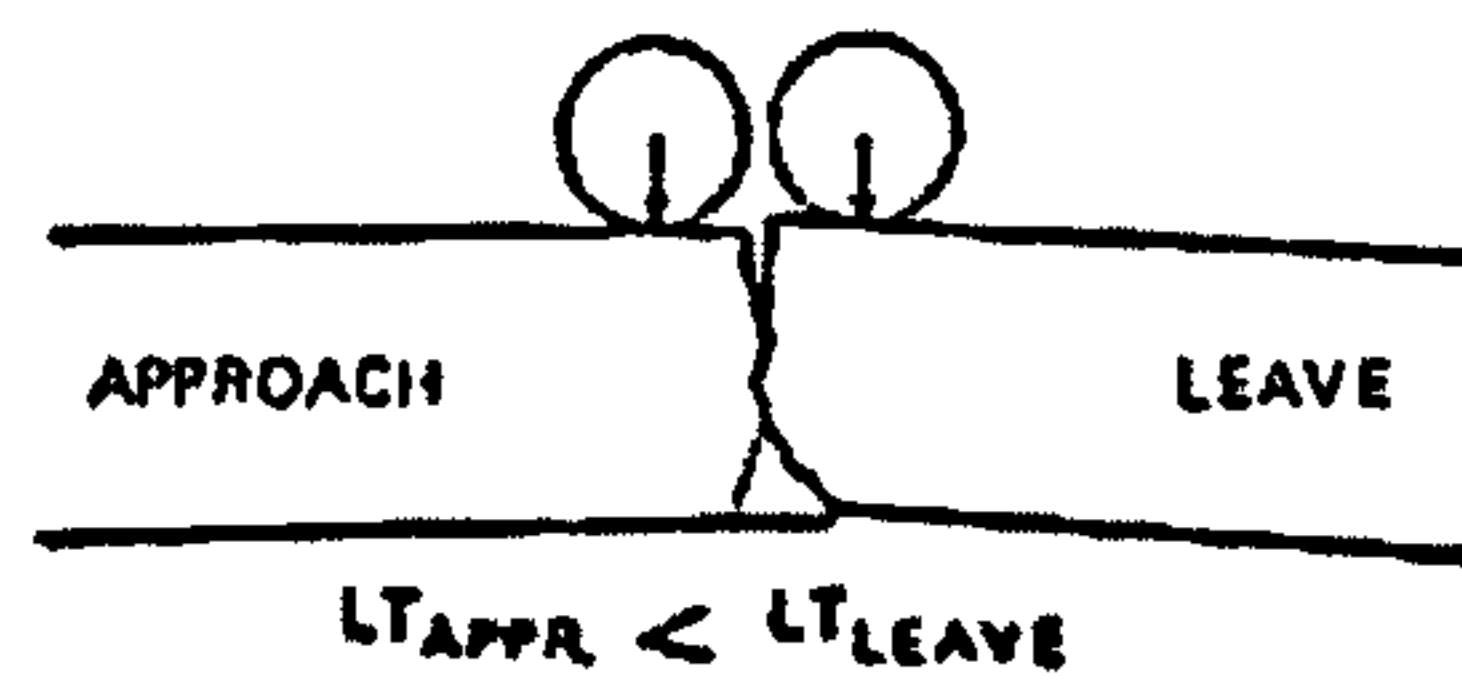


Figure 3.1 – Effect of crack verticality

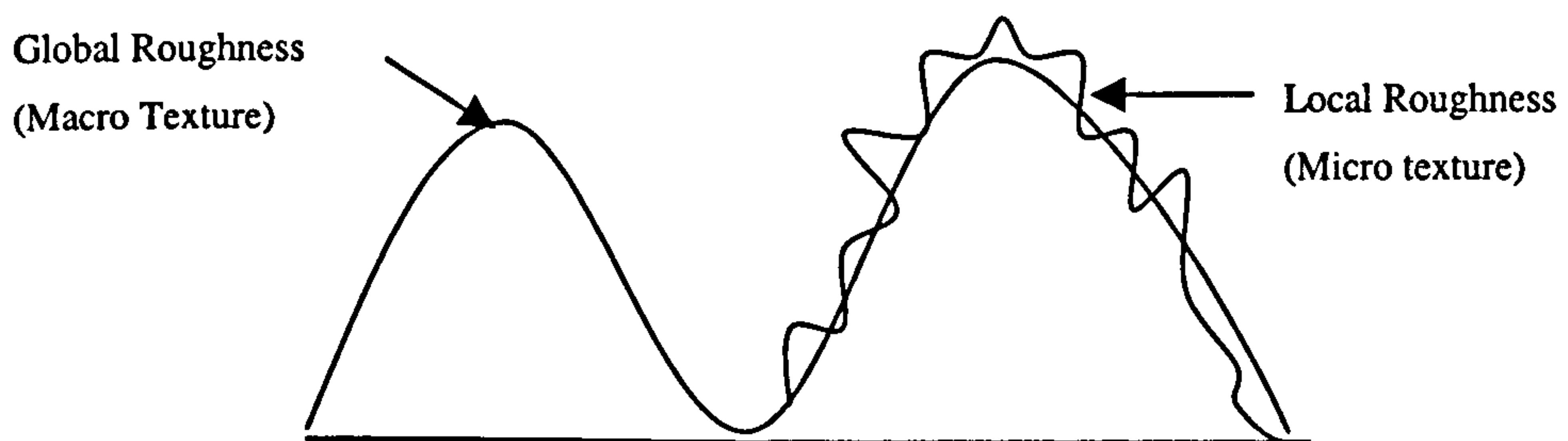


Figure 3.2 – Global (macro) and local (micro) roughness

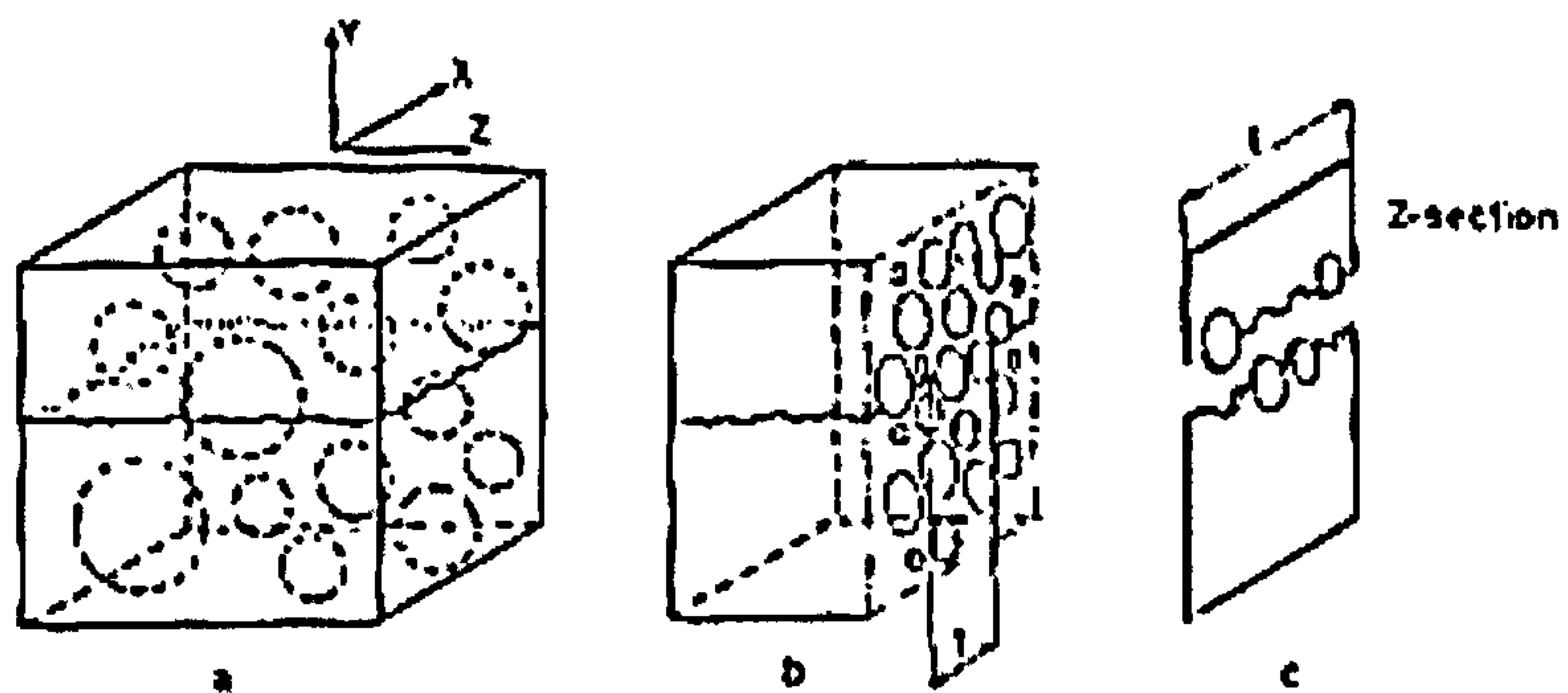


Figure 3.3 – Aggregate interlock model (Walraven 1981)

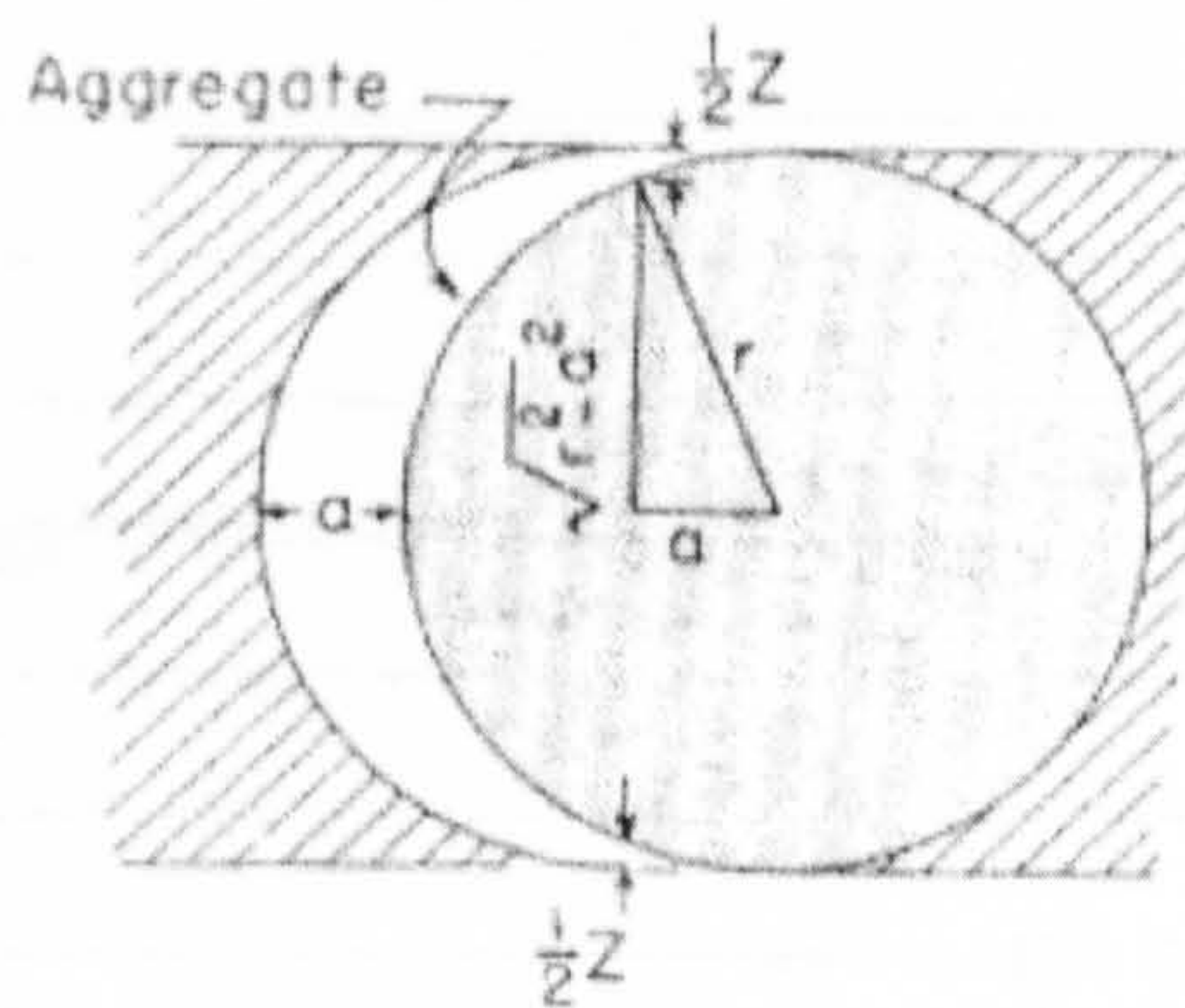


Figure 3.4 – Effect of crack opening on aggregate contact (Walraven 1981)

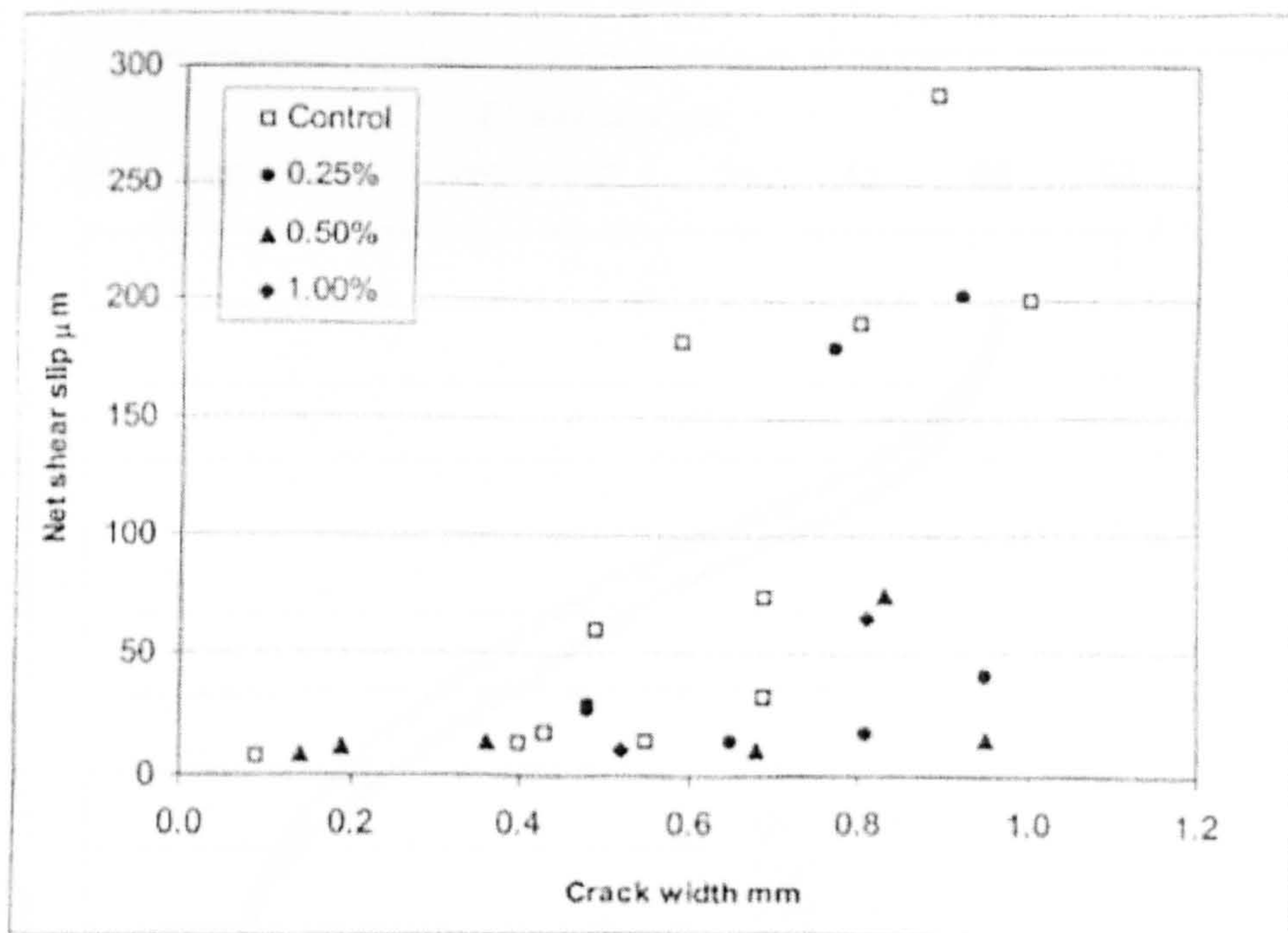


Figure 3.5 – Effect of crack width on net shear slip (Thompson 2001)

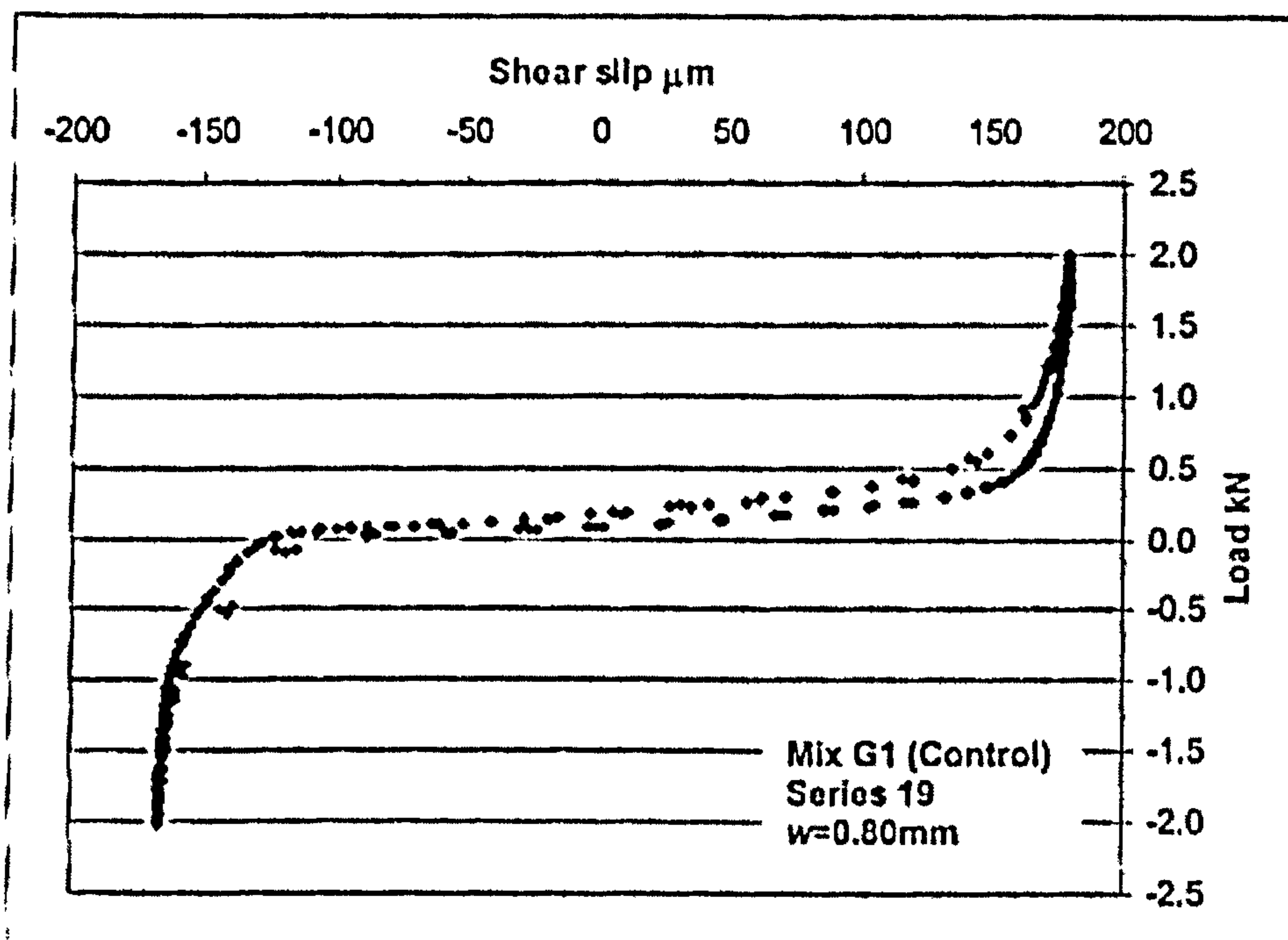


Figure 3.6 – Load/shear slip plot for non-reinforced specimen (Thompson 2001)

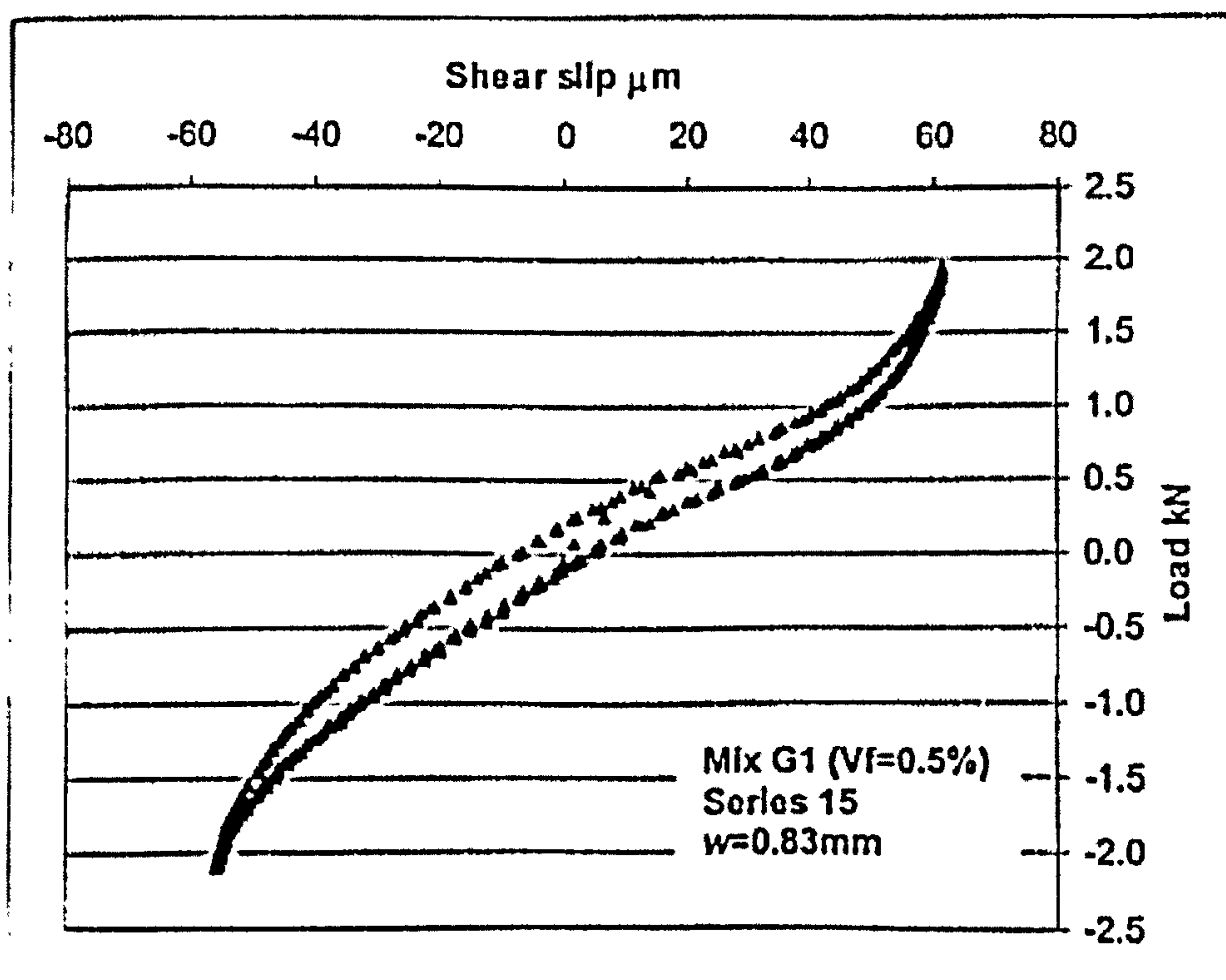


Figure 3.7 – Load/shear slip plot for fibre reinforced specimen (Thompson 2001)

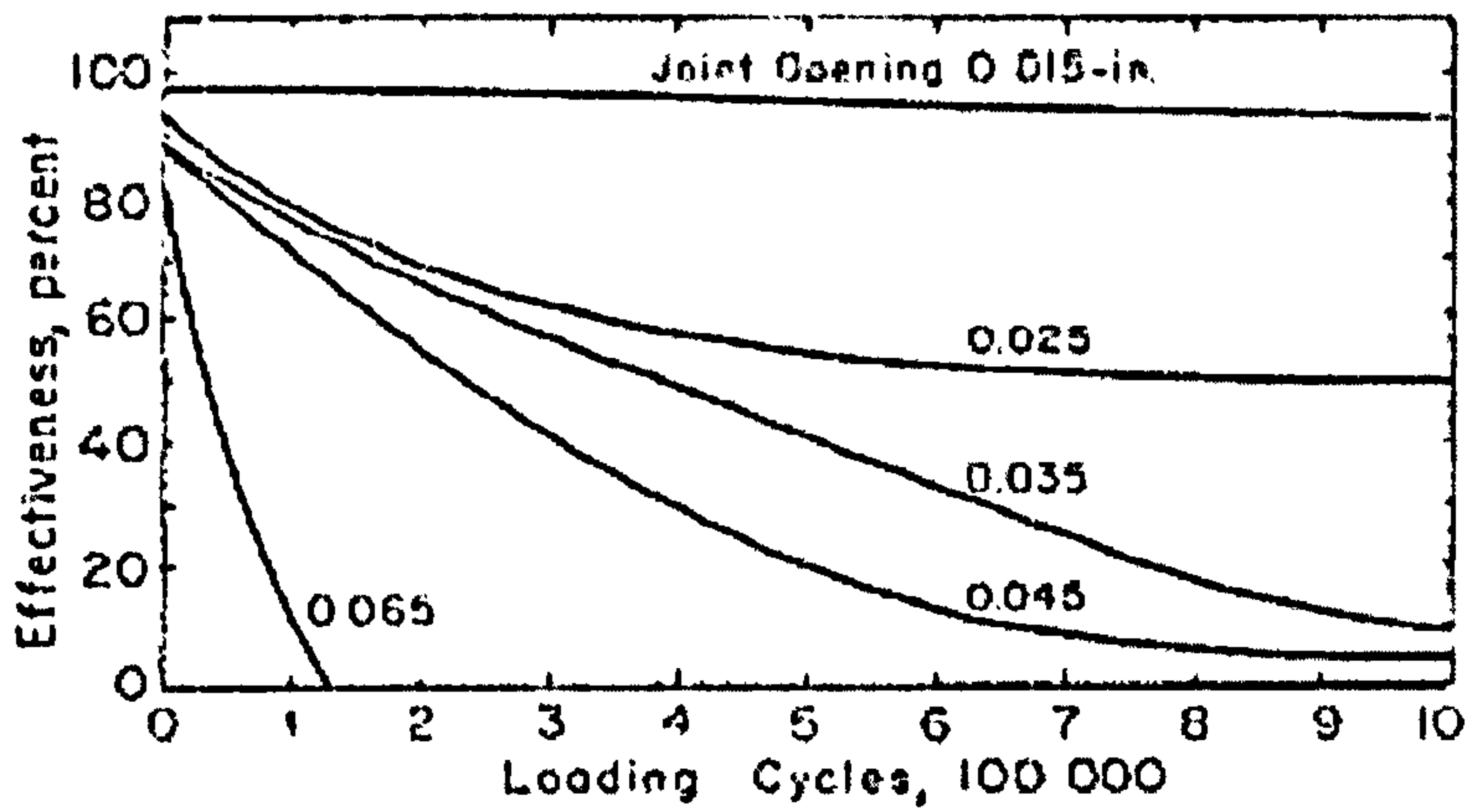


Figure 3.8 – Joint deterioration of a 175mm slab (Colley and Humprey 1967)

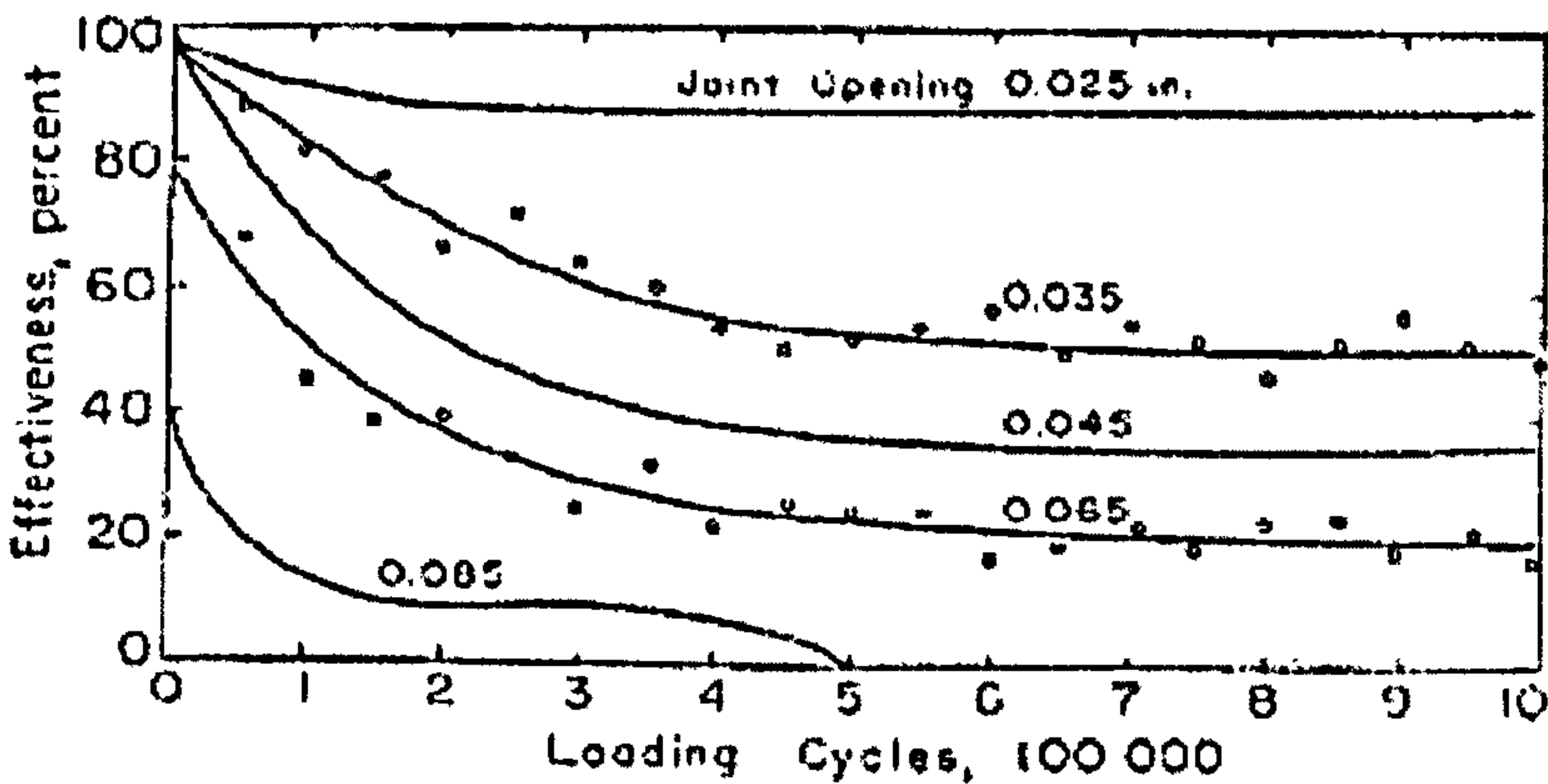


Figure 3.9 – Joint deterioration of a 225mm slab (Colley and Humprey 1967)

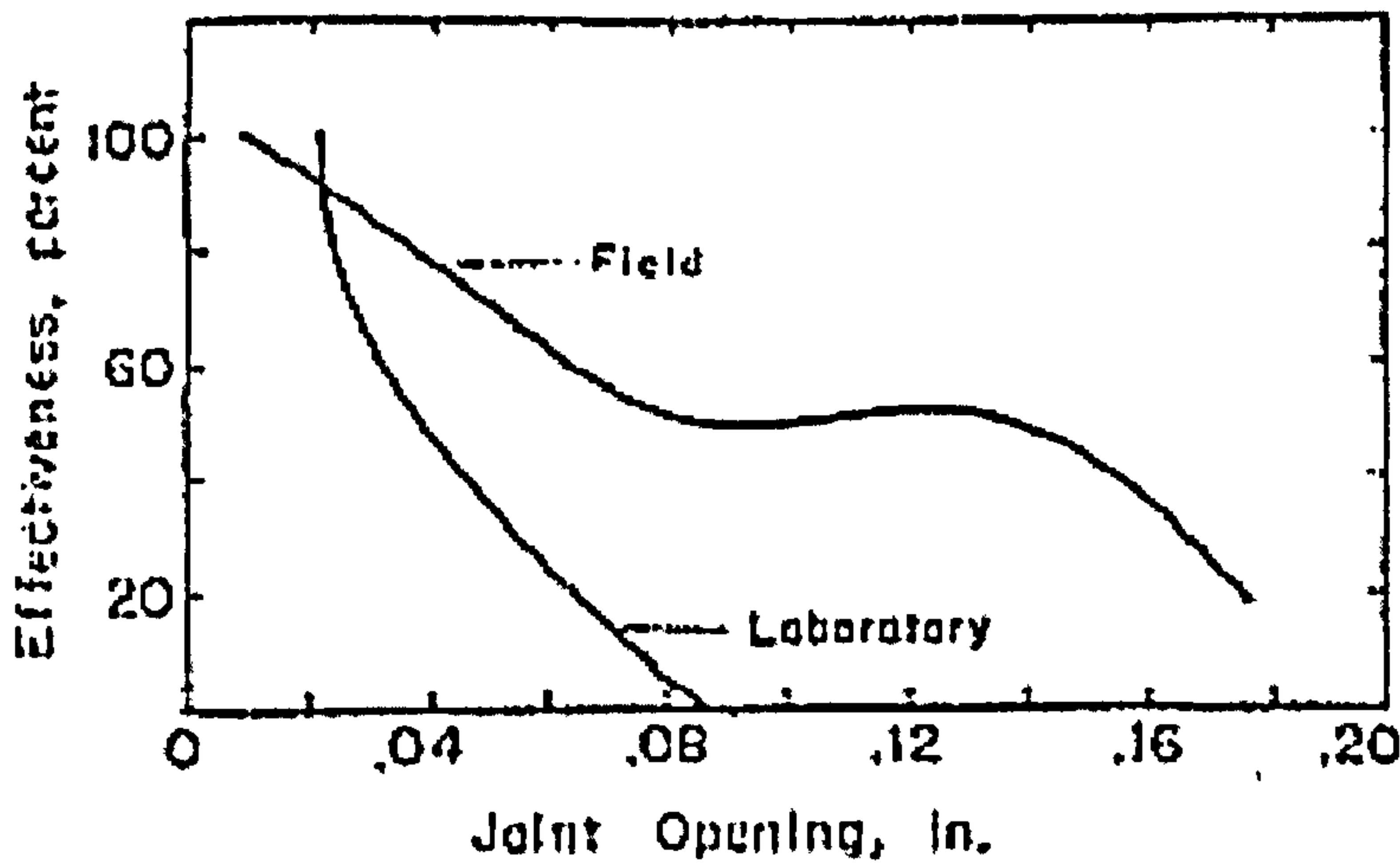


Figure 3.10 – load transfer values from laboratory and field testing (Colley and Humprey 1967)

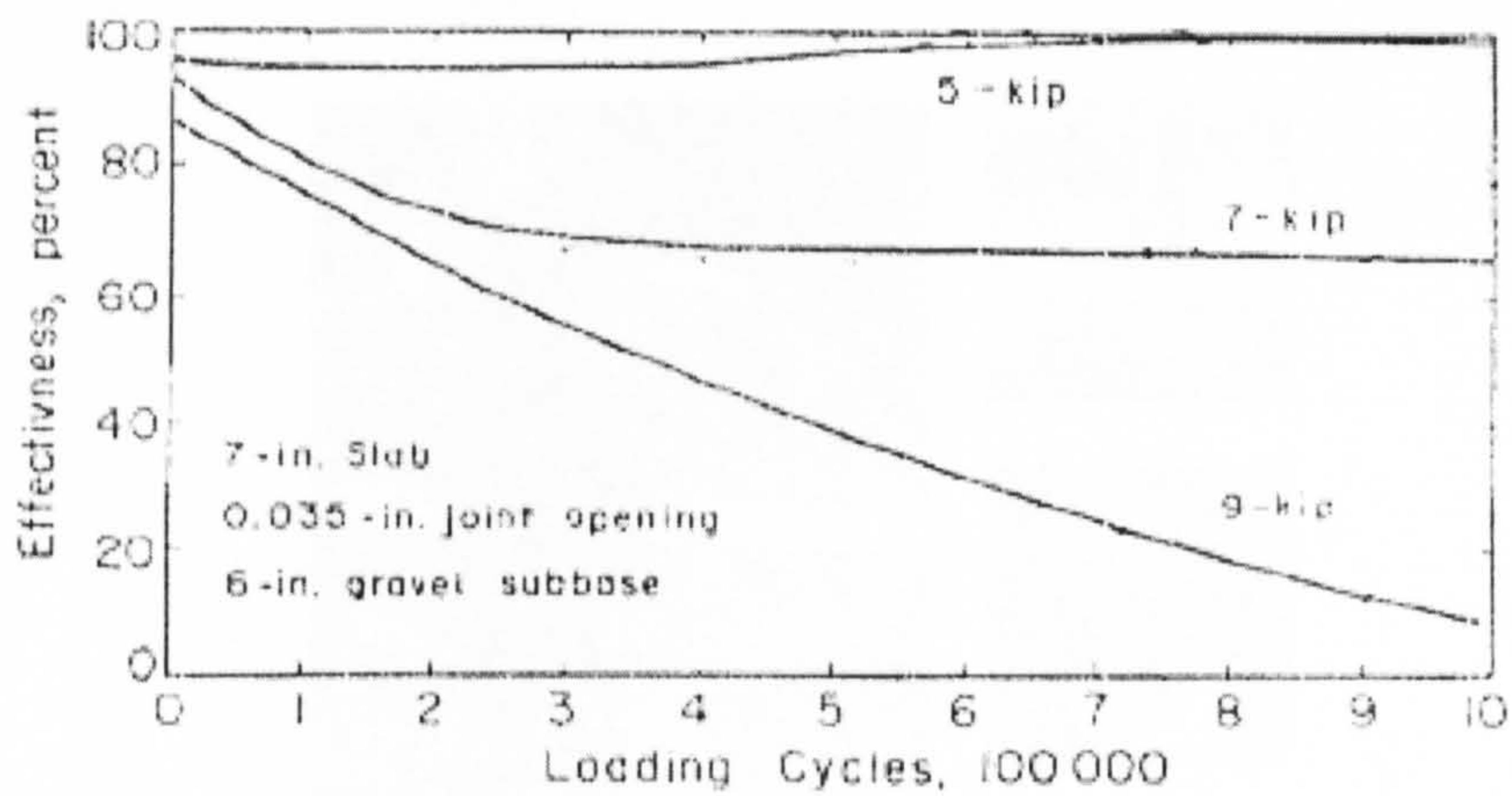


Figure 3.11 – Effect of load on joint deterioration (Colley and Humprey 1967)

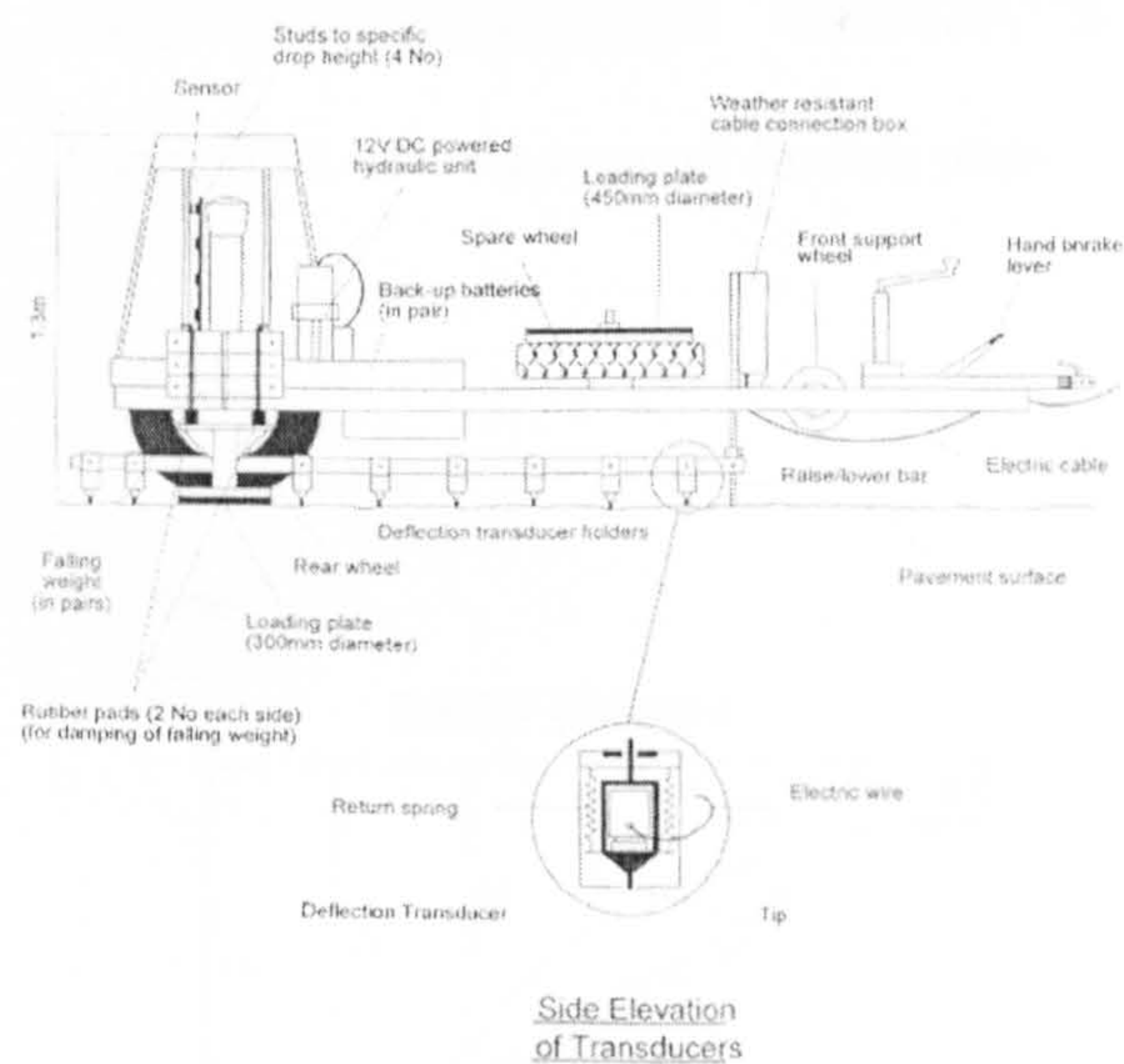


Figure 3.12 – FWD (Top - graphical representation, Bottom - Plate)

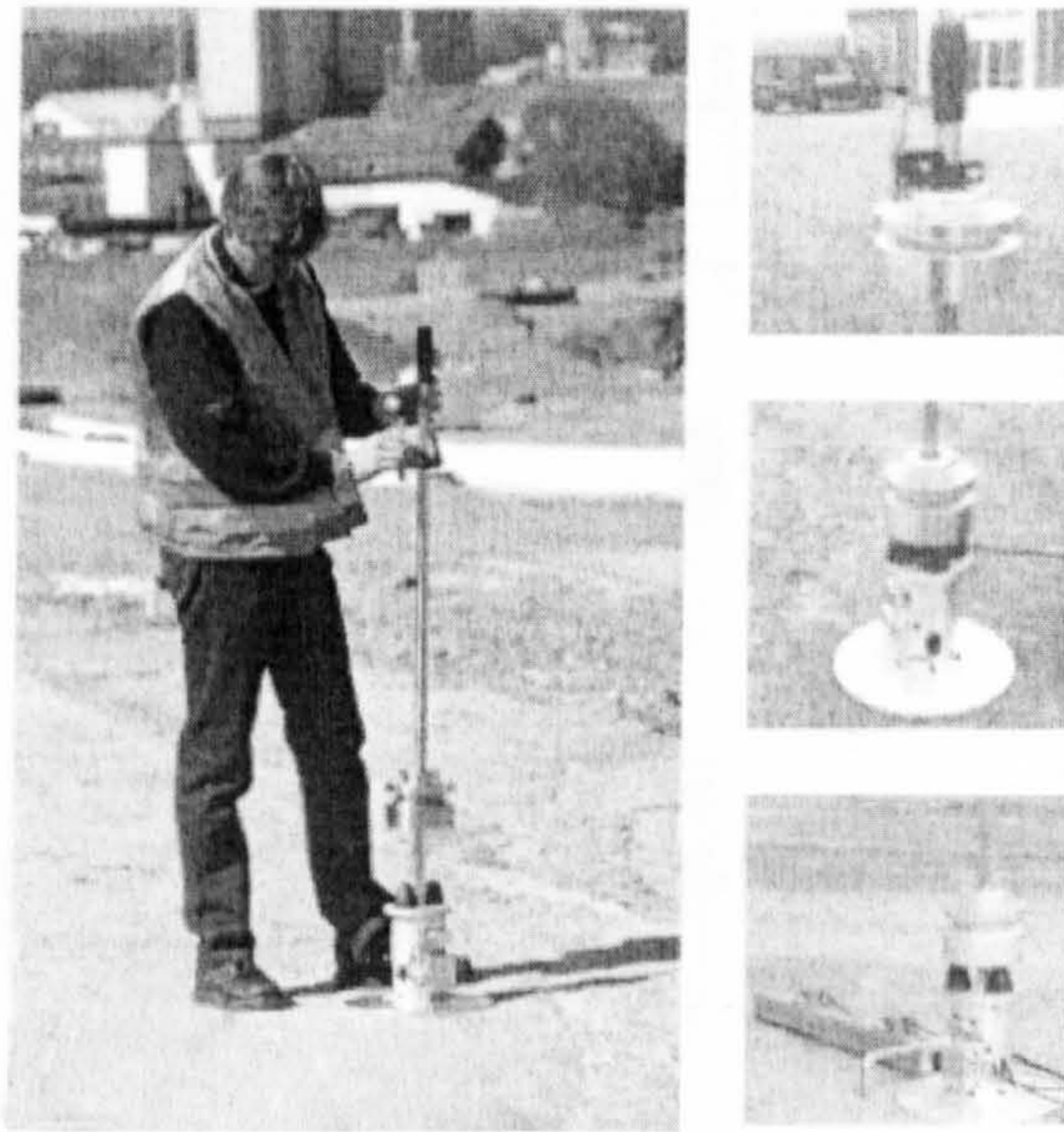


Figure 3.13 – Prima dynamic loading plate

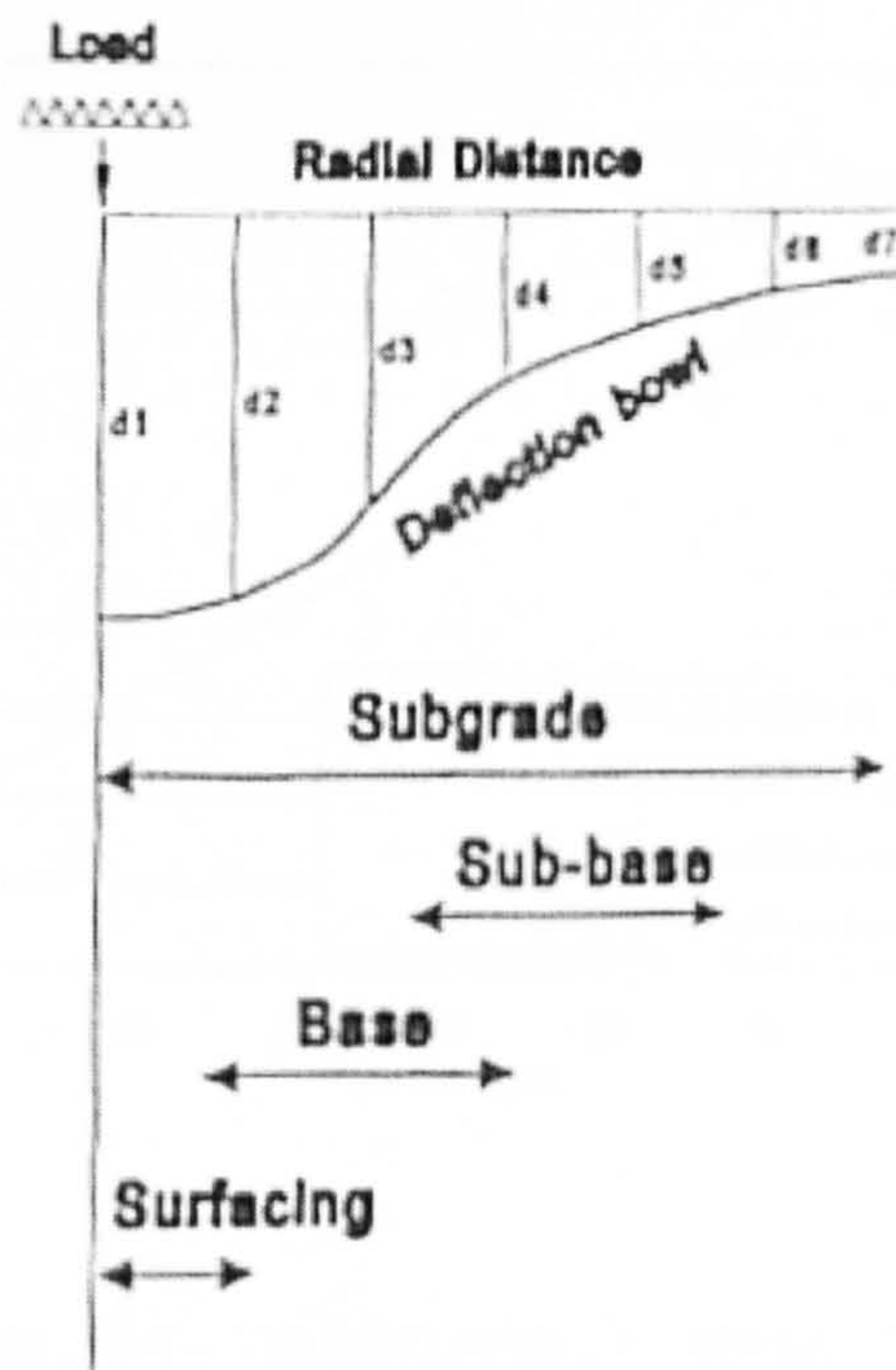


Figure 3.14 – FWD deflection basin analysis

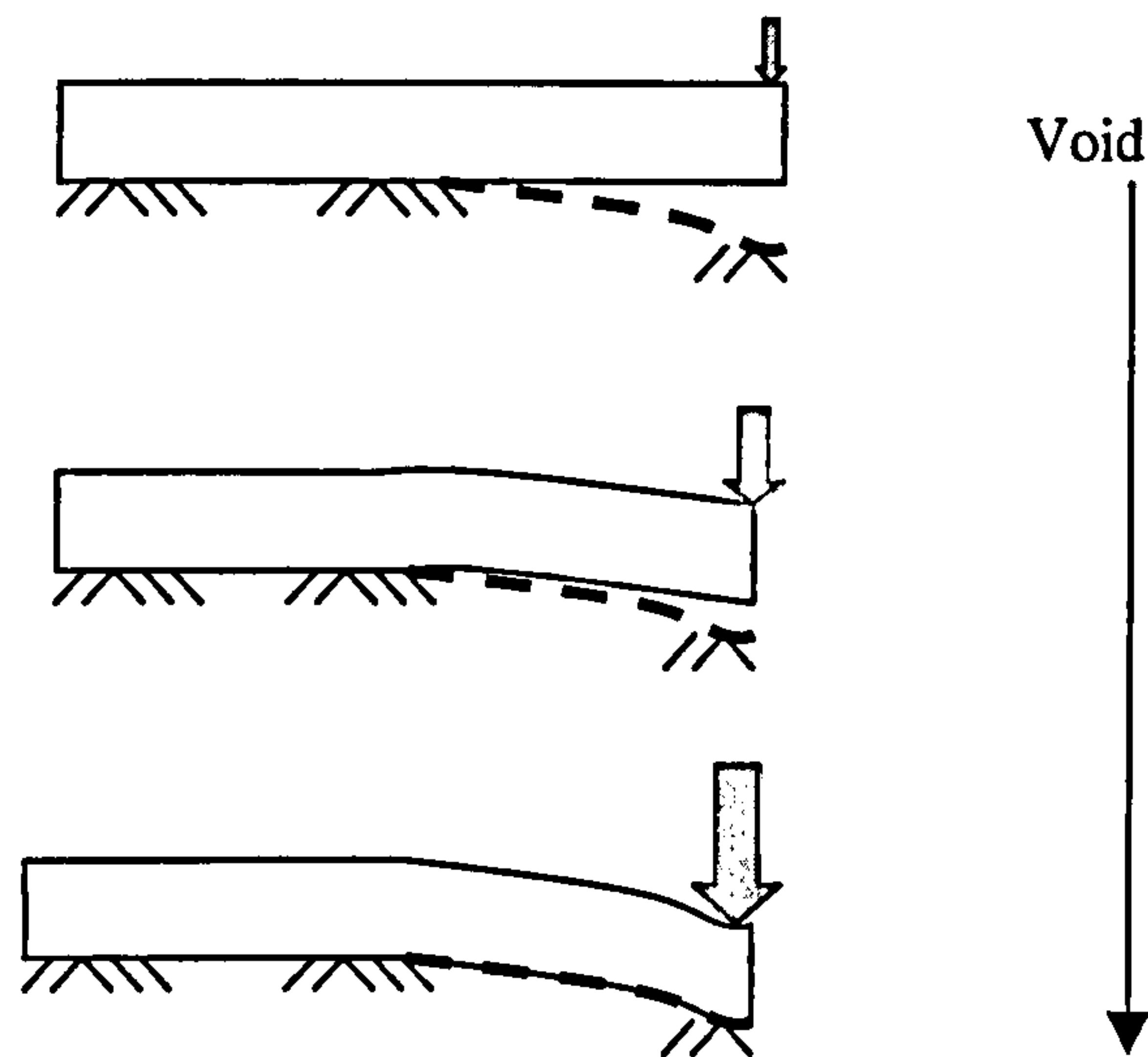


Figure 3.15 – Void closure under load

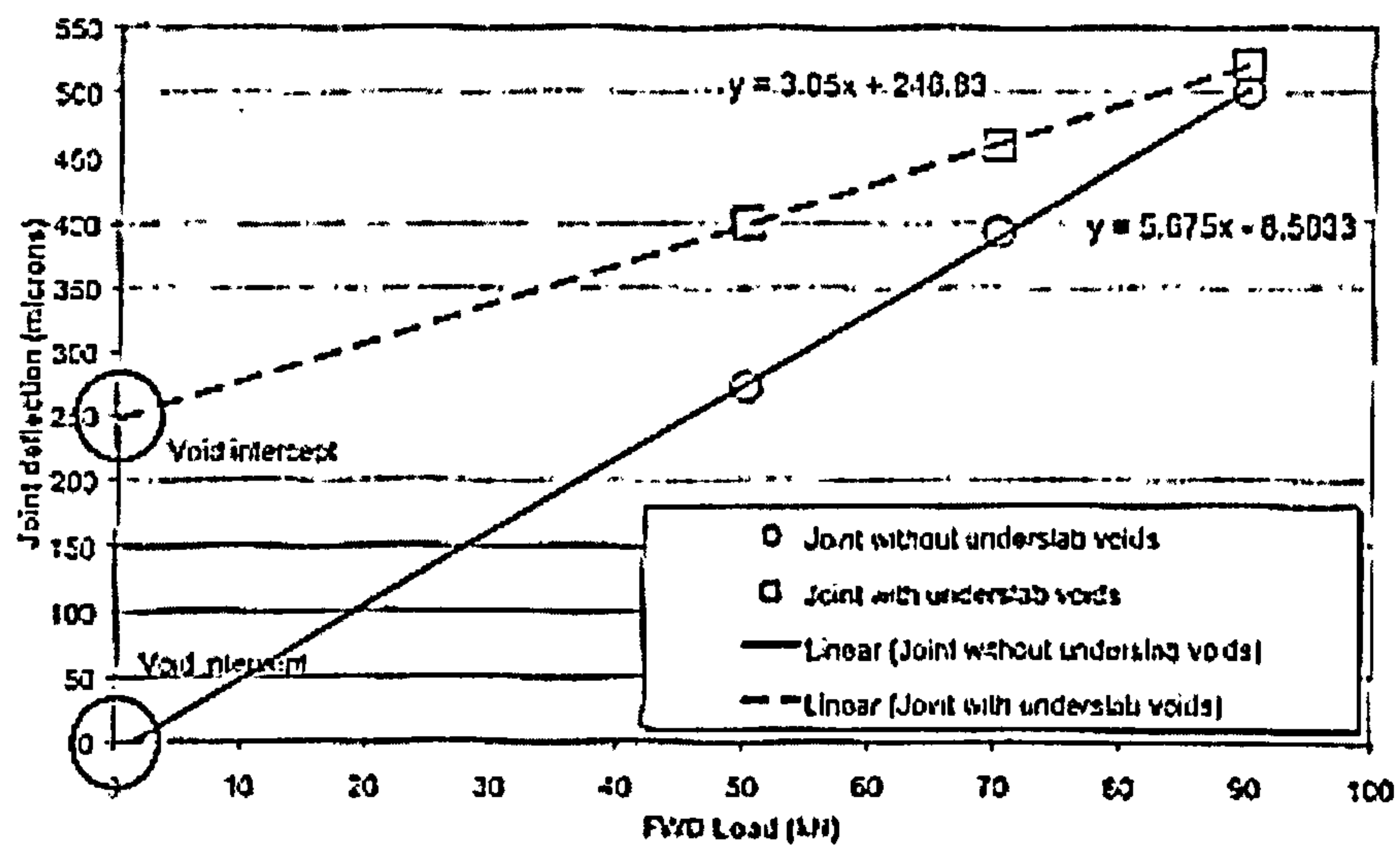


Figure 3.16 – Void Intercepts (Cudworth 2003)

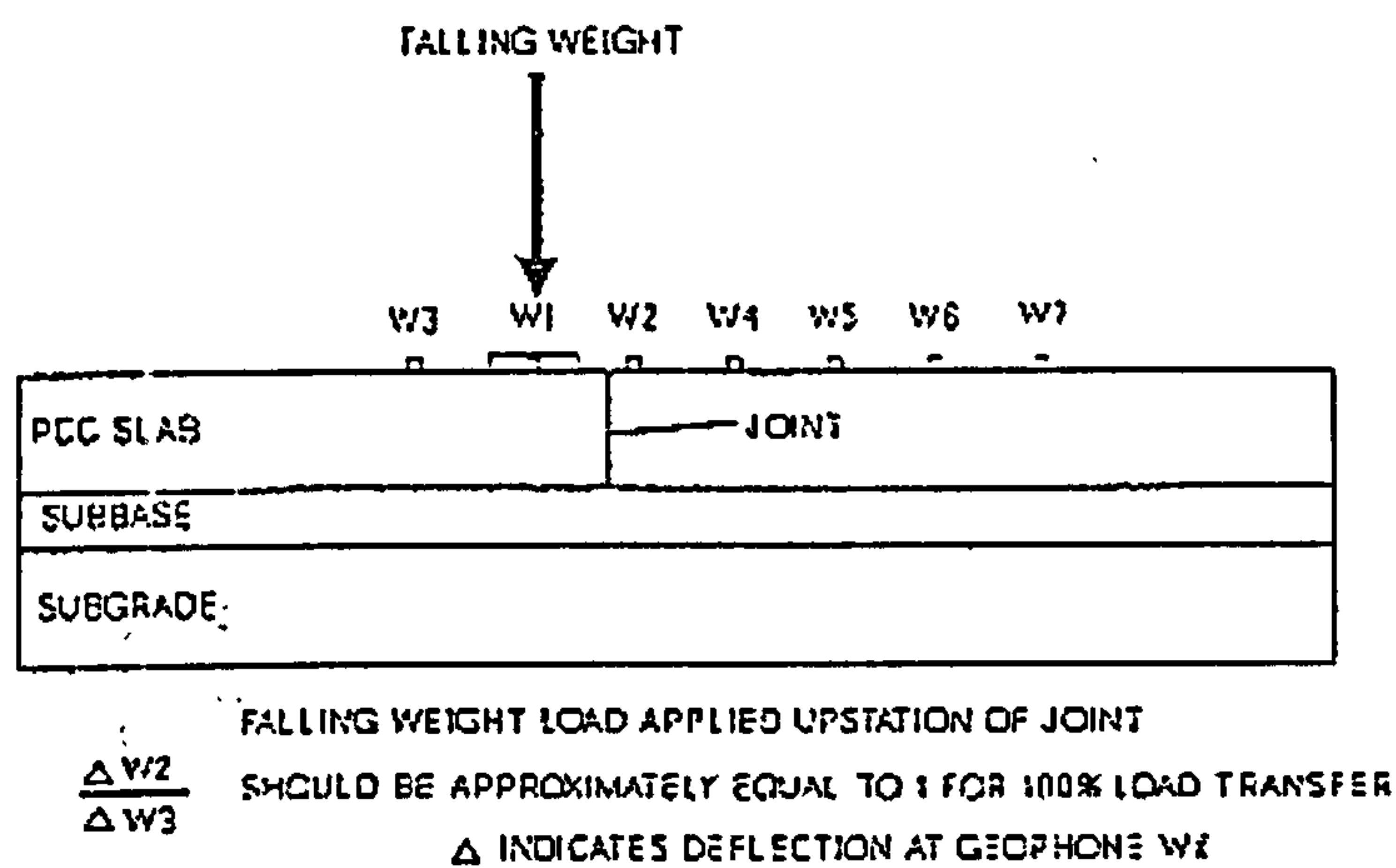


Figure 3.17 – Geophone locations (Ricci *et al.* 1985)

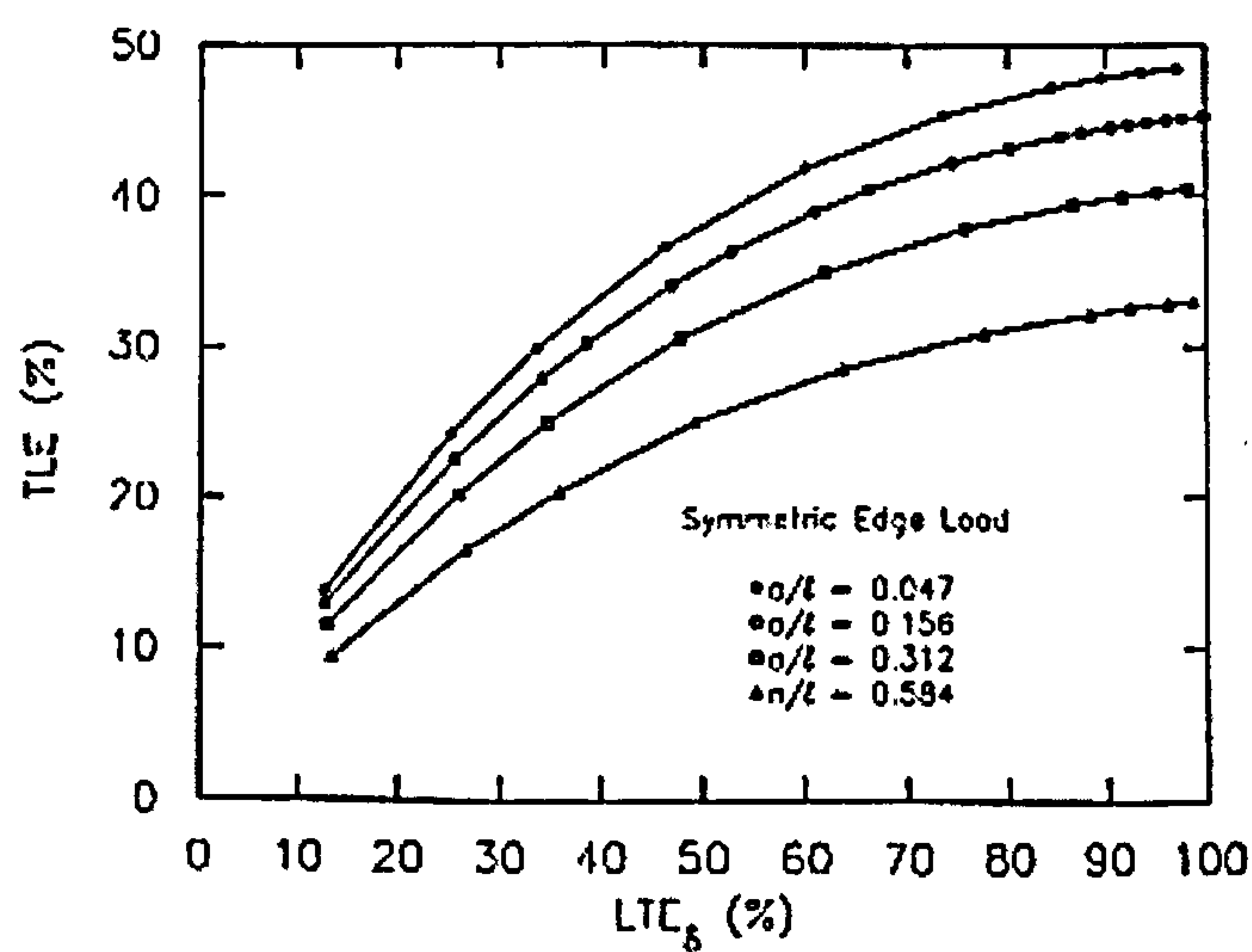


Figure 3.18 – LT versus TLE (Ioannides and Korovesis 1990)

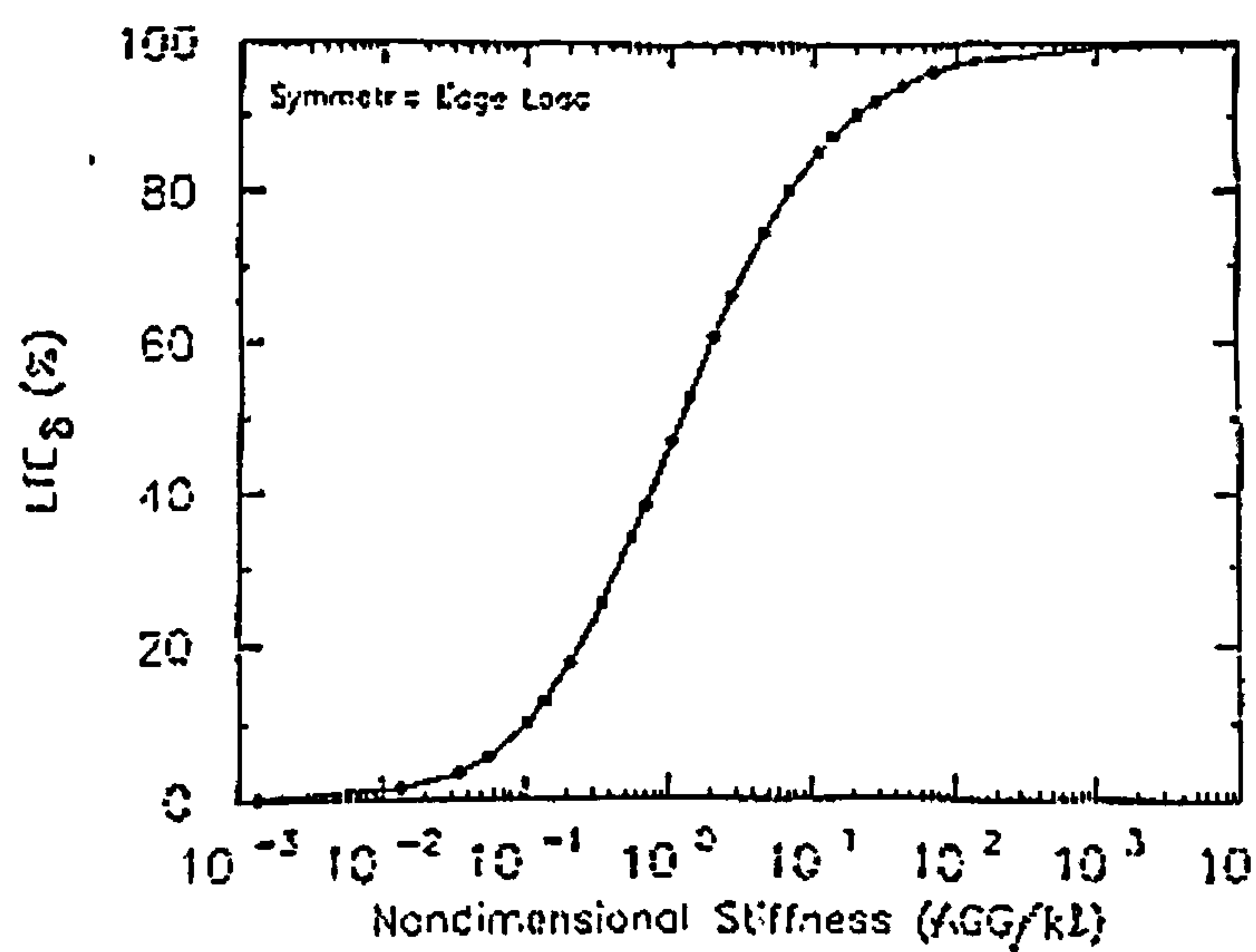


Figure 319 – LT Vs AGG (Ioannides and Korovesis 1990)

4. SLAB CONDITION

4.1 Introduction

Field testing was undertaken at four in service sites throughout the research period, these being at Daventry, Lutterworth, Ballymena and Skelmersdale. All except Daventry were examined once Engineers had been called in to assess and repair serviceability problems. Due to constraints on equipment availability and site accessibility it was not always possible to complete FWD and Prima testing on every visit. This was most prominent at Ballymena and Skelmersdale where difficulties were found in gaining access to the FWD. As it was important to gather as much information as possible, these sites were tested thoroughly using only the Prima Dynamic Plate. Coring was undertaken at Lutterworth by an external company under guidance from a consulting Engineer. The placement of the cores was dependant on the requirements of the slab assessment being carried out due to serviceability problems, although on a few occasions specific areas were selected to incorporate the research objectives. Information from three other sites, namely Leeds, Marston and Northampton was also used for determining crack geometry, although direct access was never undertaken. The data was obtained via work conducted by Bishop (2001), in which regular visits were made to record strain measurements from gauges embedded across joints. The collection of data was categorised into three main areas comprising crack measurement; surface profile measurement; and deflection testing.

Crack measurement enabled typical geometries to be ascertained, which were then used in the assessment of the deflection test results, and the development of crack profiles for use within the laboratory test program. Comparison could also be made against the test methodologies and analysis techniques used by other authors. The process required the determination of changing width with depth, rather than just a single surface measurement.

Slab surface profiles provided an indication of edge curling caused by differential shrinkage. Although the method could not be used alone to determine voiding under the slab, it was useful as a prediction tool. The surface crack measurement was also incorporated with the curled profile to enable calculation of crack geometry using simple trigonometry.

Deflection testing using either the FWD or the Prima dynamic plate enabled slab condition to be assessed. This was accomplished using a variety of analysis methods, previously described fully in section 3.6.2, and included: load transfer, load step, cantilever deflection, void intercepts and, for the FWD only, deflection bowls. The methods of calculation and the equipment set-up used for determining each parameter are discussed in sections 4.4 and 4.5. The relationships between deflection responses enabled the influence of critical factors such as crack width and voiding to be determined. These results were also used in the verification of the finite element model.

A matrix showing which information was collected from each site is shown in Table 4.1, where the black areas signify areas of data collection.

Table 4.1 – Site Testing Matrix

	Daventry	Lutterworth	Ballymena	Skelmersdale	Leeds	Marston	Northampton
Crack Measurement							
Surface Measurements							
Coring							
Strain Gauges							
Surface Profile							
Precise Level							
Builders Level							
Profilometer							
Deflection Testing							
FWD (Single Load)							
FWD (Variable Load)							
Prima							

4.2 Crack Measurement

Where applicable, full crack geometries were obtained through the Bishop (2001) results from embedded strain gauges installed at Leeds, Marston and Northampton, and from coring at Lutterworth. Unfortunately, as an external party had ordered the cores as part of a structural survey the locations were unable to be determined by the project’s objectives. Fortunately, some of these were taken through sawn joints and cracks, and several were bored through a wire guidance system which was behaving as a crack inducer. At

Daventry, Lutterworth and Ballymena surface crack measurements were taken, allowing comparison with slab deflection response.

4.2.1 Surface Measurements

Accurate measurement of surface crack widths is known to be difficult (Ibrahim and Luxmoore 1987). Ideally, some form of measurement marker is inserted across a joint or crack prior to movement occurring. In this manner an accurate value can be ascertained, with its development monitored over a period of time. Unfortunately many of the structures examined herein were already in use and therefore required the utilisation of other methods. This resulted in a greater risk of inaccuracy and therefore care was taken to ensure the most appropriate technique was selected for each location at every site.

Surface measurements of crack width can be prone to slight discrepancy due to the nature of development and edge deterioration. Some of the cracks found on site were many metres in length and consisted of a varying surface width. Occasionally these had divided into two within close proximity, creating difficulties in calculating an overall value. In circumstances where the crack had been open for some time, degradation and spalling of the sides had occurred leading to what appeared to be a much wider surface crack. Careful inspection of the overall area was therefore imperative to ensure a representative sample was recorded. This was ideally a section which had a similar width for a distance of approximately 1m, and showed little surface edge damage.

When evaluating the crack width within a filled sawn joint, accurate measurement was problematic. The saw-cut had a depth of around 1/4 of the slab thickness (approximately 50mm), which made identification and insertion of a measurement device almost impossible. To overcome this the overall joint size was measured and a reduction made for the saw cut alone, the width of which was obtained from cores and slab sections containing zero cracking (Figure 4.1).

The crack or joint width measurement was taken using a variety of instruments dependant on its ease of visibility. When clear at the surface an optical microscope was used as it was the most precise method (Figure 4.2). This contained a measuring gauge in the eyepiece, with a resolution of 0.02mm enabling a precision of +/- 0.01mm to be recorded. When the crack was too large for the microscope (such as in the case of a sawn joint), a set of callipers were inserted approximately 10mm below the slab surface (Figure 4.3). Inserting the device to this depth prevented spalling close to the joint surface being

included in the calculation, and enabled variations in measurement of 0.1mm to be detected with a precision of 0.05mm.

Two other devices occasionally used for quick and easy estimation of crack width measurement were a standard 30cm ruler and a crack comparator. Although not as accurate as the previous methods due to operator interpretation, these could be used in situations too difficult for the other devices due to spalled edges and/or rigid fillers. The crack comparator uses visual comparisons against line thickness up to 4mm to produce an estimation of crack width with a precision of 0.1mm (Figure 4.4). The ruler was used to record much larger widths, although it can only measure accurately to within 0.5mm.

4.2.2 Embedded Strain Gauges

Work conducted by Bishop (2001) required the installation of strain gauges at various locations throughout slabs at Leeds, Marston and Northampton, some of which were placed across sawn and construction joints at different depths. Measurements of movement due to environmental and climatic effects were then taken throughout the early ages of slab life to develop an understanding of the thermal and hygral effects.

Examination of the records enabled strain to be calculated at joints over a set period of time. According to Bishop (2001) all strain can then be translated directly into crack width to determine the size of the opening. In some instances two strain gauges had been inserted at the same position, but at different depths within the slab, enabling extrapolation of surface and base values if a linear variation is used (Figure 4.5). This approach was verified using 3-gauge monitoring, where the insertion of demec pips onto the surface of the slab directly above strain gauges enabled a more complete geometry to be produced (section 6.12).

Full information on the type of strain gauges used, the methodology of placement and accuracy can be found in Bishop (2001).

4.2.3 Coring

At Lutterworth, coring enabled crack geometry to be investigated throughout slab depth; this was undertaken by a specialist company. Once removed the cores were taken to a laboratory where Construction Materials Testing in Derby determined the concrete properties and constituent materials. Possession was then temporarily given to Loughborough University where the crack geometry was examined in detail, involving

the measurement of variation in width with depth, and the distance of the crack edge to an arbitrary vertical datum. This was undertaken with the use of a standard 30cm ruler, crack comparator, callipers and a crack microscope, as described in section 4.2. Measurements were taken at 20mm intervals of depth on opposing sides of the core to enable any variance to be established.

When measuring the crack it was important to ensure stress relaxation of the core had not occurred. This could have altered the width depending on the internal forces acting within the slab. To account for these movements the dimensions of several cores containing no discontinuity were taken to provide a comparable standard. Dimensions were then checked at the top and bottom of each cracked specimen, and any deviancies from the standard identified. Simple calculations could then take place to amend the crack widths recorded, producing a corrected value, as shown in equation 4.1. The accuracy of the method was dependant on the device used to measure the crack and the core diameter.

$$\text{Actual } w = \text{Core } w + (\text{Uncracked core } \phi - \text{Cracked core } \phi) \quad \text{equation 4.1}$$

Where:

w = Crack width

ϕ = Diameter

4.3 Curling/Warping

4.3.1 Introduction

Identification of the slab edge profiles enabled the degree of curl to be established using simple geometric calculations. This could be then be used alongside the crack surface measurements to determine the overall joint geometry (equation 4.2). The results from the embedded strain gauges and coring had ascertained that crack opening was approximately linear (section 6.1). Occasionally a greater degree of movement was found at the surface which would lead to the estimation of larger base measurements when using surface profiles. As this effect was only found in a few situations, the method was deemed acceptable for producing representative orientations with a lower bound crack angle.

$$w_b = w_s - [(V/H) \times 2h] \quad \text{equation 4.2}$$

Where:

w_b = Base crack width

w_s = Surface crack width

V = Difference in slab surface level

H = Horizontal distance between levelling points

h = Slab depth

Differential shrinkage may not necessarily lead to curl in the slab edge, although it may cause cracking. Movement is prevented by the self-weight of the slab forcing it down onto the subbase, resulting in the formation of a crack, but no proportional curl. Measurements of the surface profile may therefore lead to an underestimate in the crack angle, and wider crack base estimations (Figure 4.6). This will provide a lower bound for base measurement prediction, similar to that described above.

4.3.2 Precise Levelling

The use of a precise level enabled accurate surface profiles to be determined at various locations within the Daventry site. Firstly a grid of reference points was set out, with the intensity increasing with proximity to the joint. Vertical elevations were then recorded at each grid-point producing a numerical 3-dimensional plot of the surface. The Golden software SurferTM graphing package was then used to interpret the data and translate the numerical values into contour and three-dimensional views.

Unfortunately, the levelling process was found to be extremely labour intensive, with the setting out and data collection requiring a great deal of time. With most of the warehouses examined containing over 100 joint or crack positions, and only limited access time, this method was too inefficient and was therefore used solely at Daventry.

4.3.3 Builder's Level

The use of a builder's level was an effective method of obtaining curling estimations at Ballymena. In most situations the slab curled upwards at its edges due to the shrinkage differential. Placement of a builder's level at the joint enabled a vertical measure between the bottom of the level and the surface of the slab (Figure 4.7). This provided information on the magnitude and rate of curling at either side of the joint, with an increased number of measurement points along the level generating a more detailed profile.

The builder's level method contained some limitations as its short length restricted the amount of data obtained. The accuracy was also open to error as it was difficult to gauge

the distance between the underside of the level and the surface of the floor slab. A graduated wedge provided some improvement, but still only enabled measurements to the nearest 0.5mm to be obtained.

4.3.4 Profilometer

The profilometer was a useful way of identifying curl in the edge of the slabs at Ballymena. This device consists of a backboard (which was set level) and a number of needles, which when pressed against the surface provided an exact copy of the floor profile (Figure 4.8). A graduated scale set against the top of the pins enabled comparisons between sections, and therefore any variations were easily determined. This gave similar results to the builder's level except that the increased amount of pins, and the easily read scale, allowed an accuracy of 0.2mm to be achieved.

This was found to be a slightly quicker method of measurement and interpretation than both the precise level and the builder's level, although it was restricted to a single line of measurement with finite length.

4.4 Deflection Measurement

Deflection testing was undertaken using both the FWD and the Prima portable dynamic plate. Both devices utilised identical geophone placement and load plate size to reduce any error caused by set-up variations. As the FWD and Prima were borrowed from external organisations, calibration of the devices was undertaken by the individual owners to ensure the specifications stated in section 3.6.1 were met.

In all cases a 300mm diameter load plate was used for both the FWD and Prima, as recommended by the Highways Agency (1999). They also suggest using a 75kN FWD load on concrete pavements where the deflection may be below 100microns; however, White Young Green (2002) advised using the standard 50kN load instead as this more closely represents that of a forklift. Unfortunately, control of the FWD loading was limited by the requirements of the Engineers who were undertaking tests to examine slab condition. On all sites an initial settling drop was provided to seat the loading plate and check for any anomalies. The recording drops were then initiated, with three loads of the same 50kN magnitude used on the Daventry site, with values of 42, 58 and 85kN applied at Lutterworth to enable void intercepts to be obtained (see section 4.5.5).

For the Prima, each site was tested with the highest possible load to obtain the greatest amount of deflection. This provided a greater range of response and produced the most variation between points. To accomplish this, 20kg weights were applied, and the drop height was set to maximum. Davich (2000) recommends using the 100mm load plate when testing rigid materials to achieve the highest bearing stress; however, to enable direct deflection comparison with the FWD, a 300mm diameter load plate was selected. Using this method, a force of approximately 10kN was achieved on all sites.

The main requirement for testing was the determination of load transfer across joints and cracks. On sites using either the Prima or FWD the centre of the loading plate was positioned 250mm from the crack face. Geophones were then placed 50mm either side of the joint leaving a gap of 50mm to the edge of the plate (Figure 4.9). This was specified as work conducted by Poblete *et al.* (1988) concluded that load transfer effectiveness reduces as load is moved further from the slab edge. In addition, this set-up provided a real edge loading condition without the possibility of spalling affecting the results. The remainder of the FWD geophones were placed at increasing spacing along the slab surface, the exact locations varying between the Daventry and Lutterworth sites (Figure 4.10). The geophone positions provided different information with respect to deflection bowls. A profile was recorded for the loaded slab (slab with load applied) at the Daventry site, whereas for Lutterworth, the unloaded slab deflection (slab opposing load application) was produced.

The majority of joints were tested in a single direction only due to the difficulty in manoeuvring the equipment within each aisle. The load transfer variation in approach (upstream) and leave (downstream) slabs described in section 2.4.4 was prevented by the equal forward and reverse movements of the MHE. Furthermore, the change in verticality of the crack was shown to be below 25mm in the cores taken at Lutterworth (section 6.1.1) and was therefore assumed to have little effect on results. The lack of data in the literature assessing the problems associated with crack verticality compounded this conclusion. The small number of joints that were tested in both directions demonstrated good agreement as shown in Figure 4.11, where the maximum variation in load transfer was below 10%.

Slight variations in load are expected between test locations caused by the method of impact and slab response. To enable comparison between points it was necessary to normalise the data to a load magnitude applicable for all points tested under the same conditions. At the Daventry site, a 50kN FWD load was used, with that at Lutterworth

using 42, 58 and 84kN to assist in void detection. For all sites a 10kN load was selected for the Prima dynamic plate, which was close to the device limit. Normalisation consists of a proportional increase or decrease in deflection dependant on the actual magnitude of load, and assumes a linear load deflection response. Although this was not truly representative of all situations, the small variations involved had little effect on the results. The method of calculation is shown in equation 4.3.

$$ND = (AD/AL) \times NL \quad \text{equation 4.3}$$

Where:

ND = Normalised deflection

AD = Actual deflection

AL = Actual load

NL = Normalised load

The nature of the testing procedure using both the FWD and the Prima dynamic plate enabled repeatability to be checked on many joints. Initially, specific points on the Daventry site were to be retested during the second visit to check for any anomalies when using the same equipment. However, continuing fatigue and changes in temperatures are known to cause variation in results, as shown by Benkelman (1933), and therefore this could not be used as an accurate measure. The past effectiveness of the FWD equipment, the three load drop testing procedure and the additional testing of the Prima dynamic plate were therefore deemed to provide a satisfactory check.

4.5 Slab Analysis

On each site the dynamic deflection measurements were determined using either the FWD or the Prima dynamic plate. Unfortunately, it was not possible to use both pieces of equipment on every site due to availability and logistics of access to smaller aisled warehouses. The FWD is the standard method of deflection testing, with the Prima used on all sites, and therefore comparisons between the two devices were required to enable correlation, and ensure the results found across different sites could be cross referenced. As the equipment takes only one measurement at a particular point in time, the results obtained were only snapshots of the current behaviour of the slab. The level of deterioration caused within the crack from cyclic loading could not be determined; however, knowledge of slab age and the results from the laboratory testing (Chapter 6.4) enabled good estimations of joint or crack condition to be established.

4.5.1 Load Transfer

Load transfer is the relationship of deflections either side of a crack or joint caused by a dynamic load (section 3.1). To generate a value for load transfer, deflections from the dynamic force were measured on both the loaded and unloaded side of the crack. Authors have suggested different ways of calculating this, trying to place the emphasis on either the loaded or unloaded slab deflection (section 3.8.1). The simplest of these was suggested by Croveti and Darter (1985), it being a direct relationship between the two deflections expressed as a percentage (equation 3.4, and re-iterated below for clarity). Due to its effectiveness and unbiased approach, this method was used for the majority of site data analysis. Where alternative formulae were used to enable comparisons with other author's work, it has been stated explicitly within the figure or text.

$$LT = (du/dl) \times 100\%$$

Colley and Humphrey (1967) commented that load transfer is affected by the magnitude of load imparted onto the slab, particularly when curled at the edges. As the FWD has a load magnitude 4-5 times higher than that of the Prima, comparisons between the two pieces of machinery was thought necessary to examine the relationship. Numerical models of uncurled slabs were also used to examine the effect of load magnitude on transfer efficiency, with the results presented in section 7.6.

4.5.2 Load Step

Load step is the variation between the loaded (dl) and unloaded (du) deflections either side of a crack or joint (section 3.6.2), and is calculated using equation 4.4. As the step is a function of directly measured deflections, its value is highly sensitive to changes in load magnitude. With the FWD force being 4-5 times greater than that of the Prima, and increasing loads being used with the FWD to ascertain voiding, significant differences were expected. Comparison between load magnitudes were therefore required for each site to enable its effect to be ascertained, allowing the relevant data to be used when calculating any relationships.

The load step value obtained is that caused under dynamic load only. Any permanent step accumulated in the slab due to foundation compaction could not be detected by either piece of equipment. In this situation levelling or surface profile measurements were required to obtain the relevant data.

$$\text{Load step} = dl - du$$

equation 4.4

4.5.3 Edge Cantilever

As defined in section 3.6.2 cantilever deflection is used for the assessment of discontinuities (cracks), foundation influence, and determination of floor flatness requirements. For both the Prima and FWD, geophones were positioned 50mm from the loaded (*dl*) and unloaded (*du*) crack faces, with another placed 200mm back directly underneath the loading plate (*do*) (Figure 4.9). This enabled deflections of at least two points on the loaded slab to be recorded, providing an indication of the edge cantilever. Subtracting one of the geophone values from the other allowed the degree and direction of bending in the slab to be quantified (equation 4.5).

The magnitude of cantilever varies depending on the size of load used for testing. For this reason the values obtained using the FWD changed in respect to the force applied and were much greater than that obtained when using the Prima. These effects were taken into account when making assessments on slab behaviour, with results from the two devices examined separately.

$$\text{Edge Cantilever} = dl - do$$

equation 4.5

4.5.4 Deflection Basins

Deflection bowls can be used to examine slab curvature and the overall response to load (section 3.6.2). The position of the geophones differed between the two sites. At Daventry deflection basins were obtained for the loaded slab section; however, at Lutterworth the unloaded slab was monitored. In both situations at least one geophone was placed onto the opposing slab to enable load transfer calculations to take place. The remainder were then placed at increasing radial intervals from the source of the load to enable a full profile to be measured.

As described in section 3.6.2, when tests are placed at the centre of the slab, deflection bowls enable the back-calculation of layer properties. As those taken at Daventry and Lutterworth were taken at the slab edge this was not possible; however, a deflected shape caused by the imposed load was produced.

4.5.5 Void Intercepts

Void intercepts enabled the occurrence of a void and its size at the slab edge to be estimated. This was then used to evaluate the effects of slab voiding on joint and crack behaviour. Confirmation could also be made on the amount of voiding suspected at the Lutterworth site, providing explanations for possible variations in the site data collected.

The void intercept approach suggested by Croveti and Darter (1985) was used in the testing program as its effectiveness had been verified by other authors. A void intercept is the position at which the extrapolated best fit line of deflections under three increasing load magnitudes crosses the zero load axis (Figure 3.16). Values of 25-75 microns have been proposed as indicating a void, with some authors (Croveti and Darter 1985, Frabizzio and Buch 1999) suggesting the value of the intercept is in direct correlation to the size of the void. For this research the method has been deemed correct, enabling relationships between void size and slab response.

4.6 Site Information

Due to confidentiality the commercial names of the sites cannot be identified; however, information is provided on the operational requirements of the slabs and their construction methods. Where possible layouts of the floor have been provided so the location of testing can be identified.

4.6.1 Daventry

Measurements taken on the floor slab consisted of surface crack measurement, precise levelling, single load FWD deflection testing and Prima deflection testing. A plan of the South West corner of the site is provided in Figure 4.12.

This warehouse was used for the storage and distribution of an assortment of toys and packaging materials. The far West and East of the building were predominantly used for block stacking of items, with the central area containing goods on various racking devices. The South of the warehouse (running full length) was left relatively clear for the preparation of items ready for dispatch onto lorries. A mix of both dock levellers and ramps were used for loading, with pallet trucks and small-wheeled forklifts the main types of goods transporters used within the warehouse.

The floor was constructed in early 1999, with 160mm thick concrete containing 20kg/m³ of steel fibre. The sections of floor between construction joints were split into separate panels with the use of sawn induced joints, 60mm deep. These were approximately 6 by 7.5m in plan, but varied slightly to accommodate the geometry of the warehouse. Across construction joints 12 by 1500mm dowel bars were used to enhance load transfer.

The sawn joints had opened up to different sizes, some of which were less than 1mm wide, with others over 10mm (many of which were tested). Deterioration could be seen mainly on the joints that had opened up significantly, and this consisted of edge spalling and corner cracking. High deflections were observed by eye across some joints when goods transporters were passing over, indicating very poor load transfer. No mid-aisle cracking or structural damage was found throughout the site signifying a generally sound construction.

4.6.2 Lutterworth

Measurements taken on the floor slab consisted of surface crack measurement, coring, variable load FWD deflection testing and Prima deflection testing. A plan of the site is provided in Figure 4.13.

This warehouse contained racking which was a mixture of both very narrow and wider aisles interspersed. This took up the majority of the floor area and was tight against the North-West wall. Loading bays were positioned to the South, with a small storage facility to the East next to the office complex. Areas next to loading bays were generally free of goods, with those near to the offices used as storage areas for small stockpiles of material. A mezzanine floor was sited at the South East corner with minor low load works occurring on this level.

The concrete floor was 190mm thick with mesh reinforcement throughout the base of the slab. Dowelled construction joints were placed 18 to 22m apart with sawn joints inserted at distances of 5.5 to 8m. The VNA trucks were run on wire guidance systems set approximately 20mm deep into the slab and filled to level with a rigid resin

Various companies had undertaken surveys previous to the site visit and some remedial work had been actioned. This mainly consisted of crack filling with a resin and grinding to VNA vehicle tracks. Some sections of floor slab had been replaced completely, with approximately 500mm either side of a joint having been recast. Large cracks were clearly

visible, the majority of which ran parallel to the aisles for 10's of metres. These were generally found in the racking areas, with the similar sized slabs outside of this zone showing no sign of deterioration. Interestingly, cracks were also seen extending from the grooves incorporated for the wire guidance system. These ran to the edge of the building, with some of the surface cuts themselves showing signs of deterioration and spalling. Most of the sawn joints and almost all of the construction joints had opened up relatively little. Previous surveys had shown that the slab was prone to voiding under the slab edges caused by compaction of the subbase material.

4.6.3 Ballymena

Measurements taken on the floor slab consisted of builders level curling checks, profilometer curling checks and Prima deflection testing.

This site was used for the bulk storage of tobacco and its packaging products. These were placed on racking systems nine pallets high, with each holding up to one metric ton. There were 16 aisles within the store, each having a width of approximately 1.5m. To one side of the warehouse a smaller area has been constructed which seemed to be a temporary storage facility. The warehouse has previously been used for the bulk storage of tobacco and therefore the point loads produced by racking were relatively new in comparison to the life-span of the slab.

High lifting trucks were the most predominantly used pieces of machinery in the aisles. It had been found that these were swaying excessively due to movement of the slab edges. The driver had complained that the trucks were occasionally moving very close to the racking because of the lean, and commented that he suffered from back pain brought on by the movement. The trucks themselves were run on wire guidance systems set within the concrete slab. Only three cracks were found in total throughout the slab, all of which were below 1mm in width and showed little sign of deterioration.

The slab for this site was approximately 40 years old making its construction date sometime in the 1960's. Cores had been taken and the slab was found to be non-reinforced, with a thickness of 225mm and placed on a weak concrete subbase of 100mm. The subgrade material was assumed to be good as the ground surrounding the site was at a much higher level and had therefore been cut to a reasonable depth. Each aisle contained 8 joints running North to South with longitudinal joints positioned under the

racking system to reduce the risk of deterioration. The construction was representative of long strip although no one could guarantee that this was the case.

The joints themselves were all of the construction type with no dowels or load transfer system visible. All were less than 0.2mm in width and appeared to be behaving reasonably well with little arris damage or corner cracking. Some voiding was apparent, detected by the movement of the joints as vehicles were passing over. Some permanent curl was felt at the joints, and in some positions grinding had taken place to smooth the ride for vehicles.

In general the slab was in very good condition although the joints were moving enough to cause some problems with the high loading vehicles.

4.6.4 Skelmersdale

Measurements taken on the floor slab consisted of surface crack measurement and Prima deflection testing. A plan of the site is provided in Figure 4.14.

This warehouse consisted of two separate buildings which had been joined to form a larger floor area. The section that had recently been taken over (5 years) was previously used as a carpet warehouse containing only minor loading. The walls between the two buildings had been removed at specific areas to form a thoroughfare, and from this it was clear to see that the two floor levels were different at the time of construction. Racking had been constructed in the South-West corner of the site, with the North-West section consisting of an automated transfer system for items of clothing. Pallet trucks and small reach trucks were the most common means of transporting goods, with forklifts used for occasional loading and unloading of vehicles.

A lot of remedial work had taken place in both sections of the warehouse floor. This consisted of filling any problematic joints with a rubberised resin, which was left raised from the surface. Other methods of repair comprised a two part self-levelling screed, much of which had cracked and de-bonded from the original slab. Where the two floor levels had varied it appeared that a section, approximately 1m from the join on either side, had been cut-out and in-filled with new concrete. This had cracked several times and resin had been used to try and level the area. Once again this had not been kept flush with the floor surface.

Many, if not all of the joints were of the construction type, with no saw cuts or inducing materials to be seen. These had opened up a great deal and almost all were showing signs of spalling and deterioration. Many had not been filled and were full of detritus; others had foam filler between the concrete faces. In most areas of the old carpet warehouse a covering had been applied over the floor. This was a brittle material and therefore cracks in it were indicating some kind of recent movement. The joint size in the concrete underneath was extremely difficult to measure because of this surface material.

A section of slab between the racking area and the buffer lanes of the old carpet warehouse was in very poor condition. Strips of the top screed were peeling off at a width of approximately 200mm. After speaking to the survey team it had been assumed that this was the site of a strip foundation where a wall had been standing. Movement was high across this section of slab and the warehouse operatives encountered problems when trafficking.

Cracks could be clearly seen throughout the entirety of the slab. Some of these were quite large although it did appear that many were dormant and only a few showed signs of recent movement. These had been repaired using a resin which had spilled onto the surface of the slab. In general, the whole floor varied in level and flatness with most of the joints in the carpet warehouse showing signs of deterioration. Some of the older cracks around the building were showing signs of edge spalling.

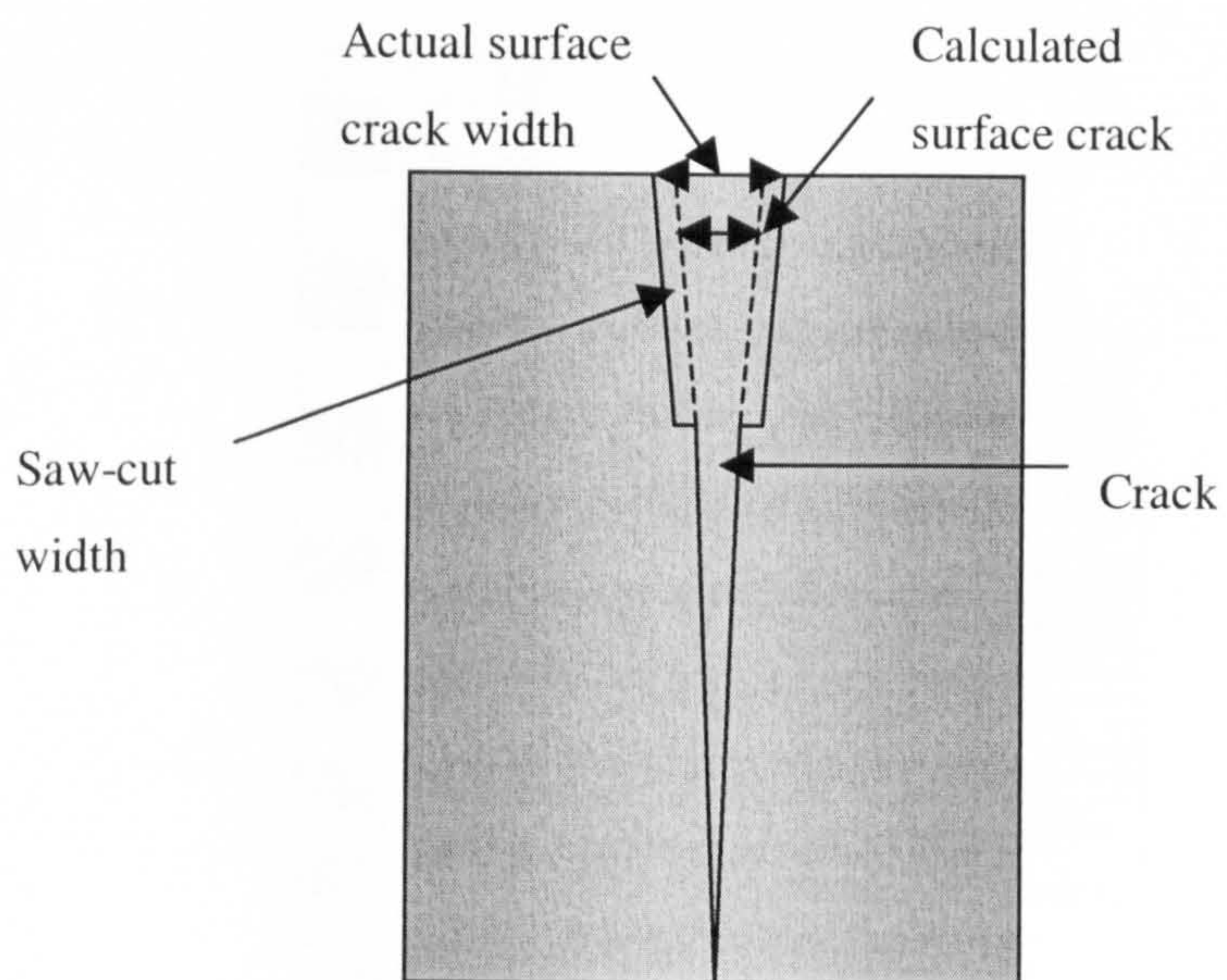


Figure 4.1 – Crack width prediction from saw-cut joints

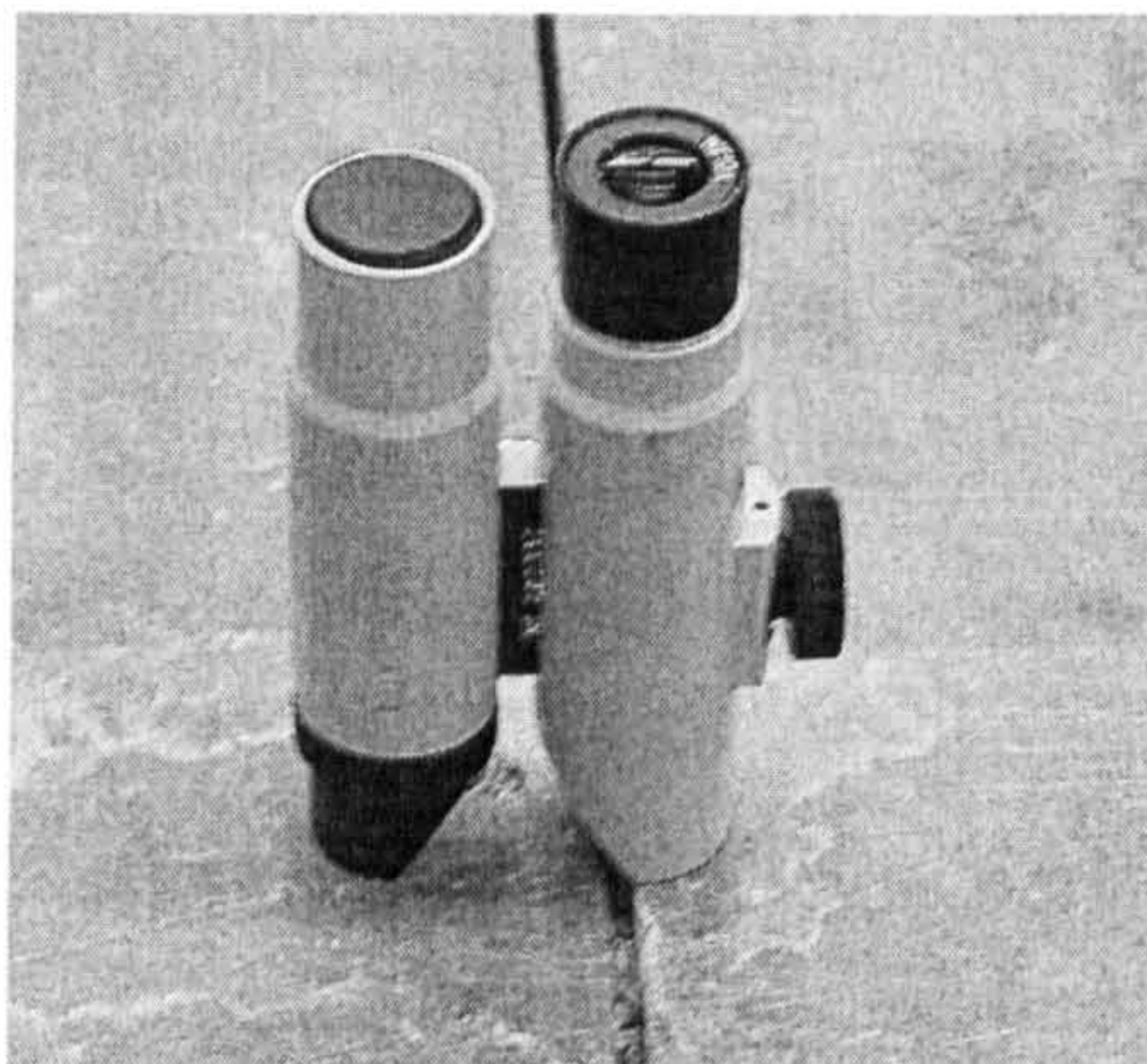


Figure 4.2 – Crack microscope measuring a saw-cut joint

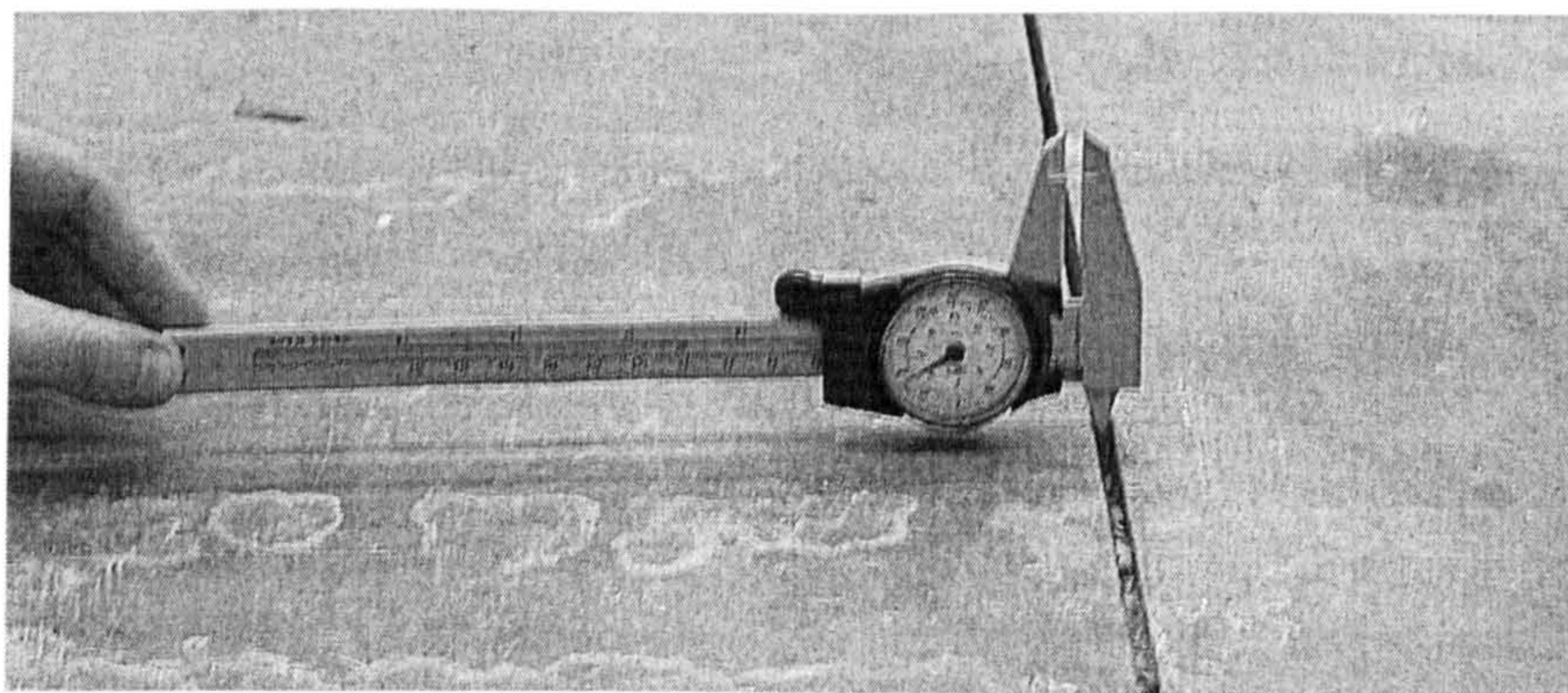


Figure 4.3 – Set of callipers measuring a saw-cut joint

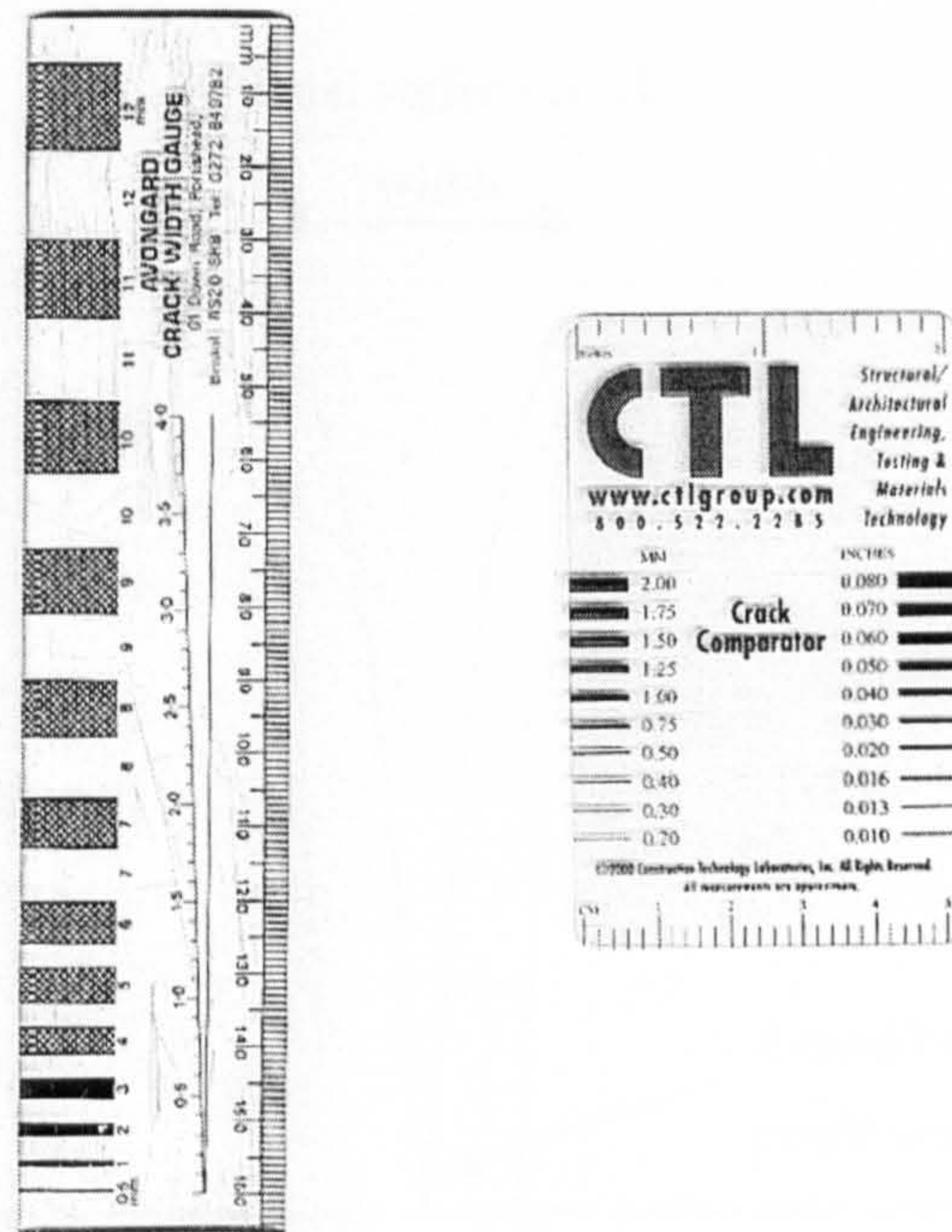


Figure 4.4 – Set of crack comparators

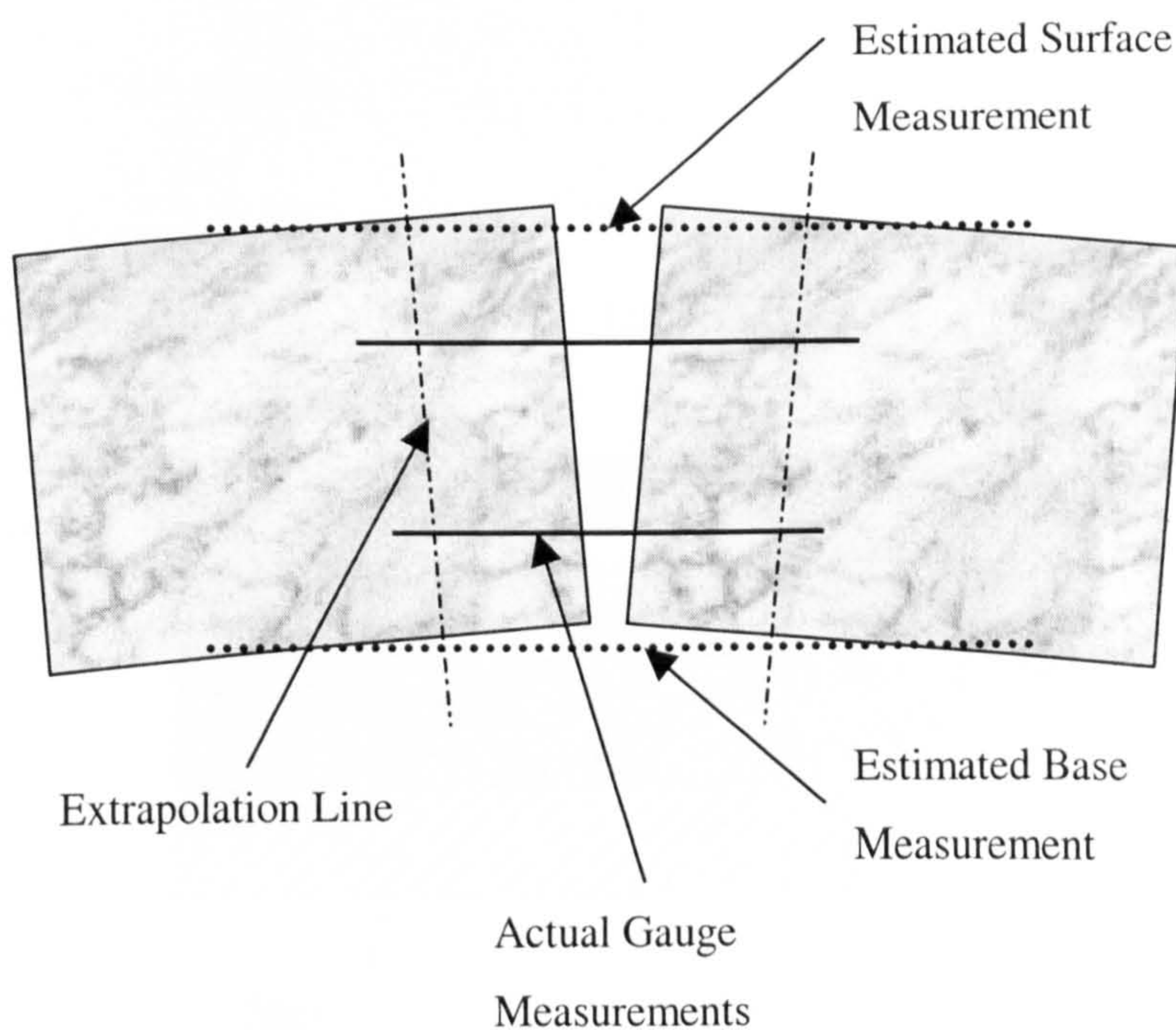


Figure 4.5 – Extrapolation of embedded strain gauges to calculate surface and base crack widths

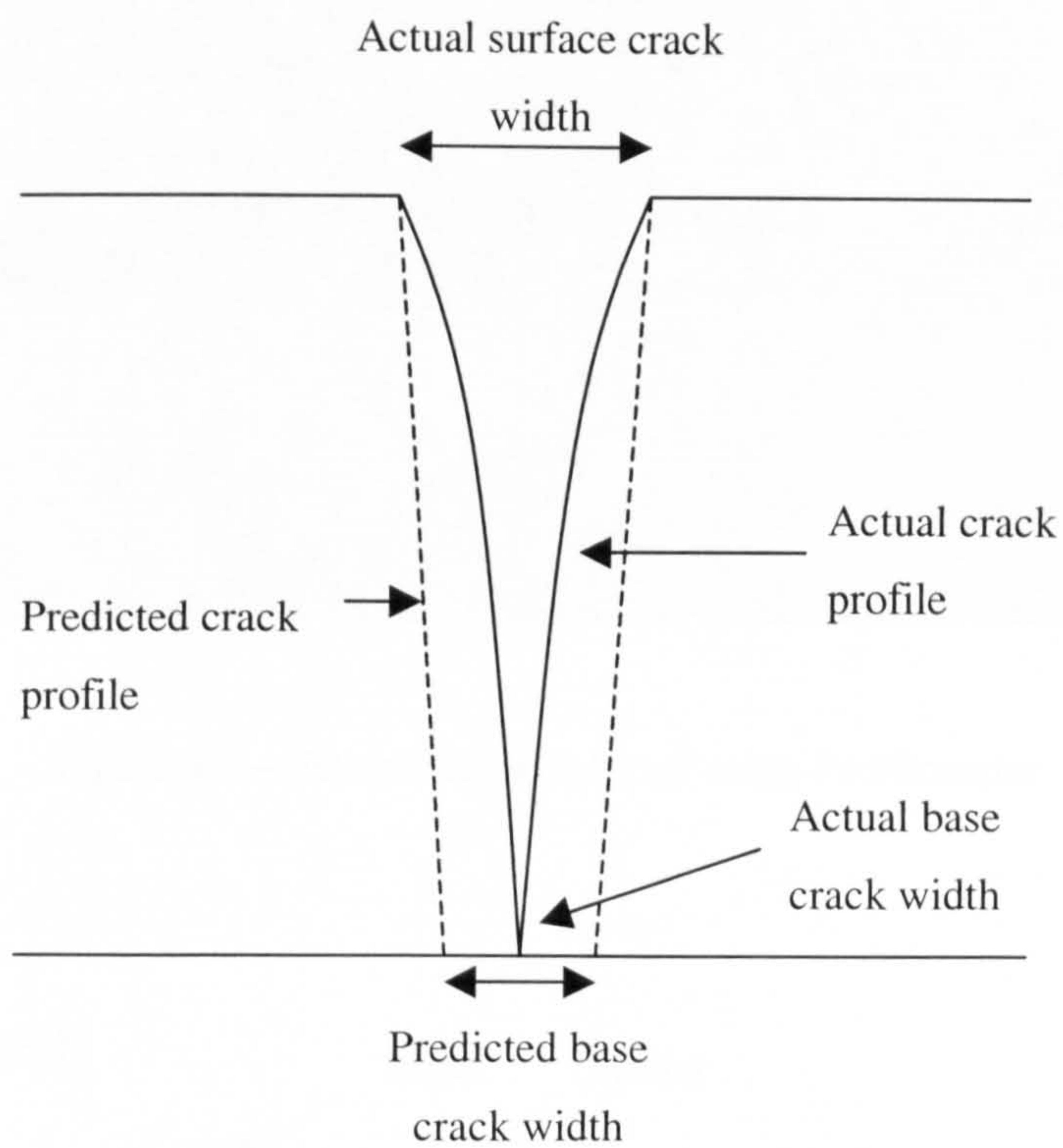


Figure 4.6 – Overestimation of base crack width caused by differential shrinkage

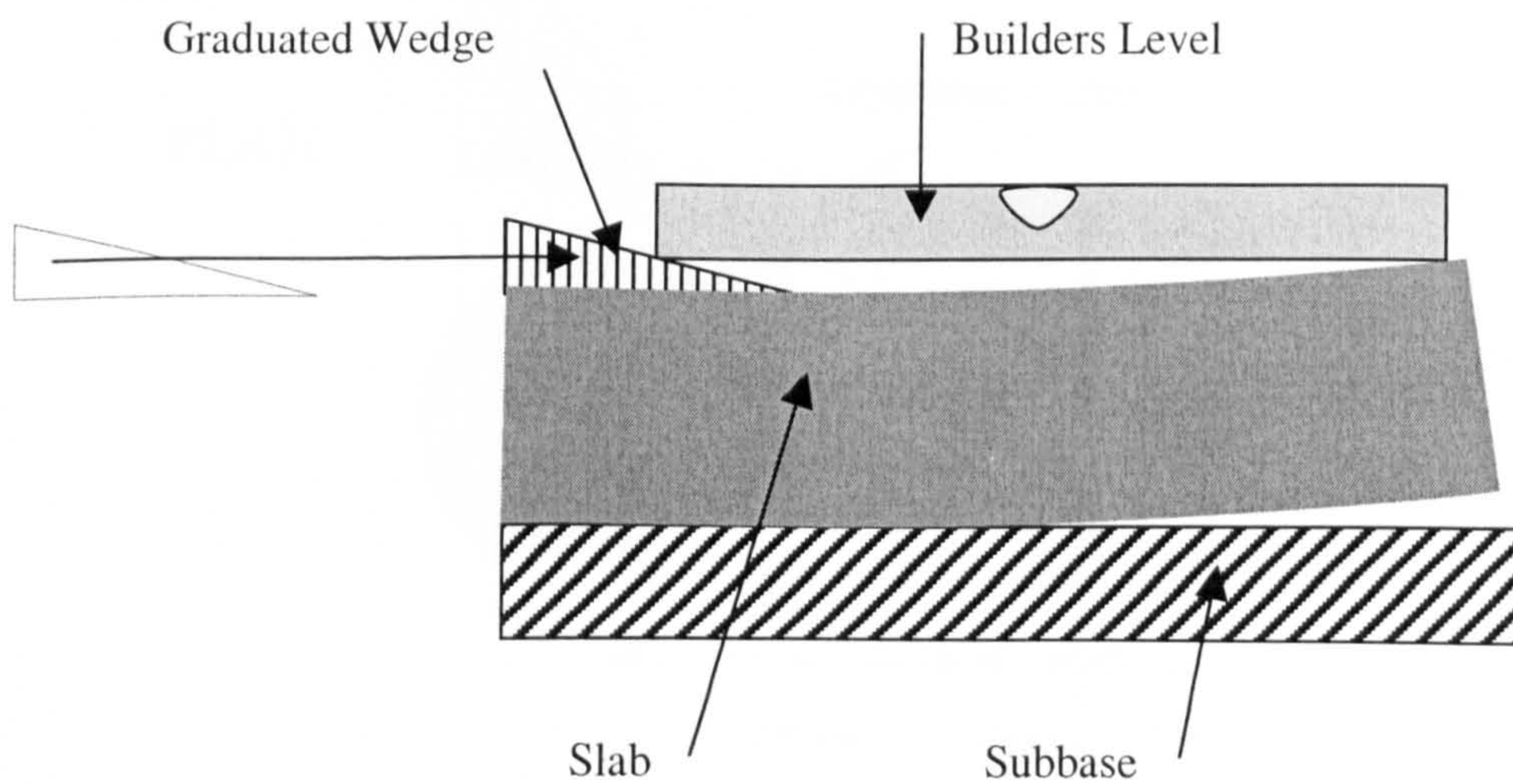


Figure 4.7 – Estimation of slab curl using builders level and graduated wedge

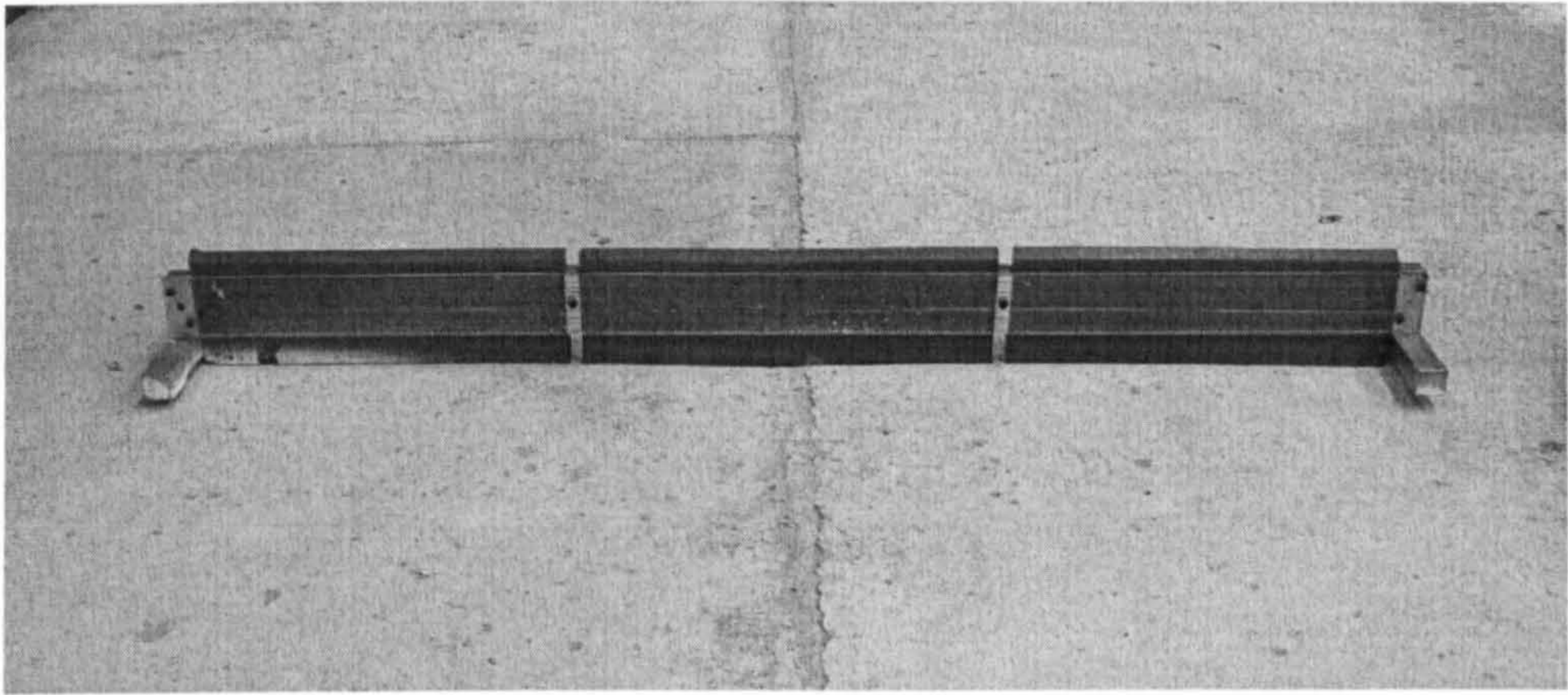


Figure 4.8 – Estimation of slab curl using Profilometer

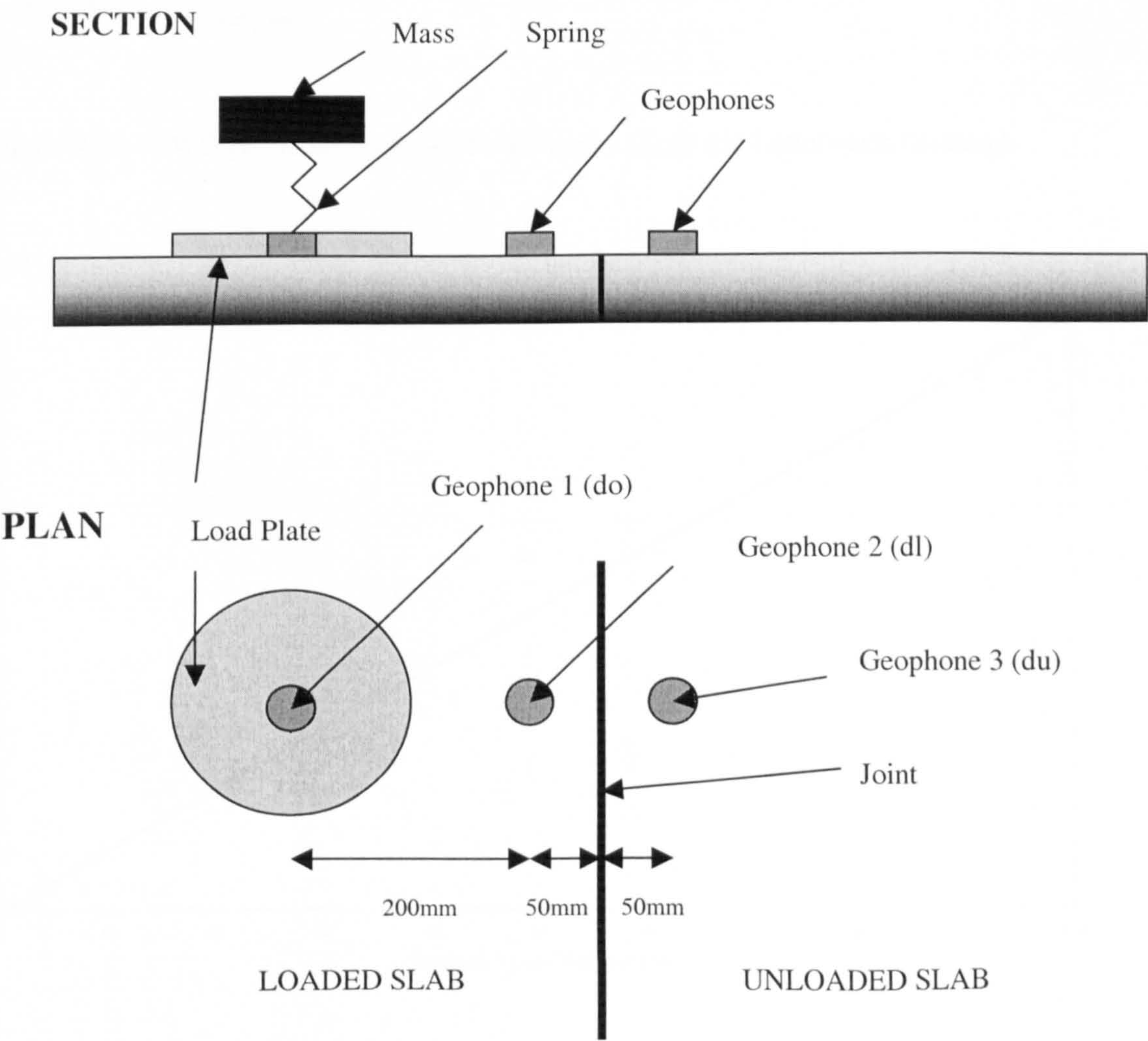


Figure 4.9 – FWD and Prima geophone placement for measurement of slab behaviour across cracks and joints

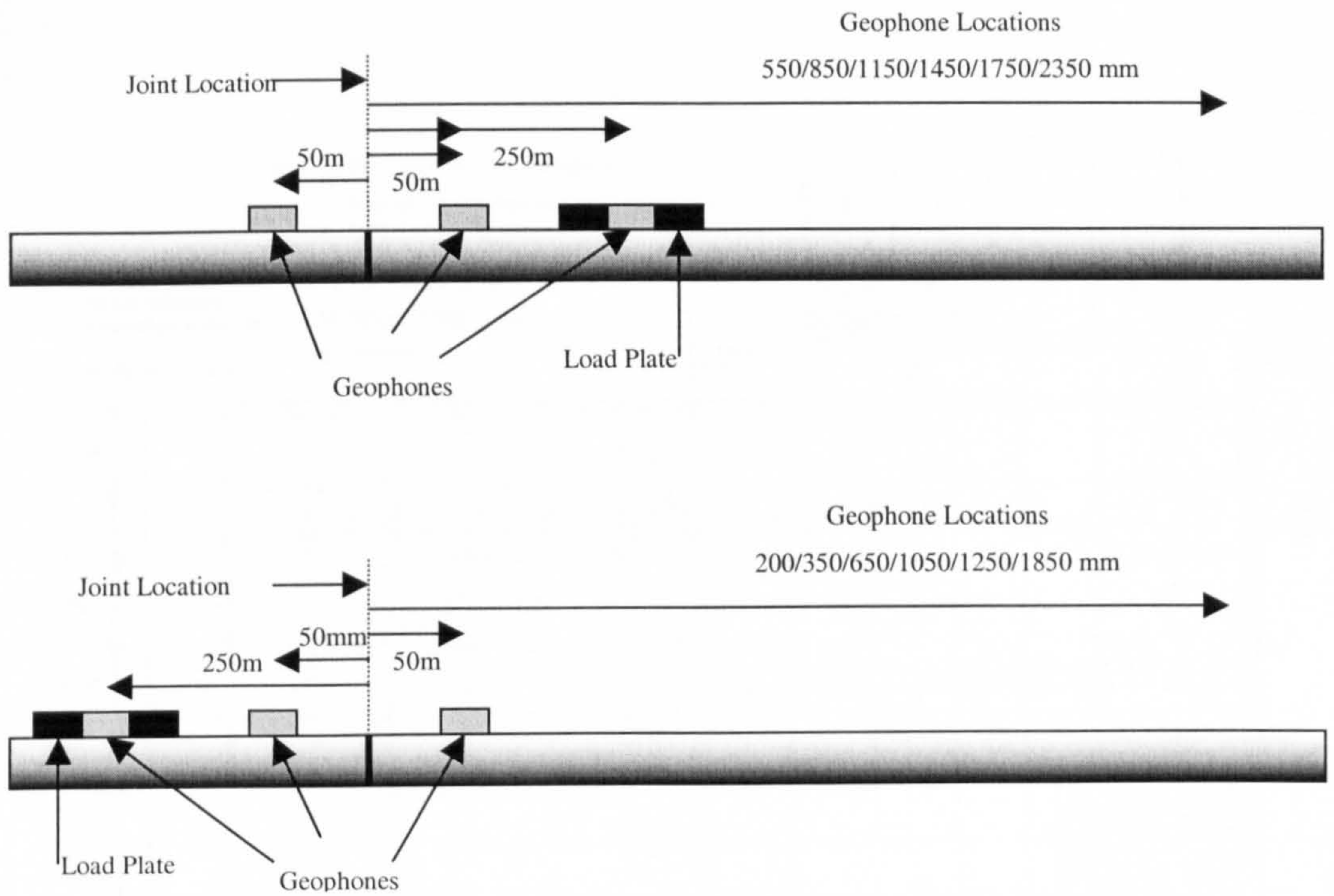


Figure 4.10 – FWD geophone locations for Daventry (Top) and Lutterworth (Bottom)

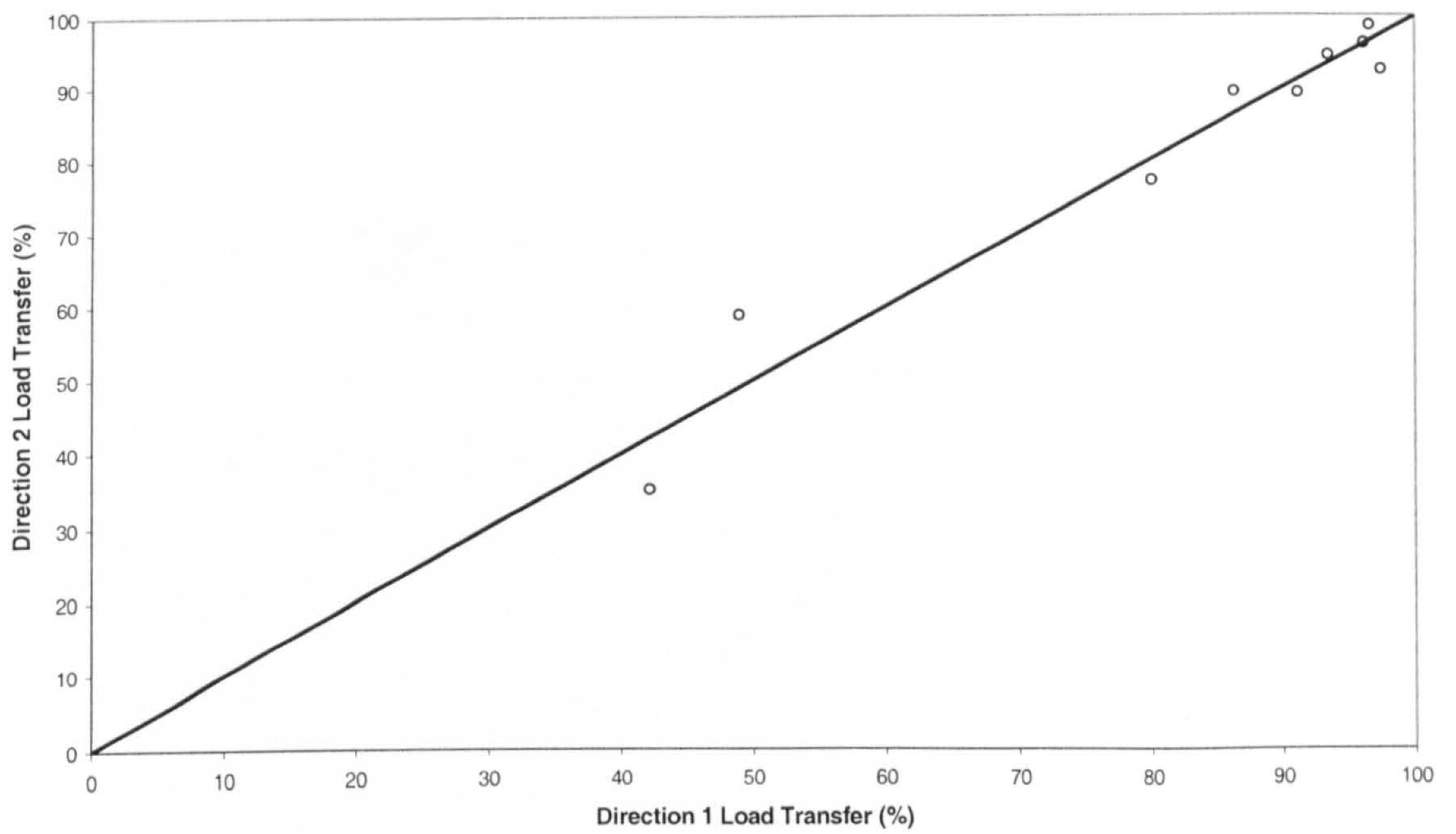


Figure 4.11 – Load transfer comparison when loaded each side of a joint

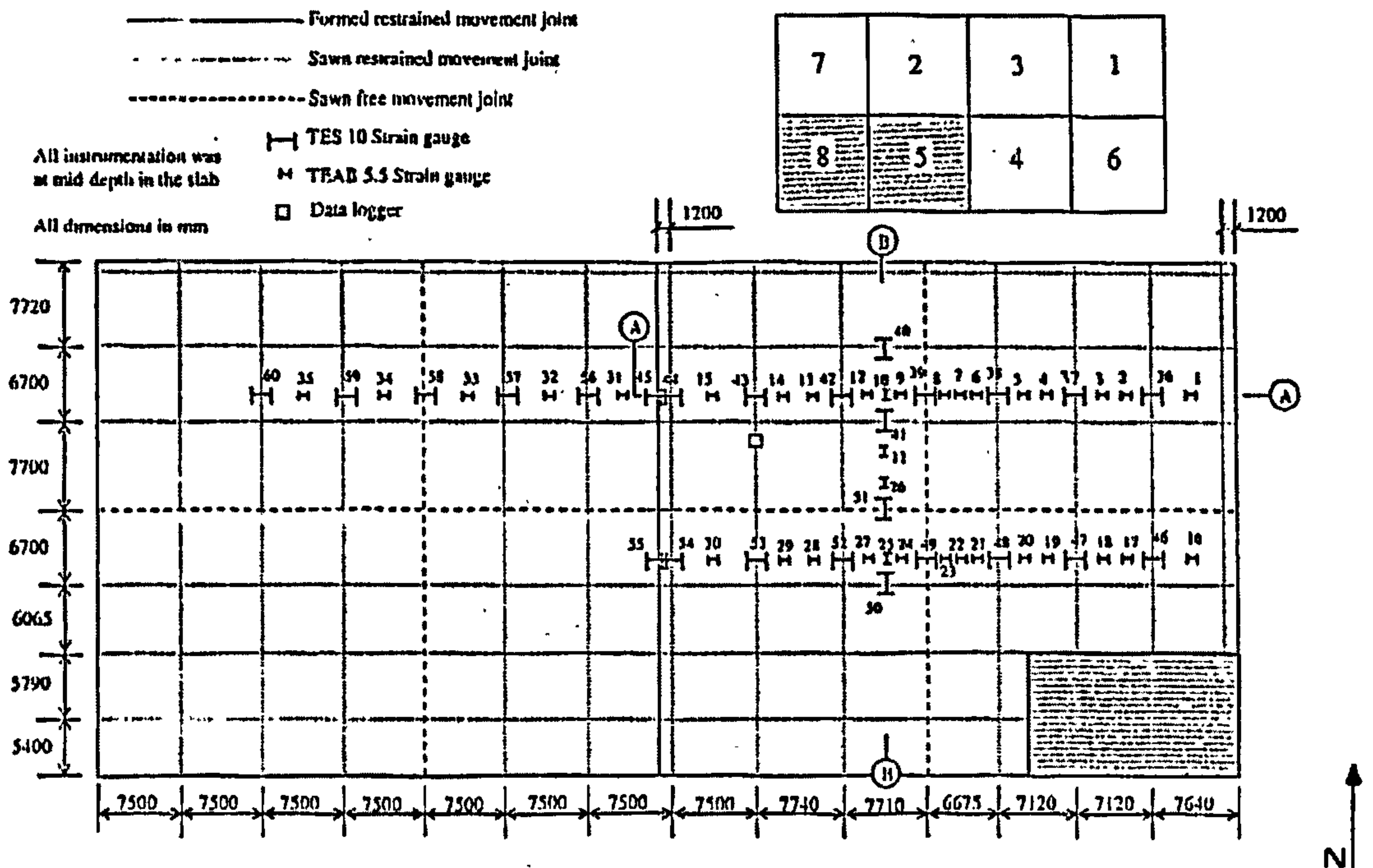


Figure 4.12 – Plan of S.W. corner of Daventry site

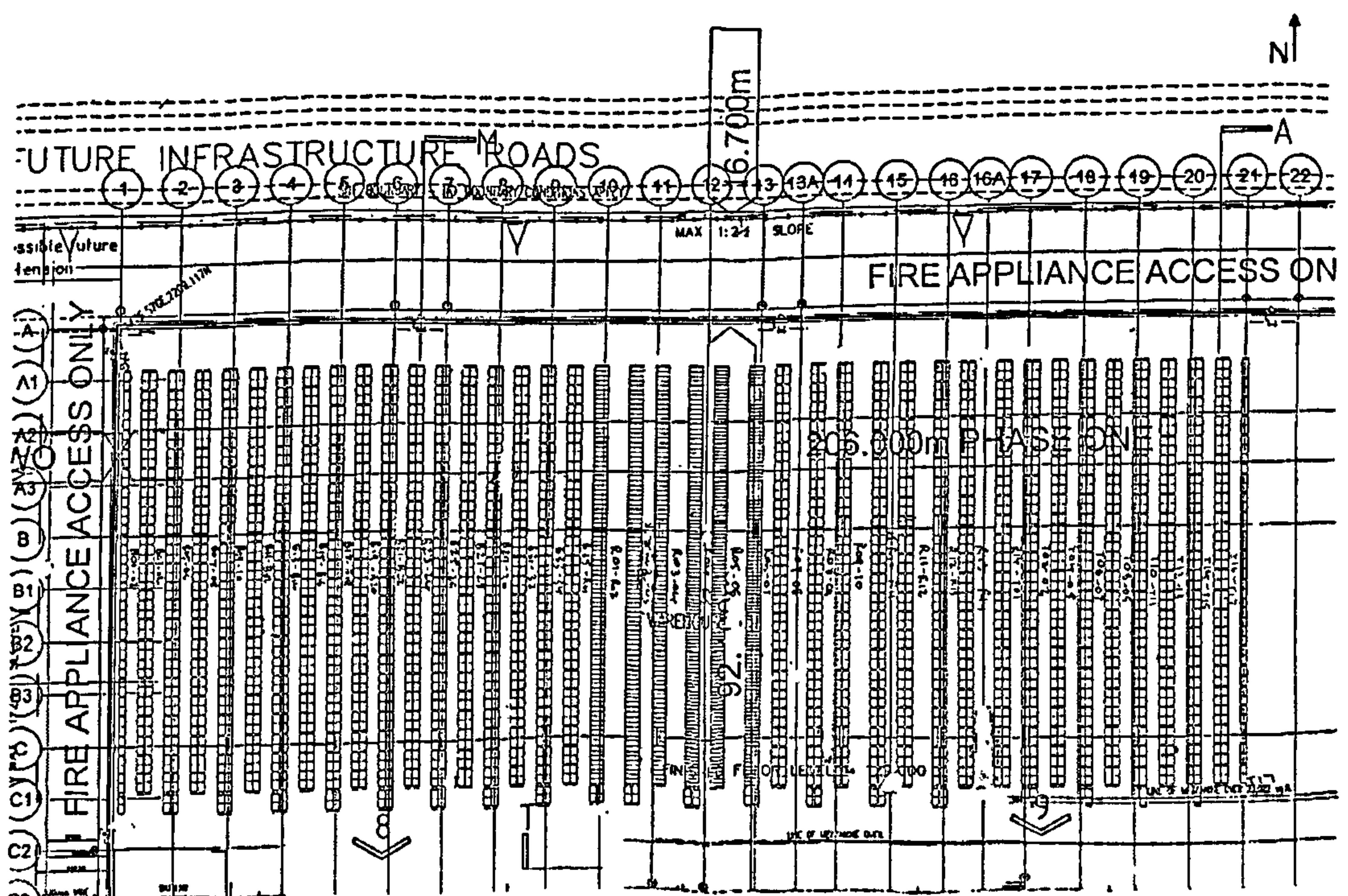


Figure 4.13 – Plan of Lutterworth site

5. JOINT DETERIORATION

5.1 Introduction

This Chapter describes the development of a small-scale testing facility used for the examination of load transfer deterioration caused by cyclic loading. The test method had the following requirements:

- Provide accurate measurement of the deterioration process
- Enable simulation of site conditions
- Facilitate variation in crack geometry
- Produce high cycle numbers whilst being time efficient
- Be cost effective
- Utilise existing equipment (where practical)

Each area of the testing methodology was carefully considered to provide close comparison with in-service site conditions for internal floor slabs. This included crack formation (both initiation and geometry), contact stresses across the crack face, number of cycles of loading, subgrade support conditions, and rate of loading. The study investigated high cycle loading on cracks and joints, examining the load transfer effect and the resistance mechanisms. The results provided significant insights into load transfer across cracks/joints under cyclic loading, which could be used in the long-term assessment of concrete slabs on grade. Comparisons could also be made with the field testing (described in Chapter 4) to assess the effect of age and deterioration of the crack, and its associated slab response effect. This also provided information required for the load transfer elements within the finite element model, described in Chapter 7. During the experimental program a range of parameters, including: crack geometry, reinforcement type and quantity, and load magnitude were examined to assess their effect on the crack deterioration process (section 5.2).

The method of testing utilised a small-scale (100x100x400mm) double ‘V’ cracked beam specimen, in which the two edge sections were clamped against a reaction frame (Figures 5.1 and 5.2). The central block was attached to a force applicator which cyclically imparted load and created a shear stress across the crack plane. Vertical displacement

measurements were then taken periodically from both cracks, enabling deterioration to be monitored over a controlled number of cycles. The reasoning behind the development of this method and the procedures used are discussed in detail in the following sections.

5.2 Test Variables

A variety of crack orientations and reinforcement types/quantities were examined during testing to establish their effect on the crack deterioration process. To enable comparisons between specimens a reference was used which comprised of a beam constructed with the standard concrete mix described in section 5.4.2, with the incorporation of 30kg of Dramix® RC-65/60-BN steel fibre. This was chosen as it represented a typical slab construction, with a mid-range reinforcement quantity. This section describes the reasoning behind each test parameter, with Table 5.1 providing a summary of all specimens examined during the test period.

5.2.1 Surface Crack Widths

For each variation in beam type, the crack width was altered between 0.66, 1.98, 3.3 and 4.62mm at the surface, reducing to zero at the base. This provided reasonable variations between each width but also enabled the trends from crack opening to be identified. The ‘V’ shaped geometry was typical of that found from the Lutterworth cores, and the embedded strain gauges at Leeds, with the surface widths representative of the range of field data collected. The exact value of the initial surface crack width was controlled by the depth of the shims used, and therefore simple combinations were chosen to make setting-up of the test easier. On a few samples the crack width was set to 3.96mm or 5.94mm using an intermediate shim size if useful data would be obtained by doing so. Occasionally, testing of the 0.66 and 4.62mm crack widths did not take place as the results would have produced small displacements or early failure of the specimen.

5.2.2 Steel Fibre Types

Three Dramix® hook ended fibres of type RC-65/60-BN, RC-80/60-BN and RL-45/50-BN, supplied by Bekaert Building Products Ltd. were tested during the research. Consultation with the manufactures identified these to be the most common sizes in internal floor slabs on grade, with the RC-65/60-BN being used most often. More information on the steel fibre types used in the research is provided in Table 5.3 and section 5.4.3.

5.2.3 Steel Fibre Quantities

Three steel fibre quantities of 20, 30 and 40kg/m³ were used during the experimentation since these are stated in the literature as being typical values for industrial floors (ACIFC and The Concrete Society 1998, The Concrete Society 2003). For the standard beam 30kg/m³ was used, it being the intermediate value and that found regularly in many of the mix designs obtained from site.

5.2.4 Non Reinforced

Non reinforced specimens were tested to examine the effect aggregate interlock alone has on the deterioration process. This enabled direct comparison of the 'V' shaped crack orientation used in this research against parallel cracks tested elsewhere.

5.2.5 Mortar

Mortar beams containing 30kg/m³ of the RC-65/60-BN fibre were examined to determine the degree of load transfer obtained from the fibre alone, without influence from aggregate interlock.

5.2.6 Parallel Cracks

Parallel cracks varying between 0.5 and 2.0mm width were tested for each of the three fibre quantities. The results provided comparison with the findings of other researchers who examined parallel crack aggregate interlock effects. This also enabled differences between 'V' shaped and parallel crack orientation to be identified.

5.2.7 Fabric

Representative sections of A142 mesh (Figure 5.3) were cast into beams and tested at 1.98 to 4.62mm crack widths. This enabled comparison of reinforcement type and gave some indication of the steel fabric load transfer effect.

5.2.8 Loads

Load magnitudes of +/-2kN and +/-6kN were tested in addition to the standard +/-4kN value to determine their effect on the rate of deterioration. The reason behind the selection of these values is described in section 5.3.5. For each load the standard 30kg/m³ of RC-65/60-BN fibre beam was used over the full range of crack widths.

5.2.9 Summary of Test Variables

Table 5.1 below shows a summary of specimens examined during the testing period.

Table 5.1 - Testing Schedule

Reinforcement Type	Surface Crack Width (mm)				
	0.66	1.98	3.3	4.62	Other
None	✓	✓			
30kg /m ³ Fibre (Mortar)	✓				
20kg/m ³ Fibre	✓	✓	✓	✓	3.96mm
30kg /m ³ Fibre		✓	✓	✓	5.94mm
40kg/m ³ Fibre		✓	✓	✓	5.94mm
30kg /m ³ RC-80/60-BN Fibre		✓	✓	✓	
30kg /m ³ RC-45/50-BN Fibre		✓	✓	✓	
Re-bar		✓	✓	✓	
Fabric		✓	✓	✓	
30kg /m ³ Fibre (2kN Load)		✓	✓	✓	
30kg /m ³ Fibre (6kN Load)	✓	✓			
20kg/m ³ Fibre (Parallel Crack)	✓	✓			
30kg/m ³ Fibre (Parallel Crack)	✓	✓			
40kg/m ³ Fibre (Parallel Crack)	✓	✓			

Unless otherwise stated beams contain fibre type RC-65/60-BN at 30kg/m3 with 'V' shaped cracking

5.3 Load Test Development

5.3.1 Simulation Method

Many of the previous test methods examining small-scale monotonic or cyclic load transfer have employed a singularly cracked specimen. Valle and Buyukozturk (1993), Van de Loock (1987) and others, used a rectangular section with a shear plane induced through the centre (Figure 5.4). This arrangement is only of use for single or low repetitions of load due to the method of horizontal restraint. Millard and Johnson (1984) used a similar set-up with a smaller specimen, although once again this was only applicable to single cycle loading (Figure 5.5). Each of these tests required displacement across the shear plane, whilst preventing movement in the normal direction. This was partially prevented with the use of slip plates and compression jacks; however, measurements taken during testing showed signs of crack widening caused by stress development as aggregate particles are forced over each other. The method of normal

restraint also creates rotation due to the eccentric loading, which is difficult to prevent in a singularly cracked specimen.

In a pavement or floor slab the frictional restraint of the concrete on the subbase, and the confinement of adjacent slabs, prevents all horizontal displacement. The joint or crack is therefore fully restricted from movement in any direction other than vertically. This is very difficult to simulate in a small-scale, one crack specimen due to the poor control of normal restraint. Colley and Humphrey (1967) and Raja and Snyder (1991) used large scale testing to overcome this problem, closely representing real conditions (Figure 5.6). This arrangement typically consists of two large (1220 x 3000mm) slabs resting on a real or simulated foundation, with a pulsating load applied alternately to each side of the joint.

Due to the available test equipment and number of specimens that required testing, it was not appropriate to utilise large-scale testing and therefore a small-scale alternative was employed. This had to allow for high cycling whilst preventing the overall rotation and normal displacement which had been found with the smaller methods of Millard and Johnson (1984) and Valle and Buyukozturk (1993). Some of these problems can be overcome with a double cracked shear specimen as used by Thompson (2001), shown in Figure 5.7. This method required a controlled crack to be induced either side of the load application position. The central section was then fixed to the loading ram with the end segments rigidly clamped against a stable surface. This caused a load differential between each side of the crack creating a double shear stress, and a reduced risk of rotation. If symmetrical degradation across both faces is assumed, the use of two crack planes is of no consequence and is equivalent to a singularly cracked specimen.

For the formation of a simple set-up with a fully restrained crack face, an arrangement similar to that used by Thompson (2001) was used, details of which are provided in the remainder of this chapter. The set-up enabled utilisation of an existing (Dartec) cyclic loading test machine, which could apply the required load magnitude and cycle rate.

To simulate the type of loading found, and the degradation mechanisms within, a crack or joint in a concrete slab on grade, load was applied in both a positive (downward) and negative (upward) direction. Figure 5.8 demonstrates how each laboratory simulation position related to that occurring within a site. Position 1 is an unloaded case whereby there is no movement. When the central block is moved in a positive direction (position 2), the left hand side of the specimen represents a slab load on the leave side, whereas the specimen right hand side represents a slab load on the approach side. As the central load

moves in a negative direction (position 3) the left hand side of the specimen represents a load on the approach side, with the right hand side representing a load on the leave side. This approach ensured that the left and right hand sides of the specimen simulated a load crossing the joint in either direction and was therefore fully characteristic of the contact stresses acting across a typical joint.

5.3.2 Specimen Geometry

A specimen was required which would enable a number of material parameters to be examined, whilst being both time and cost efficient. This prevented the use of a full size slab, which could have replicated exact site conditions. A small-scale section was therefore selected, which had to provide a characteristic value, representative of the entire slab. Although small attributes of the crack face would have a much larger influence on a small specimen, careful selection of its size and thorough examination of the production process sufficiently reduced any discrepancy. A depth of 100mm was used as this was a lower bound for a 150mm slab with 1/3 saw cut. The width had to represent a typical section of the slab incorporating a sufficient blend of concrete constituent materials (most importantly coarse aggregate and steel fibre). As the aggregate was below 20mm, with a maximum fibre length of 60mm, a value of 100mm was chosen as being fully representative and having limited scale effects. The 400mm length of the beam enabled the central 100mm section to be fixed to the load applicator, whilst providing sufficient end strapping to the reaction frame.

5.3.3 Crack Geometry

The literature reviewed in section 3.3, and the measurement techniques used in section 6.1, suggested that the majority of joints or cracks are of a 'V' geometry, caused by the differential shrinkage and curling commonly found in concrete slabs on grade. The majority of the previous tests carried out on shear transfer across joints (Colley and Humphrey 1967, Millard and Johnson 1984) assumed a parallel width over depth and are therefore inconsistent with in-service slab conditions. White and Holley (1972) examined a small number of 'V' shaped cracks and compared the results to those of parallel cracking. They found that the average width of the 'V' shaped crack had a greater load transfer capacity than that of a similar sized parallel crack, highlighting the importance of using correct geometry when testing. Work undertaken by Colley and Humphrey (1967) compared laboratory load transfers to those obtained from site and found that the site values were much larger. The parallel cracks assumed in their laboratory testing could be

a reason for their findings, as 'V' shaped cracking (probable in their field slabs) is known to provide greater load transfer.

To ensure that the testing procedure and specimen preparation used in this research provided good representation of site, the majority of specimens were pre-cracked and set-up to obtain 'V' shaped geometries. The size of the surface widths was selected from the data collected in section 6.1, with the exact values used, and the reasoning, given in section 5.2.1. A selection of parallel cracks was also tested to examine the effect of the crack angle, and identify any variations in behaviour.

5.3.4 Subgrade Support

Many of the tests undertaken by previous authors (Buch *et al.* 2000, Raja and Snyder 1991) incorporate well supported slab edges, utilising either a foundation made from soil compacted in a test box, or 'elastic' materials such as neoprene pads. The incorporation of these materials partially dictates the amount of displacement that can take place, and therefore controls the rate of deterioration. If the soil in the field is different to that used in the experimentation then any comparison will contain errors. Section 2.4.2 demonstrated that in most situations the slab edges will have curled to some degree, thereby leaving the slab unsupported, with the load transfer system alone contributing to joint efficiency up to a certain load limit. This creates higher contact stress on the crack faces resulting in an enhanced risk of deterioration failure. In the test method developed, foundation or support materials were excluded for more accurate simulation of site conditions and this therefore provided an element test. This approach produced a worst-case scenario, which could then be used in comparisons of site data.

5.3.5 Load Magnitude

The magnitude of loading has been shown to highly influence the rate of concrete crack degradation (Colley and Humphrey 1967). A suitable value was therefore essential to represent that occurring within the field. The majority of previous tests on full-scale slabs have used a 40 to 50kN load over a cross sectional area of around 0.2m², generating a contact stress in the region of 200 to 250kPa. The loading found on internal floor slabs varies greatly but example values given in Table 2.1 are between 42 and 60kN. In external slabs this can regularly exceed 100kN depending on the type of vehicle used, with pavements designed on an 80kN standard axle, thereby creating 40kN per wheel.

Yoder (1959) and Friberg (1938) proposed that for dowel bar calculations only a distance 1.8 times the radius of relative stiffness ' l ' (equation 3.1) from the load source has any influence on transfer efficiency, the effect reducing linearly with distance. From this information the Concrete Society (2003) concluded that full load transfer could be assumed at a distance 0.9l either side of the load. Calculating ' l ' using typical values of: Youngs modulus of concrete (E_c) = 30GPa, Slab depth minus saw-cut (h) = 150/300mm, Poissons ratio (ν) = 0.15 and modulus of subgrade reaction (k) = 0.07/0.01 N/mm³, produces results in the range of 0.6 to 1.6m, which when doubled (incorporating the effect either side of the load, along the slab edge) gives full load transfer lengths between 1.1 and 2.9m. If the average of these values is used to simulate a typical situation (i.e. 2m), with an effective slab depth (minus saw-cut) equal to 0.1m, and an application load of 50kN, equation 5.1 generates a contact stress (τ) of 250kPa.

To produce a similar 250kPa contact stress in the small-scale specimens, where beam width (x) and depth (d) are equal to 0.09m (doubled as there are two crack faces), an applied load (P) of +/- 4kN was required (equation 5.2). When smaller and larger loads with equivalent full-scale magnitudes of 25 and 75kN were considered, loads of +/-2 and +/- 6kN were required.

$$\tau = P / (2l \cdot d) \quad \text{equation 5.1}$$

$$P = 2\tau (x \cdot d) \quad \text{equation 5.2}$$

5.3.6 Loading repetition

The crack or joint of a slab may be subjected to hundreds of load repetitions every day. This can result in many millions of cycles throughout its expected lifespan. Given the research period it was deemed impractical for testing to continue for the equivalent number of cycles and therefore a value was adopted which enabled a comparison between laboratory and field data. Colley and Humphrey (1967) tested large-scale slabs for up to one million cycles and concluded that 90% of the degradation will have occurred within the first 500,000 cycles, as shown in Figure 3.8. Abdel-Maksoud (2000) conducted similar tests on smaller samples at cycle numbers up to 300,000 cycles, at which point the increase in degradation appeared to have ceased (Figure 5.9). Thompson (2001) examined cement bound materials and stopped testing after 10,000 cycles as the gradient of shear slip displacement had reduced dramatically (Figure 5.10).

Due to the range of load cycles used in the tests reviewed, 15 trial tests were conducted with the selected test method to ascertain the most appropriate number for this research. A minimum of 250,000 cycles was chosen initially, with a further 250,000 applied on 5 specimens to examine longer-term degradation. At least 75% of the 500,000th cycle deterioration occurred within the first 250,000 cycles (Figure 5.11), and therefore this level of repetition was selected as an appropriate representation of total degradation.

In the majority of the experiments the displacement/cycle gradient was found to reduce to negligible values towards the end of the test. However, in a few samples appreciable levels of deterioration were still visible as indicated by the steady increase in gradient. In these circumstances the test was continued until a horizontal gradient was found (normally shortly after), although the 250,000 cycle data was still used for comparison during analysis.

5.3.7 Load rate

Colley and Humphrey (1967) measured the loading pattern of a joint as a vehicle travels over at approximately 30mph (Figure 5.12). This required the approach slab to be loaded from zero to maximum in 0.25 seconds, and then instantaneously removed. On completion the leave slab was immediately loaded and gradually reduced to zero in 0.25 seconds, resulting in a total cycle length of 0.5 seconds. Due to the nature of the small-scale tests, and the limitations of the Dartec testing machine, it was not possible to fully replicate the approach used by Colley and Humphrey (1967); however, a sinusoidal curve which completes a full cycle in 0.5 seconds was employed (Figure 5.13). Abdel-Maksoud (2000) concluded from his work on cyclic loading that the load rate has very little impact on degradation results unless weak aggregate is used, and therefore this approach to loading was acceptable.

5.4 Specimen Production

5.4.1 Introduction

Each batch of specimens comprised six 100x100x400mm beams for use within the cyclic load test machine and two 100x100x100mm cubes cast for 28 day compression testing. The beams and the cubes utilised standard steel moulds; however, a 100x100x100mm wooden block was inserted into the end of the beam mould to reduce the length from 500 to 400mm in accordance with the clear access limitations of the Dartec. The use of six

beams ensured that at least two parameters (comprising of 2-3 specimens each) could be tested from the same batch, thereby reducing any errors caused by construction variations.

5.4.2 Mix Design

The mix design was selected from typical information gathered on floor slabs cast within the last six years (Table 5.2a). At each site the concrete was C40 in specification, with a 125mm slump, enabling site pumping. The maximum aggregate size was 20mm and the minimum cement content 325 kg/m³, with a water to cement ratio below 0.55. In all cases the mixes were very similar, and as such the most representative specification was chosen (Table 5.2b). The constituent material information used within the concrete is provided in Table 5.2c.

For each concrete batch, the moisture content of the coarse aggregate was calculated using a speedy test; this varied between 0 and 3%. The volume of water and aggregate was then altered accordingly to produce the correct free water ratio. The moisture content of the fine aggregate was selected from previous testing (Jones 1998) when used under similar conditions, and was found to be approximately 0.64%. This was assumed for all batches as the variation in water content would only be minor, with the mix specification altered accordingly.

Table 5.2a – Typical Site Mixes

Material	Quantity		
	Northampton	Normanton	Bedford
Cement	370 kg/m3	360 kg/m3	370 kg/m3
Coarse aggregate (5-10mm)	355 kg/m3	352 kg/m3	316 kg/m3
Coarse Aggregate (10-20mm)	711 kg/m3	704 kg/m3	736 kg/m3
Fine Aggregate	783 kg/m3	799 kg/m3	741 kg/m3
Free Water	174 kg/m3	181 kg/m3	196 kg/m3

Table 5.2b – Actual Concrete Mix Specification Used for Laboratory Testing

Material	Quantity
Cement	370 kg/m3
Coarse aggregate (5-10mm)	355 kg/m3
Coarse Aggregate (10-20mm)	711 kg/m3
Fine Aggregate	783 kg/m3
Free Water	185 kg/m3

Table 5.2c - Material Information

Material	Specification
Cement	Type 1 Ordinary Portland cement to BS12 (1991)
Fine Aggregate	Zone 2 river sand with a maximum size of 5mm
Coarse Aggregate	Trent River Gravel with 5-10mm and 10-20mm gradings
water	Tap Water held at laboratory temperatures
Plasticisor	Sikament Ultra

To ensure the characteristic concrete strength (f_c) was achieved a target mean strength (f_m) was calculated, which all specimens had to exceed. For the purpose of testing a 5% defectives value was chosen ($k = 1.64$), along with a standard deviation of 3N/mm^2 , allowable because of the controlled conditions found within the laboratory. Equation 5.3 therefore produces a target mean strength of 45MPa. The results of the concrete mixes used within during the research are provided in section 6.3.1.

$$f_m = f_c + ks$$

equation 5.3

When mortar was required, quantities of coarse aggregate were replaced with an equal weight of fines. This made the mix very stiff and a Plasticisor was introduced at a dosage of 1 litre per 50kg of cementitious material (as instructed by the material suppliers) to increase workability. The target mean strength was calculated in a similar manner to the concrete, although it was not required to conform to the 45MPa value, as the reduction in aggregate size was known to produce a significant loss in strength.

5.4.3 Reinforcement

Three fibres types were used within the test program, all of which were supplied by Bekaert Building Products Ltd. and consisted of Dramix[®] categories RC-65/60-BN, RC-80/60-BN and RL-45/50-BN (Figure 5.14). Details of each fibre are shown in Table 5.3 with further information supplied in appendix A.

Table 5.3 - Steel Fibre Data

	RL-45/50-BN	RC-65/60-BN	RC-80/60-BN
Class	Standard	Premium	Max Performance
Type	Hook Ended	Hook Ended	Hook Ended
Length	50mm	60mm	60mm
Diameter	1.05mm	0.90mm	0.75mm
Aspect ratio	48	67	80
Fibres/kg	2800	3200	4600
Tensile strength	1000 N/mm2	1000 N/mm2	1050 N/mm2
Packaged	Loose	Collated	Collated

Steel fabric sections were cut from a standard sheet of A142 structural mesh, with transverse members located 100mm either side of the saw cut (Figure 5.3). The fabric was placed 20mm from the base of the mould and was kept in position with four triangular steel restraints.

Regular 7mm grade 460 steel reinforcement was fixed into an equivalent mesh to that in Figure 5.3. Again this was placed in position using the method described above.

5.4.4 Casting

The concrete was mixed in a 100 litre drum for 1 minute before the fibres were introduced, and then continued for a further two minutes allowing the fibres to fully separate and disperse evenly. Once complete the beam moulds were half filled with concrete and placed on a vibration table for 30 seconds. A second layer was then added and vibrated again for a period of 1 minute or until the release of air bubbles onto the surface had ceased. The cubes were cast in a similar manner and in accordance with BS1881, Part 108 (1993). Each specimen was then trowelled level and placed under a polythene membrane.

After twenty-four hours the moulds were removed from the concrete. The beams were then labelled, sawn, cracked (as described in section 5.5.2) and placed with the cubes in a water curing tank at 20°C +/-2 °C for a minimum of 28 days. After this time period the cubes were removed and tested in a Denison Material Testing System 5000kN compression machine to BS 1881: Part 116 (1983). This ensured the concrete was of the correct strength and that problems developed during casting or curing could be identified.

Throughout the testing period beams in the same set were tested within 14 days of each other to reduce any increase in strength over time having an impact on the results. Where

possible they were tested just after 28 days, with a maximum allowable time limit of 56 days.

5.5 Beam Preparation

5.5.1 Crack Timing

Before the beam could be tested in the cyclic loading rig it had to be pre-cracked. Work carried out by Abdel-Maksoud *et al.* (1997) concluded that the formation of a crack is highly dependent upon the time at which it is instigated. When formed early in the life of the concrete i.e. within 48 hours, it is the bond between aggregate and cement paste which breaks down. After this period the bond has had time to strengthen and an increased percentage of cracking will occur through the aggregate. This change in crack type causes large variation in the roughness of the face and therefore affects aggregate interlock (Nowlen 1968). The Concrete Society (2003) has determined that cracking in concrete floor joints generally occurs in the first 24 to 48 hours of slab life when the concrete has limited strength but is subjected to high tensile stresses. This leads to matrix cracking producing the more roughened surface described above. To replicate the real situation it was decided that the beam should also be pre-cracked at this early time period. As the width required would not be known at such an early stage each beam was initially cracked to the smallest 0.66mm surface width. This enabled the final measurement to be determined later on in the testing schedule, but ensured the profile would follow that of an early-age crack.

5.5.2 Crack Technique

The method of crack formation has been found to influence the roughness of the crack face (Abdel-Maksoud *et al.* 1997). Abdel-Maksoud (2000) criticised the techniques used by other researchers for not providing suitable simulation to that found on site. He suggested that a three point bending technique would produce a much smoother face compared to a true tensile crack. This was caused by significant aggregate breakage resulting in a decrease in shear transfer available through interlock. Abdel-Maksoud *et al.* (1997) proposed that when creating a crack, the width at the surface could be in the region of 2mm, although 30% of the interior may remain uncracked, and therefore a more thorough method of crack detection should be used. They also stated that the method of tensile force application affected the roughness, as clamping and then pulling one side only gave a different crack shape to that obtained when pulling from both sides. The assumption made by both of these authors is that crack development in slabs on grade is

instigated from a true tensile stress caused by shrinkage. Walker and Holland (1999) have stated that cracking is often created by the curling of the concrete slab rather than direct shrinkage, resulting in a mixture of both tension and flexural forces.

From the monitoring of cracks discussed in section 6.1 and literature reviewed in section 3.3, it has been shown that the geometry of a crack or joint in concrete slabs is generally 'V' shaped. A method was required to enable this crack orientation to be produced in small-scale beams. The surface measurement would need to be controlled, with the base of the specimen remaining closed. Thompson (2001) developed a simple three point bending crack induction method proven to produce a vertical crack continuous across the specimen. This involved incremental loading at the crack location until the equipment control software detected a reduction, at which point loading ceased and a crack was assumed. The beam was then rotated 180 degrees and reloaded enabling a parallel crack to develop. Examination of different methods of crack induction (Abdel-Maksoud *et al.* 1997, Millard and Johnson 1984) resulted in the method suggested by Thompson (2001) being used as it could easily be adapted to produce a 'V' shaped crack through loading of one side only.

The technique developed required sawing to a depth of approximately 5mm around the circumference of the beam to enable the crack positions to be set. The beam was then placed on a system of steel blocks and shims set 90mm either side of the saw cut. A similar sized block, but with no shim, was placed directly underneath the saw cut and a round steel bar placed on top. Load was then applied at a controlled rate creating a flexural crack increasing in size until it hit the block underneath, at which point all load was removed. For the second saw cut position the beam was repositioned and cracked in a similar manner. Details of the process are shown in Figure 5.15, with the level of control achieved given in section 5.5.3.

The set-up for parallel crack development was similar to that mentioned previously. The initial crack was extended with the use of shims on the outer steel supports. When the cracks were of the required width the beam was rotated 180 degrees and the load reapplied, forcing the previously un-cracked side to open up. Finally, the beam was placed on a flat bed and load imparted to bring it back into the level position. When the beam was located into the cyclic load test rig, wedges were positioned into the crack faces to force it back into its fully opened state. The beam was then clamped to the supports and the wedges released. However, problems occurred regarding accurate control of the crack widths, and they were thus re-measured once fixed into the rig. If the two cracks were

identical in size the test was continued, with the measured values being adopted during further analysis.

5.5.3 Crack Width Control

A series of trial tests were undertaken to examine the applicability and accuracy of the cracking technique employed. A predicted opening was calculated for several shim sizes using standard geometry, as shown in Figure 5.16. Demec pips were then placed across each of the notches (10mm from the top and bottom of the specimen) and strain readings taken before and after crack formation. Extrapolation of these measurements enabled surface and base openings to be calculated.

Results obtained from the laboratory tests produced lower surface crack widths than predicted, as shown in Figure 5.17. The experimental results indicate that the crack width obtained is 1.73 times larger than the shim size used (with a coefficient of determination of 0.92). This is much larger than the value of 2.22 times the shim size obtained from predictions. On inspection the crack was found to close slightly once loading ceased due to the resistance of the reinforcement. To avoid this affecting the results in the cyclic load testing, the pre-cracking width was set 1 shim size (0.66mm surface crack width) smaller than required. This allowed the final crack size to be formed when clamping the beam in the cyclic load test rig, ensuring that closure and looseness of fibres or reinforcement did not influence the results.

Testing was also undertaken to confirm that the cracks created in the rig were linear. To achieve this demec pips were placed at 10mm intervals across both sides of the two cracks and measurements taken both pre and post loading. An almost perfectly linear relationship was found as shown in Figure 5.18, and this was therefore approved as a suitable method for beam cracking.

5.6 Test procedure

5.6.1 Overview

During the cyclic load testing deterioration of the load transfer interface was monitored over time. The beam specimen was 400x100x100mm in size with the central 100mm section sawn circumferentially to a depth of approximately 5mm. The beam was then cracked at both the saw cuts as described in section 5.5.2 and placed in the testing rig.

The testing rig was an adaptation of the Dartec cyclic load test machine (Figures 5.1 and 5.2). The tension/compression load cell was relocated to the upper cross-head to enable both positive and negative loading to be applied. Straps were constructed to fix the edges of the beam to the frame, and hold the central block to the load source. They also allowed 360 degree rotation of the loading plate enabling precise control of its orientation.

Calibration of the Dartec test machine was undertaken by an external organisation twice during the testing period. However, the load levels applied to the specimen were monitored every 600 cycles during all tests to ensure errors did not occur.

5.6.2 Beam Orientation

During trial testing it became clear that the beam orientation had to be carefully assessed. To obtain good control of crack width during preparation, the beam was required to have the trowelled surface uppermost providing a smooth face against the shims. After formation, the beam required a 180-degree rotation to produce the correct crack orientation within the cyclic load test rig. This resulted in the roughened trowelled face being placed directly on the supports, thereby reducing the accuracy of the final surface crack width.

When using this approach the specimen was reversed to the orientation of casting when placed in the cyclic loading test rig. According to Abdel-Maksoud (2000) this can lead to errors when comparing against real slab conditions due to the movement of mix materials when under vibration. Large aggregate tends to sink, being replaced by mortar, with fibres becoming orientated in one direction due to the consolidation process. Both of these actions could affect the characteristics of the shear surface and thereby the load transfer efficiency.

To overcome these concerns the beam was positioned trowelled surface upwards within the cyclic load test rig. This reduced the accuracy of the initial crack caused by undulations on the surface. However, since the pre-cracking width would be one shim smaller than that required in the rig (section 5.5.3), the error in the resultant test would be negated.

5.6.3 Rig Configuration

The test rig consisted of two steel side blocks on which the relevant shim combinations were placed, with the beam edges positioned on top. All were rigidly clamped to the test

frame, forcing the beam into an angled position and opening the cracks to the required size and geometry (Figures 5.1 and 5.2). The central section was strapped to the cross-head via a 50kN load cell, which was linked directly back into the Dartec test machine allowing load magnitude to be monitored and adjusted as required. Linear variable differential transducers (LVDT's) with a maximum travel of 4mm, repeatability of $<0.15 \mu\text{m}$ and sensitivity of $133.33 \text{ mV/V/mm} \pm 0.5\%$, were fixed to the face of the concrete specimen enabling the measurement of displacements. These were calibrated three times during the test by the laboratory technicians and on all occasions were found to be acceptable. The LVDT was glued on the outer section of the beam via an aluminium holding bracket, with the target sited on the central section, free to deflect in both the positive and negative directions. This method of LVDT placement was chosen to prevent agitation of the reaction frame being included in any measurements taken. Initially, the glue to attach the LVDT's and targets to the concrete face was a two-part epoxy resin. Due to the relatively slow nature of the setting process it was difficult to position the targets accurately as slippage regularly occurred. Bostik superglue (a rapid setting adhesive) was therefore used which enabled instant fixing and accurate placement. This allowed the target to snap off if excessive deflection was forced on the LVDT, providing increased protection against instrument damage upon beam failure.

Prior to testing, the LVDT was adjusted against the target to produce a near zero reading. This enabled equal movement in the positive and negative directions, with the actual value recorded to enable taring at a later stage. On application of load the central block moved in relation to the end sections, which in turn caused an elongation or compression of the vertical LVDT. This generated a change in voltage which was amplified, and recorded temporarily on a Campbell Scientific CR10X data logger. The information was passed periodically into a standard laptop computer in the form of a text file, where the data was further analysed. This process is shown in diagrammatic form in Figure 5.19 with further information on the data logging procedure provided in section 5.7.

5.6.4 LVDT Positioning

During the early tests, each crack had a vertical and horizontal LVDT placed on the front and rear face of the specimen, as shown in Figure 5.20. This enabled any opening of the crack to be measured alongside the vertical movement caused by application of load. After several trial tests the horizontal movement was found to be extremely small (below 0.003mm) with difficulties in determining whether this was caused by crack opening, rotation or misalignment of the target. Due to the test configuration it was unlikely that

significant horizontal movement could be accommodated as clamping of the beam on an angle prevented either side from moving apart. The position of LVDTs was therefore changed to enable increased vertical measurements to be taken.

The second set-up required vertically placed LVDTs on the front face of the specimen for both cracks as shown in Figure 5.21. On the rear of the specimen a single LVDT was fixed in the vertical direction, with another in the horizontal direction to retain a check against crack opening. This set-up provided increased vertical movement data and enabled the calculation of rotation in the central section. To obtain measurements in the plane of the specimen a moveable strain gauge was placed periodically on the face and rear of the beams, with values being manually monitored.

5.6.5 Safety Precautions

As a safety precaution, steel blocks were placed under the lower central section of the test specimen (Figures 5.1 and 5.2). A 5mm gap was retained to allow for vertical movement, but should significant displacements occur, damage to the LVDTs and the test facility was prevented. A trip function was also incorporated into the control settings to shut the machine off if high fluctuations in load magnitude were identified (signifying machine error or specimen failure). This allowed the test to be run for its full duration, and prevented the fluctuations in displacement which had been identified when using a stop/start loading regime. These had been caused by a drop in pressure when the machine was turned off, forcing the central block back into its original position (Figure 5.22).

5.7 Data Logging

The recording of data obtained from the cyclic loading tests was carried out using a Campbell Scientific CR10X data logger and the PC208 computer software. A program was written which enabled the logger to take a series of readings at its maximum rate. Due to the large amount of data collected only periodic collection at 5 minute intervals (600 cycles) was possible. The burst option was set to continually monitor for 0.5 seconds, enabling one complete 2Hz load cycle to be recorded. During this period fifty LVDT and load readings were taken, resulting in a measurement at approximately every 0.01 seconds. Unfortunately, the exact period between each measurement within the burst cycle could not be established as the logger only recorded a time for the first data point.

Each measurement taken with an LVDT and recorded by the data logger was calculated into a displacement using the relevant coefficients. The original LVDT reading taken prior to test start-up was then subtracted to provide a measure of movement from the original location. The maximum and minimum displacements were then determined from each burst cycle (Figure 5.23), and plotted against cycle number to show the effect of crack degradation (Figure 5.24). The total variation between each maximum and minimum point for an individual cycle was also calculated to achieve a total differential, which was then plotted against cycle number to give an overall indication of displacement change (Figure 5.25). Where required, individual plots showing an individual cycle were examined to determine the source of load resistance.

Visual examinations were made of the specimens periodically throughout each test. This involved assessing the amount, size and type of any ejected material caused by crack face deterioration. In fibre-reinforced specimens the behaviour of the fibres could also be identified at the outer sections to examine their failure modes. Once the test was complete the specimen was broken open across the crack face (if reinforcement was still holding it together) and any significant effects were identified. This could include excessive face cracking, aggregate looseness or reinforcement bond.

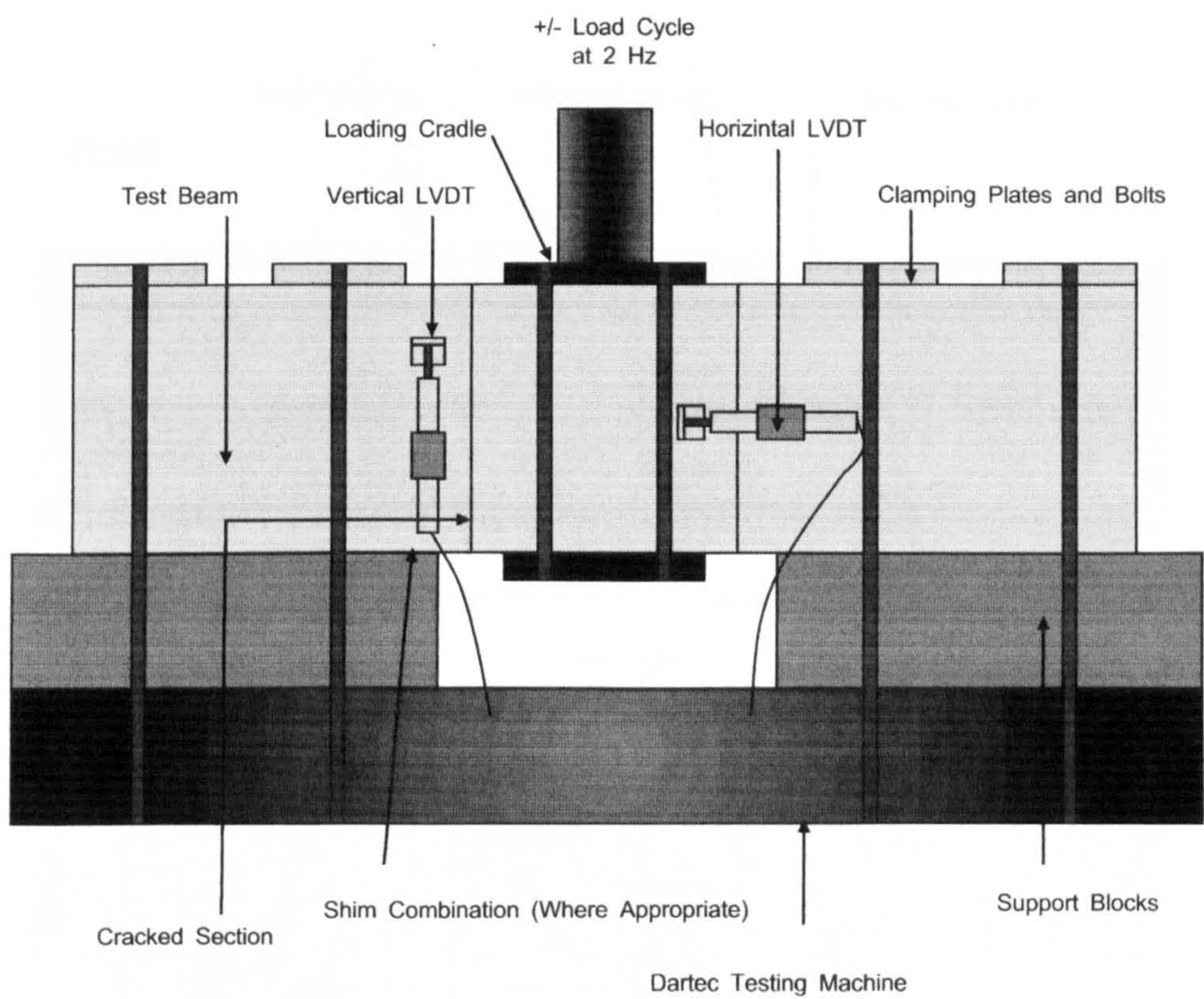


Figure 5.1 – Cyclic loading test set-up (Schematic)

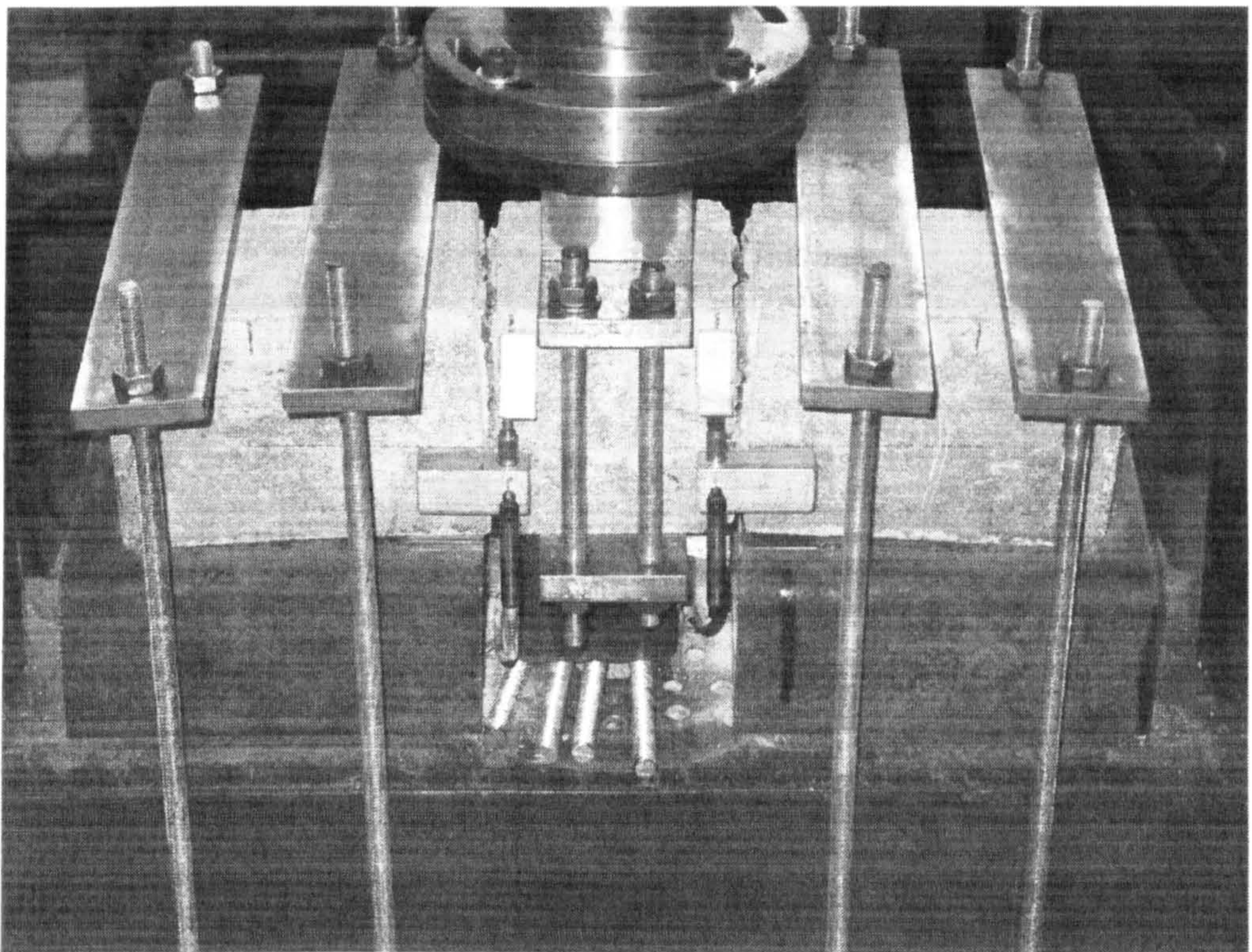


Figure 5.2 – Cyclic loading test set-up (Plate)

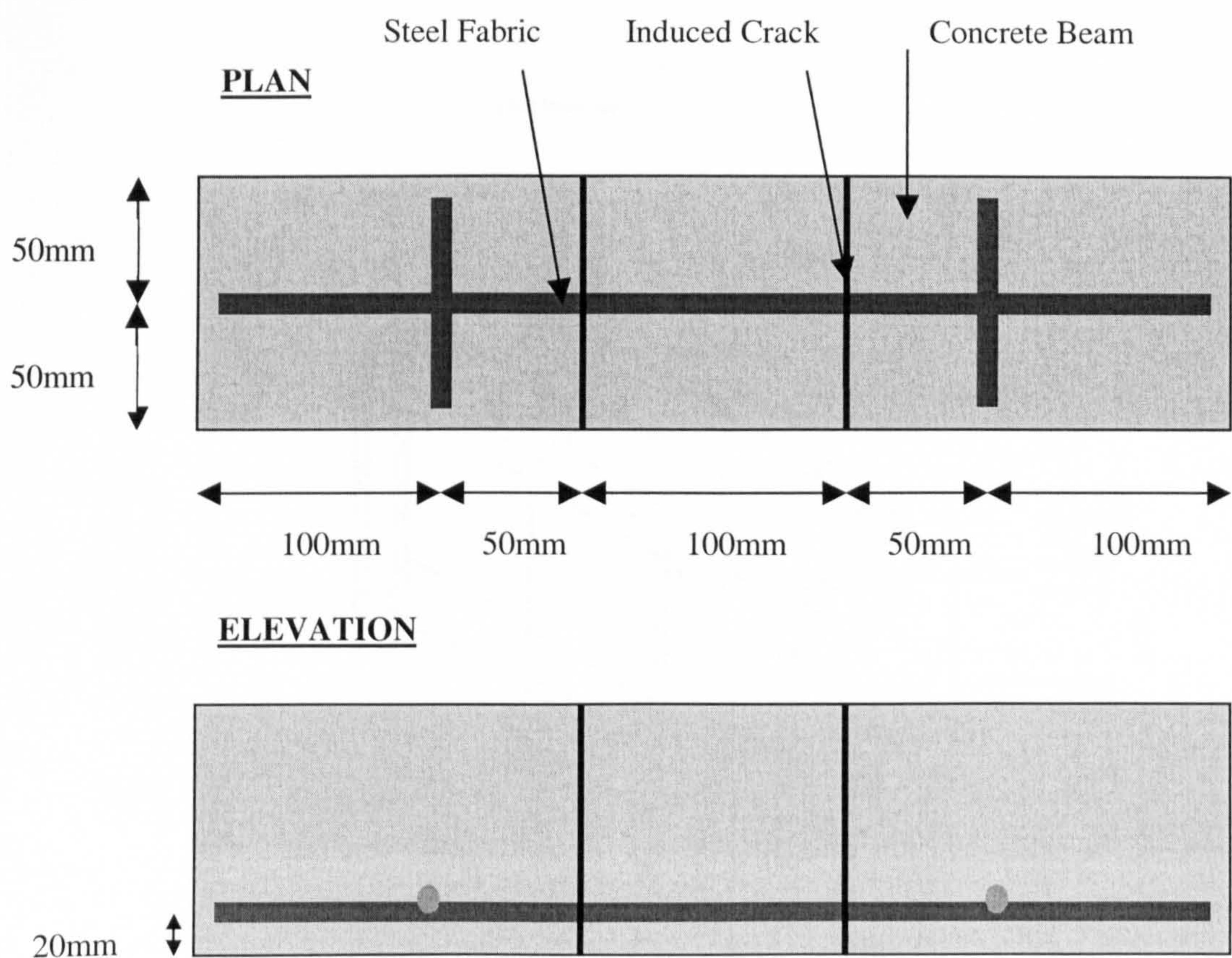


Figure 5.3 – Steel fabric and reinforcing bar layout and positioning

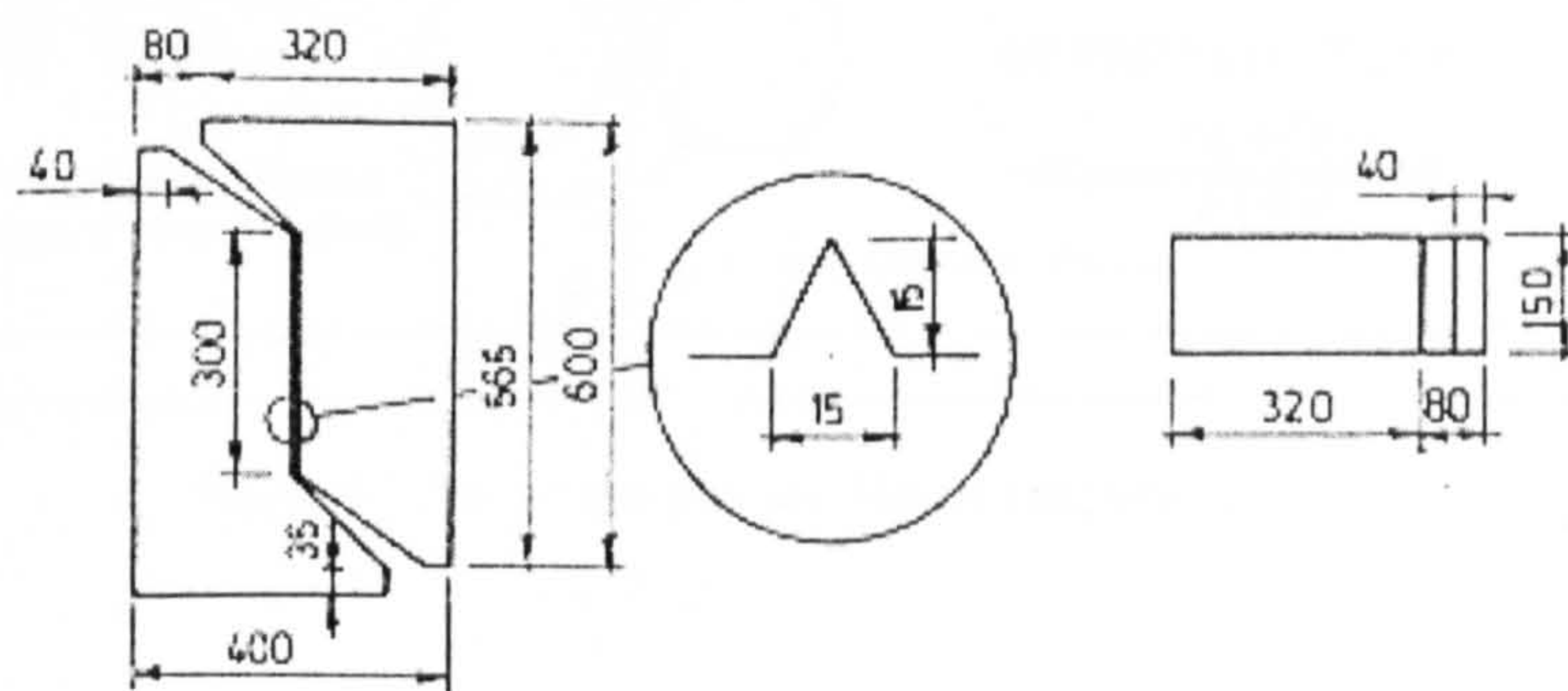


Figure 5.4 – Typical single crack test specimen (Valle and Buyukozturk 1993)

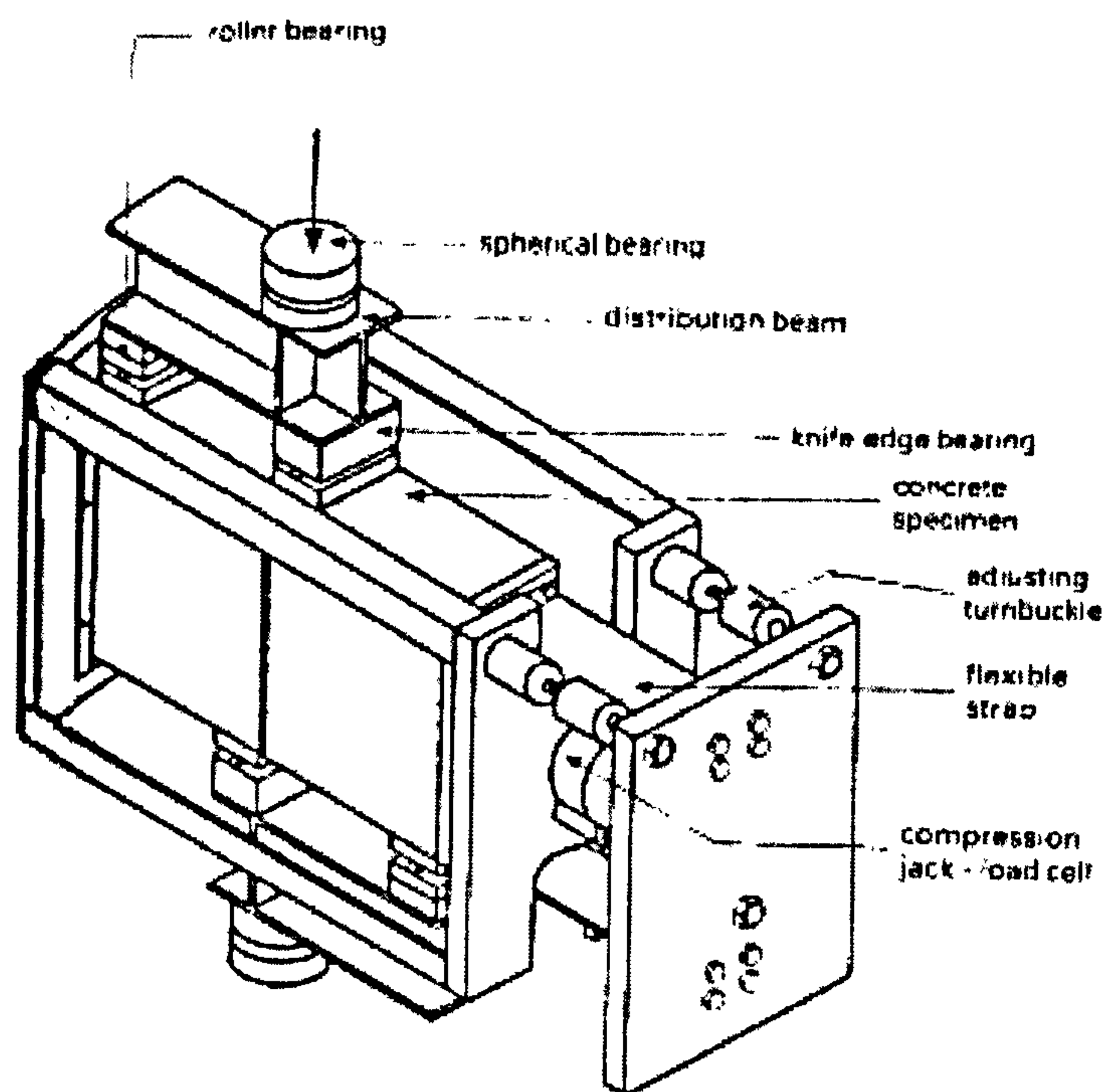


Figure 5.5 – Single cycle load test set-up (Millard and Johnson 1984)

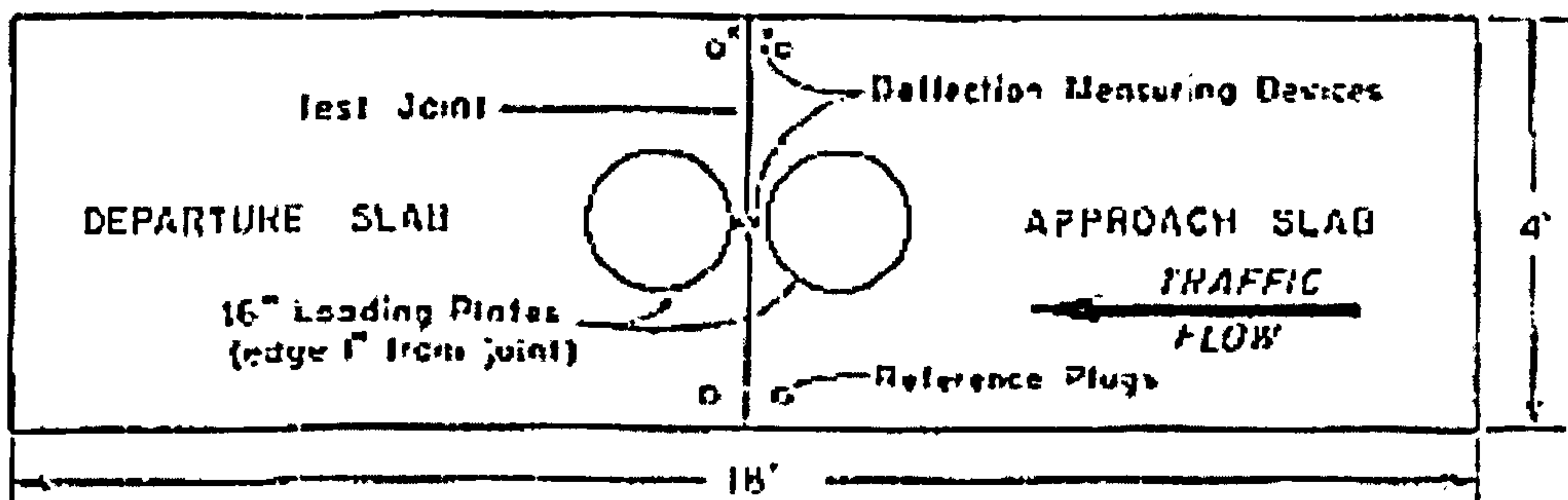


Figure 5.6. Plan of test slab and instrumentation.

Figure 5.6 – Large-scale slab laboratory set-up for cyclic load testing (Colley and Humphrey 1967)

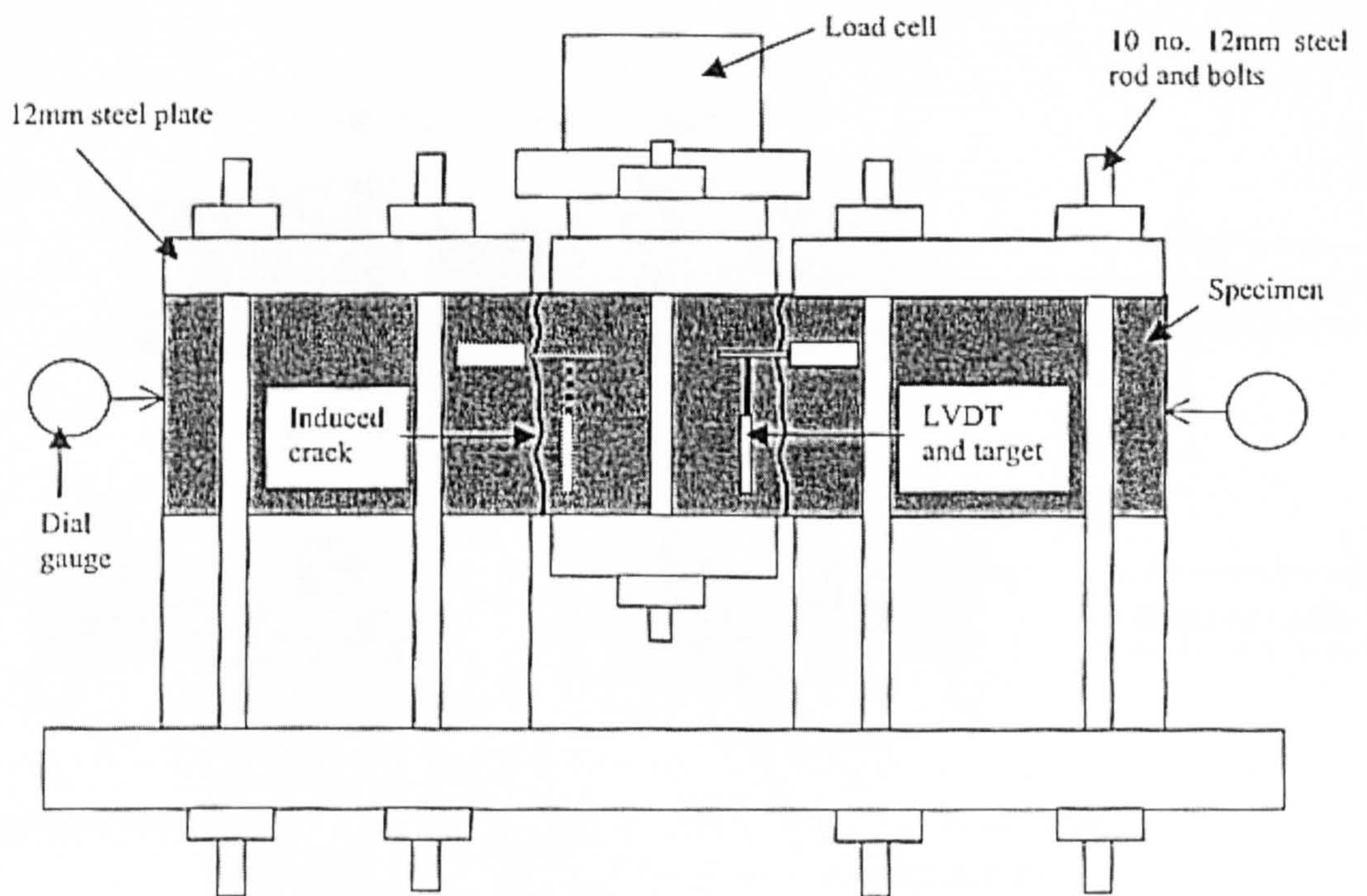
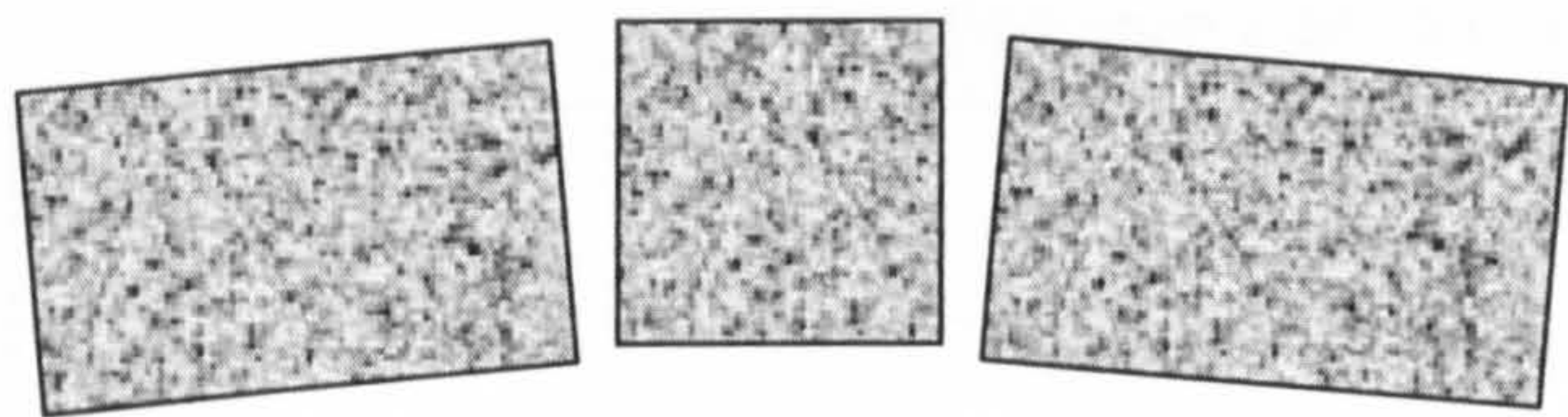


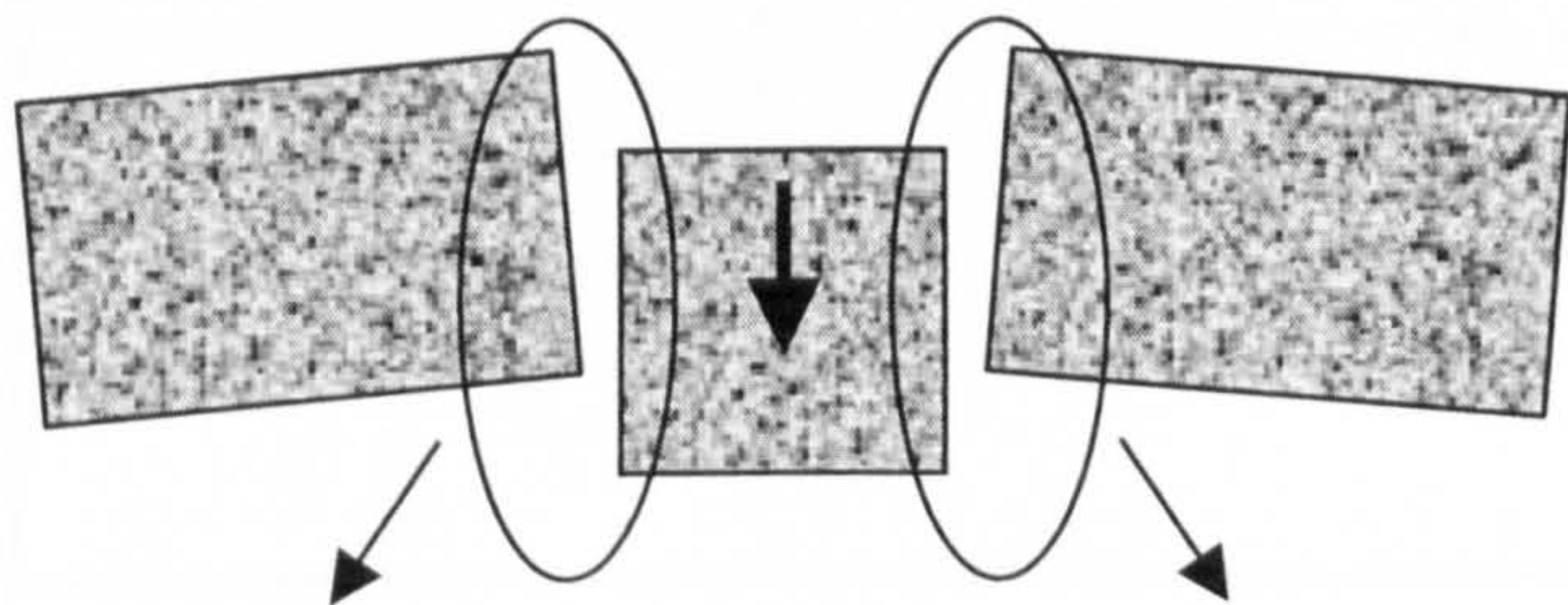
Figure 5.7 – Double crack test set-up for cyclic loading (Thompson 2001)

Position 1 - Neutral

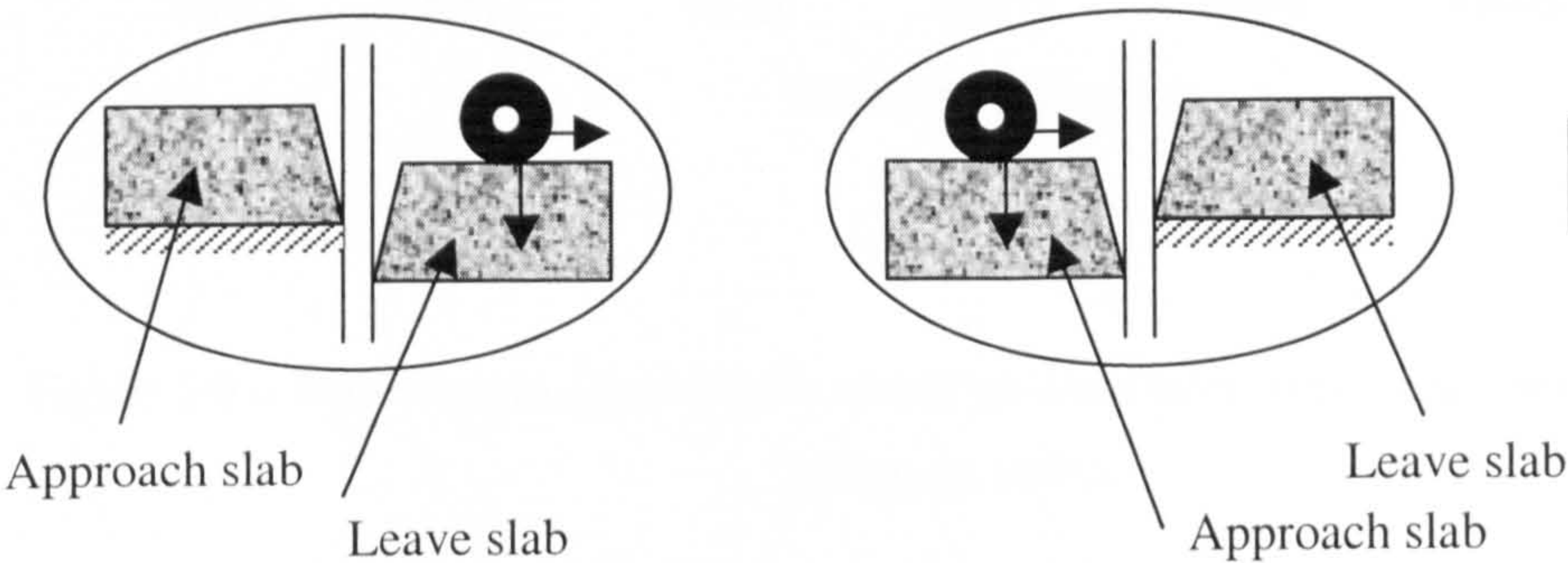


Lab specimen

Position 2 – Positive Load

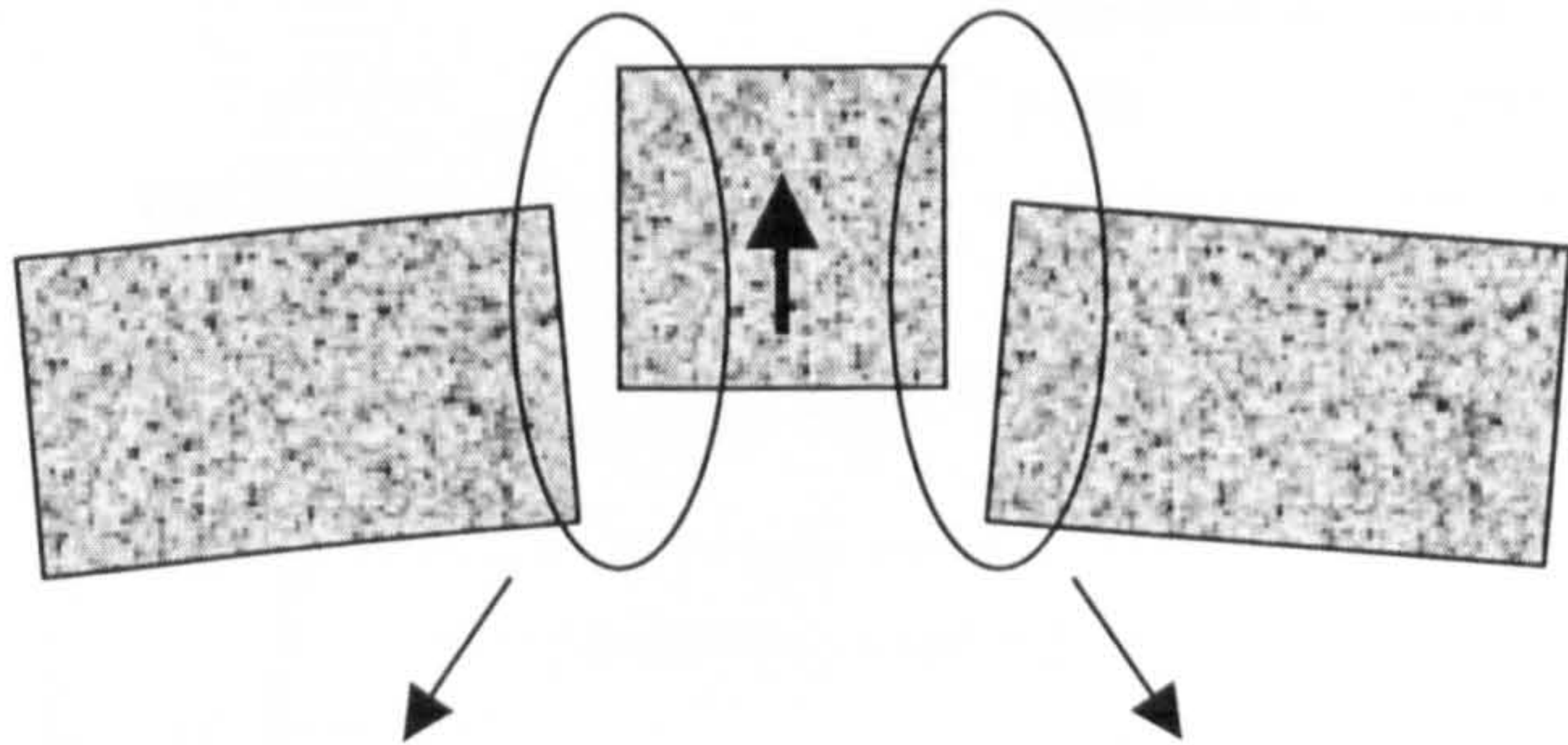


Lab specimen

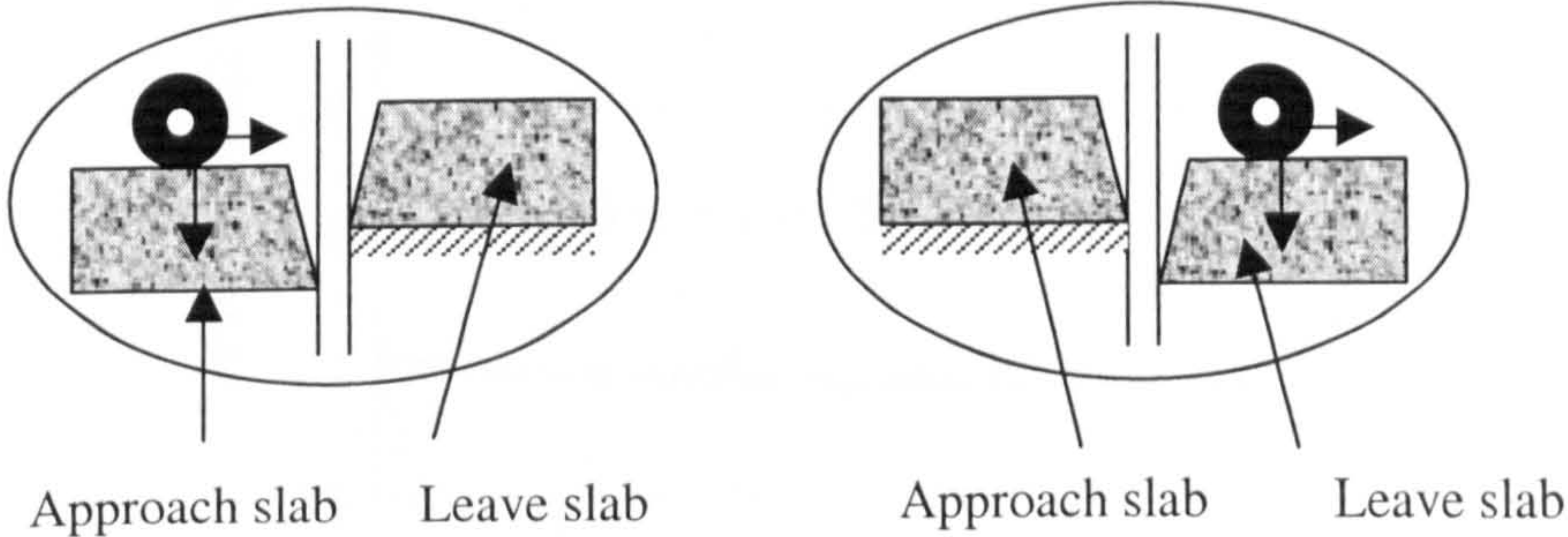


In-service slab

Position 3 – Negative Load



Lab specimen



In-service slab

Figure 5.8 – Representation of in service slab loading using positive and negative laboratory loading

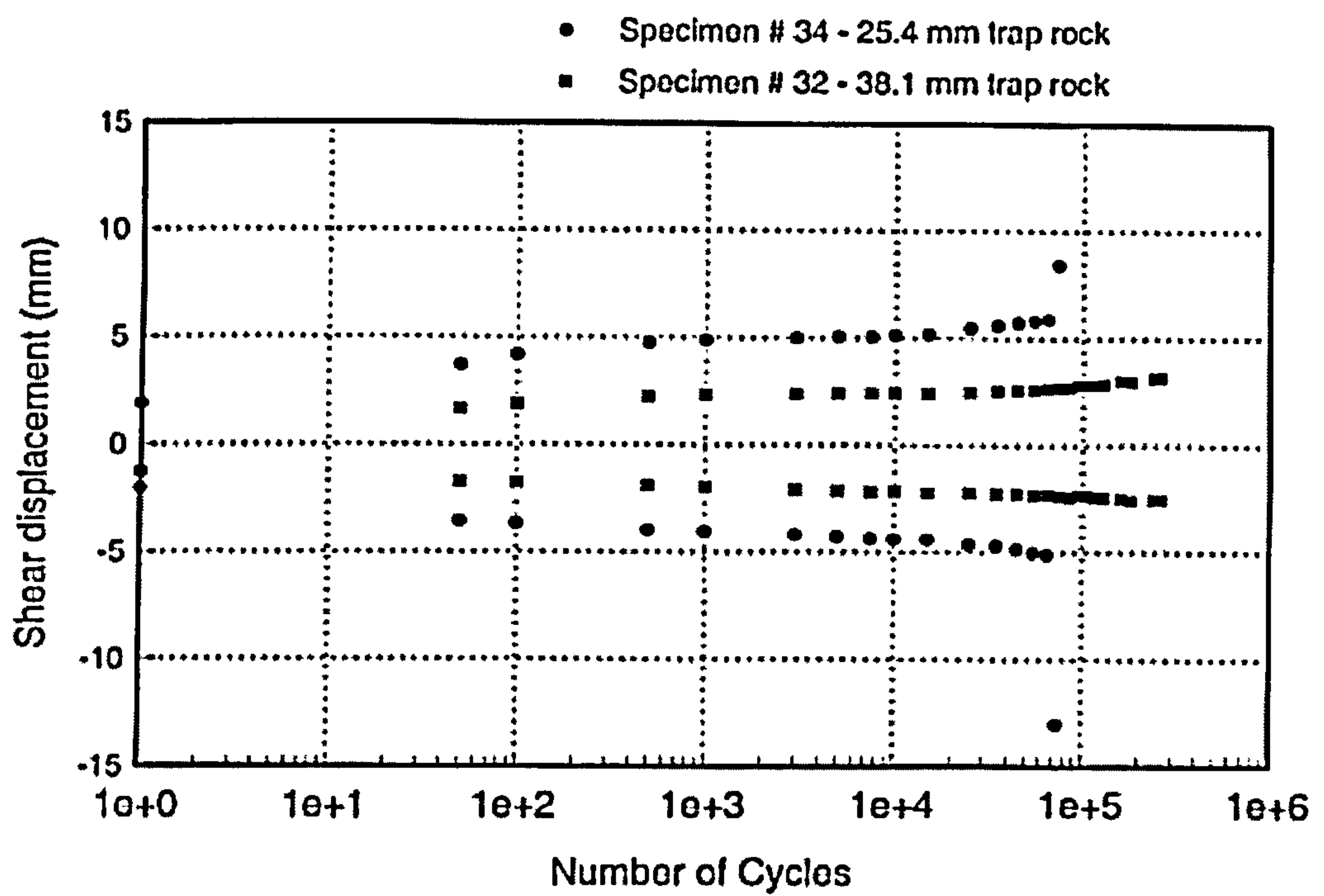


Figure 5.9 – Reduction in shear displacement gradient over increasing load cycles (Abdel-Maksoud 2000)

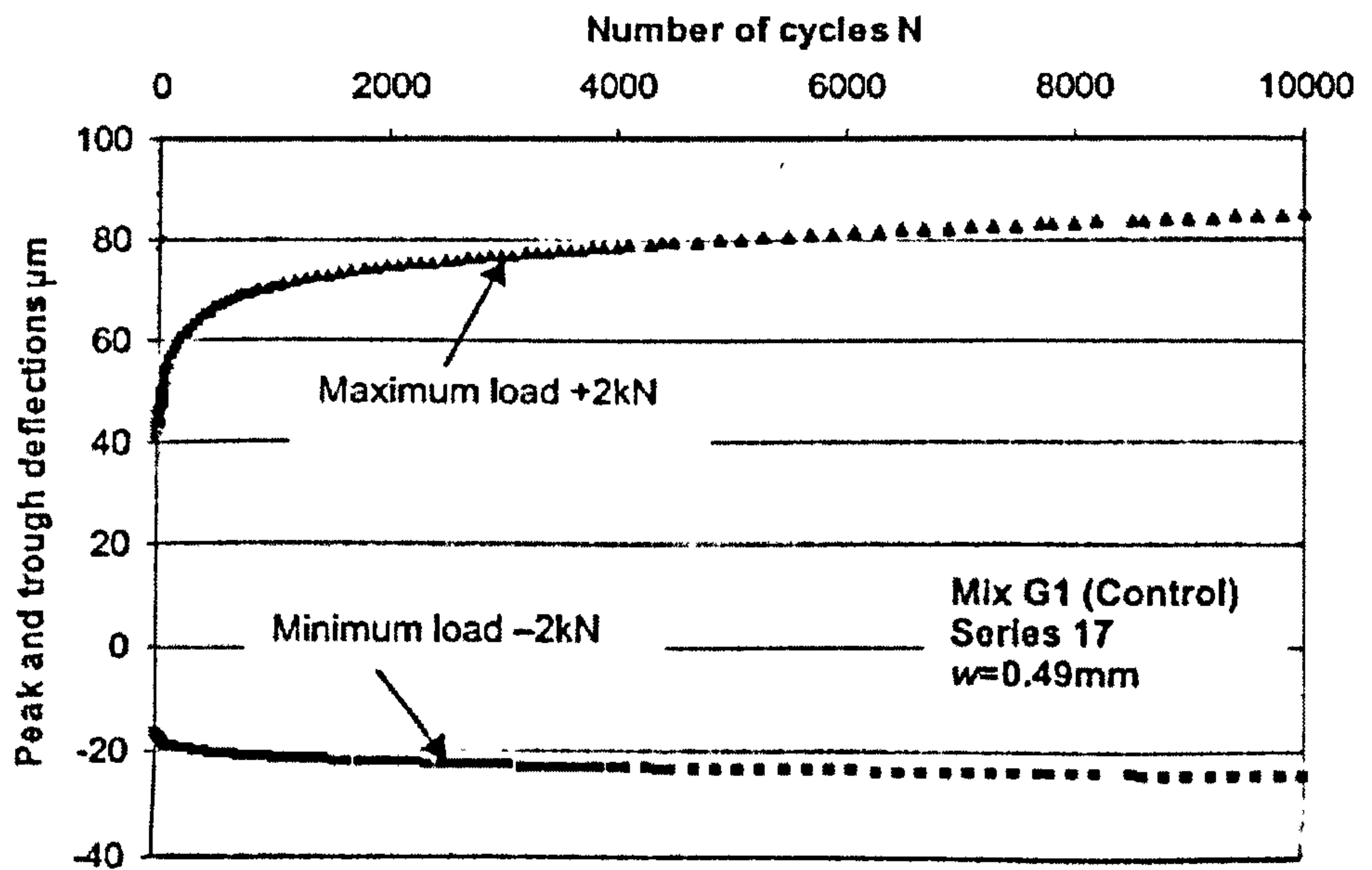


Figure 5.10 – Reduction in peak and trough deflection gradient with increasing load cycles (Thompson 2001)

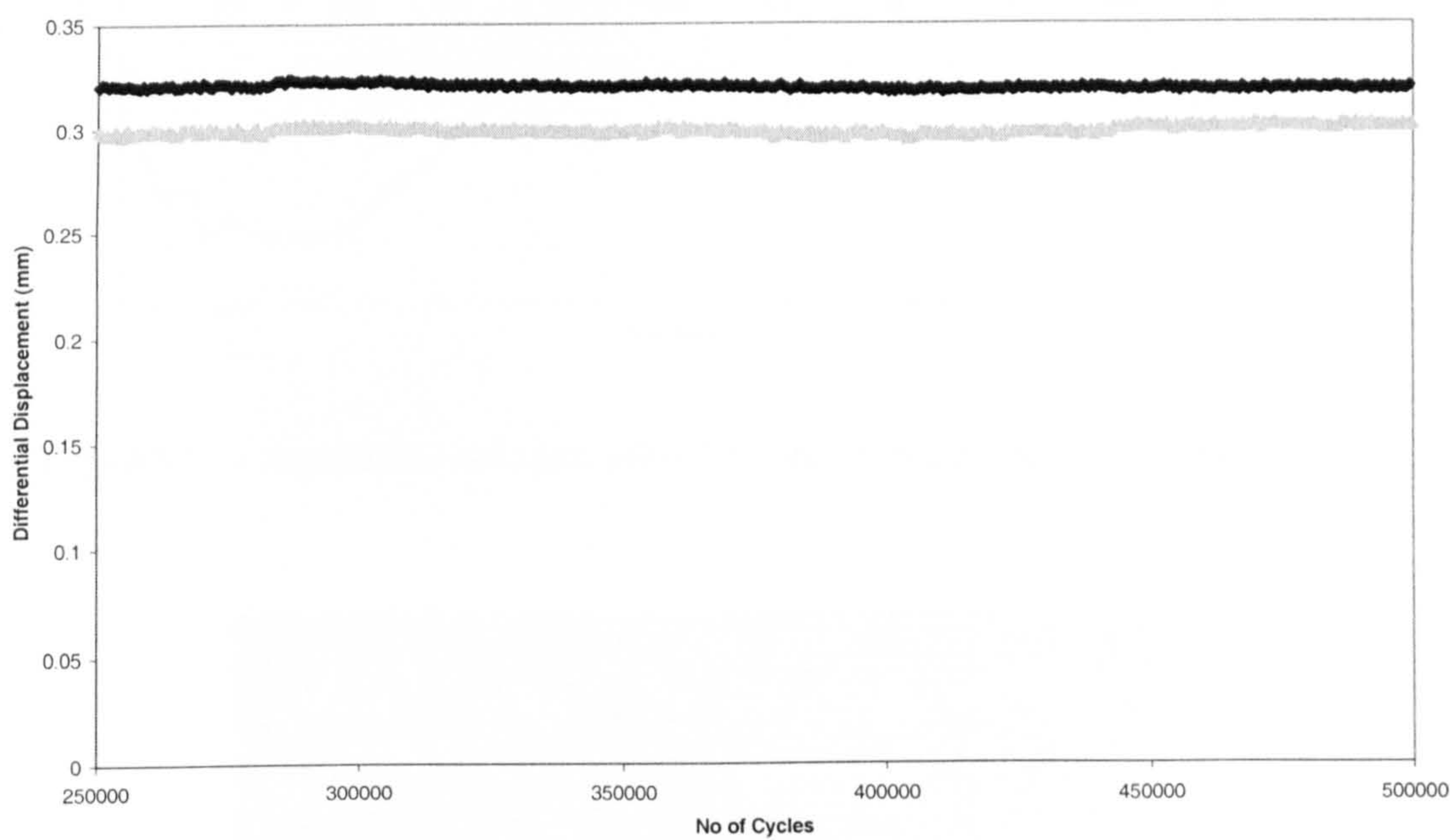
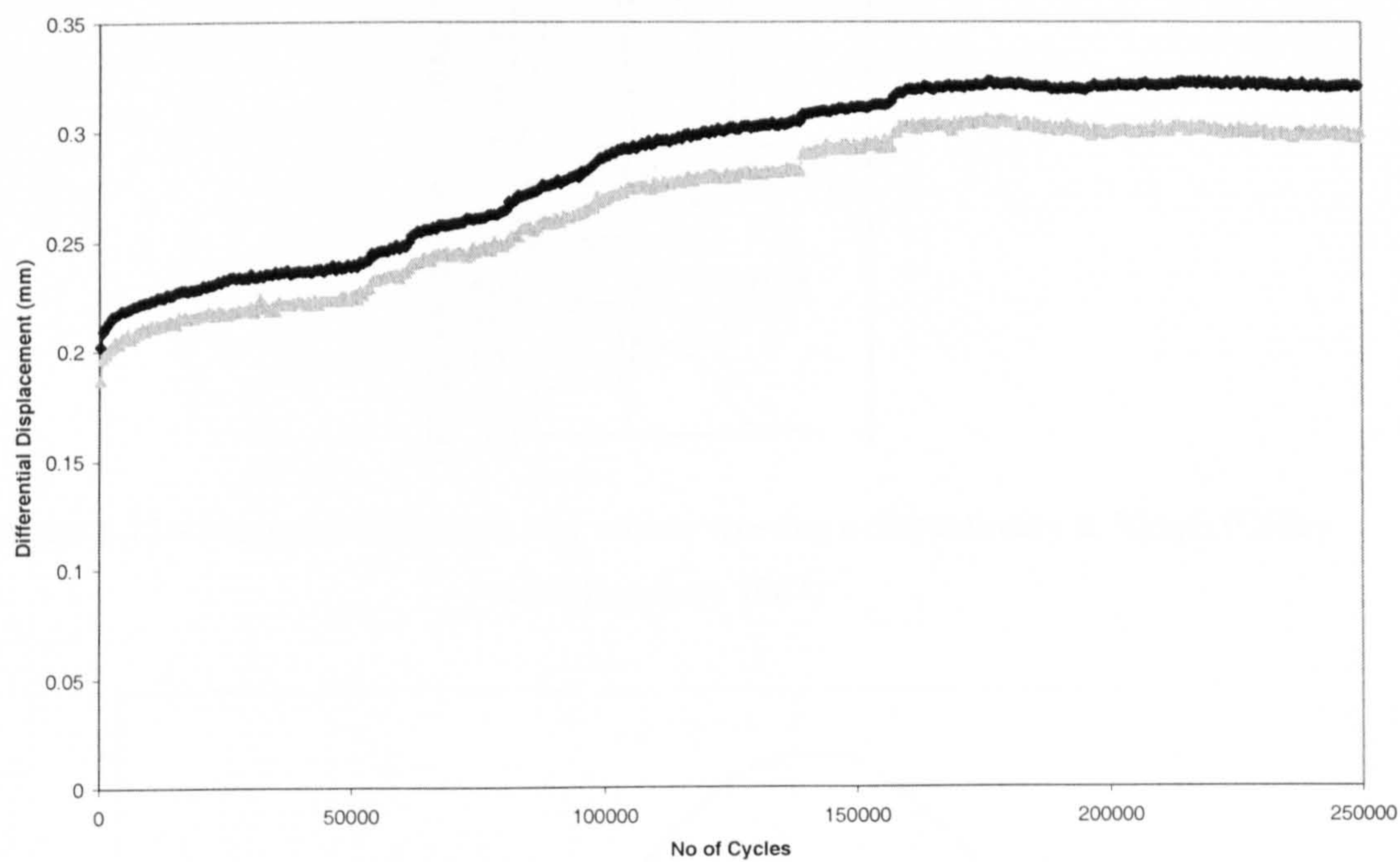


Figure 5.11 – Trial testing differential displacement plot, 0 – 250,000 cycles (Top),
250,000 – 500,000 cycles (Bottom)

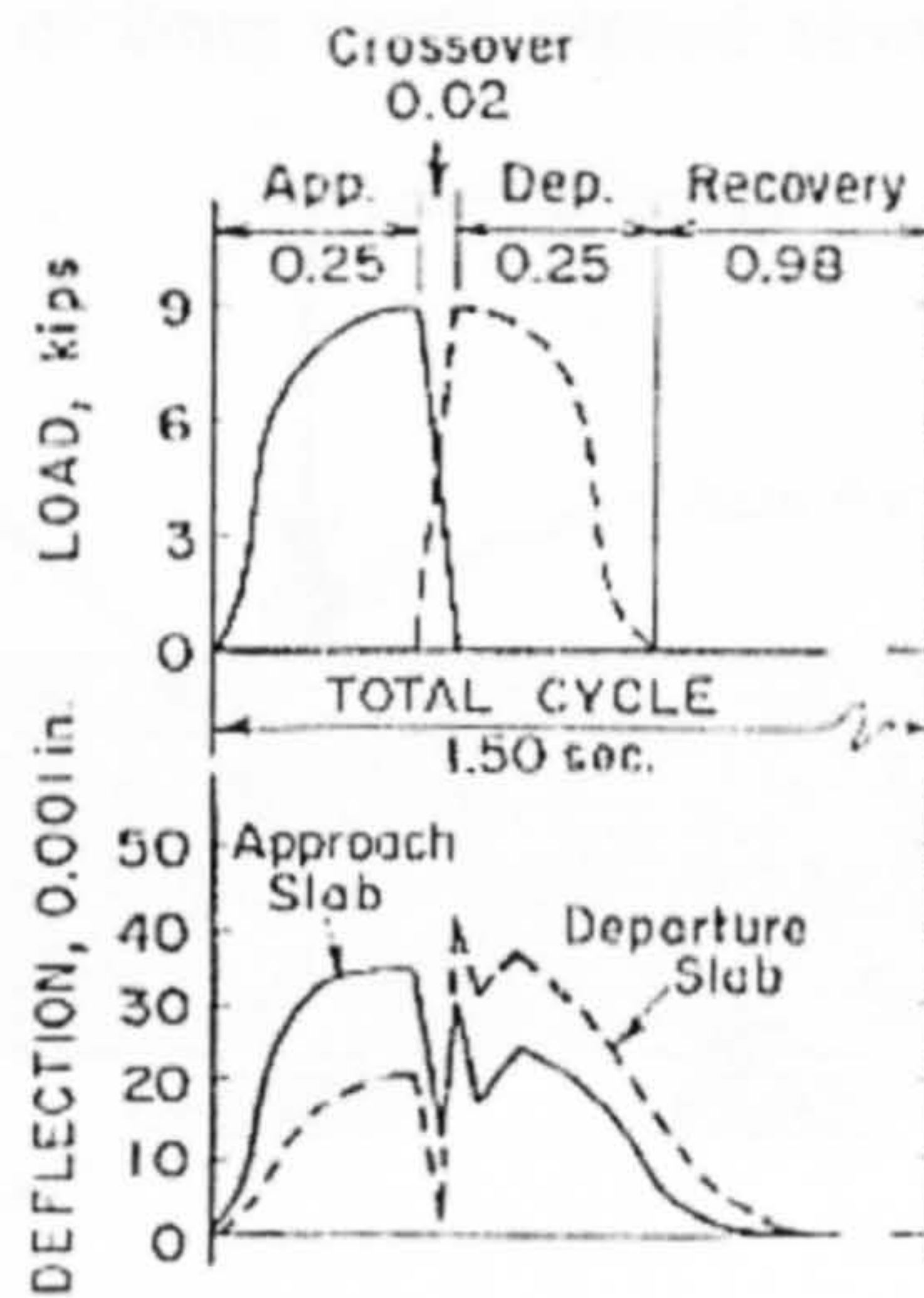


Figure 5.12 – Measured load cycle of a vehicle crossing a discontinuity at 30mph (Colley and Humphrey 1967)

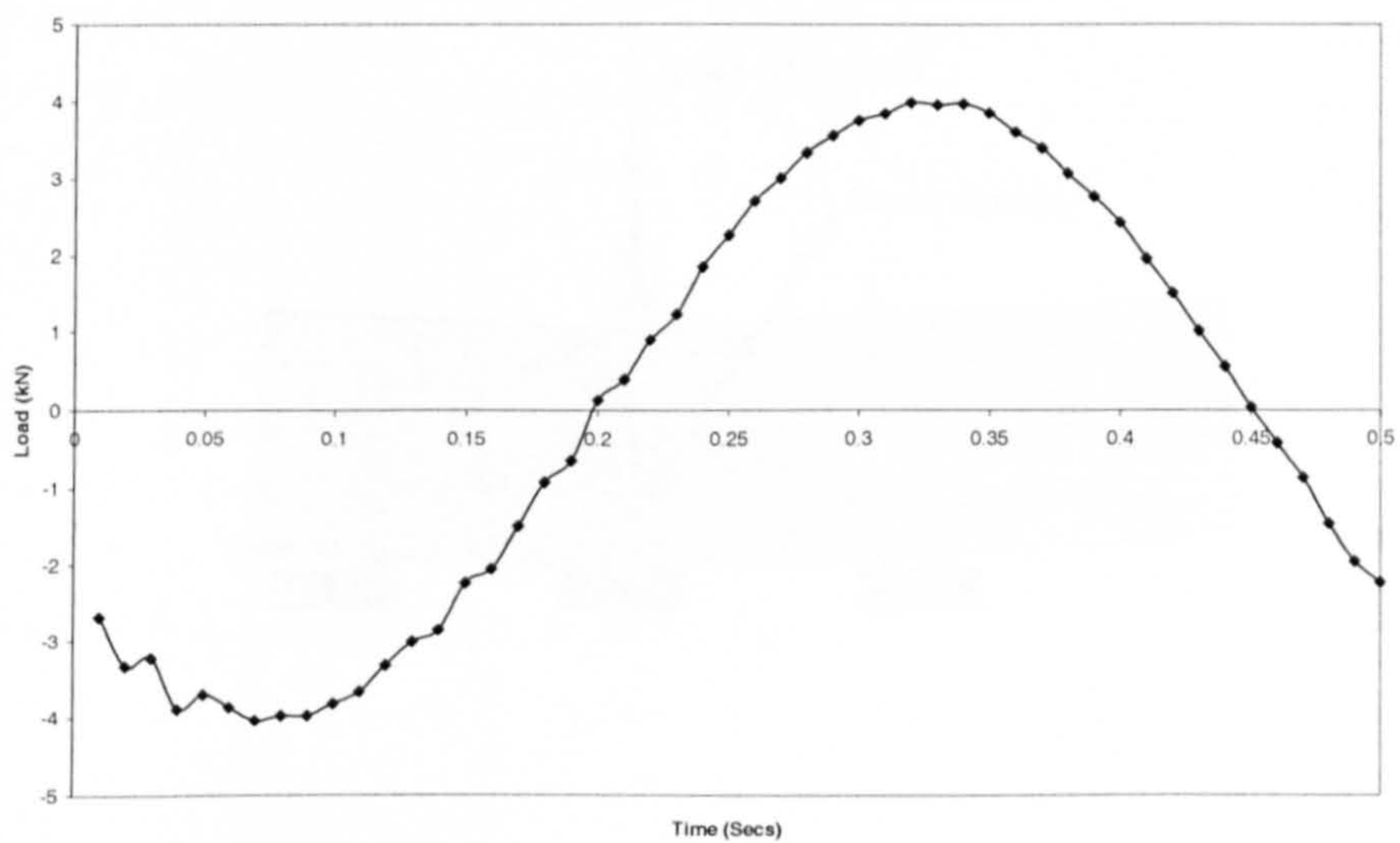


Figure 5.13 – Sinusoidal load application from the Dartec cyclic load test machine

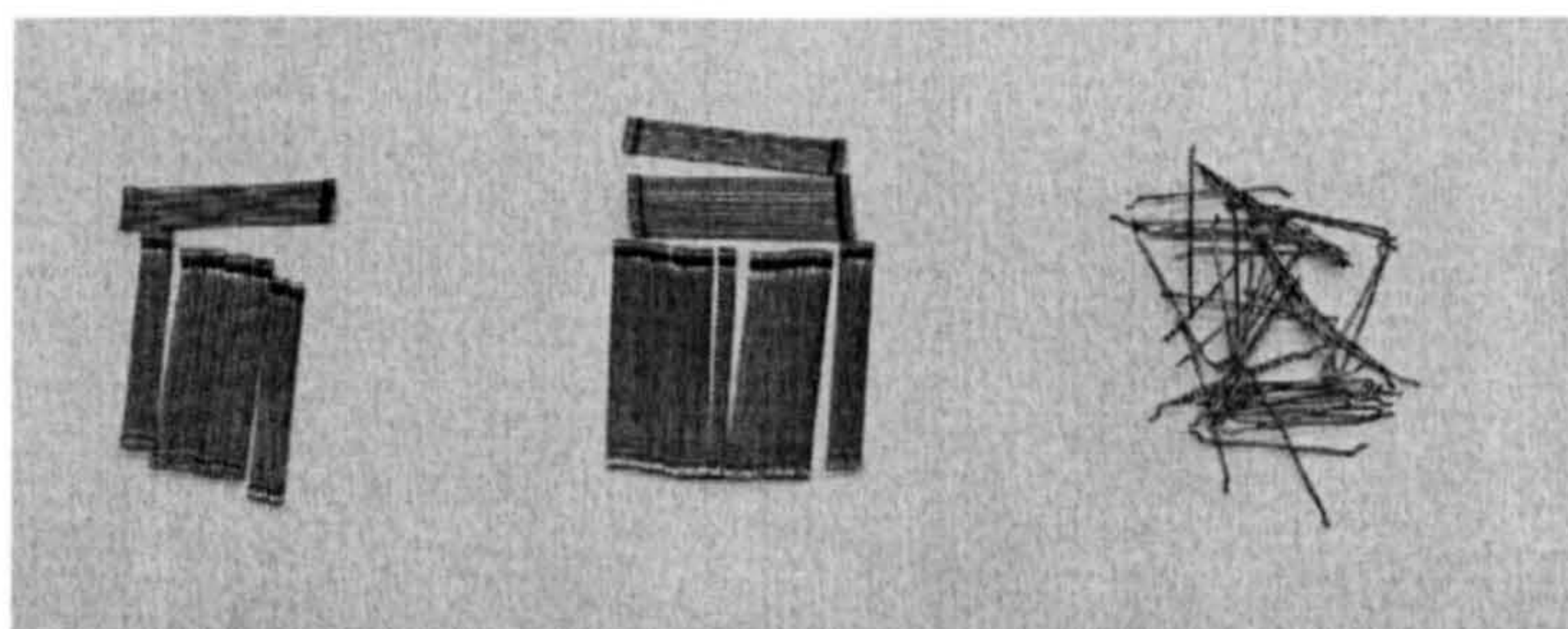
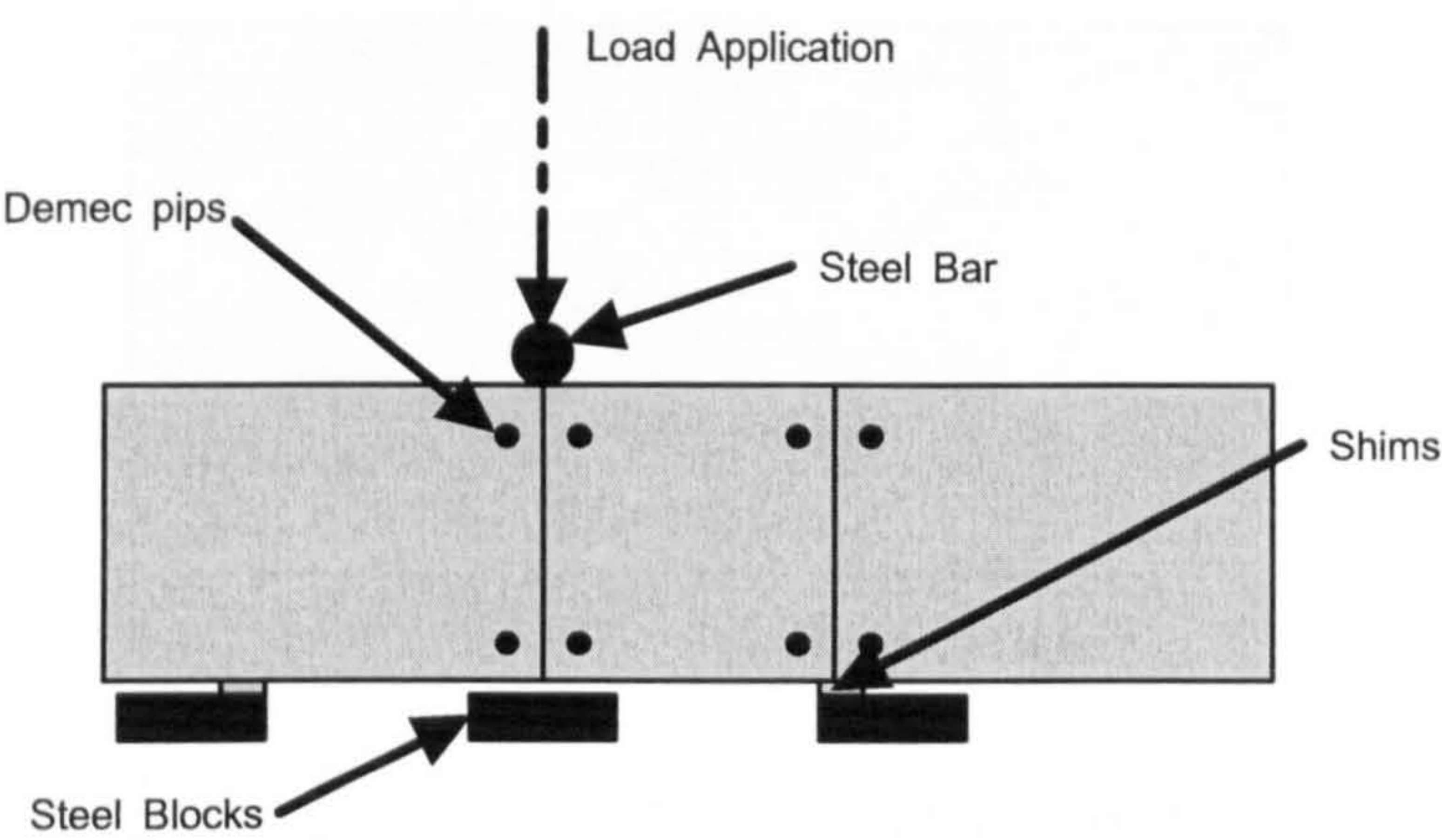
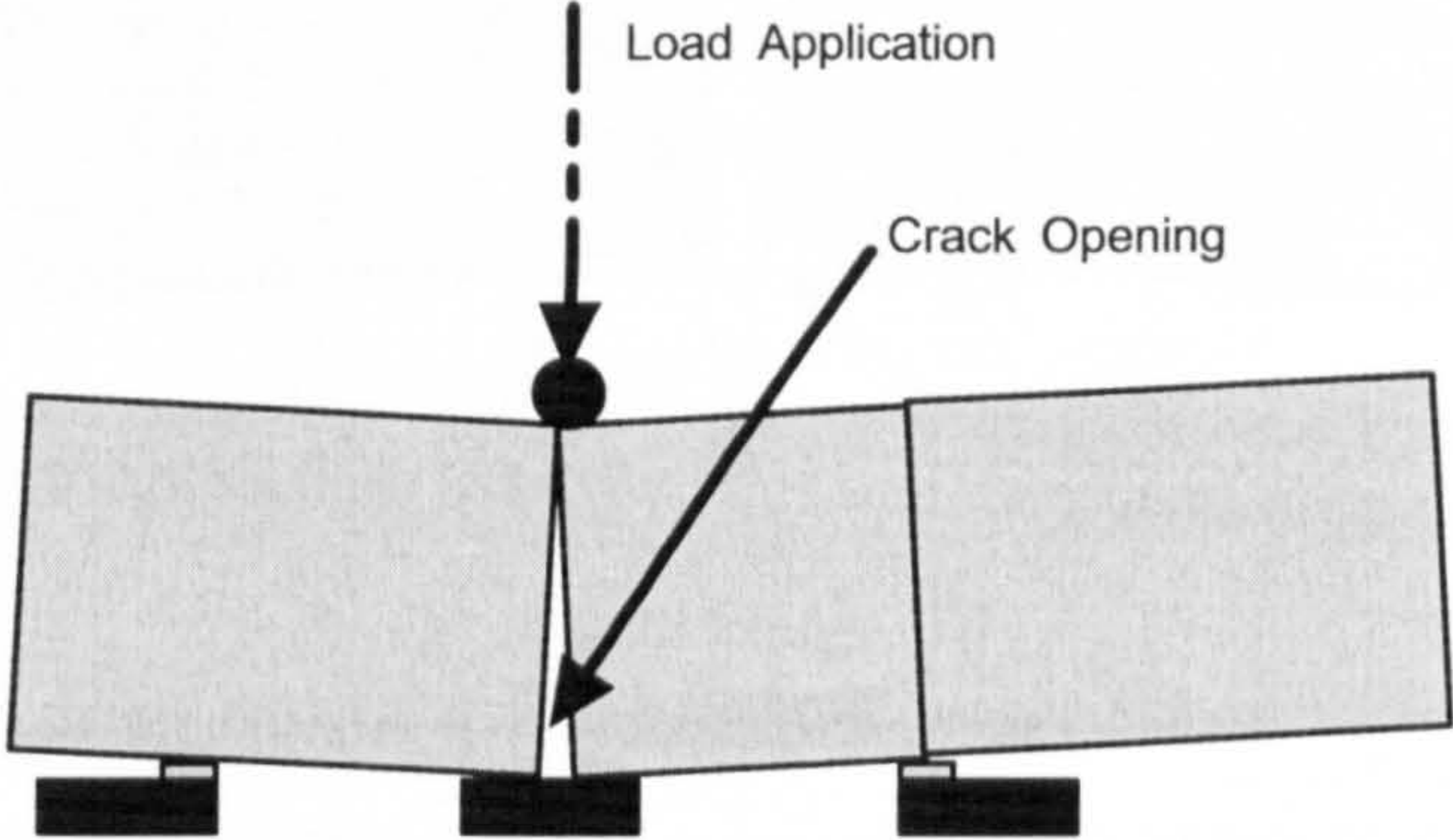


Figure 5.14 – Bekaert Dramix® Steel fibres used within the experimentation (from left: RC-65/60-BN, RC-80/60-BN, RL-45/50-BN)

Saw-cut of 6mm depth placed circumfrentially



3 Point Bending to Form First Crack, Shim Size Controls Dimensions



Second Crack Formed, Beam may be Inverted to Produce Parallel Geometry

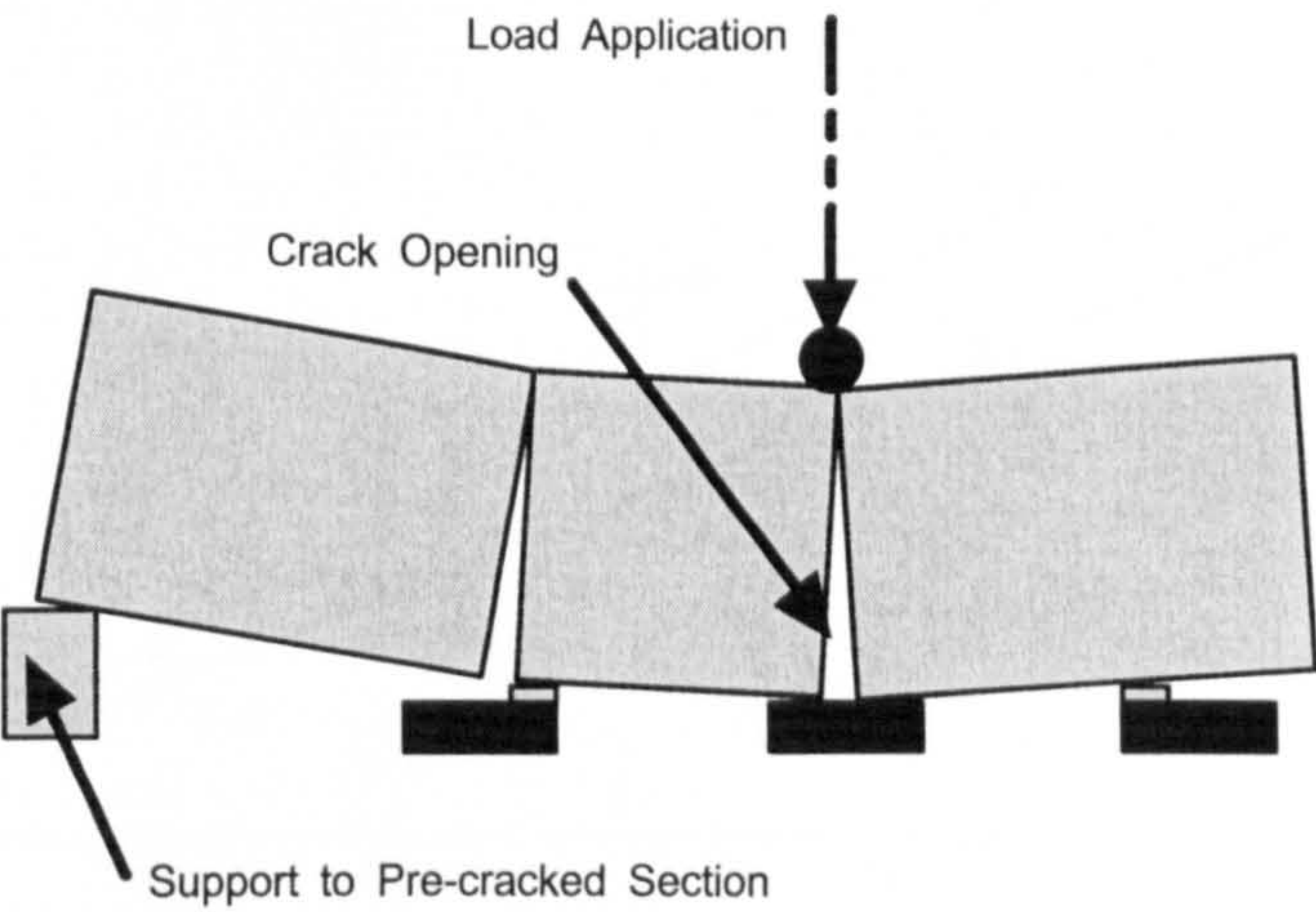
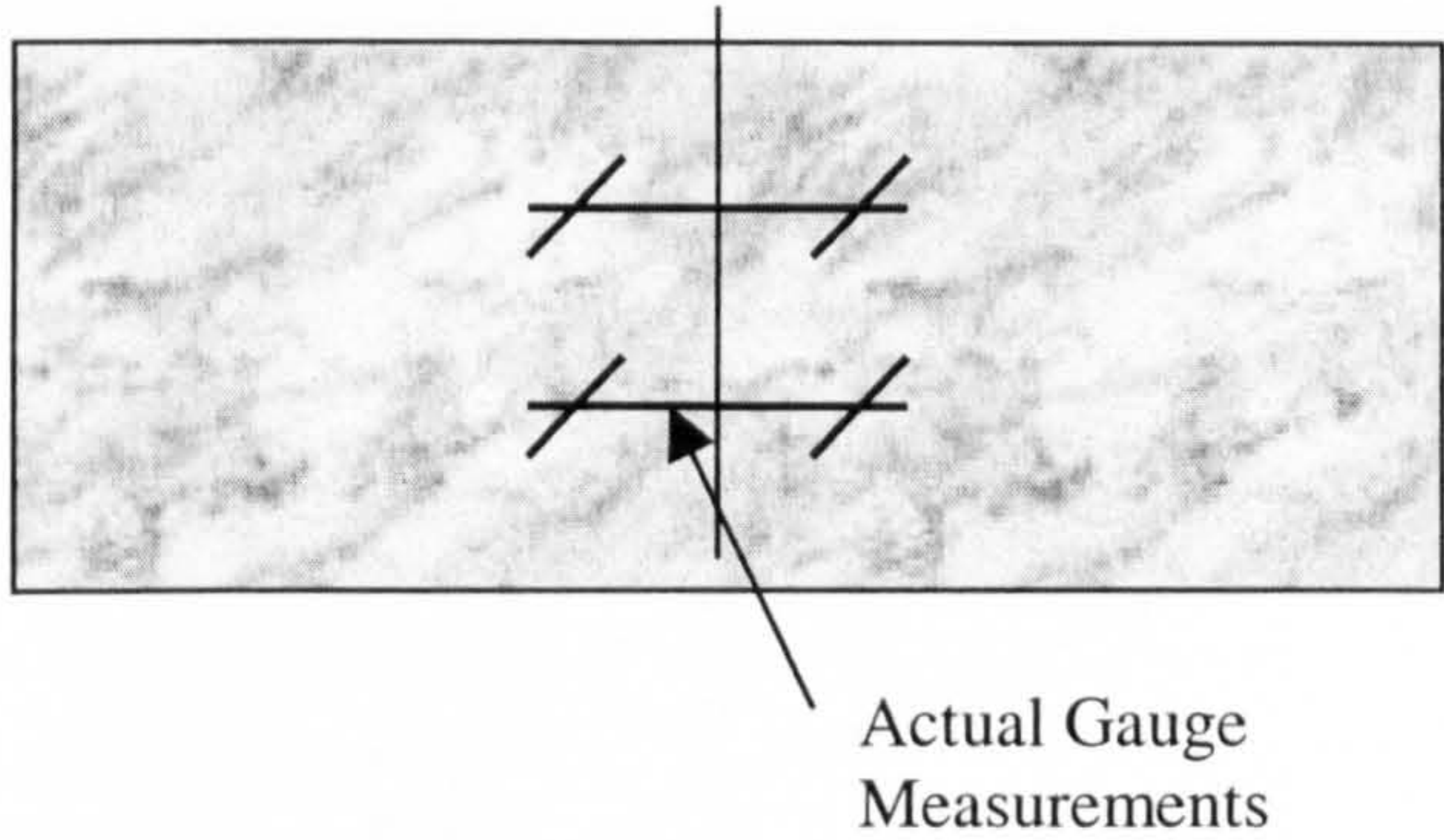


Figure 5.15 – Method of inducing cracks into test specimens

Pre-Cracking



Post-Cracking

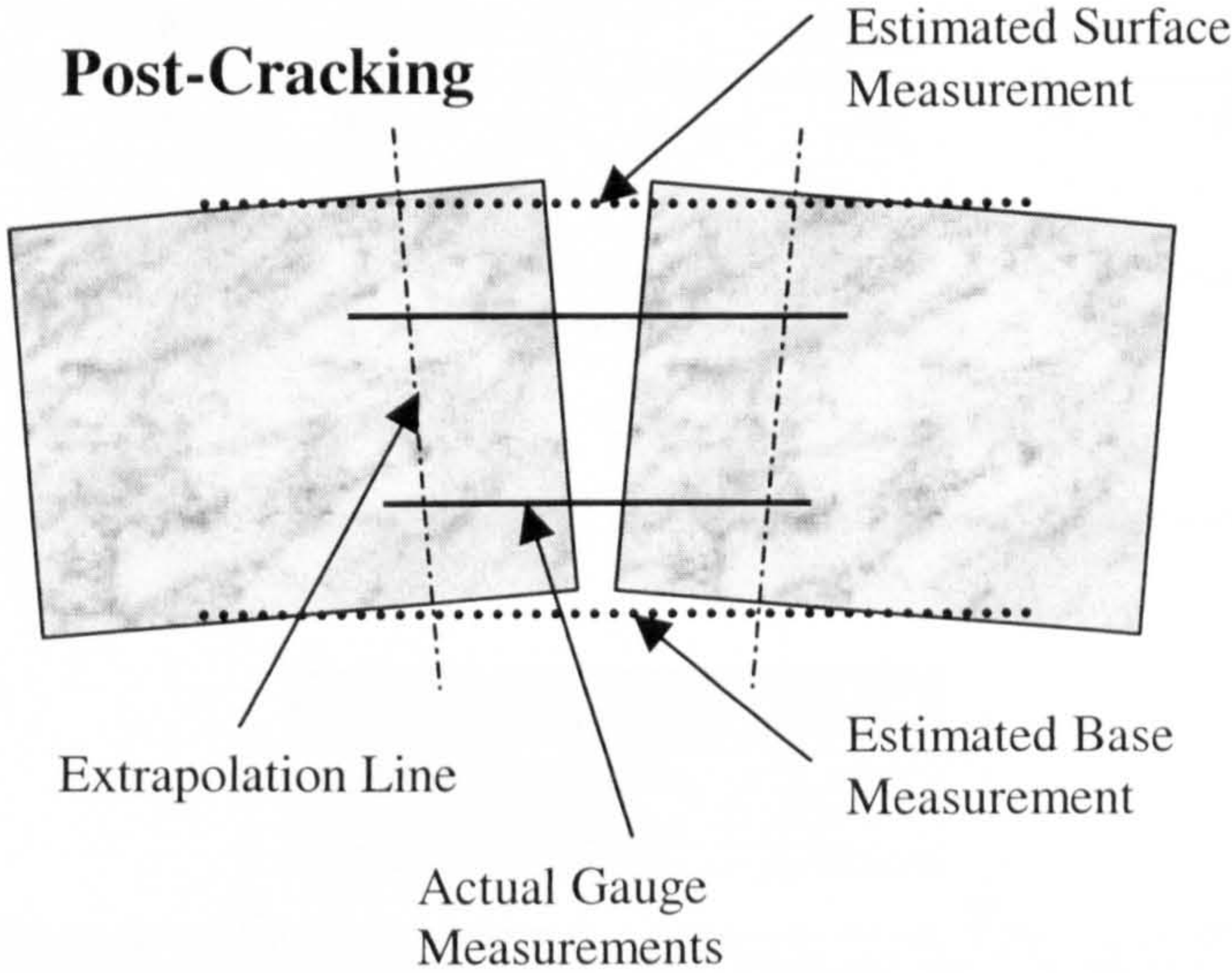


Figure 5.16 – Extrapolation of demec pip measurements to obtain surface and base crack width measurements

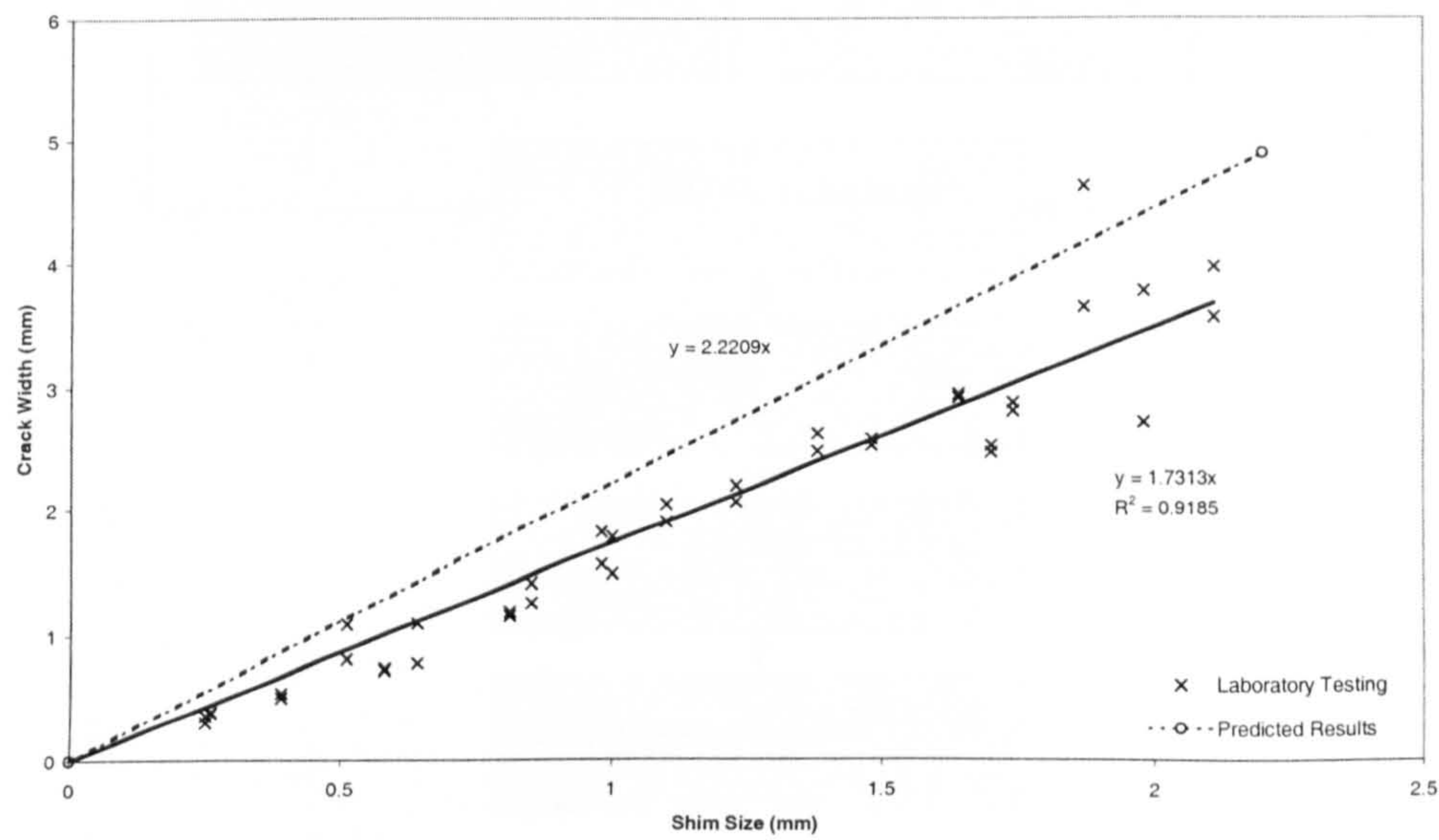


Figure 5.17 – Comparison of predicted and actual surface crack measurements

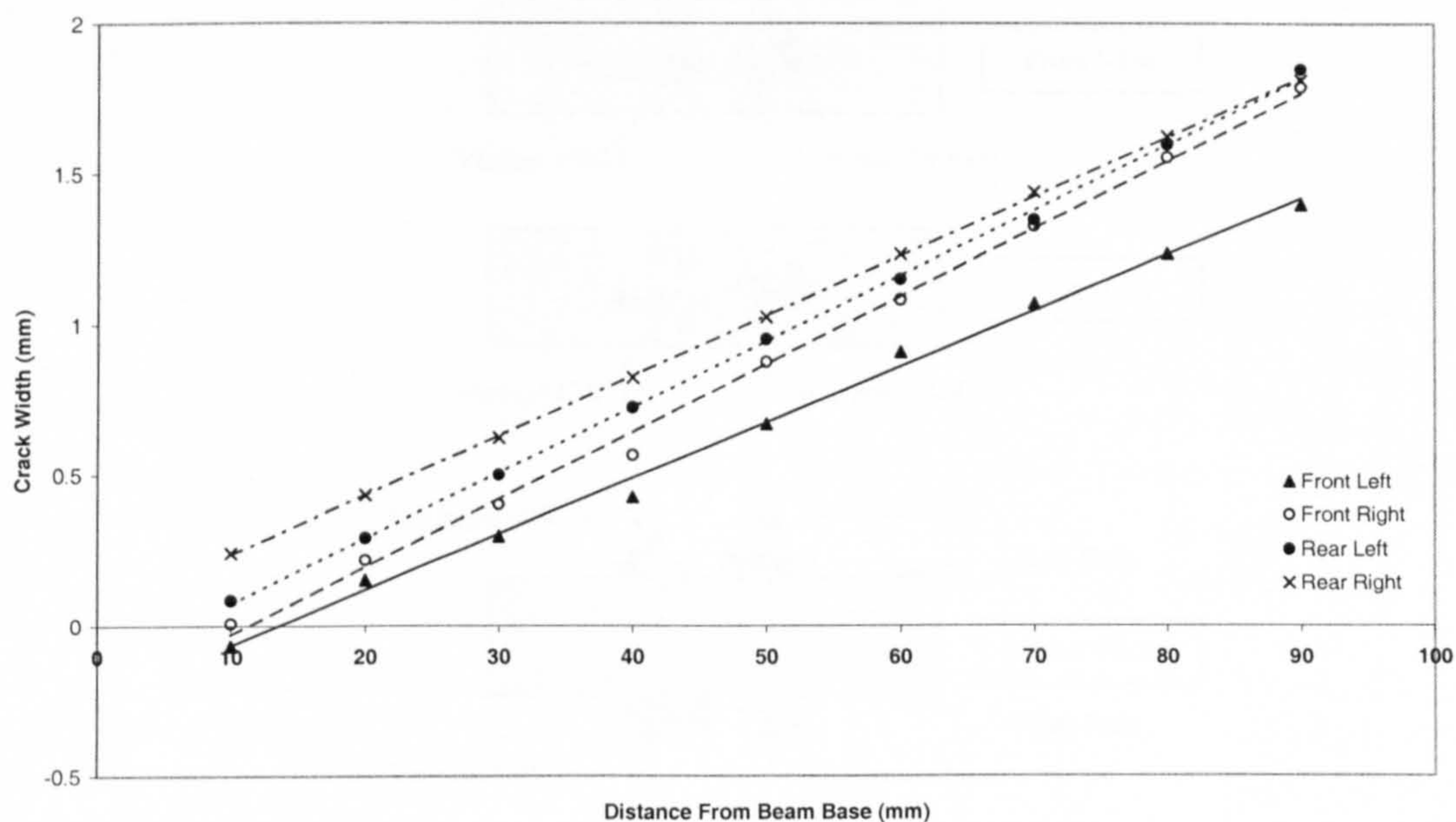


Figure 5.18 – Measurement of crack opening throughout specimen depth

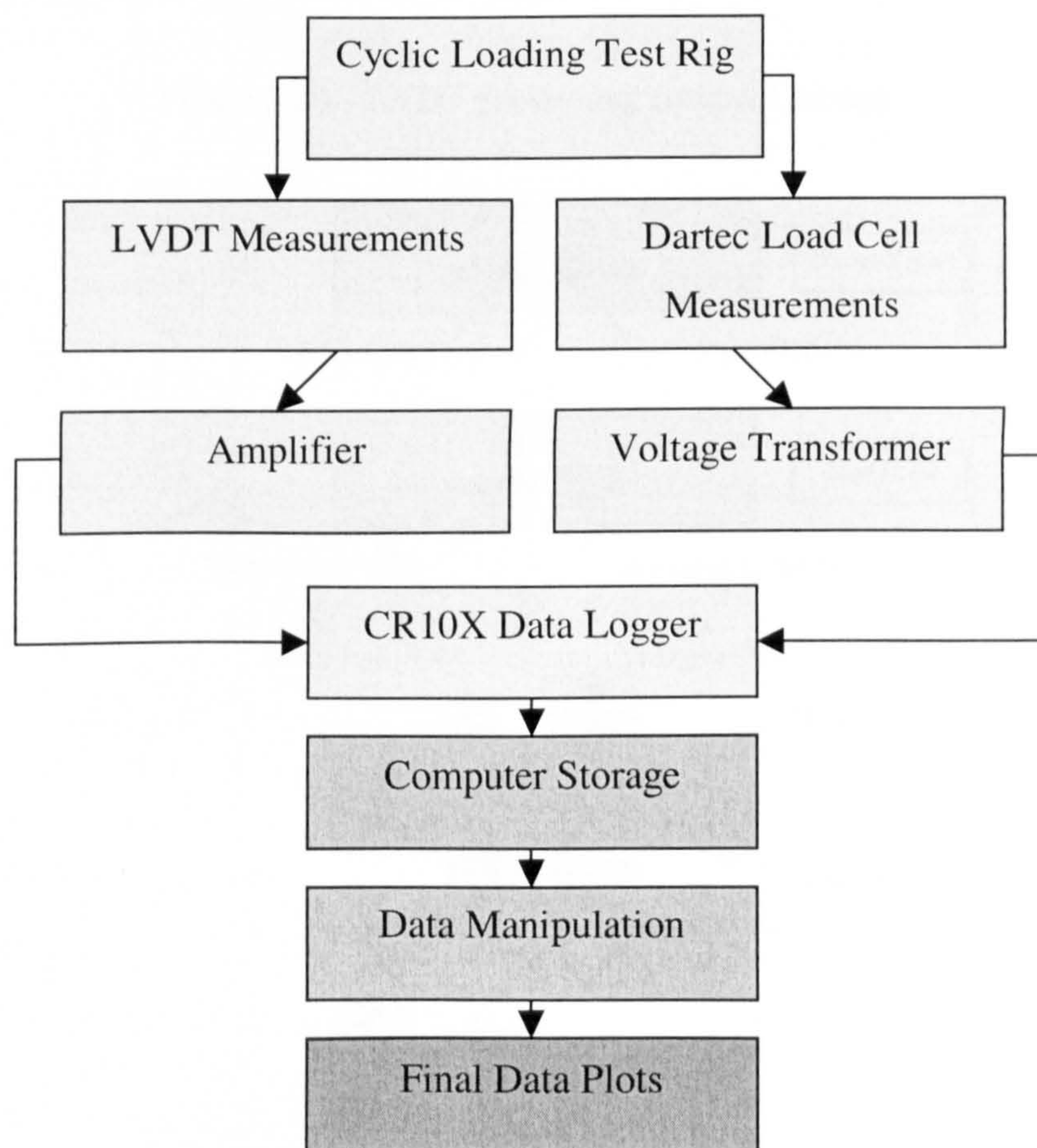


Figure 5.19 – Graphical representation of data logging process

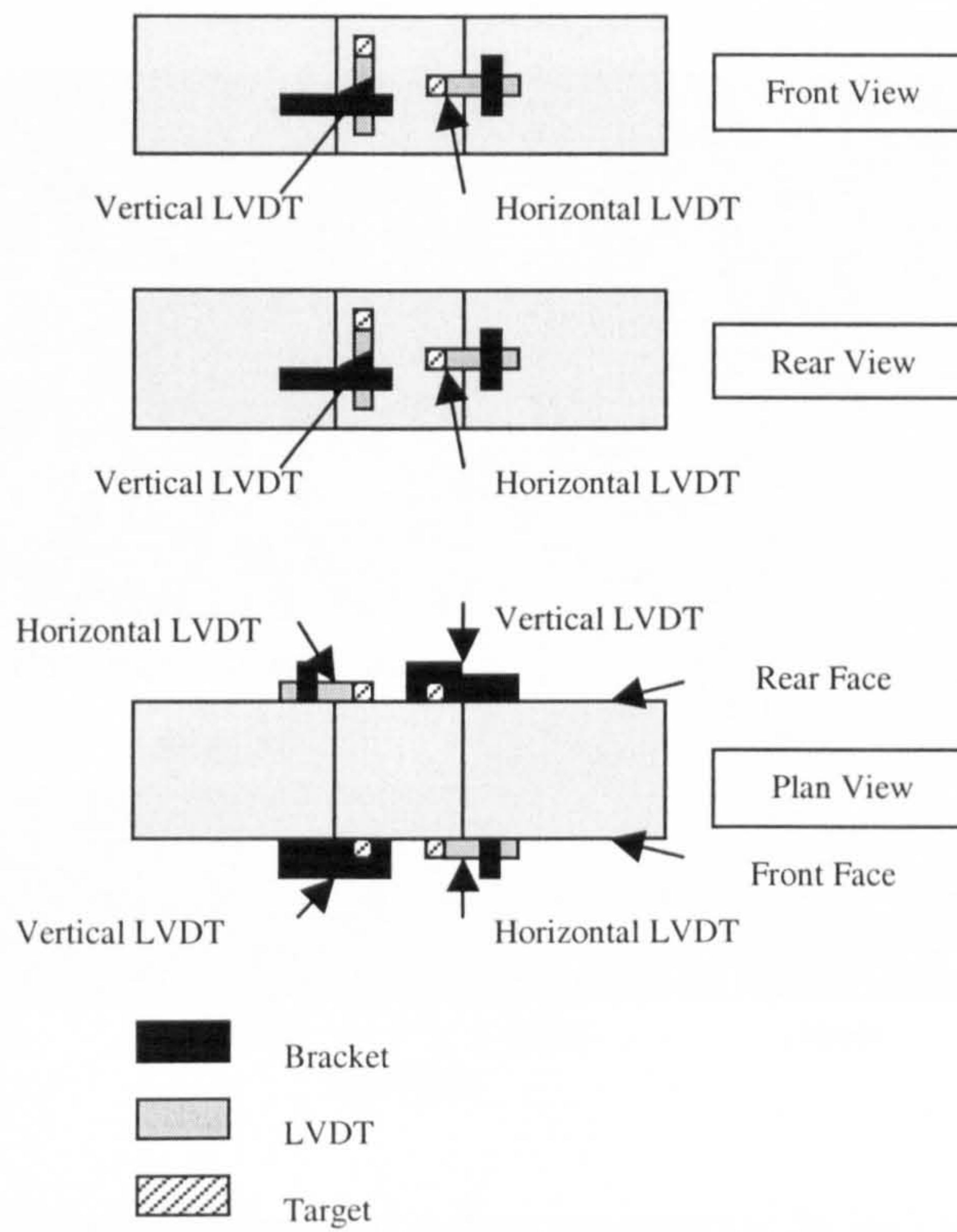


Figure 5.20 – LVDT positioning (original set-up)

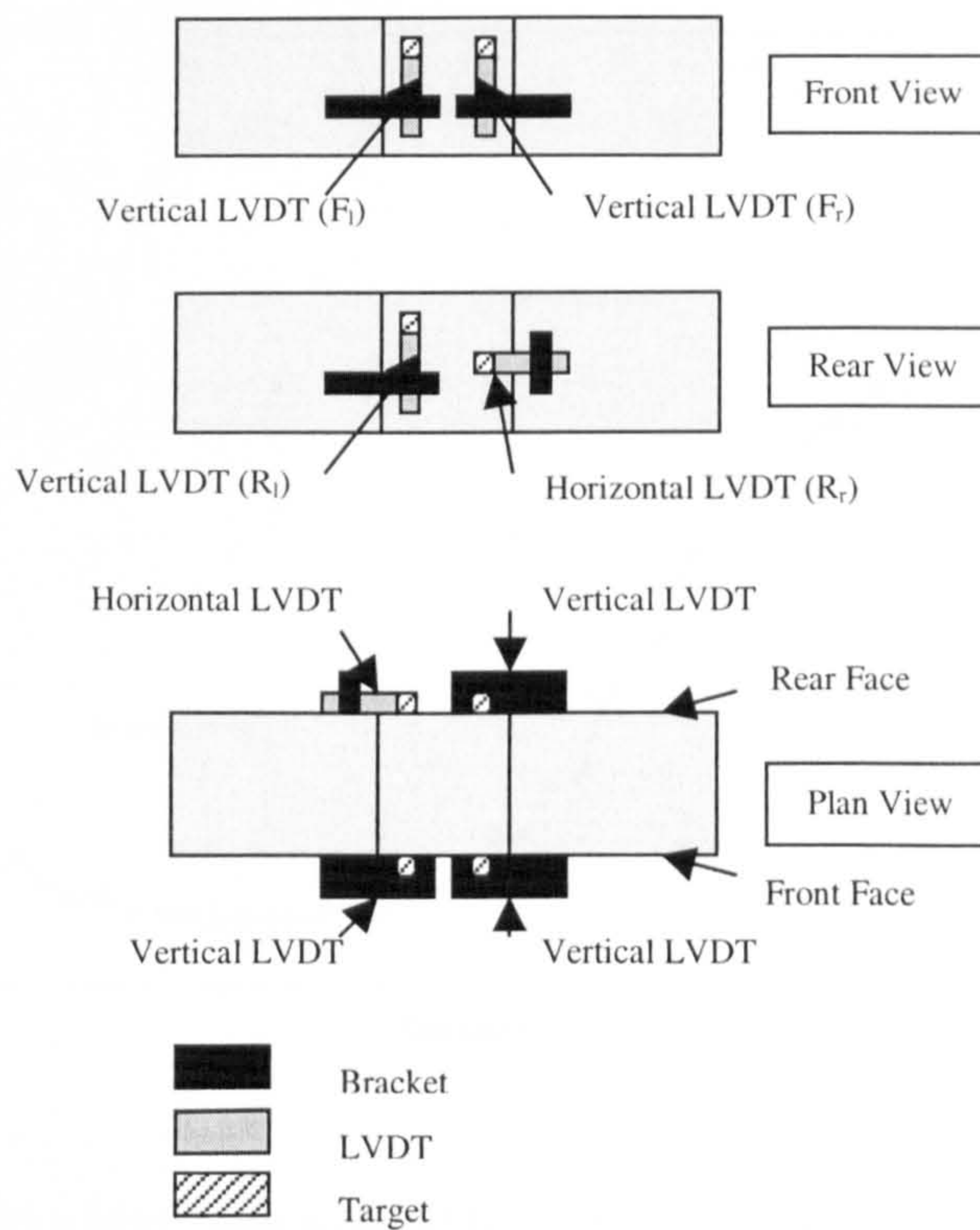


Figure 5.21 – LVDT positioning (updated set-up)

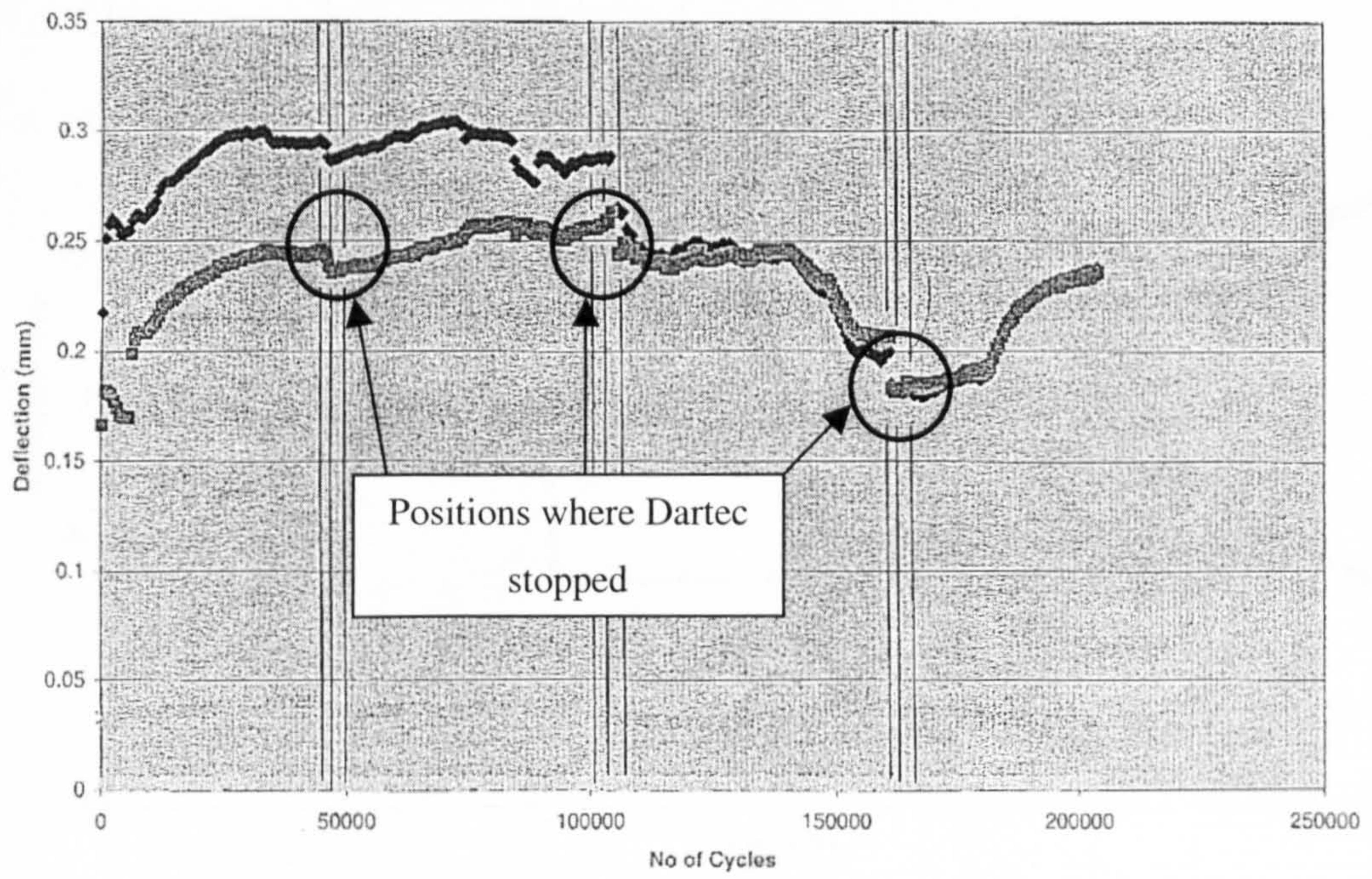


Figure 5.22 – Effect of undertaking a discontinuous cyclic load test

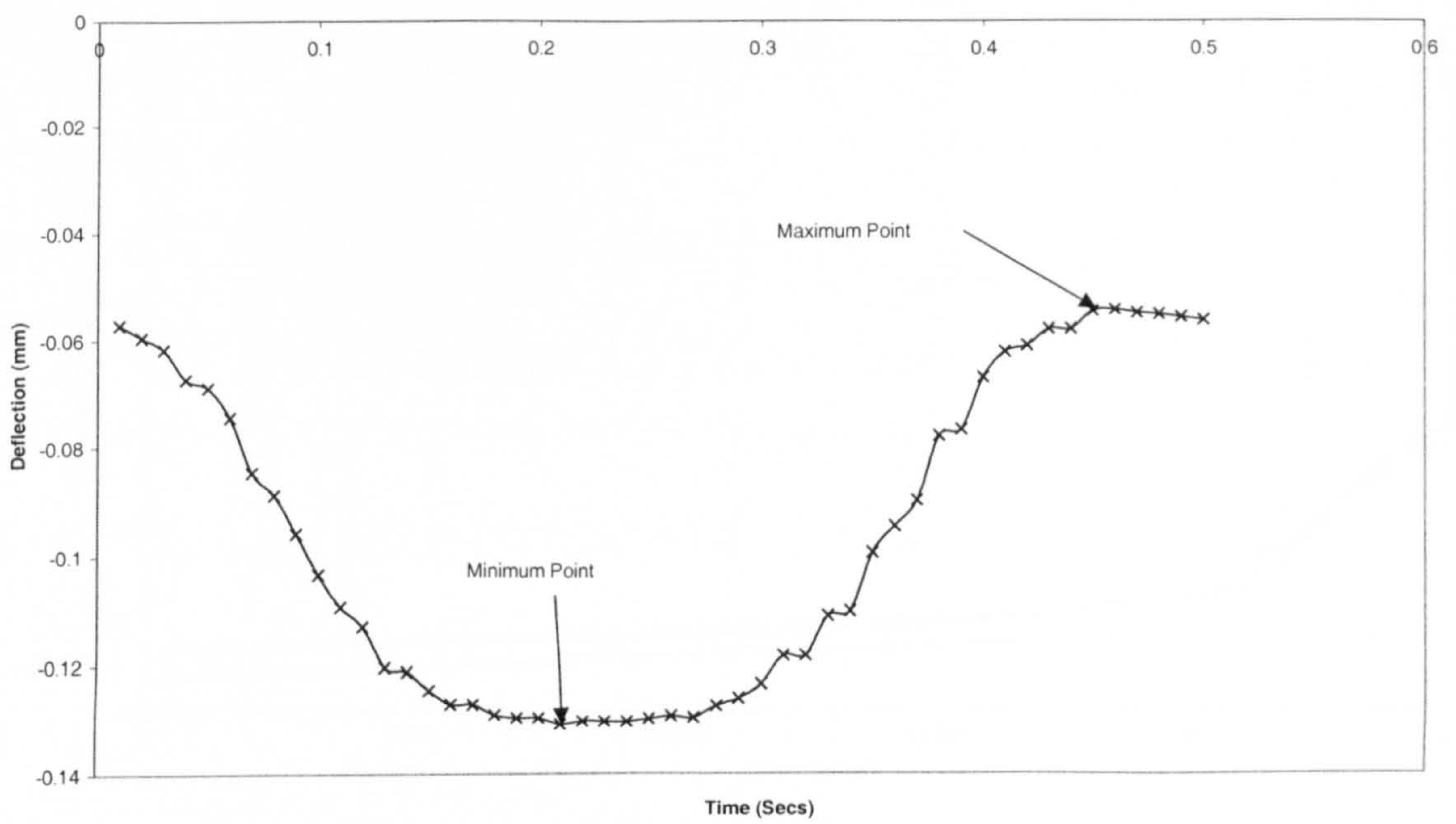


Figure 5.23 – Maximum and minimum displacement positions

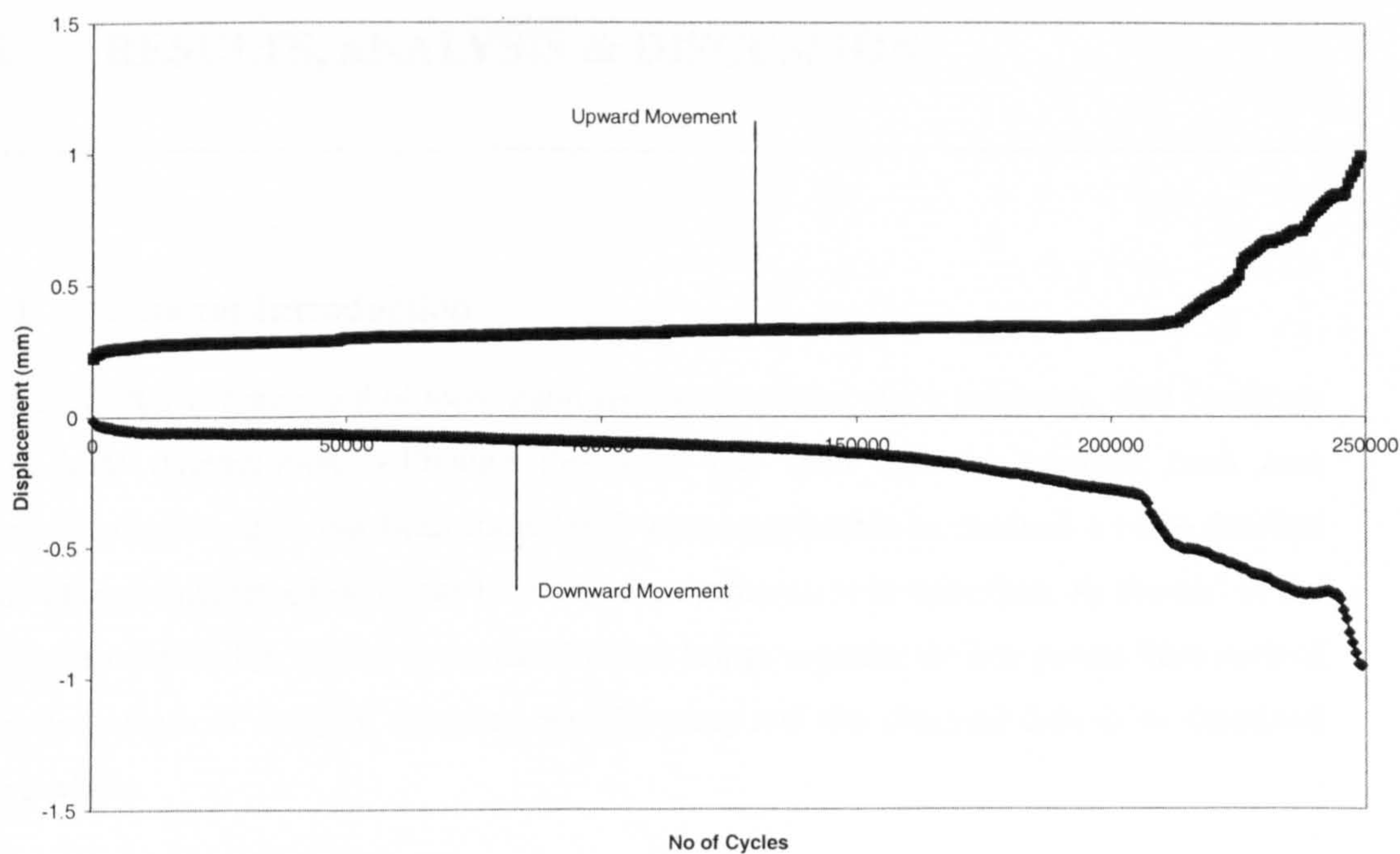


Figure 5.24 – Positive and negative displacement deterioration plot

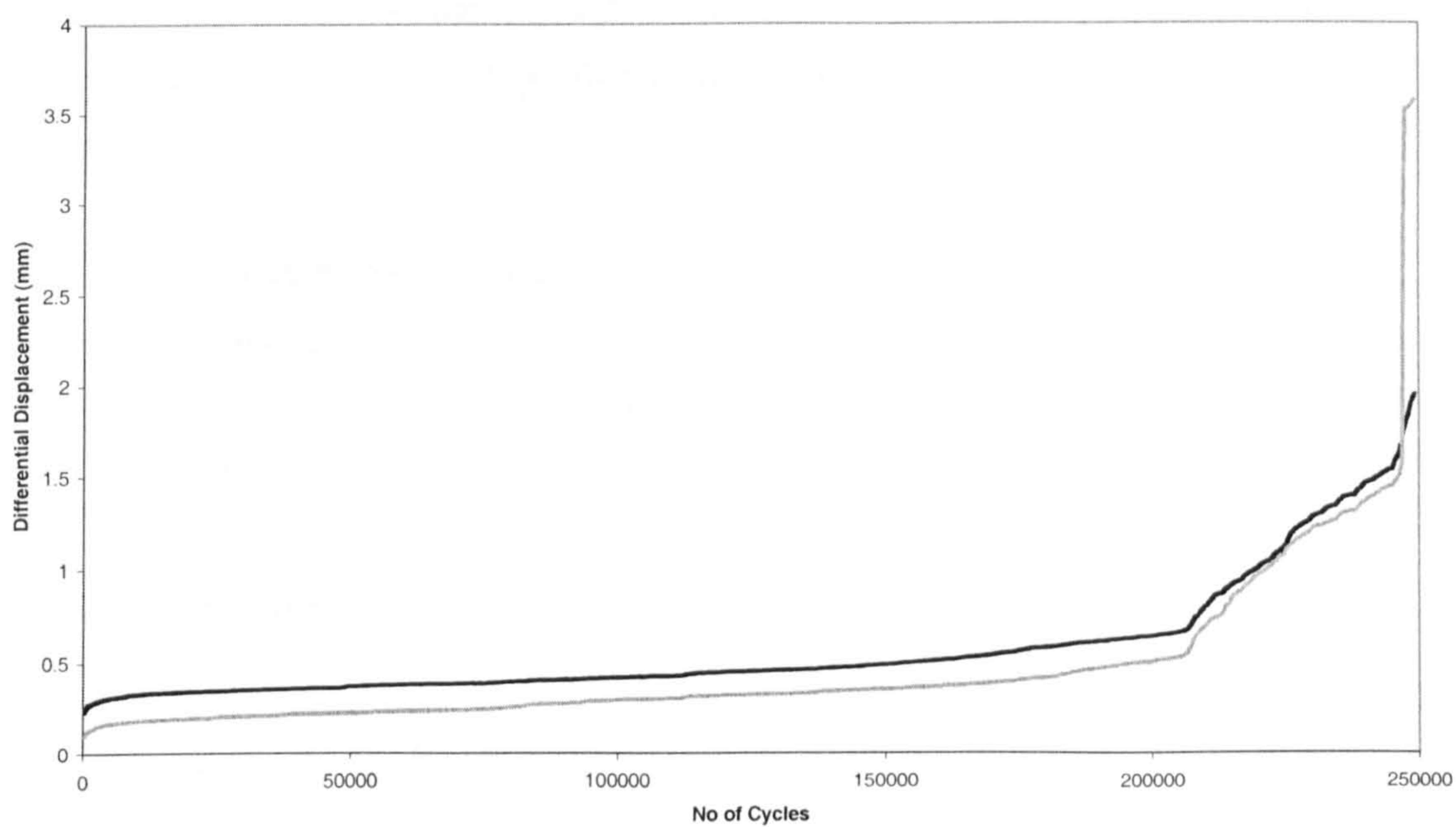


Figure 5.25 – Differential displacement deterioration plot

6. RESULTS, ANALYSIS & DISCUSSION

6.1 General Introduction

This Chapter is composed of three main sections, namely, crack geometry, slab condition and joint deterioration. Although the work has been split to examine each area individually, the data has been transferred where applicable to produce a more detailed and clearer understanding of the load transfer mechanisms in operation. At the end of the chapter a discussion section is provided which brings together the key points from each of the three areas of analysis, enabling the laboratory and site obtained data to be examined as a whole.

6.2 Crack Geometry

Crack width is known to be one of the main factors controlling the effectiveness of joints under dynamic load. The collection of site data was necessary to enable typical geometries to be identified, which would: aid in the development and set-up of the cyclic loading test rig, enable comparison with site deflection test results, validate the Finite Element model, and provide information to floor contractors and designers on typical joint opening behaviour.

According to the literature reviewed in section 3.3, surface measurements alone fail to provide all the required information in respect to crack geometries, as width regularly reduces with depth due to differential shrinkage. Several methods were therefore used to enable real site values under characteristic environmental conditions to be established.

6.2.1 Core Samples

Core samples were obtained from the Lutterworth site on two occasions. The first visit was carried out on 6th to 7th July 2002 and involved the drilling of 24 cores in total, two of which were taken through sawn contraction joints and two through cracks in the slab. The remainder were positioned at internal conditions, some areas of which had developed surface crazing. The location of each core on the site is shown in Figure 6.1, with photographs of those containing cracks or joints provided in Figure 6.2.

The second visit to Lutterworth was completed on the 21st to 22nd September 2002 with 40 cores taken in total, 10 of which were located through a wire guidance system installed into the slab for the control of VNA trucks (Figure 6.1). The cuts into the slab appeared to be working as inducers, with hairline cracks visible on the surface of the slabs extending from the edge of wire guidance grooves. At each position Prima Dynamic Plate testing was undertaken prior to coring to enable comparisons between deflection response and crack geometry, the details of which are provided in section 6.3.2.

For the first set of cores, dimensions of maximum/minimum core length and reinforcement size, were recorded by the Construction Materials Testing (CMT) laboratory in Derby. The results for those containing either a contraction joint or a crack are reproduced in Table 6.1.

For the second set of cores CMT Derby identified the thickness of slab, cover to reinforcing, depth of saw-cut and cover to wire, reproduced in Table 6.2.

Table 6.1 – CMT Core Information (Visit 1)

Core Ref.	Core Length (mm)		Reinforcement Dia. * d _{min}	Comments
	Max.	Min		
7	190	189	None	Induced Contraction Joint
17	198	174	7 * 106	Full Depth Crack
21	180	176	7 * 122	Tapered Crack to 123mm
24	196	190	18 * 95	Dowel. Induced Contraction Joint

Table 6.2 – CMT Core Information (Visit 2)

Core Ref.	Max Length (mm)	Min Length (mm)	Cover to Rebar (mm)	Depth of Saw-cut (mm)	Cover to Wire (mm)	Depth of Crack
1	176	166	90	22	18	Total
3	186	177	88	21	18	Total
5	181	165	N/A	15	14	Total
6	198	174	134	14	7	Total
10	177	165	112	18	15	Total
16	172	161	94	15	11	Total
17	186	179	111	15	11	Total
24	199	196	119	13	9	Total
27	192	180	127	13	7	Total
28	204	199	195	14	11	Total

In the cores obtained from both visits the maximum and minimum lengths show differences of up to 20mm over a core width of 100mm. Changes in the slab depth by this amount can have a substantial effect on both the structural resistance of the slab, and the friction which occurs between the foundation and the slab. This can lead to shrinkage restraint at mid span, resulting in early deterioration of the structure (section 2.4.1).

The cover and depth of the reinforcement in the visit 2 cores varied by up to 100mm. Placement of the reinforcement can influence the resistance to cracking and prevent cracks that do occur from opening up to an extent which causes deterioration problems (section 2.5.2). Variations to the level found in the cores will therefore be highly problematic and prevent the slab from responding as desired.

On completion of the CMT examinations further analysis was undertaken to meet the research objectives. Each crack or joint had measurements taken of its width and offset on both sides, with amendments made for saw cutting and relaxation of the core upon removal, in accordance with the methodology described in Chapter 4.2.3. The dimensions of crack width are shown in Figure 6.3 for the first set of cores and Figure 6.4 for the second set of cores, where the width given is the average of the measurements taken at the same depth on either side of the core specimen. Each core for the first visit is discussed in turn as each shows a different crack or joint type. The results and discussion for the second visit have been grouped together as each was of a similar type.

The crack in core 21 (visit 1) was restricted to the upper half of the slab only, with its width reducing in proportion to the distance from the surface. Although the exact cause of the crack could not be established, it was likely to be either plastic shrinkage or differential movement between the surface and base of the slab. The plot reveals that shrinkage was only high enough to create a crack at the surface, reducing to non-critical strain levels at approximately mid-depth.

Core 17 (visit 1) encompassed a mid panel crack which ran parallel to an aisle between two high racking systems. The cause may have been clamping of the slab to the subbase, preventing shrinkage movement which resulted in an increase in tensile stress. The crack itself was found to penetrate full depth, being larger at the surface and reducing proportionally until closed at the base.

The induced contraction joints in cores 7 and 24 (visit 1) both contained an underlying crack varying between maximum at the surface to zero at the base. The reduction in core

7 was proportional to depth, with the exception of several points which deviated from this line at around the 40-80mm depth. This may have been caused by aggregate spalling from the crack edge, resulting in an 'apparent' increased measurement, or differential shrinkage created by inconsistent drying. Core 24 contained the greatest crack width between the surface and 60mm depth, at which point it reduced to levels similar to that found in core 7. These large measurements go beyond that of the saw cut thus, its influence in creating the profile is shown to be negligible. The larger top section width may have been caused by the dormant/dominant phenomenon whereby adjacent joints were restrained, forcing increased movement. The shape of the crack was formed due to restriction from the dowel bar and friction against the foundation in the lower section. In the top of the slabs no restraint was provided, hence the crack opened to a much greater degree.

Figure 6.4 demonstrates that all cores taken in the second visit contain cracks which have a width larger at the surface than at the base. In 80% of these cores the base width was below 0.4mm, with the surface measurements themselves varying between 0.55mm and 1.45mm. The general trend showed a slightly steeper gradient in the top 75 to 100mm section of the core, indicating greater shrinkage in the concrete closer to the surface. This phenomenon has been discussed by Poblete et al (1988) and is discussed in section 3.3.

Three of the cores (numbered 1, 3 and 6) contained widths which varied greatly from the geometry described above. These deviations can be attributed to breakage of aggregate at the concrete edges when the cores were removed from the slab. Some degree of differential shrinkage between sections of the slab may also have had an effect, creating a non-linear variation between top and bottom faces.

The data shows that cracks under the induced joints are significantly larger than those at mid panel. This is to be expected, as the joints will contain shrinkage from the entire length of the concrete slab, whereas cracks will comprise less movement due to the shorter effective length. Smaller width generally leads to a more efficient crack, indicating that although more unsightly, they will create less problems than that of an equally trafficked joint.

For each of the cores in visit 1 a plot was produced of crack edge offset distance on either side of the specimen, to a level datum placed perpendicular to the slab surface (Figure 6.5). The results display a great deal of similarity, with the orientation varying only slightly (25mm maximum) from the initial top position. Small deviations are regularly

spaced and caused by the crack following the interface between aggregate particles, known to be the weakest point in young concrete (Abdel-Maksoud, 2000).

As expected, the magnitude of offset at the top 50-60mm of the sawn specimens (numbered 7 and 24) is controlled by the width of the saw cut, below which the variation is similar to that found in the specimens containing a crack only. The small change in offset indicates that only negligible differences in load transfer will exist due to a change in the loaded slab. The minor undulations of the crack face will therefore dominate and enable aggregate bearing to occur equally in both directions.

Examination of the offsets in the second visit cores showed similarities with that of the first. Each comprised a crack which showed little overall deviation from the surface position, but contained several small undulations in vertical orientation. A decision was made that only the crack width measurement would be taken in these cores, with no recordings of offset made.

Examination of all the cores has enabled typical dimensions and geometries of crack width to be calculated. These have been undertaken for each crack type, i.e. induced contraction joints, cracks, and semi induced cracks (wire guidance grooves) and are shown in Table 6.3. The results indicate that generally all joints have similar behaviour with respect to crack opening, the width increasing in proportion to slab depth. However, the predicted surface widths for semi-induced cracks using extrapolation of the bottom and mid slab widths (Figure 4.5) are generally smaller than the actual surface dimensions by approximately 18%, indicating slightly non-linear opening. This behaviour is similar for contraction joints and cracks, although the variation in predicted and actual surface crack opening is greater. This information is of use when extrapolating crack widths from either embedded strain gauges or surface measurements, as it confirms that the predicted surface values will generally be slightly smaller than that actually occurring within an in-service slab crack or joint.

Table 6.3 – Comparison Between Actual and Predicted Surface Crack Widths

Core Type	Actual Base	Actual Middle	Actual Top	Predicted Top	Variation (%)
Contraction					
7	0	1.2	3.1	2.4	22.5
24	0	1.55	8.3	3.1	62.7
Average	0	1.38	5.7	2.75	51.7
Crack					
17	0	0.32	0.35	0.64	-82.9
21	0.08	0.9	1.84	1.64	10.9
Average	0.04	0.61	1.10	1.14	-3.6
Induced					
1	0.28	0.4	1.45	0.64	12.5
3	0.3	0.6	0.8	0.9	-12.5
5	0.4	1.05	1.38	1.7	-23.2
6	0.1	0.55	0.85	1	-17.6
10	0.4	0.9	1.1	1.4	-27.3
16	0.2	0.35	1.2	0.5	58.3
17	0.2	0.25	0.7	0.3	57.1
24	0.2	0.3	0.55	0.4	27.3
27	0.3	0.4	0.7	0.5	28.6
28	0.15	0.65	1.3	0.85	34.6
Average	0.25	0.538	1.00	0.819	18.1

6.2.2 Strain Gauge Monitoring

Work undertaken by Bishop (2001) required the installation of strain gauges into a concrete floor slab to monitor the early age movement caused by both hygral and temperature effects. The gauges were placed at various positions, many of which were sited across contraction and induced joints. At three sites, two or three gauges and/or demec pips had been placed to increasing depths at the same location, enabling measurements to be taken of width variation. Full information on the strain gauge types and method of placement is provided in Bishop (2001), with a summary of the joint openings found by Bishop reproduced in Table 6.4a. The values for Leeds were measured at 222 days after casting, Marston at 12 days, and Northampton at 28 days. The thickness of the slabs and positions of the gauges are given in Table 6.4b and Figure 6.6.

Table 6.4a – Strain Gauge Readings Converted to Crack Width

Gauge No	Joint Type	Top Demec (mm)	Top Strain Gauge (mm)	Bott. Strain Gauge (mm)
LEEDS				
19	FF		0.11	0.01
20	SR	0.90		0.20
21	SR	0.50		0.10
22	SR	0.70	0.25	0.15
23	SR	0.90	0.30	0.10
25	FF		0.80	0.18
27	SR	0.60	0.18	0.00
28	SR	0.60	0.20	0.03
31	FF		0.30	0.02
34	SR	1.20	0.30	0.18
36	SR	1.00	0.45	0.20
MARSTON				
2	FF (wall)		2.70	2.05
12	FF		2.80	2.80
23	FF		2.70	2.70
31	FF (wall)		1.90	2.25
31 (Amm)	FF (wall)		1.90	1.75
32	FF (wall)		1.95	1.70
NORTHAMPTON				
1	SF		0.62	0.58
2	SF		0.80	0.75

SR – Sawn Restrained

FF – Formed Free

SF – Sawn Free

Table 6.4b - Strain Gauge Placement

	LEEDS	MARSTON	NORTHAMPTON
Slab Depth	225mm	175mm	260mm
Surface to Top Gauge	105mm	55mm	140mm
Surface to Bottom	165mm	115mm	200mm

Extrapolation of the measurements given by the embedded strain gauges using a linear crack formation (known to predict slightly smaller surface widths, section 6.2.1), enabled the crack widths for both the base and surface of the slab to be determined (Figure 6.7). Where demec pips were installed onto the slab surface, these were used along with the singular strain gauge, with those containing two strain gauges and demec pips utilising

the demec and top embedded gauge for the surface measurement, with the base value determined from the gradient of the two embedded strain gauges alone.

Occasionally on the Leeds site, strain gauges and demec pips were used directly above each other enabling comparisons between the predicted and actual surface values. The results of the measurements are shown in Table 6.5 with Figure 6.8 providing a plot of all three data points.

Table 6.5 – Measured and Projected Surface Measurements

Gauge No	Projected Bott. (mm)	Predicted Top (mm)	Actual Top (mm)	Variation (%)
22	0.0500	0.4250	0.7000	39.3
27	-0.1800	0.4950	0.6000	17.5
28	-0.1400	0.4975	0.6000	17.1
34	0.0600	0.5100	1.2000	57.5
36	-0.0500	0.8875	1.0000	11.3

In situations where three measurements were used, the actual surface crack width value is larger than that predicted using the embedded strain gauges, with numbers 22 and 34 showing the greatest variation. This indicates that the crack opening is non-linear, with a slightly curved orientation as shown in Figure 6.8. This agrees with the plot by Neville (1981) (Figure 6.9), who found that shrinkage values increase exponentially towards the surface, resulting in a curved profile when only one side is open to the environment. This is similar to the results found in the core examinations, where the surface of the slab contained crack width values approximately 18% larger than extrapolation of the bottom gradients predicted (Table 6.3).

The findings illustrate that surface measurement can only provide an estimation of crack width profile due to the non-linear shrinkage throughout depth. However, as the variation is only minimal (generally below 20%), it can be assumed for the analysis of surface profiles (section 6.2.3) that crack opening is linear. In reality a slightly higher gradient may be found in the top section of the slab due to the increased potential for moisture movement, and will therefore produce a larger crack angle and base width (section 4.3).

Figure 6.7 confirms that most joints have a larger width at the top surface compared to the bottom. In 80% of the joints tested at Leeds a projected surface value of up to 2mm closes completely in the bottom 50mm section. This indicates that either a crack will not exist

below this level, or that it will be closed and in a compressive state. Similarly, the results from the Northampton and Marston sites show a decrease in width over depth of between 0.2 and 3.5mm respectively; however, in both cases the joint appears to be open throughout depth, with the base width still in excess of 0.6 and 2mm.

The larger crack widths at Marston are mainly caused by the different joint type. The majority of results from Leeds originate from sawn restrained joints with only gauges 19, 25 and 31 sited across formed free joints. Marston however, contains only formed free joints, with the slab constructed using jointless methods, hence the longer effective lengths and larger magnitude of movement. Joints numbered 2, 31 and 32 were taken against a wall gauge meaning that all measurement of crack width variation occurred from one side only. However, these have been doubled in the relevant figures and tables to produce suitable comparison with the other locations. Interestingly, joints 12 and 23 show equal movement throughout depth, indicating little differential shrinkage, with joint 31 showing greater opening at the base than at the top. The cause of this reversed orientation is unknown, although on examination of the time/joint opening plot it appears that this phenomenon occurred within the last few hours of data collection, whereby a sudden increase in lower gauge movement occurred (Figure 6.10). This indicates a possible measurement error, with the earlier behaviour (Gauge 31 Amended) providing more realistic information in respect to crack opening. The Northampton site contained data from free sawn joints alone, with friction against the subbase and dowel bars perpendicular to the joint preventing slab shrinkage being converted into opening. This resulted in a small width, but still contained an increase in width with distance from the slab base.

The results from the embedded strain gauge and demec point measurements have again indicated that the crack increases in size towards the slab surface caused by differential shrinkage. This is most pronounced in the top section of the slab where the crack angle is greater than that in the bottom. The type of joint under consideration controls the magnitude of this movement with sawn restrained joint surface measurements generally below 2mm, and free movement joints over 5mm. This is generally caused by the lack of shrinkage restraint, and an increased length between adjacent crack positions.

6.2.3 Levelling Profiles and Crack Measurements

Crack orientation can be determined from the top width measurement and the surface profile of the slab if an assumption is made that opening is linear and all shrinkage strain

has been converted into curl. In construction joints this method is unreliable due to apparent curling, which is a surface condition caused by upsweeping of the trowelled face during construction. Sawn joints are formed on a level surface within a continuous slab, and therefore any vertical change measured can be attributed to curling. This method of determination will normally estimate base widths slightly larger than actually found in the joint or crack due to non-linear shrinkage (section 4.3).

At Daventry profiles were determined across two slabs and a number of joints using a precise level. The area of floor surveyed is shown in Figure 6.11, with the methods employed described in section 4.3.2.

The data recorded has been transformed into contour plots (Figure 6.12), with the joint locations superimposed to enable the positions of high points and curling to be determined. The results show a clear indication of warping at the slab edges and corners as demonstrated by the lighter patches on the contour plot. This is most apparent at the joints running in the vertical direction which show an increase in height of up to 10mm from that found at mid span, and level changes of 4mm within a distance of 0.5m from the joint itself. This effect will almost certainly be significant in the creation of a crack which opens more towards the surface. The length of slab at which point the curl reduces significantly is approximately 1m. This provides good correlation to the work of Suprenant (2002) who estimated curling to be between 10 and 20% of the slab length, which in the case of the Daventry site would provide a length between 0.75 and 1.5m.

Unfortunately, time constraints prohibited precise levelling on the remaining sites. At Ballymena the simple methods utilising the builders level and the profilometer were employed across all joints to provide an indication of curling magnitude, the results of which are shown in Figure 6.13. This method only enabled the variation between slab edges and a distance 0.5m back to be established, and therefore provided limited data on the complete curled profile. The results show a variation in slab edge level of between 0.4 and 5.1mm, similar to that obtained when examining the Daventry site.

Assuming orientation of the crack face is in direct relation to the degree of curl (as described in section 4.3.1), it was possible to determine crack measurements using only the slab profile and surface joint widths obtained from site. Results obtained using this method for Daventry are shown in Figure 6.14, where the levels closest to each side of the joint (500mm apart) have been used to enable the most accurate calculations of edge curl. The surface crack widths varied between 3 and 8mm, with 80% showing a reduction in

width with depth of between 1 and 4mm. The estimation of base measurements produce widths between 1 and 6mm; however, as found from both coring and embedded strain gauges, the estimation of proportional decrease from the surface value is expected to result in base values larger than reality (section 4.3).

The Ballymena site was constructed using the long strip method, with each joint formed rather than sawn and only opening up marginally, making it extremely difficult to measure crack width. However, the profile gradients have been determined and are provided in Figure 6.15. The plot shows a variation between surface and base measurement of between 1 and 4.5mm, although the actual values calculated are not representative of that on site because of the joint type under examination.

The typical crack profiles can be seen for both sites with the upward curl of the slab providing a width narrowing with depth, the variation being 1-4mm for both Daventry and Ballymena. These are realistic values and agree with the typical sizes obtained by coring in the Lutterworth site, and by strain gauge monitoring of Leeds, Marston and Northampton.

6.2.4 Summary

All three methods for investigating crack profiles show that the surface measurement is larger than at the base. This is caused by differential shrinkage as described in section 2.4.2, with the top surface prone to greater movement due to the drying environment. In all situations the curl was in an upward direction, with the edge of the slab being at a higher elevation than that of the centre. The value of this difference was approximately 10mm, with the variation between the edge 500mm section in the region of 1 to 5mm, and the length of unsupported slab approximately 1m. The width measurement appeared to be partially controlled by the joint type, with reinforcement holding the crack together and producing a lower opening throughout. The cores showed that the increase in crack width is generally proportional to depth, although a slightly higher degree of movement is found nearer the surface. This is also found with the embedded strain gauges, where the top demecs showed a larger surface measurement than any prediction based on embedded gauge extrapolation alone. In all cases the magnitude of variation between the surface and base crack widths was between 1 and 5mm.

These findings highlight the fact that crack geometries in concrete slabs on grade are different to that assumed in much of the literature. The effects of a 'V' shaped cracking

pattern can be highly influential to the load transfer occurring across the crack and its associated responses. Assumptions of parallel cracking with a width equal to the surface measurement are therefore conservative in design and inaccurate for structure assessment.

The maximum propagation of the crack towards one side in the core specimens was always found to be below 15mm. This small deviation, alongside the numerous aggregate undulations throughout depth, produced a similar load transfer mechanism across each face. This made the loaded side unimportant when calculating load transfer and thereby prevented field-testing having to be undertaken on both sides of the joint.

6.3 Slab Condition

6.3.1 Introduction

Slab and joint condition has been determined using calculations of: load transfer, load step, crack width, edge cantilever, deflected shape and voiding. The testing was undertaken using either the FWD or Prima dynamic loading equipment, with both devices being used on the Lutterworth and Daventry sites.

Comparison was made between the two pieces of deflection testing equipment with respect to load transfer and load step. This enabled any variations in response caused by the increased load of the FWD to be established, and therefore provided confidence in the results from the Prima. Comparing the devices and load in this way also produced some interesting findings with respect to the void effect, and that of the transfer mechanism occurring across the joint. In the remainder of the slab condition calculations, comparisons between the FWD and Prima have not been undertaken; however, the data is affected by the magnitude of the load and this has been taken into account during assessment.

Each calculation of slab response (i.e. load transfer) has been compared to other behaviour within the same slab. This has enabled many relationships to be developed, highlighting the importance of joint effectiveness on slab condition. Load transfer and load step has also been compared to surface crack width, which, although known from section 6.2 to only be partially representative of the full geometry has enabled its influence to be determined.

The foundation has a highly influential impact on deflection response. Engineers had suspected the site at Lutterworth to contain voiding underneath the slab edge and have variable support conditions. This was confirmed by the testing undertaken on site using the void intercept approach, which predicted that between 50 and 90% of the slab edges contained voids (section 6.3.6). The site at Ballymena was assumed to have a good foundation due to Engineer's assessment and the formation level at which the structure had been constructed. This information was of importance when analysing slab behaviour as it helped in determining site variability.

6.3.2 Load Transfer Evaluation

Device Comparison

Comparisons were made on the Daventry site between the load transfer values obtained using the normalised 50kN FWD and 10kN Prima dynamic plate. This enabled the devices to be correlated, ensuring that data from one site could be compared to another, whilst allowing the effect of load magnitude on slab response to be determined. The locations for each test were marked on the slab enabling the same positional set-up to be established for each piece of equipment. The results obtained are shown in Figure 6.16, where load transfer is calculated using the Croveti and Darter (1985) approach (equation 3.4).

The graph exhibits good correlation between FWD and Prima results ($R^2 = 0.94$), with only minor distribution from the equal value line. The full range of load transfer has been established and its value does not seem to affect the relationship between results. The few points that do show variation greater than 10% are not significant points on the axis; however, on inspection they were found to contain large crack widths (between 5 and 11mm), regardless of the efficiency of the joint. Examination of the full data set showed no direct link between magnitude of variation from the idealised line and surface width of the crack, and therefore the variation was attributed to site irregularities, possibly caused by the testing procedure and greater load in the FWD. Four construction joints were included within the analysis and each showed excellent load transfer (67-90%) with good comparison between test equipment, the maximum deviation being 1% or lower.

For the Lutterworth site three FWD load magnitudes of 42, 58 and 85kN were used along with the 10kN Prima dynamic plate. Comparison of the results from the largest and smallest FWD loads is shown in Figure 6.17, with the mid-range 58kN FWD load compared to the Prima in Figure 6.18.

The foundation has a highly influential impact on deflection response. Engineers had suspected the site at Lutterworth to contain voiding underneath the slab edge and have variable support conditions. This was confirmed by the testing undertaken on site using the void intercept approach, which predicted that between 50 and 90% of the slab edges contained voids (section 6.3.6). The site at Ballymena was assumed to have a good foundation due to Engineer's assessment and the formation level at which the structure had been constructed. This information was of importance when analysing slab behaviour as it helped in determining site variability.

6.3.2 Load Transfer Evaluation

Device Comparison

Comparisons were made on the Daventry site between the load transfer values obtained using the normalised 50kN FWD and 10kN Prima dynamic plate. This enabled the devices to be correlated, ensuring that data from one site could be compared to another, whilst allowing the effect of load magnitude on slab response to be determined. The locations for each test were marked on the slab enabling the same positional set-up to be established for each piece of equipment. The results obtained are shown in Figure 6.16, where load transfer is calculated using the Croveti and Darter (1985) approach (equation 3.4).

The graph exhibits good correlation between FWD and Prima results ($R^2 = 0.94$), with only minor distribution from the equal value line. The full range of load transfer has been established and its value does not seem to affect the relationship between results. The few points that do show variation greater than 10% are not significant points on the axis; however, on inspection they were found to contain large crack widths (between 5 and 11mm), regardless of the efficiency of the joint. Examination of the full data set showed no direct link between magnitude of variation from the idealised line and surface width of the crack, and therefore the variation was attributed to site irregularities, possibly caused by the testing procedure and greater load in the FWD. Four construction joints were included within the analysis and each showed excellent load transfer (67-90%) with good comparison between test equipment, the maximum deviation being 1% or lower.

For the Lutterworth site three FWD load magnitudes of 42, 58 and 85kN were used along with the 10kN Prima dynamic plate. Comparison of the results from the largest and smallest FWD loads is shown in Figure 6.17, with the mid-range 58kN FWD load compared to the Prima in Figure 6.18.

The comparison between differing FWD loads is good ($R^2 = 0.95$) with the data varying little from the equal value line. However, on closer inspection load transfers in the region of 90% or higher demonstrate that a lower load impact produces a higher value. When the load transfer reduces below 90%, the reverse takes place whereby lower loading produces a reduced value. The overall difference is found to be below 10% throughout the range of data, although only a few points provide information below 50%.

Results between the Prima and FWD display a similar relationship ($R^2 = 0.603$) to that of the high and low loading of the FWD (Figure 6.18). Towards the very high load transfer values i.e. 90% or more, the correlation between results is similar and follows the equal value line well. However, as this reduces, the FWD load transfer becomes slightly higher than that of the Prima, the difference increasing the lower the value. Unfortunately, data is limited below the 60% level and thus, it is difficult to ascertain whether this effect continues into the lower levels of load transfer. To examine if this effect is similar for all joint types, the data was separated to enable comparisons between sawn, formed and cracks. The formed joints show the greatest comparison to the idealised line, with the sawn joints and cracks showing the largest variation.

A probable reason for a higher load transfer under greater load is caused by the free slip phenomenon formed when concrete faces are placed under repetitive loading. The gradual wearing away of the micro roughness leaves only the macro roughness of the crack to resist deflection. This produces an area of free movement, or free slip, which contains little by way of support. Under a low load this free slip will be a higher proportion of the overall deflection producing a lower load transfer value; under a high load the slab will deflect more and the proportion of the free slip will become smaller, indicated by a higher load transfer; this is shown diagrammatically in Figure 6.19. As the amount of free-slip is dependant on the attrition of the crack face, slabs withstanding higher load cycles (generally older slabs) will create greater free-slip. Any reinforcement across the joint or crack will also play an important role as this can reduce the rate of crack face degradation. Table 6.6 shows the theoretical calculations from a joint which contains 100 microns of free slip movement, but provides 50% load transfer once the joint faces are engaged. The increase in transfer effectiveness can clearly be seen when the magnitude of load becomes higher.

Table 6.6 – Effect of Free Slip on Load Transfer

Load (kN)	Slab 1 Deflection	Slab 2 Deflection	Load Transfer (%)
10	100	0	0
20	150	25	16.7
30	200	50	25

This agrees with the results from the Lutterworth site as the magnitude of variation from the idealised line increases the lower the load transfer and greater the free slip percentage becomes. The separation of joint types also shows that those containing dowels produce the best agreement, as the bar will assist in the load transfer phenomenon, thereby negating the effect of any free slip. The sawn joints produce the most discrepancy as these generally open up more than the others, enabling greater free slip and an increased variation in load transfer values. This effect is reduced on the Daventry site since incorporation of steel fibres smoothes the shear slip phenomenon, as discussed in section 3.4.4 and shown in the laboratory testing results (section 6.4.4). Similarly, this can be affected by the aggregate properties which control the amount of free slip for a particular crack width. Although this method explains the phenomenon of load transfer variation between the devices, it requires further work to assess the exact effect of load magnitudes on the FWD and Prima.

Load Transfer Equations

Examination was made of the different load transfer equations provided in section 3.7 to observe their results from site obtained deflections. As the tests on site consisted of one directional testing only many of the calculations described could not be applied, thus, comparisons were only made between the equations of Croveti and Darter (1985), Teller and Sutherland (1943), and Pradhan (2002). The deflections at Daventry displayed the best correlation between test equipment, contained a good range of load transfer values, with little curling or voiding at the slab edges, and were therefore selected for the evaluation.

The findings shown in Figure 6.20 illustrate that the equation developed by Pradhan (2002) produce only a 50% or greater load transfer value regardless of the ineffectiveness of the joint. Although as simple to calculate as the Croveti and Darter (1985) method, the reduced range of results suggests that changes in load transfer stiffness are less obvious. The results obtained from the Teller and Sutherland (1943) equation exhibit a non-linear curve when compared to that of Croveti and Darter (1985). At the two extremities of 0

and 100% load transfer the results are the same, however, towards the 0-50% load transfer range a greater value per unit increase is produced, indicating that small changes in load transfer are more easily identifiable. The reverse happens towards the 50-100% range whereby the curve flattens and any increase in the Croveti and Darter (1985) equation load transfer produces only a marginal increase in the Teller and Sutherland (1943) value. In all cases, the values created by Teller and Sutherland (1943) are greater than those of Croveti and Darter (1985); however, it is the changes in gradient between low and high load transfer which show the greatest difference, providing greater clarity when determining small changes below 50%. The clearest of the equations appears to be the Croveti and Darter (1985) method as it is a simple ratio between deflections.

Crack Width

Where possible a comparison was made between crack width and load transfer. This enabled the effect of crack opening to be examined and to assess whether its measurement on site could provide estimations of slab response. Although not conclusive the Daventry site indicates that the degree of load transfer effectiveness reduces as the surface measurement of crack width increases (Figure 6.21a). A best-fit line placed through the data reveals the trend, with an appropriate lower bound showing that greater than 70% load transfer or above can be assumed when the crack width is below 2mm. This level of load transfer value for such a crack width is much greater than predicted by the laboratory data of Colley and Humphrey (1967) or Benkelman (1933); however, the field data of Colley and Humphrey (1967) shows reasonable agreement. The higher load transfer on the sites tested in this research can be attributed to the influential effect of the fibre, and the crack geometry found on site.

Only two points at 9 and 12% load transfer vary from the lower bound level and on inspection were found to be two of only four points tested at a corner location. These incorporated the reduced support of two crack faces, thus resulting in a lower load transfer. Four induced contraction joints were found to contain crack widths of approximately 11mm, but had load transfer values which varied between 35 and 95%. The most likely cause of this effect is from the geometry of the crack, which was likely to have been significantly smaller at the base than at the surface. The number of cycles that each joint had been subjected to may also have been low, thereby reducing deterioration; however, this could not be established during the site visit.

Crack and sawn joint results from the Lutterworth site show a less obvious relationship with load transfer, mainly caused by the lack of data in the load transfer region below 60% (Figure 6.21b). The greater degree of scatter in the load transfer data for the Lutterworth site may be caused by the type of reinforcement found across the joint. The mesh in the base of the slab is known to enhance load transfer capacity; however, the Concrete Society (2003) state that this will yield due to the opening of the crack. The amount of support provided is therefore questionable, and may vary enormously across individual joints, resulting in a wide variation in load transfer.

The data from the site at Skelmersdale shows large scatter with good load transfers at crack widths over 10mm (Figure 6.21c). A line of best fit was inappropriate because of the poor relationship. The data signifies that some form of additional load transfer mechanism had been inserted across some joints to enhance load transfer. The information obtained from site revealed that a lot of repair work had taken place in which the joint load transfer mechanisms may have been improved.

Cores drilled across cracked wire guidance grooves at Lutterworth provided detailed information on the changing width over depth (section 6.2.1). Testing with the Prima dynamic plate was undertaken adjacent to each core location and enabled the relationship between crack width and load transfer to be determined. The surface measurements of crack width showed poor comparison to load transfer; however, when the base crack width was used a much closer correlation of increasing crack width resulting in lower load transfer values was found (Figure 6.22). Unfortunately, all cracks produced high levels of load transfer and therefore the spread of data was restricted to 75% or more. Even with this limited information it can be seen that the base width appears to control the value of load transfer to a higher degree than that of the surface measurements, and therefore care should be taken when assessing cracks and joints on the surface measurements alone.

6.3.3 Load Step Evaluation

Load step is the difference in deflection either side of a crack when placed under load, and is a function of load transfer, foundation support and applied load. This value can be determined using either the FWD or the Prima dynamic plate and was calculated for all sites using the set-up described in section 4.5.2. Here, geophones were placed 50mm either side of the joint with the centre of the load plate situated 250mm the joint (Figure 4.9).

Device Comparison

At Daventry the joints and cracks were tested with both the FWD and Prima dynamic plate to obtain the magnitude of load step caused by each device. The comparison of data between the normalised 50 and 10kN load steps for the two devices is shown in Figure 6.23, with the line of best fit ($R^2 = 0.948$) plotted alongside the line which would have been produced had step been controlled solely by load, (i.e. the 50kN FWD load step is five times that of the 10kN Prima). The results indicate that the load step acquired from the FWD is in fact only 4 times larger than the Prima, confirming that the influence of the supporting foundation and load transfer causes significant changes in response under load.

Lutterworth displayed very similar results to those of Daventry with both the different load magnitudes applied by the FWD (Figure 6.24), and the FWD and Prima (Figure 6.25), producing lower steps than would be obtained from a direct load ratio increase. Examination of the variation between the site measured and predicted ratios of applied load magnitude reveal that the difference reduced as load magnitude was increased, shown in Figure 6.26 and summarised in Table 6.7, i.e. as the load level was increased the difference in gradient between the predicted and actual values is reduced.

Table 6.7 – Load Step Variation (Lutterworth)

Load (kN)	Step ratio	Load Ratio	Difference	Difference/kN
10-58 (Prima/FWD)	3.317	5.800	2.483	0.051
42-58 (FWD)	1.2337	1.381	0.1473	0.0092
42-85 (FWD)	1.512	2.024	0.512	0.011
58-85 (FWD)	1.238	1.466	0.228	0.0084

Figure 6.27 shows a plot of load versus absolute deflection for the increasing FWD loading, and indicates that the supporting foundation has linear stiffness. As load magnitude has little direct effect on load transfer (demonstrated in section 6.3.2), voiding under the slab and free slip in the load transfer mechanism must cause the variation between load magnitude and step ratio. In a voided slab, placed under a small load, edge deflection will be resisted mainly by the stiffness of the concrete slab. Under a large load, any void will be closed up and the deflection will be resisted by a combination of slab and foundation stiffness (Figure 3.15). Figure 6.26 and Table 6.7 demonstrate this to be the case at Lutterworth as an increase in load magnitude on site produces closer agreement to the gradient of the load ratio line. Under low loading (such as the Prima) the effect of the void is enhanced, with its size responsible for variations in slab behaviour. This is seen

when comparing the Prima 10kN load step to the FWD, as its coefficient of determination is much lower than that of the two 42 and 85kN FWD loads (0.4 and 0.915 respectively). The site at Daventry shows a better correlation between Prima and FWD load steps, as Lutterworth is thought to contain a greater degree of voiding (section 6.3.1).

Load Transfer

To ensure the slab remains serviceable the dynamic load step must not exceed a certain criterion. The development of a relationship between load transfer and load step would enable the designer to specify a load transfer dependant on the serviceability requirements of the vehicles used on the floor. For all sites a comparison was made between the magnitude of load step and the value of load transfer (Figure 6.28). This was undertaken with the Prima and FWD at the Daventry and Lutterworth sites, with the Prima alone used at Ballymena and Skelmersdale. Each plot indicates that the line of best fit contains a linear portion from the 40 to 100% load transfer range, with the horizontal axis being crossed at 100%. Values below 40% appear to have a higher gradient of step change, the overall shape fitting well to a logarithmic curve. The correlation against the data is very high (typically with an R^2 value of 0.75 or higher), with load appearing to be the controlling factor in load step magnitude. In all cases the Prima results show almost identical best fit curves, with those of the FWD increasing in magnitude in relation the size of the load.

Crack Width

Figure 6.29 shows that an increase in crack width creates a higher value of step; however, a best fit line is inappropriate due to the large scatter in the data. When the plots are split into their respective loading runs, as on the Daventry site, the effect of crack width becomes clearer (Figure 6.30). Run 1 was taken along the ends of the aisles containing little other loading source, run 2 in a bulk storage area where goods were stockpiled, and run 3 directly through a high racking aisle. The improved relationship when the results are split shows the effect of preloading. Those obtained from the areas containing the highest load (racking, run 3) resulted in lower magnitudes of step.

Invalid Load Transfer Values

On the Lutterworth site a few test locations resulted in load transfer values above 100%, thereby producing negative load step values. White Young Green (2002) found the same phenomenon when testing other sites, suggesting that the cause was a hogging effect at mid span, created by high loading of the racking either side of the crack. This irregular

load transfer effect has been the cause of a debate between various specialists in the field (FWD Users Group 2001) who state that the cause is either errors in the collection of data, or more probable, the slab acting as a beam on an elastic foundation with fixed edges. When placed under any additional load the maximum deflection will therefore occur at a position other than directly under the application point, creating the large value of joint efficiency. Any value above 100% load transfer, or with a negative load step is therefore representative of a fully supported crack or joint.

6.3.4 Slab Cantilever

Edge cantilever enables the rate of slab bending to be determined, which can then be used to assess floor flatness, currently an important issue in design. The calculation is based on the variation in dynamic deflection between the geophone next to the joint on same side of the load and that directly under the load. Comparisons between the FWD and Prima, and crack width were not undertaken as their effects have already been discussed in sections 6.3.2 and 6.3.3. The relationship between edge cantilever and load transfer or load step enables serviceability requirements for floor flatness to be checked and controlled using the known or expected behaviour of the joint. Additional mechanisms can then be inserted if required.

Load Transfer

The direction and magnitude of cantilever should be related to the load transfer effectiveness of the joint when all support conditions and free slippage are similar. In the case of a joint with good load transfer, a negative result will be produced. In a joint with poor load transfer the result will be positive, the magnitudes of which relate to the amount of load transfer. However, this is rarely the case due to crack deterioration and voiding, leading to a high degree of scatter in the data (Figure 6.31). This is highlighted by the site at Ballymena, known to contain good support conditions, producing a better coefficient of determination ($R^2 = 0.4$) than that of Lutterworth ($R^2 = 0.184$), which is suspected of voiding. In all sites lower cantilever deflections produce higher load transfer magnitudes, with cases in the positive direction (i.e. the deflection is at a maximum under the load) resulting in load transfer values above 80%, representative of an almost fully integrated slab.

Load Step

The Daventry site indicates that slab cantilever is proportional to load step with a coefficient of determination equal to 0.673 (Figure 6.32). This is similar for Lutterworth,

Ballymena and Skelmersdale; however, the reduced magnitude of step makes the results more difficult to interpret due to their close proximity. This is further reduced when the Prima is used due to the smaller load applied to the slab. The general correlation is expected since the load step is created from absolute deflection and load transfer effectiveness.

6.3.5 Deflected Shape

The deflection bowl is produced by recording geophone deflections as a dynamic load is imparted on the slab. These are then plotted against the associated distances from the load source to produce a deflection bowl (section 4.5.4). Foundation stiffness can then be examined and the position of the greatest rate of bending within the slab confirmed. This is required for the assessment of floor flatness and to verify the relevance of edge cantilever determination. This procedure was undertaken at both the Daventry and Lutterworth sites using the FWD equipment.

Figure 6.33 shows the results from the Daventry site, where the zero vertical axis is the joint location. The point at which deflection becomes negligible is approximately 2350mm from the slab edge and is the same regardless of the effectiveness of the joint. Only one point conflicted with this, and on inspection was found to be at a corner location. Here, geophones were placed linearly along the length of the joint, resulting in greater deflection due to the reduced support. The plot of geophone values generates a smooth curve between readings with the maximum rate of bending at the slab edge. A step is created at the joint location due to the discontinuity, the value of which is determined by the degree of load transfer in the joint.

Figure 6.34 from the Lutterworth site shows that the geophone locations furthest from the joint still produce a wide variation in deflection. As the results are provided for a slab loaded at the edge, it was not possible to use back-calculation methods to determine the exact foundation conditions. However, if examining the furthest geophones (D6 and D7, Figure 3.14), which are affected mainly by the subgrade, it can be assumed that the site at Lutterworth has a lower foundation stiffness than at Daventry due to the higher deflections.

6.3.6 Voiding

Under slab voiding could only be estimated at Lutterworth as this was the only site in which variation of FWD load was undertaken for the same joint. Using the methods

explained in Chapter 4.5.5 an intercept value was calculated, and used to examine the effect of voiding on other slab responses. Depending on which hypothesis is used determines how many of the slabs are estimated to contain voids. If the Wade, Cuttall et al. (1997) 75 micron limit is used 50% of the total slabs tested are affected, 60.5% if 50 microns is used (Crovetto and Darter 1985), and 88% if 25 microns is used (Cudworth 2003).

6.3.8 Summary

Increasing crack width shows a general trend of lower load transfer and higher load steps. However, the relationships are unclear with some very large crack widths still providing low deflection related response, and therefore good performance. When the data is split into separate static load areas (such as aisle racking), it shows better correlation, indicating that preloading of the slab can have a large impact on slab response. This is to be expected as any voiding or loose foundation material at the slab edge will have closed or been compacted. Tests of load transfer and crack width across joints where the full geometry was known, showed that the relationship between the base crack widths gave better correlation than that of the surface measurement. This suggests that the surface crack width must be used cautiously in the assessment of slabs.

Comparison was made between the values of load transfer obtained across different sites. Lutterworth and Daventry showed similarities in response, with the only noticeable variation being that the Daventry site contained some larger crack widths. Both sites were of a similar age but contained different reinforcement, with Daventry containing steel fibres and Lutterworth steel mesh. The site at Skelmersdale was much older and contained some very poor load transfers that had required remedial work. This was probably caused by the higher amount of load cycles it had withstood, causing deterioration of aggregate interlock.

Graphs of load transfer and load step were produced for four sites under several different load magnitudes. The results show that the foundation stiffness had little effect on the relationship in comparison to load magnitude. The trends for each plot were very similar with a linear section in the 40 to 100% load transfer region followed by a steep increase between 0 and 40%. This signifies a level of load transfer exists which should be retained to prevent problems occurring with floor serviceability.

Edge cantilever was compared against load transfer and load step to establish if it could be determined without the need for direct measurement. The majority of the sites showed reasonable correlation, with an increase in load transfer, or reduction in step, reducing the amount of cantilever. This confirms that the load transfer of the joint is important in controlling overall slab behaviour and floor flatness under dynamic load. Where the slab was thought to be voided, a much greater scatter in results was found, with the void itself increasing the amount of edge deflection.

The correlation between load transfer of the FWD and Prima is good, with equal values found for both devices. When examining load step, the correlation is satisfactory, although lower loads provide greater step than normalisation of a larger load would predict. The variation is caused by inconsistencies under low loading created by subbase support and free slip across the crack face. Once these effects are overcome, the slab structure behaves as expected with proportional response in relation to the magnitude of load.

6.4 Joint Deterioration

An extensive experimental programme was undertaken to investigate the behaviour of joints and cracks under dynamic load. A total of 82, 100x100x400mm beam samples were tested from 25 concrete mixes to examine 39 different variables, namely: crack width, aggregate size, steel fibre quantity, steel fibre type, mesh reinforcement, traditional reinforcement, load magnitude, and crack orientation. The detail and logic behind the test set-up is described in Chapter 5, and it consisted of a double cracked beam specimen cyclically loaded for 250,000 cycles at a rate of 2Hz. Measurements of vertical and horizontal displacement were recorded every 600 cycles enabling the effect of deterioration to be recorded.

This chapter discusses the results of the tests and analysis the key variables, with the aim of improving the understanding of joint behaviour and effectiveness when placed under repetitive load. Appendix B contains a summary of all the tests undertaken during testing, with the key phases (described in section 6.4.3) identified by cycle number and differential displacement magnitude.

6.4.1 Specimen Production

Over the course of the research 82 specimens were tested, all of which were cast and prepared in accordance with the methodology supplied in section 5.4. In each mix, six 100x100x400 beams were cast, together with two 100x100x100 cubes to monitor the compressive strength. This was designed to have a target mean strength of 45MPa at 28 days (section 5.4.2), with the results obtained from testing provided in Table 6.8. Each beam sample was given a specific code to enable identification throughout testing. This was in the form:

Concrete strength (MPa) / Reinforcement type / Reinforcement volume or diameter (kg/m³) or (mm) / Crack Orientation / Crack width (mm) / Load magnitude (kN).

Table 6.8 – Concrete Compressive Strengths

Mix No	Date Cast	Specimen Codes	Cube 1 (MPa)	Cube 2 (MPa)	Average (MPa)
1	27/11/2002	40/Non/0/V/0.66/4 40/Non/0/V/01.98/4	56.33	55.01	56
2	27/11/2002	40/65-60/20/V/1.98/4 40/65-60/20/V/3.3/4 40/65-60/20/V/4.62/4	55.44	55.29	55
3	04/11/2002	CANCELLED	0	0	0
4	04/11/2002	CANCELLED	0	0	0
5	06/11/2002	40/65-60/30/V/4.62/4	51.76	51.43	52
6	12/11/2002	40/65-60/20/V/3.96/4	52.76	55.33	54
7	12/11/2002	40/65-60/30/V/1.98/4 40/65-60/20/V/3.3/4	50.25	50.04	50
8	14/11/2002	REJECTED	44.11	45.3	45
9	14/11/2002	40/65-60/40/V/4.62/4 40/65-60/40/V/3.3/4 40/65-60/40/V/1.98/4	44.91	47.21	46
10	21/01/2003	CANCELLED	0	0	0
11	21/01/2003	REJECTED	41.23	40.35	41
12	03/02/2003	40/80-60/30/V/1.98/4 40/80-60/30/V/4.62/4	45.43	43.81	45
13	10/02/2003	40/45-50/30/V/4.62/4 40/45-50/30/V/1.98/4 40/45-50/30/V/3.3/4	43.98	46.82	45
14	25/02/2003	40/65-60/30/V/0.66/6 40/65-60/30/V/1.98/6	47.14	43.89	46
15	10/03/2003	40/65-60/30/V/1.98/2 40/65-60/30/V/3.3/2 40/65-60/30/V/4.62/2	43.11	47.10	45
16	17/03/2003	REJECTED	42.05	43.66	43
17	01/04/2003	40/65-60/30/Par/0.5/2 15/04/200340/65-	46.55	47.40	47

		60/30/Par/1.98/2			
18	15/04/2003	40/65-60/20/V/0.66/4 40/65-60/20/Par/0.66/4 40/65-60/20/Par/0.9/4 40/65-60/20/Par/1/4 40/65-60/20/Par/1.3/4	44.79	45.71	45
19	29/04/2003	REJECTED	42.54	45.18	43.86
20	06/05/2003	40/80-60/30/V/3.3/4 40/80-60/30/V/4.62/4	45.18	44.57	44.88
21	07/05/2003	40/Mesh/7/V/1.98/4 40/Mesh/7/V/3.3/4 40/Mesh/7/V/4.62/4	46.72	44.53	45.63
22	08/05/2003	40/65-60/30/V/3.3/4 40/65-60/30/Par/0.66/4 40/65-60/30/Par/1.98/4	45.02	45.97	45.50
23	12/05/2003	40/65-60/40/Par/0.66/4 40/65-60/40/Par/0.75/4 40/65-60/40/Par/1/4 40/65-60/40/Par/1.5/4	44.69	45.23	44.96
24	13/05/2003	40/45-50/30/V/3.3/4 40/45-50/30/V/4.62/4	43.7	48.09	45.90
25	07/07/2003	40/65-60/40/V/5.94/4	44.97	49.35	47
26	07/07/2003	40/65-60/30/V/5.94/4	44.15	48.02	46
R1	17/12/2002	40/Trad/7/V/1.98/4 40/Trad/7/V/4.62/4 40/Trad/7/V/3.3/4	52.37	51.96	52.17
M1	20/11/2002	Mor/Non/30/V/0.66/4	29.45	32.21	30.83

The testing resulted in a variation of up to 14MPa between the mean cube compressive strengths. Mix references 8, 11, 16 and 19 failed to provide the target mean strength of 45MPa specified in section 5.4.2 and were therefore rejected and replaced. The mixes constructed earlier in the testing period showed higher strengths than those cast later (Figure 6.35). The change was thought to have been caused by the moisture condition of the coarse aggregate prior to testing. This was stored externally and was therefore open to climatic conditions affecting the moisture level. Although checked using the Speedy moisture meter, and amendments made to the material quantities, it was thought this may still have affected the water/cement ratio. This resulted in a decrease in strength during the wetter months, and explains the shape of the best fit line in Figure 6.35. However, the magnitude of this variation was not thought to have any significant effects on the cyclic load test results. Mix ‘M1’ was made of mortar with all aggregate particles below 6mm. As expected this gave a lower strength of 31MPa due to the nature of its constituent materials.

Mixes referenced 3, 4 and 10 were repeated as the specimens contained honeycombing at the corners due to the dryness of the mix and poor compaction. As the condition of the beams could not be checked internally these were discarded and replaced to avoid any discrepancy in results.

6.4.2 Specimen Quantities

To ensure that representative behaviour was obtained, at least two samples were tested for each variable. Ideally three or more tests would have been undertaken; however, the duration of each (approximately 36 hours) forced a compromise. Initially a small experimental program was carried out to investigate the variability between results. This showed that usually two samples provided sufficiently similar displacements (below 150 microns) across both the same and opposing cracks within the same specimen . A strategy was developed whereby two beams were tested for each variable, with a third beam kept in reserve, used only if the variation was above certain criterion. In the case where a third beam was required for testing, the results of the two beams matching closest were used, with the third disregarded. However, comparison was also made to the results of samples looking at similar variables to ensure large discrepancies did not exist. A single beam containing reinforcement bar (40/Trad/7/V/3.3/4) was tested at the 3.3mm crack width as negligible change was found between the 1.98 (40/Trad/7/V/1.98/4) and 4.62mm (40/Trad/7/V/4.62/4) crack width. Similarly, only one specimen was tested for the 40/65-60/20/V/3.92/4 as it was an additional value to check the variation between the 3.3 (40/65-60/20/V/3.3/4) and 4.62mm (40/65-60/20/V/4.62/4) crack width values.

Table 6.9 provides a comprehensive list showing the number of beams tested for each variable.

Table 6.9 – Beam Specimens Tested

Specimen Group	0.66mm	1.98mm	3.3mm	4.62mm	Other
None	2	2			
30kg /m ³ Fibre (Mortar)	2				
20kg/m ³ Fibre	2	2	2	2	1 x 3.96mm
30kg /m ³ Fibre		2	3	2	2 x 5.94mm
40kg/m ³ Fibre		2	2	2	2 x 5.94mm
30kg /m ³ RC-80/60-BN Fibre		2	2	3	
30kg /m ³ RC-45/50-BN Fibre		2	3	3	
Re-bar		2	1	2	
Fabric		2	2	2	
30kg /m ³ Fibre (2kN Load)		2	2	3	
30kg /m ³ Fibre (6kN Load)	2	3			
20kg/m ³ Fibre (Parallel Crack)	2	2			
30kg/m ³ Fibre (Parallel Crack)	2	2			
40kg/m ³ Fibre (Parallel Crack)	2	2			

When testing across two separate cracks, as in this method of testing, there was inevitably a difference in differential displacement measurements between front to back ‘F_l Vs R_l’ and between the two cracks on the same face ‘F_l Vs F_r’ (locations shown in Figure 5.21). This was due to variations in surface profile within a single crack, and between two cracks. This was caused in particular by the distribution of aggregate particles and fibre reinforcement, along with any minor eccentricities in loading. During testing the degree of maximum variation between displacements in the same crack was 112 microns and across different cracks was 261 microns. The average variation was 52 microns and 29microns respectively. To ensure the results were representative across all cracks a 150micron boundary was applied which no variation in differential could exceed. This was reduced to 100microns in conditions where the 250,000 differential deflection was below 500 microns. This was chosen as any specimens showing values higher could be assumed to contain some discrepancy in crack face condition. To obtain a representative displacement for the specimen under consideration, the values across the same crack were averaged, with this value again averaged with the value from the opposing face (equation 6.1).

$$\{[(F_l + R_r)/2] + F_r\}/2$$

equation 6.1

Calculating the value in the way reduced the effect of any discrepancy between cracks and provided a displacement closer to the characteristic value.

6.4.3 Deterioration Phenomena

Each beam was tested to 250,000 cycles, with specific specimens continued for a further 250,000 cycles to examine longer-term deterioration patterns. To enable comparison between variables the differential displacement between positive and negative loading at key points relating to the transition between deterioration phases was used (Figure 5.25). Occasionally the beam was deemed to have failed prematurely, with load transfer becoming negligible and deflections extremely large, limited only by the restraints placed on the loading apparatus. A differential of 1.6mm or above was found to sustain very little extra loading was therefore classed as the boundary for failure. In this situation the number of cycles to failure provided some perception of strength and durability of the load transfer system.

Sixteen of the beams reached a point where they were deemed to have failed prematurely. The displacement differential versus cycle degradation plots produced similar patterns, as shown in Figure 6.36, with four distinct phases.

During phase I, rapid deterioration occurs resulting in a steep gradient (figure 6.37). After approximately 10,000 cycles this moves into phase II where a low magnitude increase, linear degradation is observed. In tests causing specimen failure phase III is identifiable, whereby deflection accelerates rapidly until reaching a magnitude of approximately 1.2mm. At this point the specimen enters phase IV where failure is likely to occur within the next 10,000 cycles. This shows similarities to the plots of Colley and Humphrey (1967) and Thompson (2001), section 3.5, although in their research deterioration occurred at different rates due to the constituent materials and reinforcement types.

The shape of the overall plot is caused by the changing aggregate interlock mechanisms as the system degrades. During phase I the mortar deteriorates quickly, it being a relatively weak material. Once this has transpired the increase in deflection slows due to the greater strength and bonding of the larger aggregate particles (phase II). As failure commences in phase III the aggregate begins to debond from the surrounding mortar, cracks are initialised and the concrete face begins to degenerate. This increases the stresses on the remaining particles creating further cracking until such a point that phase IV is entered, whereby negligible load transfer is available through the aggregate interlock mechanism. The influence of reinforcement such as steel fibres or fabric delays the onset of the preceding phase. The mortar deterioration still occurs as shown by the steep gradient in phase I; however, the reinforcement transfers some of the load and

lowers the contact stress in the crack face. This reduces the rate of deterioration and delays the onset of phase III. Variations between fibres and fabric reinforcement are found when phase III is entered as the fabric still retains its load transfer mechanism, whilst the fibres begin to deteriorate.

The differential deflection is a combination of movement in both the upward and downward directions caused by a positive and negative loading pattern. In the majority of cases (81%) the displacement in each direction of load was similar, with less than 70% variation between initial and final displacements. However, a number of specimens exhibited significant differences in deterioration, with greater displacement in one direction compared to the other (Figure 6.38). This was most likely caused by a variation in restraint to movement from the surrounding material. In one direction two pieces of hard aggregate bear upon one another, whereas in the other direction little support is provided and displacement can occur (Figure 6.39). Load eccentricity may also have created this effect, although this was thought unlikely due to the test configuration.

In 8% of the tests a reduction in displacement was found in one direction, signifying a greater resistance over time (Figure 6.40). Two possible reasons for this are as follows: the first is described by Laible, White et al. (1977) whereby small material and dust falls into the sockets from the degraded crack face, thereby reducing the amount of free slip. The other, as identified by White and Holley (1972) occurs when one section of aggregate has overridden another and requires a greater force to push it back into its original location due to the undulations and orientation of the crack face. The gradual reduction in displacement, rather than a sudden step, as observed in Figure 6.40 suggests that in this experimental programme small material accumulation is the dominant effect.

The examination of expelled material and specimen cracking provided further evidence surrounding the degradation process. In the majority of beams a crack propagated from the edge of the supporting shim to the base of the saw cut and then back to the edge of the bottom, central encasement strap. The crack itself was hairline at first, but could be seen to open and shut very slightly under load. The depth into the face of the beam was generally below 10mm and it therefore appeared to be a surface phenomena associated with the stresses created through clamping. In specimens where differential displacement was low, very little material fell from the crack; however, on completion of the test a small layer of dust could be seen directly under the specimens. On those where movement was higher (0.2mm or above) the amount of fine-grained material was much greater, but all of the larger 10-20mm aggregate appeared to be intact. In specimens which were close

to failure, sections of concrete up to 20mm in size spalled from the base of the beam on either side of the crack, along with large amounts of cement dust. Loose large aggregate particles of 10-20mm diameter, which had become detached from the surrounding matrix, could also be seen on the sides and top of the beam, and were only prevented from ejection by the support of the surrounding material. Upon failure the entire surface of the crack began to break away, resulting in a large amounts of debris.

6.4.4 Influence of Initial Crack Angle

The reference mix containing 30kg/m³ of RC-65/60-BN steel fibre showed an increase in differential deflection as the initial crack width was increased (Figure 6.41). The variation between individual specimens was acceptable with only one specimen at a crack width of 3.3mm showing significant discrepancy. The reason for this error is unknown but could be due to a lack of large aggregate or steel fibre at the crack face, caused by insufficient mixing or separation under vibration, the effects of which are exaggerated with a small sized specimen. At around the 5 to 6mm surface width the joint resistance to cyclic loading reduces rapidly, with failure (defined as greater than 1.6mm differential displacement) occurring at a width of 6mm after 10-30,000 cycles.

There is a distinct change in shape between individual cycle load/deflection plots of small (1.98) and large (5.94) crack widths (Figure 6.42). At the beginning of the narrower crack width tests the cycle shows a smooth transfer of deflection as load is applied, following the shape of the load application sine wave. Toward the end of the test this has changed slightly with a steeper gradient at the point where load transfers from a positive to negative direction. This unrestricted movement is known as free slip and is detected when the majority of deflection resistance occurs at the extremities of the deflection cycle; with the transfer line being almost vertical. The larger crack widths contained much higher levels of this free slip regardless of when the cycle plot was taken and as such were more prone to increased degradation.

This change in cycle geometry indicates that during early stages of small crack width cyclic loading, much of the deflection resistance is provided through micro roughness friction, hence the smooth curve. As the mortar is worn away macro roughness becomes dominant resulting in a much steeper transition between positive and negative deflection. The wider crack width accentuates this effect as the free movement under the aggregate will have become much greater. The inclusion of fibre reinforcement restrains some of the load throughout the cycle, particularly when the crack width is small. As the width opens

the fibres tend to break and their effect becomes less influential, creating a much steeper gradient as load is transferred from the positive to negative directions.

The non fibre reinforced beams showed a much lower resistance to differential deflection than that of the reference fibre reinforced concrete mix, with failure occurring when the surface crack width was less than 2mm (Figure 6.41). The two beams tested at the 2mm crack width show good comparison with a variation below 50 microns. Prior to placement in the rig the pre-cracking had caused the specimen to split into three sections as no restraining reinforcement was available. Upon loading, early degradation could be seen to take place at a fast rate with large amounts of rubble falling from the crack surface, accompanied by high visual movements of the central block.

At both the beginning and end of the tests the deflection cycle shape indicates that most of the resistance to deflection occurs at the extremities of movement (Figure 6.43). The minimal resistance to free slip shows that bearing rather than friction is the dominant factor in load transfer at this stage. As crack width increases the distance between the bearing surfaces becomes larger (Figure 3.4), as shown by the greater amount of differential movement in the initial cycles. This deflection is then accentuated over the test period until aggregate interlock is lost and failure produced.

The mortar beams containing steel fibre investigated the relative contribution of steel fibres and the coarse aggregate in resisting displacement. Both specimens failed early on in the test period, despite being set at the smallest 0.66mm surface crack width, with the increase in deterioration occurring extremely rapidly even though only a small amount of rubble was created (Figure 6.41). The fibres bridging the crack were seen to move freely as the central block was loaded, and upon failure the majority had snapped rather than pulled out of the mortar, with the large movements the probable cause. This failure mode illustrates that the hook anchored to the mortar extremely well, although the increase in deflection over time, rather than a sudden catastrophic failure indicates that some degree of gradual pullout occurred.

The examinations of single cycle deflection at the beginning and end of the tests indicate that although the majority of resistance occurs at peak deflection, some frictional capacity is provided (Figure 6.44). Restraint must therefore be provided from the fibre, which once extended to its full length prevents continued movement. This pattern continues throughout the test, although its capacity reduces with the onset of failure.

6.4.5 Volume of Fibre Reinforcement

The increase in fibre volume from 20 to 40kg/m³ had little influence upon the magnitude of differential displacement in surface crack widths below 3mm; however, above this value increasing the fibre volume had a pronounced beneficial effect in delaying failure (Figure 6.45). This was similar to the findings of Thompson (2001) who examined the behaviour of fibre reinforced cement bound materials and found that increasing the fibre volume had little effect on decreasing displacements.

At the 0.66mm crack width the 20kg/m³ mix experienced a higher differential displacement than either the 30 or 40kg/m³ beams predict when a linear line is extrapolated back to the zero axis. However, as the relationship at these low crack widths is unknown it may be that a non-linear function exists, with the 0.66 and 1.98mm values being similar. In either situation the deflections at this level are so small as to make the variation negligible regardless of fibre quantity.

The main effect of the steel fibres occurs as the surface crack widths become larger. At the 3.3mm level all mixes produced similar behaviour, but when increased to 4.62mm the 20kg/m³ beam failed within 50-113,000 cycles. To evaluate the behaviour between these points a single specimen was tested at 3.96mm crack width. This confirmed the expected trend displaying a large increase in differential displacement when compared to lower crack width values, and that of the 4.62mm crack widths containing higher fibre quantities. The contrast between the 30 and 40kg/m³ beams only becomes apparent when the crack width reaches 4.62mm, at which point the lower fibre quantity produces an increase in displacement. This continues to the 5.94mm crack width at which point both beams fail, with that of the 30kg/m³ occurring much more quickly (10-30,000 compared to 212,000 cycles). The two beams at 40kg/m³ show large variation between results; however, one of the beams failed towards the end of the test with the other showing rapid increases in differential displacement gradient in the last 40,000 cycles (signifying phase III behaviour and imminent failure). A further 20,000 cycles was applied to this beam at which point phase IV was achieved, indicating that the two values are in fact much closer to each other than would appear on the plot.

Figure 6.46 illustrates the effect of increasing fibre quantity for each crack orientation. The shape of the plot shows that adding fibres is most beneficial for larger widths, with a delay in failure and reduction in displacement. Increasing the fibre volume with smaller

cracks had little effect; however, when compared with non-reinforced beams the advantages of adding even a small percentage is clear.

Examination of single cycle deflection displays a variation between shear slip of the different specimens. The 20kg/m³ of fibre showed that in large crack widths most of the resistance occurred at the extremities of displacement, indicative of a bearing type restraint (Figure 6.47). During small width tests a reduced gradient was found in the early stages of testing, signifying that friction was also assisting in the transfer of load. The 30kg/m³ mix exhibited an improved transfer mechanism as a smoother curve was found throughout the smaller widths; however, much of the restraint was still created in bearing for those beams with larger cracks approaching failure (Figure 6.42). A fibre volume of 40kg/m³ provided a reduction in shear slip regardless of width and time of cycle measurement (Figure 6.48). Even when failure was approached in the largest crack, the curve still compared well to that of load application, indicating that friction was a considerable action in the restraint on movement.

The cause of this change in displacement resistance can only be attributed to the steel fibres, as no other variable was altered. Fibre contents of 30 and 40kg/m³ produced a significantly greater restraint to movement, with the maximum differential controlled by the aggregate interlock and fibre pullout. The fibres can help in two ways: they can avert degradation of the face by restraining crack growth; and secondly, the fibres will cross the crack and act as mini dowels transferring load. In low quantities these effects are reduced as fewer fibres will have less bridging points thereby lessening the force required to cause bending. There will also be fewer fibres to hold the crack face intact once micro-cracking has developed.

6.4.6 Fibre Aspect Ratio

The aspect ratio of a fibre is the ratio of length to diameter. Figure 6.49 indicates that an increase in this value reduces the differential displacement significantly at surface crack widths above 3mm. The higher aspect ratio produces a greater number of fibres in the mix for a given dosage (as shown in Table 6.10). This improves the number of bridging points across the crack enhancing resistance to deflection, as shown with the fibre quantity comparison plot in Figure 6.50. With a simple calculation of fibre volume it is possible to determine that the use of the RC-80/60-BN results in 1.4 times as many fibres as the RC-65/60-BN, which contains 1.4 times as many as the RL-45/50-BN. In essence this causes the RC-80/60-BN to relate more closely to the 40kg/m³ RC-65/60-BN beam, which when

compared to the fibre quantity plot shows closer representation than that of the 30kg/m³ beam used as a reference. Similarly the RL-45/50-BN is equivalent to a beam containing closer to 20kg/m³ of fibre, which shows good comparison to the results of the 20kg/m³ values.

Table 6.10 – Typical Fibre Count across Crack Face

Fibre Type	Fibre Volume (kg/m³)	Diameter (mm)	Length (mm)	Fibres/kg	Fibres across Crack Face
RC-65/60-BN	20	0.9	60	3200	31
RC-65/60-BN	30	0.9	60	3200	47
RC-65/60-BN	40	0.9	60	3200	62
RL-45/50-BN	30	1.05	50	2800	34
RL-80/60-BN	30	0.75	60	4600	67

These observations might suggest that aspect ratio only influences differential displacement through changing the fibre count across the crack, with the results from Figure 6.50 showing similar values to that of the equivalent standard RC-65/60-BN. A plot of fibre number against differential displacement (Figure 6.51) shows that as fibre numbers increase the magnitude of differential displacement reduces significantly, with the 4.62mm crack showing reductions in displacement from over 1.1mm to below 0.15mm when the fibre count is increased across the crack face from 31 to 67. Fibre length and diameter effects appear to be negligible, although the greater thickness may show some slight increase in fatigue resistance.

Figure 6.52 clarifies the influence of aspect ratio on the reduction of differential deflection with those containing higher values showing better performance. Specimens with larger cracks show the greatest increase in performance; however, even at smaller widths the advantages of using a high aspect ratio fibre can be seen.

Examination of the single cycle plots (Figure 6.53) illustrates that towards the end of the high crack width tests the cycle is still smooth for those specimens containing 30kg/m³ of the RC-80/60-BN fibre ($L/d = 80$), indicating that resistance from the fibre is increasing the frictional component. The RL-45/50-BN fibre shows a different behaviour; towards the beginning of the test resistance to deflection provides good agreement to the load application plot, indicating energy absorption throughout the loading cycle from both friction and fibre bending (Figure 6.54). Later cycles produce a much steeper gradient as the load changes direction, with the majority of resistance at the extremities of deflection.

This indicates that the frictional component has degraded over time with a bearing effect becoming the dominant means of load transfer, similar to that found at a volume of 20kg/m^3 .

6.4.7 Load Magnitude

The application of a relatively low 2kN load causes little change in differential displacement regardless of surface crack width, with the overall pattern in an individual test showing only minor degradation, and even some reduction in displacement, over time (Figure 6.55). The reason for this can be assigned to the gradual accumulation of cement dust and rubble in the aggregate sockets, which eventually builds up and reduces the available free movement. Examination of individual loading cycles shows that even when nearing the 250,000 cycle limit, the resistance to displacement is shared equally through the entire cycle with friction accounting for much of the energy dissipation (Figure 6.56).

The 6kN load resulted in much faster degradation with only the 0.66mm surface crack width able to resist failure up to 250,000 cycles. Regardless of crack width, examination of all individual load cycles show that at the beginning and end of the test resistance to movement at the transition between positive and negative loading is extremely low, with the majority coming at the extremities of displacement (Figure 6.57). This signifies a bearing effect with high load degrading the frictional capacity of the crack face early in the test.

The summary plot in Figure 6.58 illustrates the effect load magnitude has on deflection, with the higher levels showing large increases in deflection. With the exception of extremely small crack widths the prevention of failure for a load application of 6kN is negligible, with a reduction to 2kN producing only minor deflection.

These results contain similarities to the prediction of Ioannides and Koreveis (1990) who stated that there is a particular level of stress where degradation occurs, below which the structure is relatively unaffected. In the case of the testing undertaken, this value is somewhere between the 2-4kN range, which calculates as a shear stress of 100 to 200kN/m^2 .

6.4.8 Parallel Cracks

The effect of crack geometry in resisting differential deflection can clearly be seen when comparing the 30kg/m^3 'V' shaped crack against that of a similar surface sized parallel

crack. Figure 6.59 demonstrates that the parallel crack width is highly influential in the resistance to deflection, with up to 40kg/m^3 of fibres unable to resist failure when over 1.2mm in size. A point exists near the 0.7mm crack where displacement increases greatly, with widths below this level showing only a gradual increase in movement. This agrees well with the static tests of Pearson (1999) and ACI Committee 360 (2000), and the fatigue test results of Colley and Humphrey (1967), who all show that levels of load transfer reduce significantly at crack widths over 0.5mm (section 3.5).

The single load cycle plots illustrate that as most tests commence, particularly those with smaller crack widths, deflection resistance produces a relatively smooth curve with friction providing substantial restraint (Figure 6.60). For smaller crack widths this continues for a reasonable period throughout the test; however, near the 250,000 limit bearing begins to dominant. For larger crack widths both early on and nearing failure the majority of deflection occurs at the extremities of deflection with bearing again being most influential.

6.4.9 Reinforcement Type

The introduction of either a 7mm rebar or section of A142 mesh (containing one longitudinal and two transverse members) shows an improvement in resistance to displacement when compared to those reinforced with steel fibres (Figure 6.61). The increase in crack width has very little impact on the amount of displacement, with even the 4.62mm tests resulting in values below 0.7mm. The difference between the mesh and rebar displacement is very small with mesh giving fractionally lower deflection at small widths, this swapping over at the 3.3mm crack position. When comparing with steel fibres the mesh and reinforcing bar shows reduced displacements to that of 20 and 30kg/m^3 . However, when examining 40kg/m^3 the variation is much smaller showing that the inclusion of steel fibres above certain levels can produce similar effects in respect to the prevention of deterioration.

Both types of reinforcement show almost identical single cycle load deflection curves uninfluenced by cycle number or crack width (Figure 6.62). These are generally smooth, with a gradual increase in deflection on application of load, demonstrating that displacement is controlled by the deflection of the bar rather than bearing of the aggregate in its socket. Friction may also assist in the resistance; however, the previous plots show that at large crack widths this phenomenon will have reduced considerably.

6.4.10 Serviceability Limitations

As has been stated in section 6.4.3, the beams that failed providing no load transfer comprised four main phases. Phase III was indicative of imminent failure (within the next 20,000) cycles, and could therefore be used to identify problematic cracks. If the differential deflections could be contained below this level then it would appear that the joint could be classed as ‘fully serviceable’ (Figure 6.63). Table 6.11 provides a summary of differential deflection values at which Phase III deterioration began to operate. Unfortunately some of the specimens failed early on during the test and therefore clear identification between phases was not possible.

Table 6.11 – Differential Deflection at Phase III

Specimen Code	Phase III Differential Displacement (mm)
40/Non/0/V/1.98/4	1.15
40/65-60/20/V/4.62/4	1.10
40/65-60/30/V/5.94/4	0.80
40/65-60/40/V/5.94/4	0.65
40/45-50/30/V/4.62/4	0.60
40/65-60/30/V/1.98/6	0.80
40/65-60/40/Par/1.5/6	1.40

The table shows that the onset of phase III deterioration is dependant on the reinforcement type/quantity and the load magnitude. A lower bound level can be drawn at 0.6mm differential displacement, at which point none of the specimens tested would show phase III behaviour. This suggests that if differential deflection is kept within this limit (0.3mm load step on site) then the joint will remain fully serviceable.

The literature in section 3.8.1 provided two values of load step within concrete slabs on grade which would provide acceptable behaviour in respect to ride quality. However, there is little information to confirm these values, and the variation in vehicle type using the floor will be critical to the levels chosen. To examine the effect of reinforcement type and load magnitude on these serviceability requirements, both values have been used to assess their applicability. The lower value was 0.1mm, with an upper level being 0.3mm. As the laboratory testing in this research has examined differential displacements caused when loading in the positive and negative directions, the values obtained must be doubled to produce comparisons with site slabs, becoming 0.2 and 0.6mm respectively. In this case the 0.6mm allowable displacement is very close to the phase III deterioration change

point (described above). The 0.2mm differential displacement provides a far greater safety factor against complete joint failure, whilst also ensuring vehicle load stepslimitations are met. The 0.2mm (limit ‘A’) and the 0.6mm (limit ‘B’) have been used in the test results to indicate tolerable crack widths for serviceability.

Insertion of these serviceability limits onto the plots of crack width and differential displacement (Figures 6.41/6.45/6.49/6.55/6.59/6.61) for the entire range of testing, made it possible to determine acceptable values of surface crack width for a given reinforcement or load magnitude. This information is provided in a summary form in Table 6.12.

Table 6.12 – Allowable Crack Widths Preventing Serviceability Problems

Specimen Type	Limit ‘A’ (0.2mm) Crack Width (mm)	Limit ‘B’ (0.6mm) Crack Width (mm)
Mortar	0.09	0.21
Parallel 30kg/m ³ Fibre	0.38	0.9
Non	0.46	1.00
Parallel 20kg/m ³ Fibre	0.80	1.08
Parallel 40kg/m ³ Fibre	0.85	1.16
6kN Load	0.98	1.45
20kg/m ³ Fibre	2.82	3.9
RL-45/50-BN Fibre	3.10	4.26
30kg/m ³ Fibre	3.48	4.78
40kg/m ³ Fibre	4.62	5.74
RC-80/60-BN Fibre	4.26	6.98
2kN Load	8.2	> 10.00
Steel Fabric	> 10.00	> 10.00
Steel Rebar	> 10.00	> 10.00

These results show that there can be significant variation in allowable crack widths between limit ‘A’ and Limit ‘B’ requirements. The magnitude of load is highly influential, increasing the allowable crack width for serviceability limit ‘A’ from 0.98 to 8.2mm with a reduction in load from 6kN to 2kN. Steel bar and fabric show excellent resistance to displacement in respect to limits ‘A’ and ‘B’ with extrapolation of the data indicating that 10mm crack widths still produce displacements well below serviceability limit ‘A’. The use of RC-80/60-BN shows similar behaviour to that of mesh when widths are below 4.26mm; however, after this point an increase in displacement occurs with the limit ‘B serviceability requirement being exceeded at a 6.98mm crack width. Steel fibres of type RC-65/60-BN also prevent the serviceability limits being reached until high

surface crack widths are produced, the effectiveness increasing with the fibre quantity used. Parallel cracks can only withstand both 'A' and 'B' limits for crack widths below 1.2mm, with fibre quantity having very little impact. Mortar specimens, although containing steel fibres restrain very little displacement and show that the aggregate interlock effect is still important regardless of the reinforcement used.

6.4.11 Summary of Laboratory Investigation

The cyclic load testing of small-scale specimens has established that deterioration can be split into four main phases. Phase I, consists of fine material degradation and produces a rapid increase in differential displacement. Phase II shows little deterioration of the concrete face and differential displacement becomes linear. Phase III produces concrete face cracking and aggregate and fibre pullout, resulting in an increase in differential displacement. Phase IV is failure whereby the face can no longer sustain any load.

'V' shaped cracks have been shown to be much more effective in transferring load and reducing crack face degradation than parallel cracks; however, surface crack width is still highly influential to both. Steel fibre reinforcement provides significant increases in restraint to degradation when compared to non-reinforced specimens, although it is a combination of the fibres and aggregate interlock that cause this effect. The fibre quantity and type controls the amount of differential deflection restraint, with the number of fibres crossing the crack being the major contributory factor. Specimens containing steel fabric and reinforcing bars show almost no change in deflection throughout the 250,000 cycles regardless of the crack widths tested. This is due to the load carrying capacity of the bars crossing the crack, preventing macro roughness degradation. The magnitude of load controls the amount of differential displacement and the rate of deterioration. A 2kN load shows relatively small changes in displacement throughout the duration of the test, with a 6kN load showing rapid failure in larger crack widths.

Examination of the single cycle plots shows that friction from the local roughness dominates in the early stages of testing, especially under small crack widths. As the stresses across the crack are increased this degrades, the rate of which depends on load magnitude, reinforcement type and crack width, with resistance then converting to bearing of the macro roughness. In situations where failure is approached the aggregate providing this bearing resistance, cracks and pulls out from the surrounding mortar leading to reduced aggregate interlock, increasing stress and further degradation. There

are no specific values where the changes in restraint occur, instead resulting in a gradual transfer.

Serviceability limits show the importance of each factor examined during testing in providing resistance to displacement. This shows that if crack widths can be prevented from opening up excessively, or loads kept within certain criteria then the type or quantity of reinforcement used is inconsequential. However, in normal circumstances crack widths open up to varying degrees and therefore the use of any reinforcement is highly influential. As expected the greater the surface crack width measurement, the more reinforcement is required within the concrete to keep the displacements within tolerable limits.

6.5 Summary of Field and Experimental Work

Examination of concrete slabs within the field combined with laboratory testing has enabled a more complete picture to be developed in respect to crack and joint behaviour. Typical crack geometries have been determined and display a 'V' shaped formation caused by differential shrinkage. This indicates that surface measurements alone cannot be used in the assessment of cracks, as those previously thought to be unsatisfactory (greater than 2mm in width) can provide adequate load transfer as shown by the deflection test results on site. The geometries found in the field have then been used within the small-scale laboratory test procedure to provide an understanding of the deterioration processes.

Links have been made between the effectiveness of the joint in transferring load, to other deflection dependant responses such as load step and edge cantilever. This has shown that the joint is highly influential in the behaviour of the slab as a whole; both in resisting failure mechanisms and ensuring serviceability requirement are met.

Reinforcement within concrete slabs on grade has been shown to influence both the single cycle load transfer behaviour, and the deterioration rate of the concrete face. In all situations the local roughness was found to deteriorate early on in the cyclic loading tests, relying on the global roughness for longer-term load transfer. The incorporation of reinforcement delayed the attrition of global roughness and therefore retained much of the load transfer. This also enabled serviceability requirements to be controlled for given crack widths. In site conditions steel mesh was found to be more beneficial in larger cracks than quantities of 20kg/m³ of steel fibre reinforcement; however, larger quantities

of 40kg/m³, or the use of a different fibre type, were found to produce similar results within the laboratory.

The variation in foundation condition under the slabs tested in the field produced different deflection responses. This confirmed that edge support cannot be relied upon and therefore the laboratory testing was sufficiently accurate in producing a lower bound of displacement degradation. In both laboratory and field work, load was found to have a highly influential effect in respect to both deflection magnitude and crack face deterioration, and therefore needs to be carefully assessed prior to slab construction to ensure load transfer mechanisms are satisfactory.

The following Chapter utilises the information gathered in the small scale testing of laboratory specimens to develop a representative load transfer mechanism within a finite element model. This is then used to model the sites investigated during field testing enabling verification of the method and further analysis of the load transfer effect.

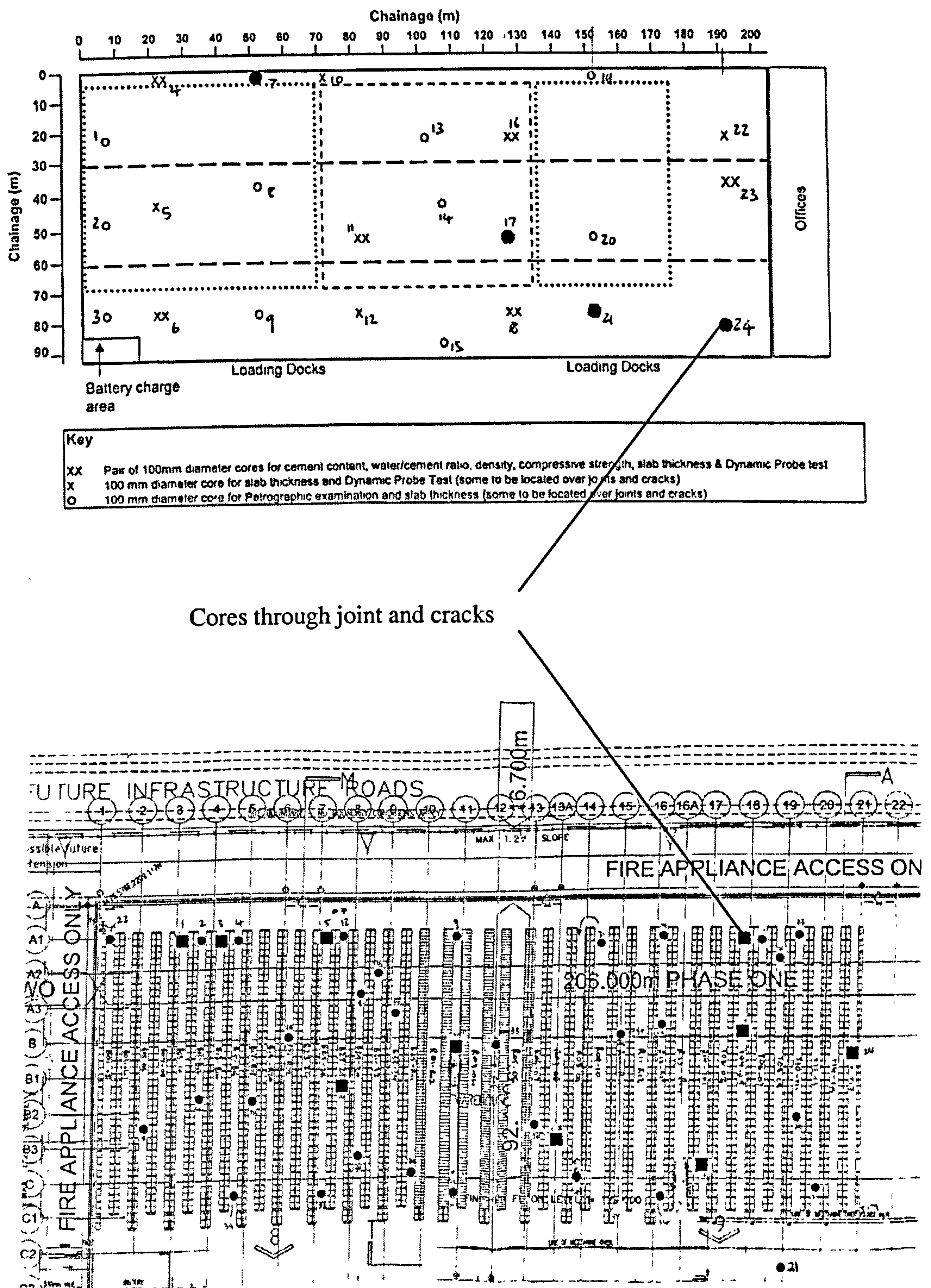


Figure 6.1 – Lutterworth Core Locations (Top – visit 1, Bottom - visit 2)

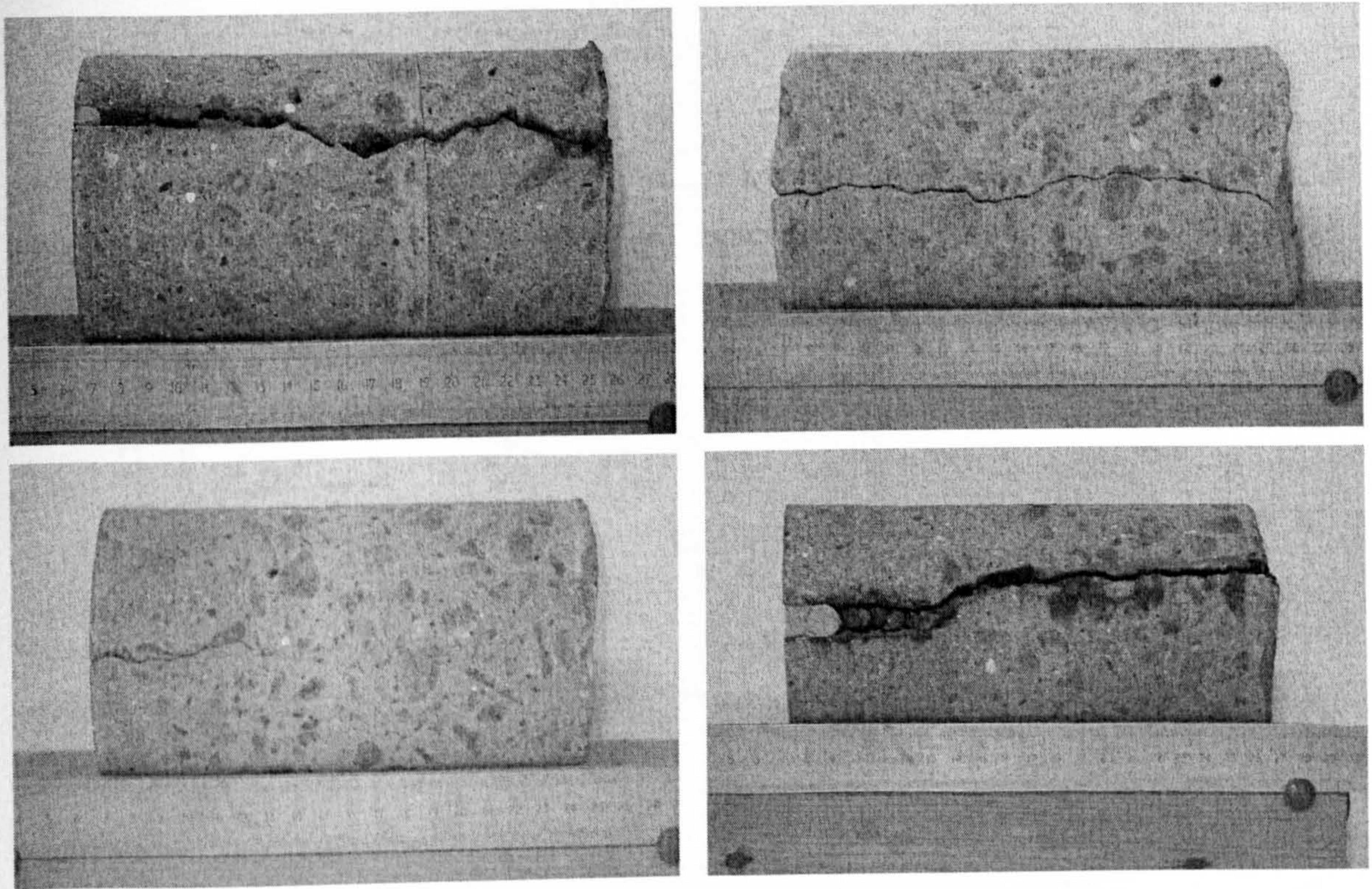


Figure 6.2 – Core taken during visit 1 (Clockwise from top left, Core 7, Core 17, Core 24, Core 21)

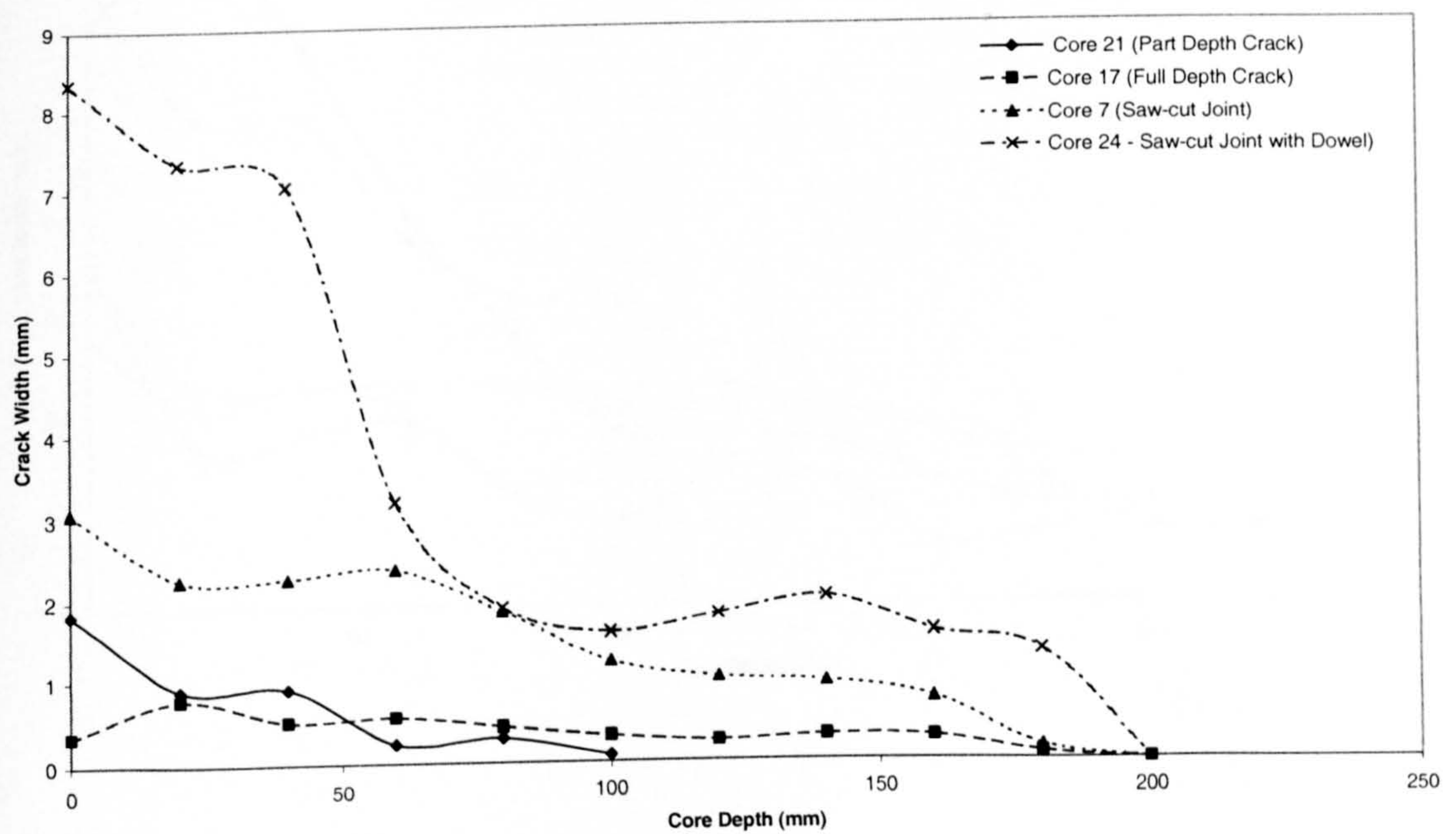


Figure 6.3 – Crack profiles from cores taken in visit 1

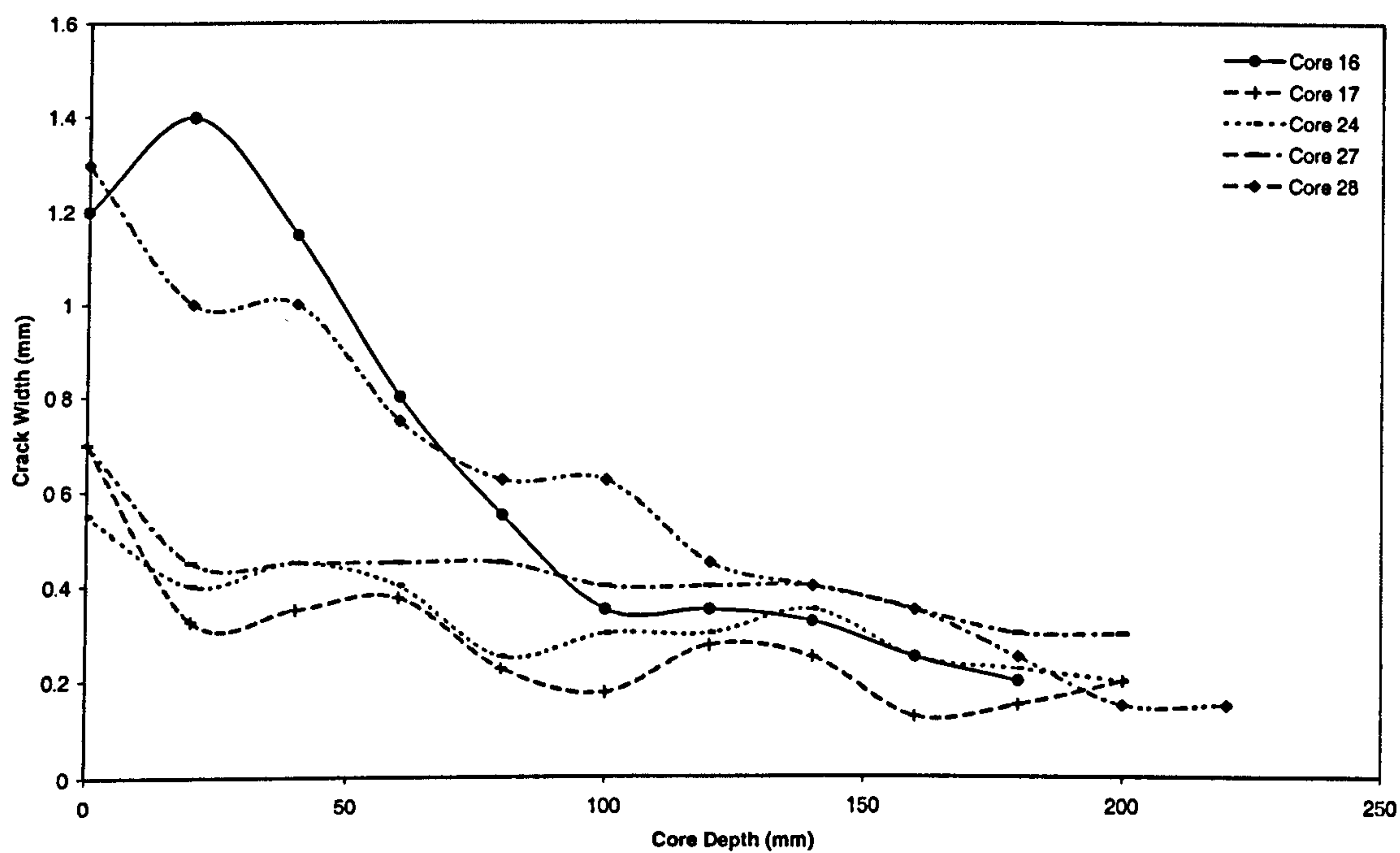
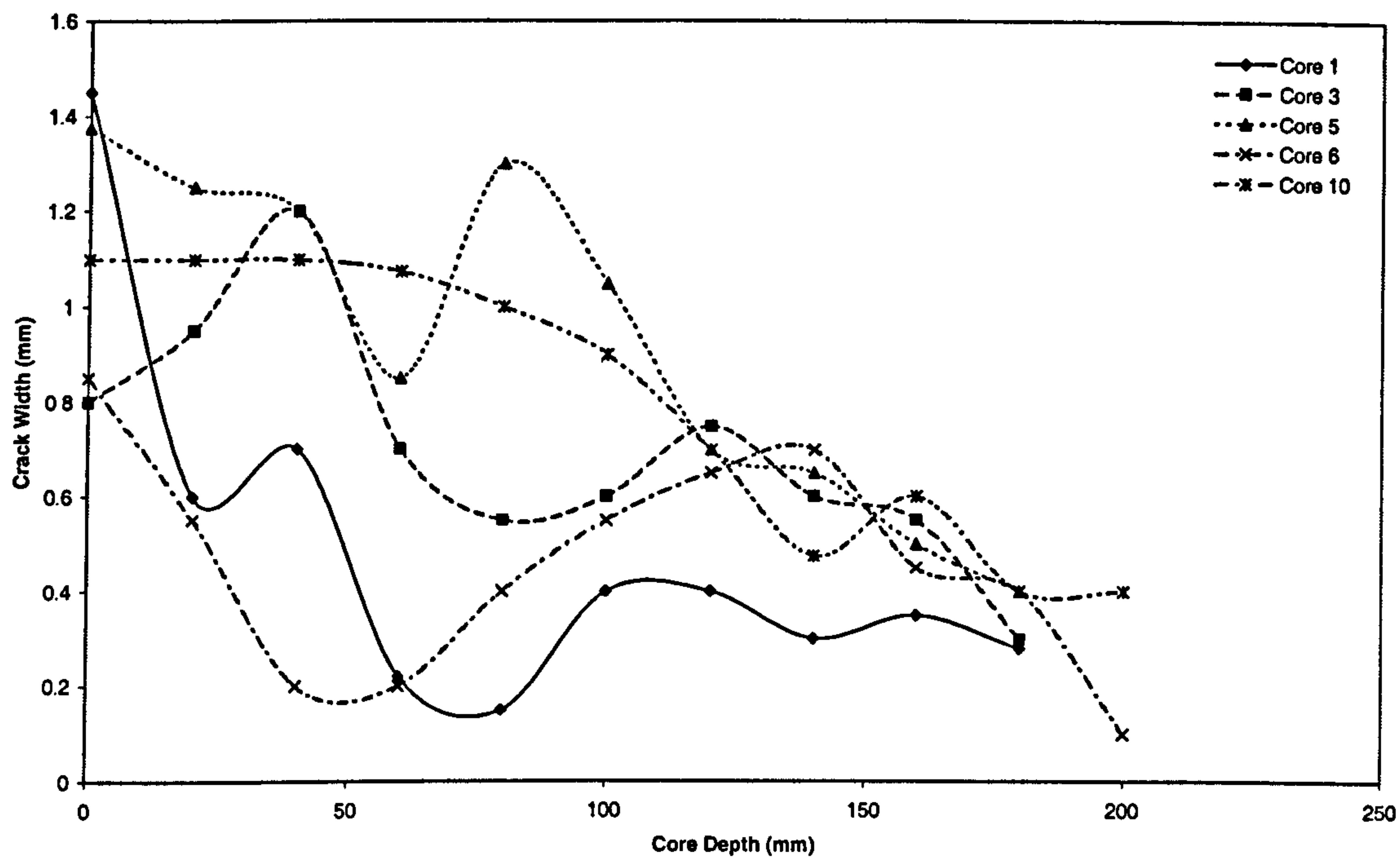


Figure 6.4 – Crack profiles from cores taken in visit 2

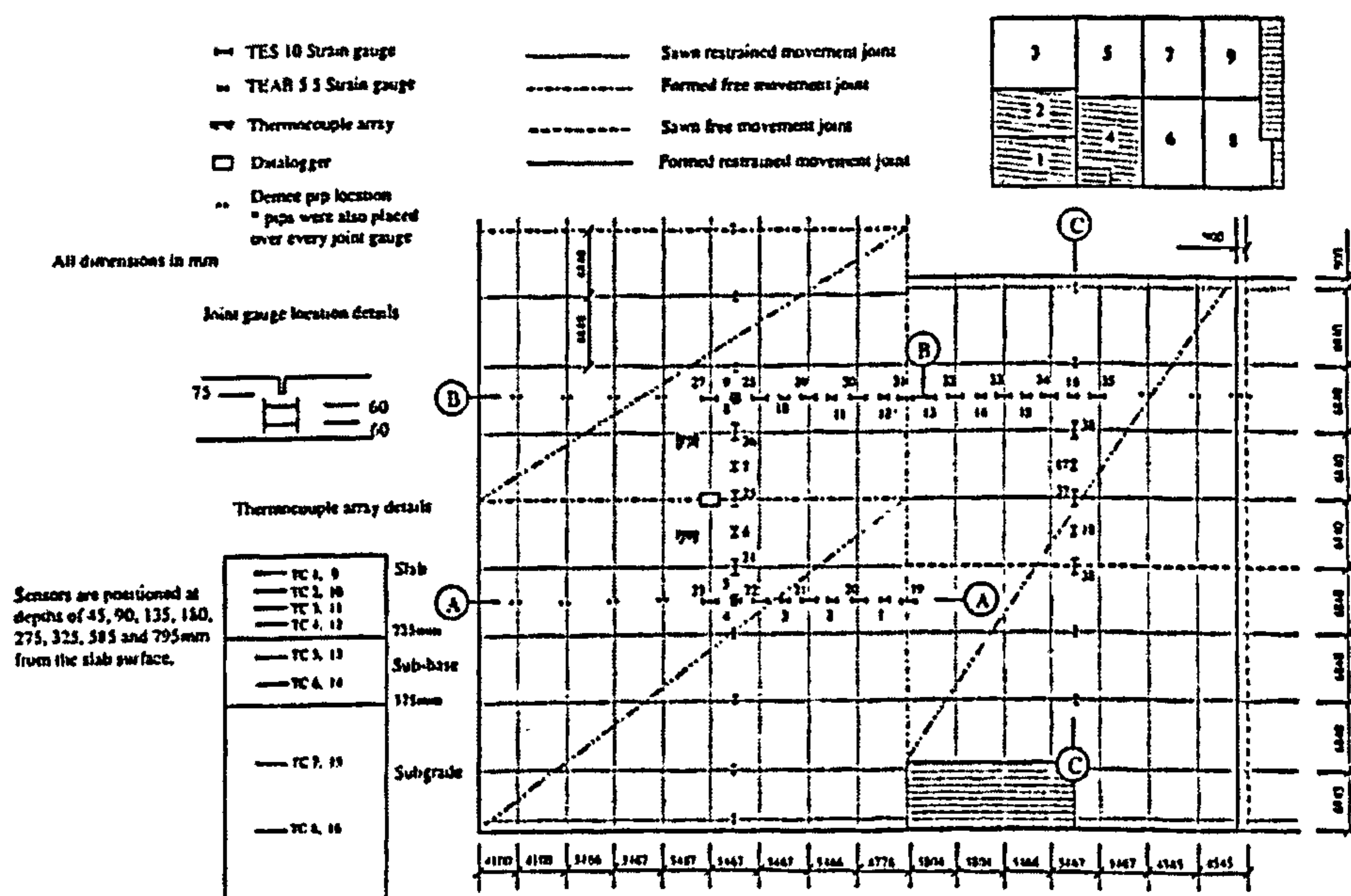
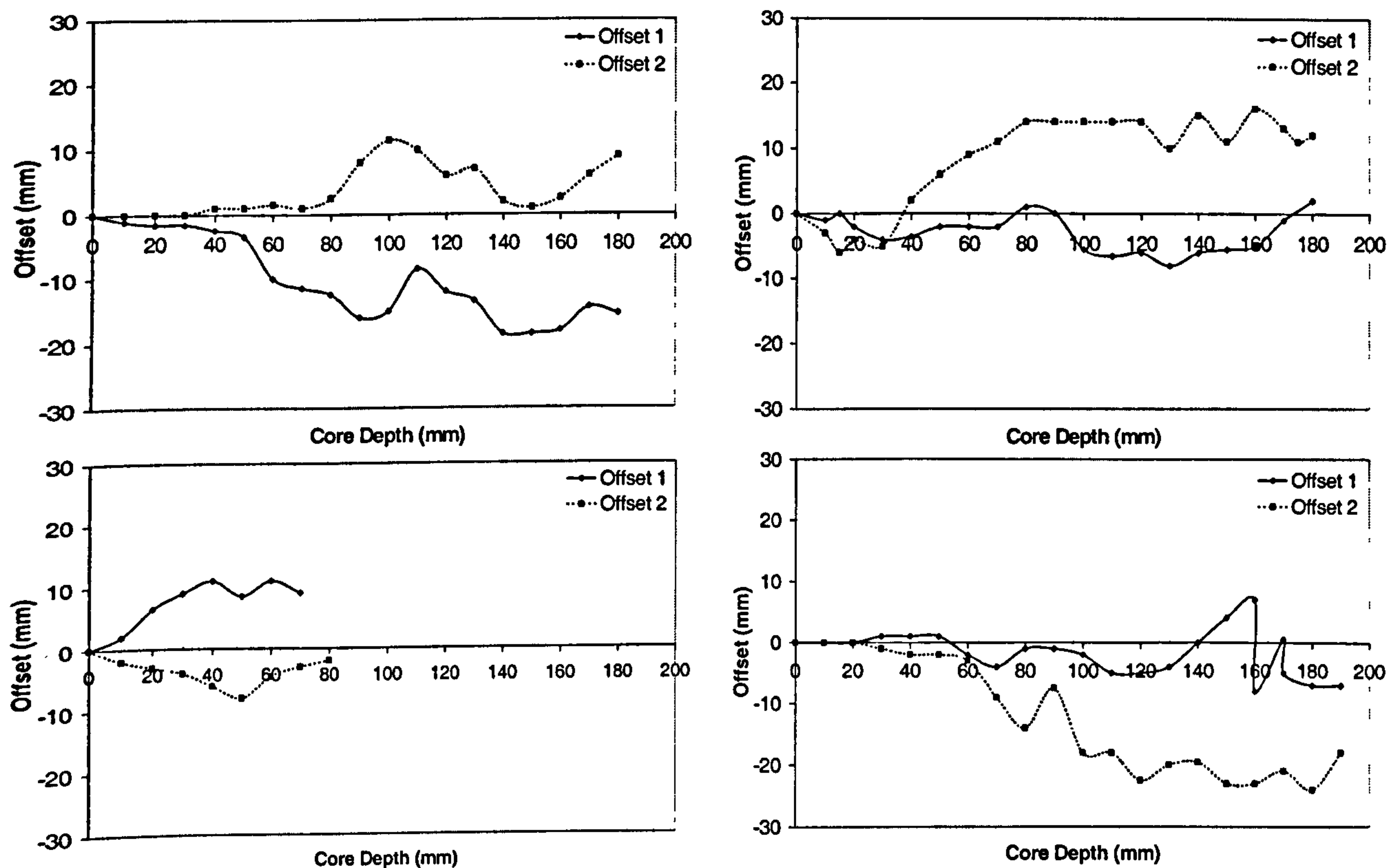


Figure 6.6a – Strain Gauge Positions (Leeds)

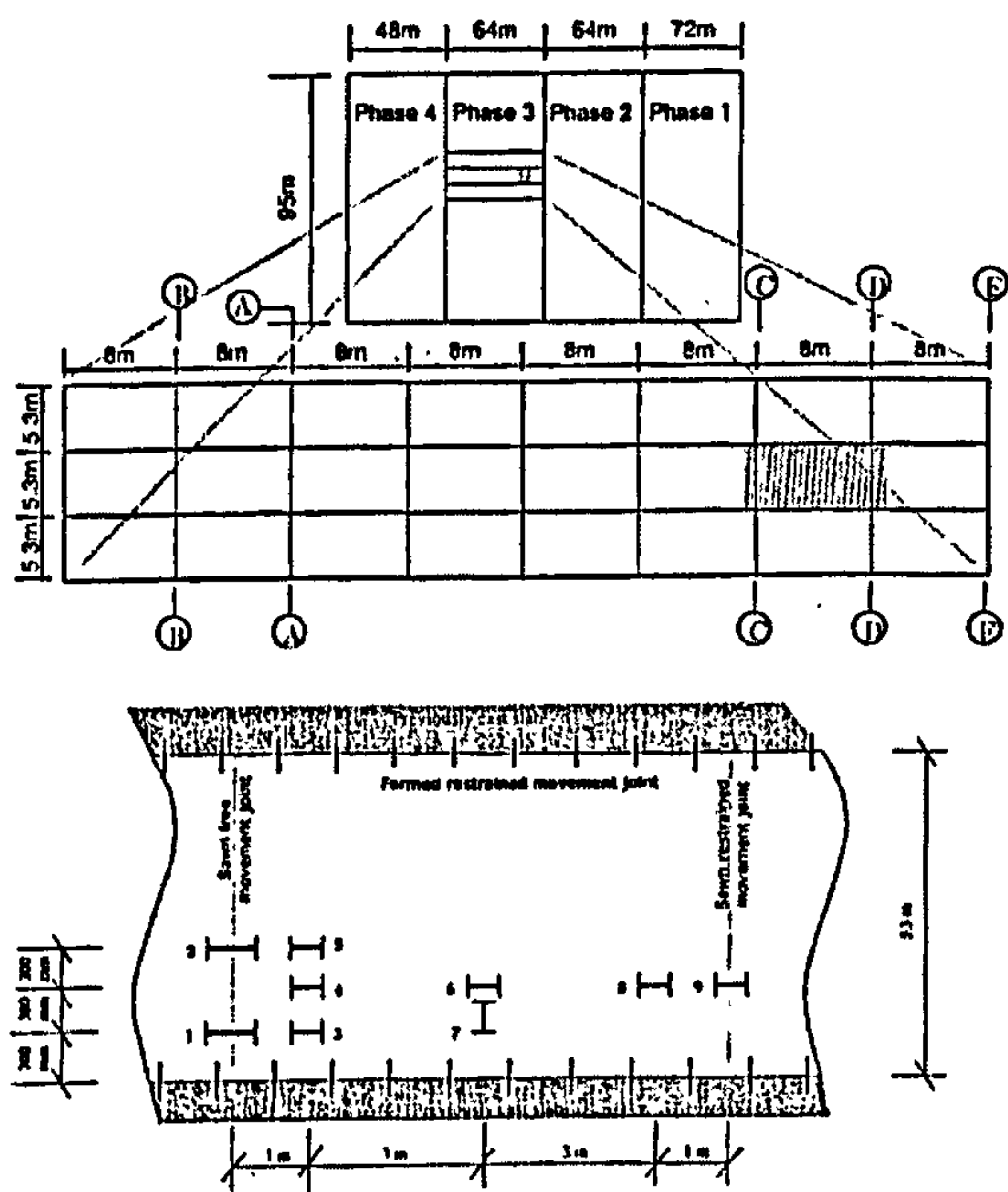


Figure 6.6b – Strain Gauge Positions (Northampton)

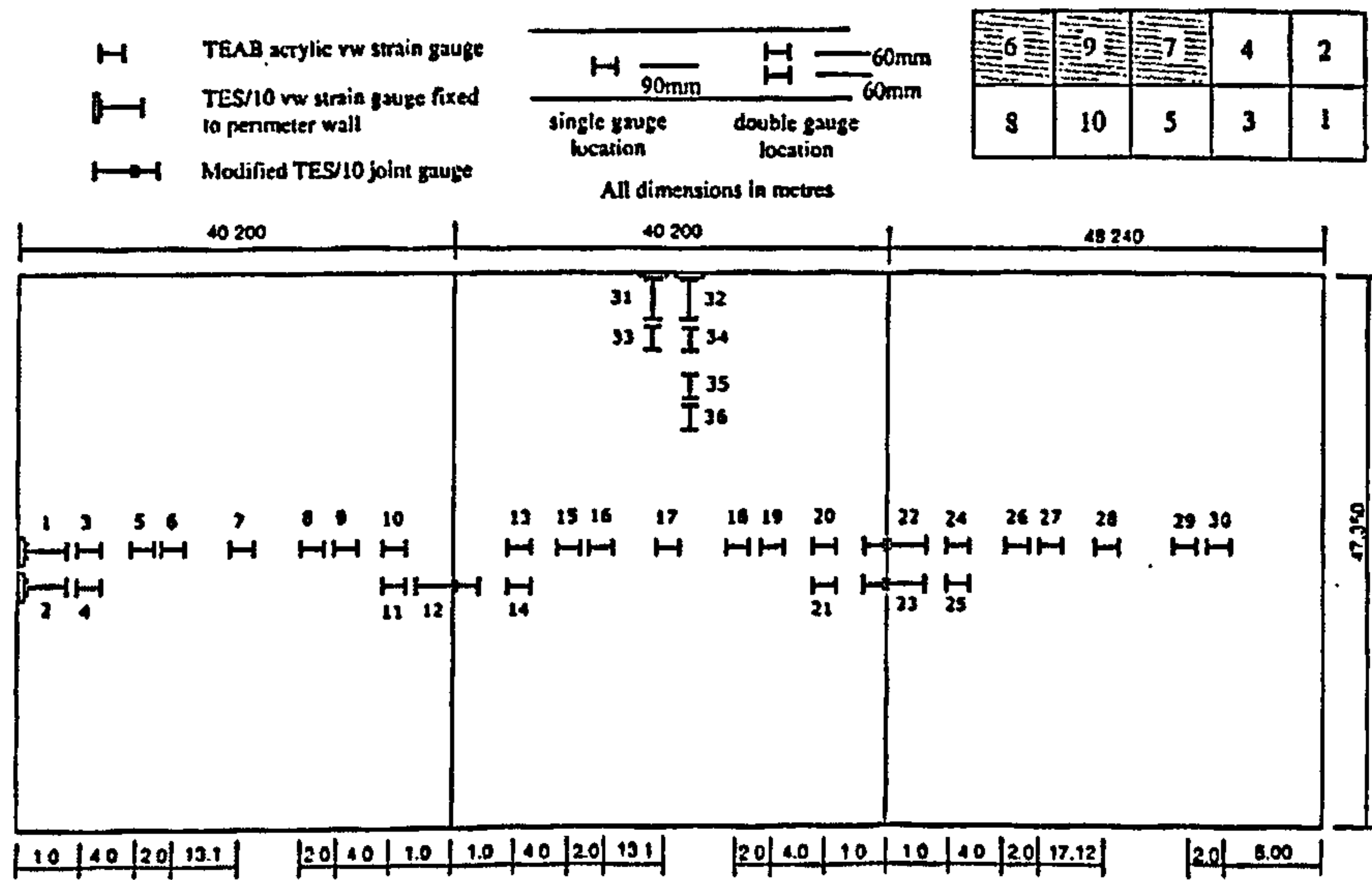


Figure 6.6c – Strain Gauge Positions (Marston)

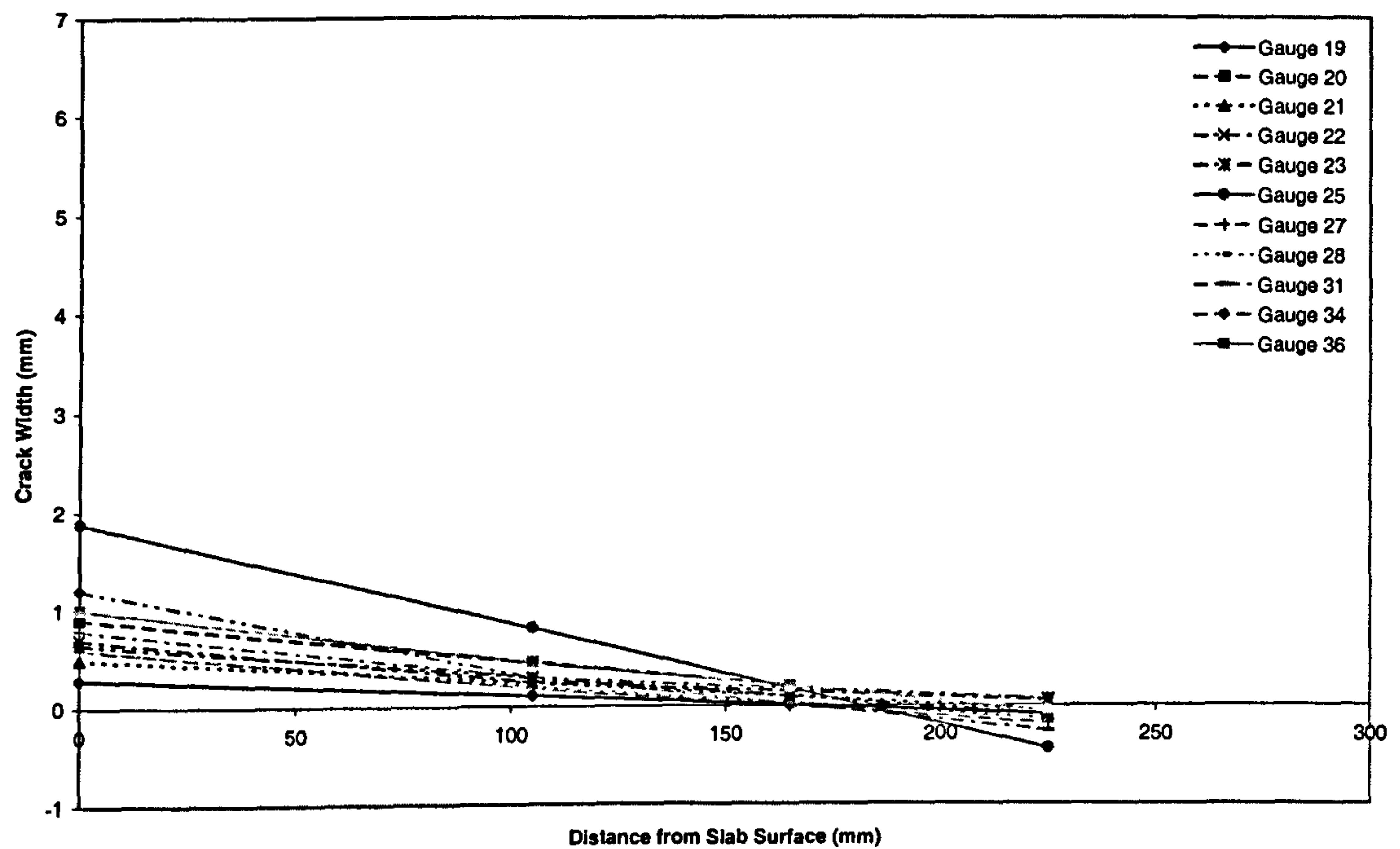


Figure 6.7a – Crack width extrapolation (Leeds)

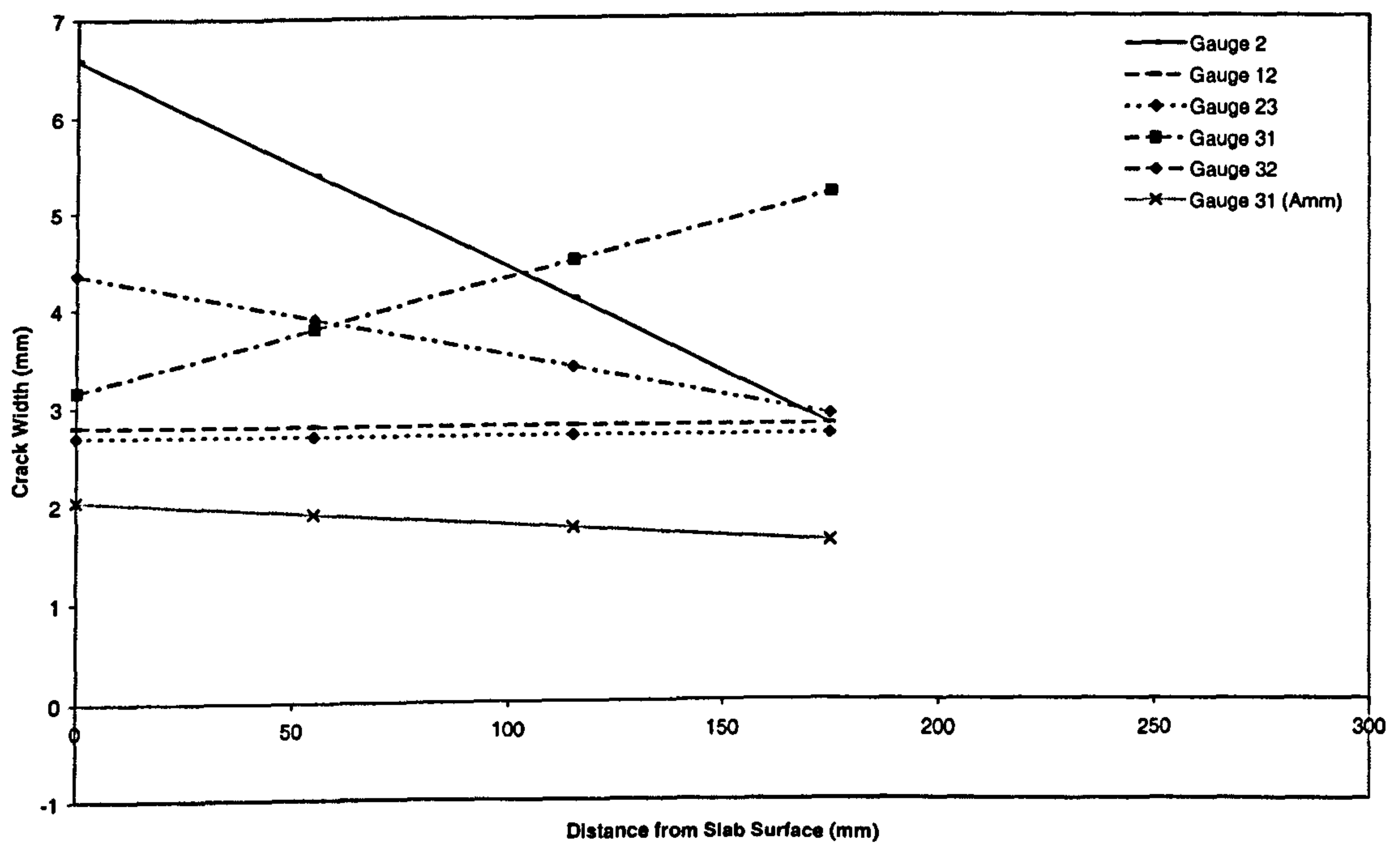


Figure 6.7b – Crack width extrapolation (Marston)

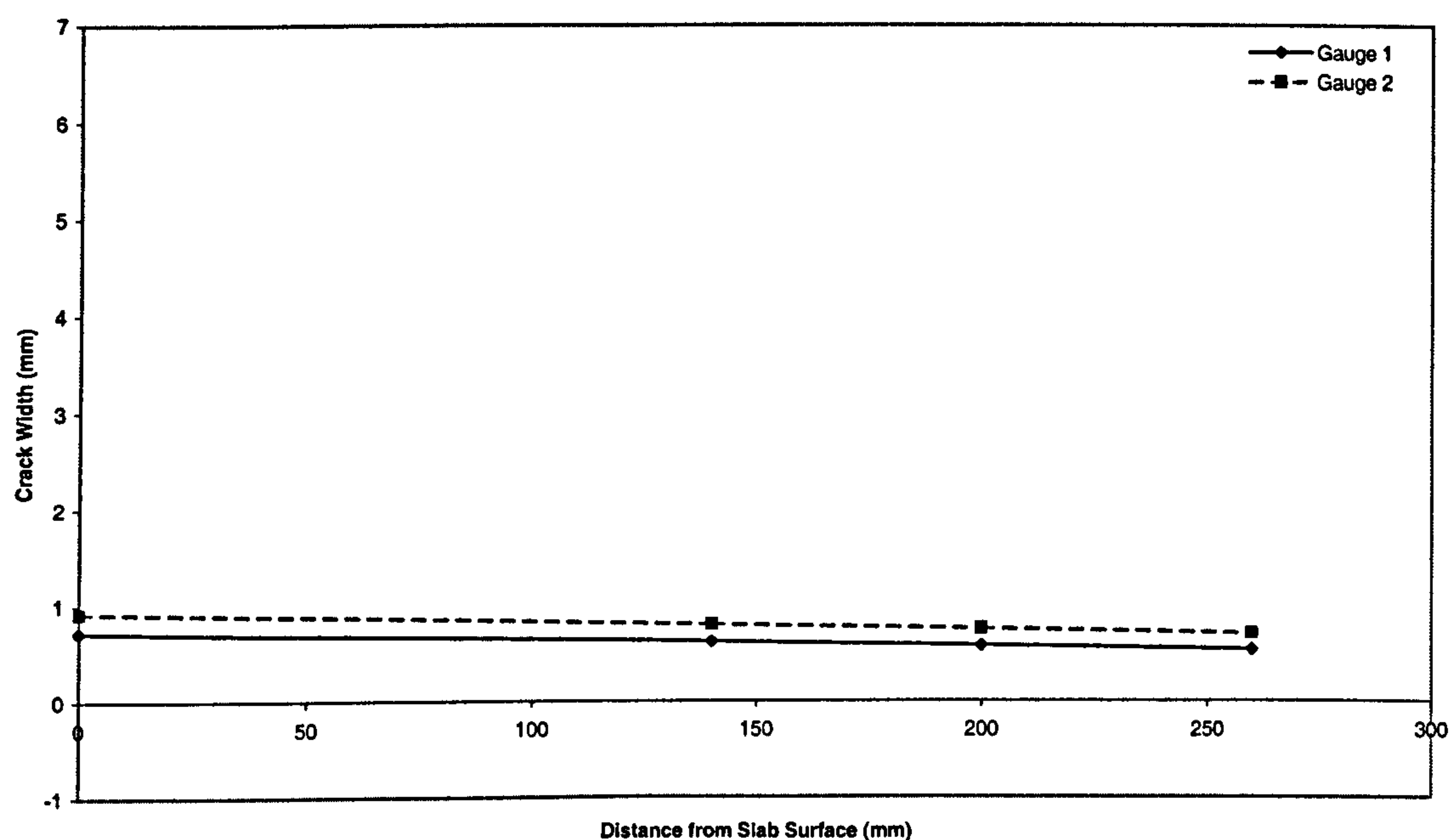


Figure 6.7c – Crack width extrapolation (Northampton)

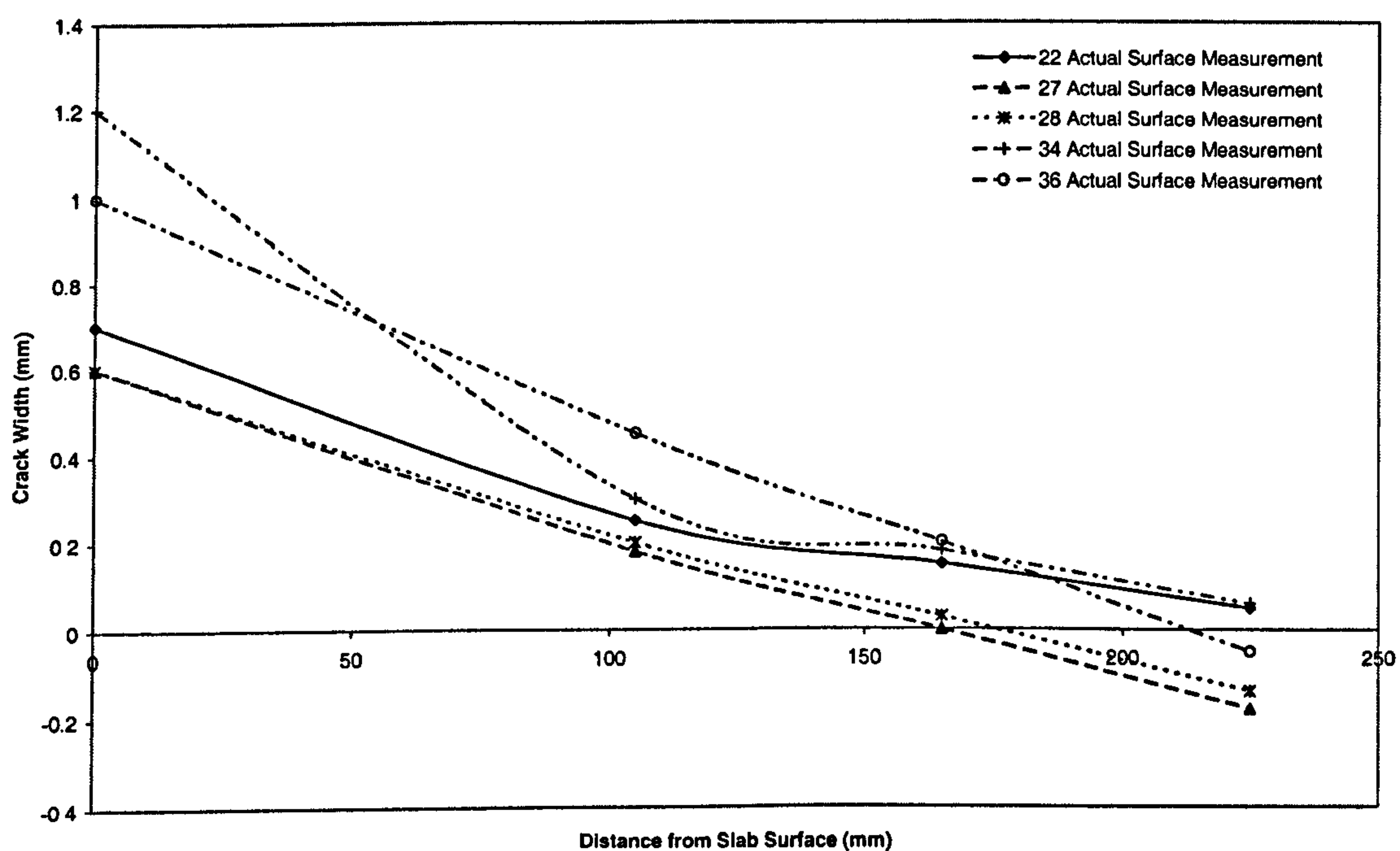


Figure 6.8 – Actual crack profile using embedded stain gauges and surface measurements (Leeds)

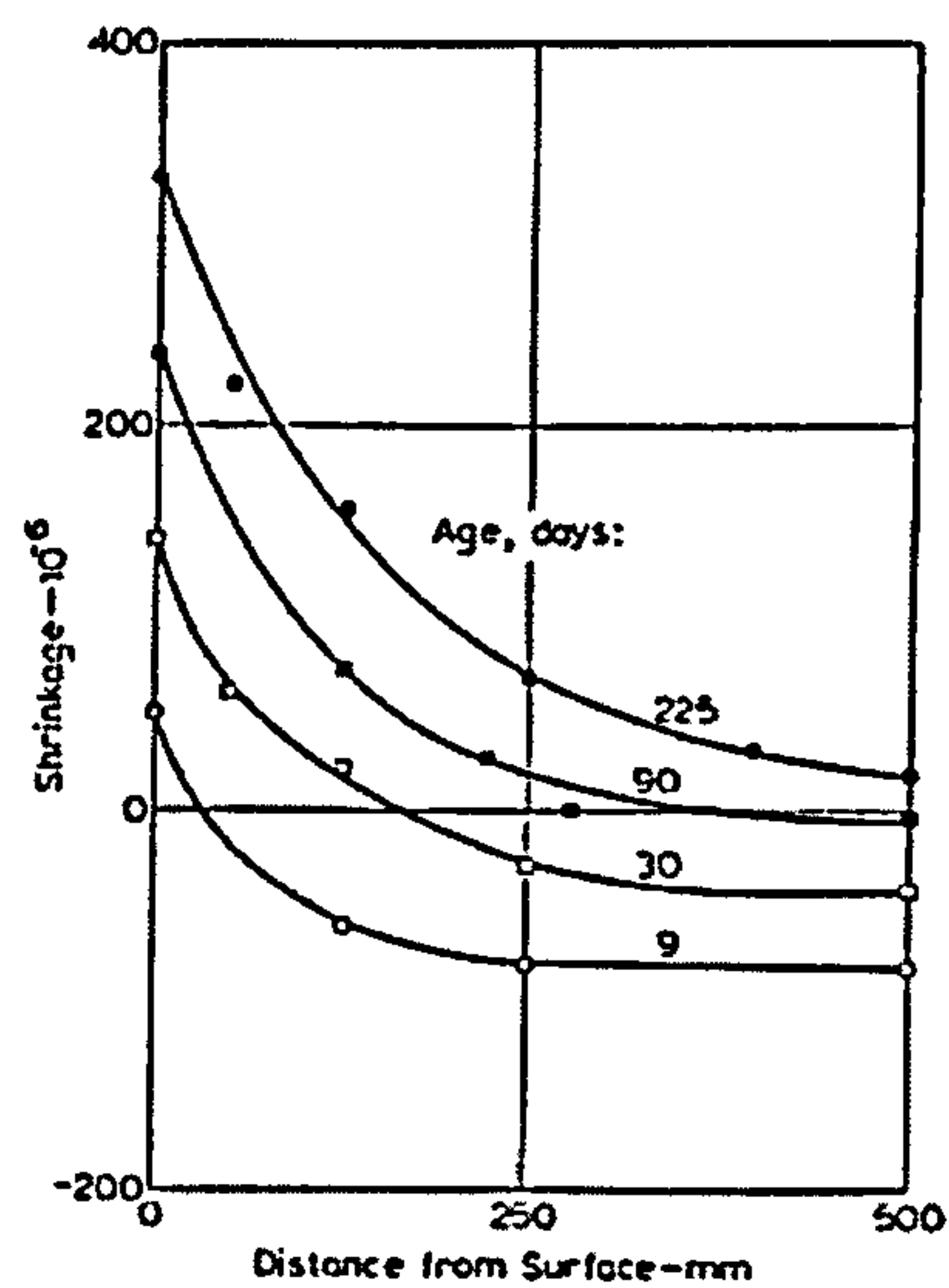


Figure 6.9 – Differential shrinkage of concrete open to the environment on one side (Neville 1995)

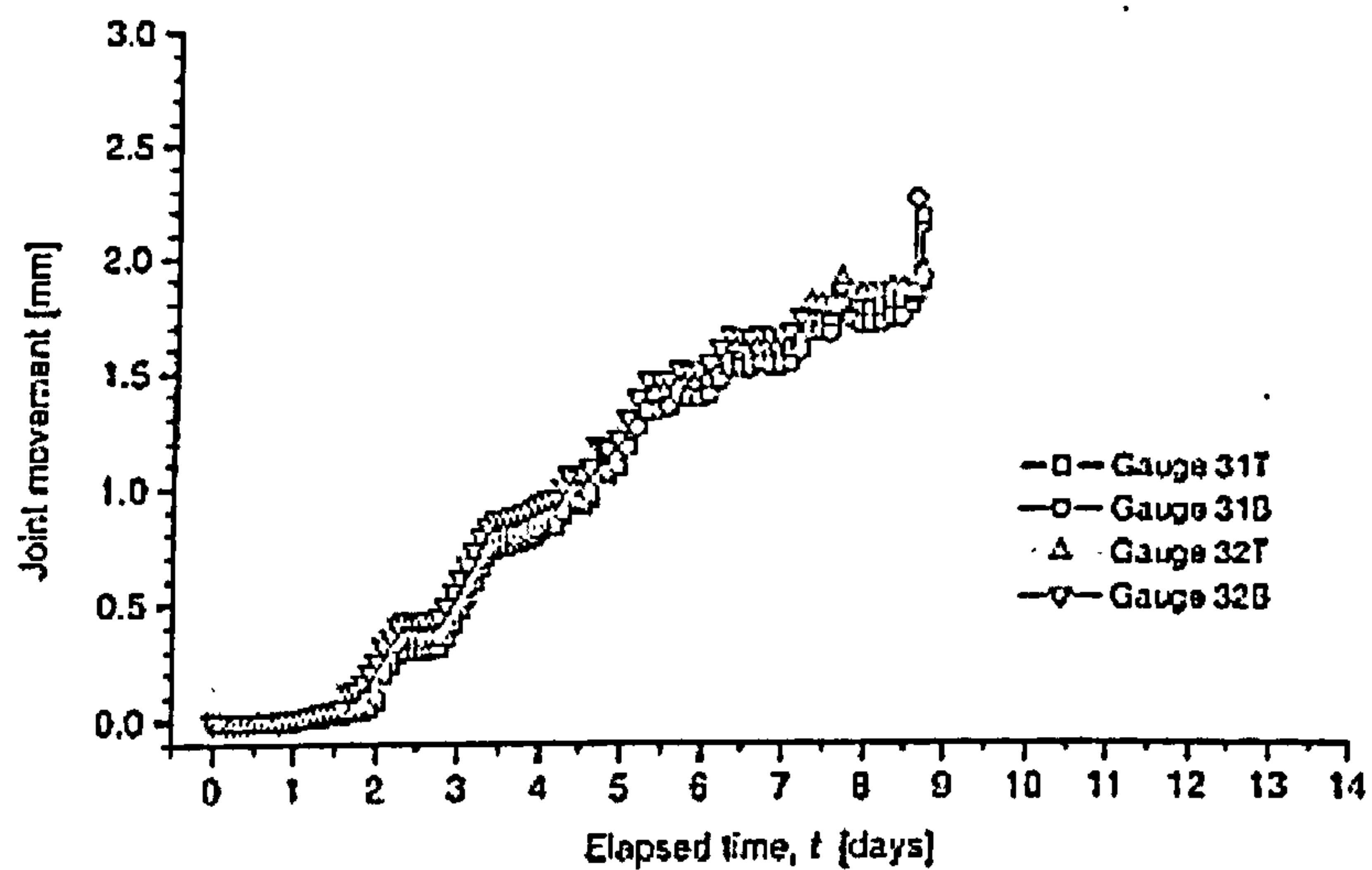


Figure 6.10 – Erroneous strain gauge reading from Bishop (2001)

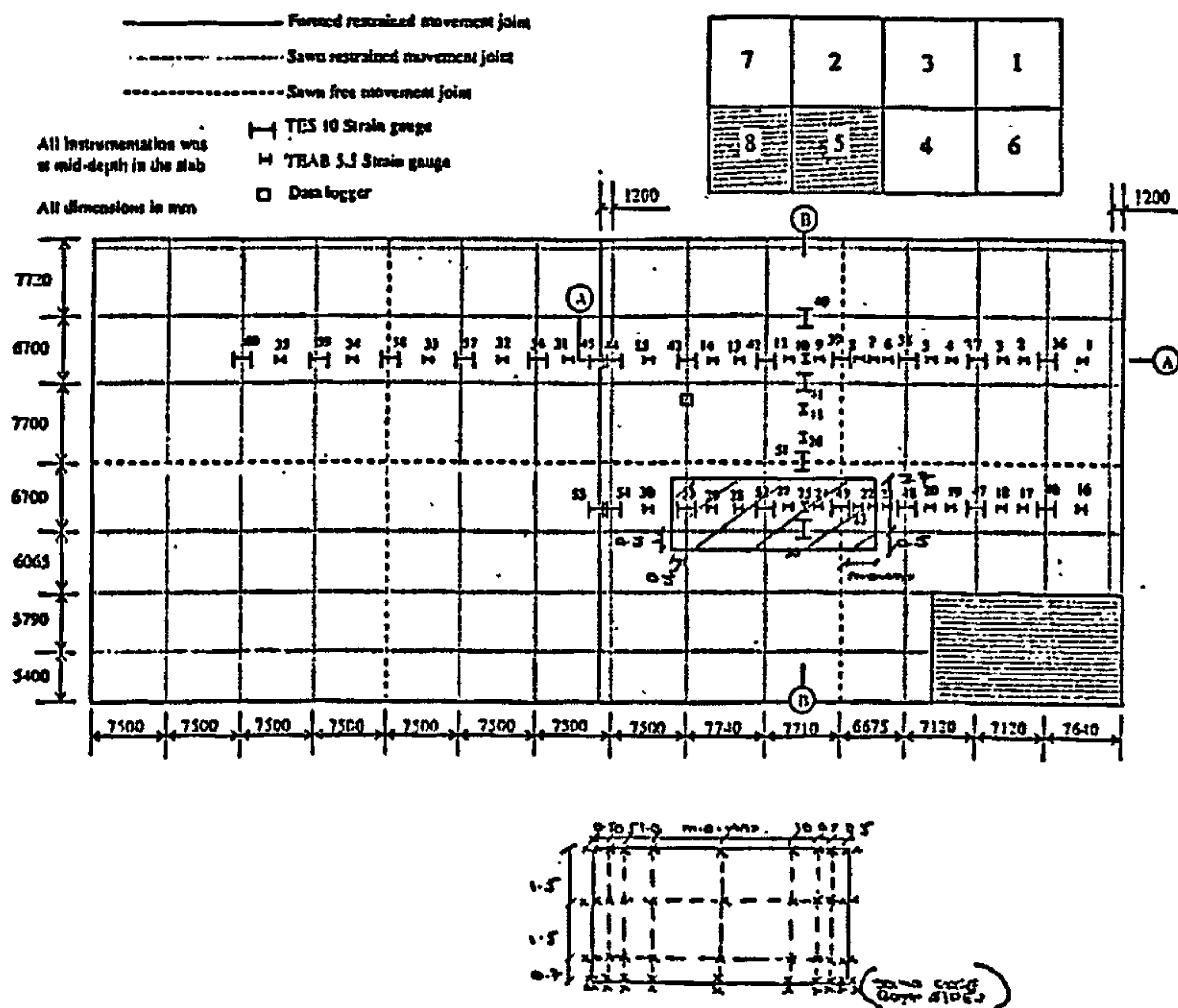


Figure 6.11 – Area of floor level surveyed with a precise level (Daventry)

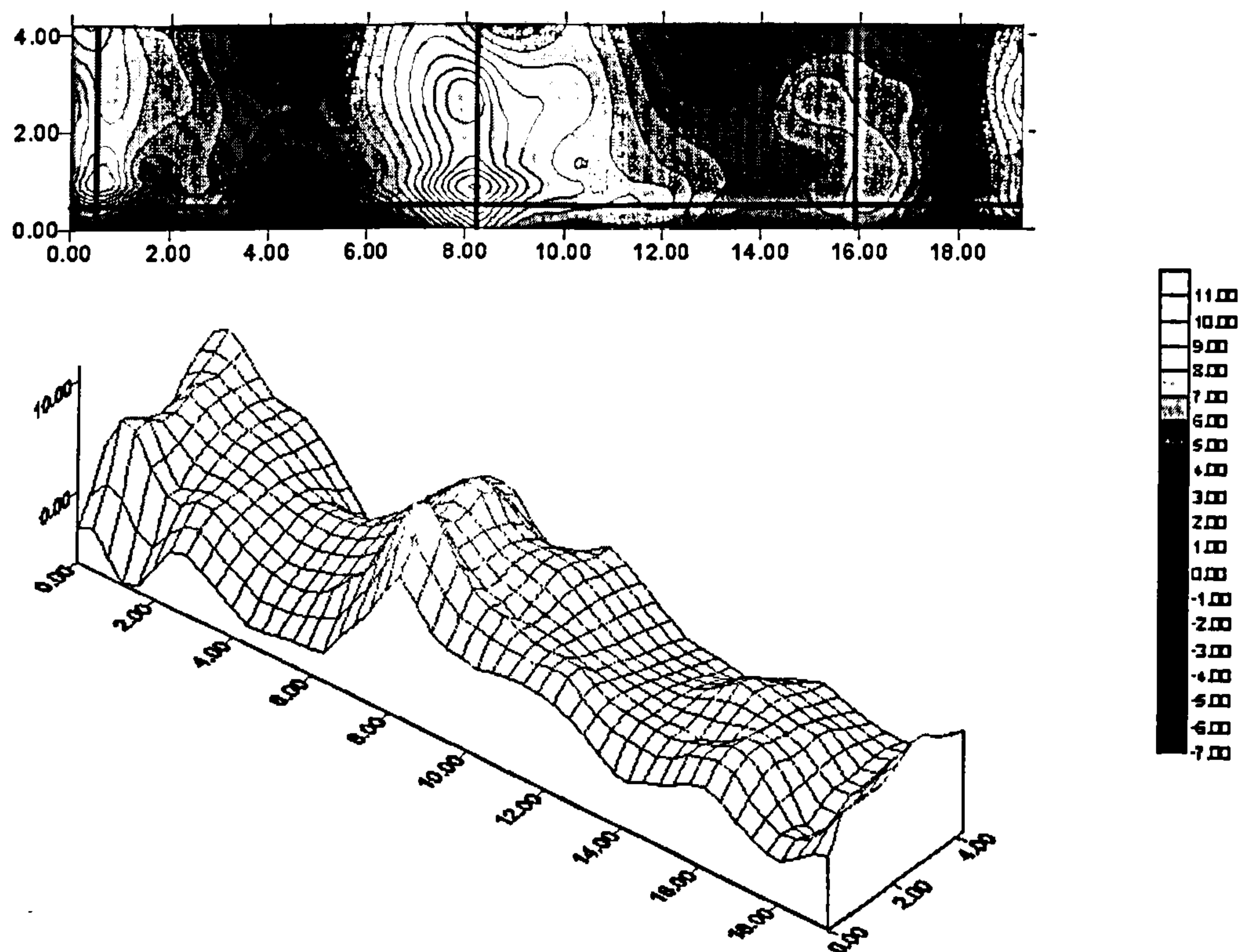


Figure 6.12 – Floor surface profiles (Daventry)

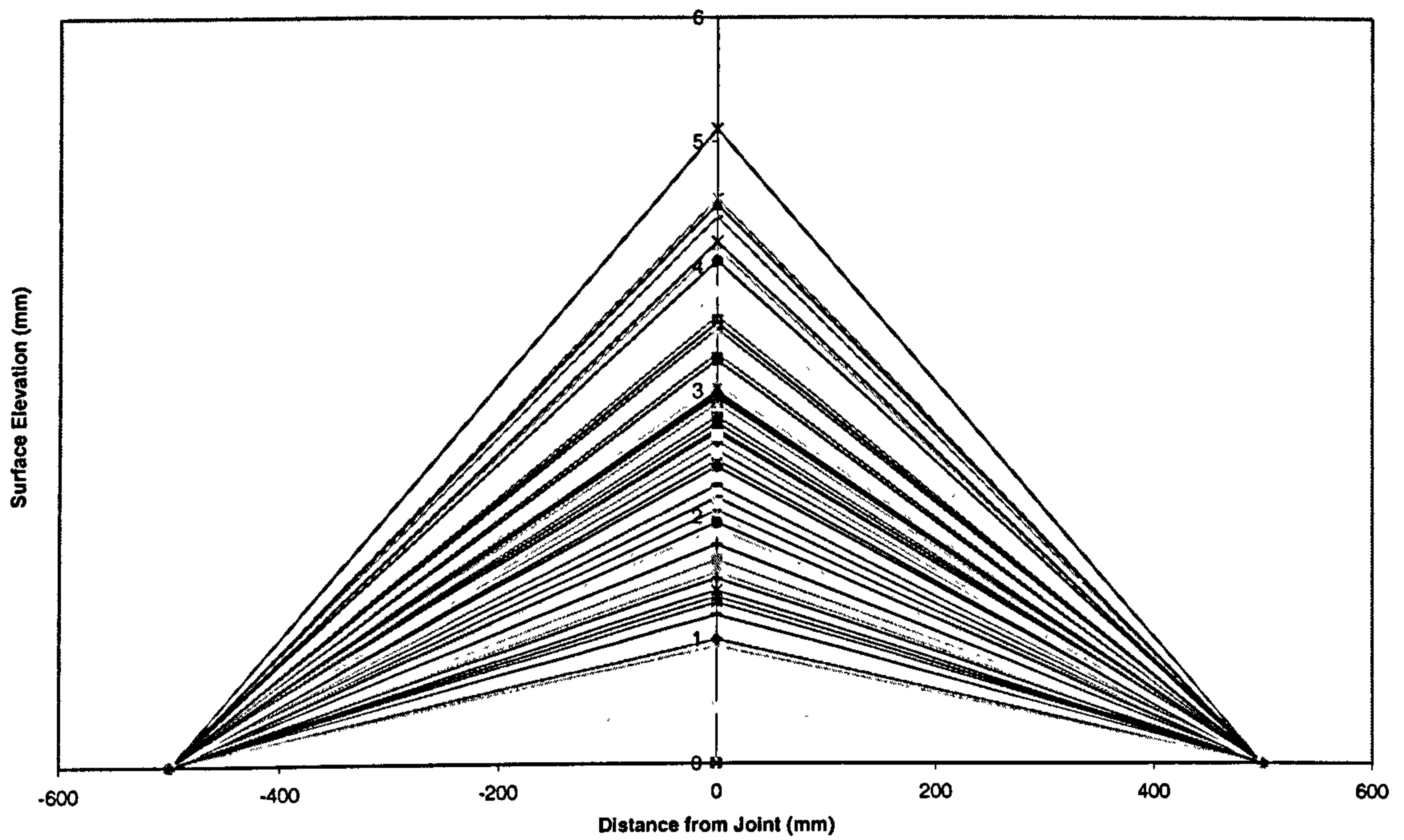


Figure 6.13 – Measured edge curl using a builders level (Ballymena)

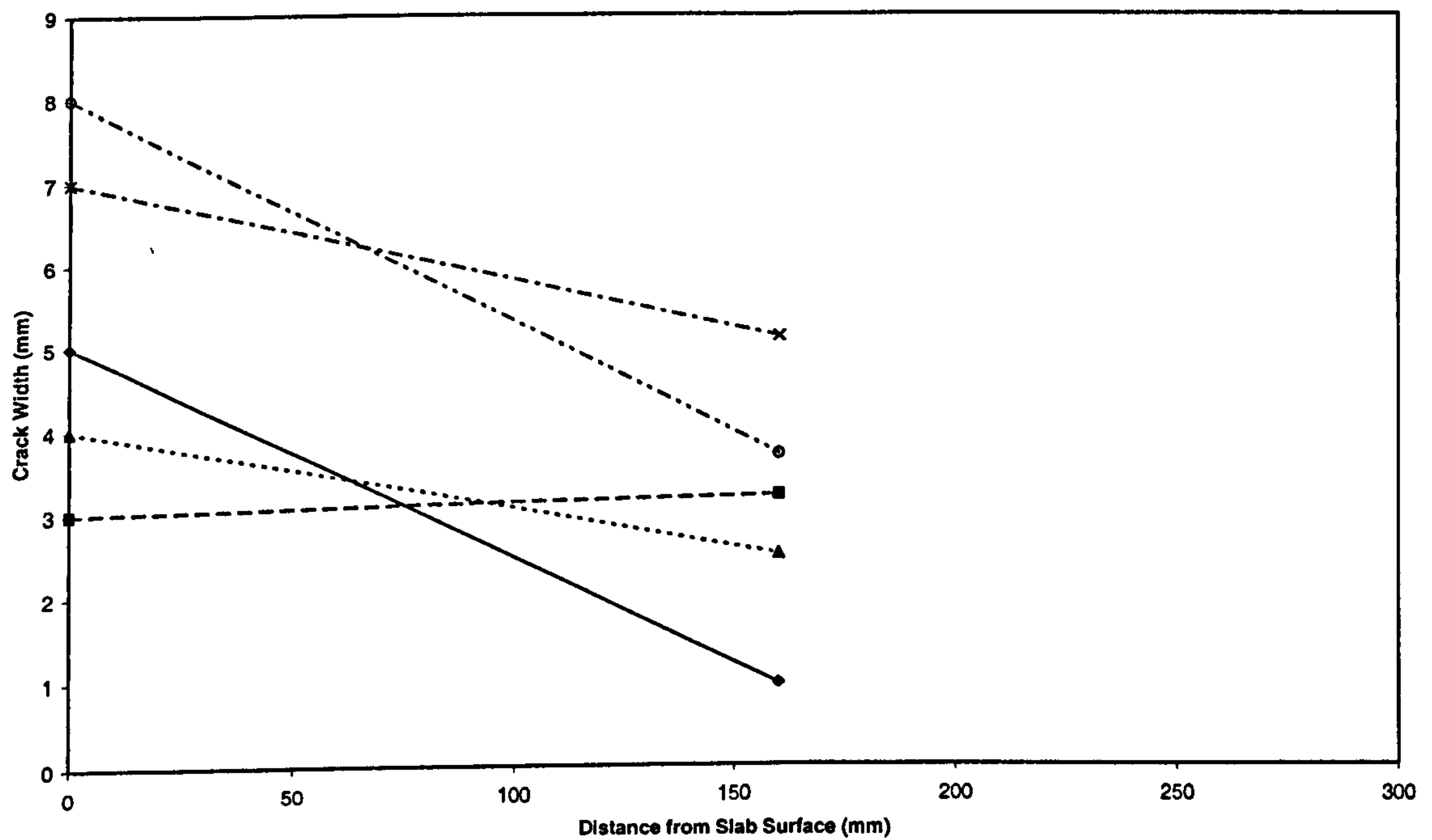


Figure 6.14 – Predicted crack profile using slab levels and surface width (Daventry)

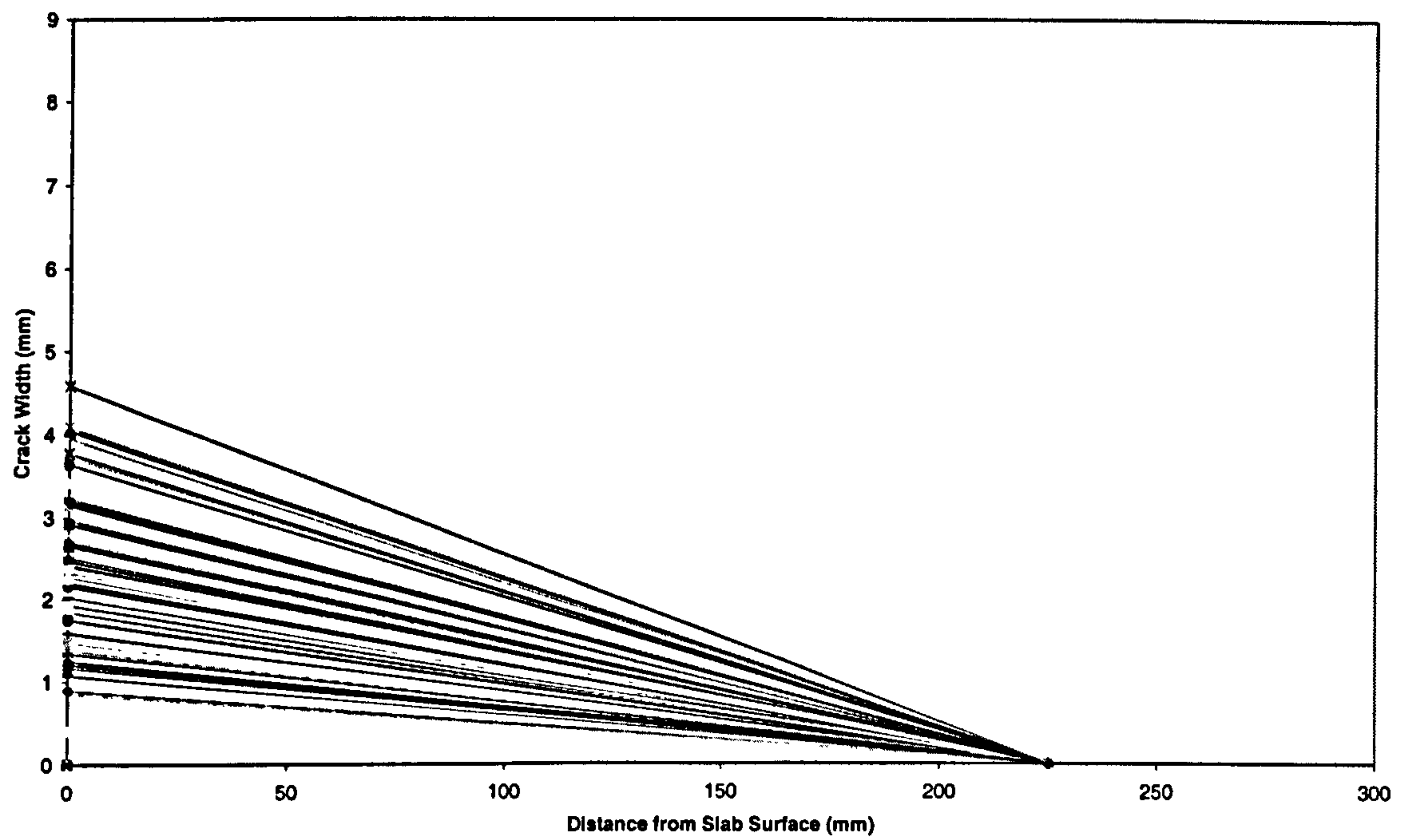


Figure 6.15 – Predicted crack profiles using edge curl (Ballymena)

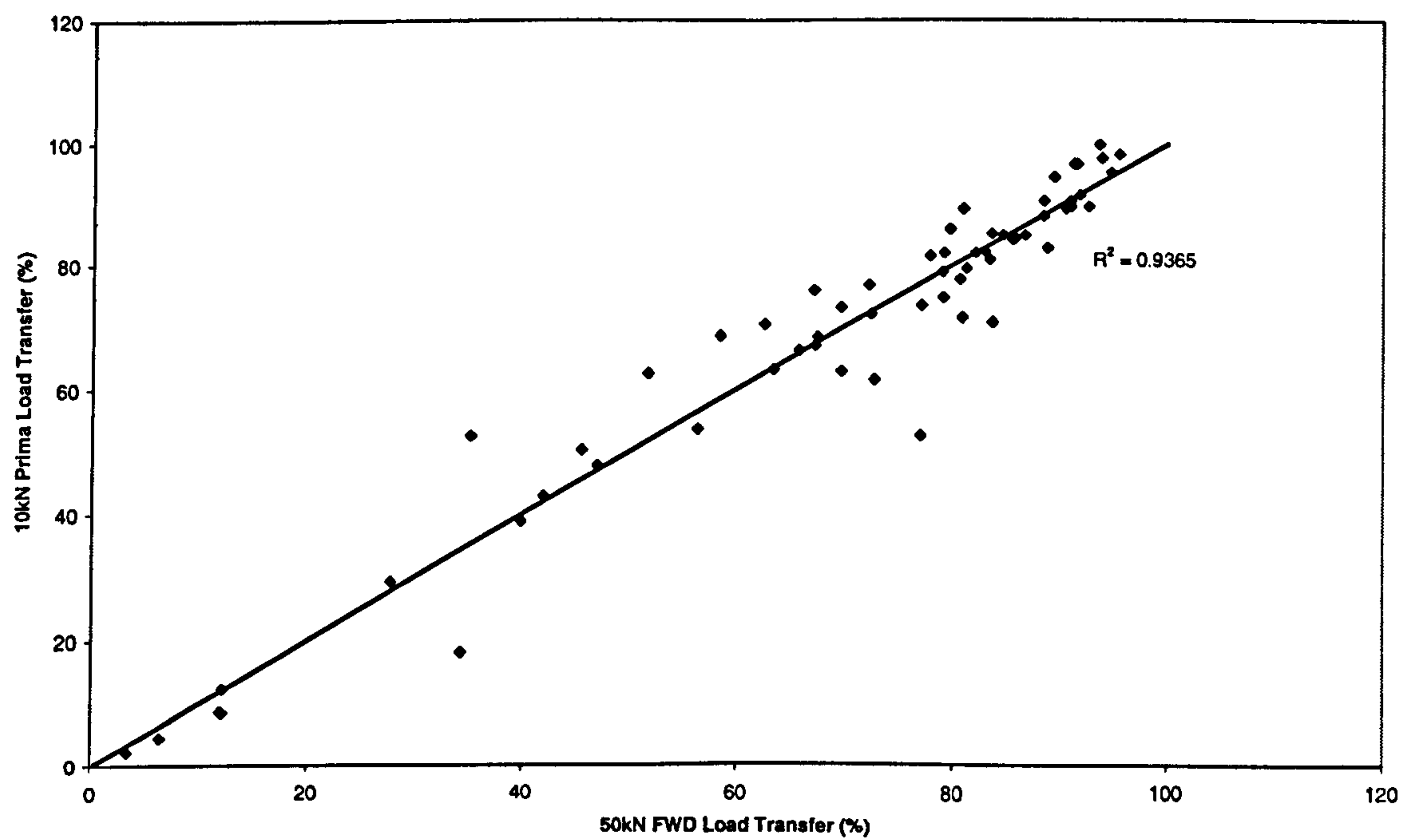


Figure 6.16 – Load transfer comparison between FWD and Prima (Daventry)

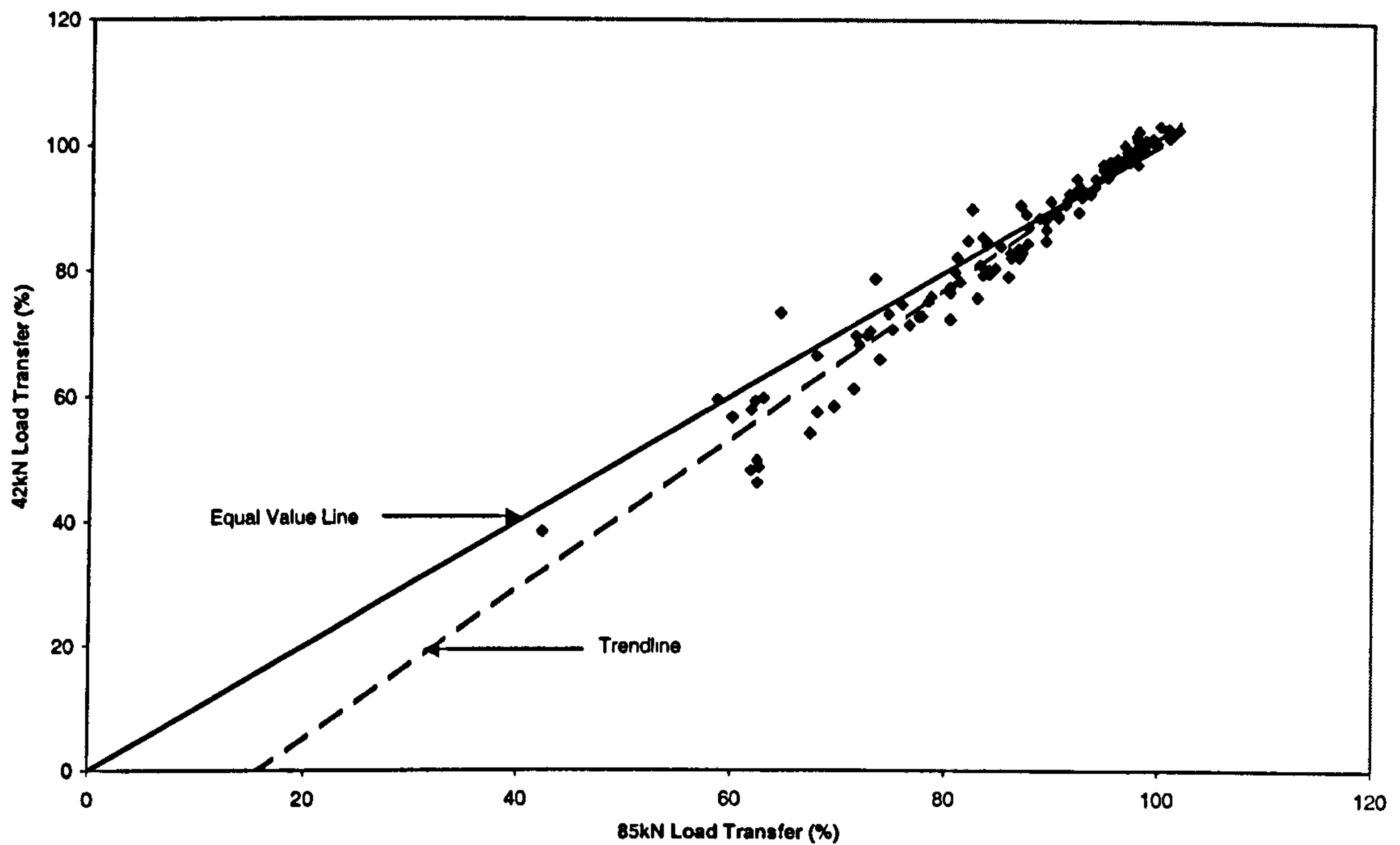


Figure 6.17 – Load transfer comparison between FWD loads (Lutterworth)

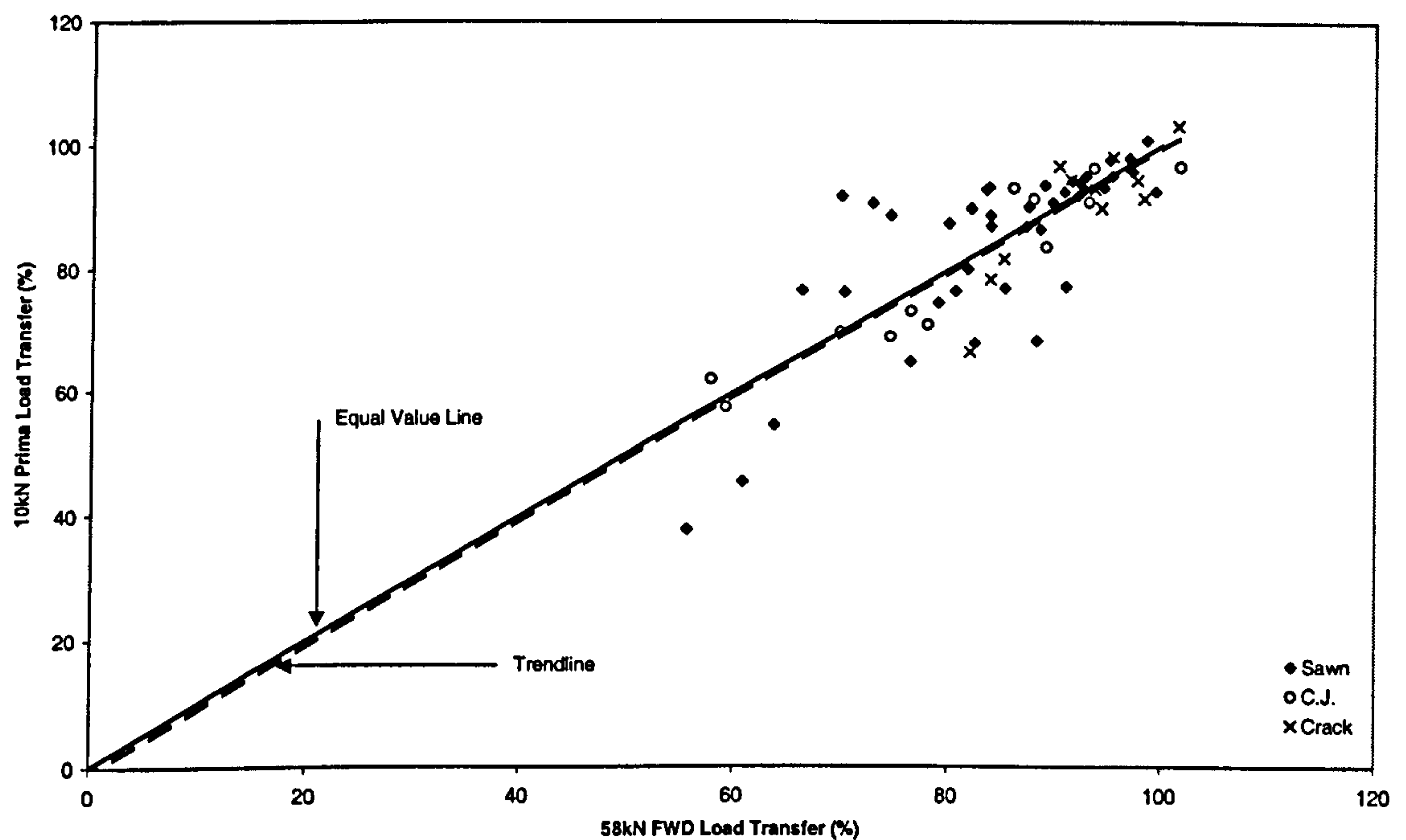


Figure 6.18 – Load transfer comparison between FWD and Prima (Lutterworth)

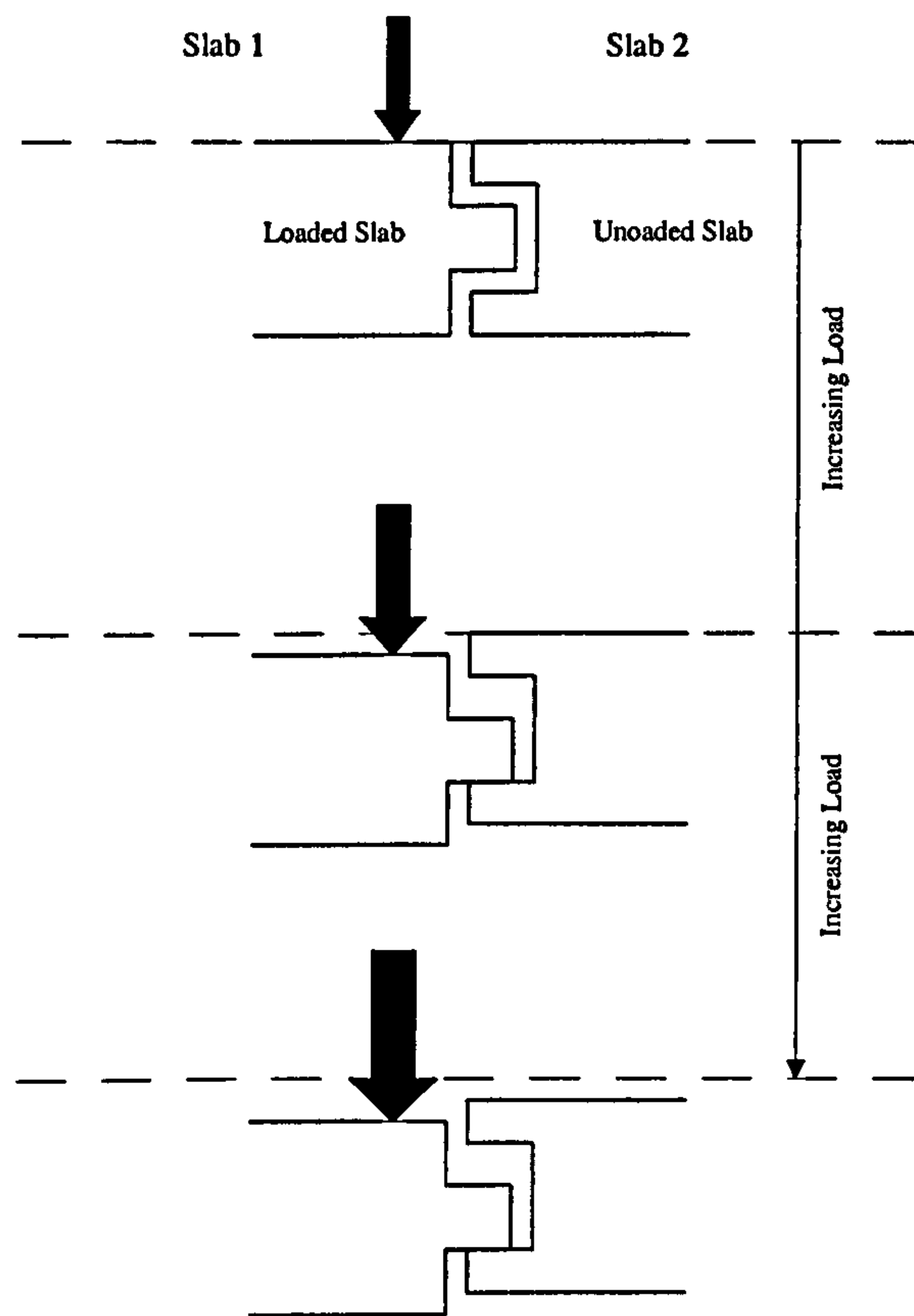


Figure 6.19 – Effect of free-slip on load transfer

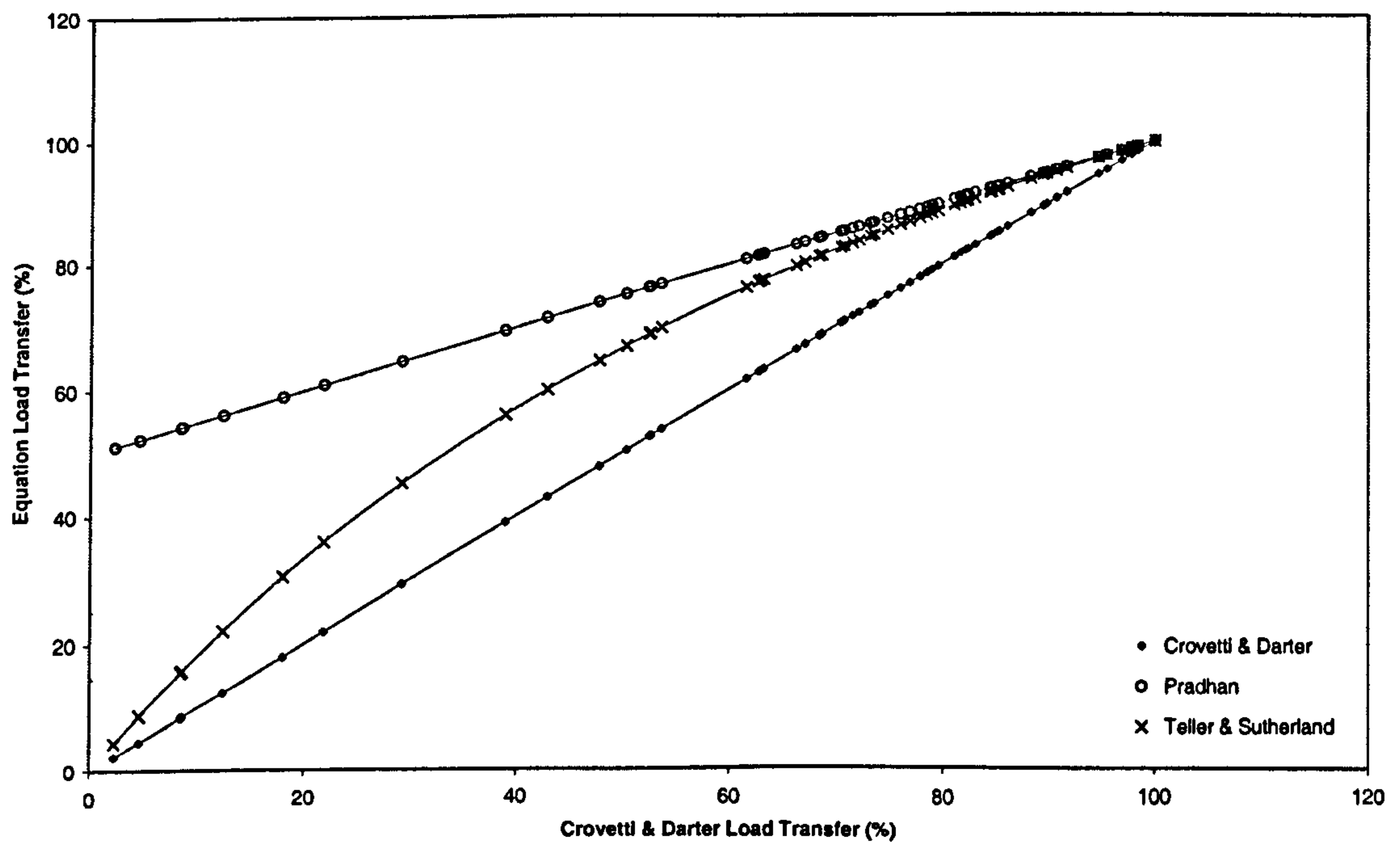


Figure 6.20 – Comparison of load transfer equations

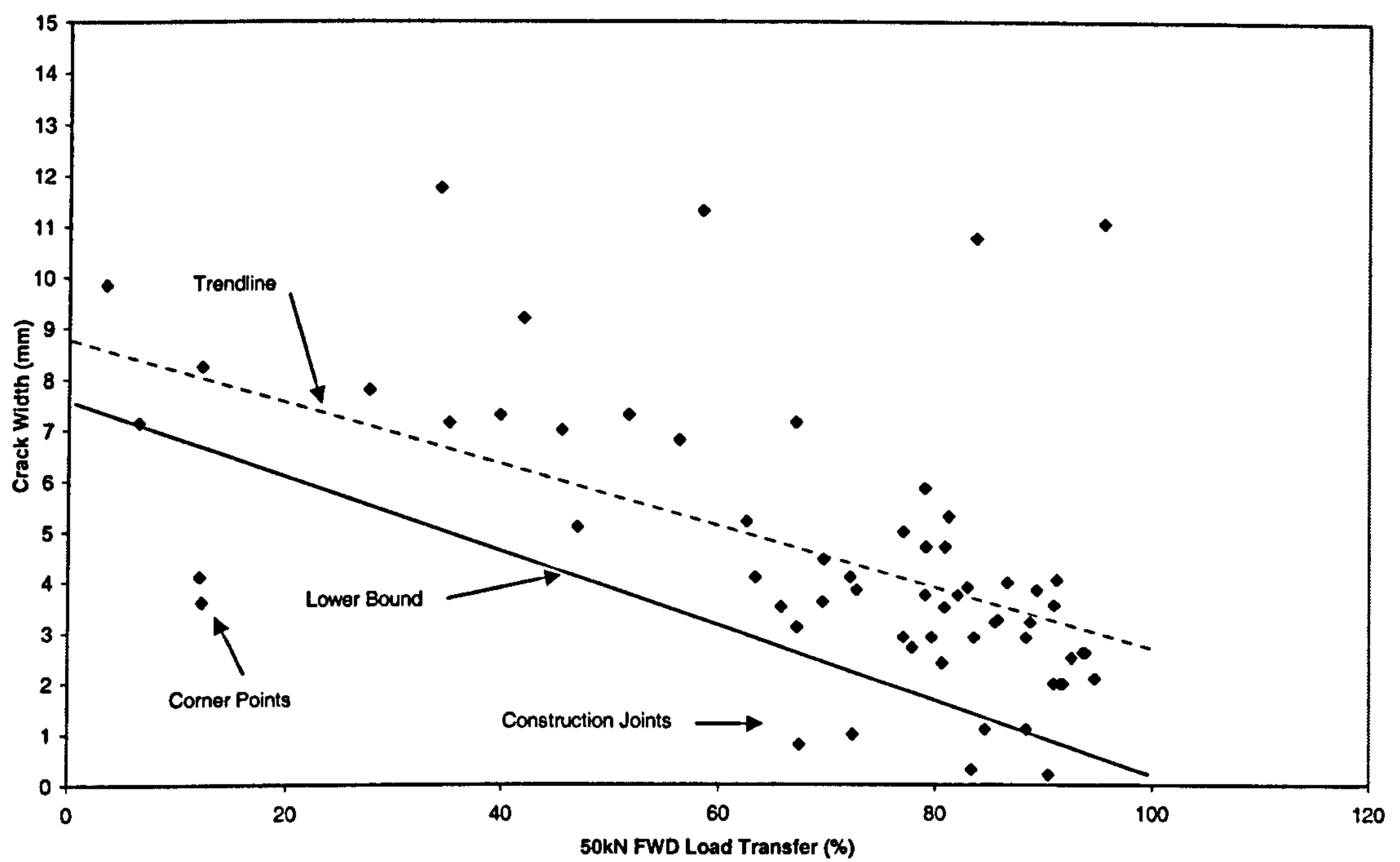


Figure 6.21a – Comparison of load transfer and crack width (Daventry)

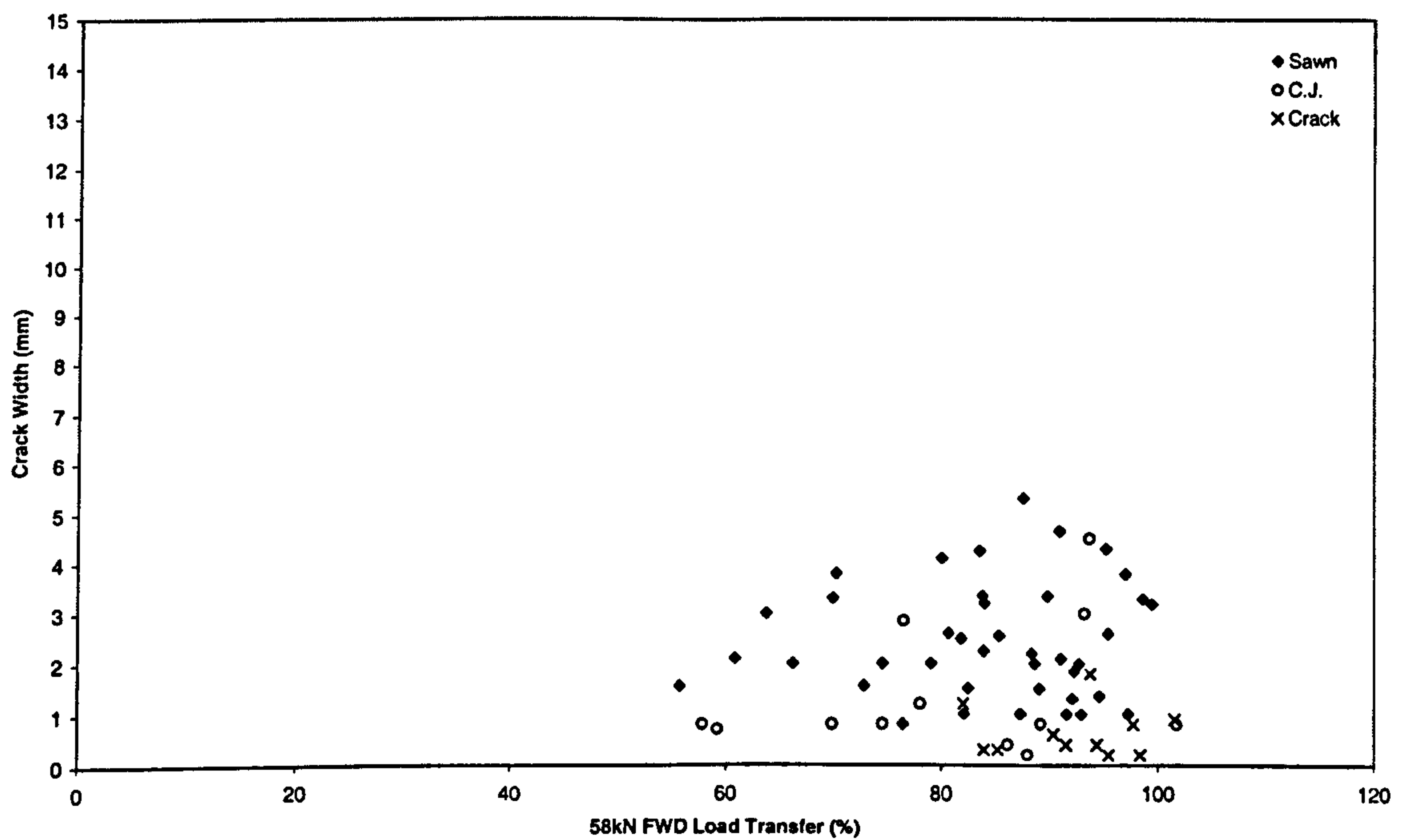


Figure 6.21b – Comparison of load transfer and crack width (Lutterworth)

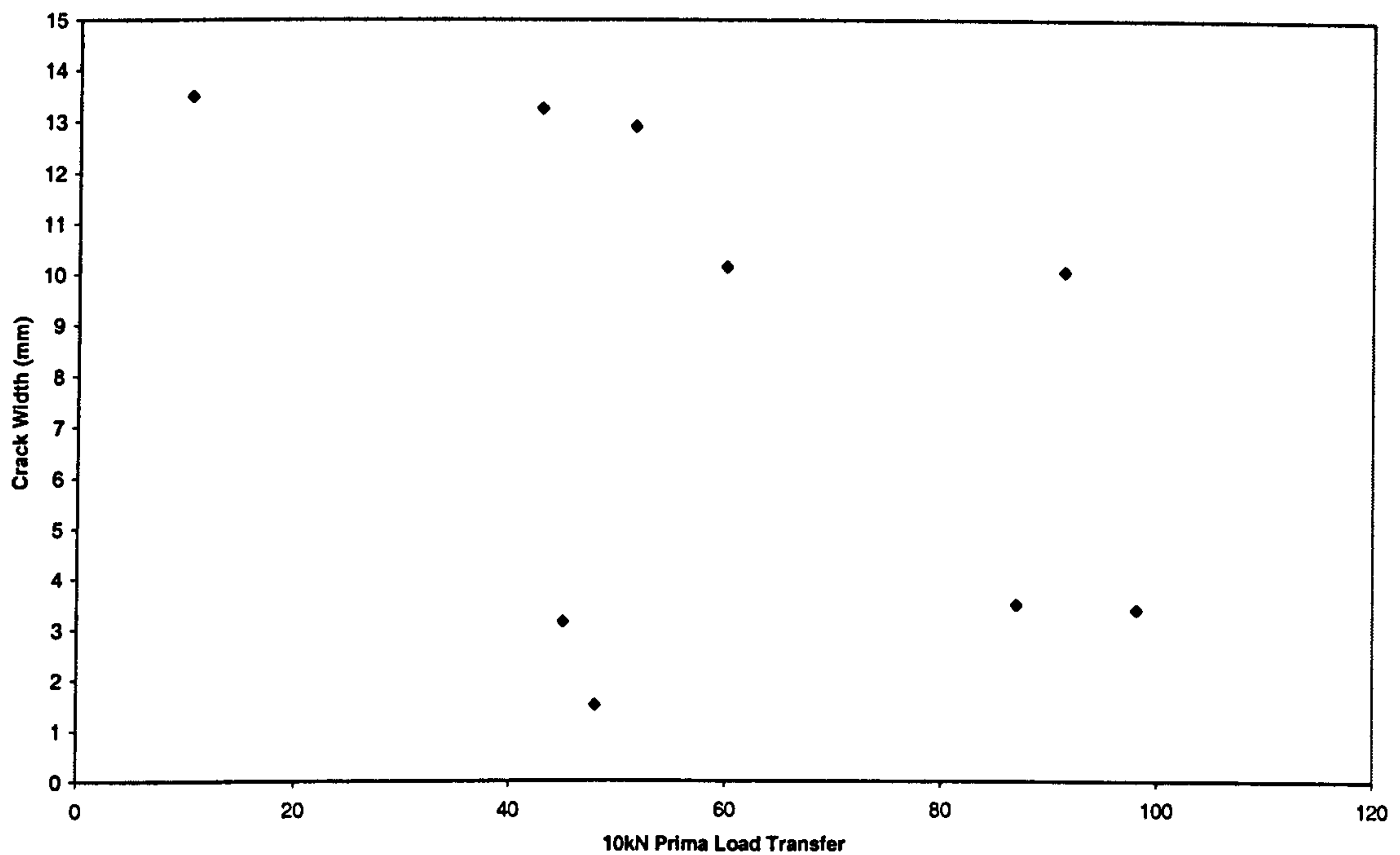
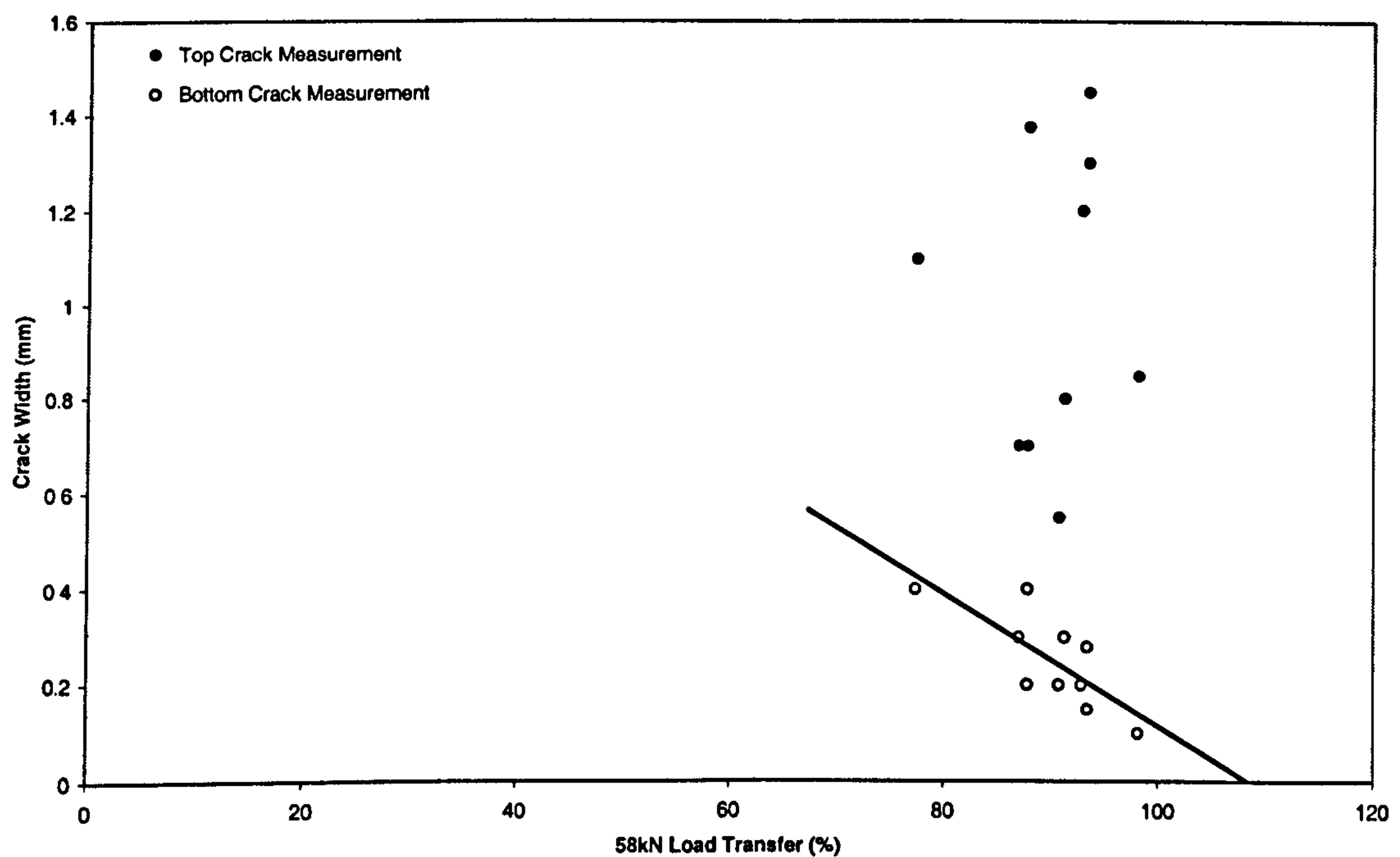


Figure 6.21c – Comparison of load transfer and crack width (Skelmersdale)



**Figure 6.22 - Comparison of load transfer with surface and base slab crack widths
(Lutterworth)**

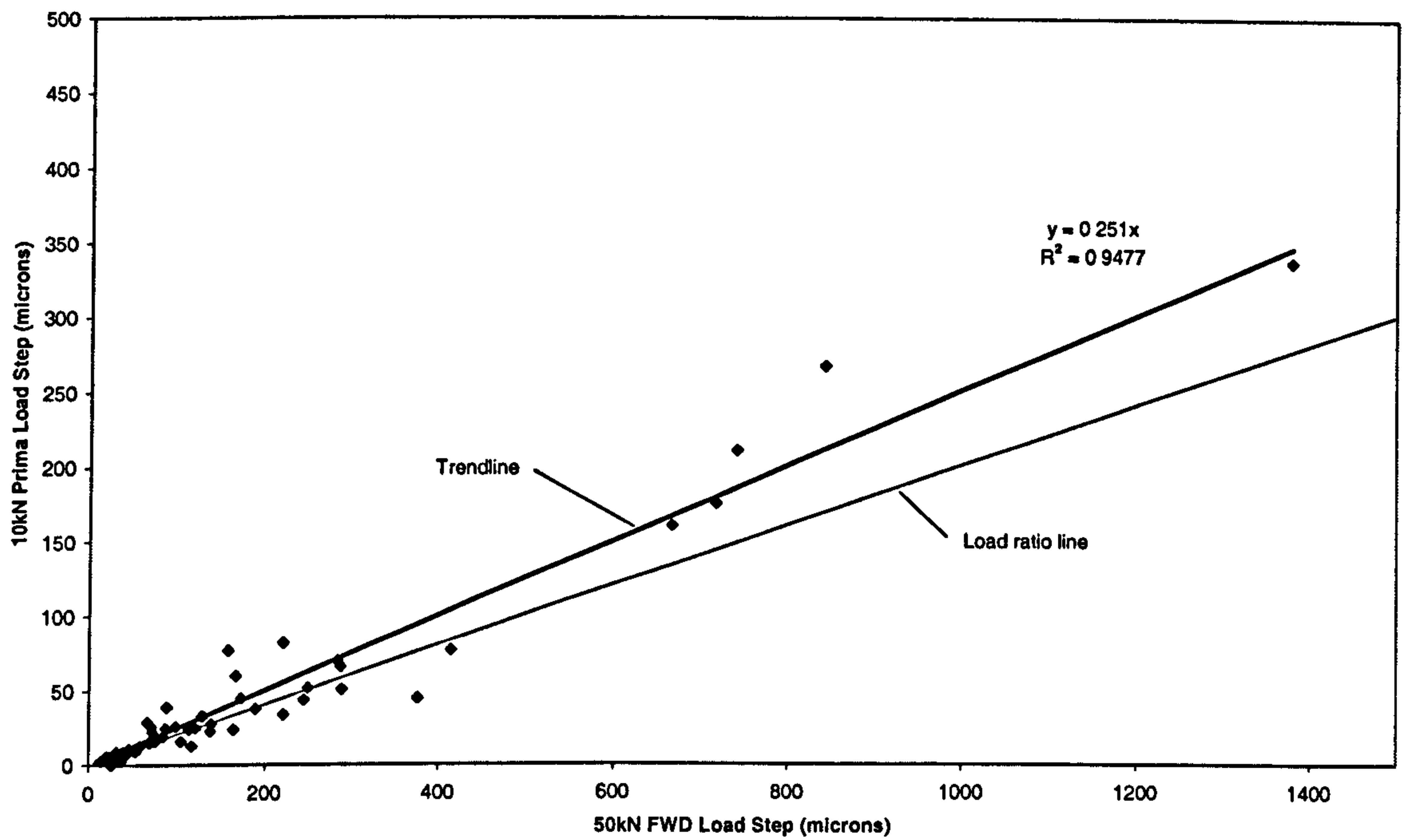


Figure 6.23 – Load step comparison between FWD and Prima (Daventry)

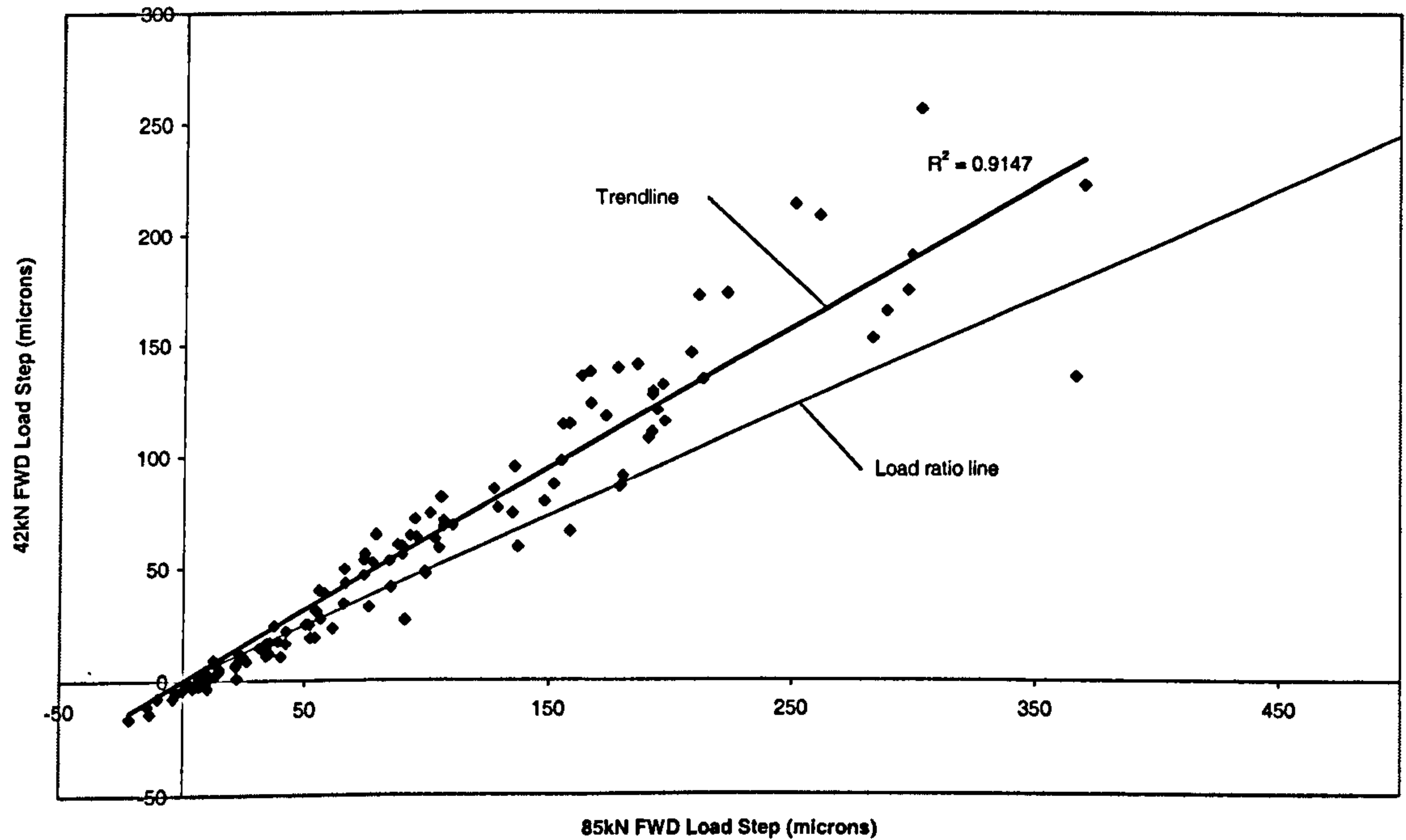


Figure 6.24 – Load step comparison between FWD load magnitudes (Lutterworth)

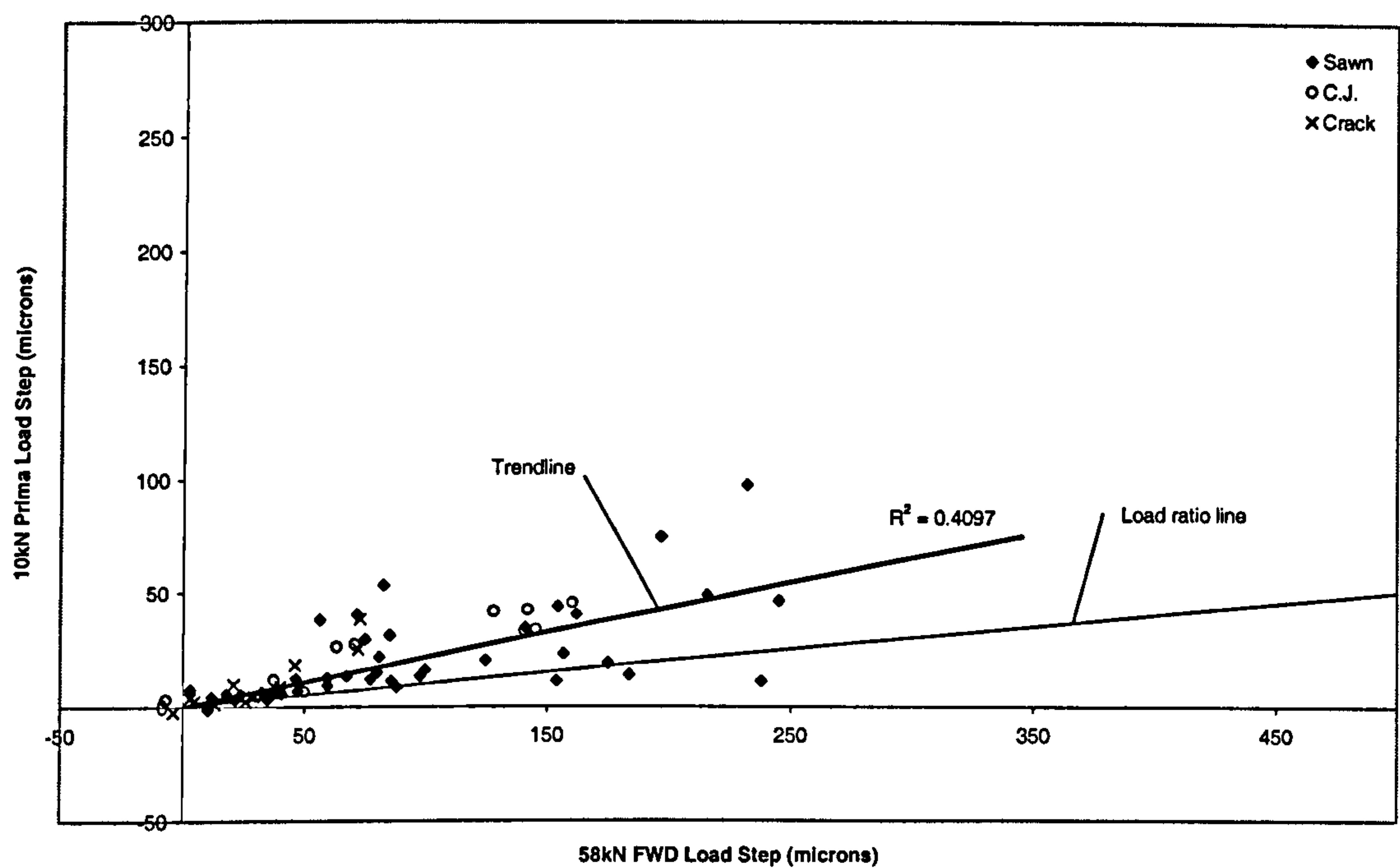


Figure 6.25 – Load step comparison between FWD and Prima (Lutterworth)

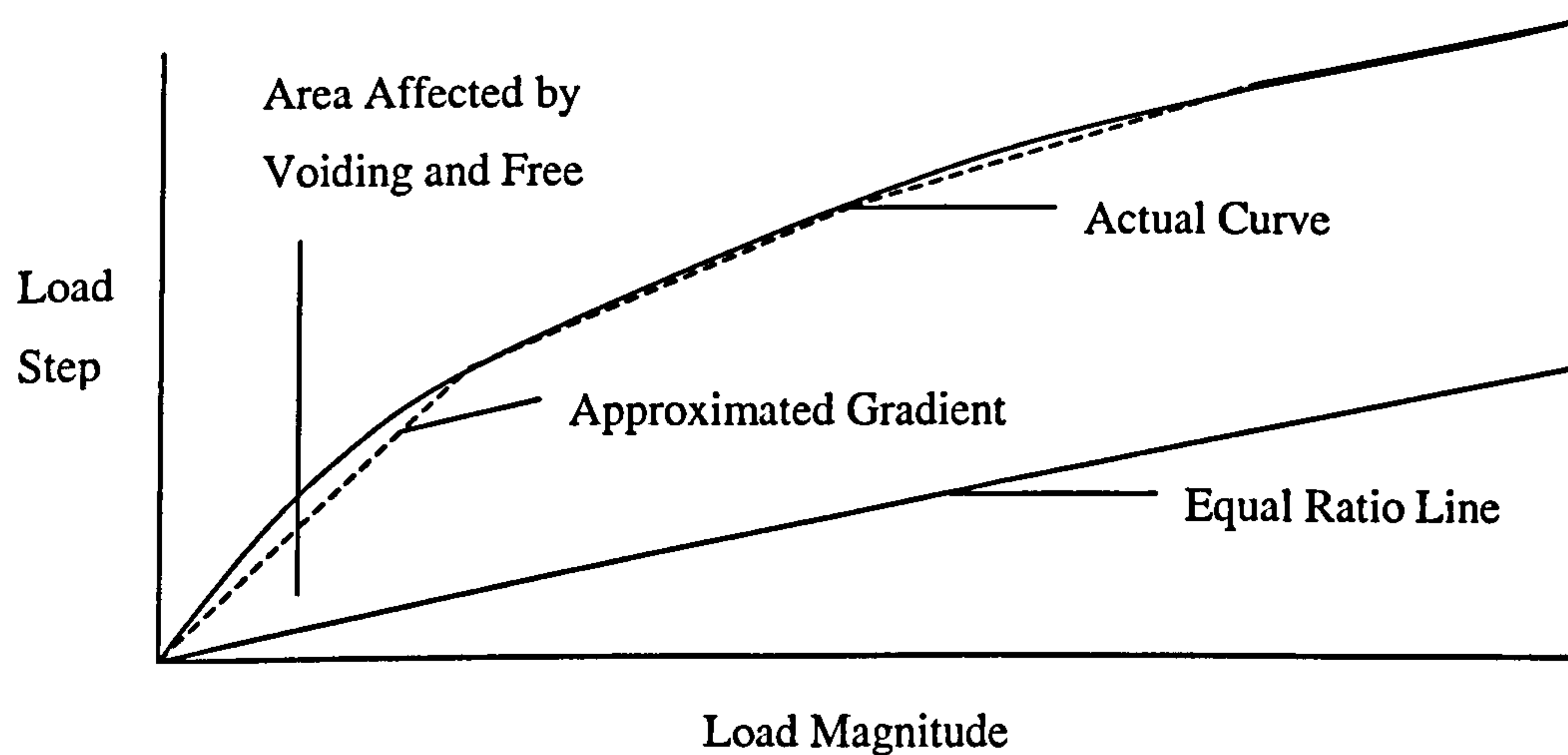


Figure 6.26 – Effect of voiding on load magnitude / load step gradients

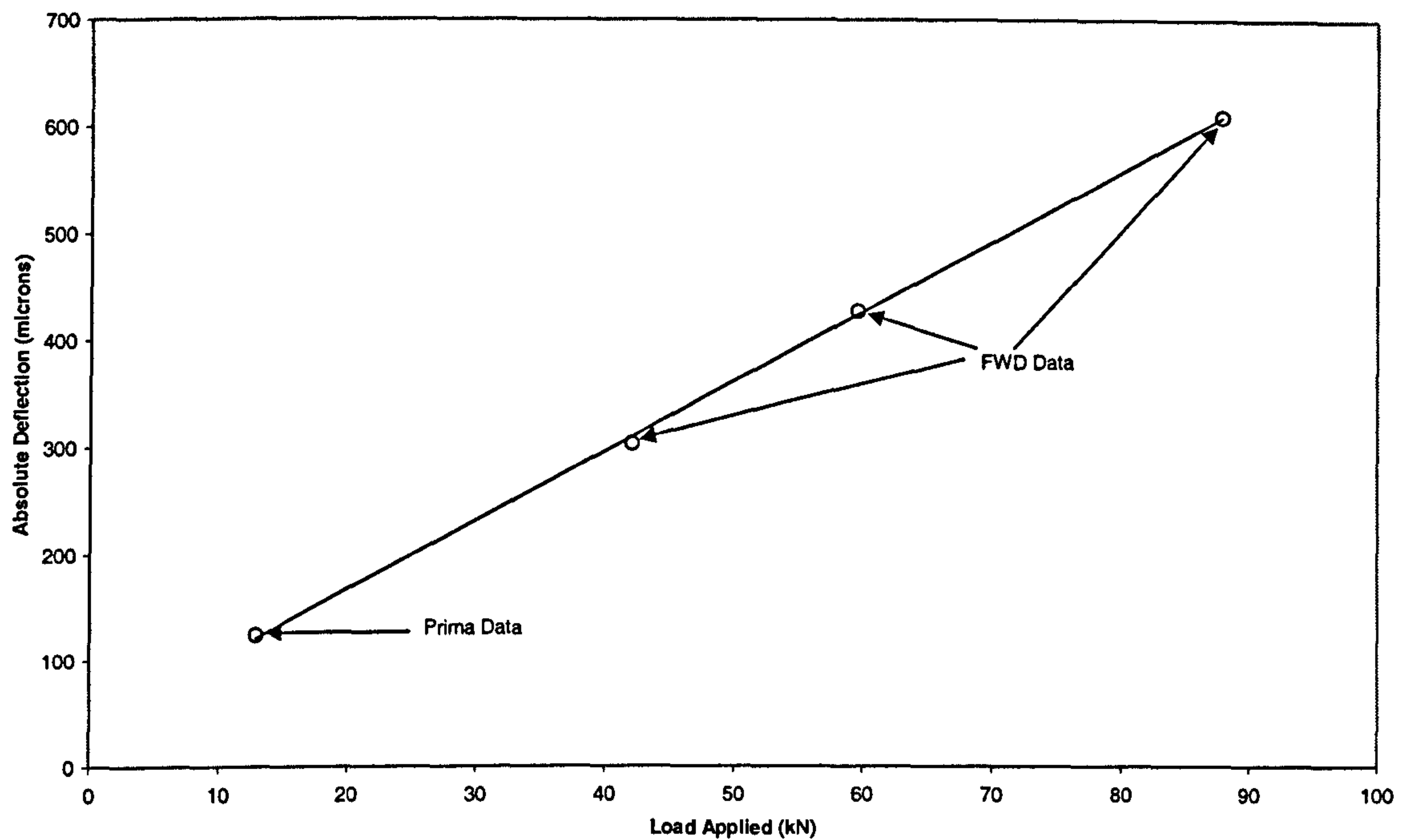


Figure 6.27 – Effect of load on absolute deflection

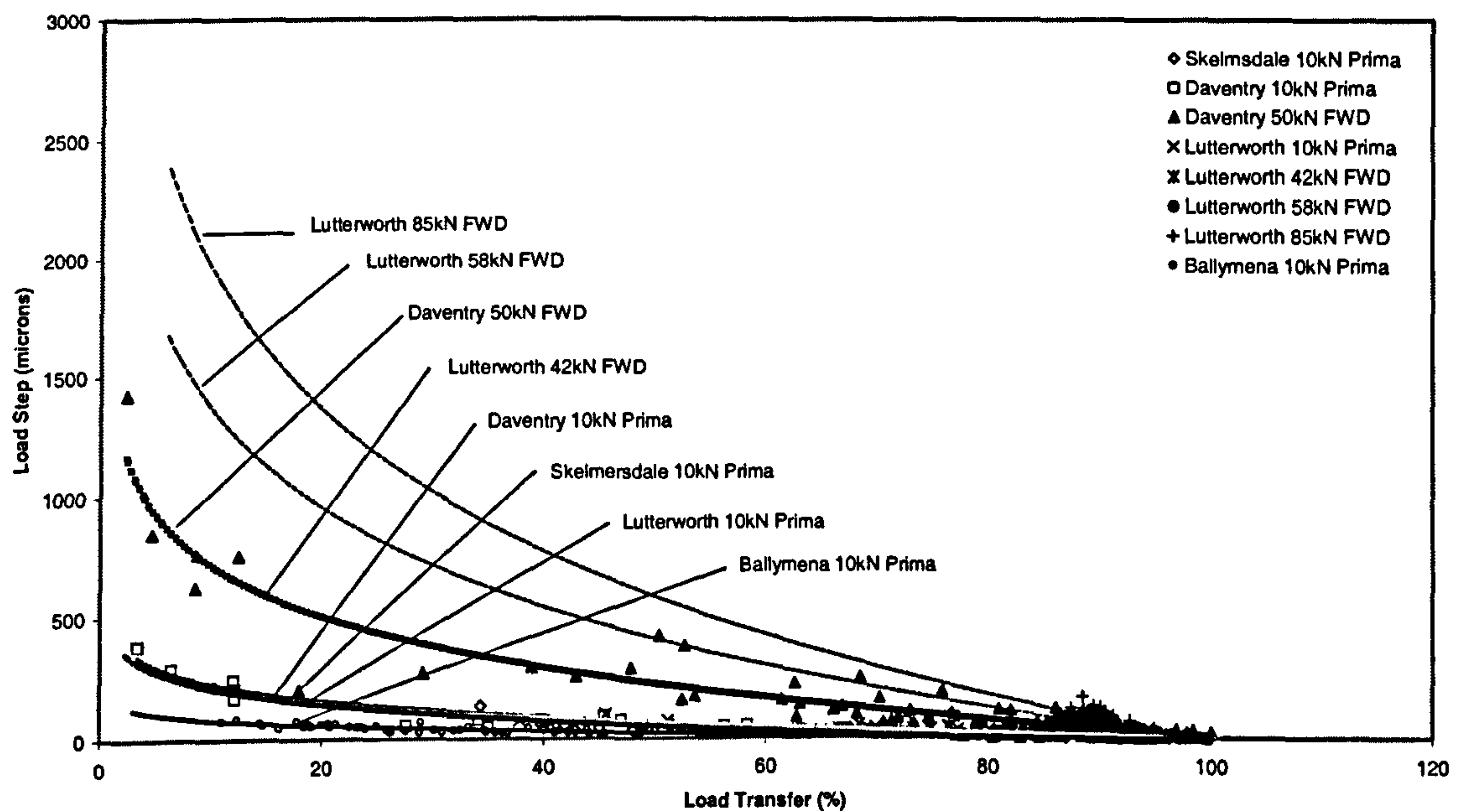
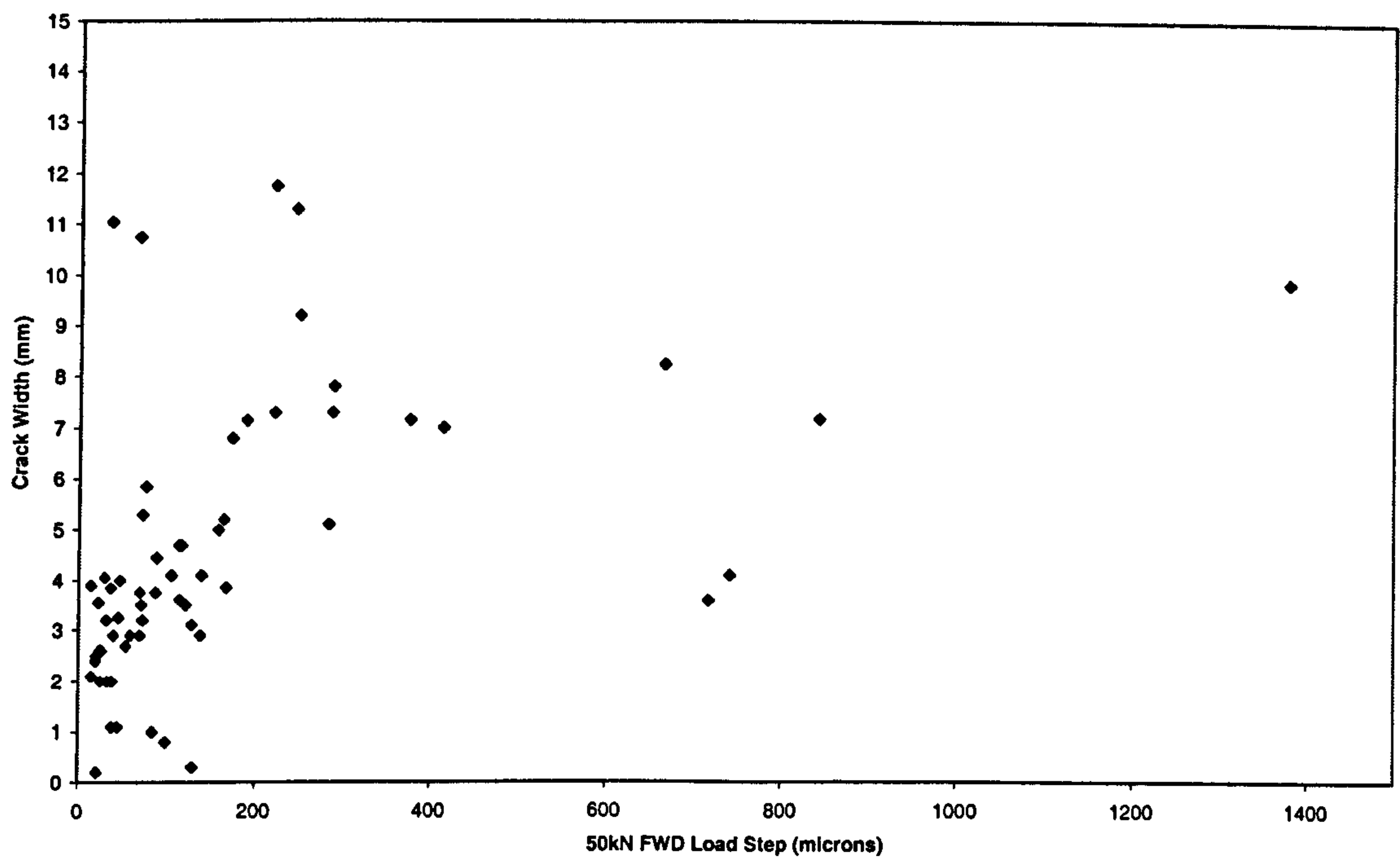


Figure 6.28 – Comparison of load transfer and load step
(Daventry/Lutterworth/Ballymena/Skelmersdale)



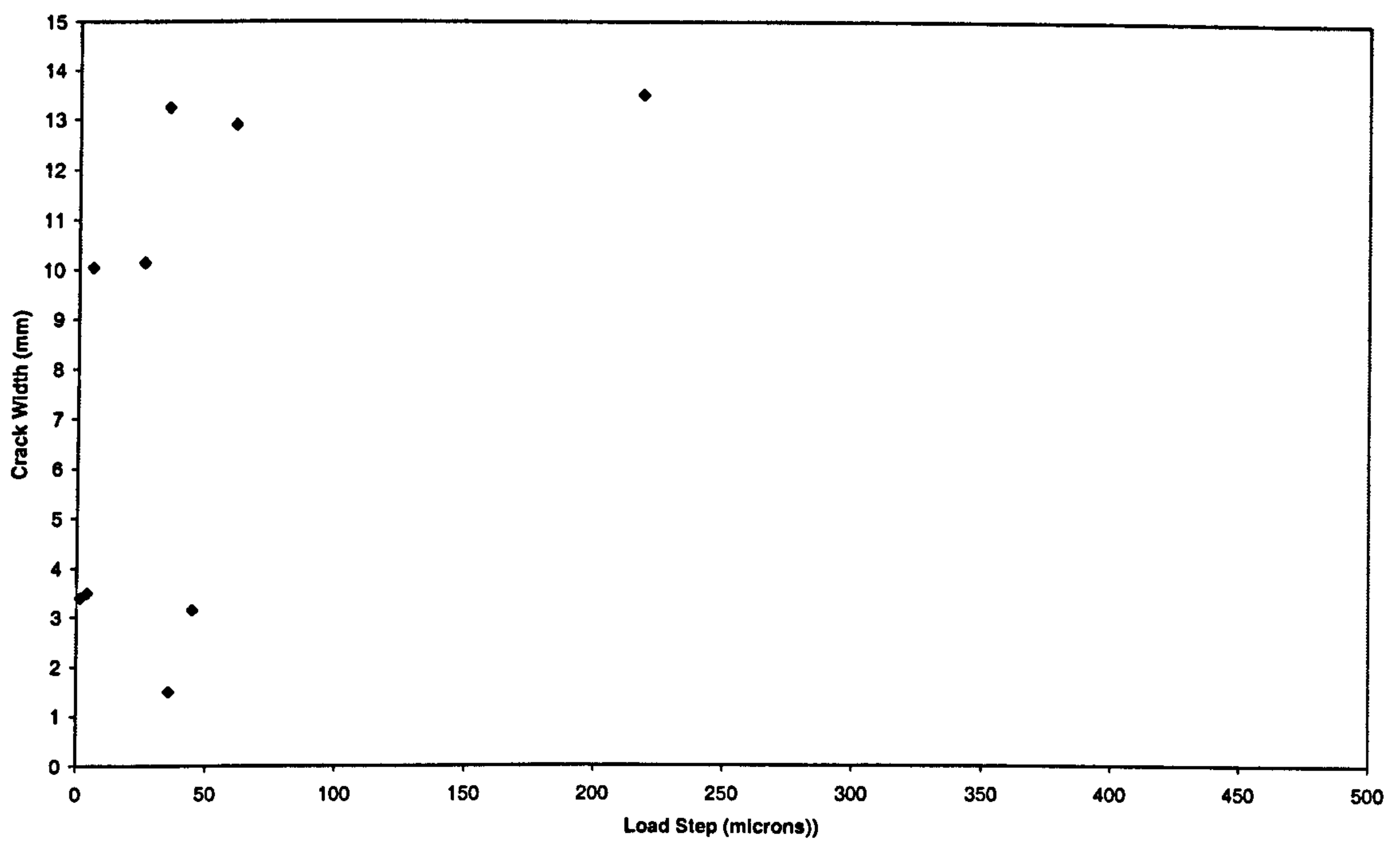


Figure 6.29c – Comparison of load step and crack width (Skelmersdale)

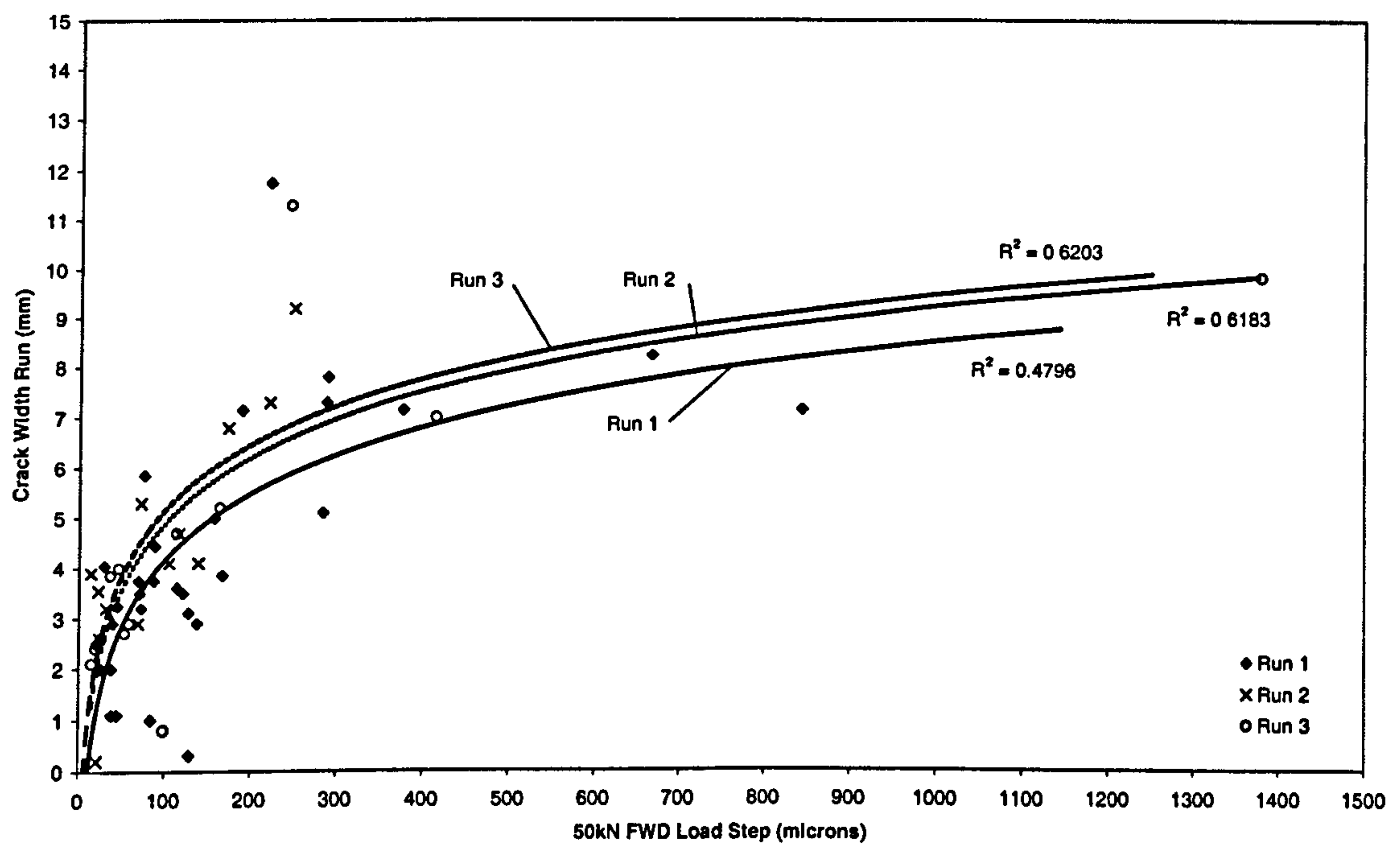


Figure 6.30 – Comparison of load step and crack width taking into account pre-load (Daventry)

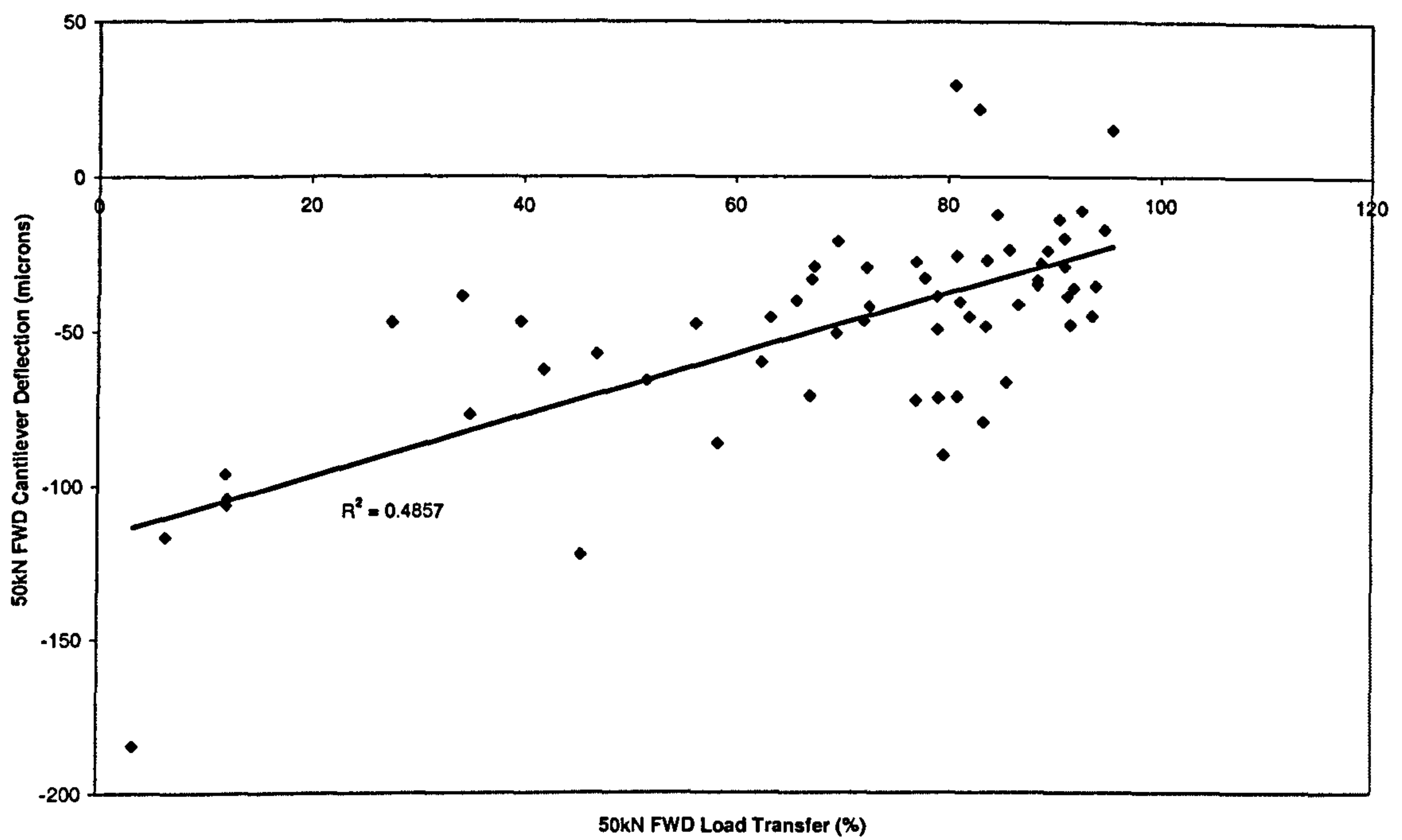


Figure 6.31a – Comparison of load transfer and edge cantilever (Daventry)

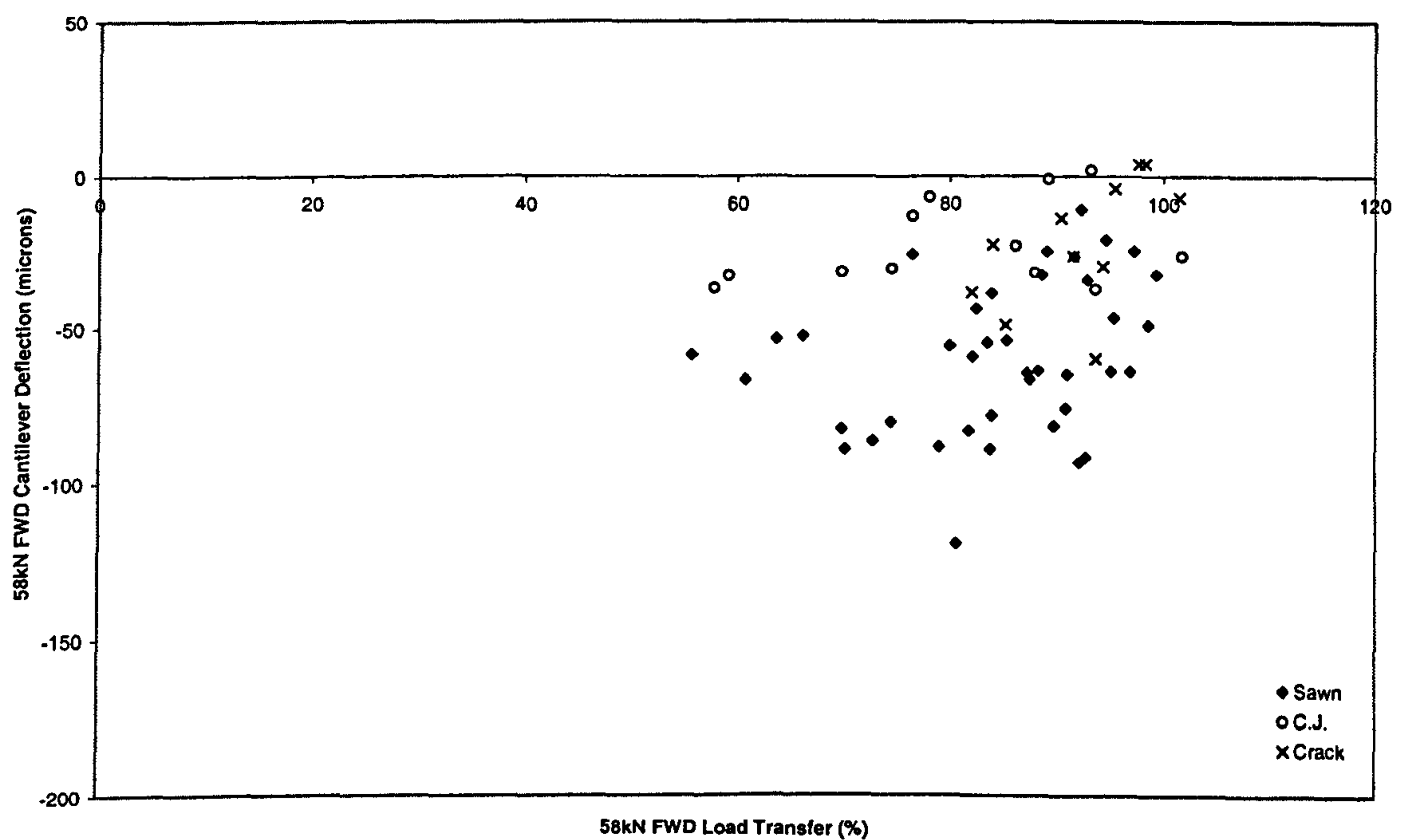


Figure 6.31b – Comparison of load transfer and edge cantilever (Lutterworth)

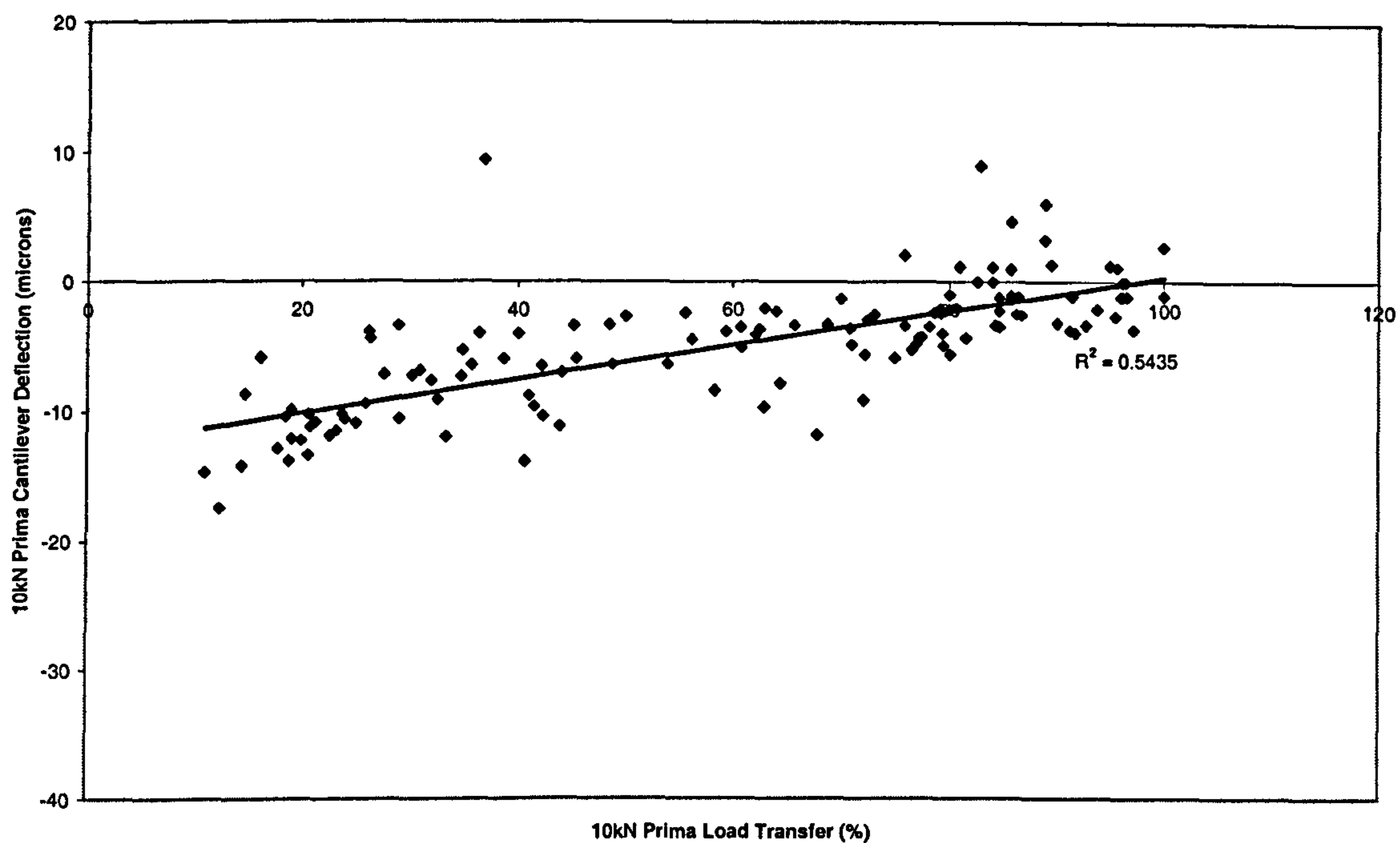


Figure 6.31c – Comparison of load transfer and edge cantilever (Ballymena)

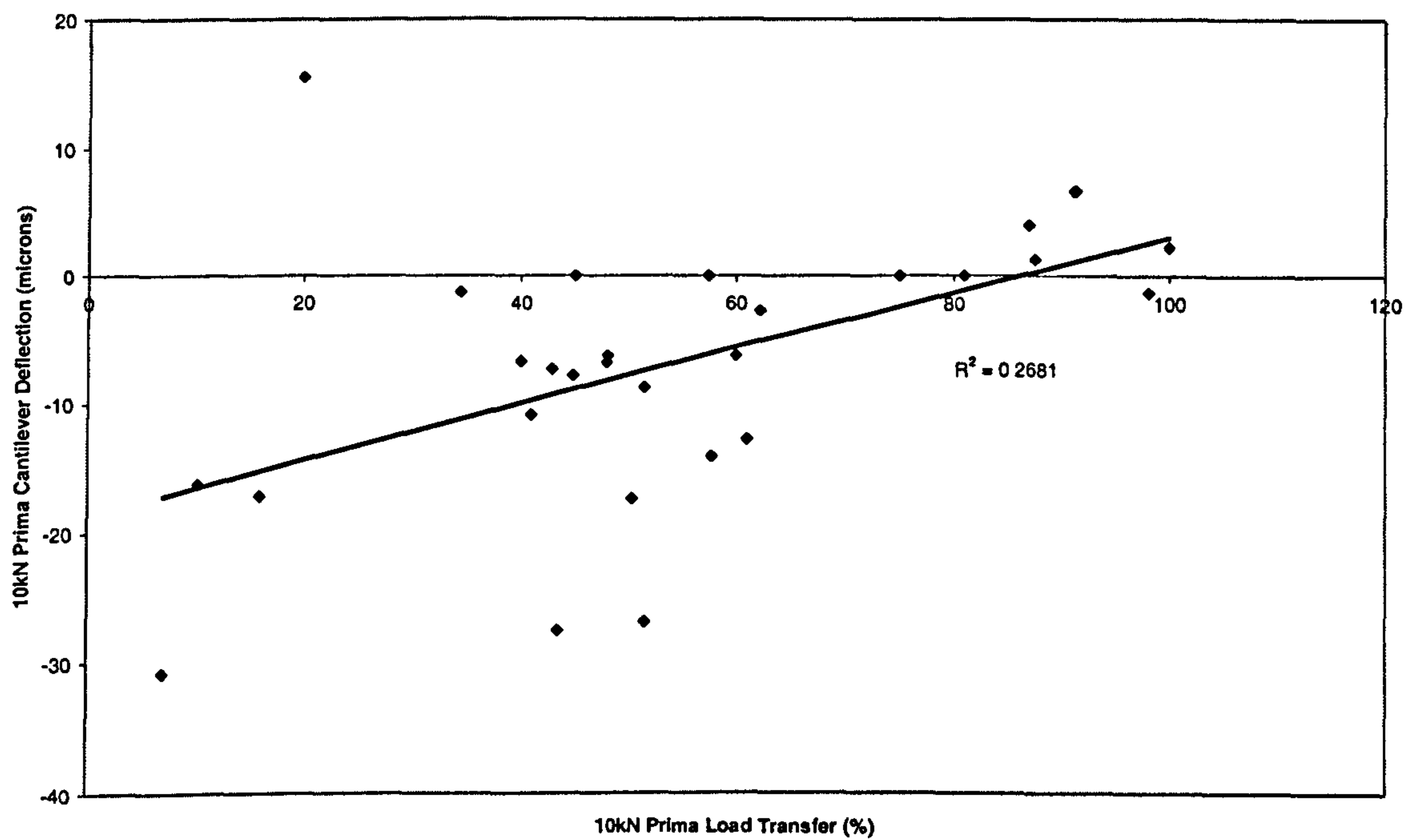


Figure 6.31d – Comparison of load transfer and edge cantilever (Skelmersdale)

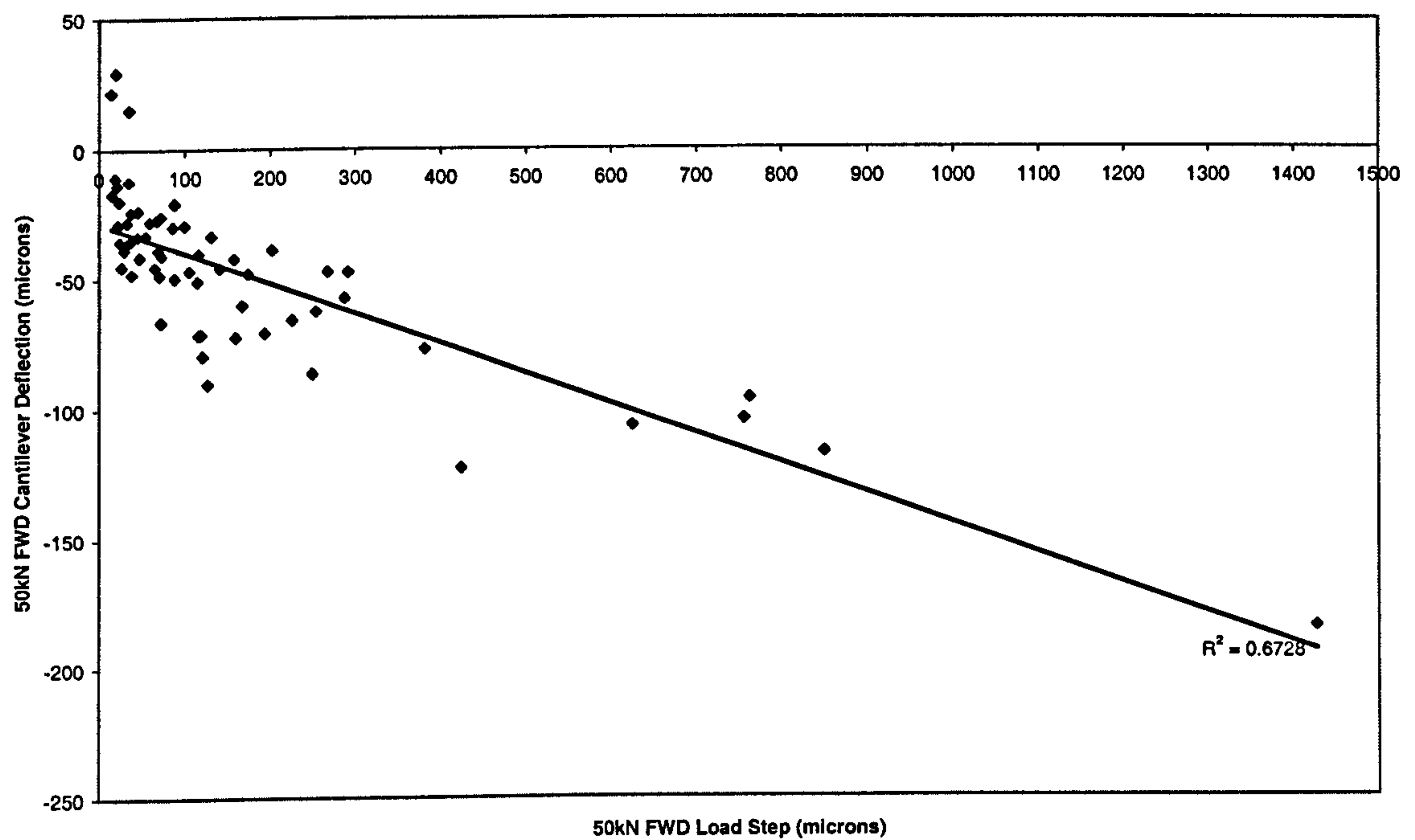


Figure 6.32a – Comparison of load step and edge cantilever (Daventry)

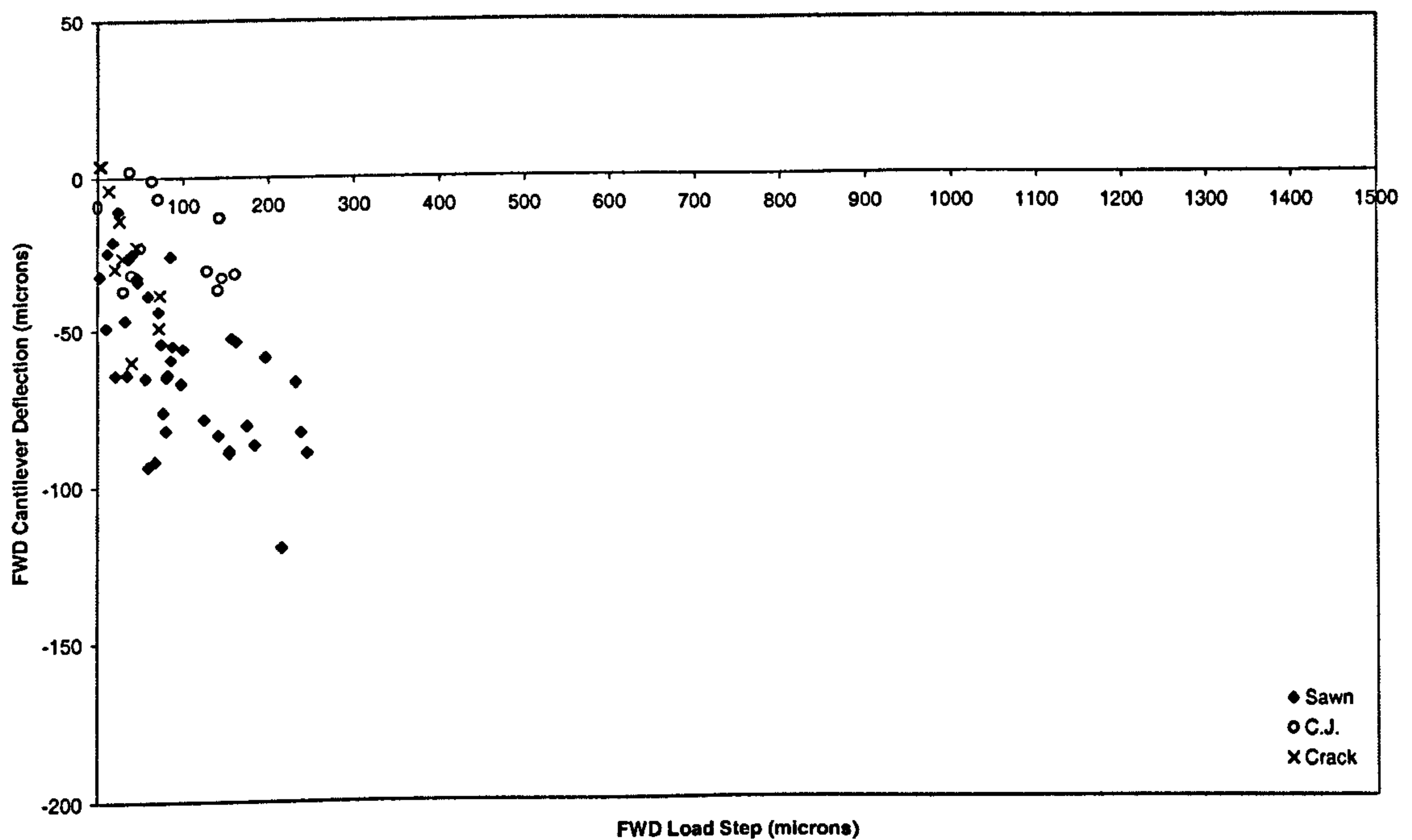


Figure 6.32b – Comparison of load step and edge cantilever (Lutterworth)

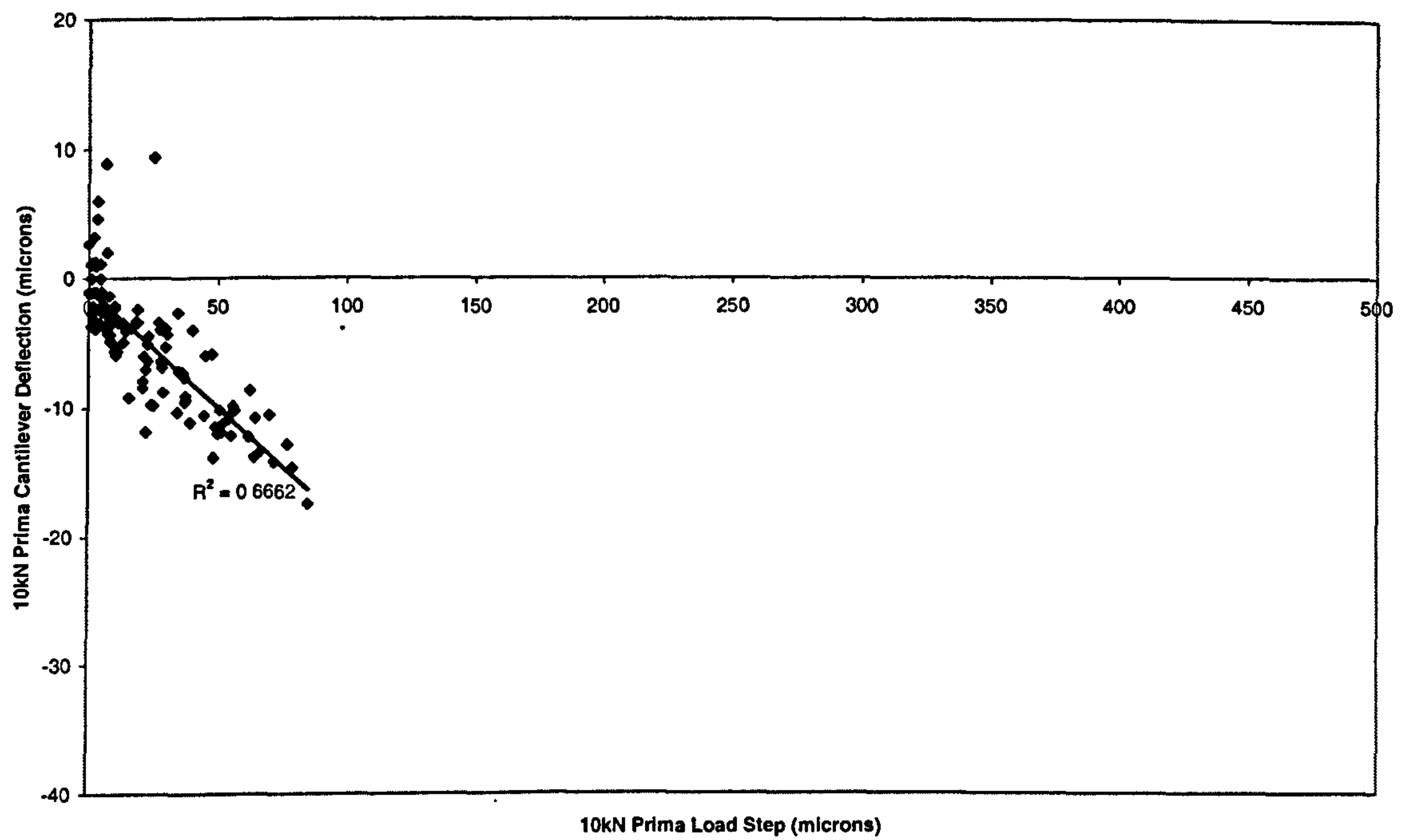


Figure 6.32c – Comparison of load step and edge cantilever (Ballymena)

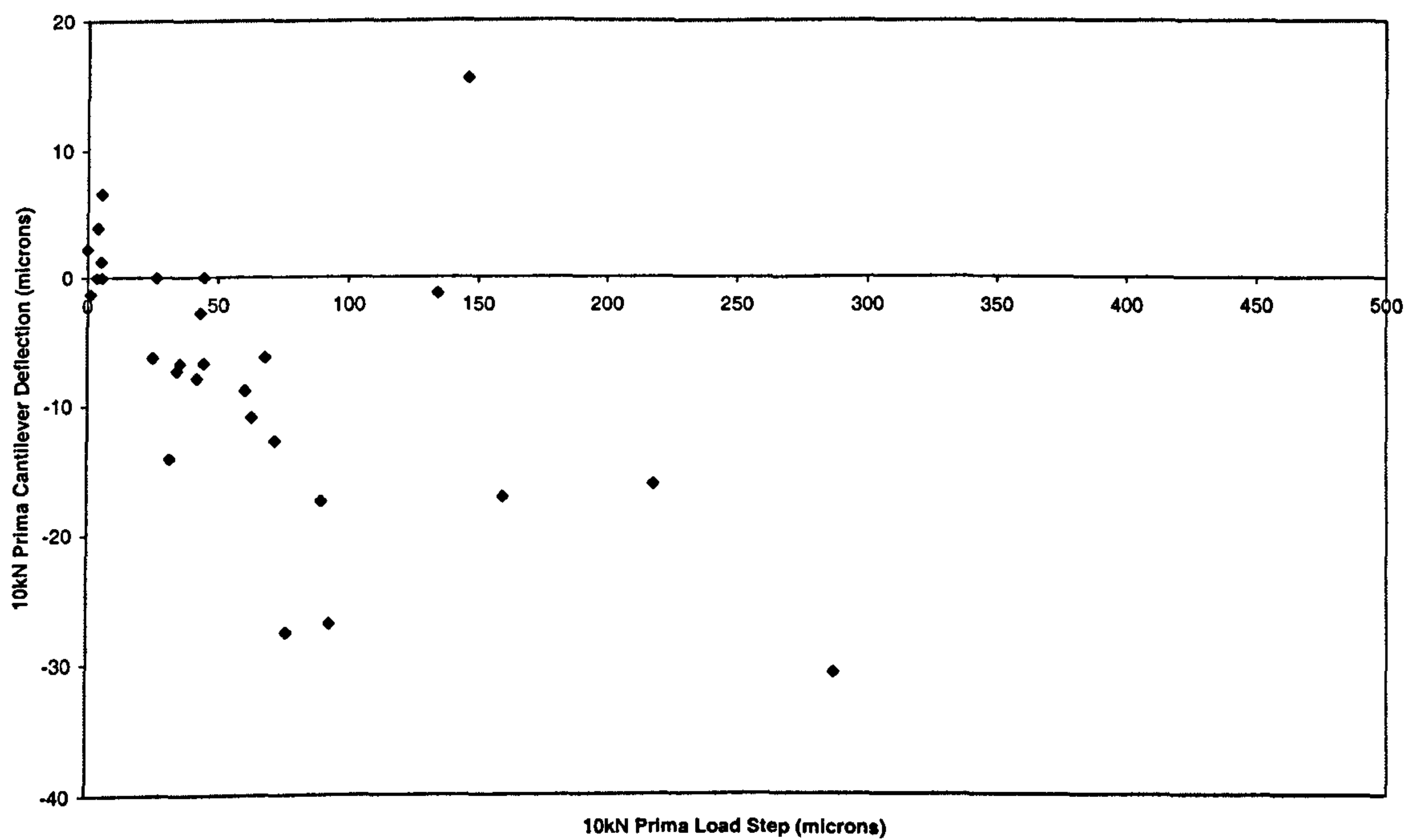


Figure 6.32d – Comparison of load step and edge cantilever (Skelmersdale)

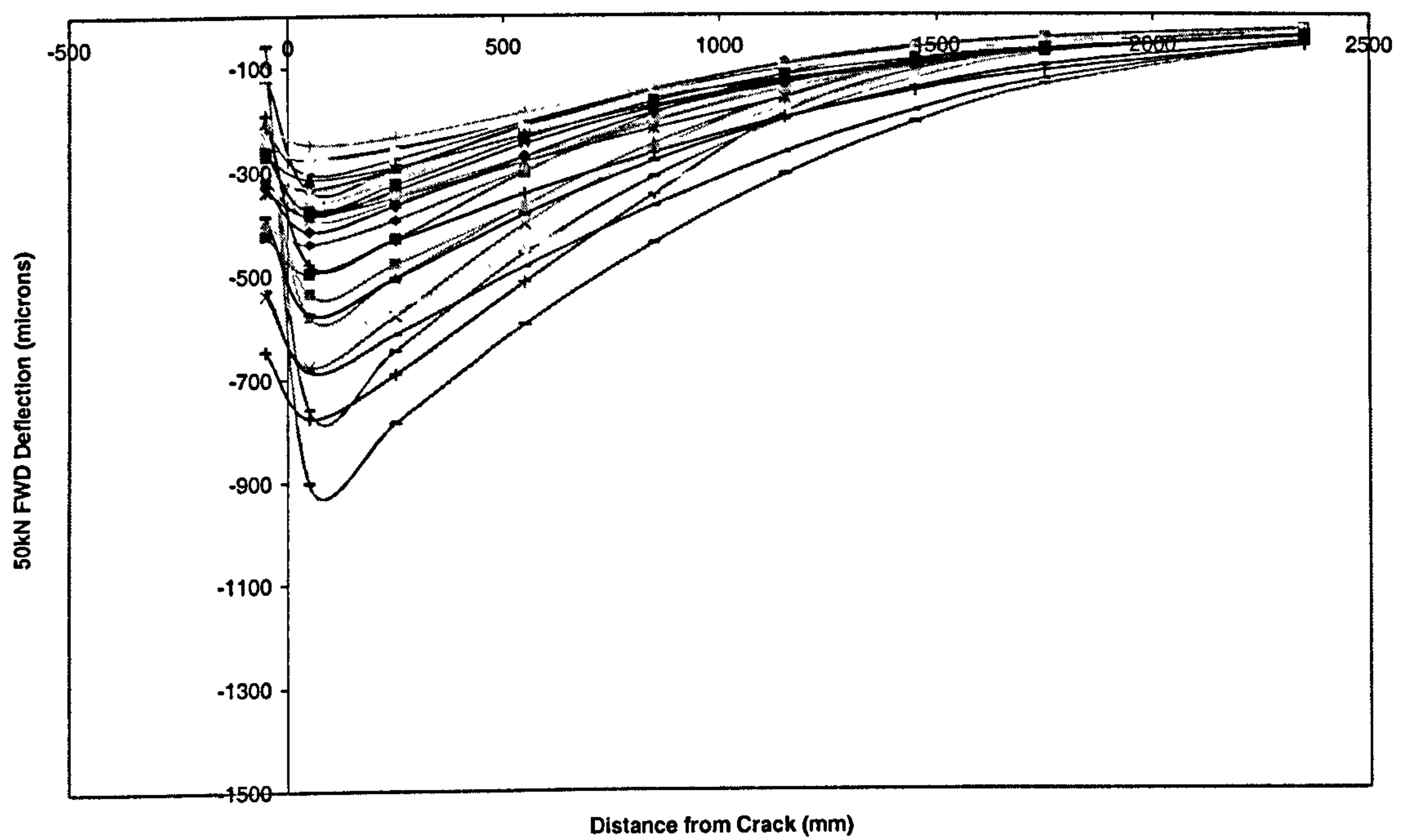


Figure 6.33 – Typical deflection bowls (Daventry)

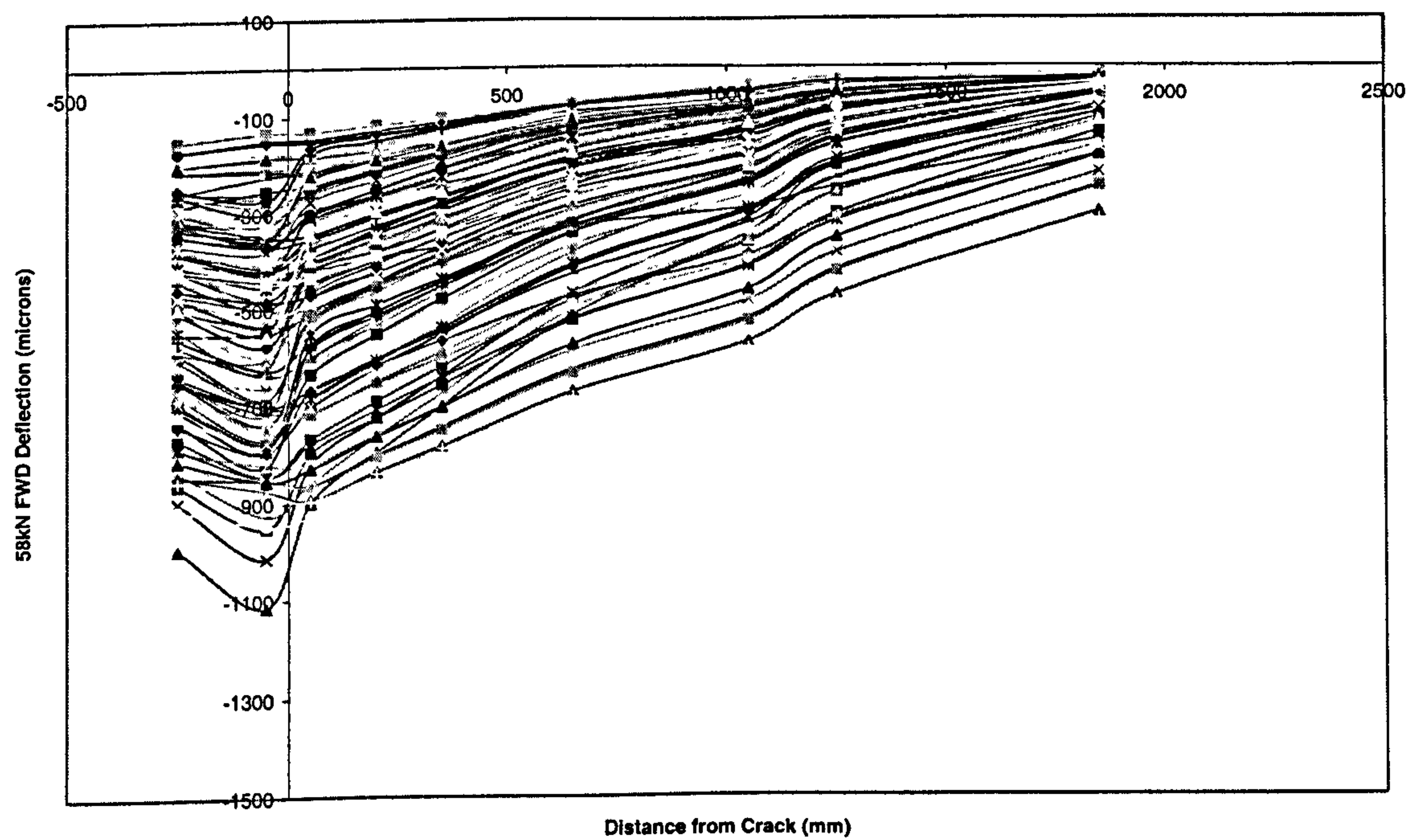


Figure 6.34 – Typical deflection bowls (Lutterworth)

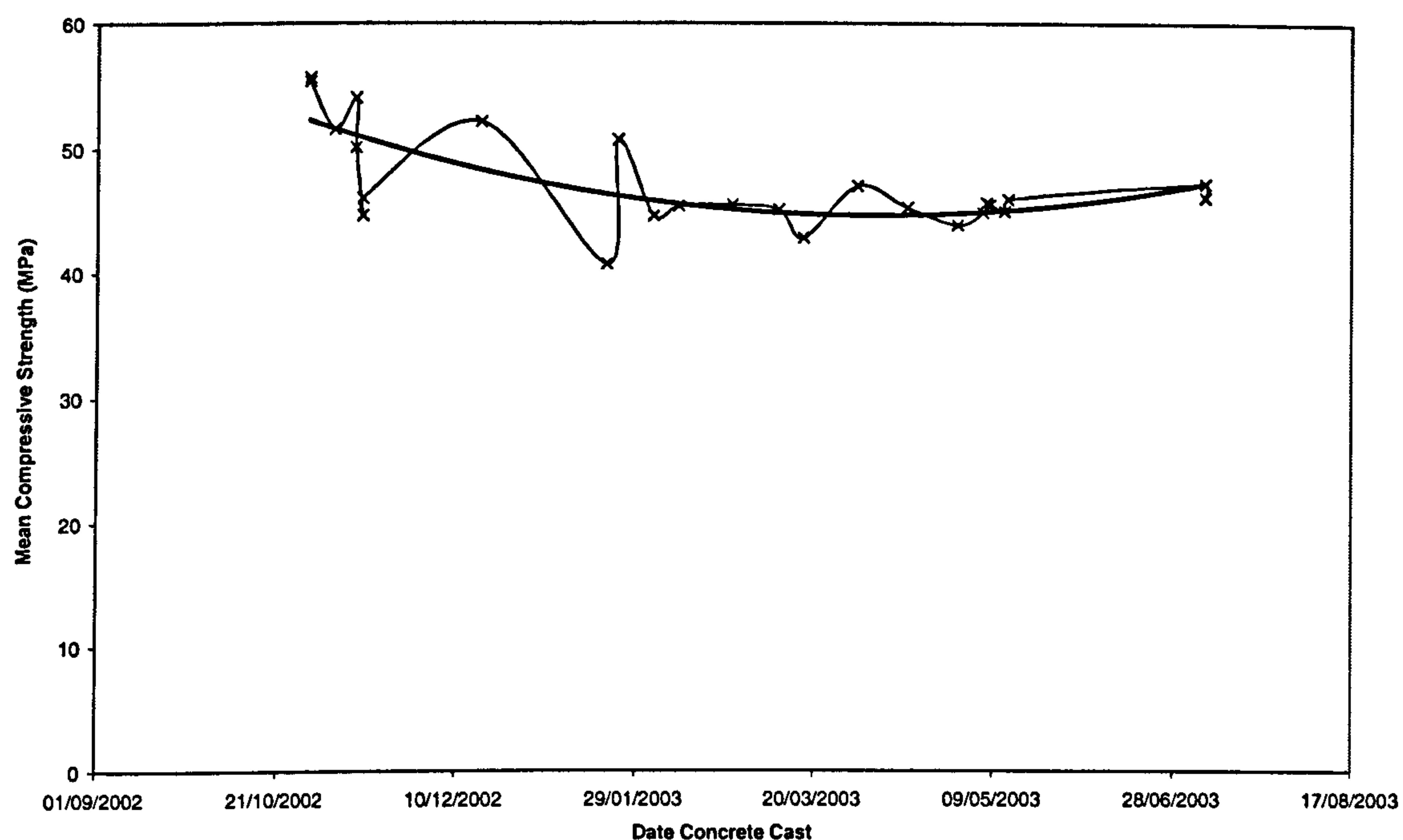


Figure 6.35 – Effect of casting date on cube compressive strength

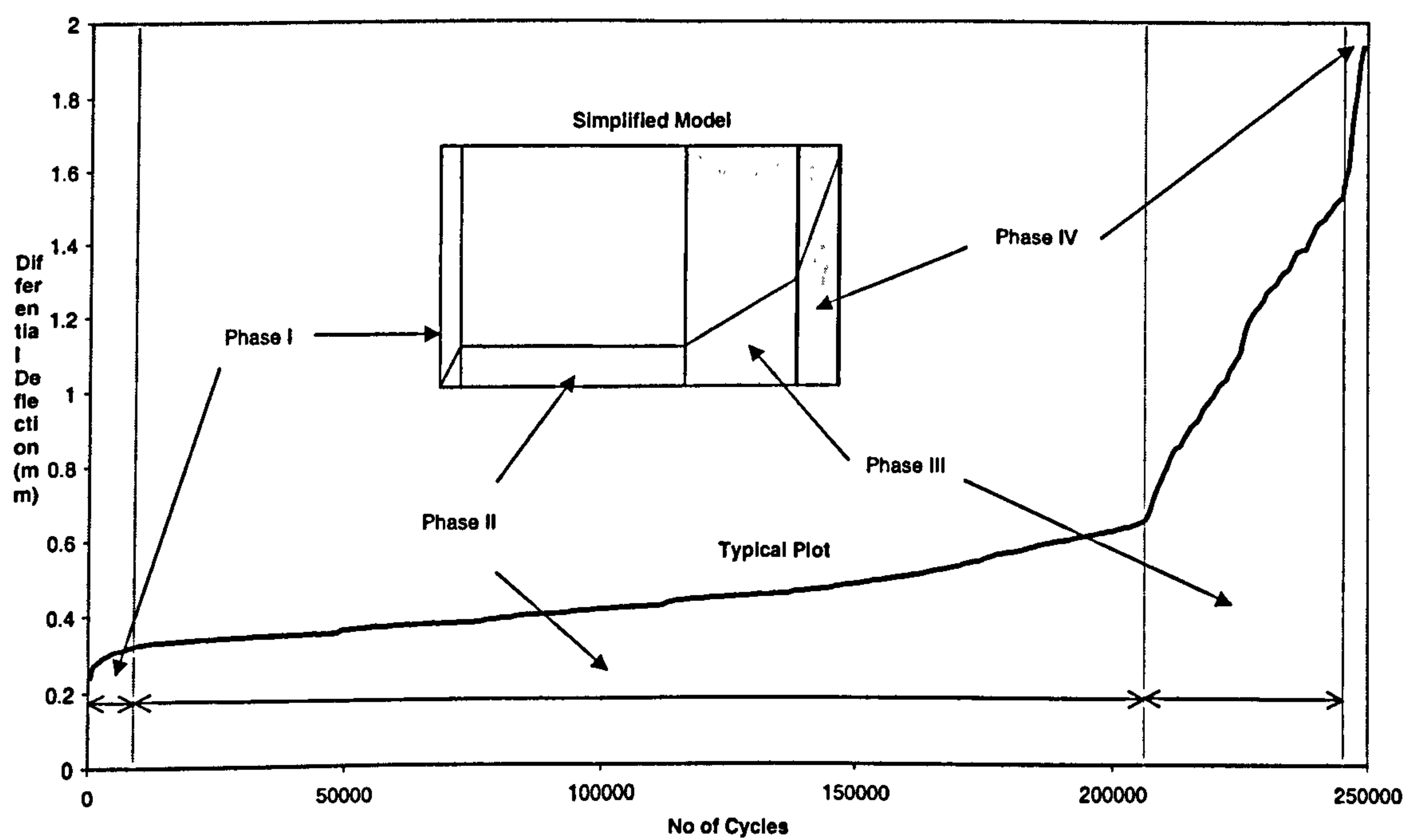


Figure 6.36 – Deterioration phases of a concrete crack

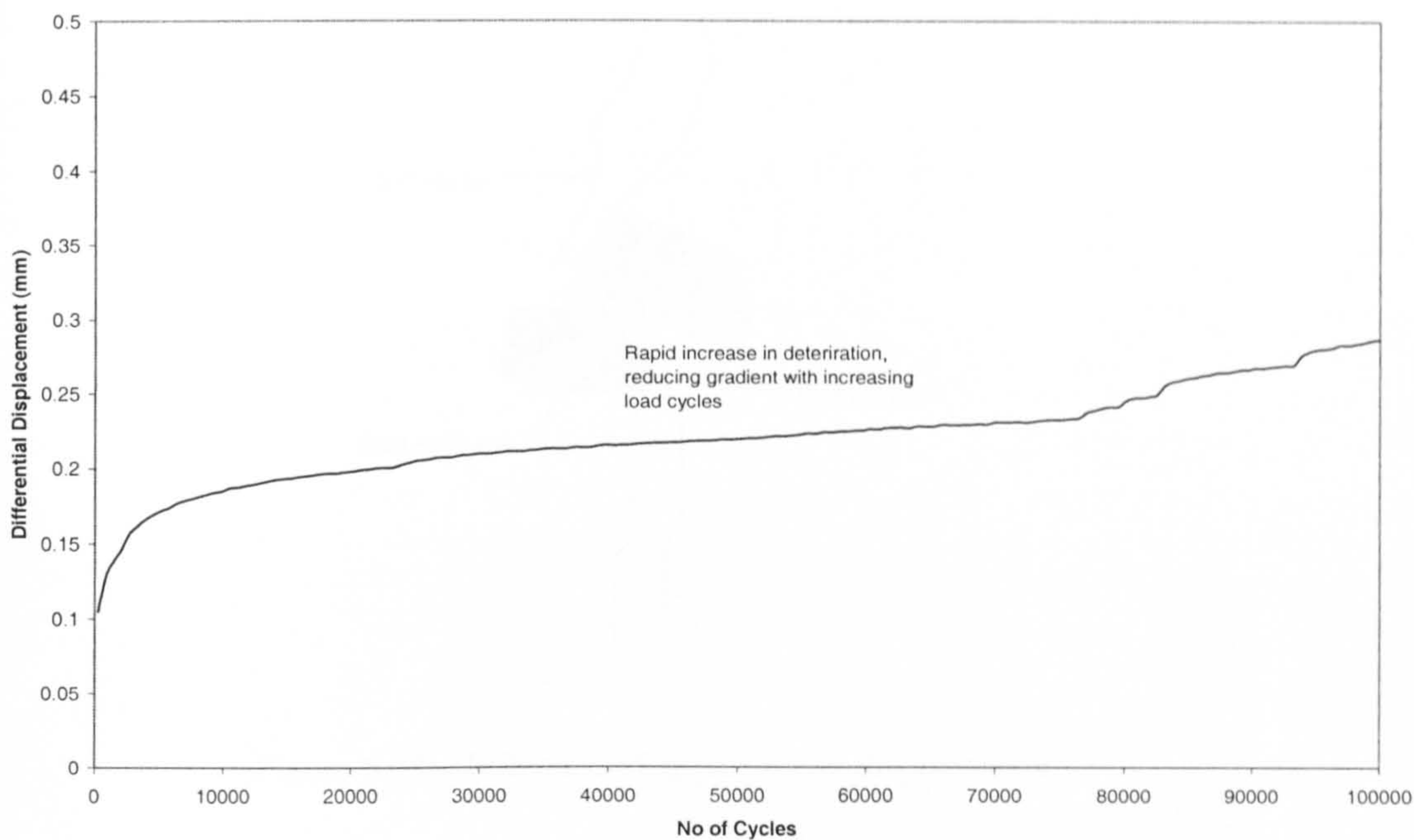


Figure 6.37 – Early deterioration in a concrete test specimen

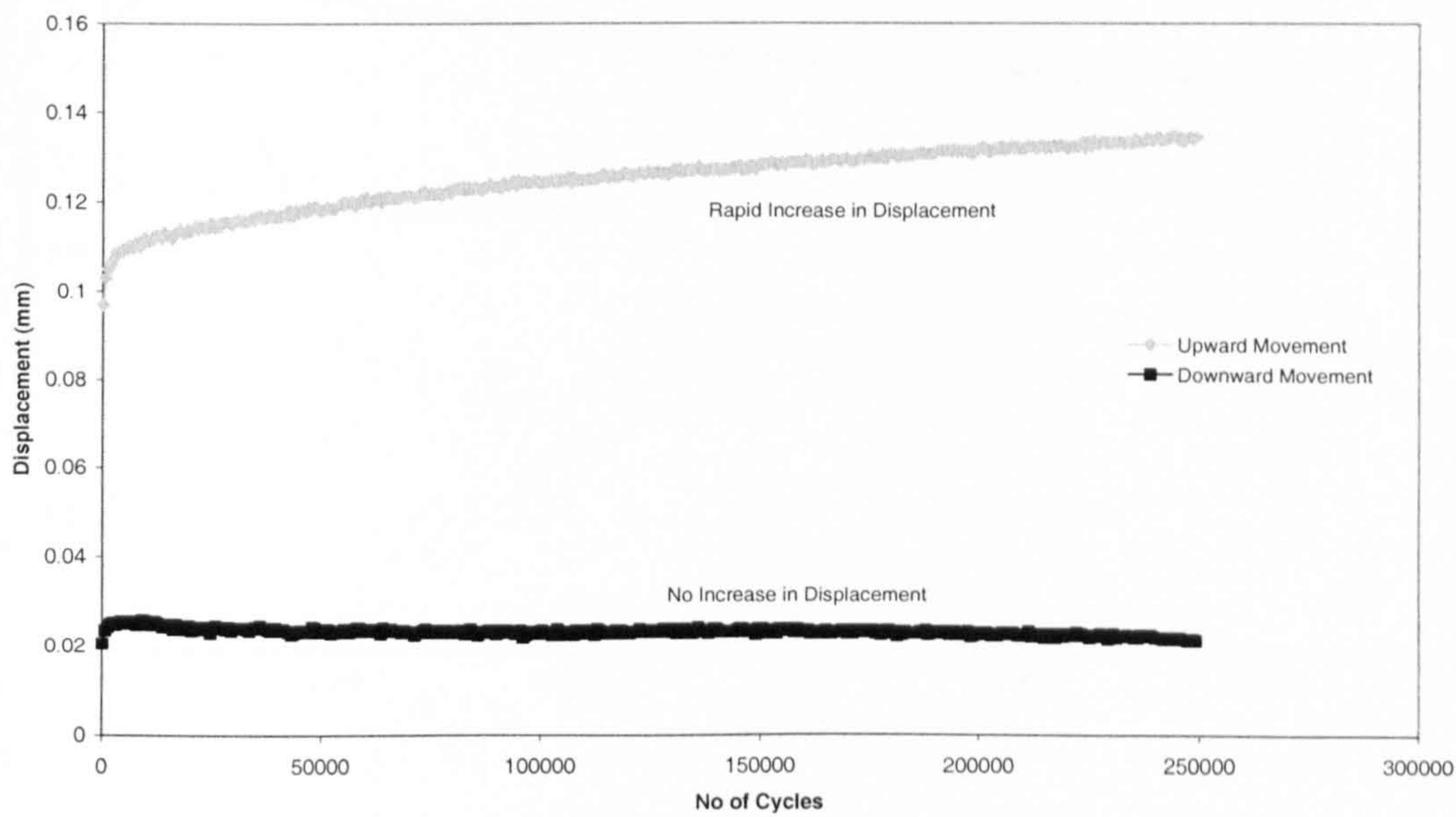


Figure 6.38 – Unequal displacement

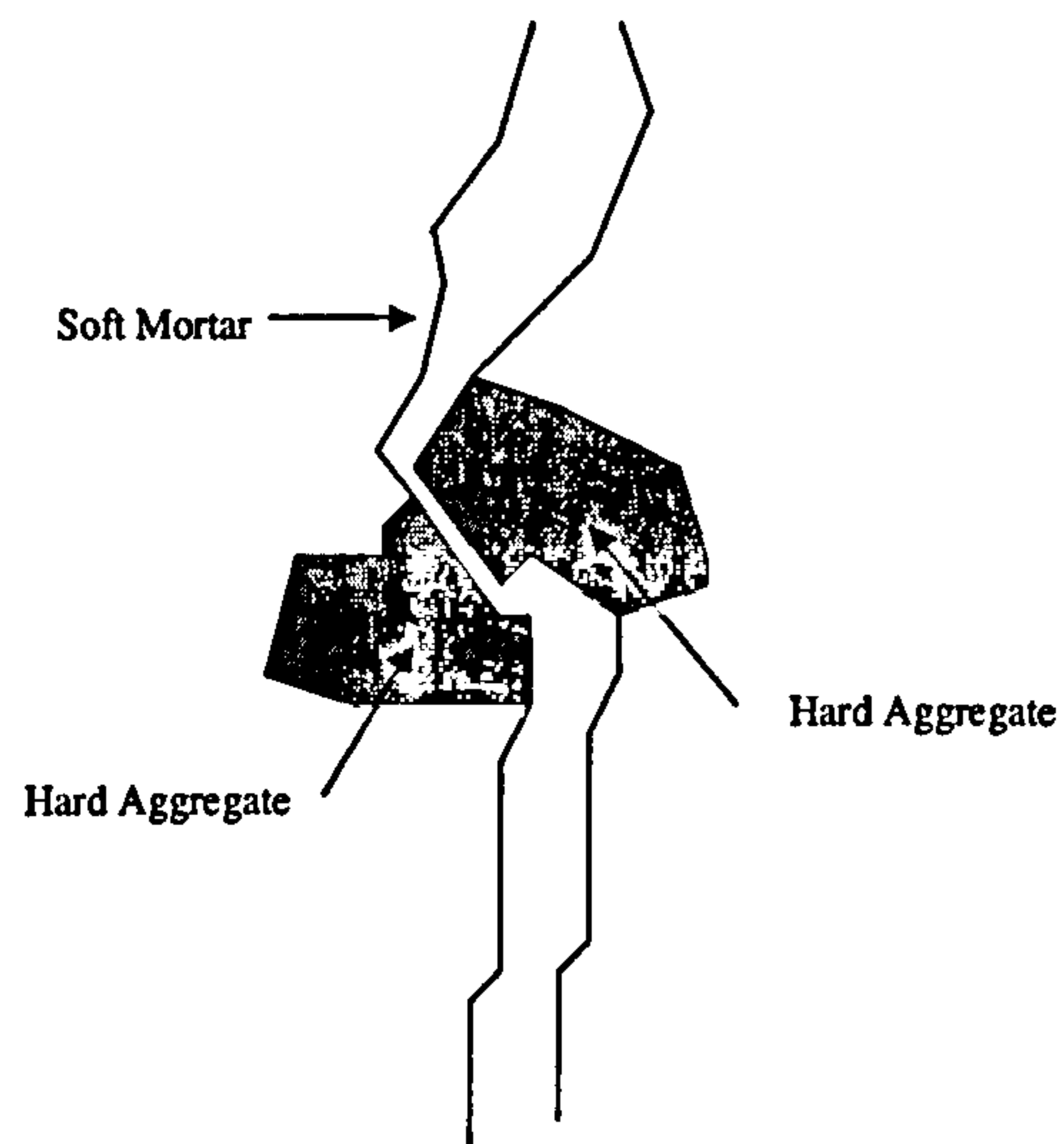


Figure 6.39 – Influence of aggregate on displacement

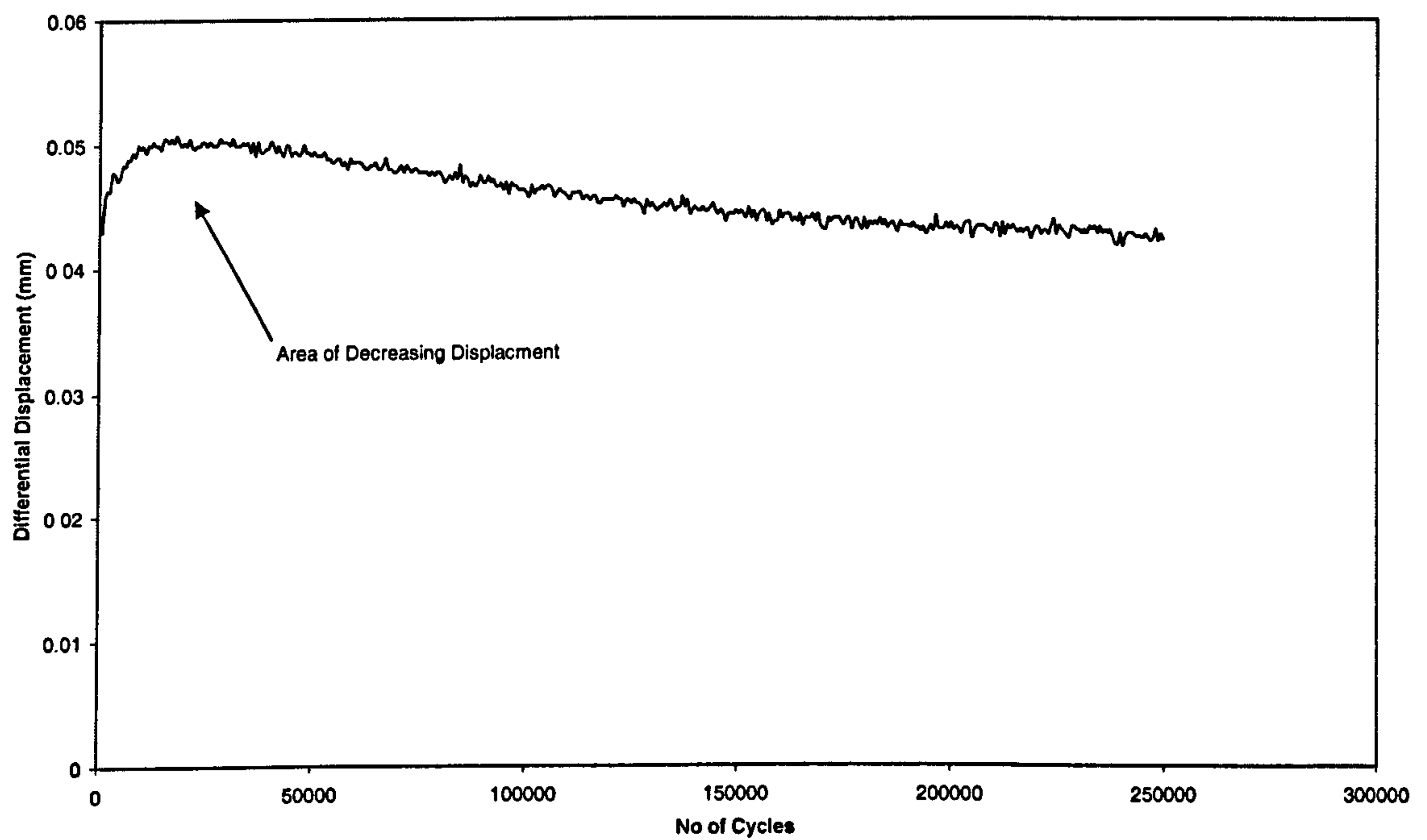


Figure 6.40 – Negative deterioration caused by small material accumulation

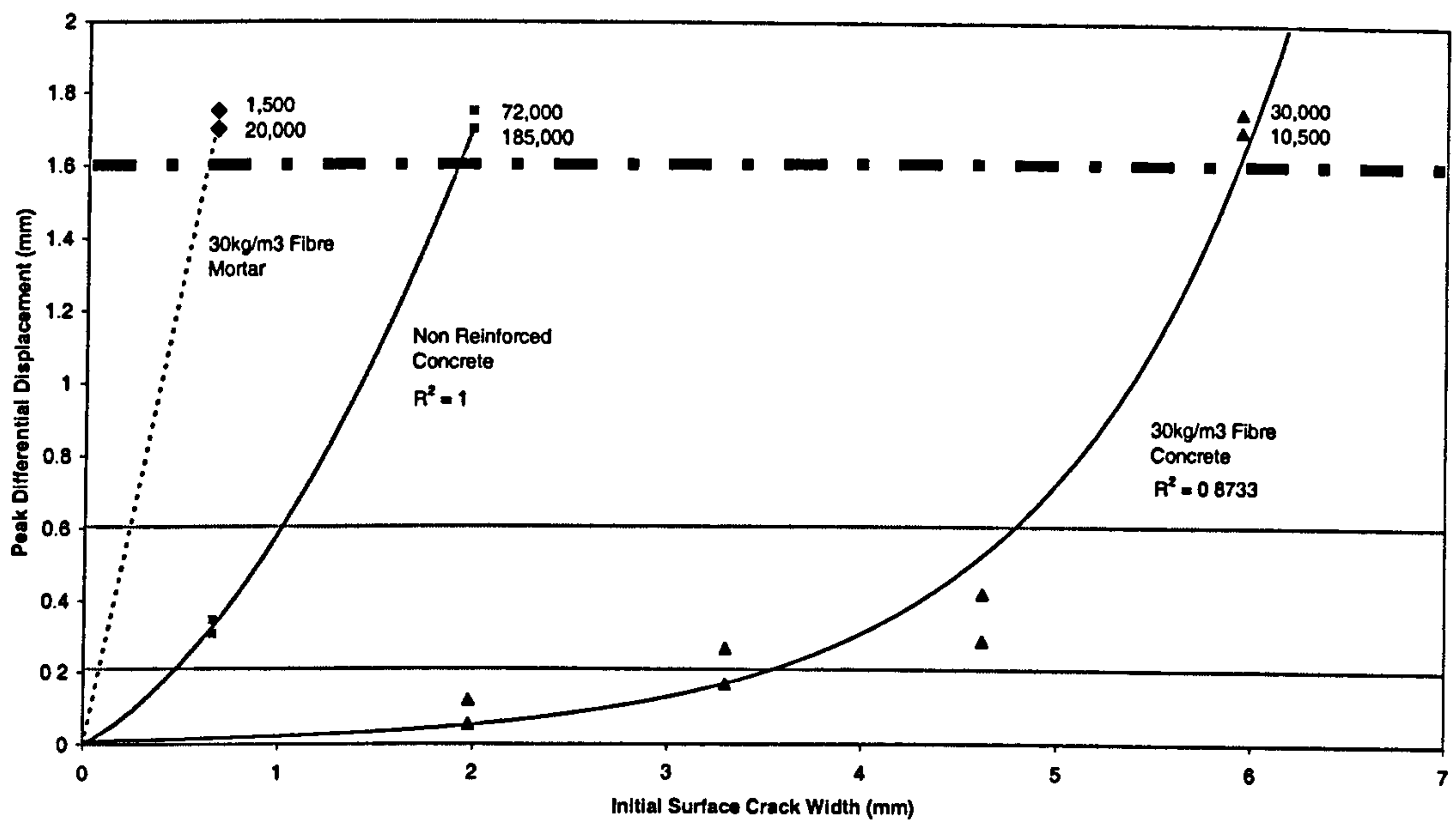


Figure 6.41 – Effect of aggregate and steel fibres on differential displacement

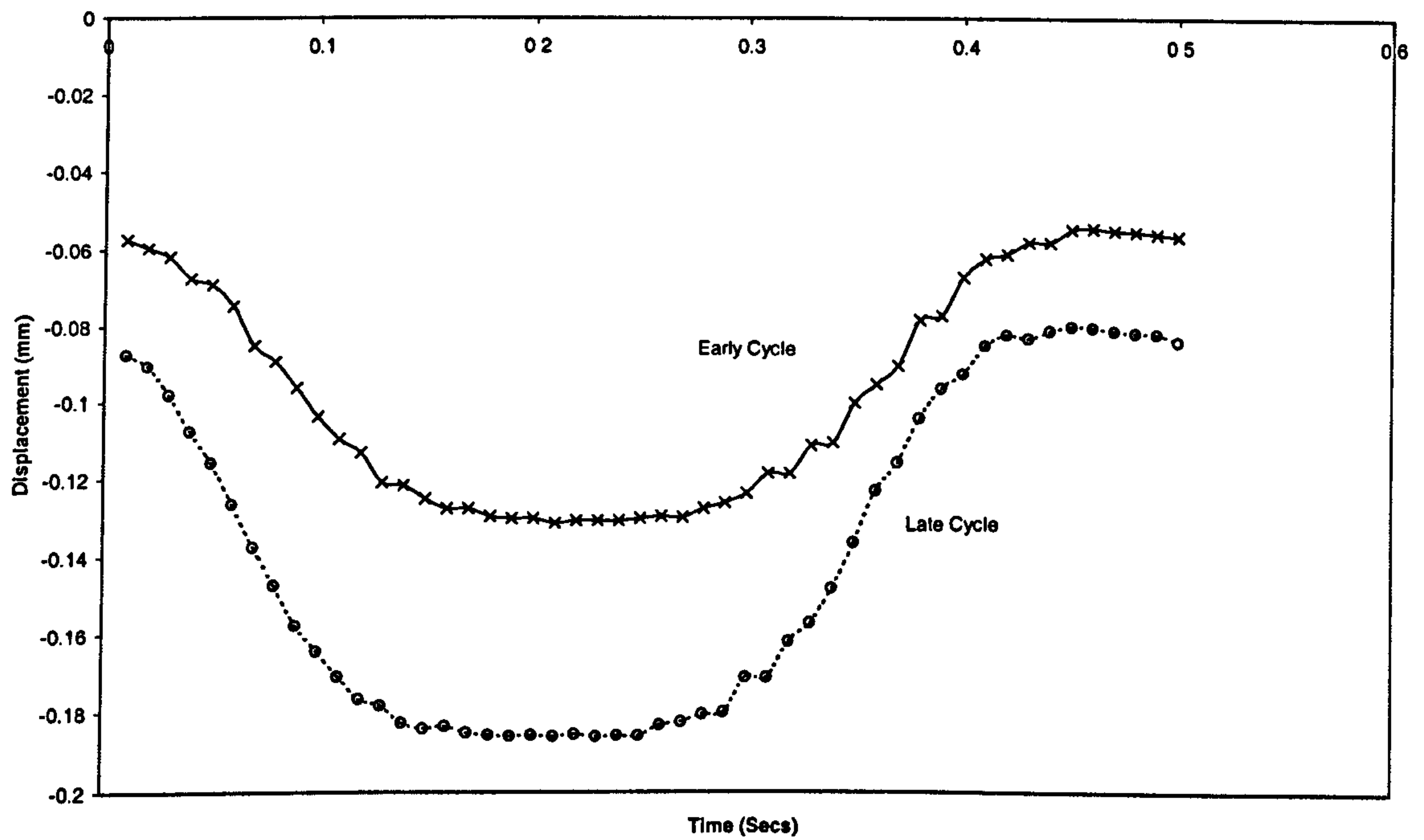


Figure 6.42a – Effect of deterioration on displacement resistance (30kg/m³ steel fibre with 1.98mm crack width)

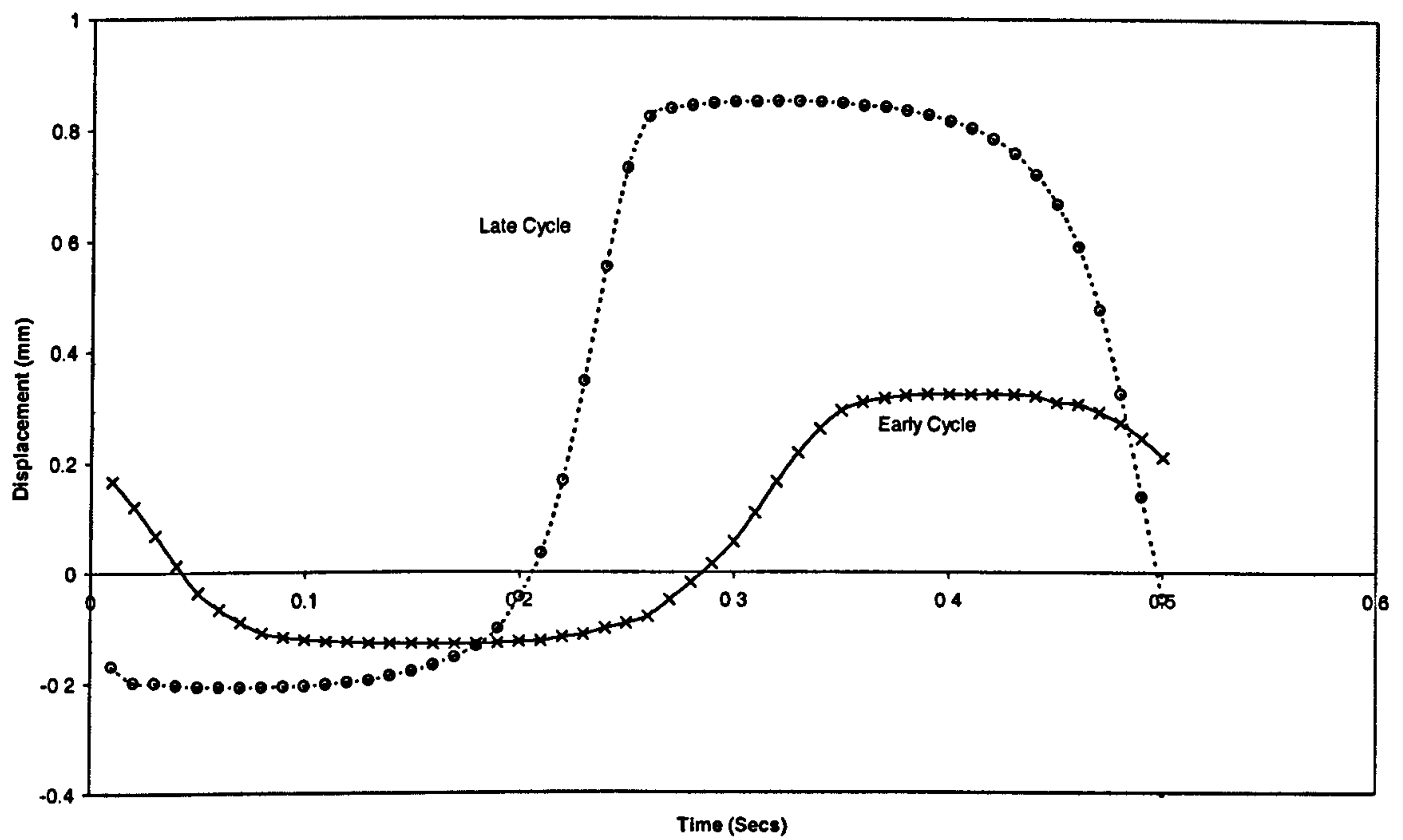


Figure 6.42b – Effect of deterioration on displacement resistance (30kg/m³ steel fibre with 5.94mm crack width)

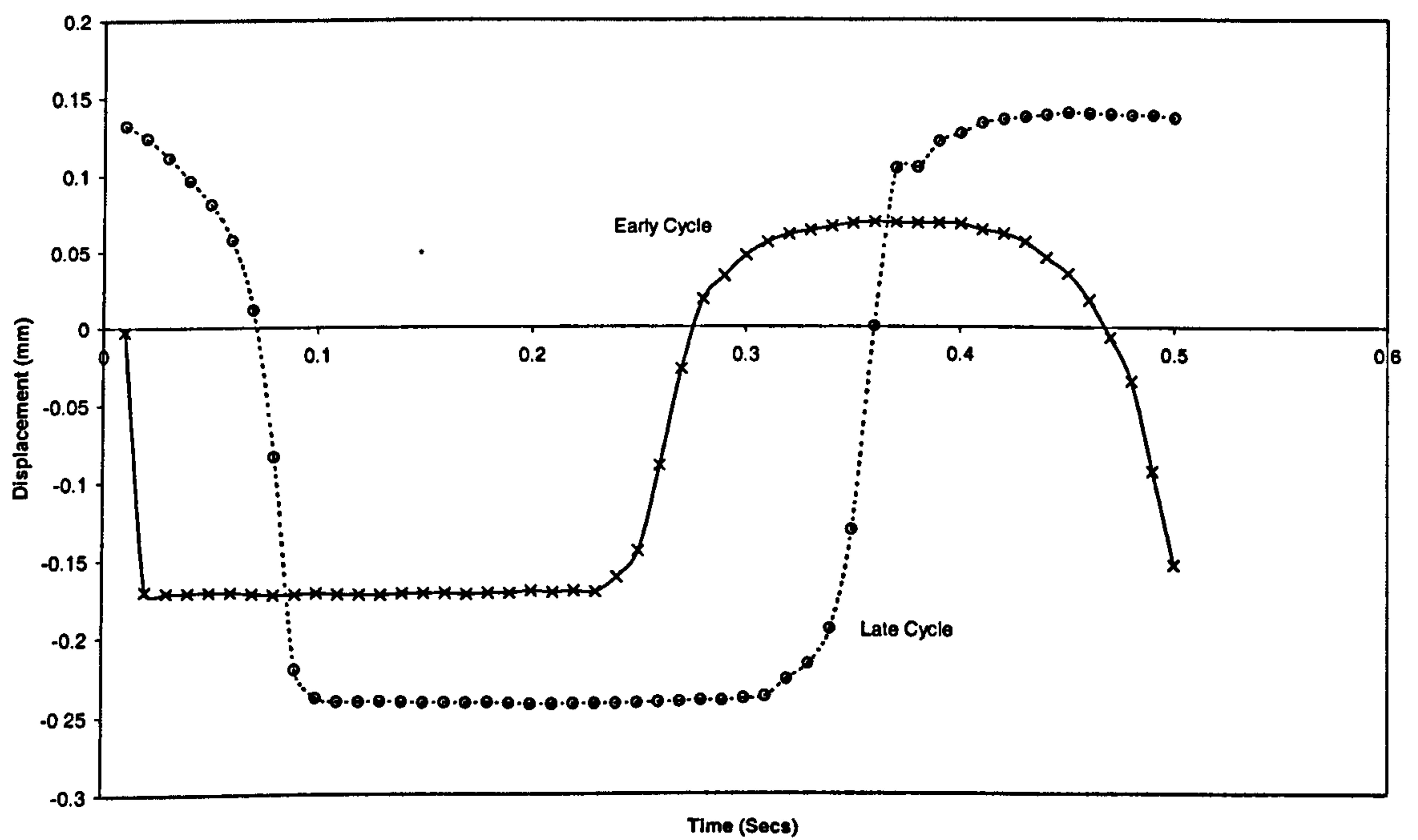


Figure 6.43a – Effect of deterioration on displacement resistance (non-reinforced with 0.66mm crack width)

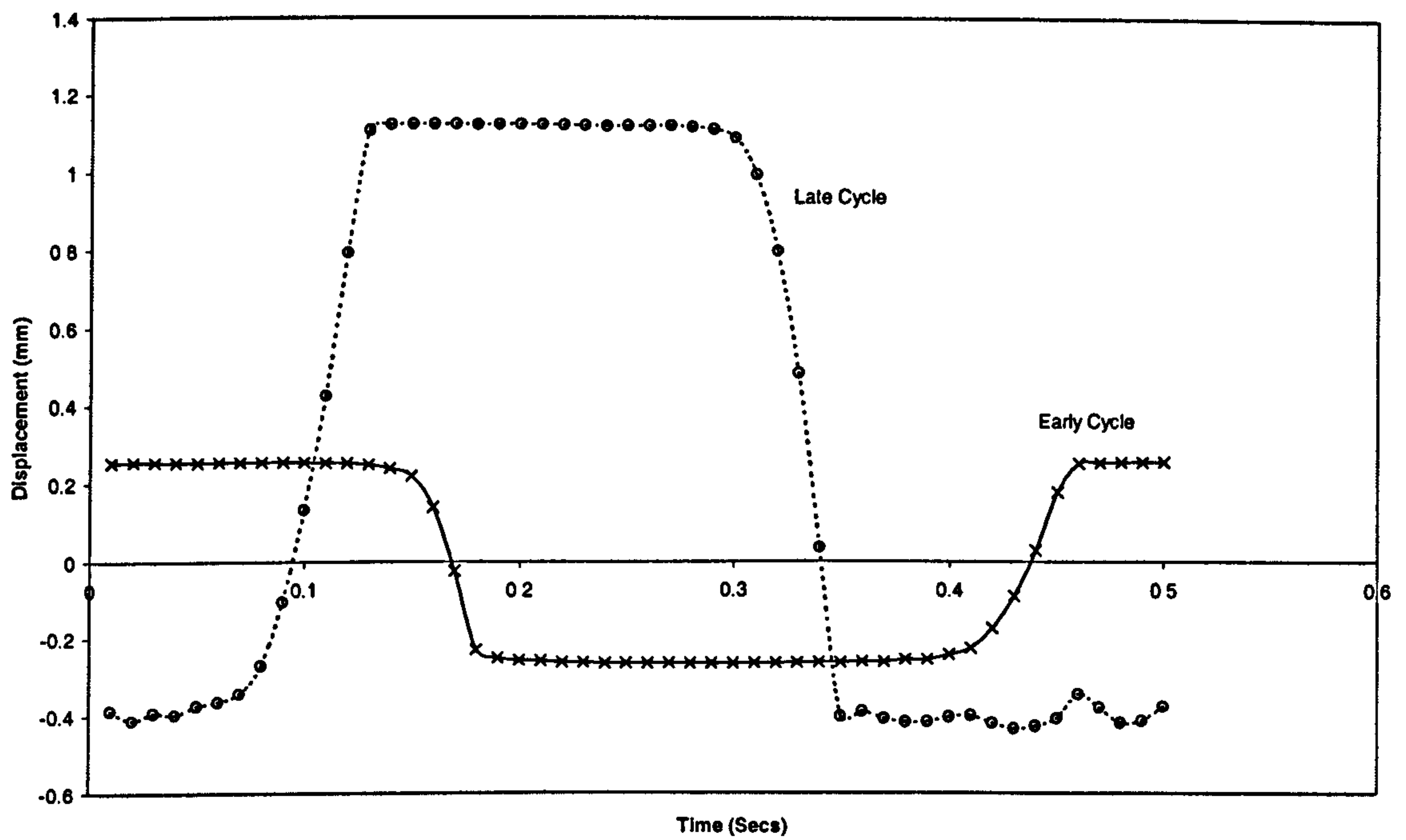


Figure 6.43b – Effect of deterioration on displacement resistance (non-reinforced with 1.98mm crack width)

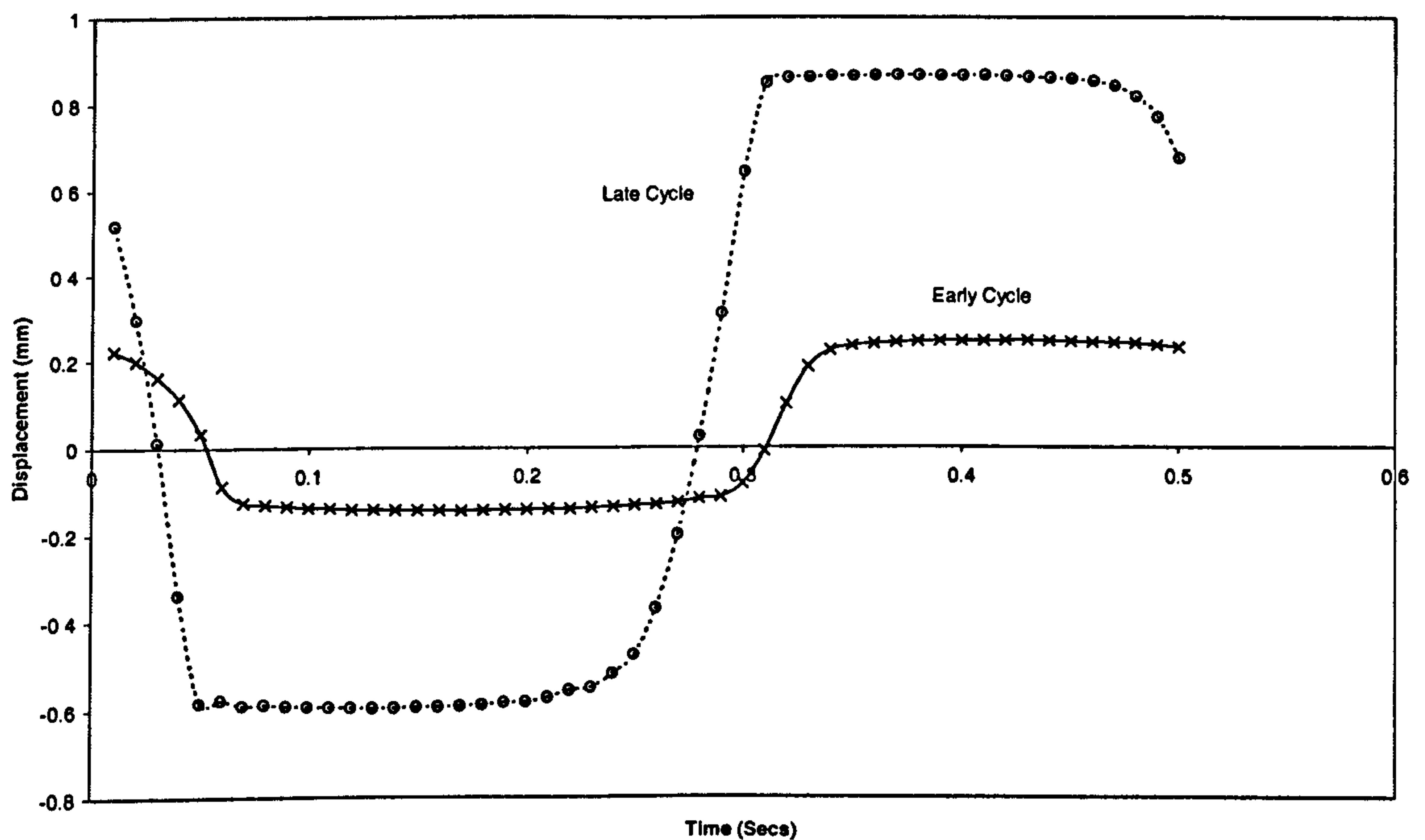


Figure 6.44 – Effect of deterioration on displacement resistance (mortar with 0.66mm crack width)

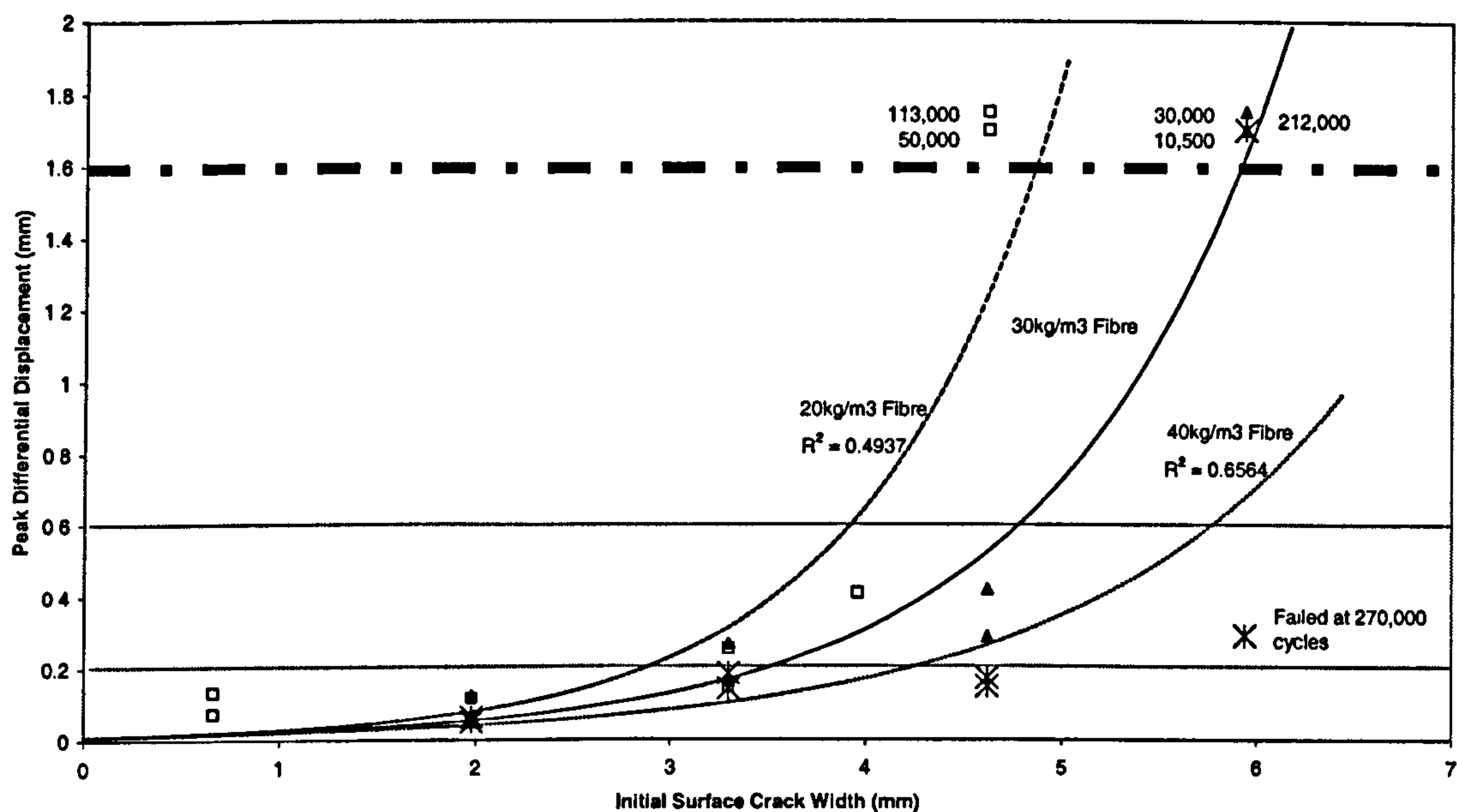


Figure 6.45 – Effect of steel fibre quantity on differential displacement

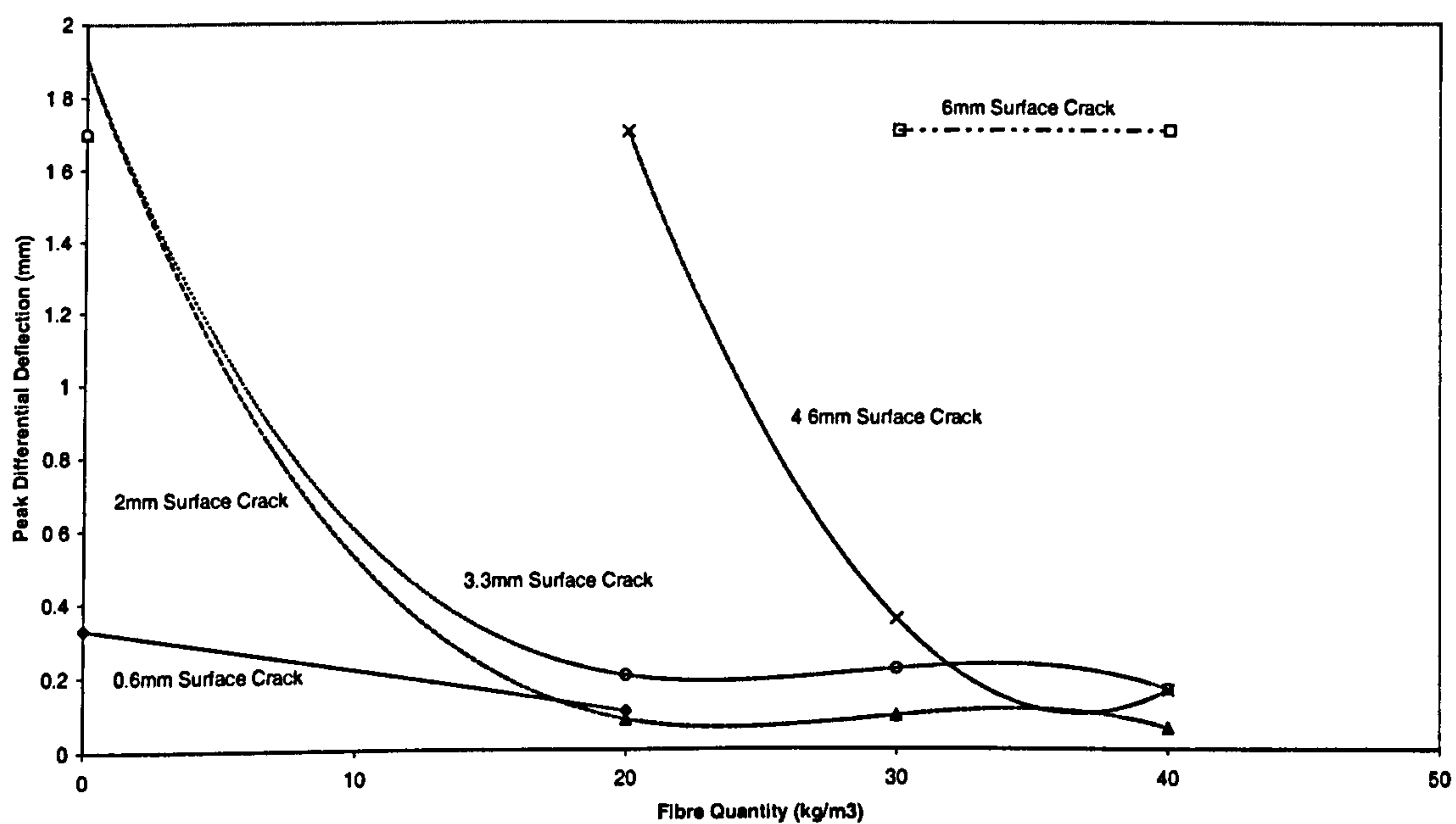


Figure 6.46 – Effectiveness of fibre quantity in resistance to displacement

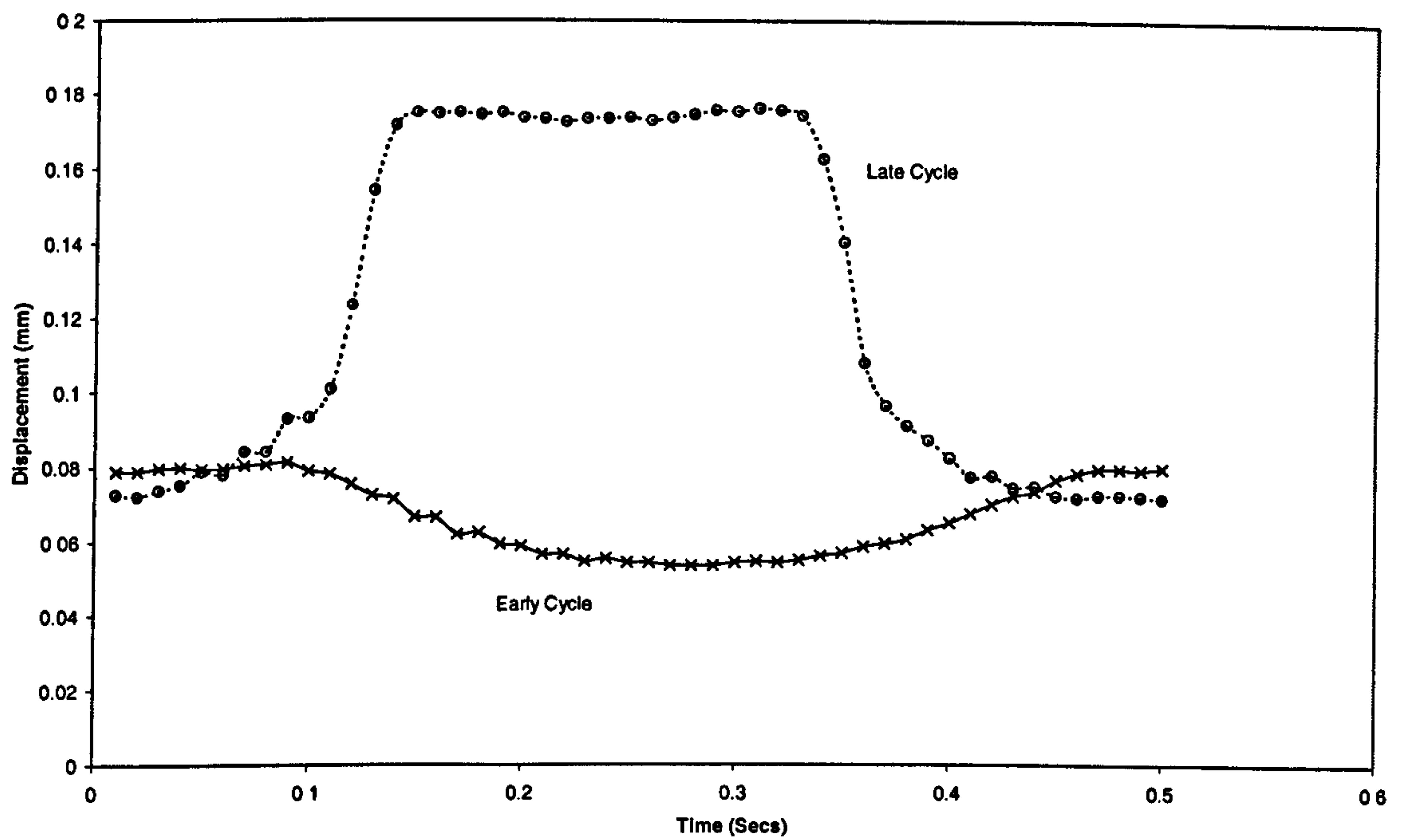


Figure 6.47a – Effect of deterioration on displacement resistance (20kg/m³ steel fibre with 0.66mm crack width)

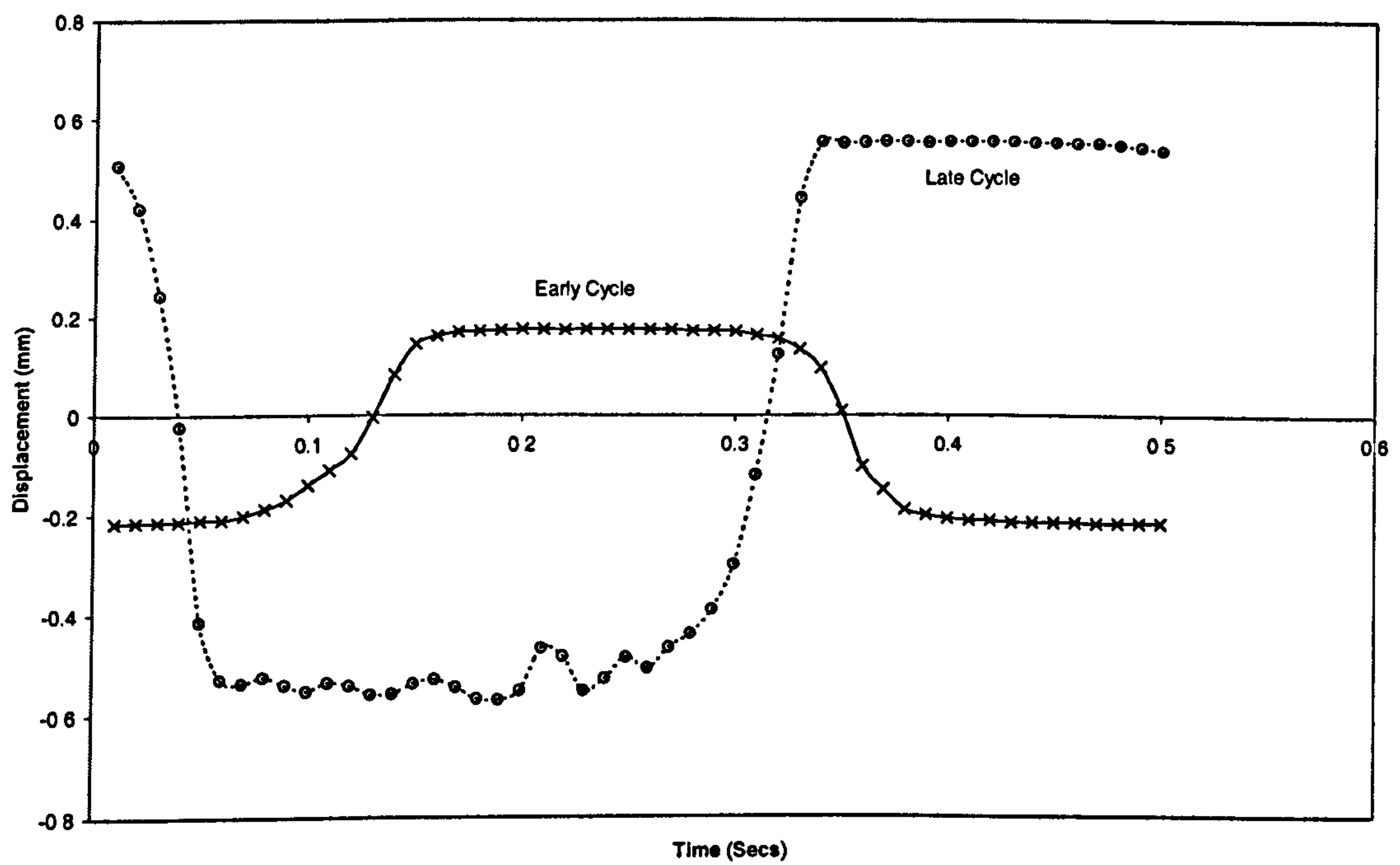


Figure 6.47b – Effect of deterioration on displacement resistance (20kg/m³ steel fibre with 4.62mm crack width)

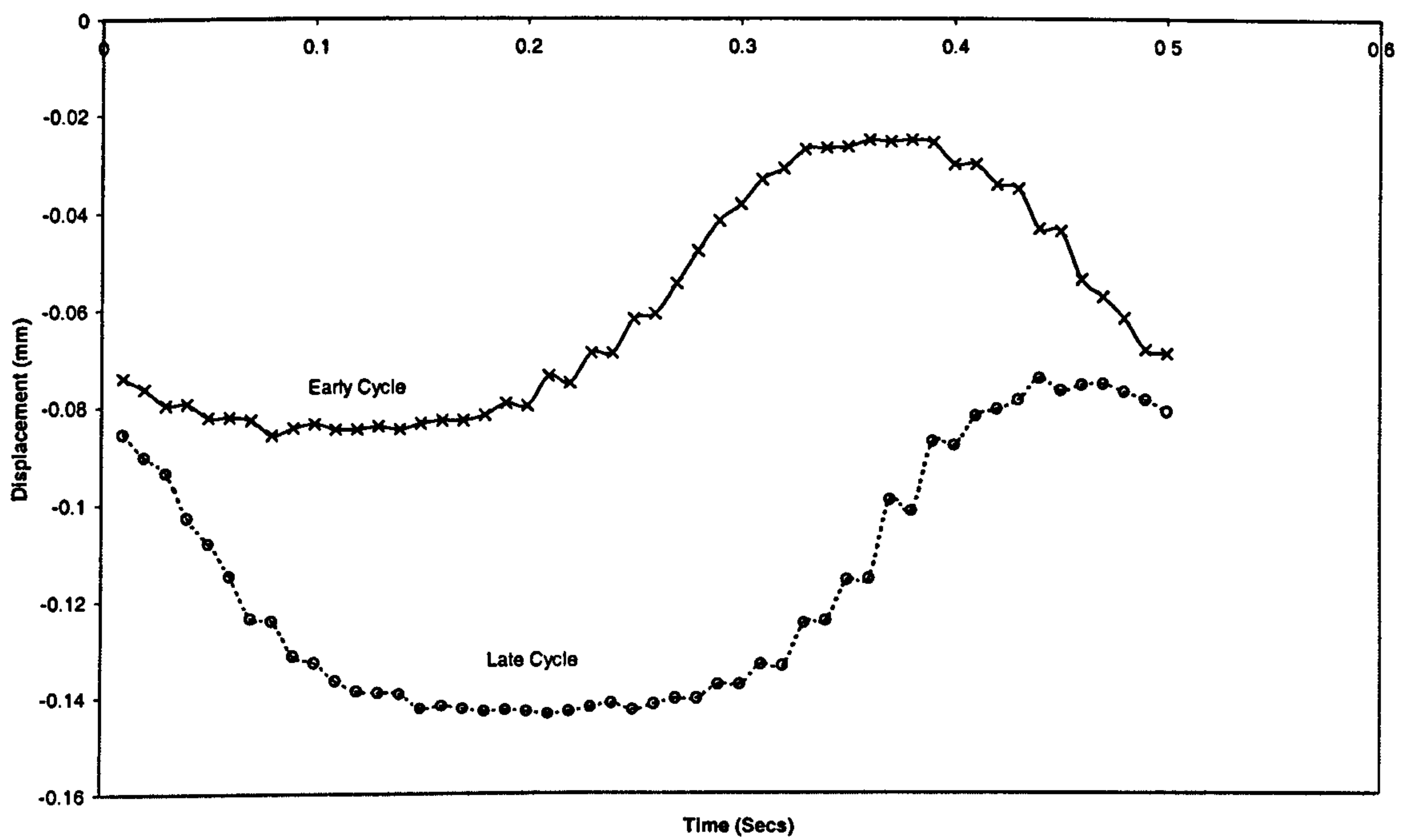


Figure 6.48a – Effect of deterioration on displacement resistance (40kg/m³ steel fibre with 1.98mm crack width)

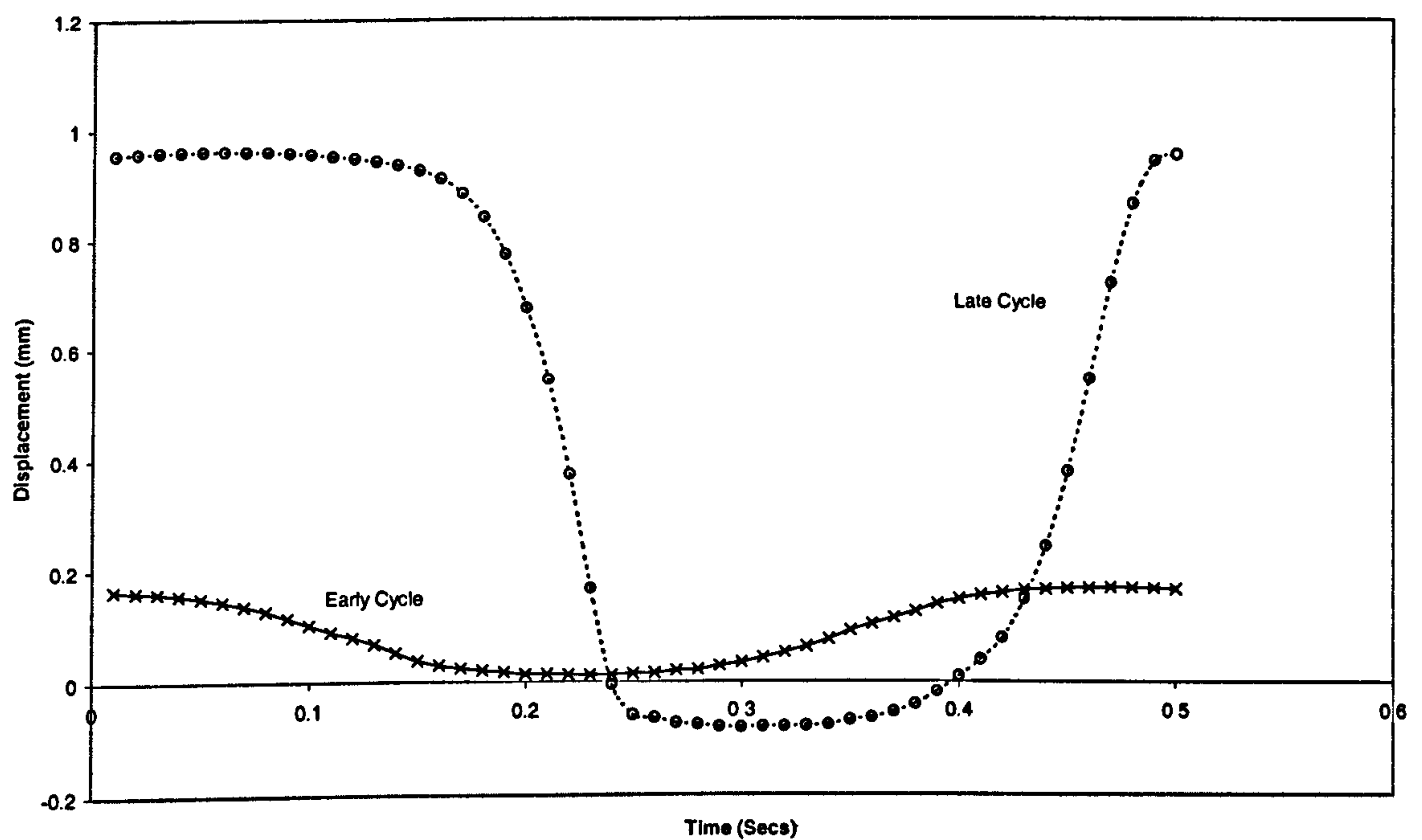


Figure 6.48b – Effect of deterioration on displacement resistance (40kg/m³ steel fibre with 5.94mm crack width)

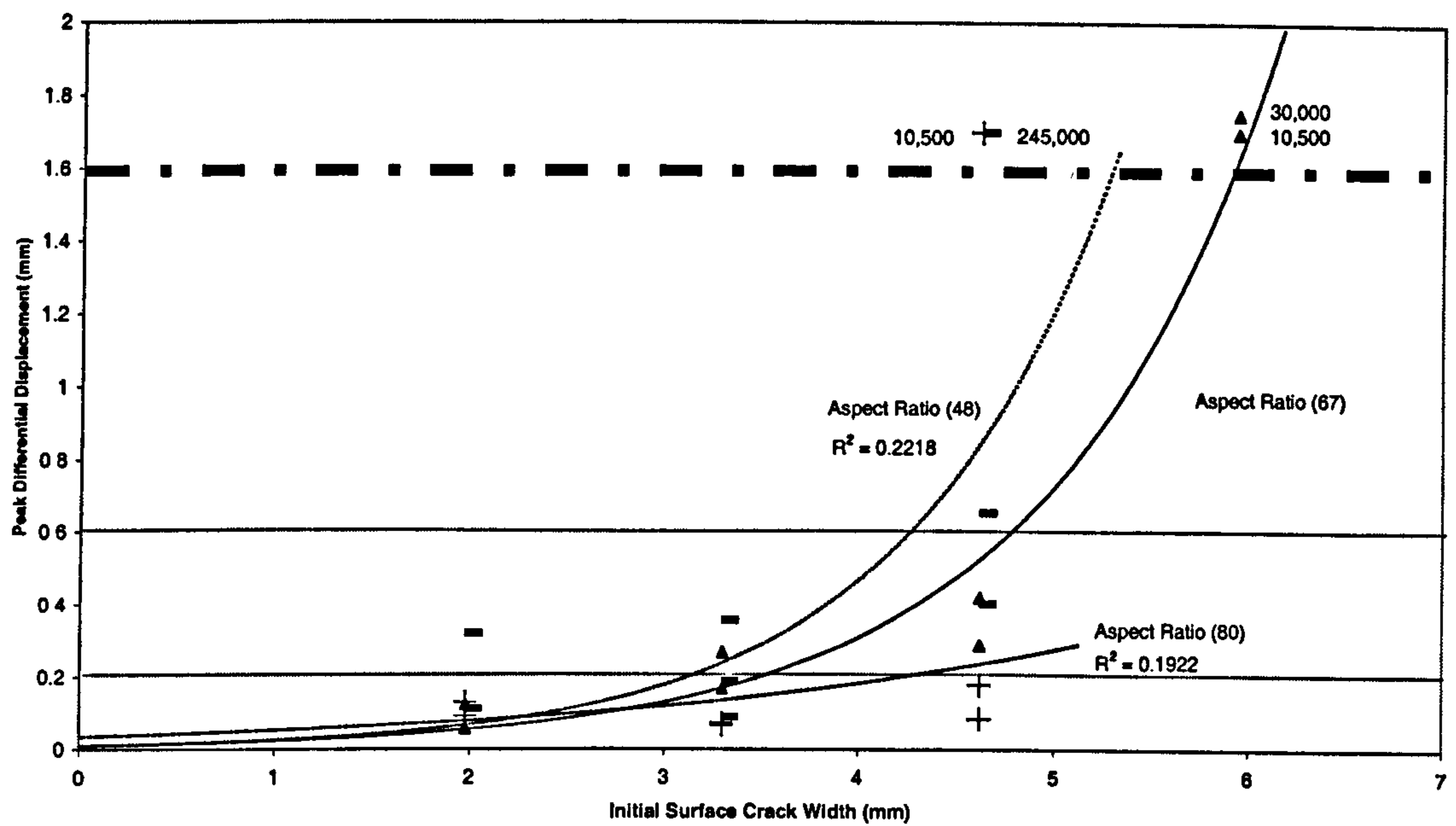


Figure 6.49 – Effect of steel fibre aspect ratio on differential displacement

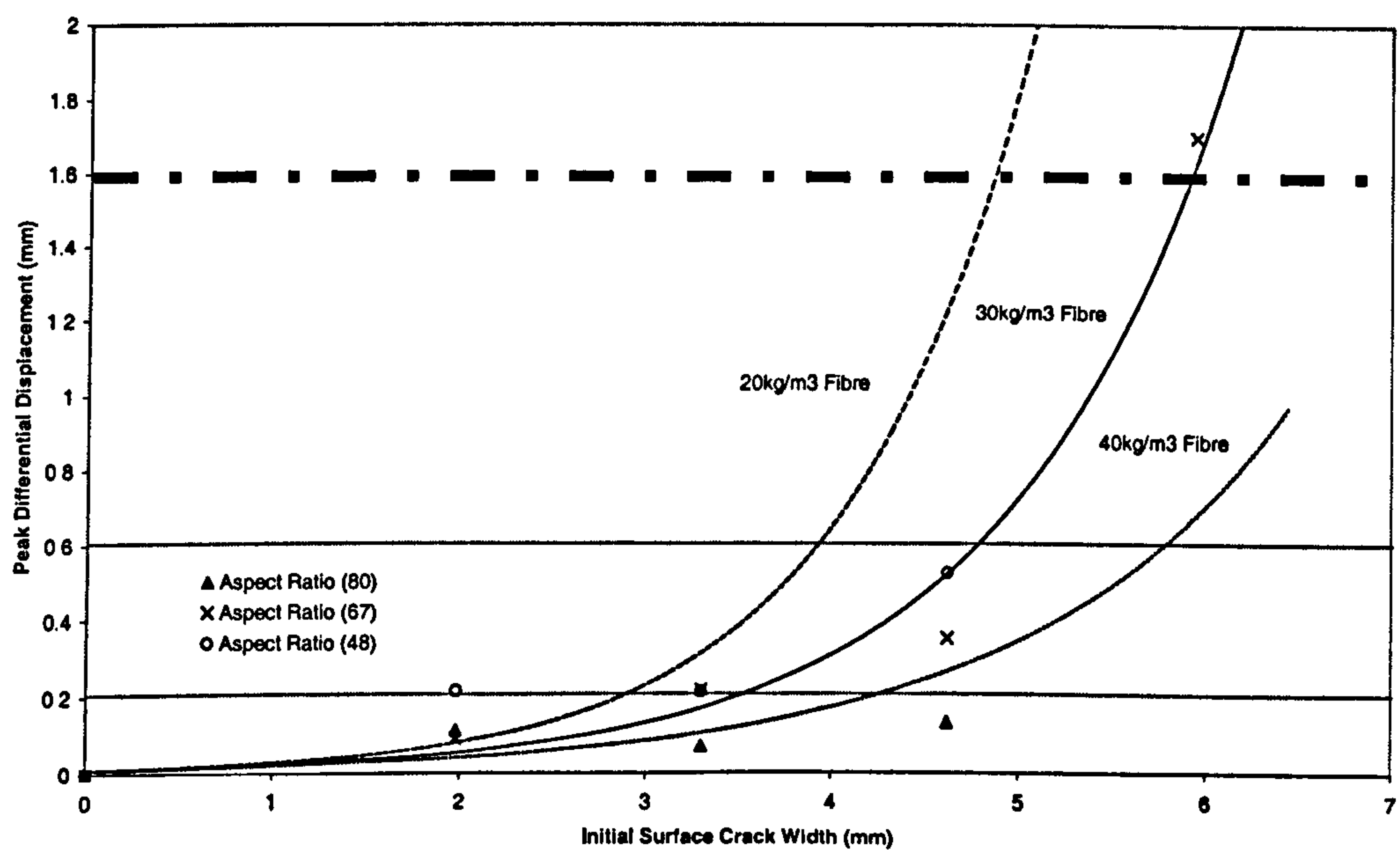


Figure 6.50 – Comparison between steel fibre aspect ratios and steel fibre quantities

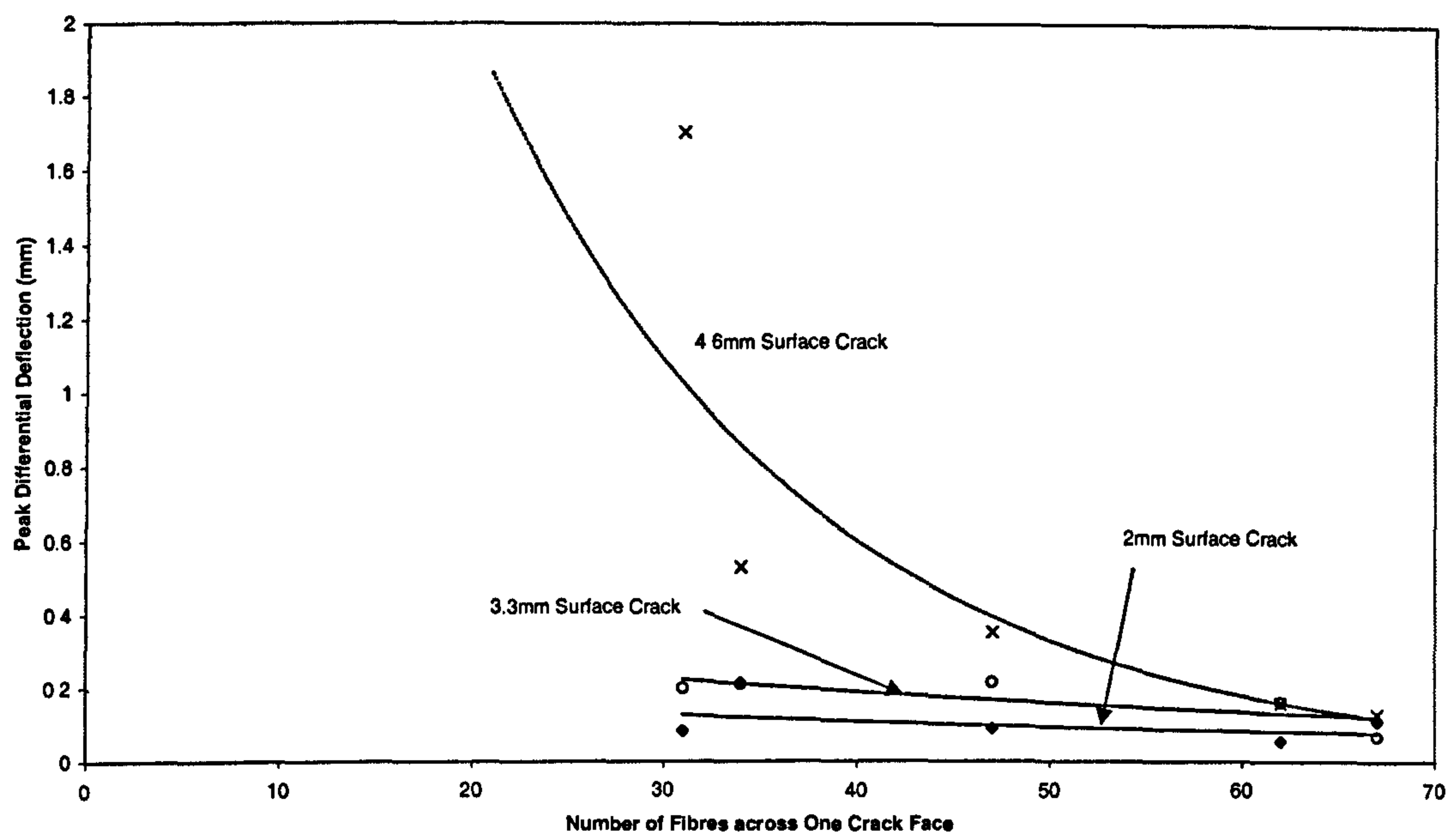


Figure 6.51 – Effect of crack face fibre count on resistance to deflection

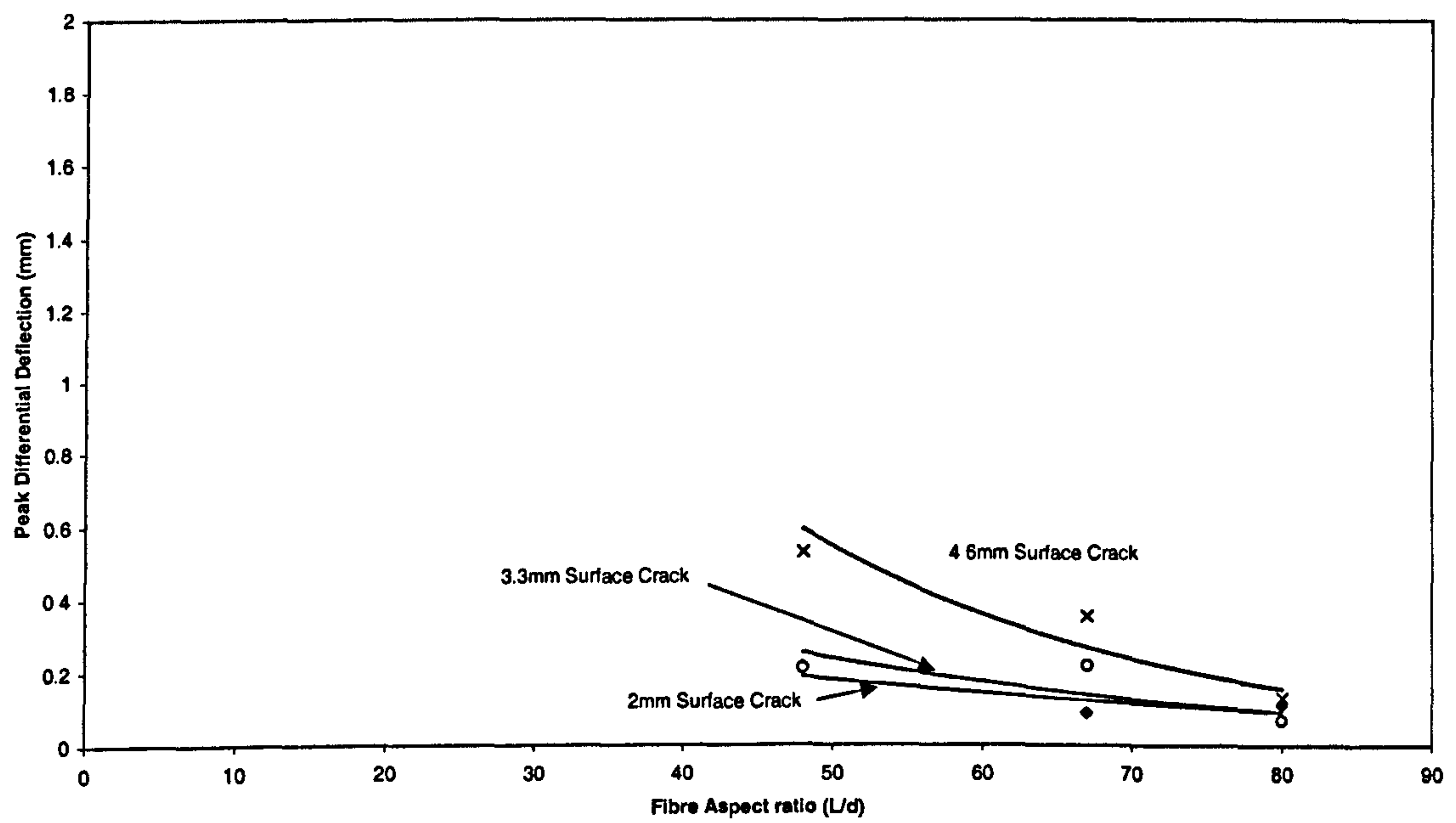


Figure 6.52 – Effectiveness of aspect ratio in resistance to displacement

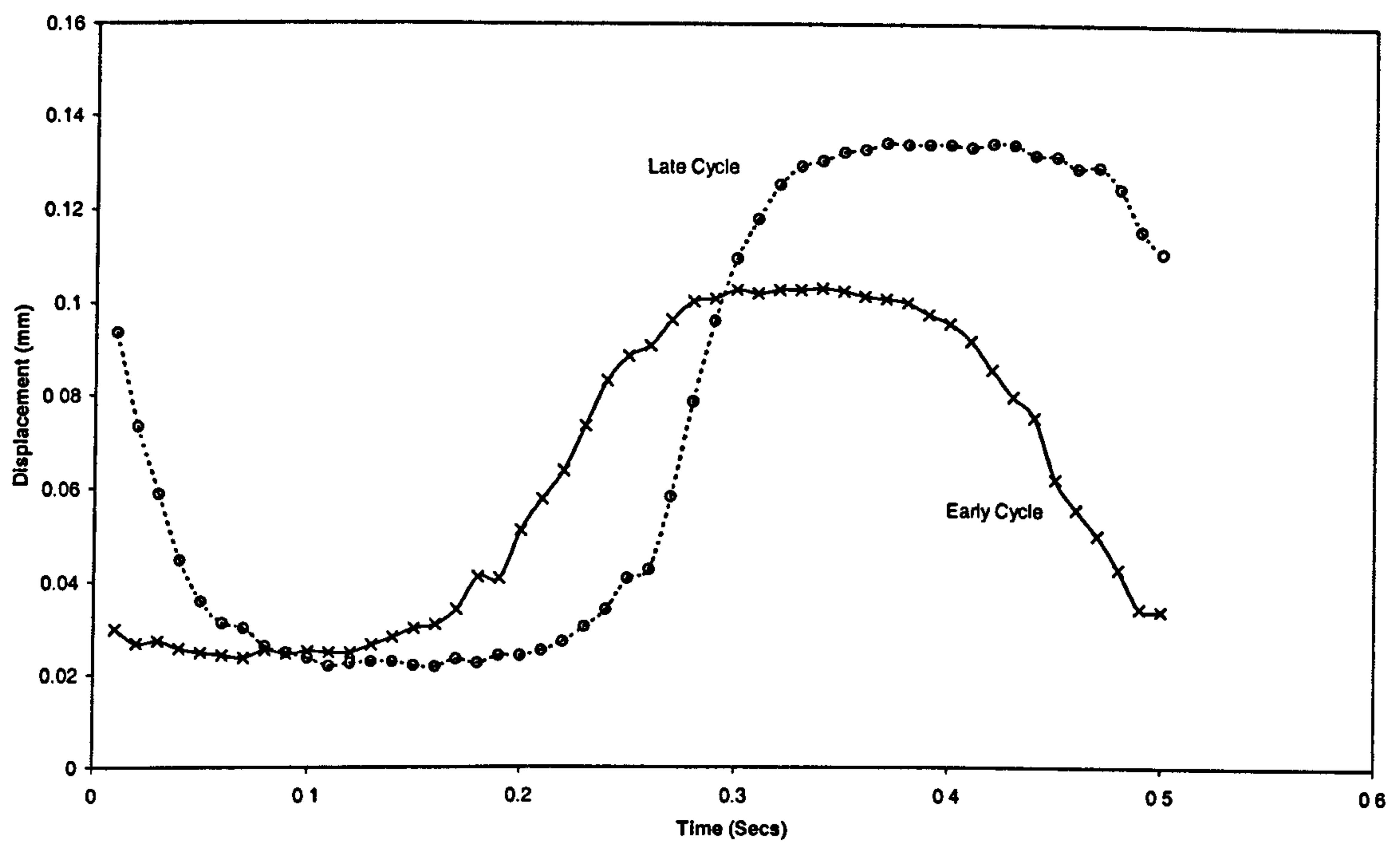


Figure 6.53a – Effect of deterioration on displacement resistance (steel fibre of aspect ratio 80 with 1.98mm crack width)

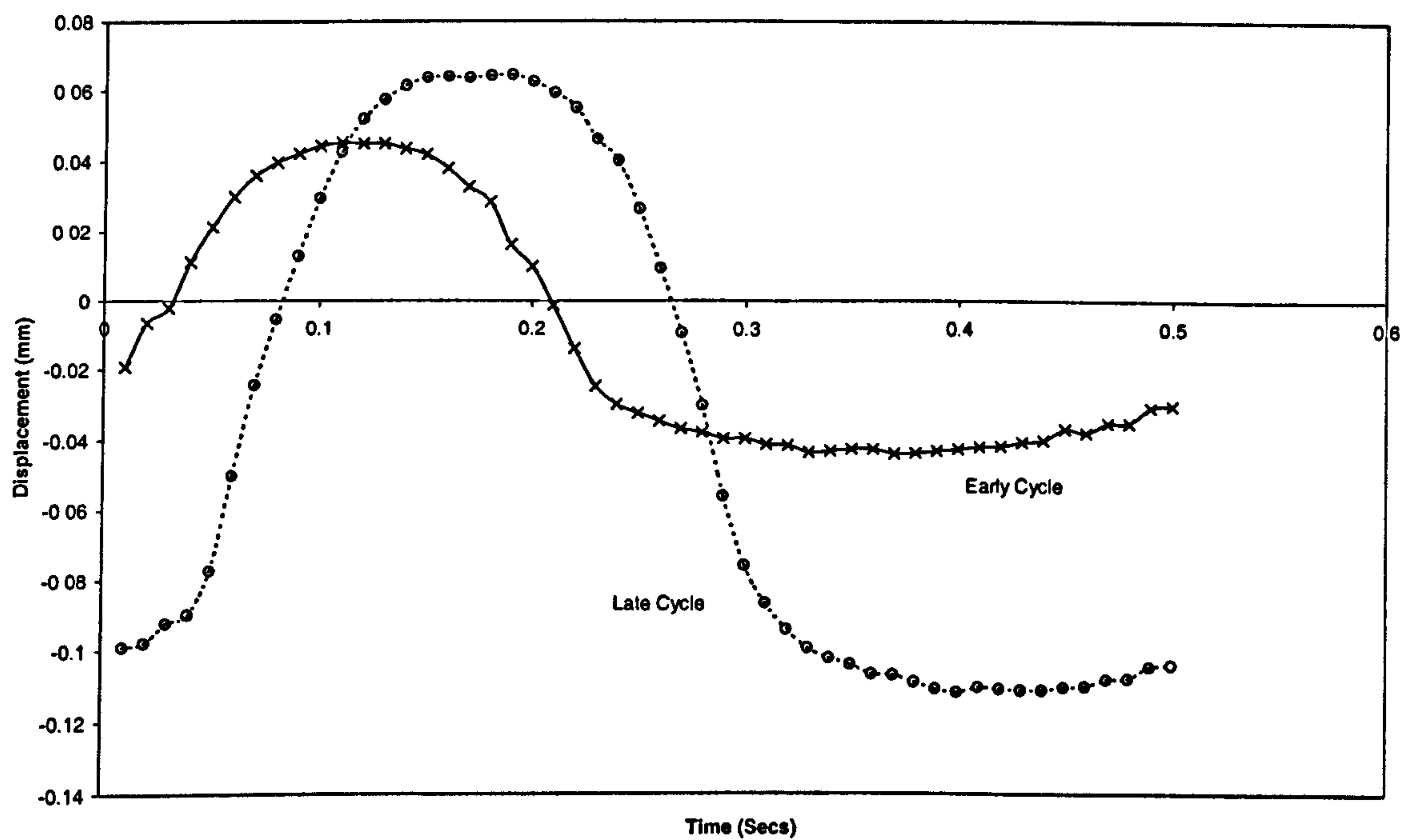


Figure 6.53b – Effect of deterioration on displacement resistance (steel fibre of aspect ratio 80 with 4.62mm crack width)

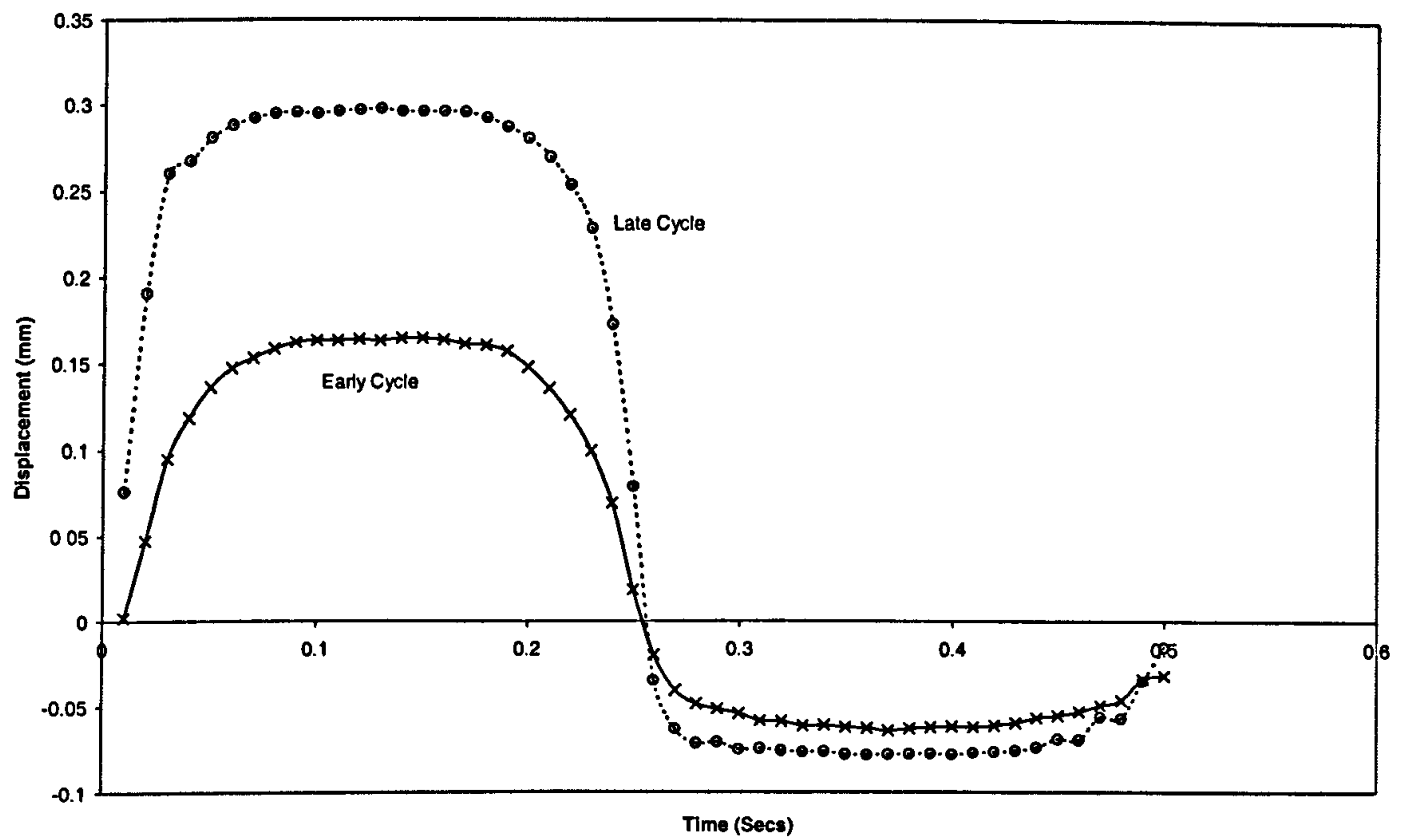


Figure 6.54a – Effect of deterioration on displacement resistance (steel fibre of aspect ratio 48 with 1.98mm crack width)

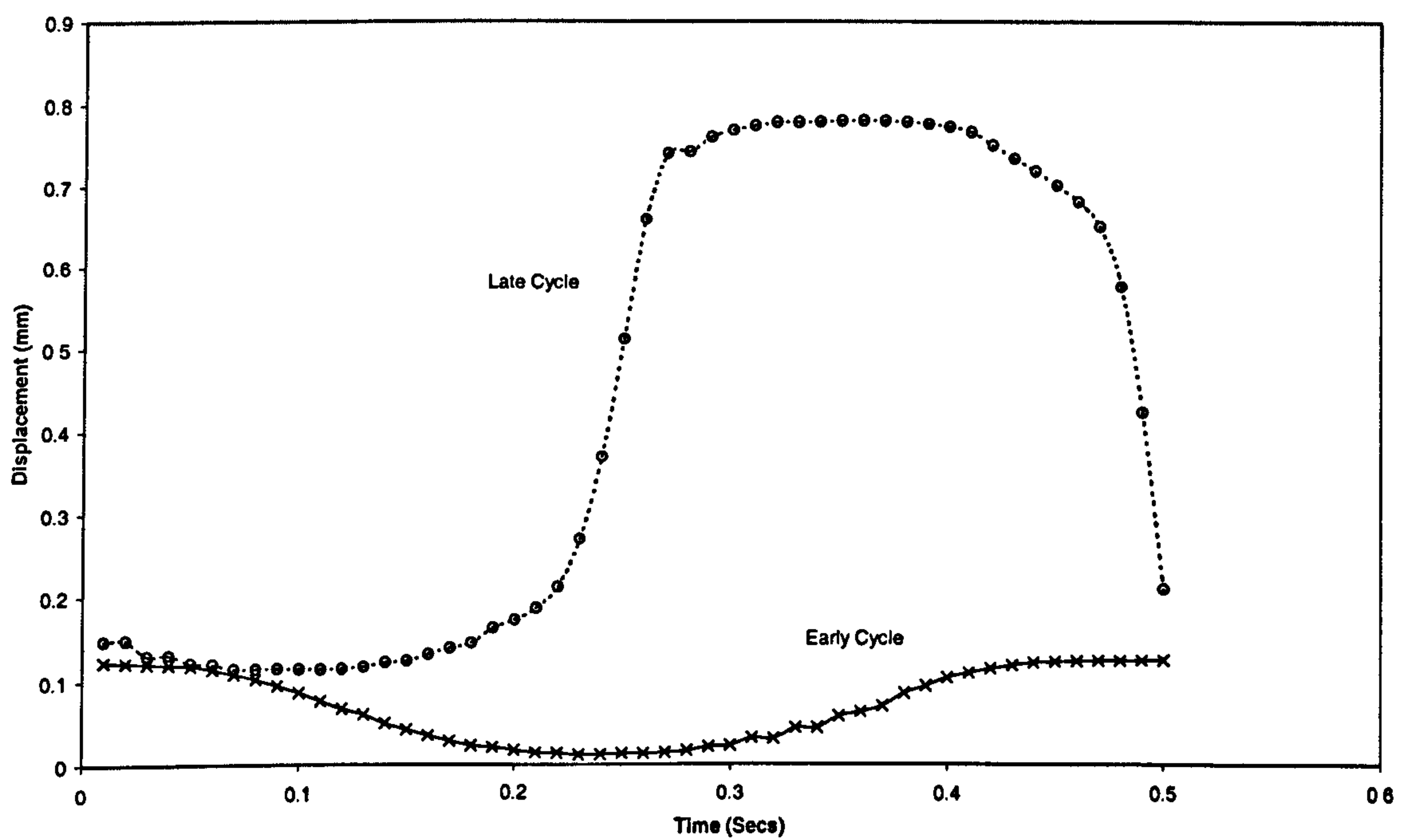


Figure 6.54b – Effect of deterioration on displacement resistance (steel fibre of aspect ratio 48 with 4.62mm crack width)

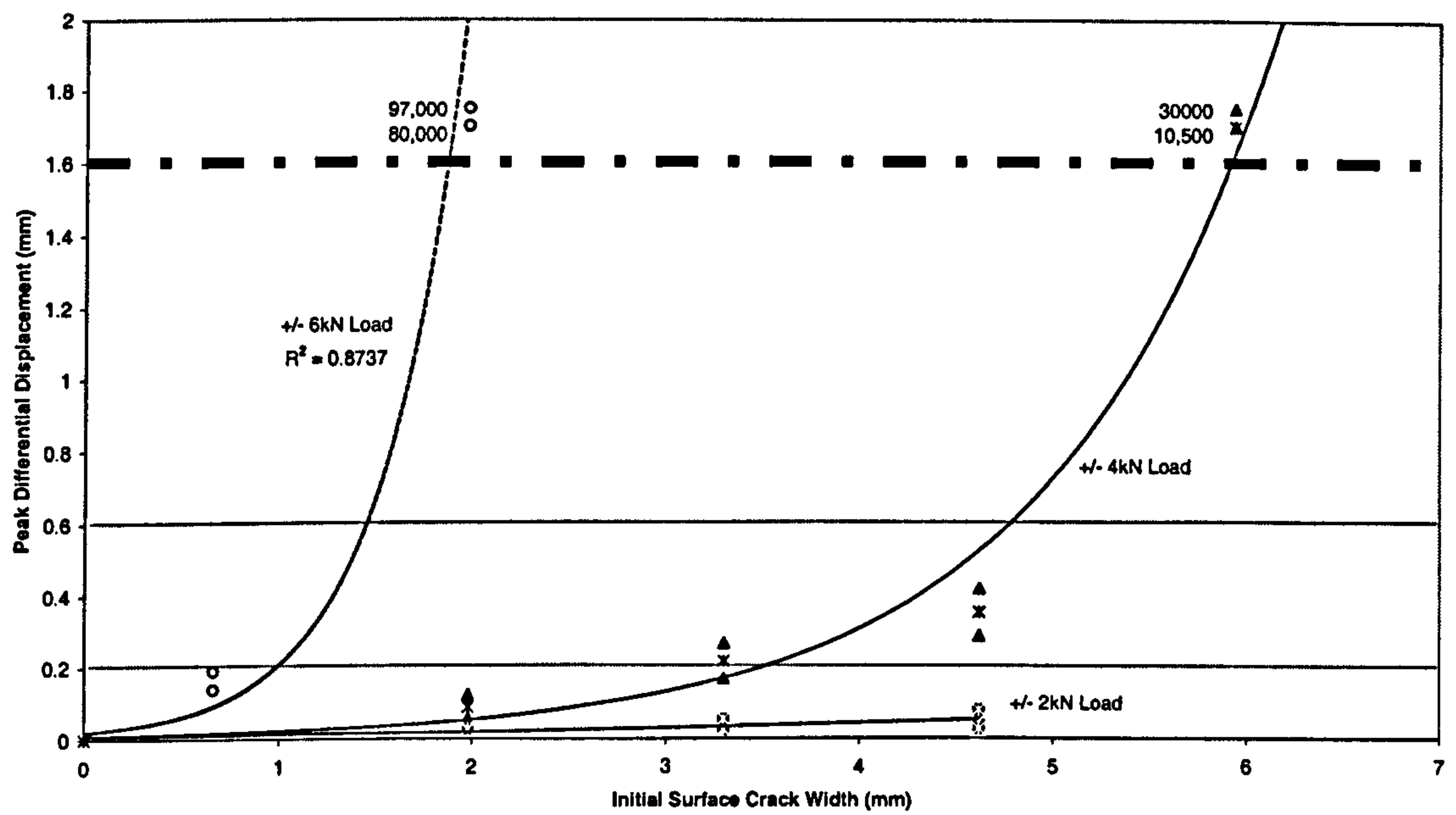


Figure 6.55 – Effect of load magnitude on differential displacement

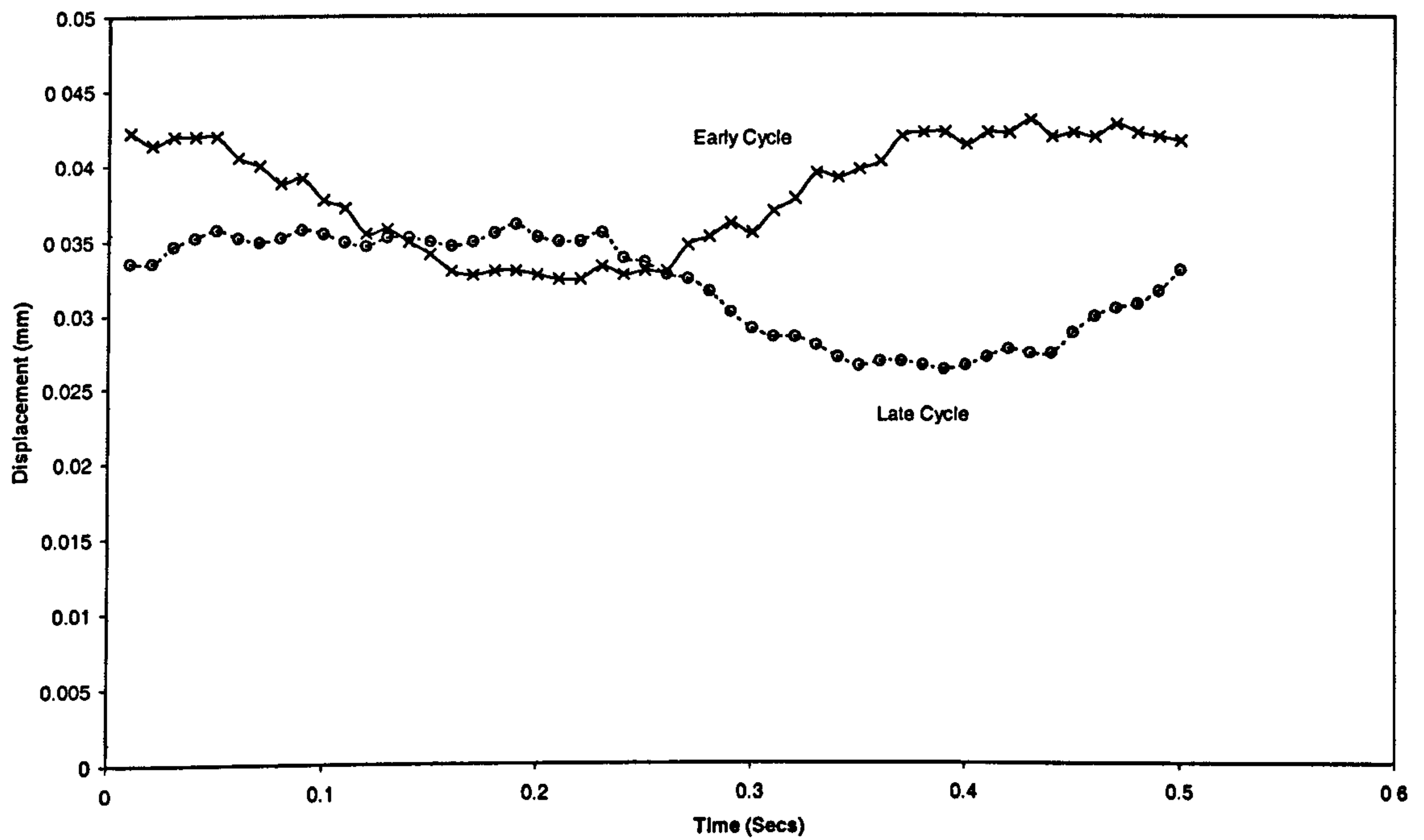


Figure 6.56a – Effect of deterioration on displacement resistance (load magnitude of 2kN with 1.98mm crack width)

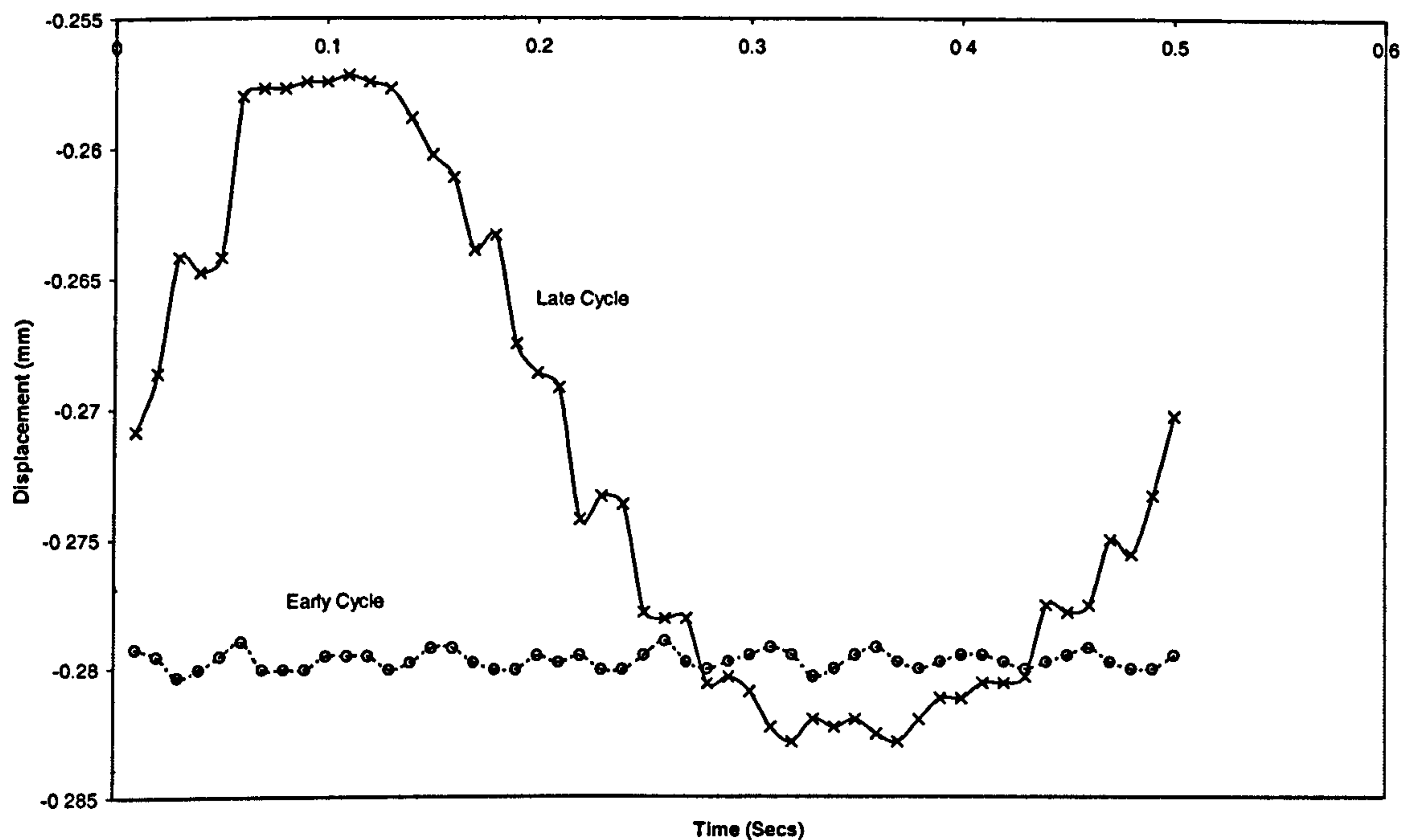


Figure 6.56b – Effect of deterioration on displacement resistance (load magnitude of 2kN with 4.62mm crack width)

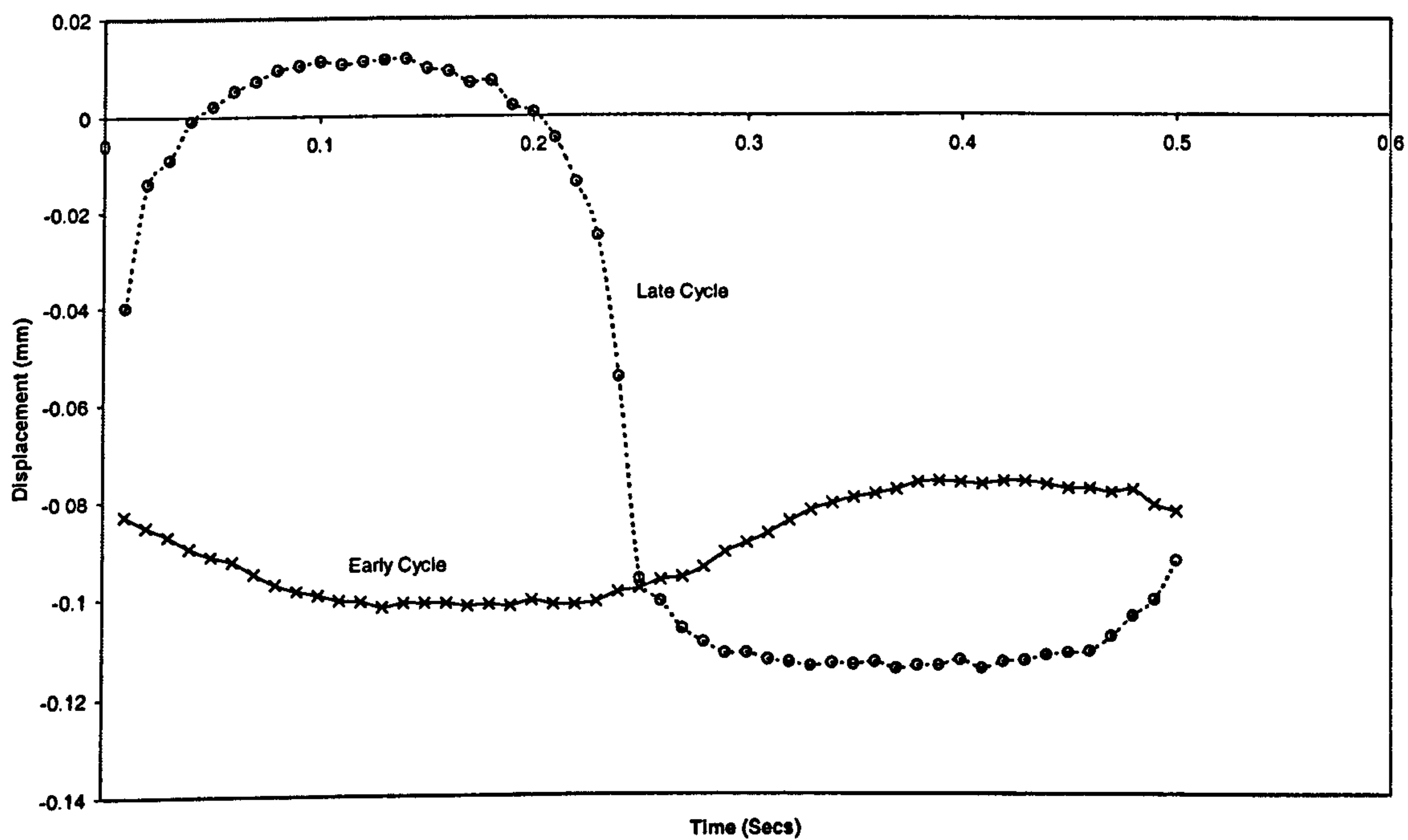


Figure 6.57a – Effect of deterioration on displacement resistance (load magnitude of 6kN with 0.66mm crack width)

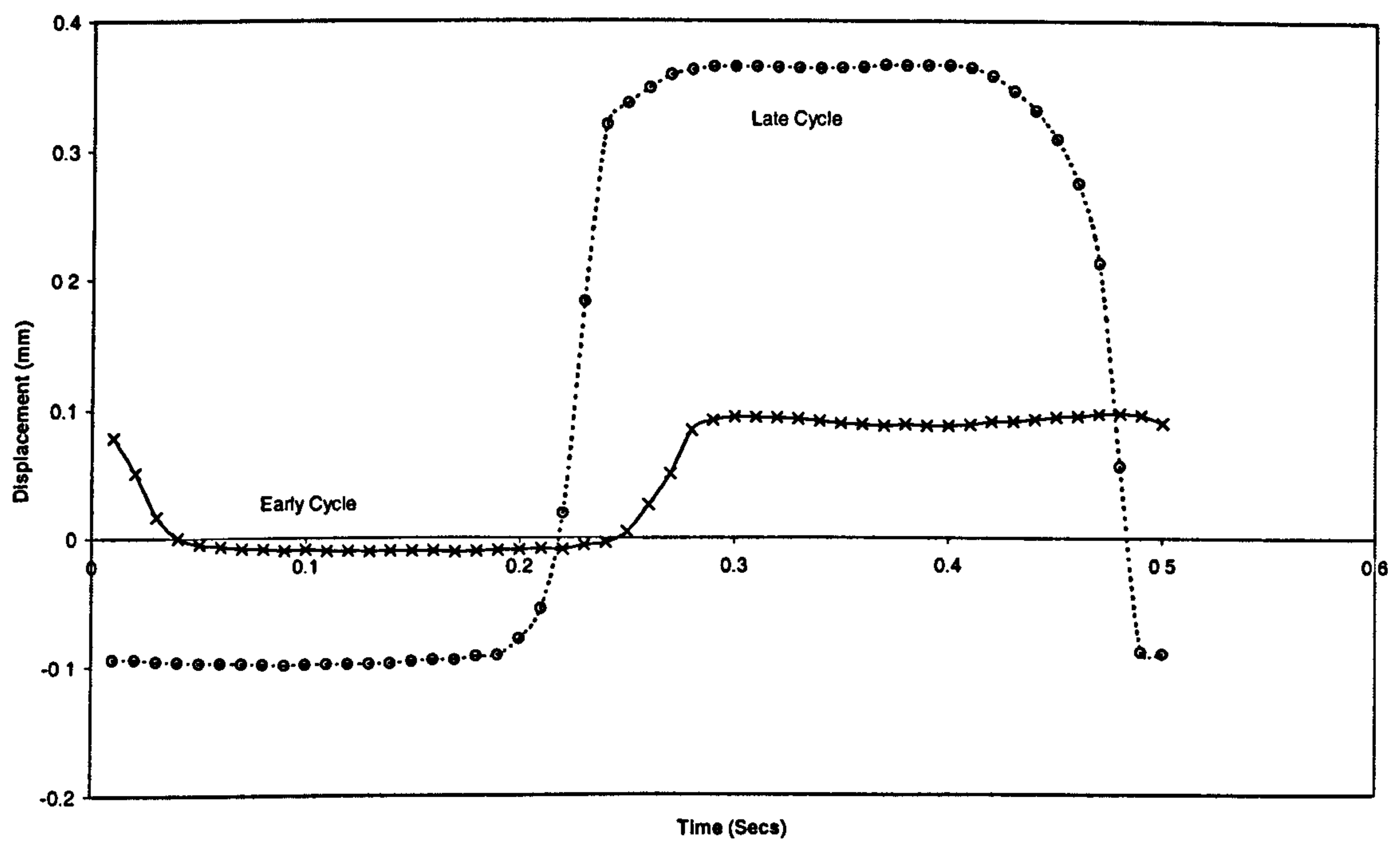


Figure 6.57b – Effect of deterioration on displacement resistance (load magnitude of 6kN with 1.98mm crack width)

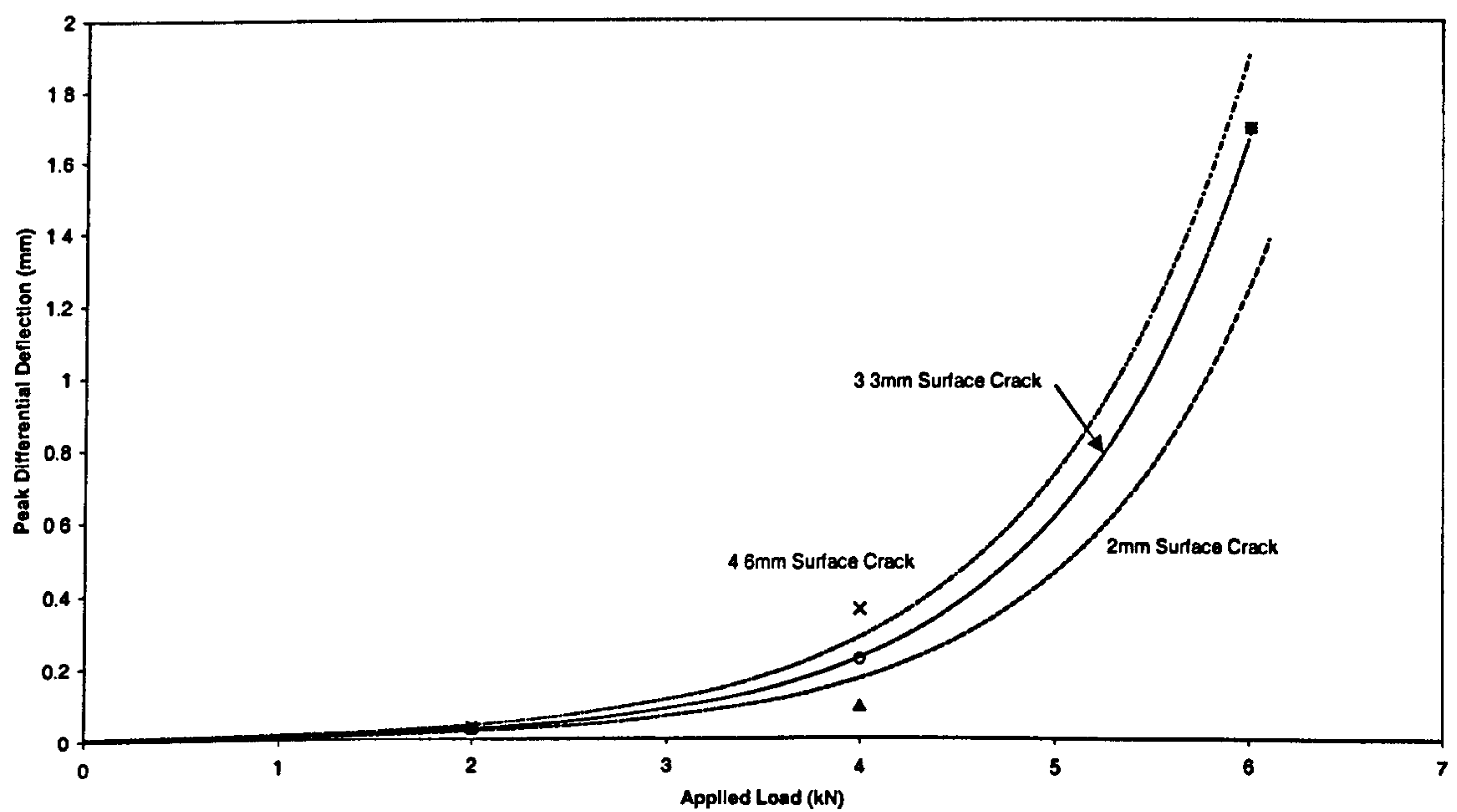


Figure 6.58 – Effect of load magnitude on displacement

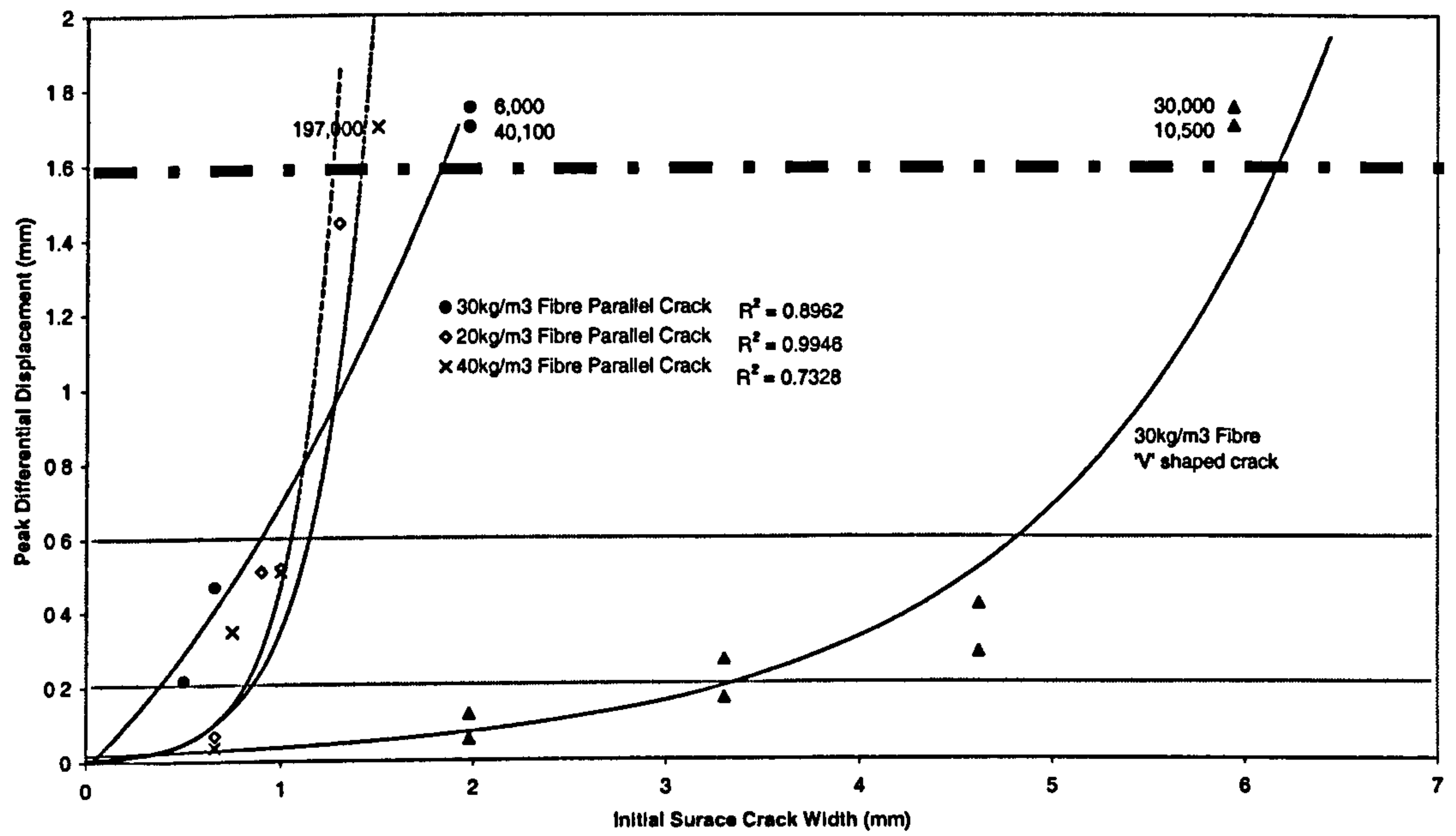


Figure 6.59 – Effect of crack profile on differential displacement

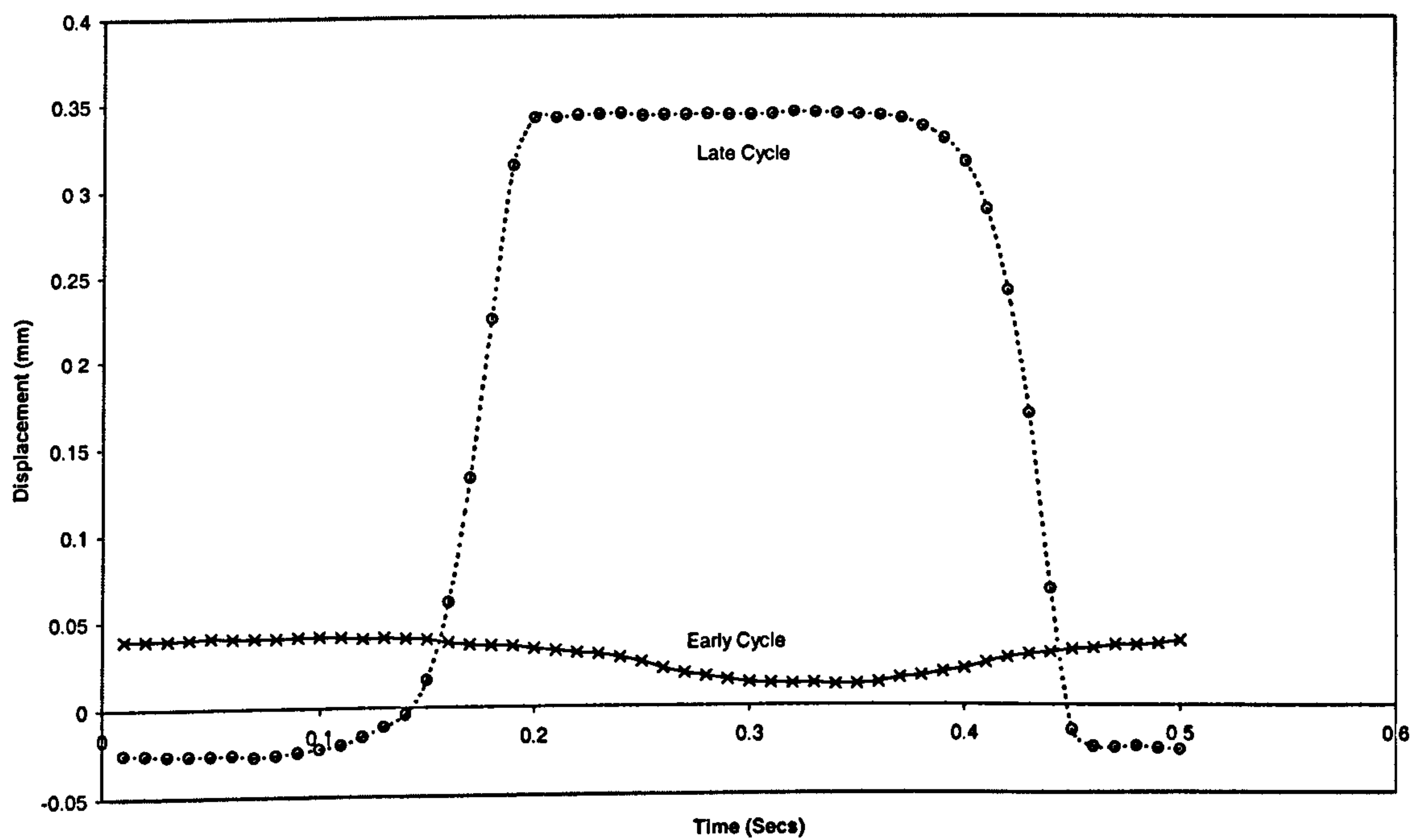


Figure 6.60a – Effect of deterioration on displacement resistance (Parallel crack of 0.66mm width)

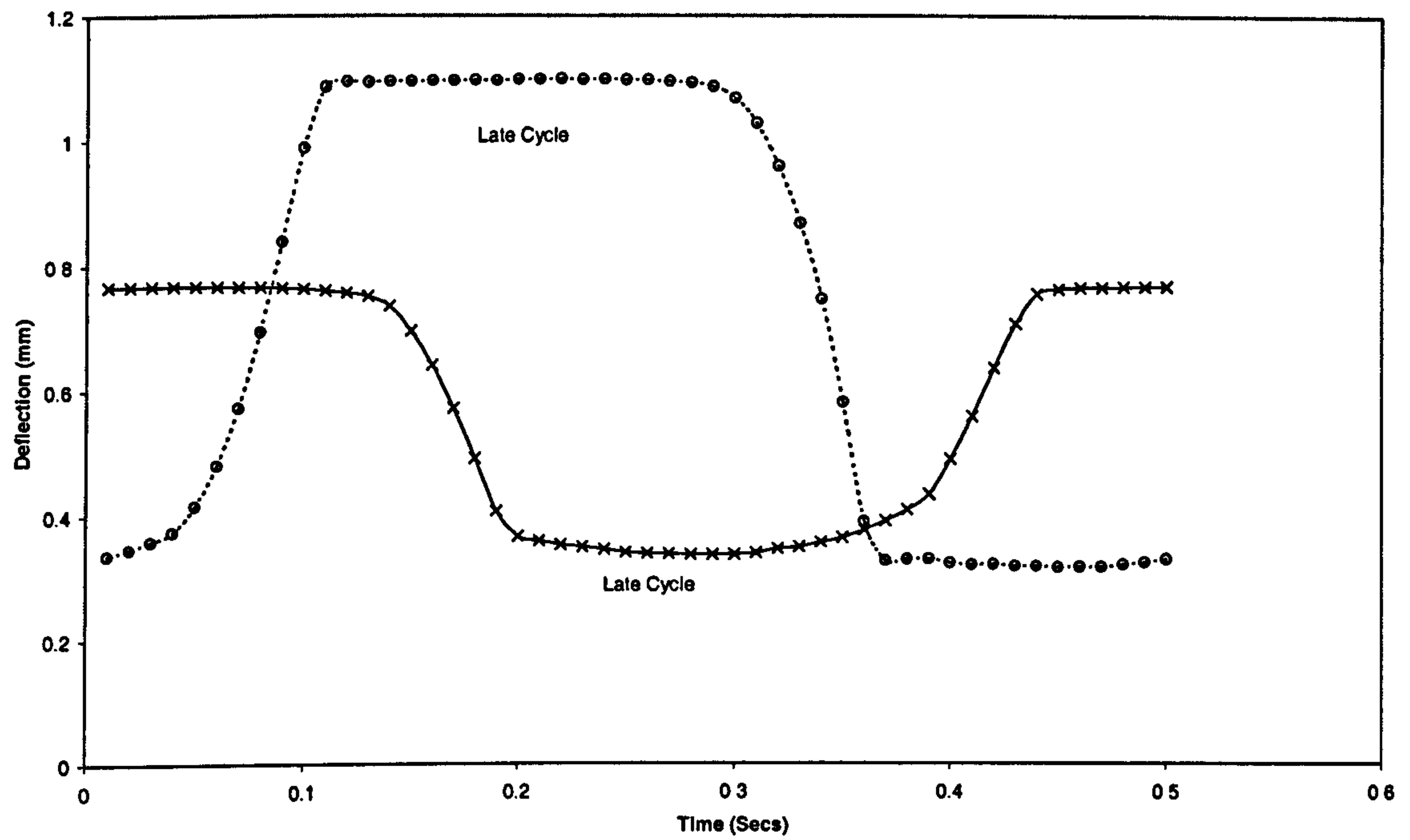


Figure 6.60b – Effect of deterioration on displacement resistance (Parallel crack of 1.98mm width)

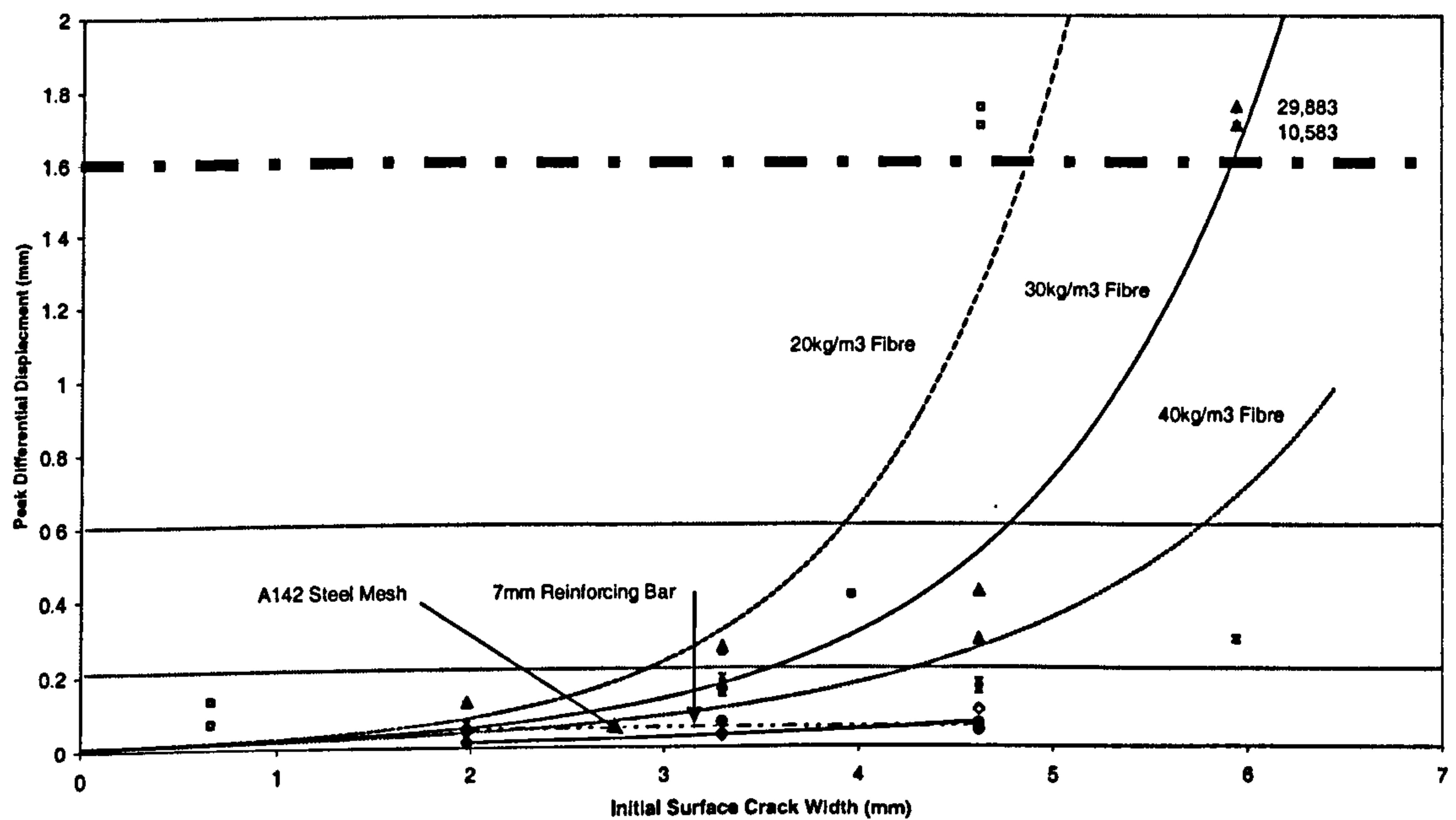


Figure 6.61 – Effect of steel fabric and reinforcing bar on displacement

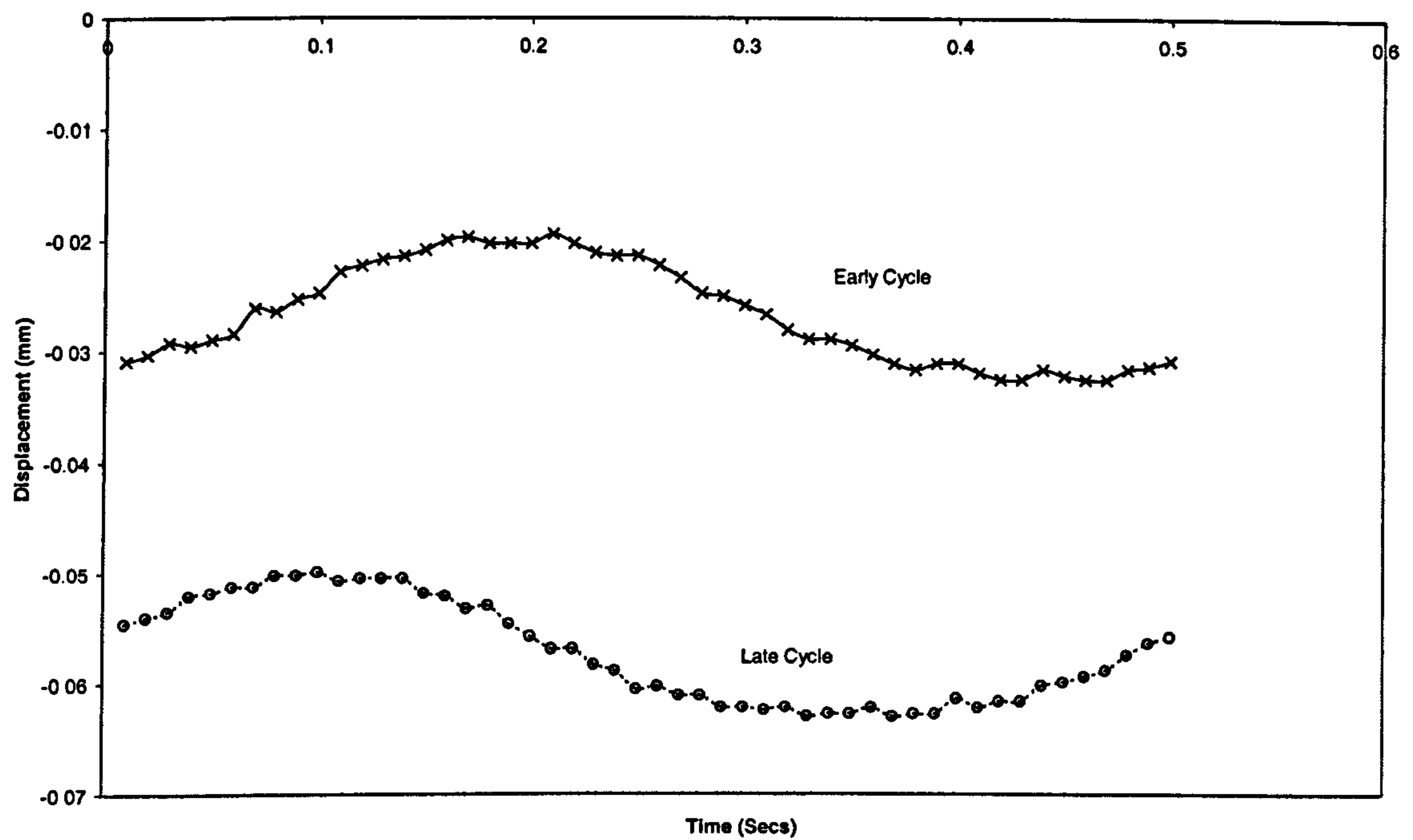


Figure 6.62a – Effect of deterioration on displacement resistance (steel fabric with 1.98mm crack width)

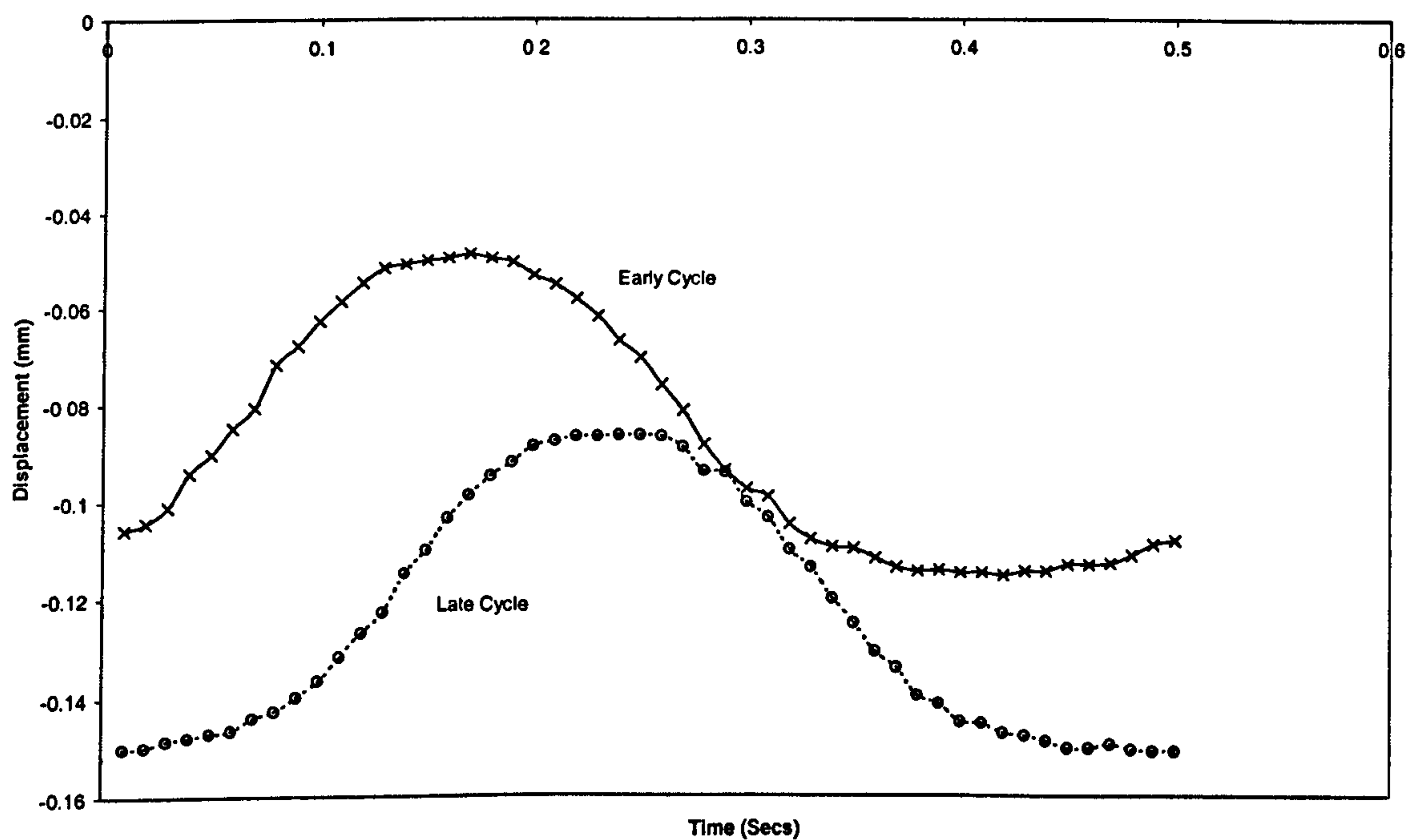


Figure 6.62b – Effect of deterioration on displacement resistance (steel fabric with 4.62mm crack width)

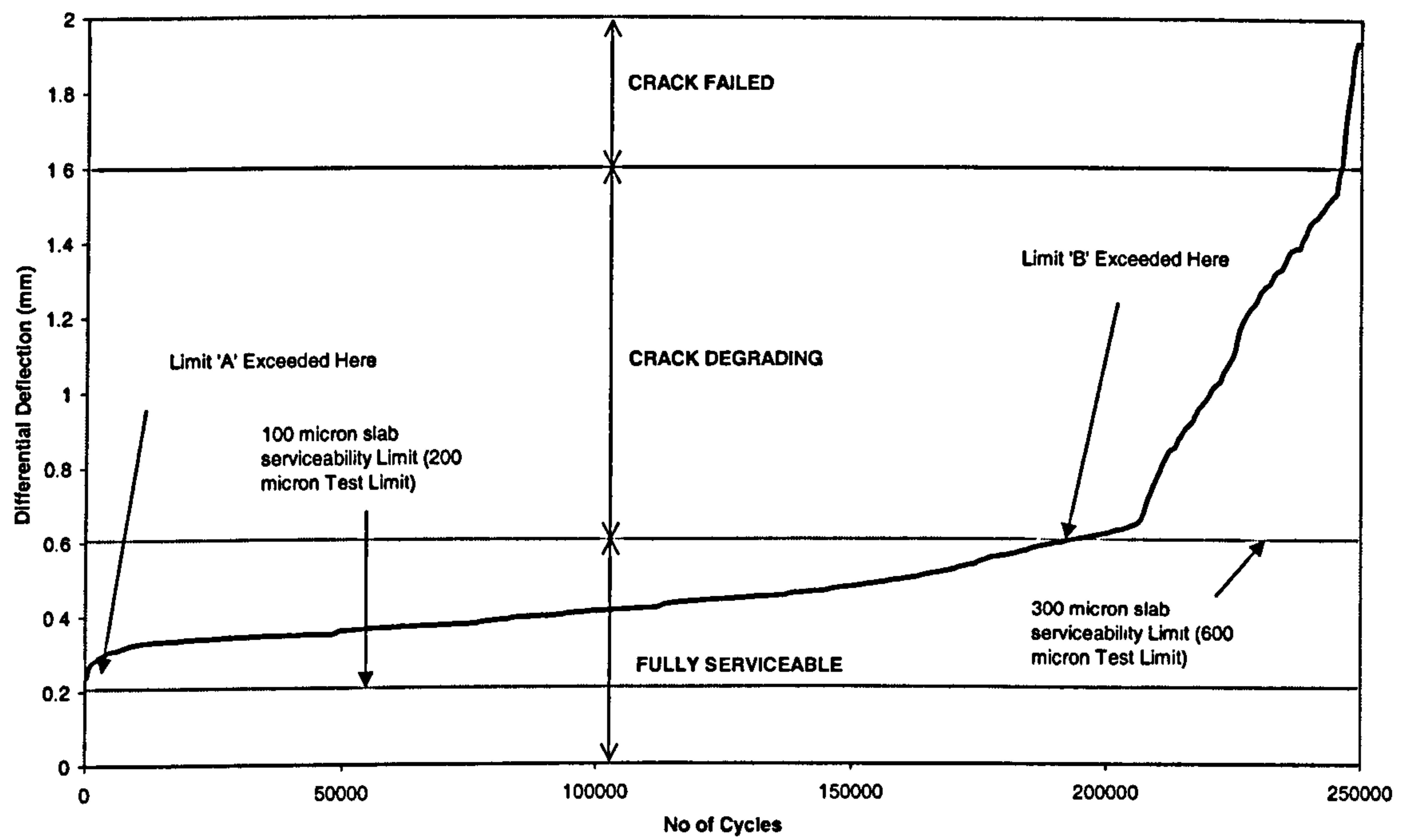


Figure 6.63 – Serviceability thresholds for crack degradation

7. NUMERICAL MODELLING

7.1 Introduction

This chapter discusses the finite element model developed for predictions of slab response under a variety of loading and environmental conditions. The data obtained from the laboratory testing of small-scale specimens was used to provide input of the load transfer mechanism for the relevant crack width and reinforcement type. Field testing enabled comparisons between the numerical model and actual site response to determine the effectiveness of the approach. Parameters could then be changed in a standard slab to enable their effects on behaviour to be identified.

7.2 Model Set-up

Part of the requirement for the finite element configuration was to facilitate future incorporation of the load transfer mechanism into the model constructed by Bishop (2001). This provided predictions of internal concrete stresses and strains, resulting in a crack opening dependant on the environmental conditions and structure properties. When impacted by load the resultant performance of the slab is heavily influenced by the load transfer system which is partially controlled by the width of the crack. To enable progression of slab prediction it was necessary to fully understand and develop a simulation of typical joint behaviour.

As with the Bishop (2001) model, this testing investigated the performance of a slab edge alone, with the large distance from the corner making its influence minimal in affecting response. A two-dimensional finite element program could therefore be utilised since plain strain elements have been shown to provide an adequate simulation to real situations when the distance from the adjacent joint is greater than 0.25m (Kim *et al.* 1998). This method reduced computational requirements and enabled a more meticulous examination of the effects of singular load transfer mechanisms than that of a three dimensional model.

A standard set-up was developed which permitted comparison with other deflection equations and finite element models, providing verification of the approach. The standard consisted of two 6 metre long, 200mm deep slabs sited next to each other, joined only by

the load transfer spring system placed between the opposing bottom nodes of the crack face (Figure 7.1). The DIANA software package was used to model each slab with 225 eight noded quadrilateral plane strain elements, with the load transfer utilising a two noded translational spring. The support conditions required a one noded translational spring at all base slab nodal positions. An interface gap element with a coefficient of friction equal to 1.0 (as recommended by Bishop 2001) was placed between the underside of the slab and the foundation springs to enable the slip membrane friction to be modelled, and allow upward vertical unrestricted movement where applicable. A spring was used for the load transfer system to enable large fluctuations in value to be incorporated in a relatively simple way. This could also be used effectively regardless of the structure's constitutive model. Furthermore, it enabled the wide variety of load transfer mechanisms found in concrete slabs to be integrated in the same way, without the need for separate modelling. This method does not allow direct interaction between the crack width opening from slab shrinkage behaviour and the response of the spring. However, this was acceptable for a first stage analysis and could be adapted in future modelling as required. Generally the approach will not be entirely accurate for calculating the stresses between slabs since each mechanism will exert different forces; however, in respect to deflection response the accuracy should be high.

As mentioned in section 2.7.4 the use of a Winkler spring to represent the soil foundation is not completely accurate. However, to enable comparisons with the Westergaard (1926 and 1947) equations, and many of the other analytical models, it was found to be the best approach. This also enabled easier determination of the soil behaviour when estimating the foundation strength direct from back-analysis of the site deflection response. Where the standard model has been used, a subbase material was in several situations incorporated between the Winkler spring and the slab to enable its effects to be determined.

7.3 Model Verification

To verify the model set-up and ensure adequate predictions of slab response, comparisons were made to the Westergaard 1926 and 1947 equations. These were evaluated against an ILLIS-SLAB finite element package by Ioannides *et al.* (1985) and were found to show good correlation, with the Westergaard (1947) equations providing the greatest accuracy. Ioannides *et al.* (1985) proposed that the infinitely long slab used within the Westergaard equation was the cause of the slight variation between results. The Concrete Society (2003) continue to use these equations to predict serviceability slab deflections in

uncracked situations, and these can therefore be used with confidence in ascertaining the accuracy of the finite element results.

Comparisons were made at both the edge and centre of the slab as it can be assumed that these are equivalent to the extremities of zero and 100% load transfer. Slab lengths were taken as 6m long for the initial tests with thickness varying between 100, 200 and 300mm. Figures 7.2a-f show the results from the analyses and the comparison with the Westergaard original (1926) and new (1947) equations, where applicable.

The plots show that the relationship between the methods improves for both the central and edge locations as the depth of the slab increases. In most situations the Westergaard 1926 and 1947 values show a higher deflection than that of the DIANA model. The only exception to this is with the 300mm slab loaded at the centre, whereby the DIANA model shows higher deflections when the modulus of subgrade is below 0.01 N/mm^3 . The best correlation is observed in the 300mm slab loaded at the edge, in which changes between both Westergaards 1947 and 1926 equations, and the DIANA model are negligible.

The Westergaard 1926 and 1947 equations assume an infinitely long slab; however, that used in the model is chosen to simulate a real situation as closely as possible and is therefore limited to 6m. Ioannides *et al.* (1985) showed that a greater radius of relative stiffness and slab length produced a reduction and increase in the associated deflections respectively. Figure 7.3 shows the effect of increasing the DIANA model slab length for a fixed thickness of 200mm, with those that are longer producing results closer to that found when using the Westergaard 1926 and 1947 equations. This suggests that the Westergaard 1926 assumption of infinite slab length is the cause of the variation between the methods and thus, the results from the DIANA analysis can be used to predict deflection from load.

7.4 Comparison to Laboratory testing

A finite element model of the laboratory test was produced to confirm the effect of spring stiffness on deflection and enable the resistance provided from subgrade support to be identified. The model itself consisted of two end sections which were restrained in both the horizontal and vertical directions. The central section was free to move in both directions, with springs placed between the two lowest nodes adjacent to each other across the crack faces (Figure 7.4). This was undertaken on both sides of the central block to control load transfer through alterations in stiffness of each spring. The concrete was

modelled using an eight noded quadrilateral isoparametric plane strain element, with load transfer utilising a two noded translational spring. Where foundation support conditions were required, a one noded translational spring was used, the stiffness of which was determined by the modulus of subgrade reaction. These were attached to each node of the lower central block and provided equal restraint throughout.

To determine the spring stiffness (K) required for replication of load transfer in a singularly cracked slab, the laboratory cyclic loading test data was translated using the standard spring equation. The total differential displacement at the end of the testing was halved to provide an average movement in one direction from the initial block position. A rearrangement of the standard spring equation (equation 7.1) then produced the associated stiffness from a knowledge of this deflection (Δ) and the applied load (P).

$$K = P/\Delta \quad \text{equation 7.1}$$

The force is equivalent to half the applied load (due to symmetry), and assumes the effect between each crack face is similar, and can therefore be split equally.

The data calculated from the equation produces exactly the same values as that obtained when modelling the lab test with zero subbase support (Figure 7.5). This enables the associated spring stiffness to be determined directly from the results of the laboratory testing for any of the load magnitudes and crack types investigated. These can then be input directly into any analytical model of site slabs to produce representative load transfer results.

Due to the set-up of the laboratory test it was not possible to examine the effects of under slab support on joint stiffness, nevertheless, by means of the finite element model this could be represented adequately for a single load application. The effect of degradation within the joint face cannot be incorporated since the resistance provided will occur throughout the duration of the test, thereby reducing displacements and the rate of degradation. The model can therefore only provide a single representation of the loading cycle and is therefore a snapshot of behaviour, with the load transfer spring stiffness determined beforehand using another source of data. The result of incorporating a subbase under the slab edge can be seen in Figure 7.6, which clearly shows the beneficial effects of having under-slab support. Any change in foundation strength has very little effect when the subgrade modulus values are between 0.05 and 0.15N/mm³, a range representative of good to excellent strength. When this drops to 0.01N/mm³ there is a

clear indication that the amount of displacement increases accordingly; however, even at such a low level, it produces a large reduction in displacement when compared to non-supported beams. This demonstrates how important voiding is when examining under slab edge deflections, as a complete loss of foundation produces large increases in displacement to that found when even a low level of support is provided.

7.5 Relationship with Site Data

To accurately model site behaviour, four finite element models were produced containing the appropriate slab lengths and depths. In all cases the model consisted of two slabs joined at the bottom nodes with a translational spring, similar to the standard model described in section 7.2. Details of the foundation were not known and therefore a Winkler spring system was used in lieu of a separate subbase and subgrade system. This enabled a support condition to be incorporated, without the need to input individual subbase and subgrade information from site. As mentioned in section 4.5.4 back-calculations from the FWD can be used to ascertain foundation strengths for the separate materials. However, Tang (1993) states that this is not applicable when used at the edge condition, as the values of modulus of subgrade reaction are often different under the joint to that found in the more central conditions. A trial and error approach was therefore employed, whereby an estimation of modulus of subgrade reaction was incorporated within the model, from the outcomes of slab deflection behaviour examined against real site data. If the comparisons were poor, the support conditions were altered accordingly until a reasonable correlation was produced. The variety of behaviours examined enabled the approach to be used with confidence. The values of support within each site correlated well with expectations (Figures 7.7 - 7.10, a/b/c), with the sites thought to have a good foundation showing greater stiffnesses than those that did not. The magnitudes of modulus of subgrade reaction found through the finite element model comparisons were representative of typical site conditions, as suggested by Knapton (1999).

Predicted and site measured results of load transfer and load step showed good agreement (Figure 7.7 – 7.10, a). As expected from the examination of field data there is some degree of scatter caused in part by the variations in subbase support. The occurrence of voiding affects the results with an increase in step produced, the size of which depends on the magnitude of the void (section 6.3.2 and 6.3.3). The proximity of the site data to the analytical result line is much closer in those sites containing the highest modulus of subgrade reaction (Ballymena, Daventry). This indicates that voiding and reduced support creates a variation in values. Interestingly, the greatest amount of disparity occurs at the

very low end of the load transfer region, with site data from Ballymena, Daventry and Skelmersdale showing a greater amount of step for its associated load transfer than found from the analytical results. This indicates that where load transfer is negligible some level of voiding appears to accumulate. This may either be caused by the lack of load transfer causing increasing deflection and leading to permanent subbase compaction, or the voiding under the slab increasing the stresses across the crack face resulting in degradation and therefore a reduced load transfer mechanism. In all cases the site data shows that simulation of a consistent foundation support throughout the load transfer range is reasonable except where low levels of joint stiffness are found, at which point a voided model needs to be introduced.

The comparison between the analytical model and site data of loaded and unloaded slab deflections shows much greater disparity (figure 7.7-10, b/c). Even at Ballymena where the foundation produced reasonable agreement to load step comparisons, some scatter can be seen. As predicted the smaller load from the Prima produces a greater correlation than the FWD due to its reduced overall deflection; however, the percentage error between the two is similar. As with the load step relationship, the site containing the strongest foundation generates the greatest correlation, with those having weak support, or slab edges thought to contain voiding, producing the most discrepancy. These plots confirm that edge deflections are controlled by many factors other than the load transfer mechanism, with the foundation support and void quantity being influential.

Where FWD measurements were taken, comparisons were made of the actual slabs' deflected shape and that estimated using the DIANA model (Figure 7.11, a/b). At Daventry comparisons were made between typical good and poor joints, with associated load transfers of 90 and 10% respectively. The deflections measured were all taken on the loaded slab except for the end geophone, which was situated on the unloaded slab to enable calculation of joint load transfer. The plot of the good joint illustrates high variation in the 3m section of slab closest to the slab edge. However, extrapolation of the line beyond this distance indicates that the two will become relatively comparable at approximately one metre further back. The deflections found at the very edge of the slab are similar, with those from site being slightly higher than that of the finite element model. This changes within the first 100mm as the numerical analysis value produces a higher gradient of deflection when compared to the actual slab, which remains fairly consistent. Similarities are found in the results of the poor joint; however, in this situation the deflections throughout the length of the slab are greater on site than in the finite element model. The results from Lutterworth are similar to those of Daventry, although in

this case the deflections are recorded on the unloaded slab, with load transfers calculated at a high value only as no site data was available below 60%.

The variation in gradient indicates that for both sites the slab contains a greater stiffness than that estimated with the model. This is probably due to the two dimensional assumption used within the finite element analysis which contains some known limitations when examining a three-dimensional element.

7.6 Comparison of Laboratory Obtained Joint Stiffness

For the Daventry and Lutterworth sites, data obtained of crack width and joint effectiveness was compared to the results of the finite element model, with the laboratory calculated stiffness used in the development of the load transfer representation. Initially, a laboratory data plot was chosen which most closely represented the slab construction in respect to the reinforcement type and quantity. The number of loading cycles applied to the site slab was assumed to be in the region of 250,000 or greater. Subsequently, it was possible to use the plots of crack width and differential deflection provided in section 6.4 to determine a representative spring stiffness value for that on site. These were incorporated within the DIANA model most closely representing the site conditions in respect to geometry, material properties and support condition, enabling the resultant slab deflections to be identified. Translations of the data into load transfer and load step allowed the response of a laboratory and analytical model to be compared to that obtained from site. This process is shown in diagrammatic form in Figure 7.12.

A second finite element plot using a voided slab was produced to examine its effects and ascertain whether it gave better correlation to site data. This consisted of an affected area 10% of the total slab length, as suggested by Suprenant (2002) and found from the site data in section 6.2.3. Ideally, the foundation support under this section would have been reduced to zero to represent a full void. However, constructing a model in this way created a mechanism within the analysis producing erroneous results. Incorporation of the lowest modulus of subgrade reaction possible was therefore required to simulate the reduced support but prevent the mechanism from developing. A period of trial and error deduced that the smallest value achievable was 0.005N/mm^3 .

The results of load transfer and crack width from both the voided and unvoided Daventry finite element models, along with the site data, are shown in Figure 7.13. The crack values from the laboratory testing have been extrapolated to provide the equivalent width

had the beam been of the same depth as the slab. As expected the data shows that the model containing the void produces higher load transfer values than the unvoided. However, the majority of the site data is above both of these lines, and thus indicates some increased load transfer effect in addition to that discovered in the laboratory tests. The simulation test beams were 100mm in depth, and therefore contained a crack approximately 30mm shallower than was found on site. Any increased surface area could therefore raise the load transfer potential and result in values closer to the field data. The effect would be more pronounced in areas where the surface crack is below 1.5mm, as it has been suggested by Pearson (1999) and Colley and Humphrey (1967) that widths above this show minimal aggregate interlock. This observation supports the findings from site as the data displays greatest divergence from the analytical line when the crack width is low. However, a discrepancy also exists as modelling of voiding requires a value of support to be inserted to prevent a mechanism being developed. As mentioned previously this should ideally be zero to fully represent a true condition, although in the analytical model a low value had to be incorporated thereby resulting in a lower load transfer in comparison. This would create a significant shift in the line, and produce results closer to that found on site.

The comparison of site deflections with the prediction lines of load step and crack width from the numerical analysis shows significant differences between the voided and unvoided slabs (Figure 7.14). Here, the unvoided slab produces a better comparison to the site data, although the voided line produces an upper boundary which no site data point exceeds. This change in response between the load transfer and load step indicates that the increase in joint stiffness brought about by the greater slab depth in the real site joint is more likely than voiding to be the explanation of the discrepancy. A higher joint stiffness would increase the load transfer and reduce the load step for a given crack width, thereby producing better correlation to the site data.

The assumptions made in the determination of load transfer from the laboratory simulation may also affect the accuracy of any prediction. In the determination of the test duration, it was assumed that 250,000 cycles of the +/- 4kN load produced an equivalent stress to that found within the slab. If that on site was at a lower stress, or received fewer cycles of load, then fatigue is reduced thereby increasing joint stiffness, resulting in greater load transfer values and lower load steps.

The load transfer results obtained from the Lutterworth site were compared against the laboratory testing of both non-reinforced and mesh reinforced concrete as the condition of

the actual joints on site was unknown (Figure 7.15). The Concrete Society (2003) state that any steel crossing an open joint may have yielded and therefore the degree of load transfer capacity will reduce accordingly. Similar to the results of Daventry, both of the load transfer mechanisms were tested for unvoided and voided foundations to enable comparison. As expected most of the data obtained from site lies somewhere between the extreme lines, these being the voided mesh and the unvoided non-reinforced joints. As mentioned previously, voiding under the slab edge produces higher values of load transfer, although this has only a minor impact when compared to the change between mesh and non-reinforced specimens.

Comparison of Lutterworth load step shows that the mesh reinforced specimens produce better correlation with the site data than that of non-reinforced (Figure 7.16). The non-reinforced analytical line appears to be an upper boundary which none of the site data exceeds. Similar to the Daventry results several of the points show an increased load transfer and reduced load step when compared to any of the analytical predictions. This may be caused by the increased section of crack face found on site compared to that simulated in the laboratory, which leads to an improvement in the load transfer mechanism.

The results from both tests show that numerical modelling of site conditions using laboratory testing and the DIANA finite element software produces acceptable results for estimating slab response. The accuracy of the site data alone is very scattered due to the variation in crack geometry, inconsistencies in under slab voiding, and the load transfer mechanism. By obtaining further information about the exact loading frequency and magnitude, alongside the support conditions, a better approximation can be made using the analytical techniques. In both cases investigated, the importance of selecting the correct parameters for comparison between laboratory and site joint stiffness is shown. However, even in cases where exact details are unknown the predictions produce good lower and upper bound levels enabling assumptions of worst-case scenarios to be developed.

7.7 Effect of Constituent Material Parameters

The standard model consisted of two 6m slabs, with an arrangement and specification similar to that described in Chapter 7.2 (Figure 7.1). In the examples where a subbase was incorporated, this was modelled with eight noded quadrilateral plane strain elements with the strength and stiffness input as appropriate. Two depths were chosen as 150 and

225mm as these represented typical maximum and minimum values suggested by the Concrete Society (2003). The strength of the Winkler spring subgrade was reduced to 0.01 N/mm³ for these models as this is typical of a subgrade material with the stiffness used previously being a combination of the two foundation layers.

The methodology behind the standard slab testing was to vary individual parameters in turn and examine their effect on deflection response. The values used for each analysis were typical of those found in site conditions, with comparisons made of modulus of subgrade reaction, concrete modulus of elasticity, joint spring stiffness, slab depth, subbase Young’s modulus and load position. The parameters used for the standard slab are listed below in Table 7.1.

Table 7.1 – Standard Slab Basic Parameters

Parameter	Standard Value
Slab Depth	200mm
Modulus of S/G Reaction	0.05 N/mm ³
Concrete Poisson’s Ratio	0.15
Load Magnitude	50kN
Joint Spring Stiffness	0 and 1,000 MN/m ²
Concrete Young’s Modulus	30 GPa
Load Position	Slab Edge
Subbase Young’s Modulus	100 - 300 MPa
Subbase Poisson’s Ratio	0.2
Frictional Interface	1.0

Figure 7.17 shows the effect of the modulus of subgrade reaction in resisting deflection. Towards the reasonable (0.05 N/mm³) to good (0.2 N/mm³) level the plot shows a moderate increase in deflection as the soil modulus is reduced. However, in poor soil the change in deflection gradient is steep with high levels of movement for a relatively small reduction in modulus. The differential between the 0 and 100% joint effectiveness also increases slightly as the modulus of subgrade reaction reduces, indicating how performance becomes more prominent when the foundation is weak.

The effect of the concrete’s Young’s modulus is minimal in resisting deflection, with even the maximum stiffness investigated of 35 GPa only producing a 0.035mm reduction in slab edge deflection compared to that obtained with the minimum value of 24 GPa (Figure 7.18). This demonstrates that increases in the stiffness of the concrete provide little assistance in the reduction to deflection, regardless of joint efficiency.

An increase in joint stiffness is most beneficial in reducing deflections between the zero and 200 MN/m² level, typically 0–80% load transfer (Figure 7.19). After this range the effect slows, with any additional increases in joint stiffness producing only minor improvement, the overall plot showing reasonable correlation to a logarithmic curve. In a perfect joint where the load transfer is 100% the slab edges will result in a deflection of 0.18mm compared to that of 0.36mm for a low stiffness joint. These results show that in most situations high load transfers can halve the unrestricted deflection. There is however a point where large enhancements in stiffness (or load transfer mechanism) will only produce minor reductions in the edge deflections, and therefore a suitable compromise has to be made by the designer.

Increases in slab depth, resulting in a stiffening of the structure, produce significant reductions in the edge deflections under both good and bad load transfer conditions (Figure 7.20). For the standard slab, doubling of the depth from 150 to 300mm reduces the edge deflection by 0.16mm when the joint has zero load transfer. In situations where the joint stiffness is high then reduction is still in the region of 0.08mm.

Figure 7.21 demonstrates the effect of subbase inclusion in reducing the magnitude of deflection at the slab edge. Where the joint is working efficiently the subbase stiffness has very little influence regardless of thickness. However, this changes when the joint stiffness is poor with the introduction of the subbase decreasing the magnitude of the deflection dramatically. The model containing the thickest subbase shows the most reduction, though the effect of both is reduced as its modulus is lowered from 300 to 100MN/m².

Hammons (1998) has suggested that the distance of the load from the slab edge affects the value of load transfer. The spring stiffness examined during this finite element analysis shows that equal load transfer values are produced regardless of the location of the load (Figure 7.22). The disagreement with the work of Hammons (1998) may be caused by the free slip phenomenon, as discussed in Chapter 6.3.2. Here, the deflection reduces as the load is moved away from the joint, making the proportion of free slip larger, resulting in a reduction in the load transfer efficiency.

7.8 Summary

A finite element model has been developed and verified against the established equations developed by Westergaard (1926, 1947), and the Ioannides *et al.* (1985) ILLISLAB finite element model. The results of this analysis have shown good comparison and, as predicted, indicate the greatest correlation with Westergaard's (1947) equations when a reduced stiffness, created from an increasing slab length and reduced thickness are used.

Several models have been established containing the parameters assumed and measured on site. These models have enabled analysis of deflection response and, via a back-calculation approach, the determination of the magnitude of modulus of subgrade. The results from the deflections obtained under the same loading conditions as that of site have then been compared and found to show reasonable agreement in most situations. Any scatter found in the data has been attributed to under slab voiding and the assumptions in materials and layout when developing the finite element model.

Using the laboratory based degradation plots, spring stiffness has been determined using the standard spring equation and a finite element simulation model. The stiffness for the associated crack width has then been imported into the relevant analytical model with the deflection response compared against that obtained from site. Voiding is well known to affect the magnitude of deflections on some sites and therefore models were set-up in which 10% of the slab length contained a reduced level of foundation support to incorporate this situation.

Although the data is scattered, the finite element model provides a reasonable representation of site behaviour. Examination of the information shows that analysis of both the load transfer and load step graphs needs to be undertaken to ensure continuity and enable voiding effects to be ascertained. The additional support available from the larger crack face on the site joints appears to produce an appreciably higher load transfer value than is found within the laboratory. The effect of the reduced fatigue created by the foundation support condition and the unknown loading behaviour is also thought to have some effect, increasing the load transfer values and decreasing the load step. In general the finite element testing enables good estimation of the slab behaviour, with upper and lower bound levels determined.

A standard slab containing typical dimensions and material parameters was used to establish the effect of each on slab response. Subgrade support conditions were found to

have a large impact on response, with those containing below average values producing greater increases in deflection for relatively small enhancements in stiffness. This is similar when utilising a subbase as the strength and depth of the material heavily influences the associated deflections, indicating that its careful selection can assist in increasing the longevity of the slab. Concrete strength has little effect in respect to deflection; however, increasing the thickness of the slab (thereby stiffening the structure) provides resistance to a significant degree. Joint efficiency is highly influential in the slab response as a 100% load transfer can reduce the deflection of a non-efficient joint by 50%. The effects are more influential when the joint stiffness is low, as even small increases can provide large reductions in deflection. According to the finite element model, in a normal situation the distance of the force from the slab edge has very little impact on the load transfer magnitude obtained, although the shear slip phenomenon may influence the results due to the change in total deflection.

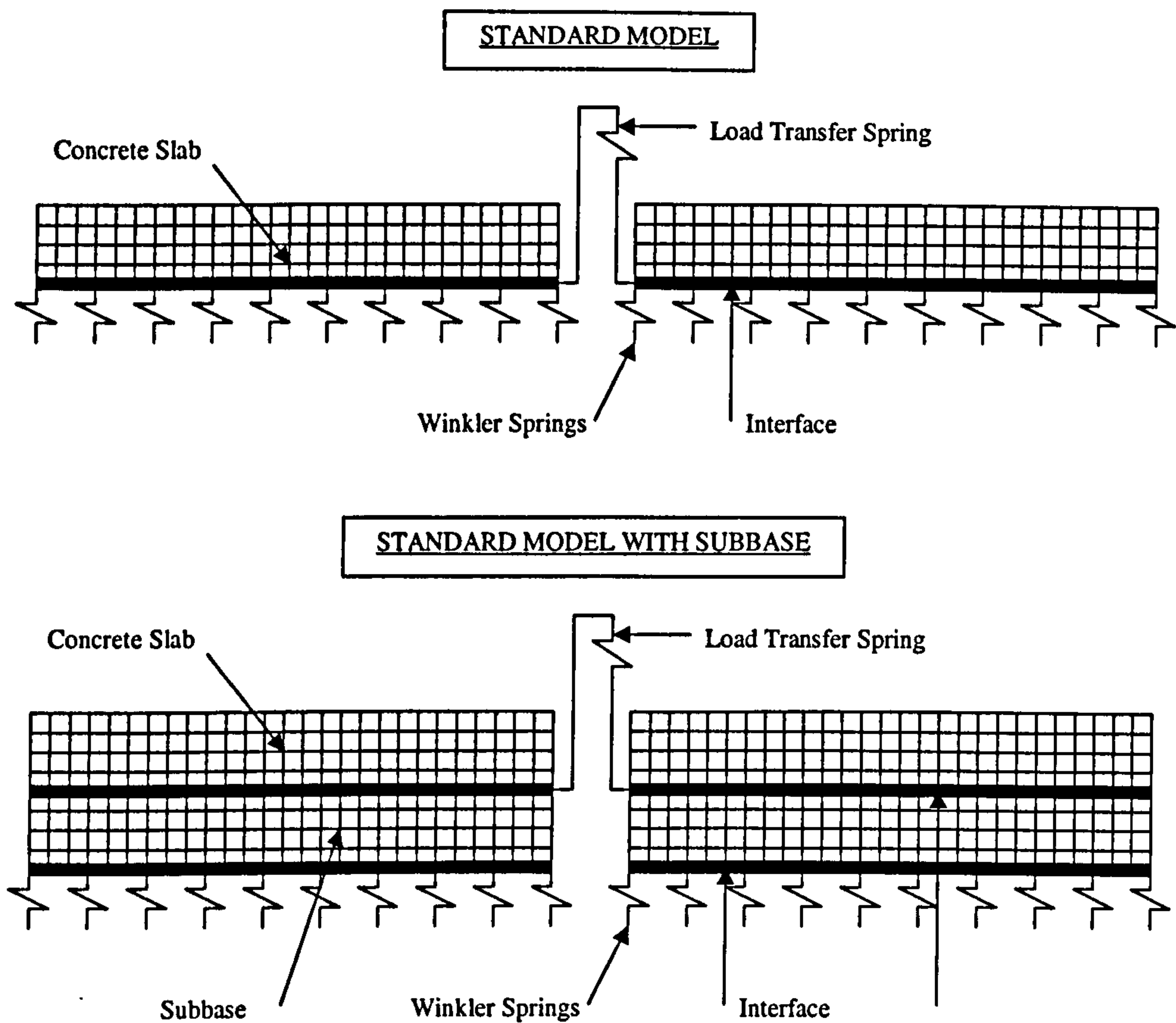


Figure 7.1 – Finite Element model of a concrete slab on grade with a discontinuity

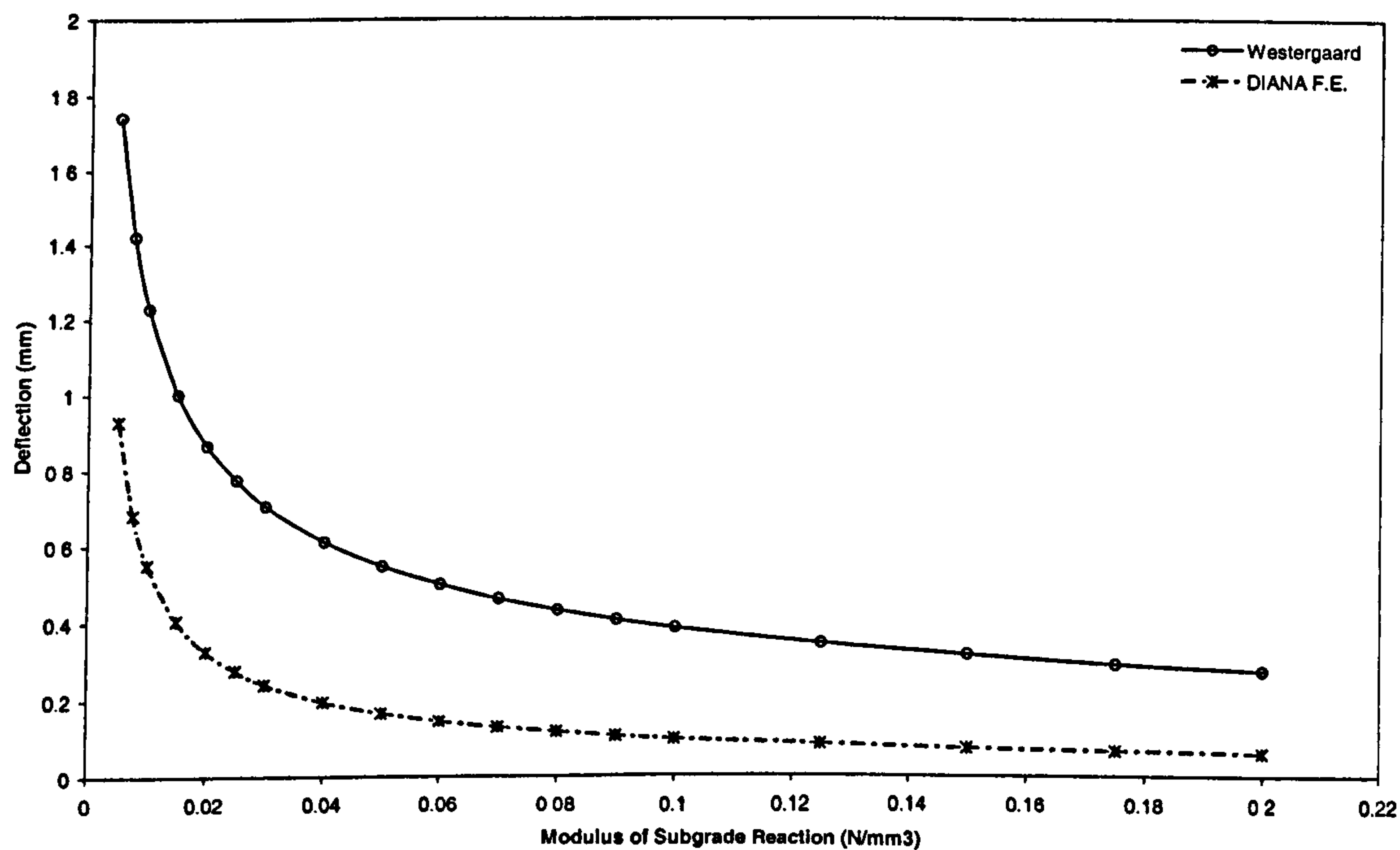


Figure 7.2a – Comparison of DIANA with Westergaard (1926) for a 100mm slab loaded internally

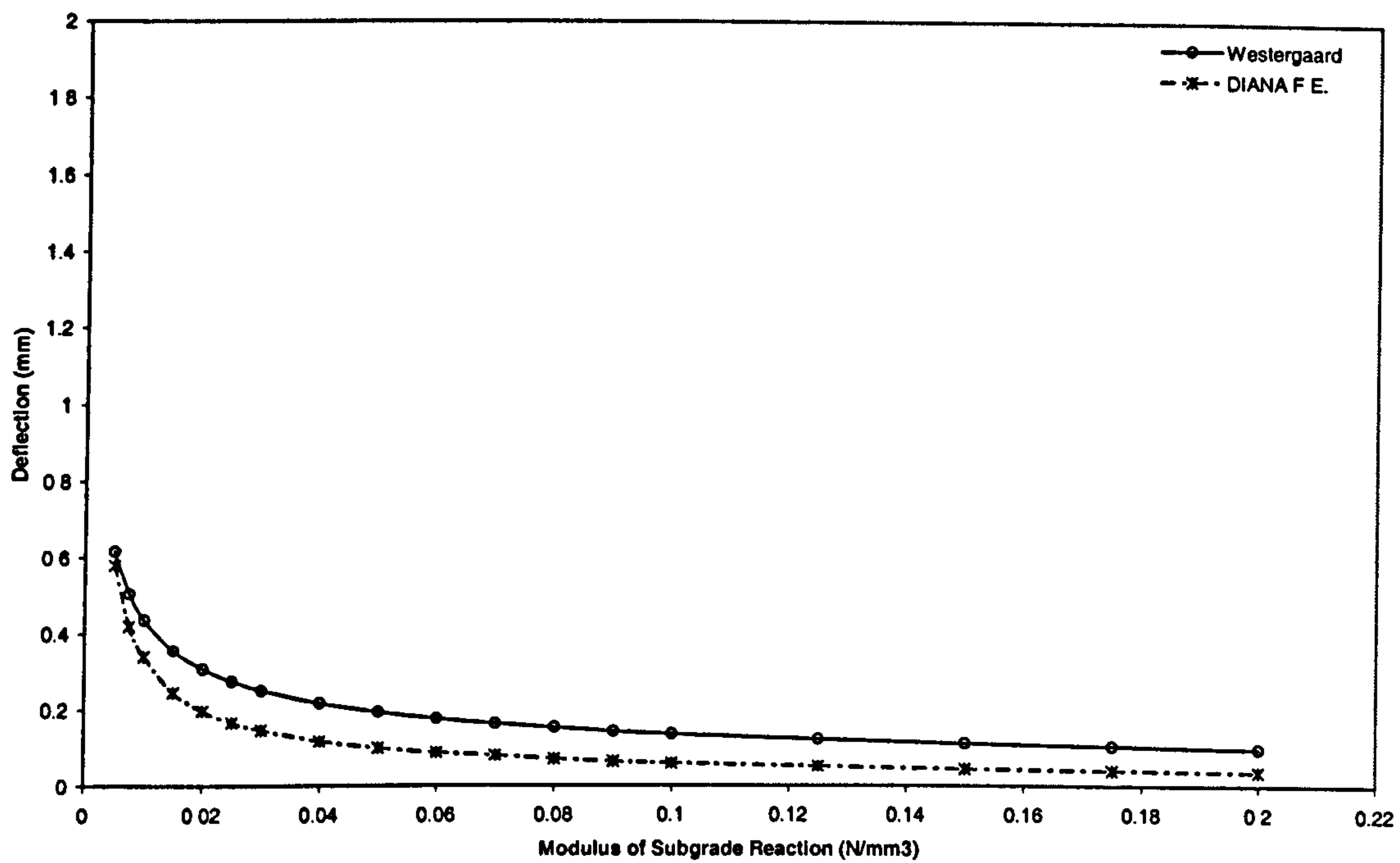


Figure 7.2b – Comparison of DIANA with Westergaard (1926) for a 200mm slab loaded internally

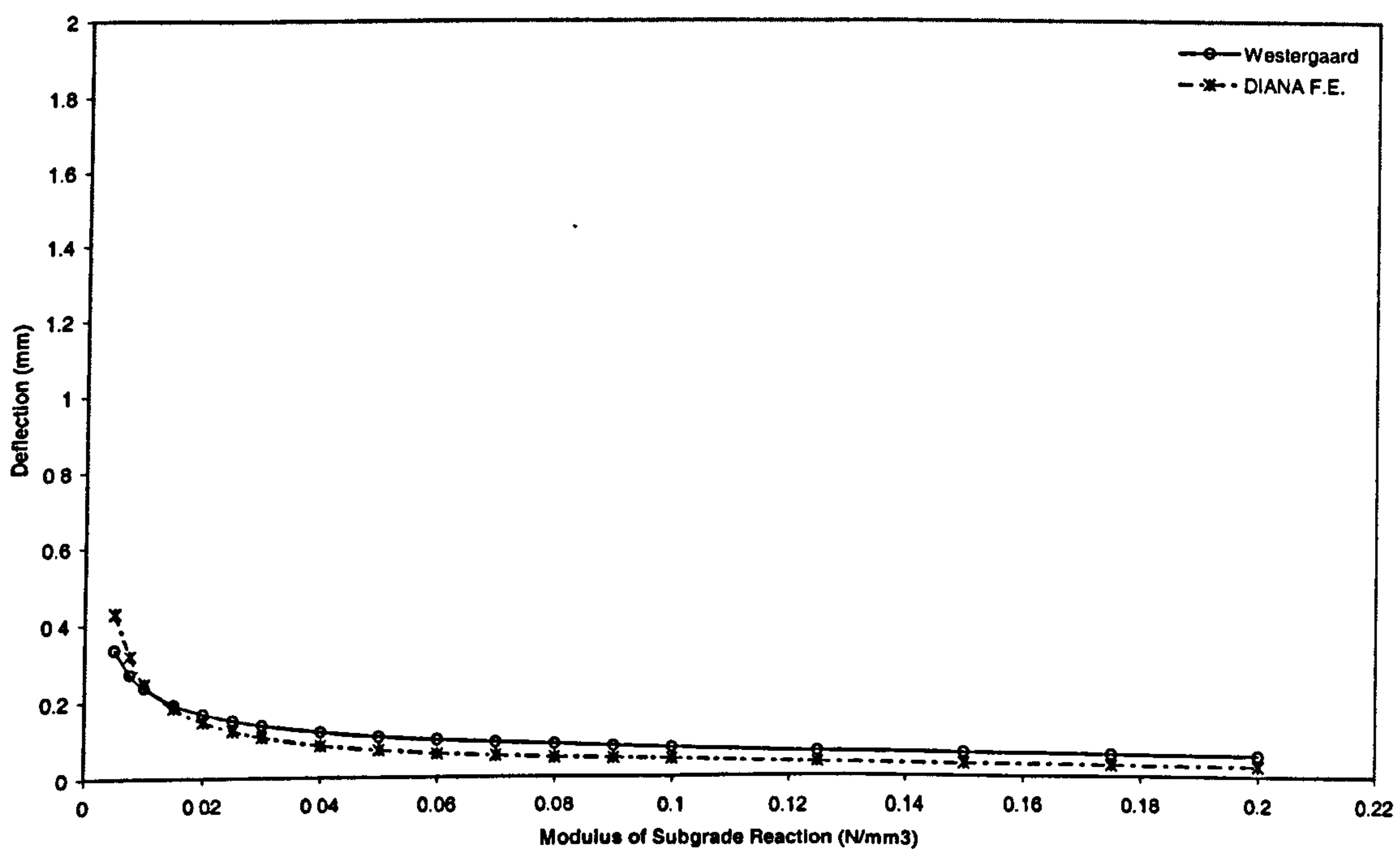


Figure 7.2c – Comparison of DIANA with Westergaard (1926) for a 300mm slab loaded internally

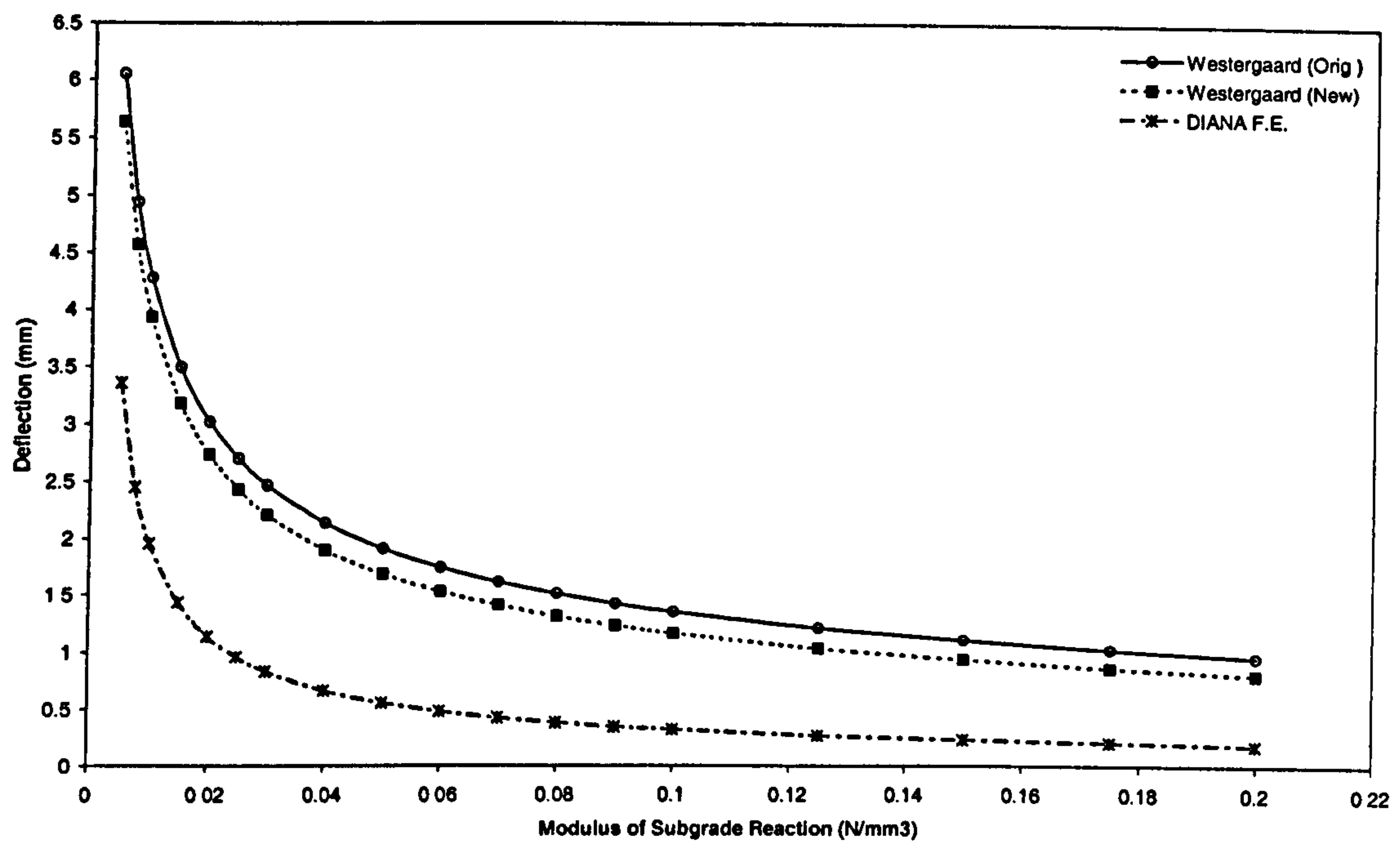


Figure 7.2d – Comparison of DIANA with Westergaard (1926 and 1947) for a 100mm slab loaded at the edge

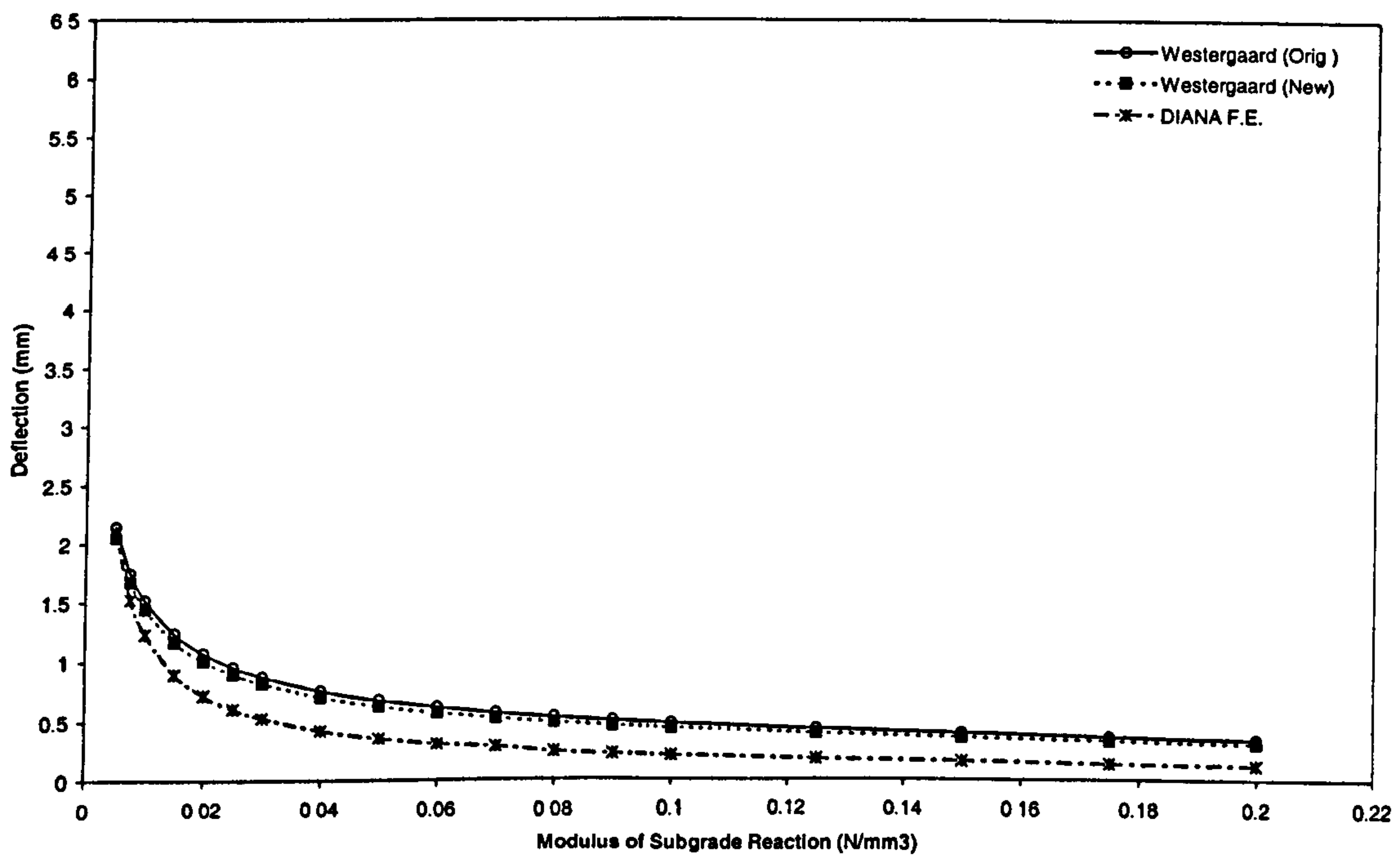


Figure 7.2e – Comparison of DIANA with Westergaard (1926 and 1947) for a 200mm slab loaded at the edge

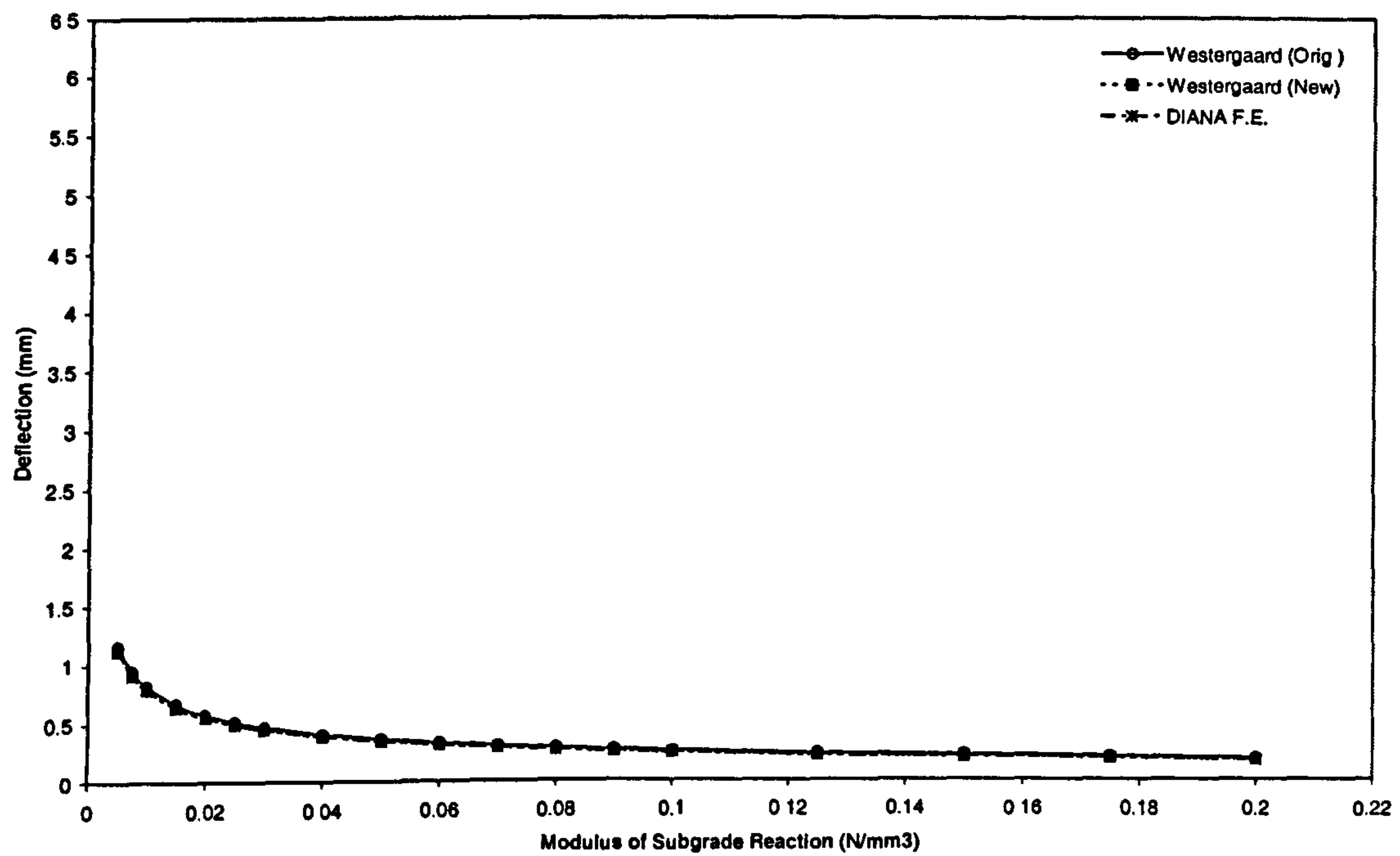


Figure 7.2f – Comparison of DIANA with Westergaard (1926 and 1947) for a 300mm slab loaded at the edge

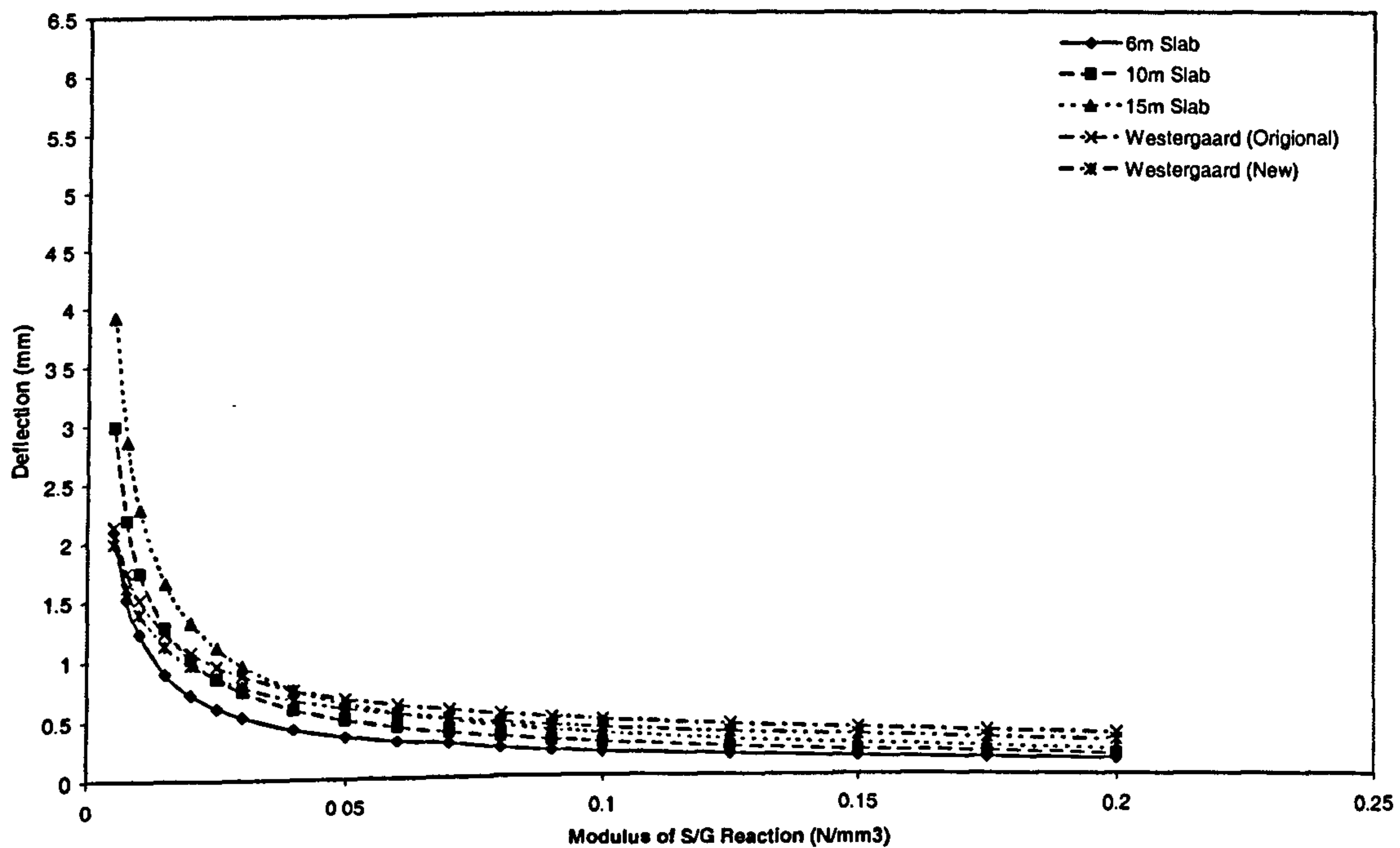


Figure 7.3 – Comparison of DIANA with Westergaard (1926 and 1947) for a 200mm slab loaded at the edge with lengths of 6, 10 and 15m.

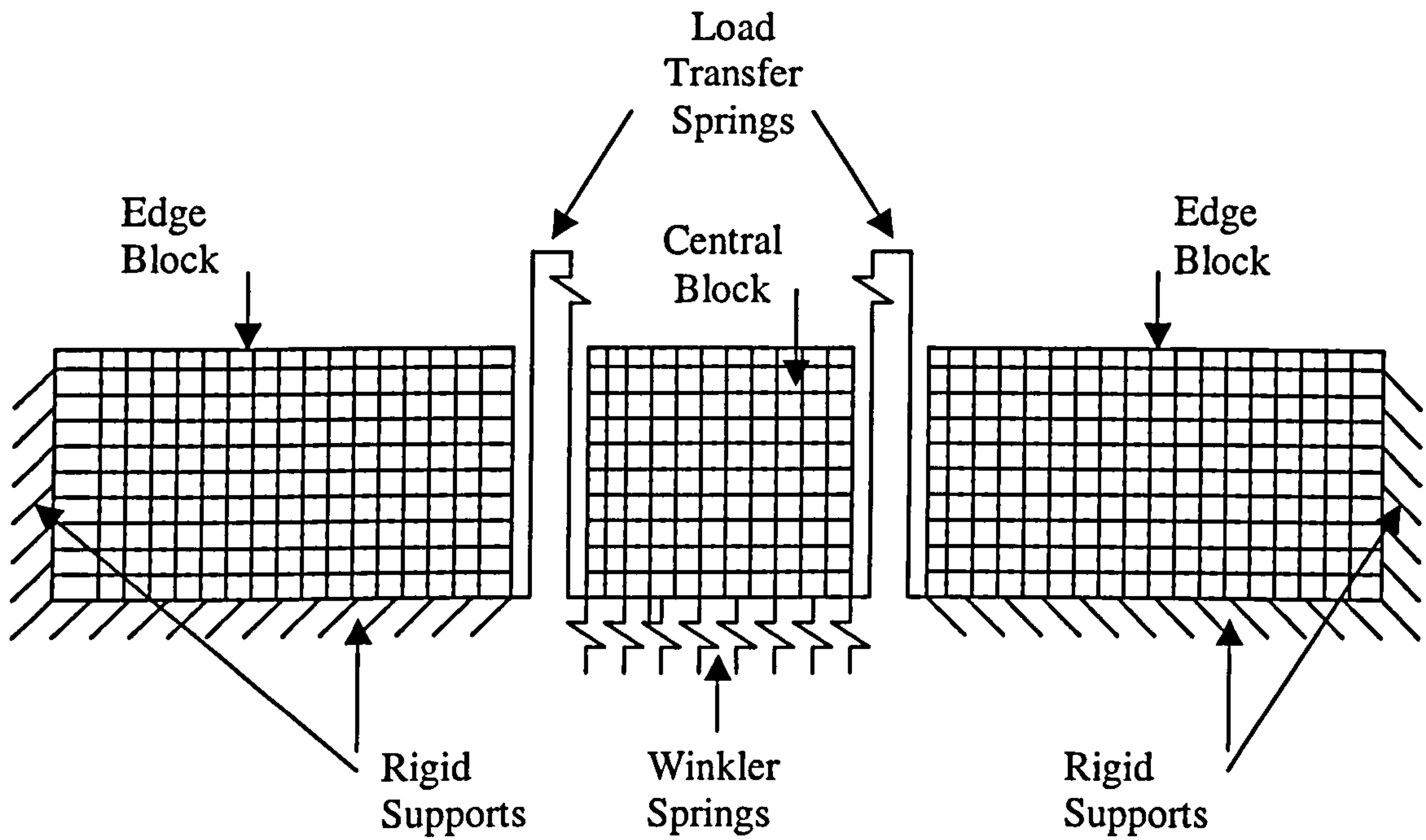


Figure 7.4 – Schematic of the Finite Element model of crack behaviour within the laboratory test rig

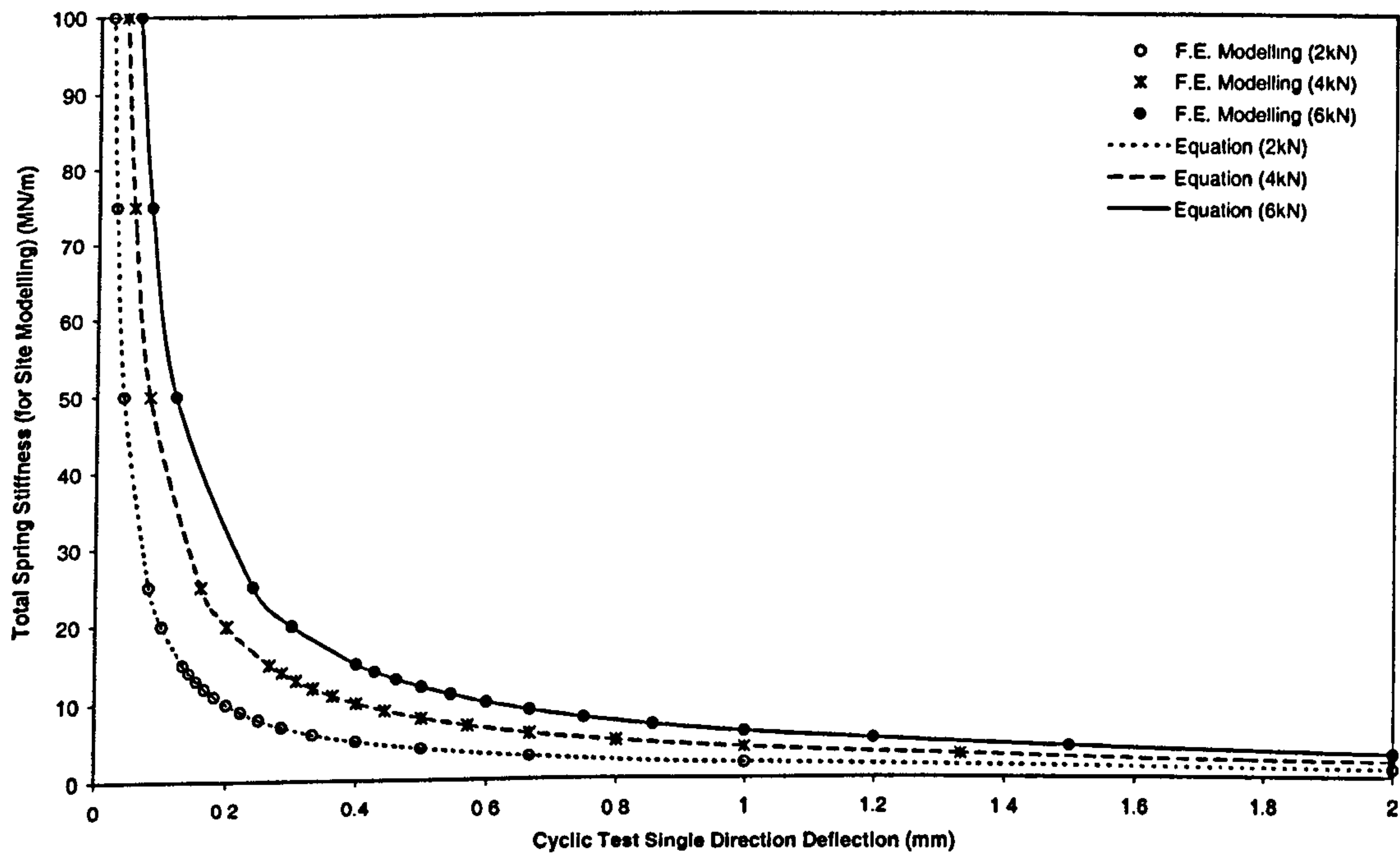


Figure 7.5 – Comparison of the laboratory Finite Element model with the standard spring equation

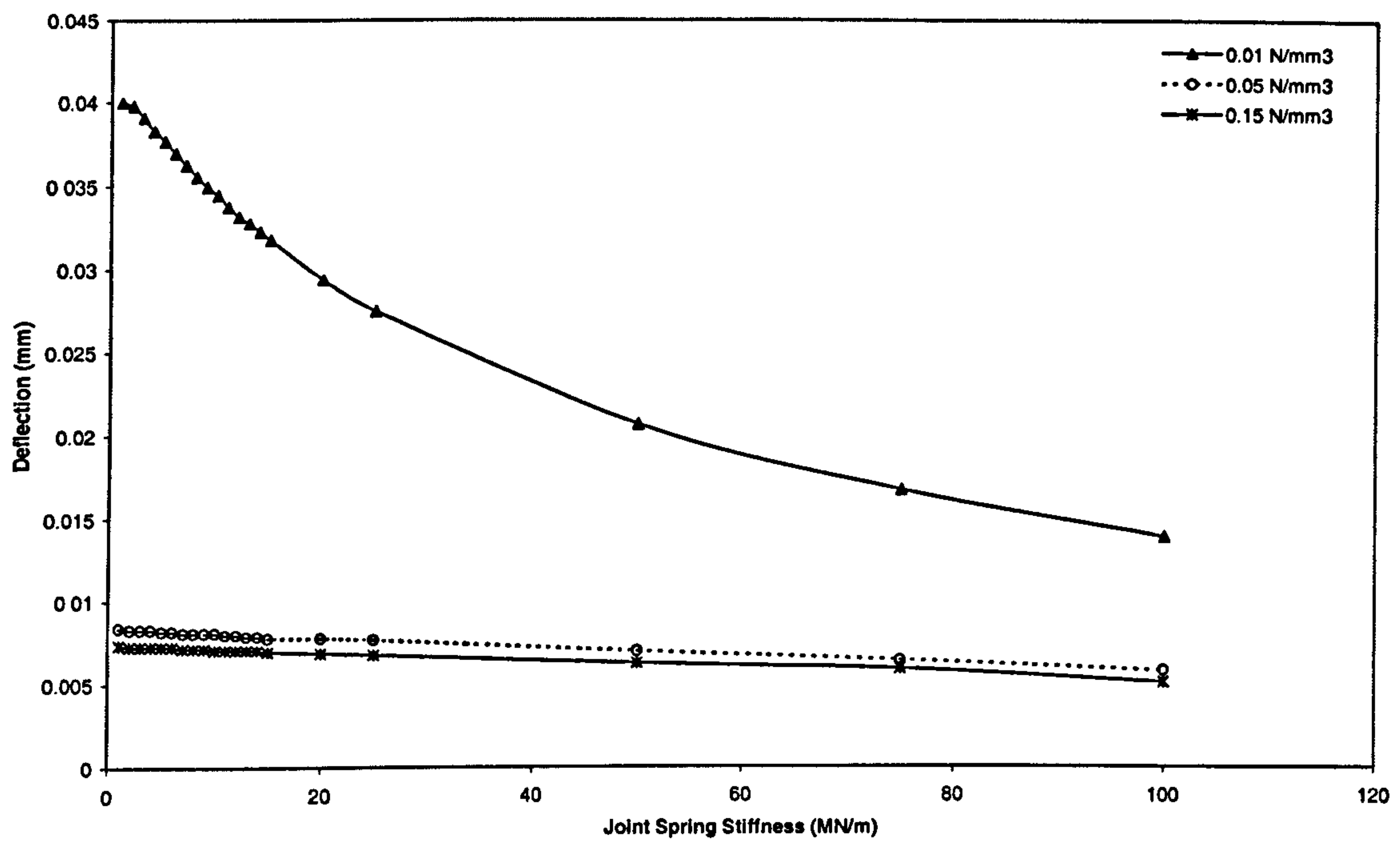


Figure 7.6 – Effect of foundation material under the crack in the laboratory Finite Element model.

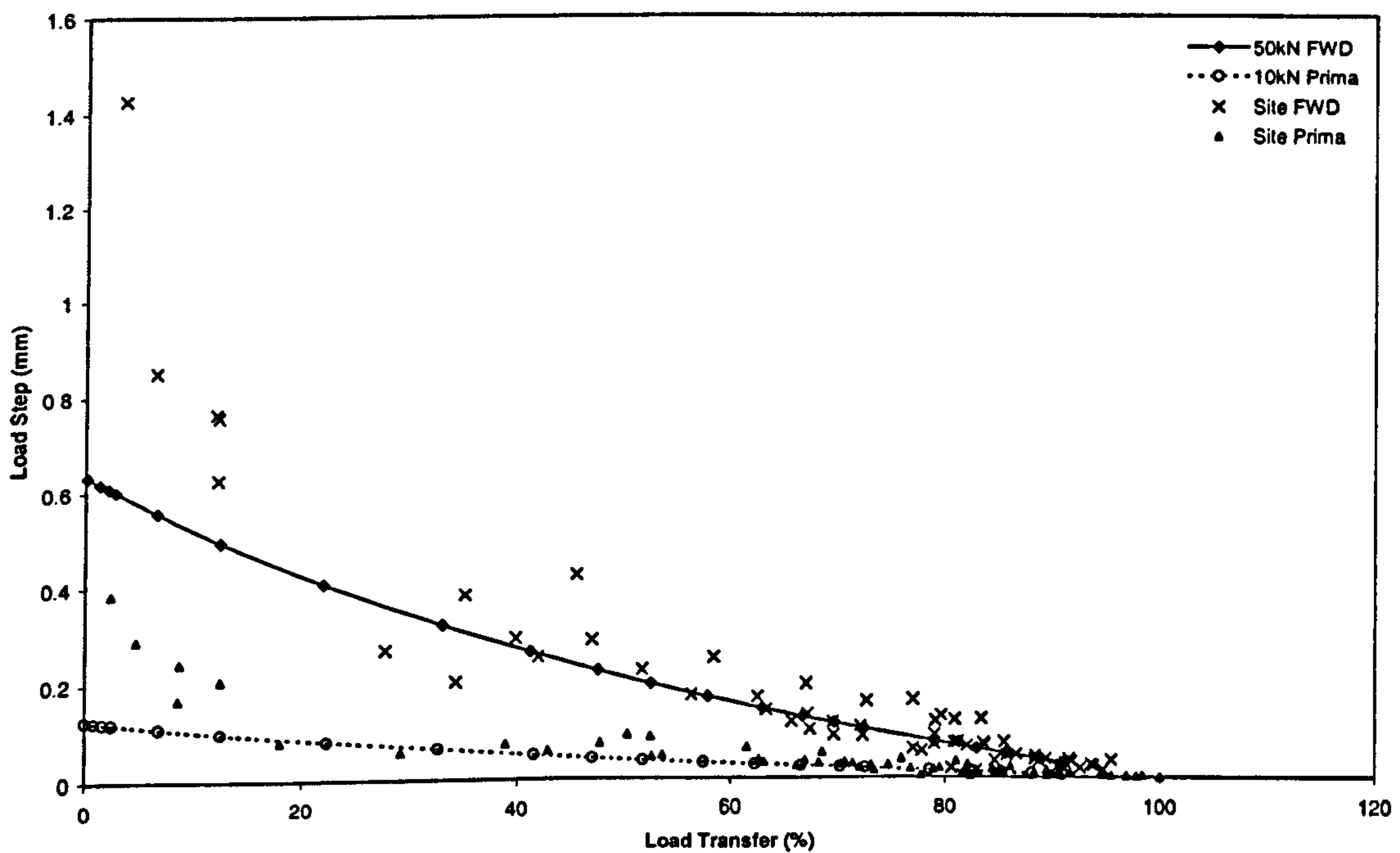


Figure 7.7a – Comparison of load transfer and load step between the Daventry Finite Element model and in-service slab response

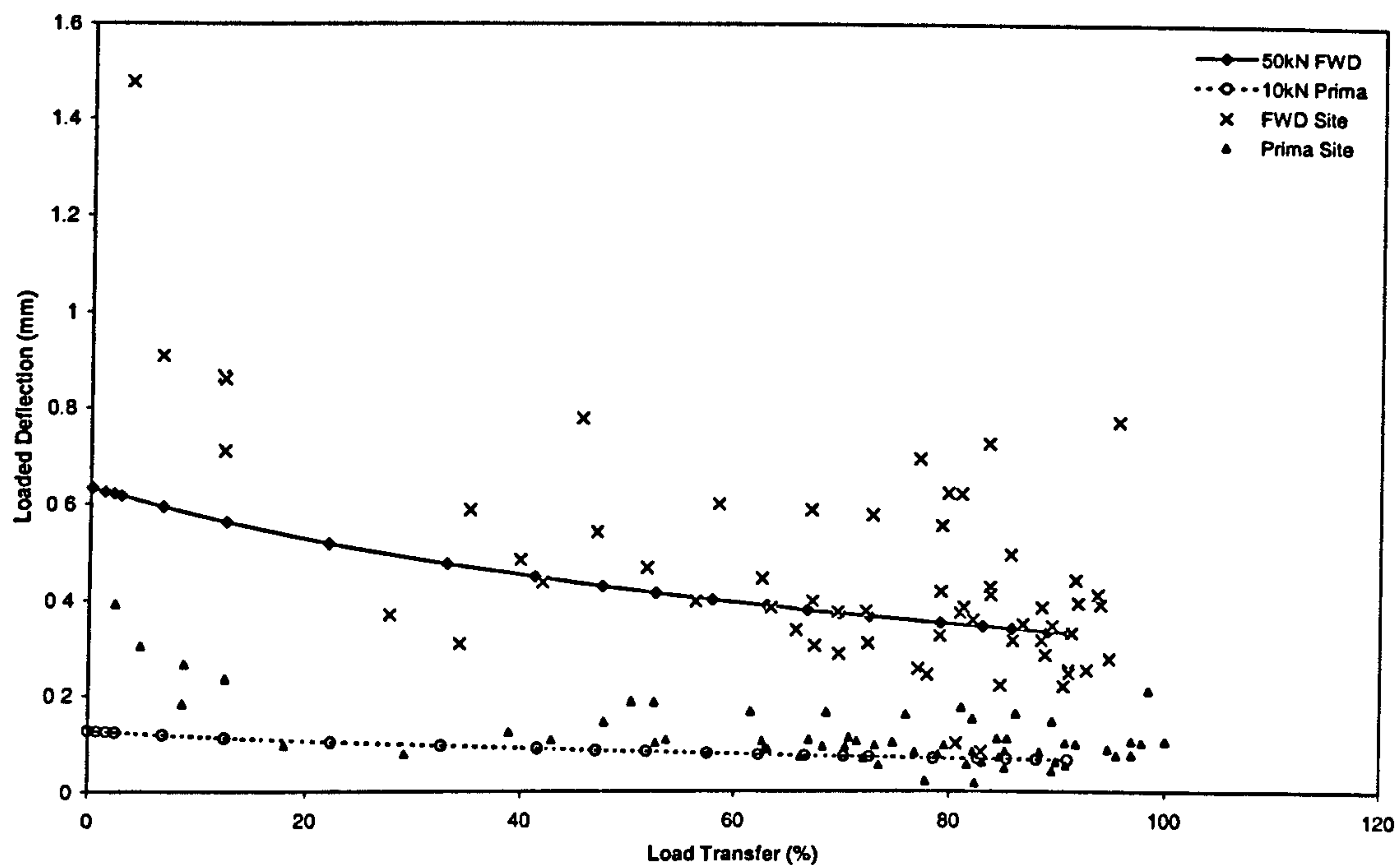


Figure 7.7b – Comparison of loaded edge deflection and load transfer between the Daventry Finite Element model and in-service slab response

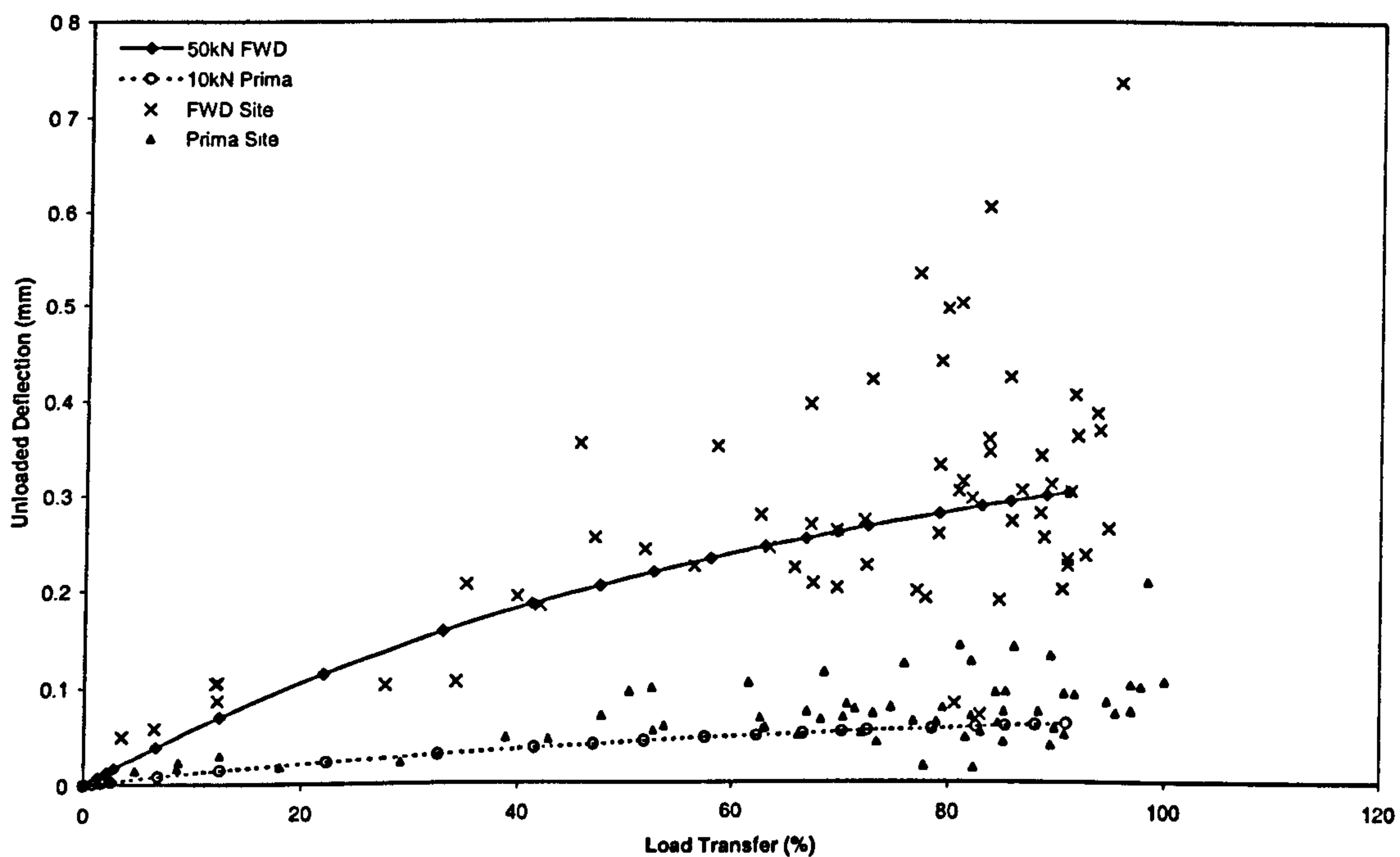


Figure 7.7c – Comparison of unloaded edge deflection and load step between the Daventry Finite Element model and in-service slab response

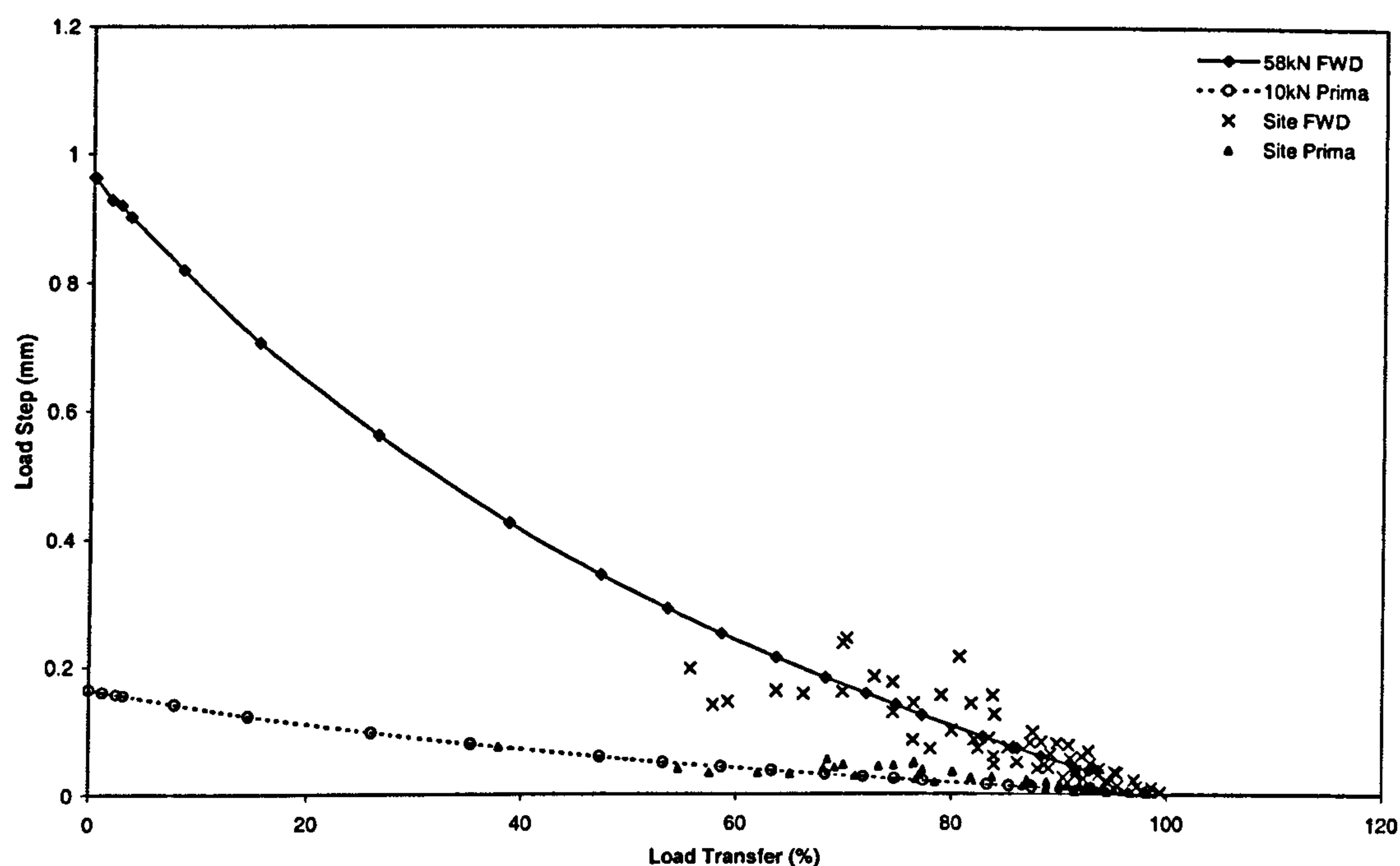


Figure 7.8a – Comparison of load transfer and load step between the Lutterworth Finite Element model and in-service slab response

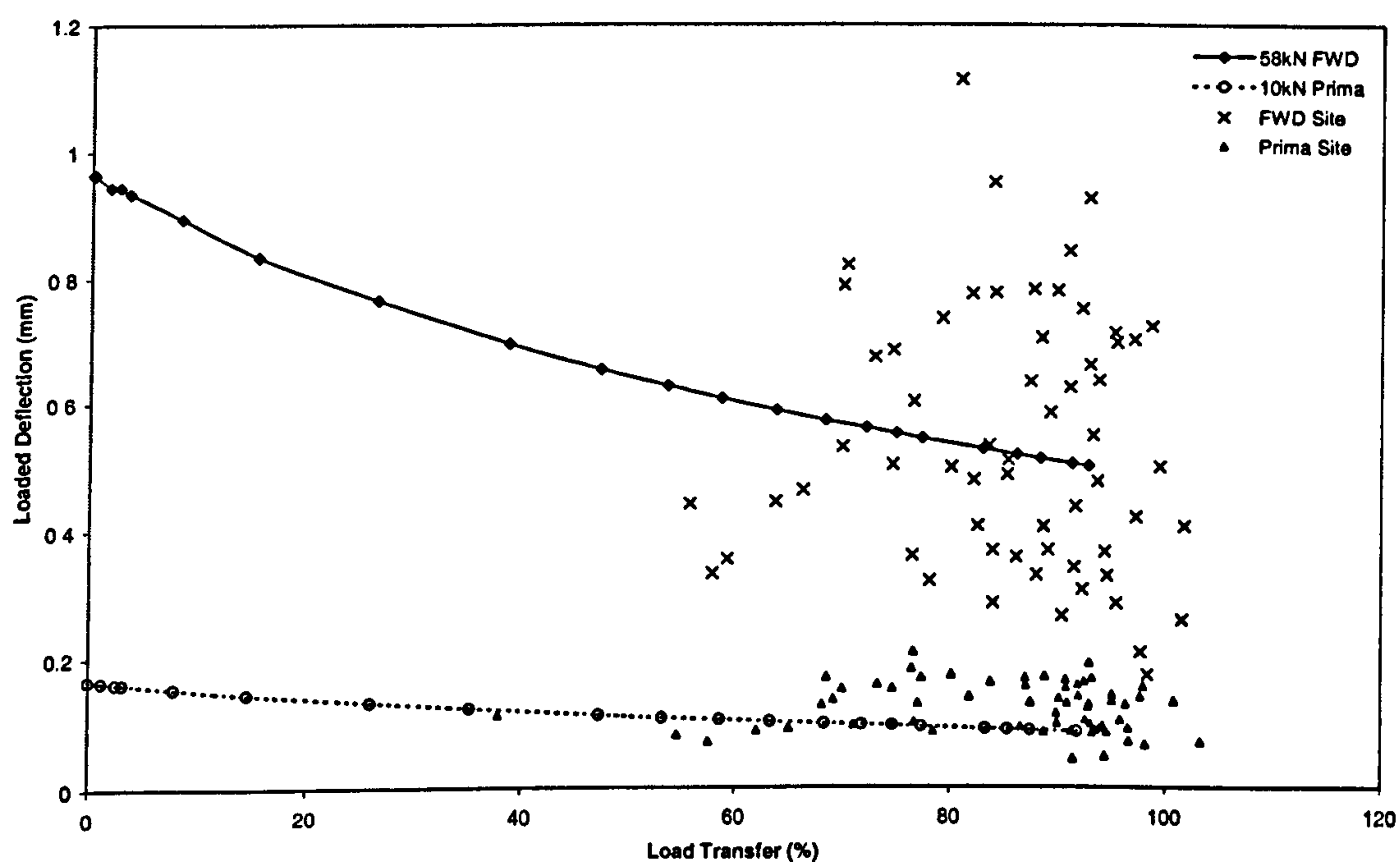


Figure 7.8b – Comparison of loaded edge deflection and load transfer between the Lutterworth Finite Element model and in-service slab response

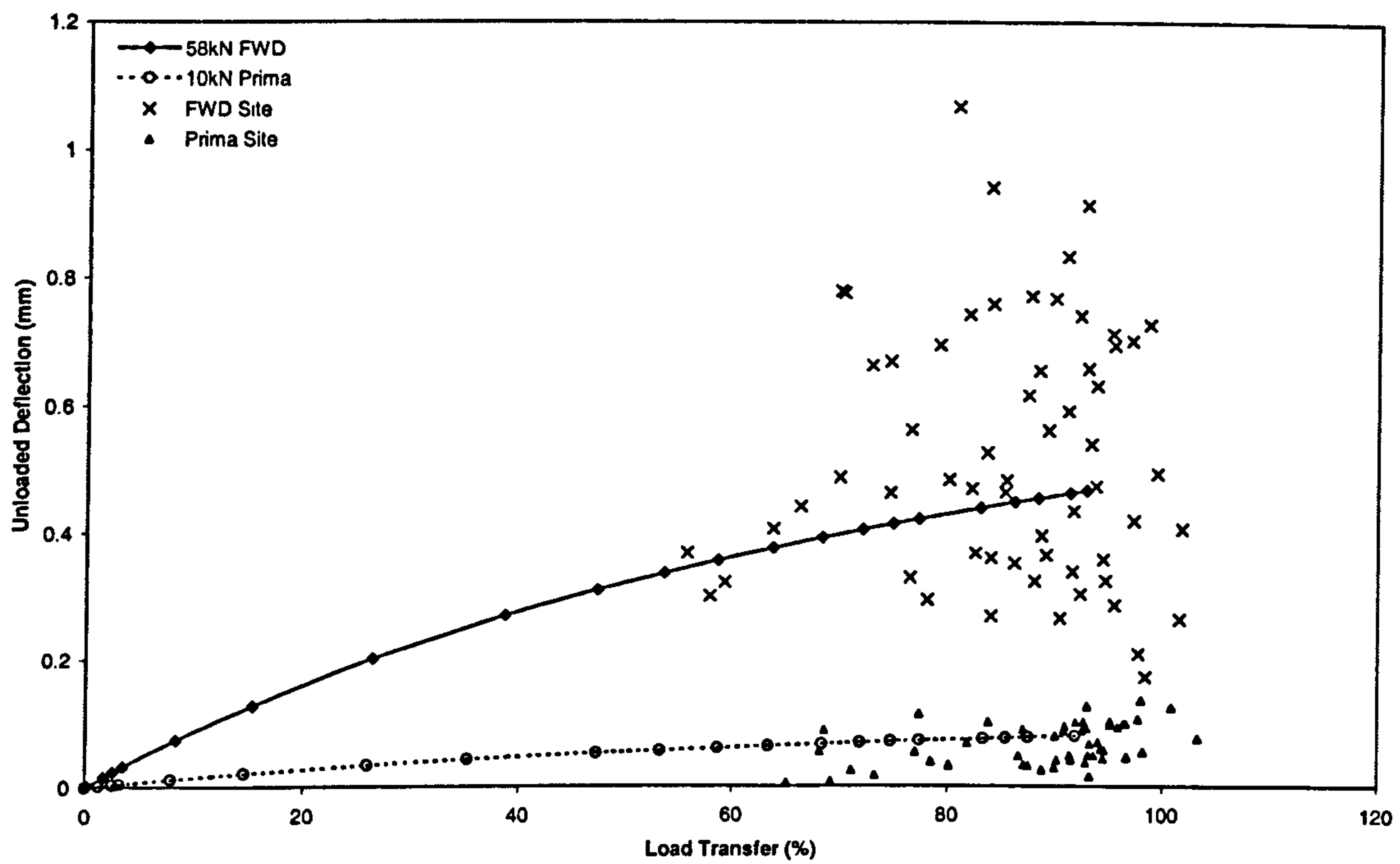


Figure 7.8c – Comparison of unloaded edge deflection and load step between the Lutterworth Finite Element model and in-service slab response

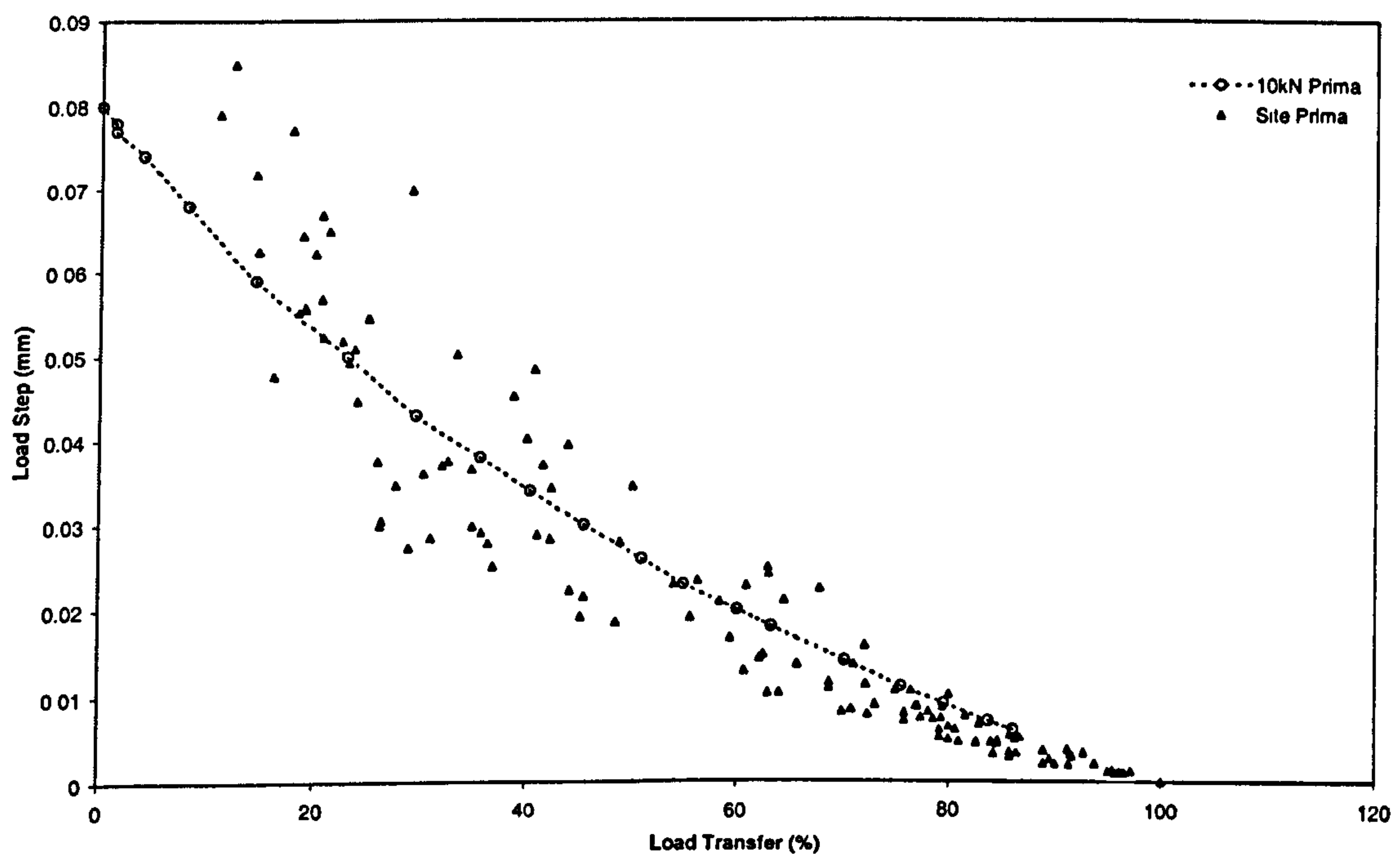


Figure 7.9a – Comparison of load transfer and load step between the Ballymena Finite Element model and in-service slab response

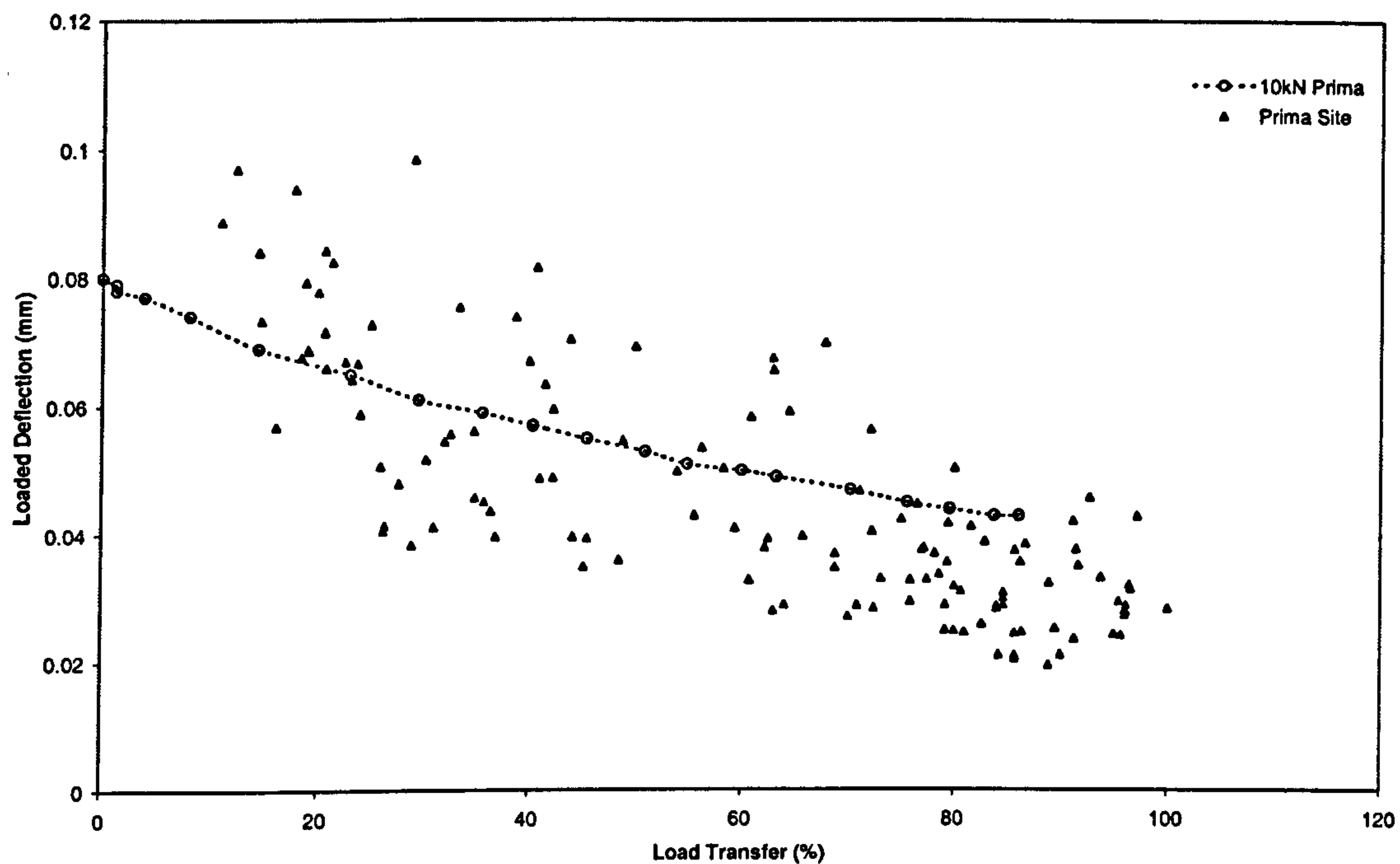


Figure 7.9b – Comparison of loaded edge deflection and load transfer between the Lutterworth Finite Element model and in-service slab response

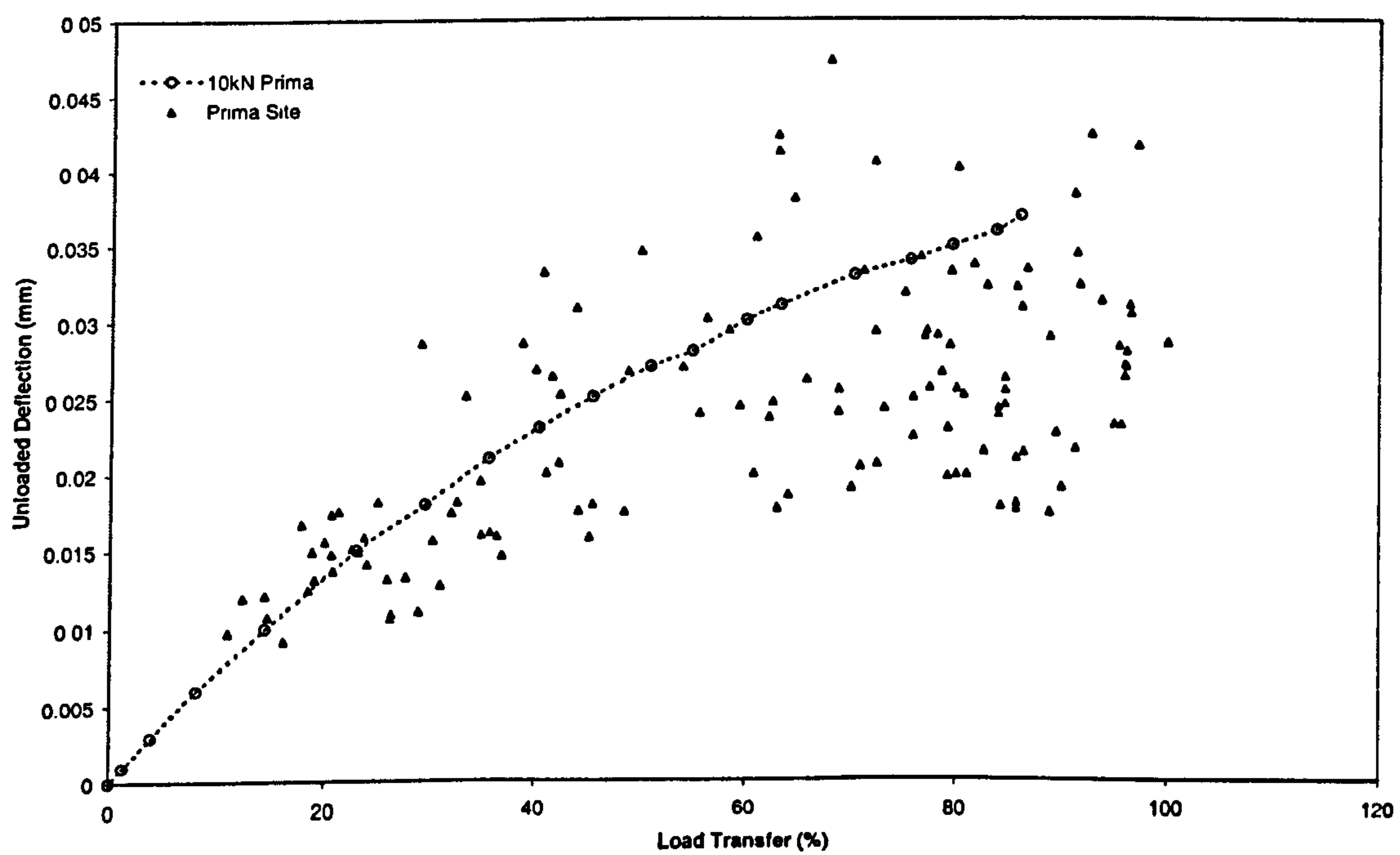


Figure 7.9c – Comparison of unloaded edge deflection and load step between the Ballymena Finite Element model and in-service slab response

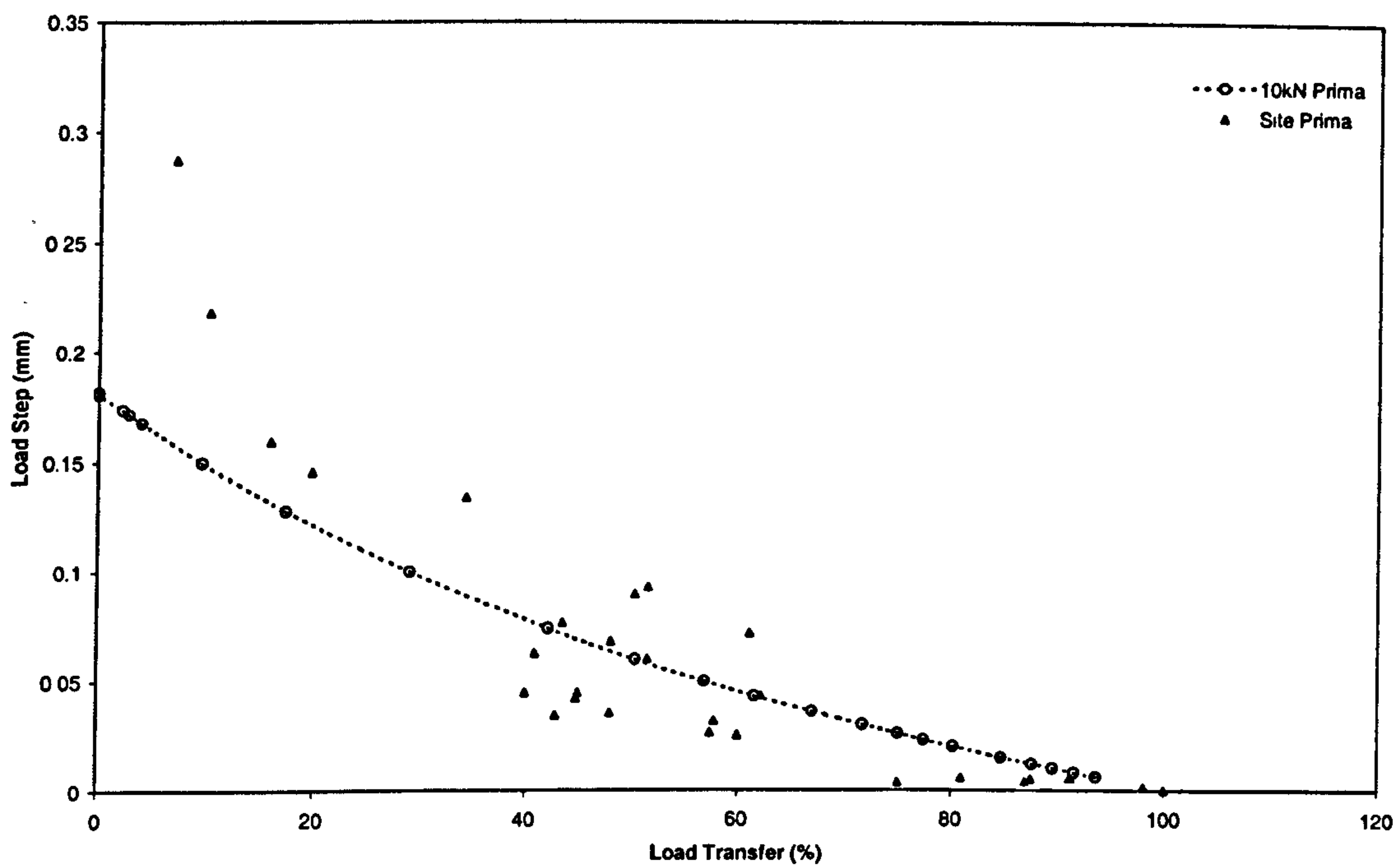


Figure 7.10a – Comparison of load transfer and load step between the Skelmersdale Finite Element model and in-service slab response

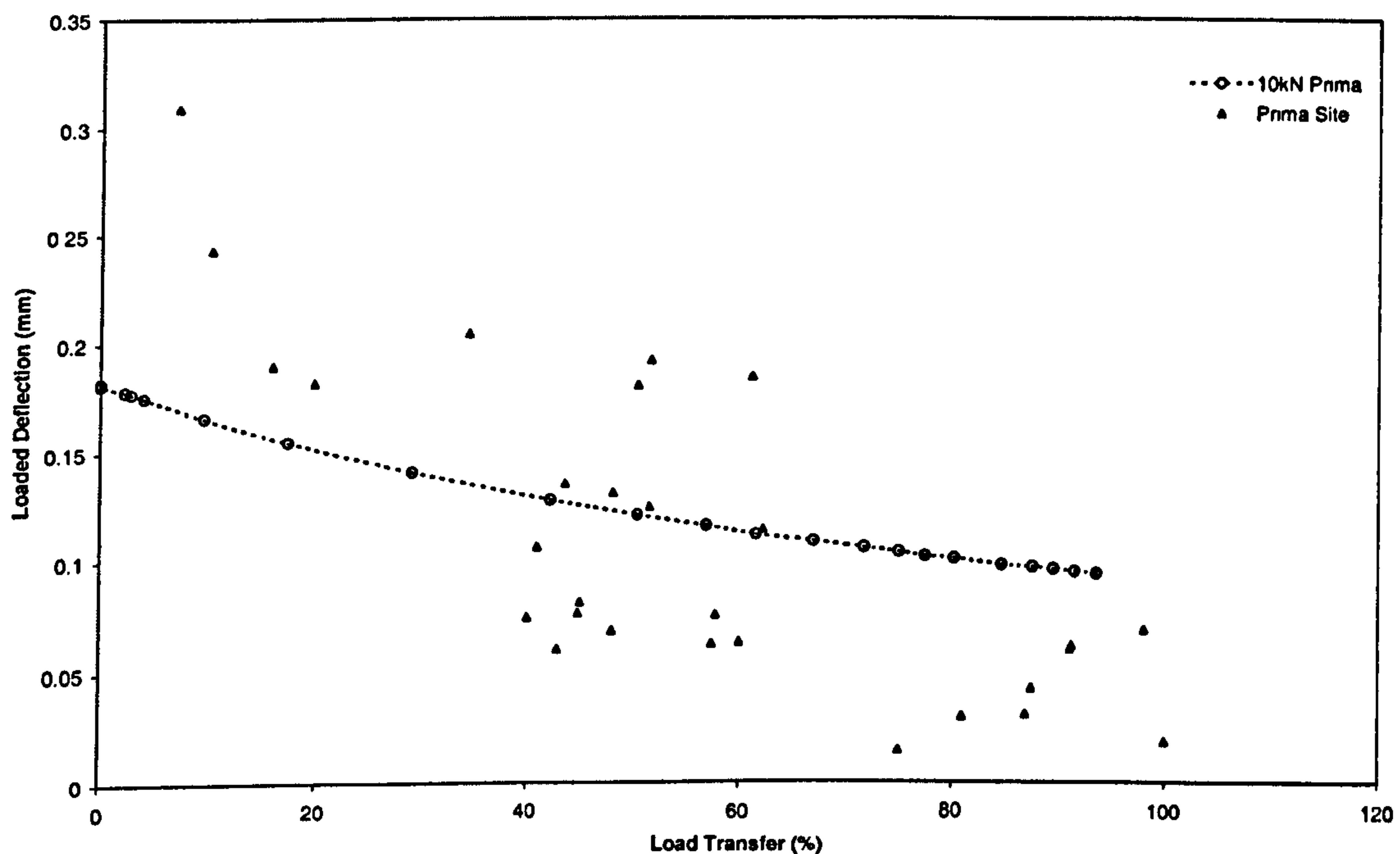


Figure 7.10b – Comparison of loaded edge deflection and load transfer between the Skelmersdale Finite Element model and in-service slab response

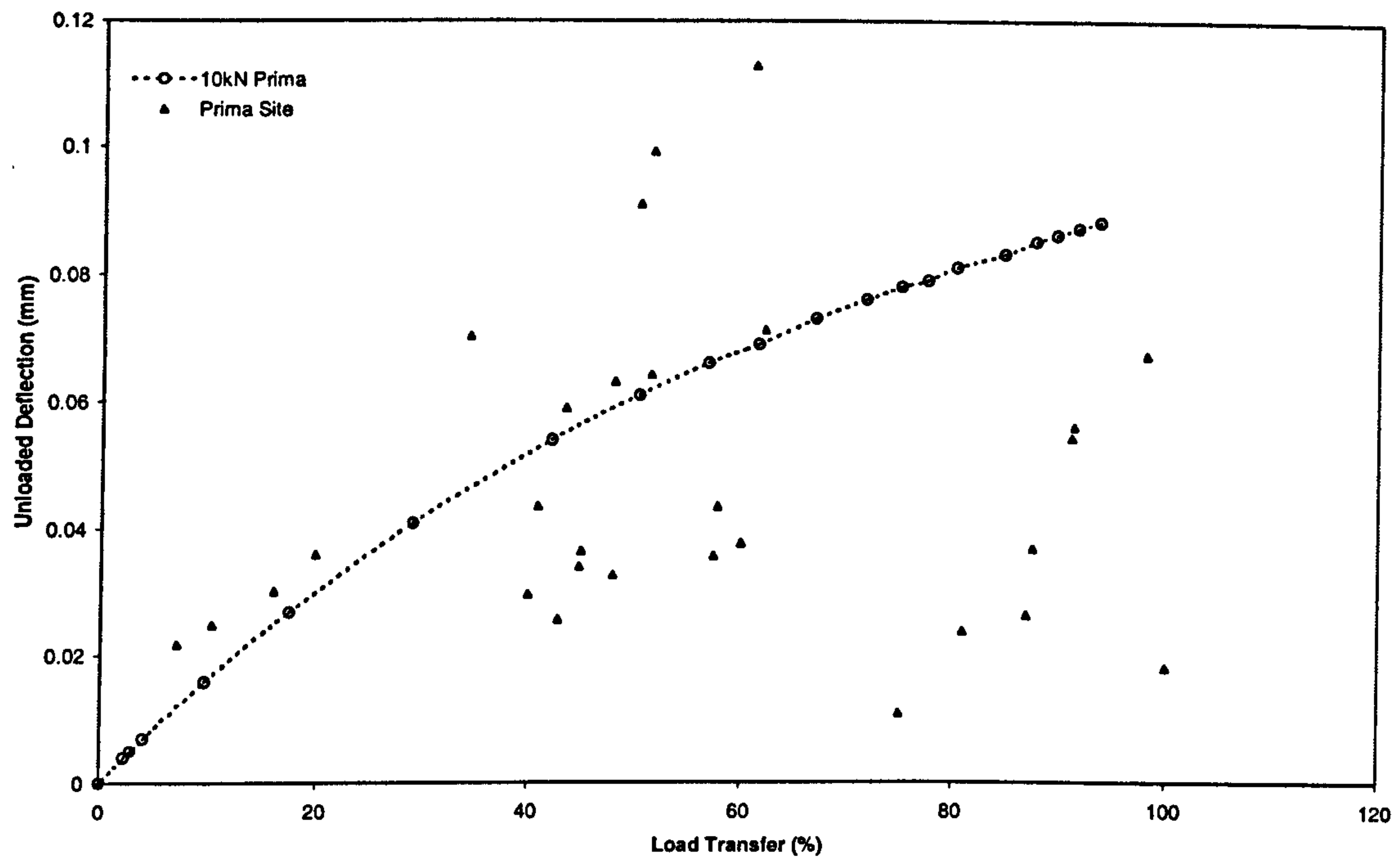


Figure 7.10c – Comparison of unloaded edge deflection and load step between the Skelmersdale Finite Element model and in-service slab response

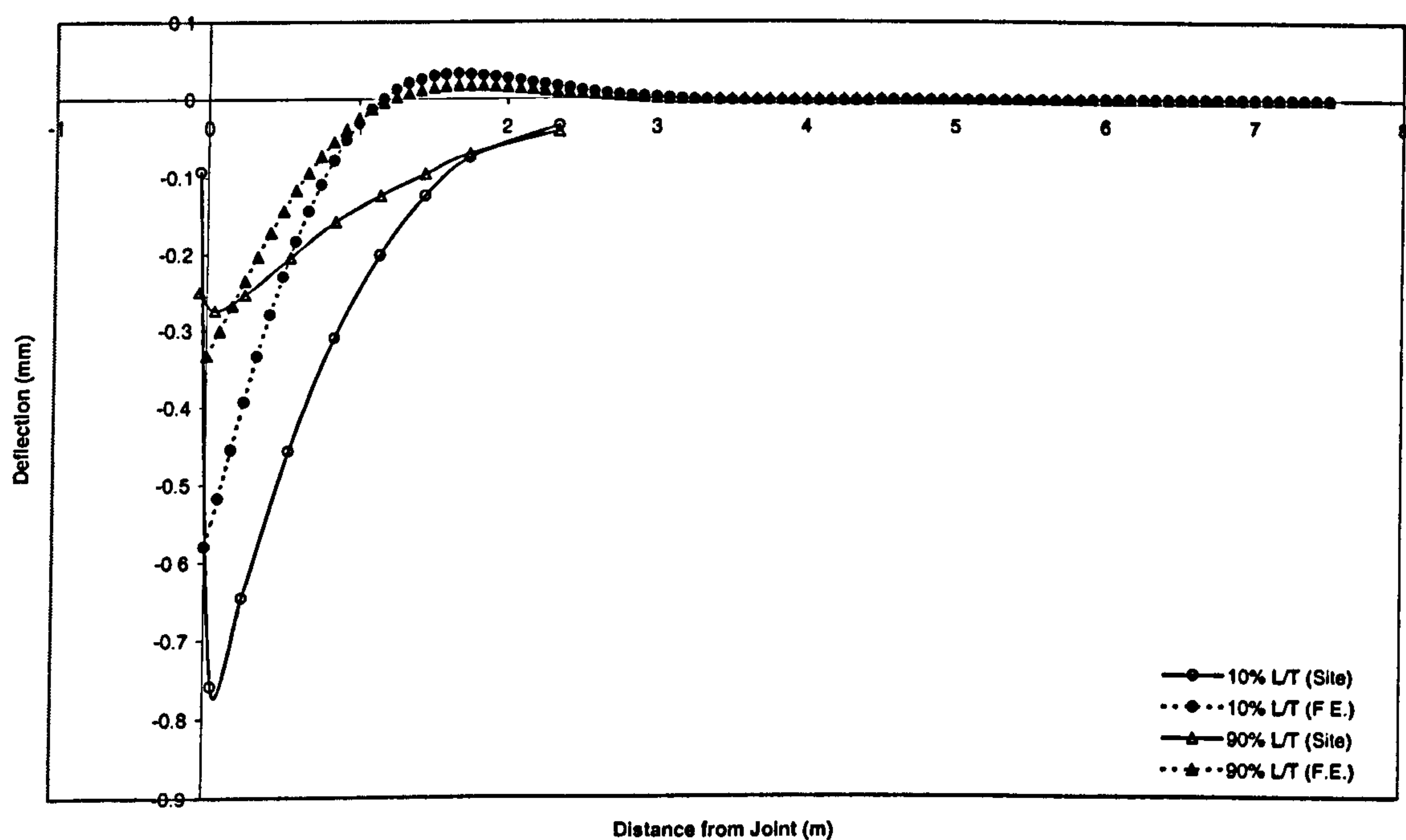


Figure 7.11a – Comparison of deflection bowls between the Daventry Finite Element model and in-service slab response

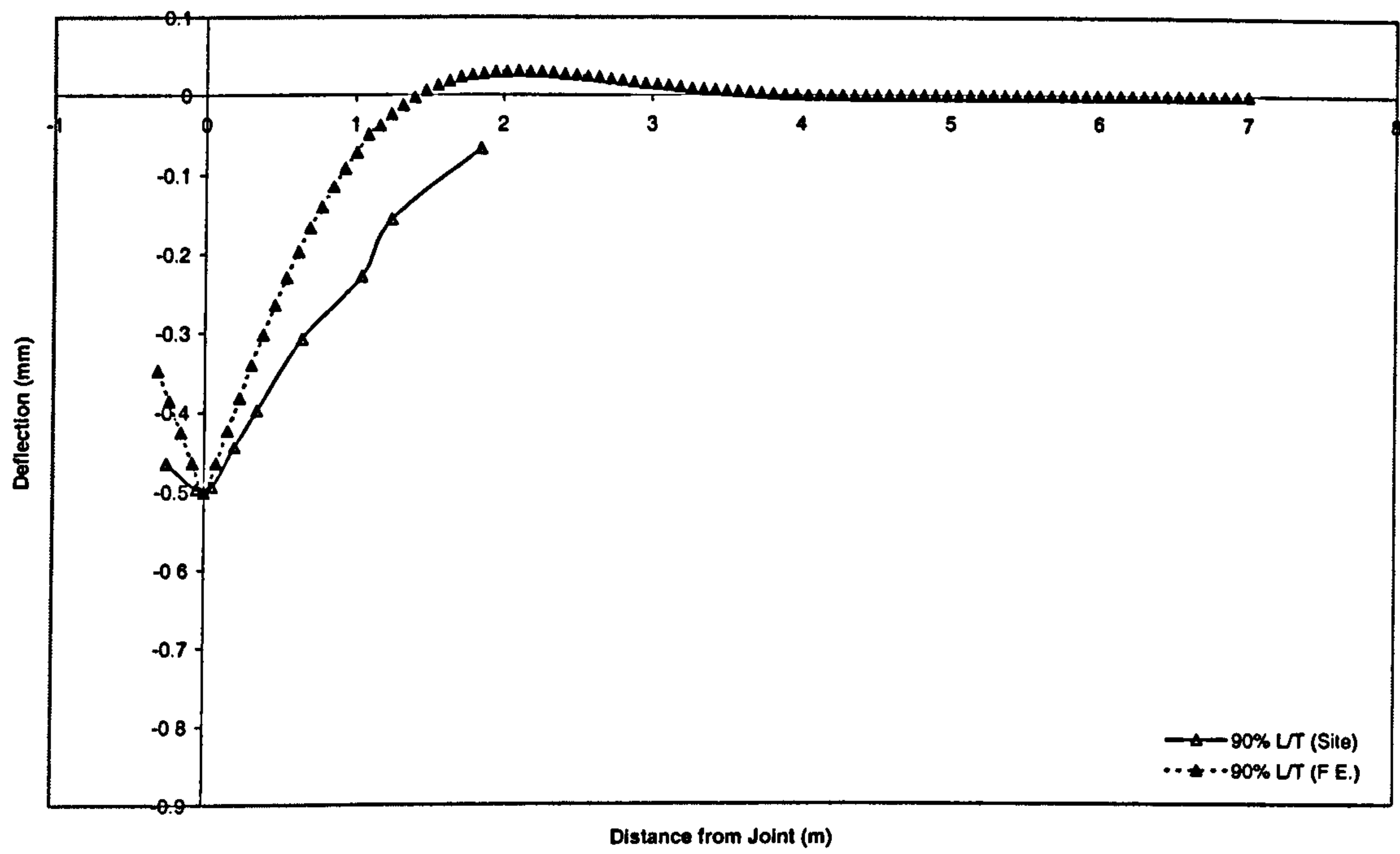


Figure 7.11b – Comparison of deflection bowls between the Lutterworth Finite Element model and in-service slab response

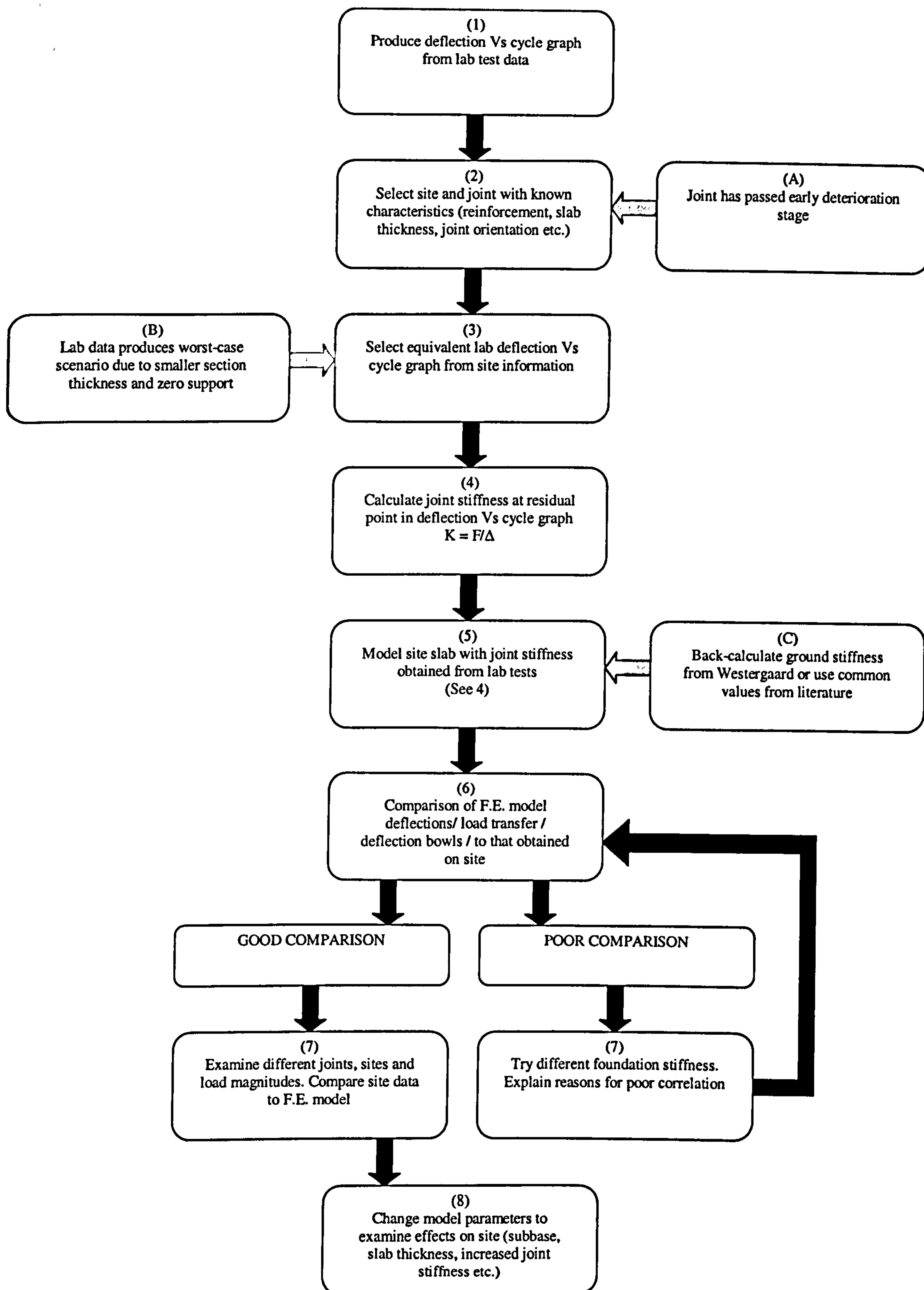


Figure 7.12 – Process diagram for establishing slab response using laboratory cyclic load testing and the Finite Element model

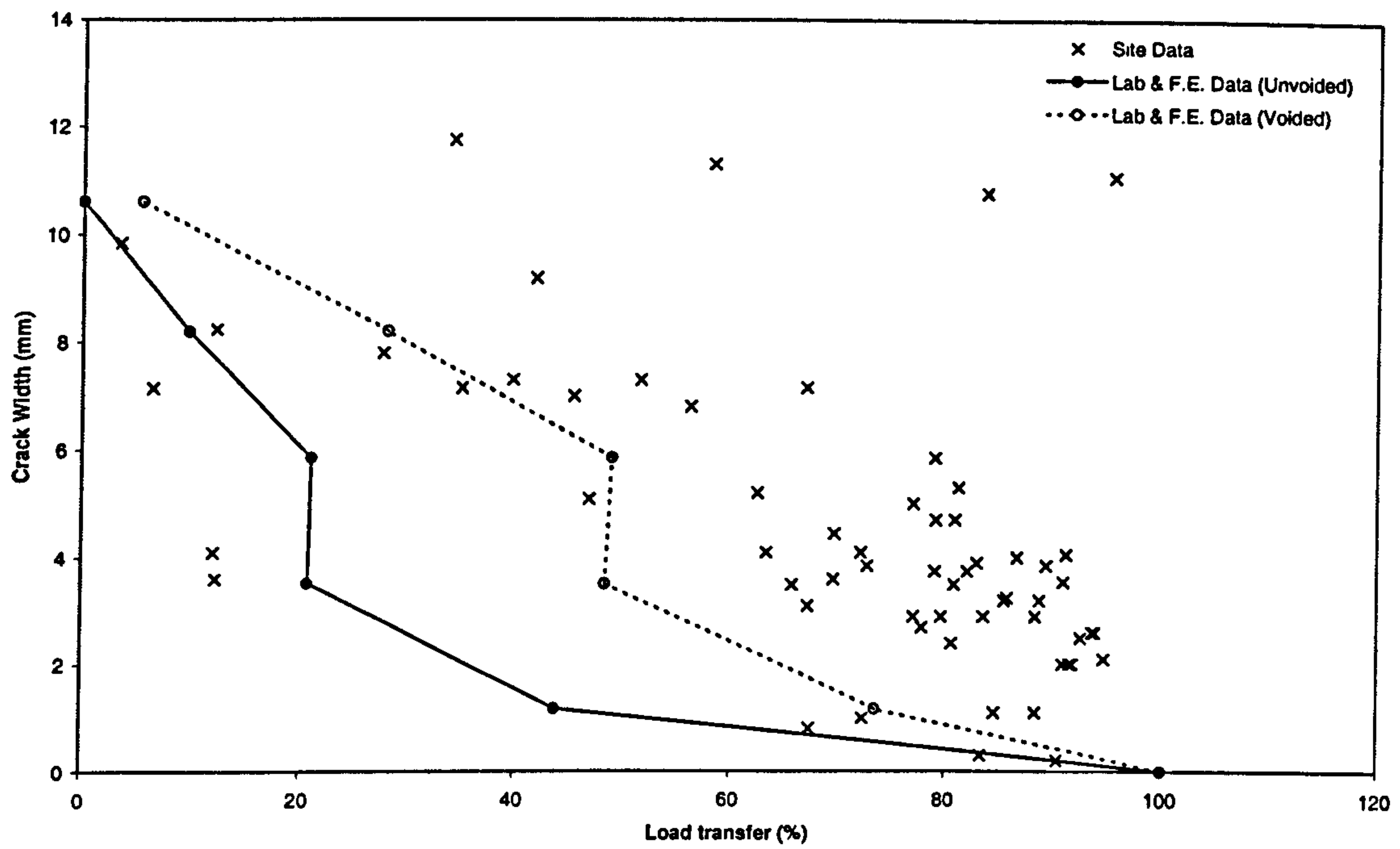


Figure 7.13 – Comparison of predicted and actual surface crack width/load transfer behaviour for Daventry

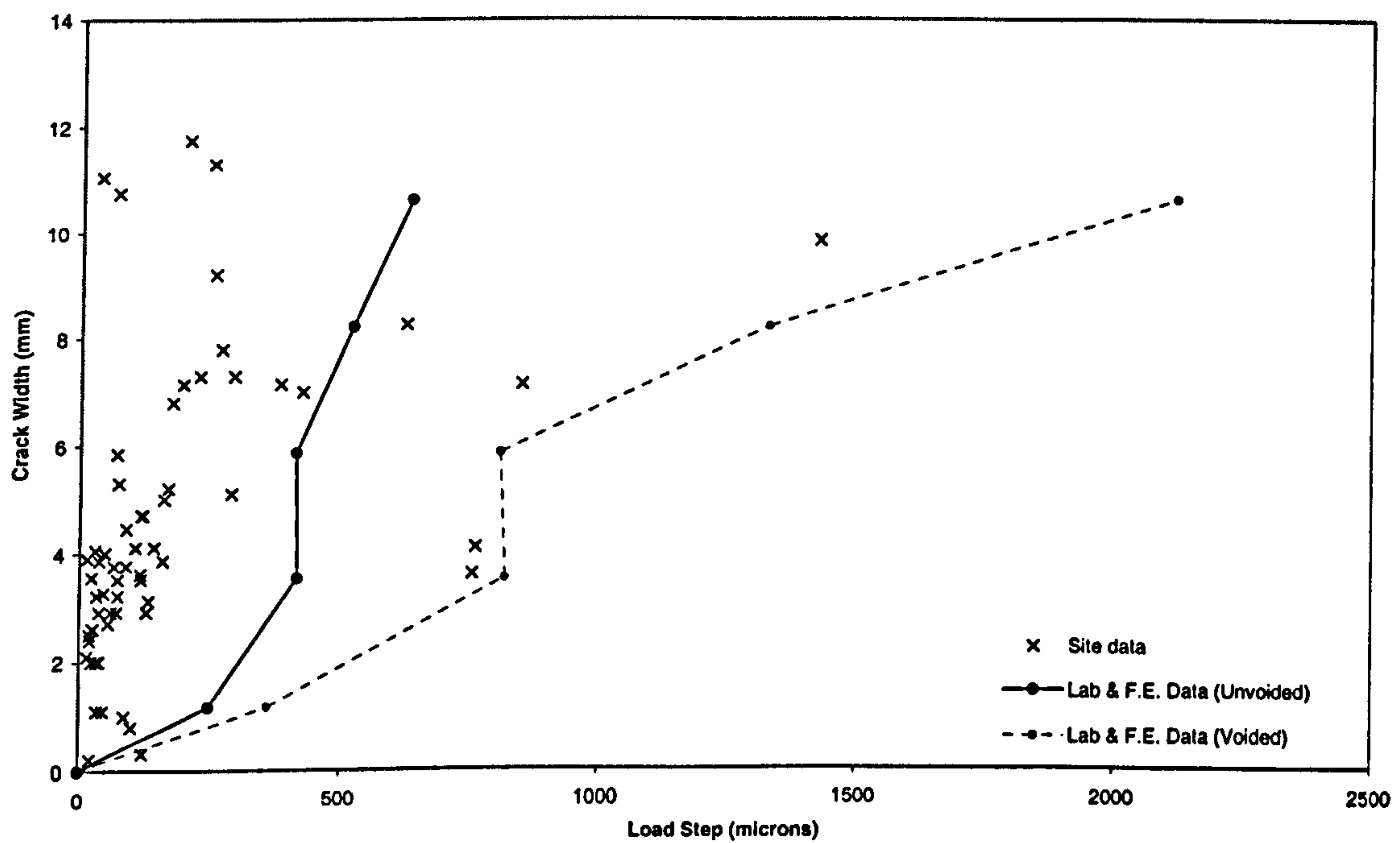


Figure 7.14 – Comparison of predicted and actual surface crack width/load step behaviour for Daventry

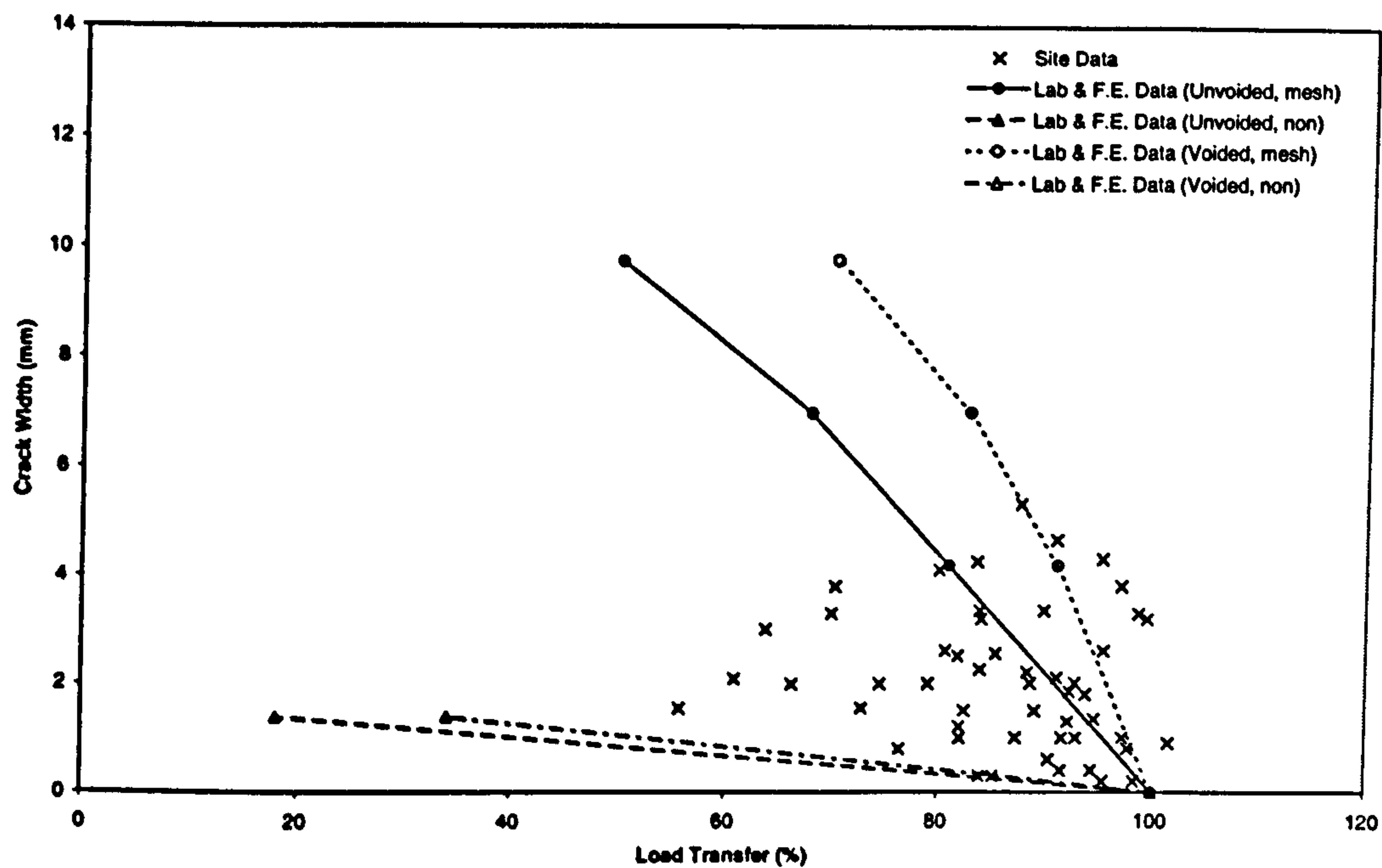


Figure 7.15 – Comparison of predicted and actual surface crack width/load transfer behaviour for Lutterworth

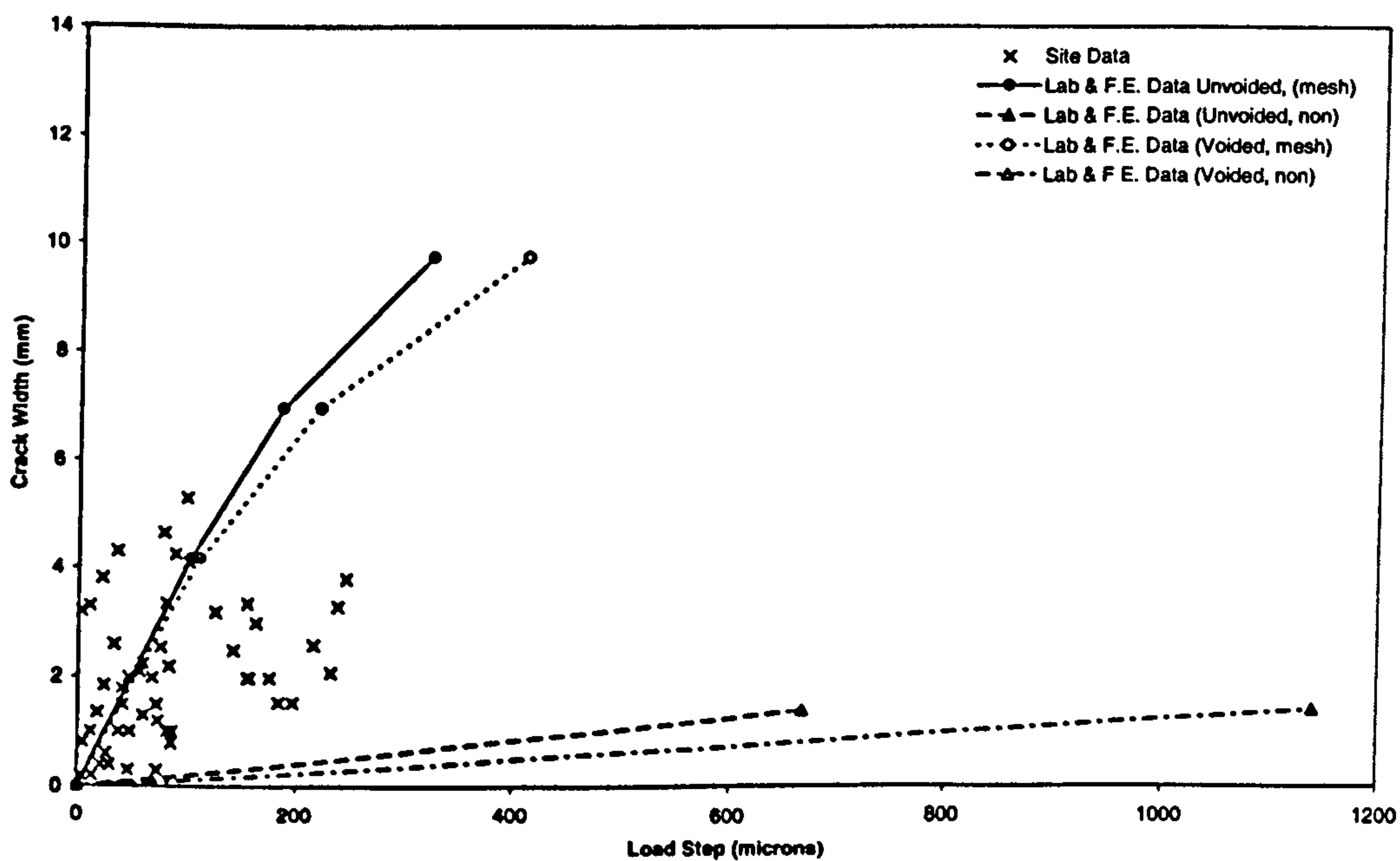


Figure 7.16 – Comparison of predicted and actual surface crack width/load step behaviour for Lutterworth

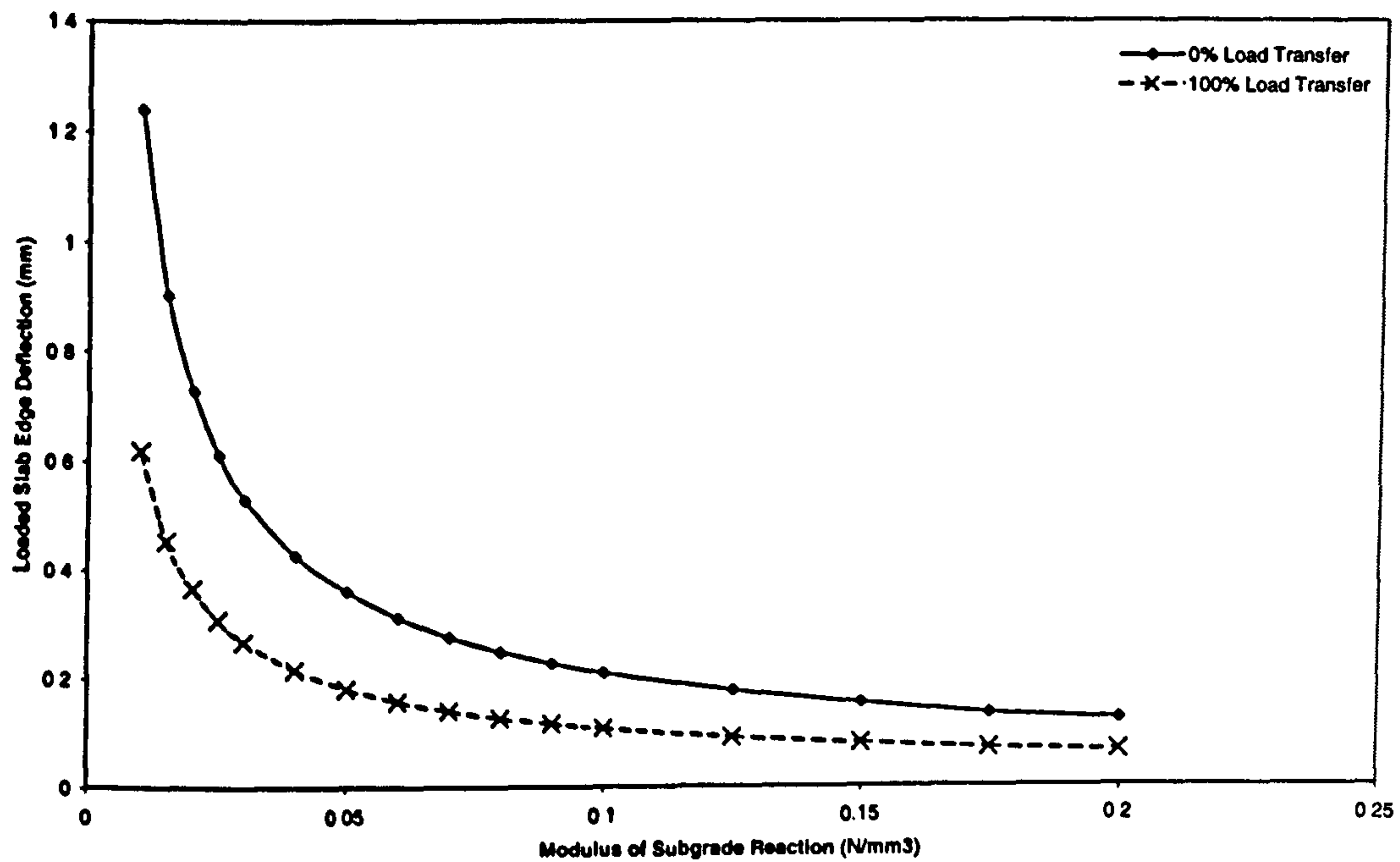


Figure 7.17 – Effect of modulus of subgrade reaction on the loaded slab edge deflection for a typical in service slab

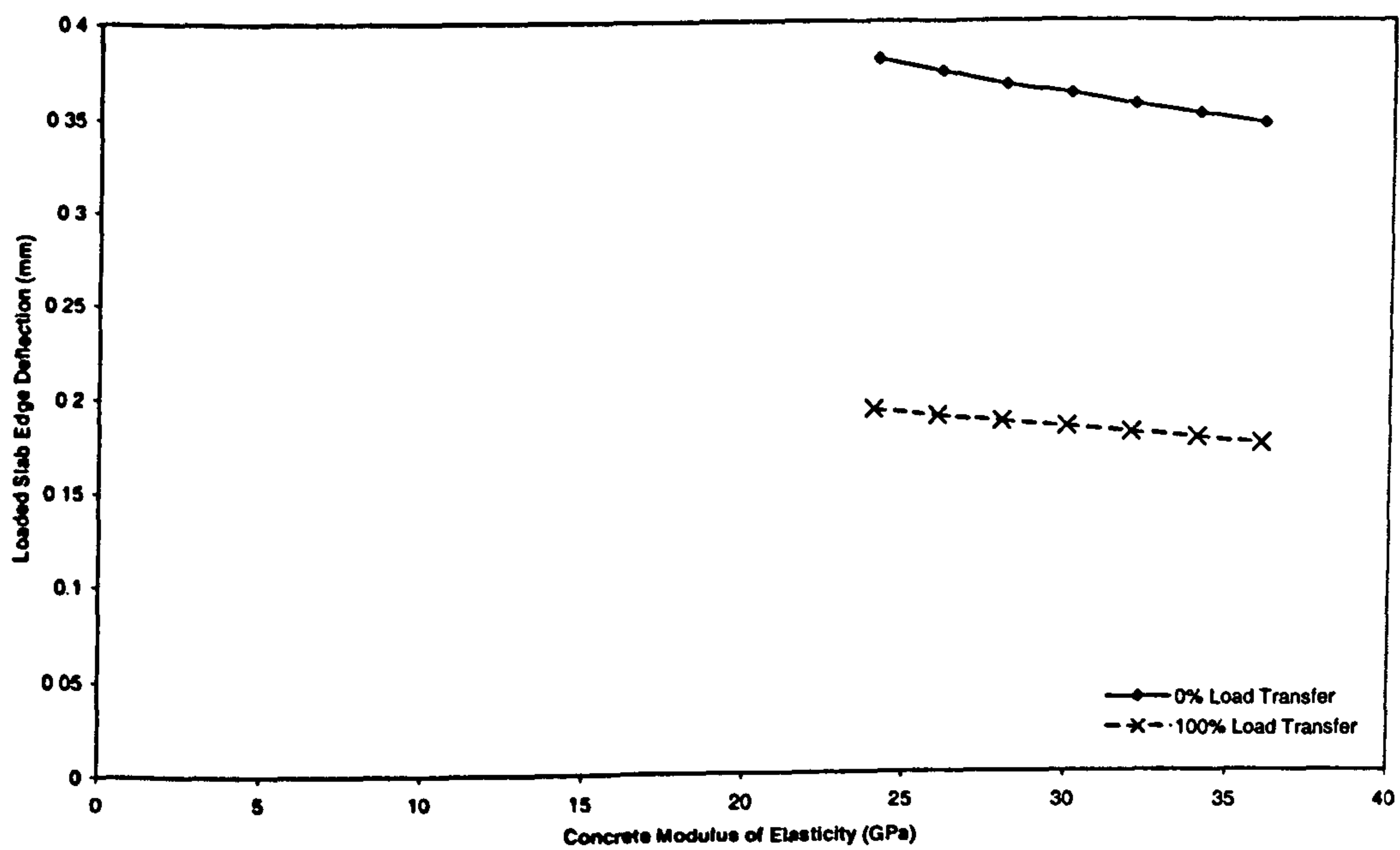


Figure 7.18 – Effect of concrete modulus of elasticity on the loaded slab edge deflection for a typical in service slab

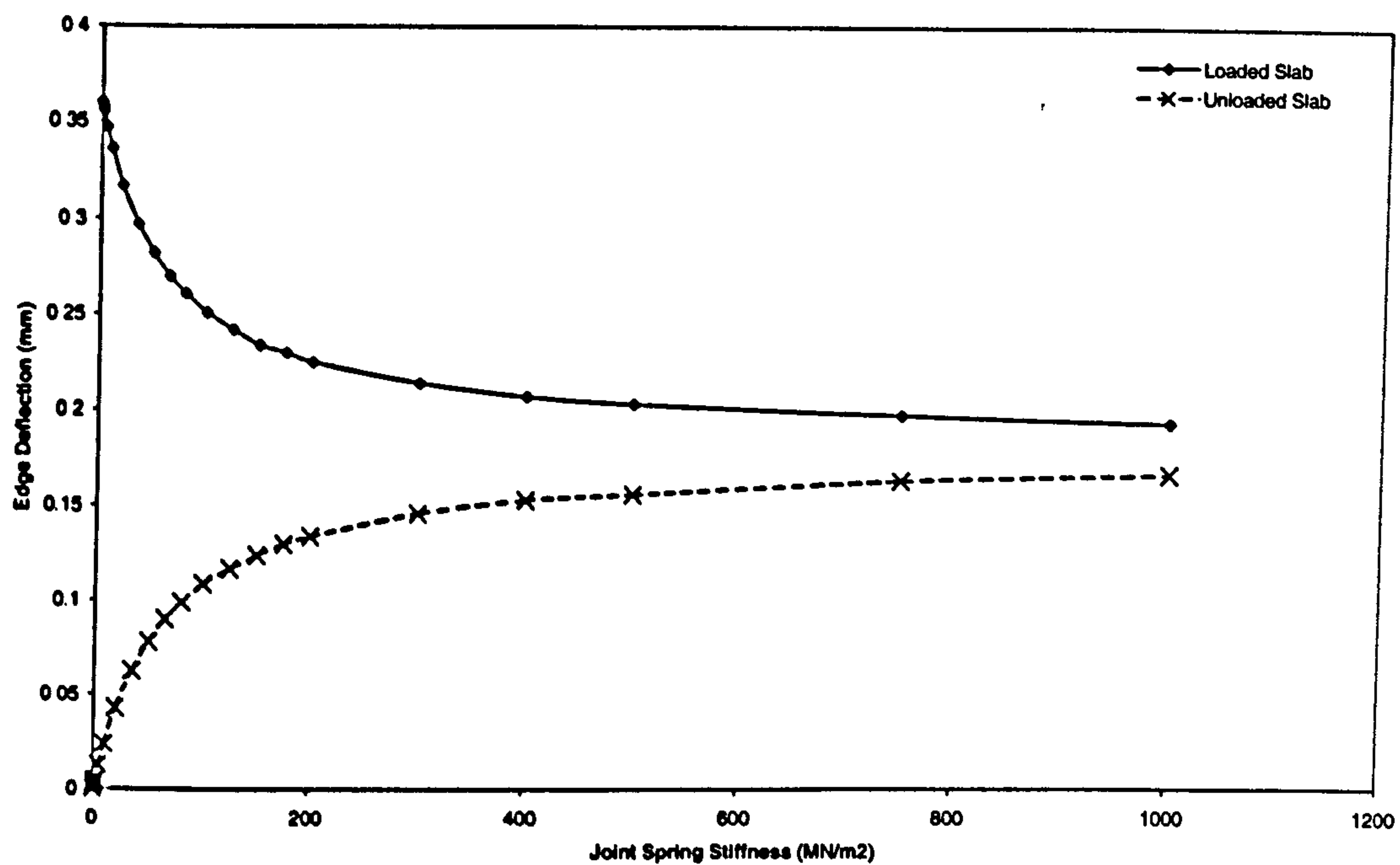


Figure 7.19 – Effect of joint spring stiffness on slab edge deflections for a typical in service slab

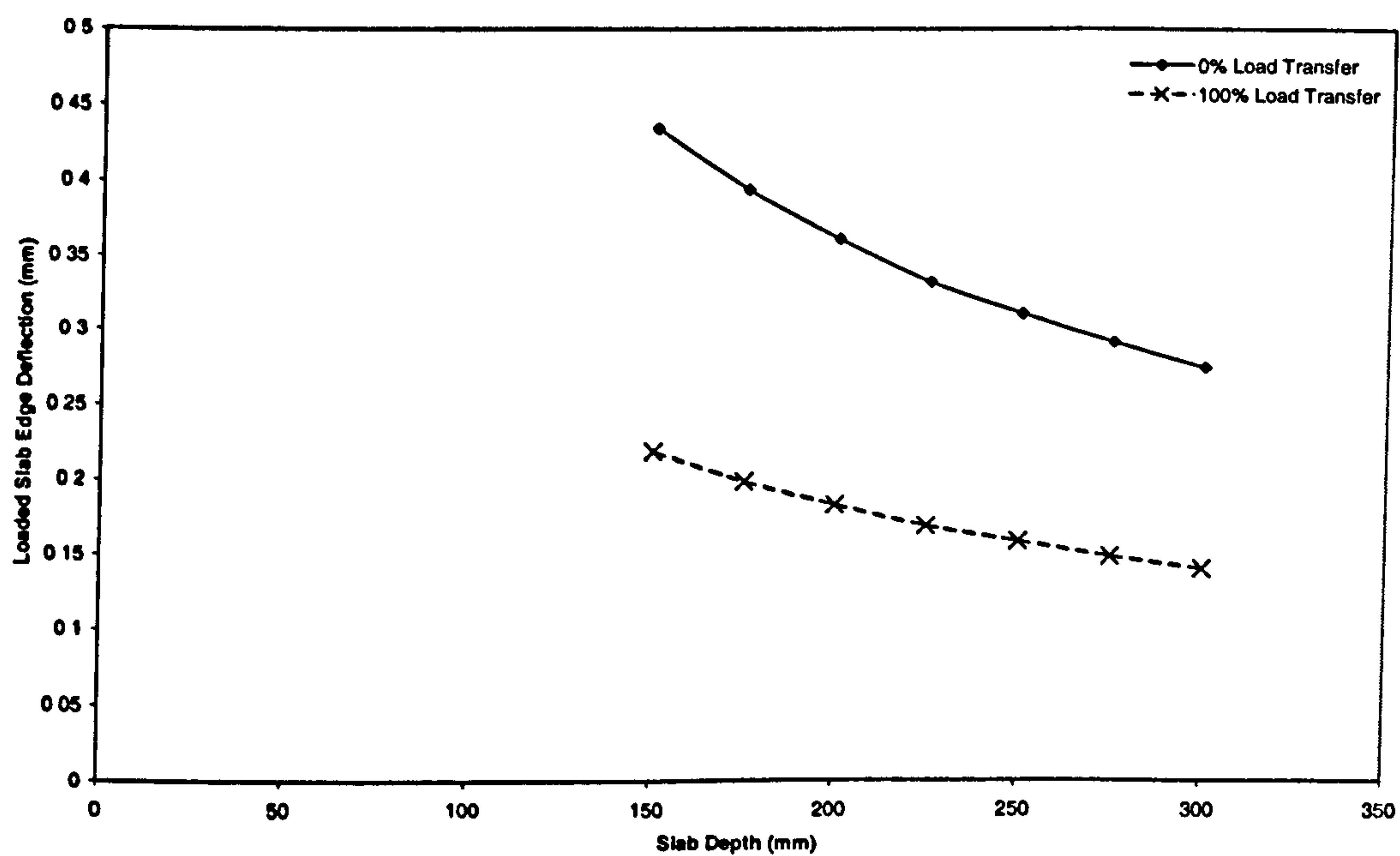


Figure 7.20 – Effect of slab depth on the loaded slab edge deflection for a typical in service slab

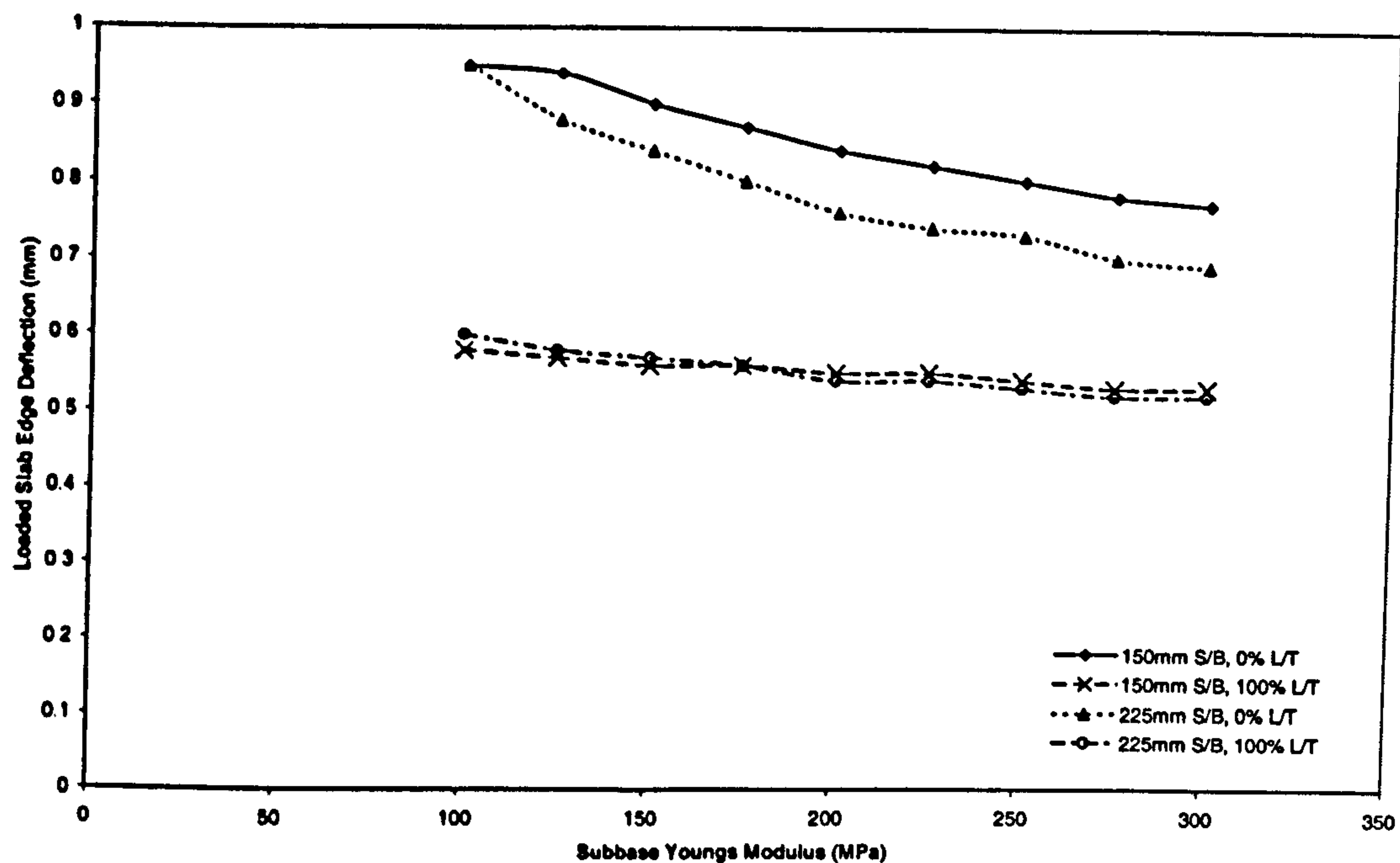


Figure 7.21 – Effect of subgrade modulus of elasticity on the loaded slab edge deflection for a typical in service slab

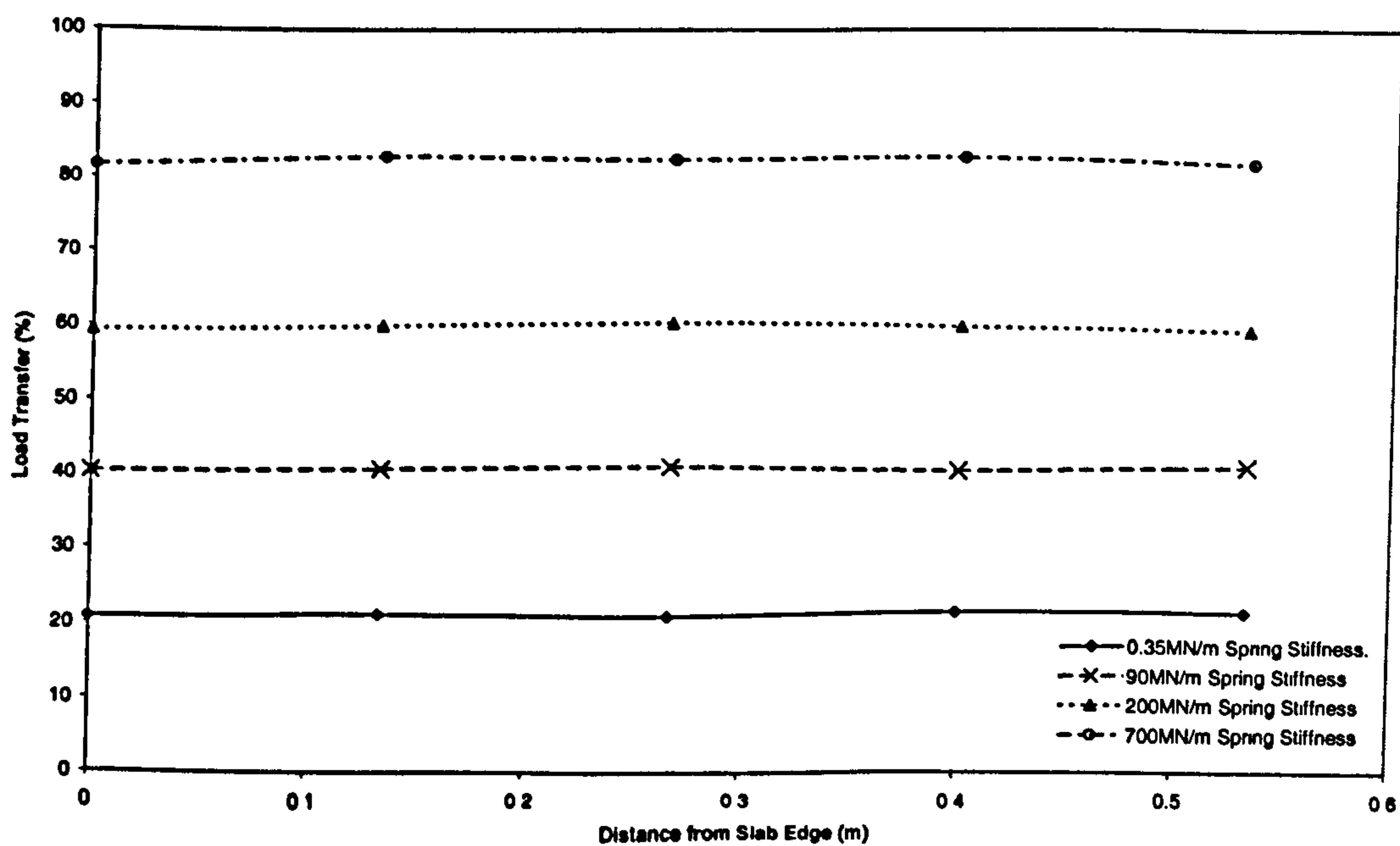


Figure 7.22 – Effect load position on load transfer for a typical in service slab

8. CONCLUSIONS AND RECOMMENDATIONS FOR FURTHER WORK

8.1 Overview

A review of the current documentation and guidance on concrete floor/pavement construction and maintenance has highlighted the need for further understanding of the behaviour of load transfer mechanisms within induced joints and cracks. Much of the literature reviewed has examined only low cycle, high intensity fatigue loading, ignoring the constant repetitive action from vehicular traffic.

This chapter presents the conclusions from the site, laboratory and analytical model testing of a variety of joint properties to assess their effect on fatigue and slab response. The research has encapsulated the initial assessment of crack/joint geometries and the associated slab response from real site conditions. This has enabled simulation of the loading regime on test specimens within the laboratory, and resulted in the development of an analytical model to predict slab behaviour under a number of varying parameters and conditions.

8.2 Site Testing

Measurements from site utilising embedded strain gauges, drilled cores and surface profile approximation have established that differential shrinkage creates a significantly larger crack width at the slab surface than at the base. This is shown to vary depending on the category of joint and the placement and type of reinforcement used in the slab.

Slab deflection from the impact of load was monitored with the use of dynamic plate devices. The comparison between each device was good with respect to load transfer. However, deflection related values did not respond in direct relation to the increase in load magnitude. This was caused by voiding underneath the slab edges and the free-slip phenomenon, created from degradation of the crack face.

Correlation was found to exist between load transfer, load step, and edge cantilever. The variation in results changed depending on which parameters and which site were being examined, with disparity from the idealised plot caused by voiding and free-slip.

The relationship between slab deflection behaviour and surface crack width measurement was poor, although overall trends could be observed. This was due to the limited knowledge of the crack geometry, with surface measurements alone used as the comparable measure, already shown to only partially signify the true status.

Preloading of the slab proved to be highly influential in altering deflection response. Splitting the data into similarly loaded slab areas produced better comparison in results, especially when compared against crack width.

8.3 Laboratory Testing

A laboratory test rig was developed to investigate the high cycle load transfer degradation of a number of small-scale specimens. Unlike many previous tests the geometries used were typical of those found during the real slab joint and crack analysis, with most being 'V' shaped, although several parallel cracks were also tested for comparison.

Plots of the increase in differential displacement over 250,000 loading cycles were obtained for a variety of concrete and reinforcement specifications. A rapid amplification in displacement over the first few thousand cycles was found, caused by degradation of the fine aggregate. After this there was a period of little change whereby larger aggregate particles began to bear upon one another. In those specimens where failure transpired a third section of rapidly increasing differential displacement occurred. Here, the aggregate cracked and debonded from the remainder of the concrete, creating higher stresses across the crack face and therefore quicker degradation.

Parallel cracks were found to deteriorate at a much faster rate than 'V' shaped cracks, with widths above 1mm unable to resist failure for the entire 250,000 cycles, highlighting the importance of correct geometry selection.

The inclusion of steel fibres was found to enhance the load transfer mechanism in two main ways. The restraint to micro cracking prevented degradation and spalling of the crack face leading to retainment of aggregate interlock. Secondly, the fibre itself provided some load bearing through dowelling across the crack interface. The fibre was generally found to pull out of the concrete; however, as deflection increased fatigue took place leading to fibre snapping.

Increasing the quantity of fibres from 20 to 40kg/m³ enabled surface crack width to be opened further before failure was initiated, and created a minor reduction in magnitude of differential deflection. Increasing the aspect ratio of the fibre was also found to increase the resistance to failure; however, the results established that it was the change in number of fibres crossing the joint that was having the effect, rather than modification of either length or diameter.

Introducing steel A142 mesh, or 7mm reinforcing bar produced significant reductions in the differential deflection over all the other reinforcement types tested, regardless of the number of cycles applied. For the entire range of crack openings there was no significant change between the start and end deflections and visual observations showed little sign of fatigue.

The effect of load was highly influential in the rate of deterioration with all specimens loaded at 2kN (125kN/m²) showing very little fatigue damage. However, when increased to the standard 4kN (250kN/m²) load this changed dramatically, with 6kN (375kN/m²) causing failure in all specimens other than that with the lowest crack width.

8.4 Analytical Modelling

A finite element model developed using the DIANA software package was assessed against the Westergaard (1926 and 1947) equations. When simulating the equation assumptions of a long slab with a shallow depth it produced good comparison. This also agreed well with results obtained from other researcher's work when using other finite element packages such as ILLISLAB, proving the method to be adequate in simulating slab response.

A model of the laboratory test facility produced results identical to that obtained from the standard spring equation. The introduction of a model foundation material reduced the deflection by over ten times on a single analysis, showing that during a set number of cycles the damage caused by fatigue would be significantly reduced if some level of support was introduced.

Models representing slab geometries provided accurate comparison to the load transfer and load step data obtained from site throughout the entire range of spring stiffness. The small variation found was unavoidable, due to the unpredictable nature of site foundations. When examining the individual slab edge deflections the correlation with the

analytical model was less precise, however this was improved when comparing sites with stronger foundations.

Estimation of site slab response was derived using spring stiffness from the laboratory tests for the associated crack width and reinforcement type. The results produced deflections that matched well with those achieved from site, and enabled upper and lower bounds for slab behaviour to be developed.

The effects of material and geometric variations were tested to examine which were most influential in respect to slab response. Increases in soil strength, joint stiffness and slab depth all produced significant reductions in the edge deflection; however, concrete strength and load position had negligible effects.

8.5 Final Comments

This research has introduced a method of determining slab deflection response in relation to load transfer by means of small scale laboratory testing and finite element modelling. Utilising data collected from in-service sites the method has been validated and shown to produce reasonable correlation to the measured values under a variety of conditions. Similar to previous research, crack geometry has been found to be a highly influential factor controlling the efficiency of the slab, thus making its accurate measurement vital. This has included the assessment of 'V' shaped cracking which was discovered to be more predominant on site than the commonly assumed parallel crack. The introduction of reinforcement into the concrete was shown to vastly improve the resistance to deflection; with steel fibres providing reasonable comparison to steel mesh when used in the correct quantities.

The concept of small scale testing facilitates cost efficient examination of load transfer mechanisms, thus providing the designer with a simple method of assessing the behaviour of joints and cracks under a number of structural and environmental conditions.

8.6 Recommendations for Further Work

To enable typical crack geometries to be established and used in design and maintenance analysis, additional monitoring of crack widths is needed. The use of strain gauges has been shown to provide reliable data; however, an increased number should be placed throughout depth to enable the full geometry to be determined.

Further deflection testing undertaken on both site and in the laboratory would allow the effect of voiding and loose material under the slab edges to be examined. Comparison between the Prima and FWD requires completion under controlled slab conditions to determine correlation between the two devices and to examine whether the variation found in site results is caused solely by the change in load applied to the slab. The relationship between parameters such as load transfer, load step, cantilever deflection, absolute deflection and crack width can then be determined, incorporating the effect of pre-load.

A statistical survey of load sources should be carried out on a number of industrial floor slabs, external hardstandings and pavements. This would provide information on typical load magnitude (i.e. vehicle type and weight) and number of applications across joints, to enable representations to be modelled and therefore predictions made of slab deterioration. Without this knowledge the simulations made both in analytical modelling and laboratory testing may be inaccurate.

The finite element model could be further developed to incorporate the subbase and subgrade as separate entities. This may then be compared to site behaviour where the foundation stiffness is well known to enable the comparison and accuracy of the model to be determined. Values of joint stiffness obtained from the laboratory tests containing the relevant crack and material properties could then be inserted into the model to enable its effect on slab response to be calculated. A model of spring stiffness changes with associated crack opening may be used within the Bishop (2001) early age behaviour model to automatically predict the stiffness and relevant performance. This could incorporate a load cycle plot, obtained from the laboratory tests, to enable the degradation and associated effects to be analytically examined over time. The model may then be enhanced to incorporate three-dimensional elements, making the analysis of corner deflections possible.

A combination of these recommendations would enable a simulation of deflection response for the majority of slabs using finite element software directly from the input of known site parameters, and small scale testing of the load transfer mechanism. If undertaken for many different scenarios predictions of slab behaviour under a variety of geometric and environmental conditions will be generated.

9. REFERENCES

- Abdel-Maksoud, M.G. (2000), "Behaviour of Concrete Joints Under Cyclic Shear", PhD Thesis, University of Illinois, USA.
- Abdel-Maksoud, M.G., Hawkins, N., Barenberg, E.J. (1997). "Behaviour of Concrete Joints under Cyclic Shear." American Society of Civil Engineers, August 1997, pp 190-204.
- Abdul-Wahab, H.M.S. (1992), "Strength of Vertical Joints with Steel Fiber Reinforced Concrete in Large Panels", ACI Structural Journal, Vol.89, No.4, pp367-374.
- ACI Committee 302.1R-96 (1996), "Guide for Concrete Floor and Slab Construction", ACI Manual of Concrete Practice Part 2, American Concrete Institute, Farmington hills, Michigan.
- ACI Committee 360R-92 (1992), "Design of Slabs on Grade", ACI Manual of Concrete Practice Part 2, American Concrete Institute, Farmington hills, Michigan.
- ACI Committee 360 (2000), "Draft Copy – Chapter 10", American Concrete Institute, Farmington hills, Michigan.
- ACI Committee 544 (1988), "Design Considerations for Steel Fiber Reinforced Concrete" ACI Structural Journal, Vol.85, No.5, pp 563-580.
- ACIFC and the Concrete Society (1999). "Steel Fibre Reinforced Concrete Industrial Ground Floors: An Introductory Guide" Concrete, Vol.33, No.10.
- Al-Nasra, M. and Wang, L.R.L. (1994), "Parametric Study of Slab-on-Grade Problems due to Initial Warping and Point Loads", ACI Structural Journal, Vol.91, No.2, pp 198-210.
- American Association of State Highway and Transportation Officials (1986), "AASHTO Guide for Design of Pavement Structures", American Association of State Highway and Transportation Officials, Washington D.C.

American Concrete Institute (1977), "Hot Weather Concreting", Journal of the American Concrete Institute, Vol.74, pp 317-332.

Armaghani, J.M. (1993), "Factors Affecting Performance of Concrete Pavements", 5th International Conference on Concrete Pavement Design and Rehabilitation, 20-22nd April, Purdue University, West Lafayette, Indiana, USA.

Armaghani, J.M., Lybas, J.M., Tia, M. and Ruth, B.E. (1986). "Concrete Pavement Joint Stiffness Evaluation.", Transportation Research Record, Vol.1099, Transportation Research Board, pp 22-36.

Arnold, S. (2002), "Report of the 2nd Meeting of the Industry Liaison Group on Load Transfer across Cracks/Joints in Concrete Slabs on Grade", 8th April 2002, Loughborough University, England.

Atkins, H.N. (1997), "Highway Materials, Soils and Concretes", 3rd ed., Prentice Hall, Upper Saddle River, N.J., USA.

Balaguru, P.N. and Shah S.P. (1992), "Fiber-Reinforced Cement Composites", 1st ed., McGraw-Hill Inc., USA.

Barenberg, E.J. and Zollinger D.G. (1990), "validation of Concrete Pavement Responses using Instrumented Pavements." Transportation Research Record, Vol. 1286, Transportation Research Board, pp 67-77.

Barnbrook, G. (2000), "Overview of Industrial Concrete Floor Developments", Seminar on Developments in Industrial Ground Floor Slabs, 31st October 2000, Aston University, England.

Bazant, Z P. and Gambarova P. (1980), "Rough Cracks in Reinforced Concrete" Journal of the Structural Division, ASCE, Vol.106, No.4, pp 819-842.

Beckett (1999), "Corner and Edge Loading on Concrete Industrial Ground Floors Reinforced with Steel Fibres" Concrete, Vol.33, No.10, pp 22-24.

- Beckett, D. (2000), "Thickness Design of Concrete Industrial Ground Floors - Notes for Guidance", Seminar on Developments in Industrial Ground Floor Slabs, 31st October 2000, Aston University, England.
- Benkelman, A.C. (1933), "Tests of Aggregate Interlock at Joints and Cracks" Engineering News Record Vol.3, No.8, 227-232.
- Bhatti, M.A., Barlow J.A and Stoner, J.W. (1996), "Modelling Damage to Rigid pavements Caused by Subgrade Pumping" Journal of Transportation Engineering, Vol.122, pp 12-21.
- Bhatti, M.A., Molinas-Vega, I. And Stoner, J.W. (1998), "Nonlinear Analysis of Jointed Concrete Pavements" Transportation Research Record Vol.1629, pp 50-57
- Bischoff, P. Valsangker, A.J, and Irving, J. (1997), "A Performance Evaluation of Steel Fibre Reinforced Concrete Slabs on Grade", Asia-Pacific Speciality Conference on Fibre Reinforced Concrete, 28-29th August 1997, Singapore.
- Bishop, J. (2001), "The Early Age Behaviour of Concrete Industrial Ground Floor Slabs", PhD Thesis, Loughborough, England.
- Bodocsi, A., Minkarah, I.A. and Arudi, R.S. (1994). "Effect of pavement Variables on Average Joint Deflections in Experimental Concrete Pavement" Transportation Research Record, Vol.1449, Transportation Board, pp 182-188.
- BS 1881: Part 108 (1983). "Method for Determination of Compressive Strength of Concrete", British Standards Institution, Milton Keynes.
- BS 1881: Part 116 (1983). "Method for Determination of Compressive Strength of Concrete", British Standards Institution, Milton Keynes.
- Buch, N. (1999), "Factors Affecting Load Transfer across Transverse Joints in Jointed Concrete Pavements", ASTM Special Publications, Vol.181, No.3, pp 43-64.
- Buch, N., Frabizzio, M.A. and Hillier J.E. (2000). "Impact of Coarse Aggregates on Transverse Crack Performance in Jointed Concrete Pavements", ACI Materials Journal, Vol.97, No.3, pp 325-331.

- Chandler, J.W.E. and Neal, F.R. (1988). "The Design of Ground Supported Industrial Floor Slabs", Interim Technical Note 11, British Cement Association, Slough.
- Channakeshava, C., Barzegeer, F. and Voyiadjis, G.Z. (1993), "Nonlinear FE Analysis of Plain Concrete Pavements with Dowelled Joints", *Journal of Transportation Engineering*, Vol.119, No.5, pp 763-781.
- Chou, Y.T. (1983), "Comparative Analysis of Rigid Pavements." *Journal of Transportation Engineering*, Vol.109, No.5, pp 669-687.
- Chou, Y.T. (1989), "Failure of Concrete Pavements in Test Tracks." *Journal of Transportation Engineering*, Vol.115, No.5, pp 493-505.
- Colley, B.E. and Humphrey H.A. (1967), "Aggregate Interlock at Joints in Concrete Pavements", Development Department Bulletin D124, Portland Cement Association, Illinois.
- Colley, B.E. and Nowlen J.W. (1958), "Performance of Subbases for Concrete Pavements under Repetitive Loading", Development Department Bulletin D23, Portland Cement Association, Illinois.
- Concrete Society (2003), "Concrete Industrial Ground Floors - A Guide to design and Construction", Technical Report No.34, 3rd ed. Crowthorne, UK.
- Critchell, P.L. (1958), "Joints and Cracks in Concrete", 2nd ed., Elsevier Applied Science, London.
- Croney, D. and Croney P. (1997), "Design and Performance of Road Pavements", 3rd ed., McGraw-Hill Inc., USA.
- Crovetti, J.A. and Darter M. I. (1985), "Void Detection for Jointed Concrete Pavements", *Transportation Research Record* Vol.104, Transportation Research Board, pp 59-68.
- Cudworth, D. (2000), "The Dangers of Ignoring Asymmetric Dynamic Loading in Industrial Floor Slabs." *Concrete*, Vol 35, No.9, pp 25-27.

Chandler, J.W.E. and Neal, F.R. (1988). "The Design of Ground Supported Industrial Floor Slabs", Interim Technical Note 11, British Cement Association, Slough.

Channakeshava, C., Barzege, F. and Voyiadjis, G.Z. (1993), "Nonlinear FE Analysis of Plain Concrete Pavements with Dowelled Joints", Journal of Transportation Engineering, Vol.119, No.5, pp 763-781.

Chou, Y.T. (1983), "Comparative Analysis of Rigid Pavements." Journal of Transportation Engineering, Vol.109, No.5, pp 669-687.

Chou, Y.T. (1989), "Failure of Concrete Pavements in Test Tracks." Journal of Transportation Engineering, Vol.115, No.5, pp 493-505.

Colley, B.E. and Humphrey H.A. (1967), "Aggregate Interlock at Joints in Concrete Pavements", Development Department Bulletin D124, Portland Cement Association, Illinois.

Colley, B.E. and Nowlen J.W. (1958), "Performance of Subbases for Concrete Pavements under Repetitive Loading", Development Department Bulletin D23, Portland Cement Association, Illinois.

Concrete Society (2003), "Concrete Industrial Ground Floors - A Guide to design and Construction", Technical Report No.34, 3rd ed. Crowthorne, UK.

Critchell, P.L. (1958), "Joints and Cracks in Concrete", 2nd ed., Elsevier Applied Science, London.

Croney, D. and Croney P. (1997), "Design and Performance of Road Pavements", 3rd ed., McGraw-Hill Inc., USA.

Crovetti, J.A. and Darter M. I. (1985), "Void Detection for Jointed Concrete Pavements", Transportation Research Record Vol.104, Transportation Research Board, pp 59-68.

Cudworth, D. (2000), "The Dangers of Ignoring Asymmetric Dynamic Loading in Industrial Floor Slabs." Concrete, Vol 35, No.9, pp 25-27.

- Cudworth, D. (2001), "Joint Load Transfer in Dynamic Conditions", Floors Forum, 10th January 2001, Loughborough University, England.
- Cudworth, D. (2003), "Detecting Voids Beneath Concrete Pavements using Surface Deflection" Proceedings of the Symposium on Transportation Geotechnics, 11th September 2003, Nottingham Trent University, UK.
- Darter, M.I., LaCoursiere, S. A and Smiley, S.A. (1979), "Structural Distress Mechanisms in Continuously Reinforced Concrete Pavement." Transportation Research Record, Vol.175, Transportation Research Board, pp 1-7.
- Davich, P., (2000), "Prima 100 - Mn/DOT Testing procedure", Minnesota Department of Transportation, Office of Materials and Road Research, Minnesota Road Research Section, Minnesota, USA.
- Davids, W.G., Turkiyyah, G. M. Mahoney, J.P. (1998), "EverFE - Rigid pavement Three-Dimensional Finite Element Analysis Tool" Transportation Research Record, Vol.1629, Transportation Research Board, pp 41-49.
- Deacon, R.C. (1990), "Fibres for Floors." Concrete, Vol.24, No. 4, pp 19-20.
- Deen, R.C., W.V. Azevedo, Rahal, A.S. and Havens, J.H. (1980), "Cracking in Concrete Pavements", Transportation Engineering Journal, Vol.106, No.2, pp 155-169.
- Duncan, J.M., Monismith, C. L. and Wilson, E.L. (1968), "Finite Element Analyses of Pavements.", Highway Research Record, Vol.228.
- Fleming, P.R. (2000). "Impact Assessment of Layer Granular Materials", PhD Thesis, Loughborough University, England.
- Frabizzio, M.A. and Buch N.J. (1999) "Performance of Transverse Cracking in Concrete Pavements", Journal of Performance of Constructed Facilities, Vol.13, No.4, pp 172-180.
- Friberg, B.F. (1938) "Design of Dowels in Transverse Joints of Concrete Pavement" Proceedings of the American Society of Civil Engineers, Vol.64, No.9, pp 1809-1828.

- Fwa, T.F., Shi, X.P. and Tan, S.A. (1996), "Use of Pasternak foundation model in concrete pavement analysis" *Journal of Transportation Engineering*, Vol. 122, No.4, pp 323-328.
- FWD Users Group (2001). Electronic mail, FWD Users Mailing 727/738/742/744/745.
- Gregory, J.M. (1984) "Continuously Reinforced Concrete Pavements", *Proceedings of the Institution of Civil Engineers*, Vol.76, No.1, pp 449-472.
- Grzybowski, M. and Shah S.P. (1989), "Model to Predict Cracking in Fibre Reinforced Concrete due to Restrained Shrinkage.", *Magazine of Concrete Research*, Vol.41, No.148, pp 125-135.
- Gulden, W. and Brown D. (1985), "Establishing Load Transfer in Existing Jointed Concrete Pavements", *Transportation Research Record*, Vol. 1043, Transportation Research Board, pp 23-32.
- Hammons, M.I. (1998), "Validation of Three-Dimensional Finite Element Modelling Technique for Joints in Concrete Airport Pavements", *Transportation Research Record*, Vol.1629, Transportation Research Board, pp 67-75.
- Hannant, D. (1994), "Fibres in Industrial Ground Floor Slabs" *Concrete*, Vol.28, No.1, pp 16-19.
- Harichandrian, R.S., Yeh, M.S. and Baladi, G.Y. (1990), "MICH-PAVE: A Nonlinear Finite Element Program for Analysis of Flexible Pavements", *Transportation Research Record*, Vol.1286, Transportation Research Board, pp 124-131.
- Helwany, S., Dyer, J. and Leidi, J. (1998), "Finite-Element Analyses of Flexible Pavements" *Journal of Transportation Engineering*, Vol.124, No.5, pp 491-499.
- Highways Department (1999), "Falling Weight Deflectometer", HD29/94, Highways Department, pp 5/1-5/10.
- Houde, J. and Mirza, M S. (1974), "A Finite Element Analysis of Shear Strength of Reinforced Concrete Beams", *Shear in Reinforced Concrete*, ACI Symposium, Detroit, USA, pp 103-128.

- Howell, R.D. (1982), "Fibre Reinforced Concrete Proves Worth for Airport Pavements", *Civil Engineering*, Vol. 52, No.5, American Society of Civil Engineers, pp 52-55.
- Hulett, T. (2001), "Floor Choices: Living with Joints and Cracks", *Concrete*, Vol.35, No.3, pp 15-18.
- Ibrahim, O.T. and Luxmoore A. (1987), "Control of Crack Width in Reinforced Concrete Structure by the use of Fibres" *Industrial Problems - Treatment and Control Techniques*, pp 499-511.
- Illston, J.M. (1994), "Construction Materials: Their Nature and Behaviour", 2nd ed., E & FN Spon, London.
- Ioannides, A.M. and Koreveis G.T. (1990), "Aggregate Interlock: A Pure Shear-Load Transfer mechanism." *Transportation Research Record*, Vol. 1286, Transportation Research Board, pp 14-24.
- Ioannides, A.M., Lee, Y. and Darter, M.I. (1990), "Control of Faulting Through Joint Load Transfer Design." *Transportation Research Record*, Vol.1286, Transportation Research Board, pp 49-56.
- Ioannides, A.M., Thompson M.R. and Barenberg, E.J. (1985), "Westergaard Solutions Reconsidered." *Transportation Research Record*, Vol.1043, Transportation Resrach Board, pp 13-23.
- Jackson, D.J., Murphy, M.R. and Wimsatt, A. (1994), "Strategies for Application of the Falling Weight Deflectometer to Evaluate Load Transfer Efficiency at Joints in Jointed Concrete Pavements" *ASTM Special Technical Publication 1198*, Vol.2.
- Jimenez, R., White, R.N. and Gergely, P. (1982), "Cyclic Shear and Dowel Action Models", *Journal of the Structural Division*, American Society of Civil Engineers, Vol.108(ST5), pp 1106-1123.
- Johnston, C.D. (1984), "Steel Fibre Reinforced Pavement Trials" *Concrete International*, Vol.6, No.12, pp 39-43.

- Kelley, E.F. (1939), "Application of the Results of Research to the Structural Design of Concrete Pavements", *Journal of the American Concrete Institute*, Vol.35, pp 437-464.
- Kim, S.M., Won M. and McCullough, B.F. (1998), "Numerical Modelling of Continuously Reinforced Concrete Pavement Subjected to Environmental Loads" *Transportation Research Record*, Vol.1629, Transportation Research Board, pp 76-89.
- Knapton, J. (1999a), "In-situ Concrete Industrial Hardstandings", Thomas Telford, London
- Knapton, J. (1999b), "Single Pour Industrial Floor Slabs", Thomas Telford, London.
- Krauthammer, T. and Western, K.L. (1988), "Joint Shear Transfer Effects on Pavement Behaviour" *Journal of Transportation Engineering*, Vol.114, No.5, pp 505-529.
- Kuo, C.M. (1995), "Three-Dimensional Finite Element Model for Pavement Analysis of Concrete Pavement Support", *Transportation Research Record*, Vol.1505, Transportation Research Board, pp 119-127.
- Kuo, C.M. (1998), "Study of Load Transfer Parameter in AASHTO Design Guide for Concrete pavement", *Transportation Research Record*, Vol.1629, Transportation Research Board, pp 1-5.
- Kwak, K., Suh, J. and Hsu, C.T. (1991), "Shear-fatigue Behaviour of Steel Fiber Reinforced Concrete Beams", *ACI Structural Journal*, Vol.88, No.2, 155-160.
- Laible, J.P., White, R.N. Gergely, P. (1977), "Experimental Investigation of Seismic Shear Transfer across Cracks in Nuclear Containment Vessels", *ACI Special publications*, Vol.53, No.9, pp 203-226.
- Larralde, J. and Chen W. (1987), "Estimation of Mechanical Deterioration of Highway Rigid Pavements", *Journal of Transportation Engineering*, Vol.113, No.2, pp 193-209.
- Losberg, A. (1978), "Pavements and Slabs on Grade with Structurally Active Reinforcement", *ACI Journal*, Vol.75, No.66, pp 647-657.

Meyerhof, F. (1962) "Load-Carrying Capacity of Concrete Pavements", Journal of the Soil Mechanics and Foundations Division, Proceedings of the American Society of Civil Engineers, Vol.88, pp 89-116.

Millard, S.G. and Johnson R.P. (1984), "Shear Transfer Across Cracks in Reinforced Concrete due to Aggregate Interlock and Dowel Action", Magazine of Concrete Research, Vol.36, No.126, pp 9-21.

Minkarah, I.A., Cook, J.P. and McDonough, J.F. (1982), "Magnitude of Horizontal Movement in Jointed Concrete Pavements", Transportation Research Record, Vol. 821, pp 61-67.

Moody, E.D. and McCullough B. F. (1993), "Long Term Performance of Uncontrolled Longitudinal Cracking and Failed Longitudinal Joints in Continuously Reinforced Concrete pavements", Conference Proceedings 20-22nd April 1993, Purdue University, West Lafayette, Indiana.

Neal, F.R. (1996), "ICE Design and Practice Guides - Concrete Industrial Ground Floors", Institution of Civil Engineers, Thomas Telford, London.

Neville, A.M. (1995), "Properties of Concrete", 4th ed., Longman Scientific and Technical, New York, USA.

Nishizawa, T., Fukada, T. and Matsuno, S. (1989), "A Refined Model of Doweled Joints for Concrete Pavement using FEM Analysis", 4th International Conference on Concrete pavement Design and Rehabilitation, Purdue University, West Lafayette, USA.

Nishizawa, T., Kajikawa, Y., and Fukada, T. (1993), "Effects of Lateral Distribution of Heavy Vehicles on Fatigue Cracks on Concrete Pavements", 5th International Conference on Concrete Pavement Design and Rehabilitation, 20-22nd April 1993, Purdue University, West Lafayette, Indiana, USA.

Nowlen, W.J. (1968) "Influence of Aggregate Particles on Effectiveness of Interlock Joints in Concrete Pavements", Journal of the PCA Research and Development Laboratories, Report D139, Vol.10, No.2.

Ozbeki, M.A., Kilareski, W. P. and Anderson, D.A. (1985), "Evaluation Methodology for Jointed Concrete pavements", Transportation Research Record, Vol.1043, Transportation Research Board, pp 1-8.

Papagiannakis, T., Oancea, A., Ali, N., Chan, J. and Bergan, A.T (1991), "Application of ASTM E1049-85 in Calculating Load Equivalence Factors from In-situ Strains", Transportation Research Record, Vol.1307, Transportation Research Board, pp 82-89.

Pearson, D. (1999), "Industrial Floor Slabs Towards a Performance Specification", Proceedings of 3rd European Symposium on Performance and Durability of Bituminous materials and Hydraulic Stabilised Composites, Leeds, U.K. pp 629-611

Perenchio, W.F. (1997). "The Drying Shrinkage Dilemma." Concrete Construction, Vol.42, No.4, pp 379-383.

Petterson, D. and Alemo J. (2000), "Characterization of Restraint from Friction Tests with Slabs Cast on Ground", Structural Concrete, Volume 1, No.4, pp 181-187.

Poblete, M., Valenzuela, R. (1988), "Load Transfer in Undoweled Transverse Joints of PCC Pavements" Transportation Research record, Vol.1207, Transportation Research Board, pp 39-49.

Porter, M.L., Hughes, B. W. and Barnes, B.A. (1996), "Fiber Composite Dowels in Highway Pavements", Semisequicentennial Transportation Conference Proceedings, May 1996, Iowa State University, Ames, Iowa, USA.

Portland Cement Association (1951), "Concrete Pavement Design for Roads and Streets", Portland Cement Association.

Pradhan, M.M. (2002), "Evaluation of Rigid Pavement Condition using the Falling Weight Deflectometer", Bearing Capacity of Roads, Railways and Airfields, Lisse, Swets and Zeitlinger, pp 43-52.

Prozzi, J., DeBeer, M. and Balmaceda, P. (1993), "Non Destructive Tests Procedure for Field Evaluation of Transverse Joints in Concrete Pavements", 5th International Conference on Concrete Pavement Design and Rehabilitation, April 20-22nd 1993, Purdue University, West Lafayette, Indiana, pp3-12.

Raja, Z.I. and Snyder, M. B. (1991), "Factors Affecting Deterioration of Transverse Cracks in Jointed Reinforced Concrete Pavements", Transportation Research Record, Vol.1307, Transportation Research Board, pp 162-168.

Ricci, E.A., Meyer, A.H., Hudson, W.R. and Stokoe II, K.H., (1985), "The Falling Weight Deflectometer for Non-destructive Evaluation of Rigid Pavements", Centre for Transportation Research, Report 387-3F, Bureau of Engineering Research, Austin, Texas.

Ringo, B.C. and Anderson, R. B. (1996), "Designing Floor Slabs on Grade", The Aberdeen Group, Illinois, USA.

Road Research Laboratory (1955), "Concrete Roads - Design and Construction", Department of Scientific and Industrial Research.

Robins, P.J., Bishop J.W., Austin, S.A. (2002), "Early Age Finite Element Modelling of Industrial Ground Floors", Draft Copy, Loughborough University, England.

Rogers, M. (2000). "Joints", Draft section of a Report for The Concrete Society, 27th September 2000, Concrete Society.

Rollings, S.R. (1993), "Curling Failures of Steel-Fiber Reinforced Concrete Slabs" Journal of Performance of Constructed Facilities, Vol.7, No.1, pp 3-19.

Savage, R. J. (1985) "Dynamic Failure of Joints in Reinforced Concrete Pavements." Concrete, January 1985, pp 16-18.

Schrader, E.K. (1985), "Fiber Reinforced Concrete Pavements - A State of the Art Report", 3-5th June 1985, Steel Fiber Concrete - US-Sweden Joint Seminar (NSF-STU), Stockholm, Sweden.

Scott Wilson Pavement Engineering (2002), "Structural Evaluation with the Falling Weight Deflectometer" Internal Correspondence, Scott Wilson Pavement Engineering, Nottingham, England.

Simpson, D. (2001a). "Cracks in Concrete Ground Floors". Floors Forum, 10th January 2001, Loughborough University, England.

Simpson, D. (2001b) "Thickness Design of Ground-Supported Floor Slabs" Concrete, Vol.35, No.8, pp 22-24.

Sprigg Little Partnership (2000), "Designing Cracks out of Floors", Seminar on Developments in Industrial Ground Floor Slabs, 31st October 2000, Aston University, England

Stock, A.F. (1988), "Concrete Pavements", 1st ed, Elsevier Applied Science, London.

Suprenant, B.A. (2002), "Why Slabs Curl", Concrete International, Vol.24, No.3, pp 57-61.

Sutherland, E.C. and Cashell, H.D. (1945), "Structural Efficiency of Transverse Weakened-Plane Joints" Public Roads, Vol.23, No.4, pp 88-97.

Swamy, R.N., Al-taan, S., Sami, A.R.A. (1979), "Steel Fibres for Controlling Cracking and Deflection." Concrete International, August 1979, pp 41-49.

Swamy, R.N. and Andriopoulos A.D. (1974), "Contribution of Aggregate Interlock and Dowel Forces to the Shear Resistance of Reinforced Beams with Web Reinforcement" American Concrete Institute, Special Publication, pp 129-145.

Tabatabaie, A.M. and Barenberg E.J. (1980), "Structural Analysis of Concrete Pavements", Journal of Transportation Engineering, September 1980, pp 493-505.

Tang, B. (1993), "Structural Evaluation of Airfield Rigid pavements using Falling Weight Deflectometer", Journal of Transportation Engineering, Vol.119, No.3, pp 467-476.

Teller, L.W. and Sutherland, E.C. (1943), "The Structural Design of Concrete Pavements", Public Roads, Vol.23, No.8, pp 167-212.

Thompson, I. (2001). "Use of Steel Fibres to Reinforce Cement Bound Roadbase", PhD Thesis, The University of Nottingham, Nottingham, England.

U.S. Department of Transportation, F.H.A. (1990), "Concrete pavement Joints", U.S. Department of Transportation, Federal Highway Administration, pp 1-11.

Valle, M. and Buyukozturk, O. (1993), "Behaviour of Fiber Reinforced High Strength Concrete under Direct Shear", ACI Materials Journal, Vol.90, No.2, pp 122-133.

Van-Wijk, A.J., Larralde, J. and Lovell, C.W. (1989), "Pumping Prediction Model for Highway Concrete Pavements", Journal of Transportation Engineering, Vol.115, No.2, pp 161-174.

Verhoeven, K. (1993), "Cracking and Corrosion in Continuously Reinforced Concrete Pavements", Proceedings of the 5th International Conference on Concrete Pavement Design and Rehabilitation, 20-22nd April 1993, Purdue university, West Lafayette, Indiana pp 201-209.

Wade, M.J., Cuttell, G.D., Vandenbossche, J.M., Yu, H.T., Smith, K.D., Snyder, M.B. (1997), "Performance of Concrete Pavements Containing Recycled Concrete Aggregate", Report FHWA-RD-96-164, Federal Highway Administration, McLean, Virginia, USA, pp 296.

Walker, W.W. and J.A. Holland (1999), "Thou Shalt not Curl Nor Crack...(Hopefully)", Concrete International, January 1999, pp 47-53.

Walker, W.W. and J.A. Holland (2001), "Plate Dowels for Slabs on Ground - Dowels for the 21st Century", Draft Copy, Loughborough University.

Walraven, J.C. (1981), "Fundamental Analysis of Aggregate Interlock." Journal of the Structural Division, American Society of Civil Engineers, Vol.107, No.11, pp 2245-2270.

Watson, J. (1994), "Highway Construction and Maintenance", 2nd ed., Longman Scientific and Technical, Harlow, England.

Westergaard, H.M. (1926), "Stresses in Concrete Pavements Computed by Theoretical Analysis" Public roads, Volume 7, No.2, pp 25-35.

Westergaard, H.M. (1947), "New Formulas for Stresses in Concrete Pavements of Airfields" Proceedings of the American Society of Civil Engineers, Vol.73, No.5, pp 687-701.

White, R.N. and Holley, M.J. (1972), "Experimental Studies of Membrane Shear Transfer", Journal of the Structural Division, American Society of Civil Engineers 98(ST8), pp 1835-1853.

White Young Green (2002), "Ground Floor Slab Pavement Evaluation - Diversey Lever", Internal Communication, Loughborough University, England.

Wirtgen (2001), "Competence in concrete paving machinery: Wirtgen slipform pavers in operation" Company Brochure.

Yoder, E.J. (1959), "Principles of Pavement Design", John Wiley & Sons Inc, Chichester, England, pp 435-452.

York, D. (2001), "New Slant on Slab Foundations." Concrete, Vol.35, No.1, pp 54-55.

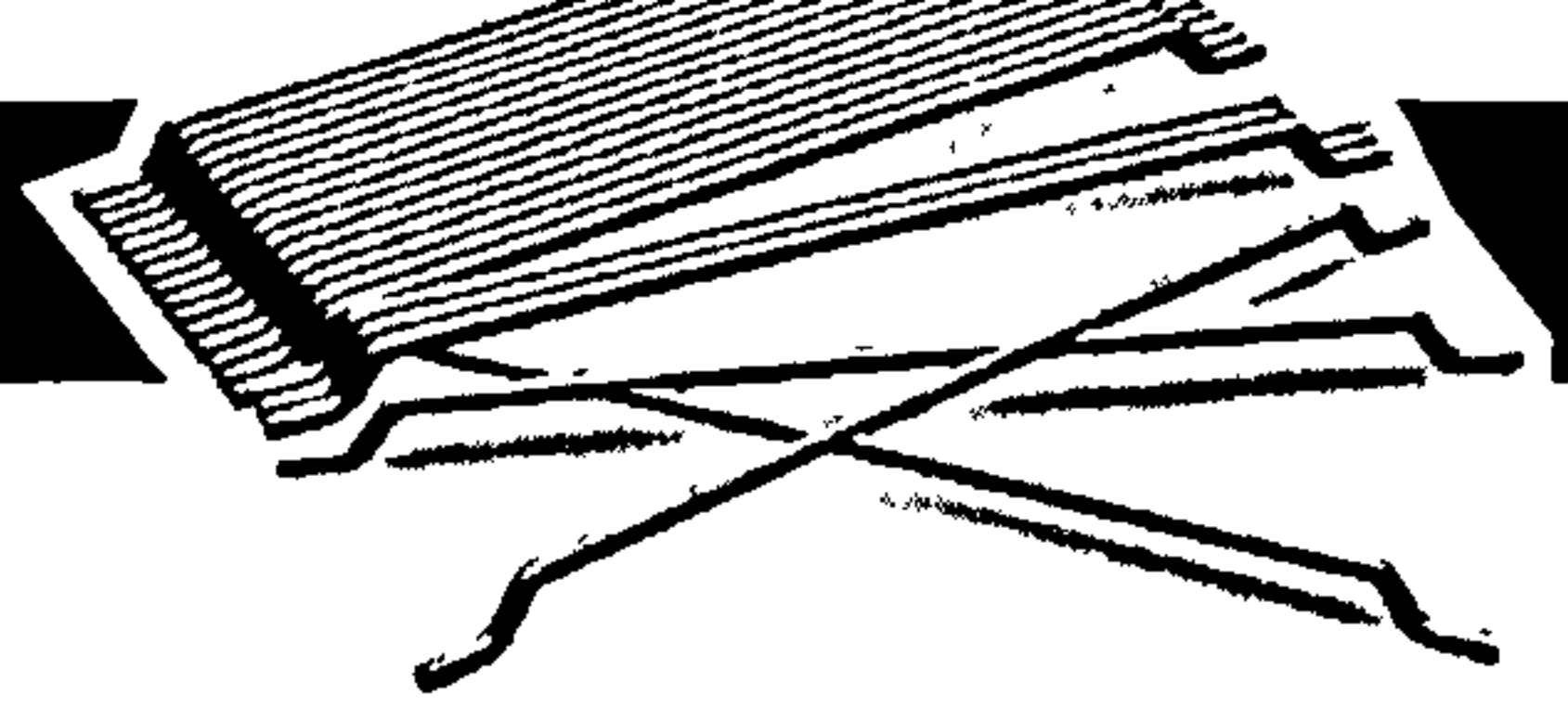
Ytterberg, R.F. (1987), "Shrinkage and Curling of Slabs on Grade: Part 1 - Drying Shrinkage", Concrete International, April 1987, pp 22-31.

Zollinger, D.G. and Barenberg, E.J. (1990), "Mechanistic Design Considerations for Punchout Distress in Continuously Reinforced Concrete Pavement", Transportation Research Record Vol.1286, Transportation Research Board, pp 25-37.

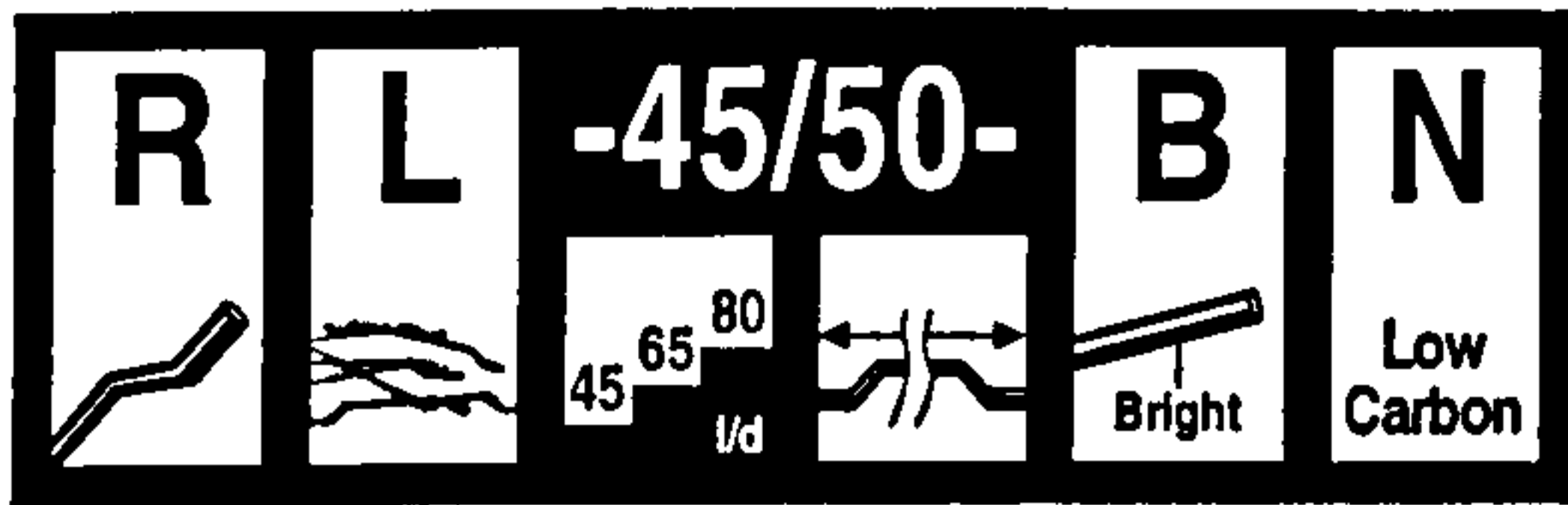
Zollinger, D.G. and Senadheera S.P. (1994), "Spalling of Continuously Reinforced Concrete Pavements" Journal of Transportation Engineering, Vol.120, No.3, pp 394-410.

APPENDIX A

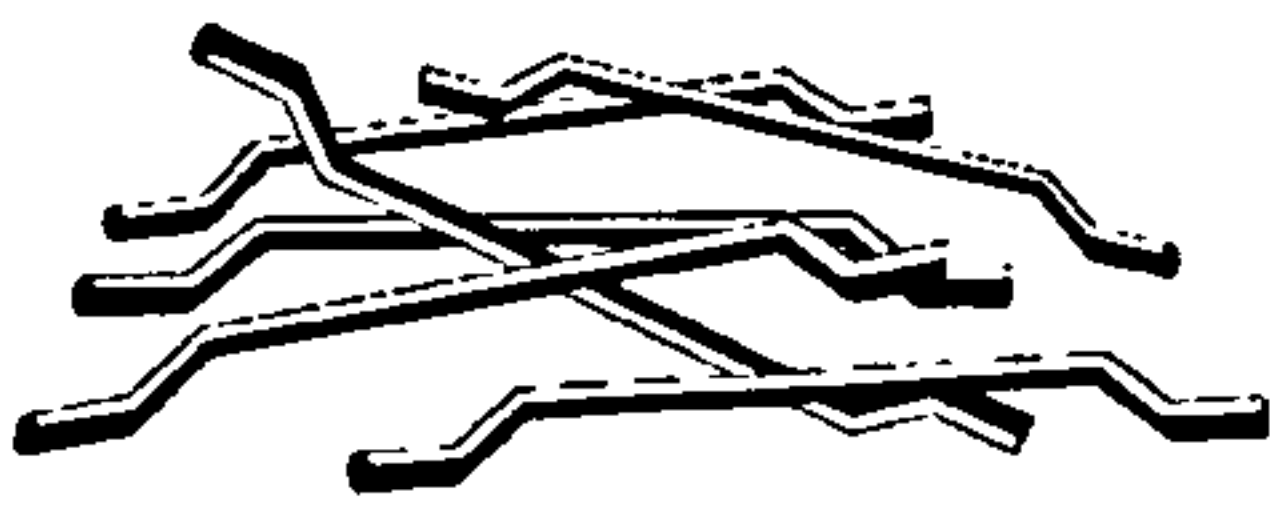
Steel Fibre Data Sheets



Dramix®



Description:



Dramix® fibres are filaments of wire, deformed and cut to lengths, for reinforcement of concrete, mortar and other composite materials. Dramix® RL-45/50-BN is a loose cold drawn wire fibre, with hooked ends.

Applications:

- industrial floors
- slabs on vibrocompacted piles

Geometry:



50 mm



1,05 mm

45 Performance class: 45
Aspect ratio (= l/d): 48



2800 fibres/kg

Tensile strength:

- on the wire: 1000 N/mm²
- low carbon conforms to: - DIN 17 140-D9
- EN 10016-2 - C9D

Coating: None

Approvals:

Conforms to
ASTM A820

Product

Belgium

ATG 1857

Slovak Republic

Č.P/01249/105/1/98

Czech Republic

TZUS Č.07-C-60/98

Turkey

TS 10513

Quality System in

Belgian
PlantsBrazilian, American
and Czech Plants

Product

Russia

TC-07-0116-98

Poland

AT-15-2117/2001

Romania

015-07/012-1997

Germany

Z-71.4-3

Technical data:

For industrial floors, ...ask for specialized documentation

Recommendations - mixing

1. General

- ✓ preferably use a central batching plant mixer
- ✓ recommended maximum dosage:

Max. aggregate size (mm)	Dosage (kg/m ³)	
	pour	pump
8	160	120
16	100	75
32	80	60

- ✓ a continuous grading is preferred

2. Fibre addition

2.1. In batching plant mixer



- ✓ never add fibres as first component in the mixer
- ✓ fibres can be introduced together with sand and aggregates, or can be added in freshly mixed concrete
- ✓ only for drummixer: unopened degradable bags can be thrown directly in the mixer

2.2. Truckmixer



- ✓ run mixer at drum speed: 12-18 rpm
- ✓ adjust slump to a min. of 12 cm (preferably with water reducing agents or high water reducing agents)
- ✓ add fibres with maximum speed of 60 kg/min
- ✓ unopened degradable bags can be added provided that drum speed is min. 12 rpm
- ✓ optional equipment: belt-hoist elevator
- ✓ after adding the fibres, continue mixing at highest speed for 4-5 min. (± 70 rotations)

Recommendations - storage



Protect the pallets
against rain



Do not stack the
pallets on top of
each other

Delivered In



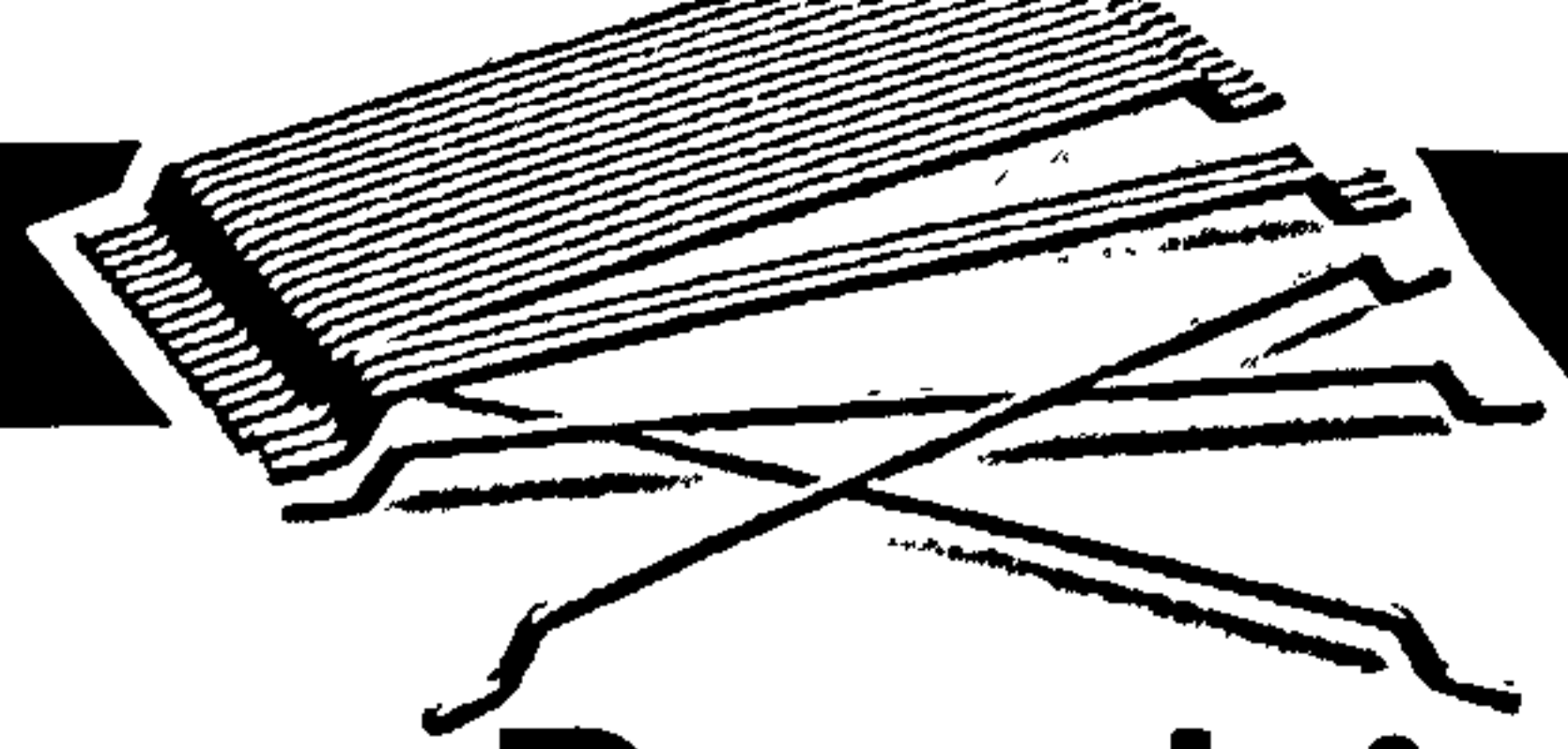
degradable
bags of 20 kg
on pallet
1200 kg



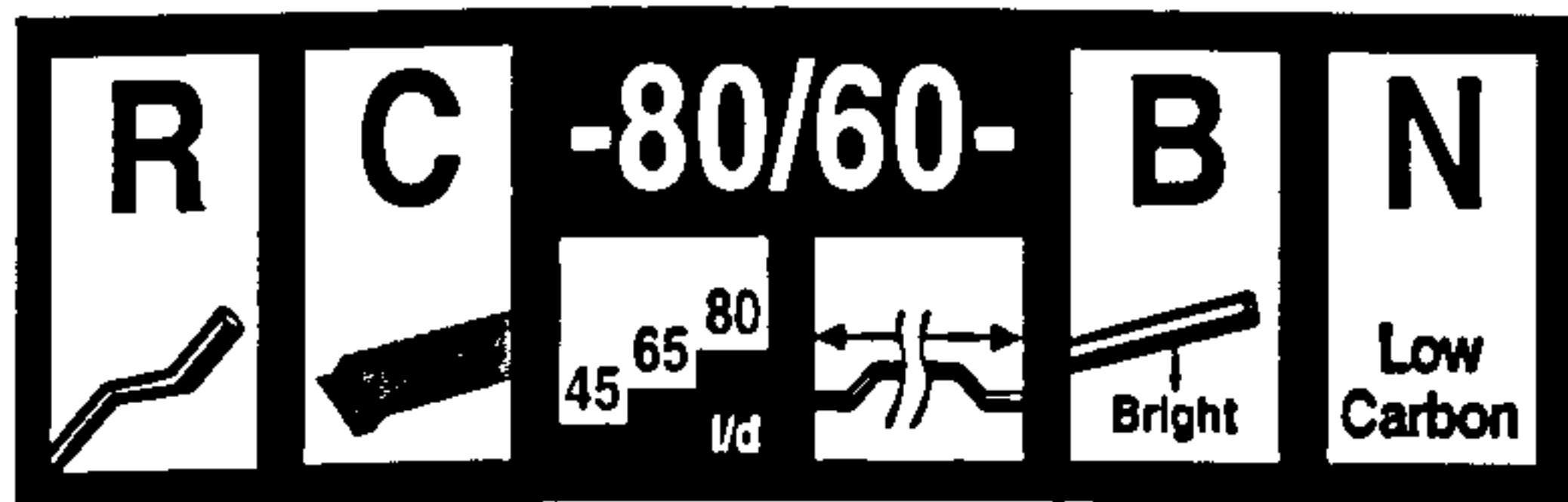
big bag
900 kg

N.V. Bekaert S.A. - Bekaertstraat 2 - 8550 Zwevegem - Belgium
Tel. +32 (0) 56 / 76 69 86 - Fax +32 (0) 56 / 76 79 47
Internet: <http://www.bekaert.com/building>

Values are indicative only. Modifications reserved. All details describe our products in general form only. For ordering and design only use official specifications and documents. N.V. Bekaert S.A. 2002



Dramix®



- Description:** Dramix® fibres are filaments of wire, deformed and cut to lengths, for reinforcement of concrete, mortar and other composite materials. Dramix® RC-80/60-BN is a cold drawn wire fibre, with hooked ends, and glued in bundles.

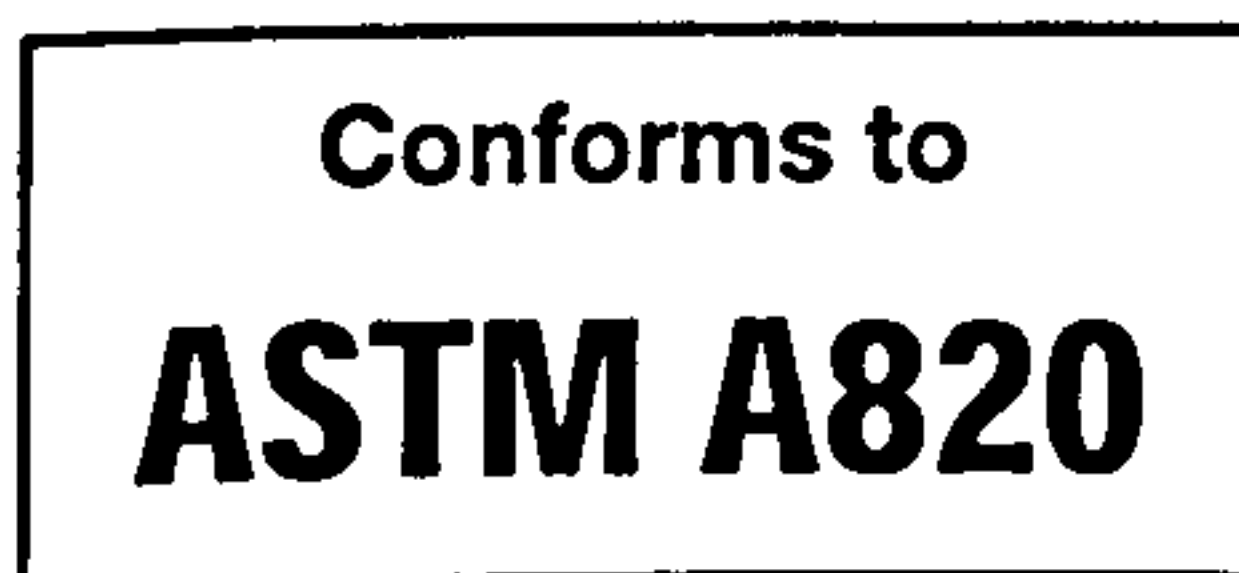
- Applications:**
 - jointless floors
 - suspended ground slabs
 - jointless floors on vibrocompacted piles
 - industrial floors
 - slabs on vibro-compacted piles
 - liquid tight floors
 - overlays
 - pavements
 - segmental linings
 - compression layers
 - cellar walls
 - precast

- Geometry:**
 - Length (l): 80 mm
 - Diameter (d): 0,75 mm
 - Performance class: 80
 - Aspect ratio (= l/d): 80
 - 4600 fibres/kg

- Tensile strength:**
 - on the wire: minimum 1050 N/mm²
 - low carbon conforms to: - DIN 17 140-D9
 - EN 10016-2 - C9D

- Coating:** None

- Approvals:**



Product



Product



- Technical data:** For industrial floors, floors on vibrocompacted piles, jointless floors... ask for specialized documentation.

Recommendations - mixing

1. General

- ✓ preferably use a central batching plant mixer
- ✓ recommended maximum dosage:

Max. aggregate size (mm)	Dosage (kg/m ³)	
	pour	pump
8	60	45
16	50	35
32	35	30

- ✓ a continuous grading is preferred
- ✓ mix until all glued fibres are separated into individual fibres. Fibres don't increase mixing time significantly.
- if special cements or admixtures are used, a preliminary test is recommended

2. Fibre addition

2.1. In batching plant mixer

- ✓ never add fibres as first component in the mixer
- ✓ fibres can be introduced together with sand and aggregates, or can be added in freshly mixed concrete
- ✓ only for drummixer: unopened degradable bags can be thrown directly in the mixer

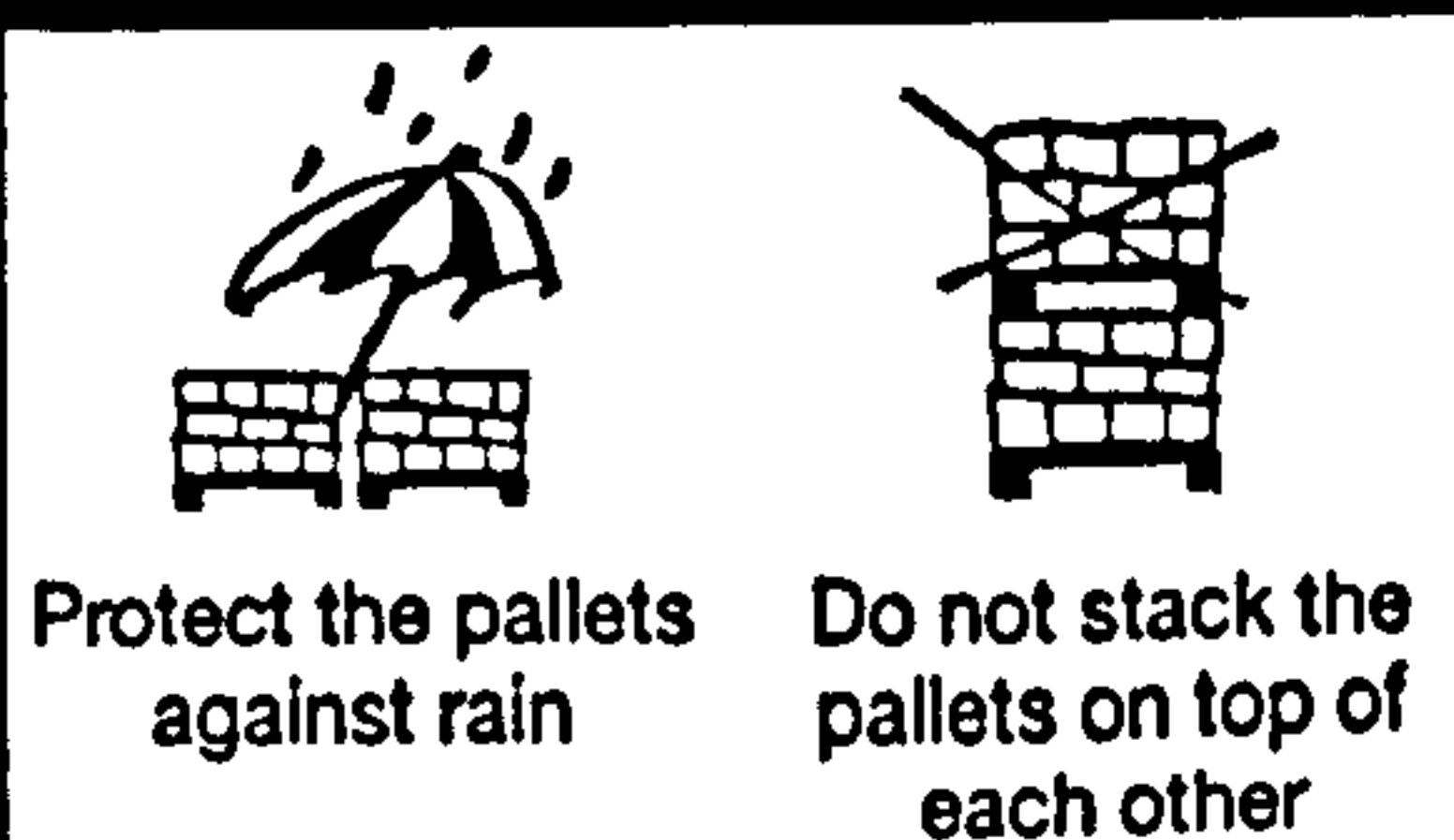
2.2. Truckmixer

- ✓ run mixer at drum speed: 12-18 rpm
- ✓ adjust slump to a min. of 12 cm (preferably with water reducing agents or high water reducing agents)
- ✓ add fibres with maximum speed of 40 kg/min
- ✓ unopened degradable bags can be added provided that drum speed is min. 12 rpm
- ✓ optional equipment: belt-hoist elevator
- ✓ after adding the fibres, continue mixing at highest speed for 4-5 min. (± 70 rotations)

2.3. Automatic dosing

- ✓ Fibres can be dosed from bulk at rates from 0 up to 3,5 kg/sec with a specially developed dosing equipment

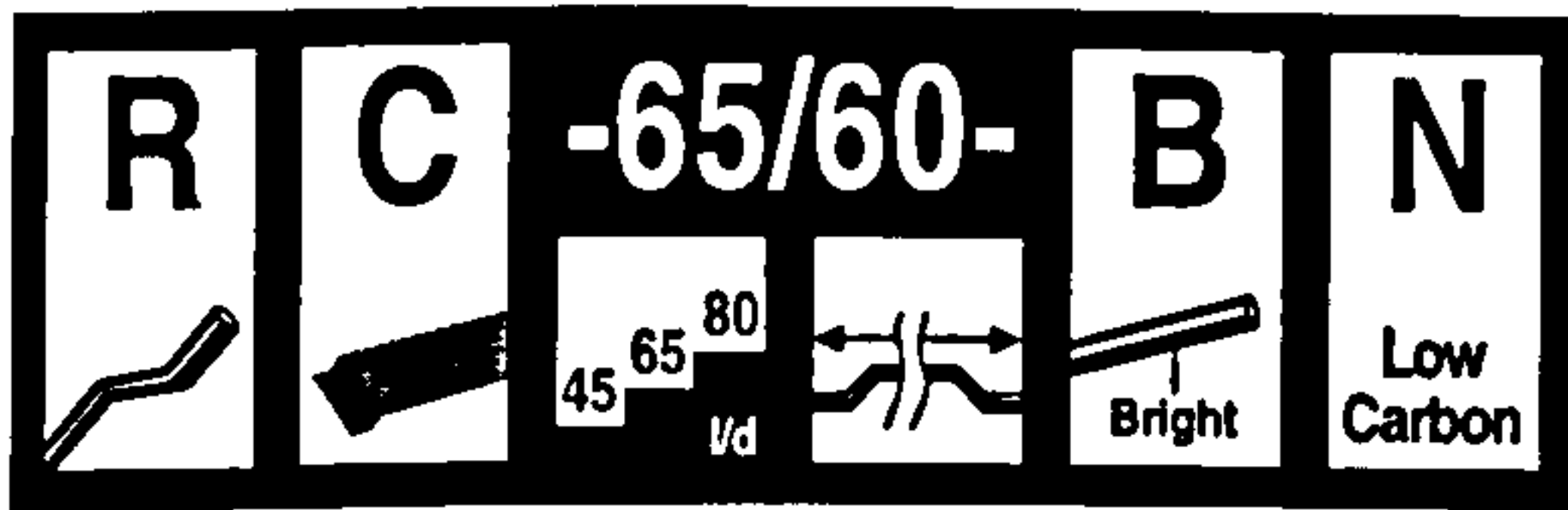
Recommendations - storage



N.V. Bekaert S.A. - Bekaertstraat 2 - 8550 Zwevegem - Belgium
Tel. +32 (0) 56 / 76 69 86 - Fax +32 (0) 56 / 76 79 47
Internet: <http://www.bekaert.com/building>

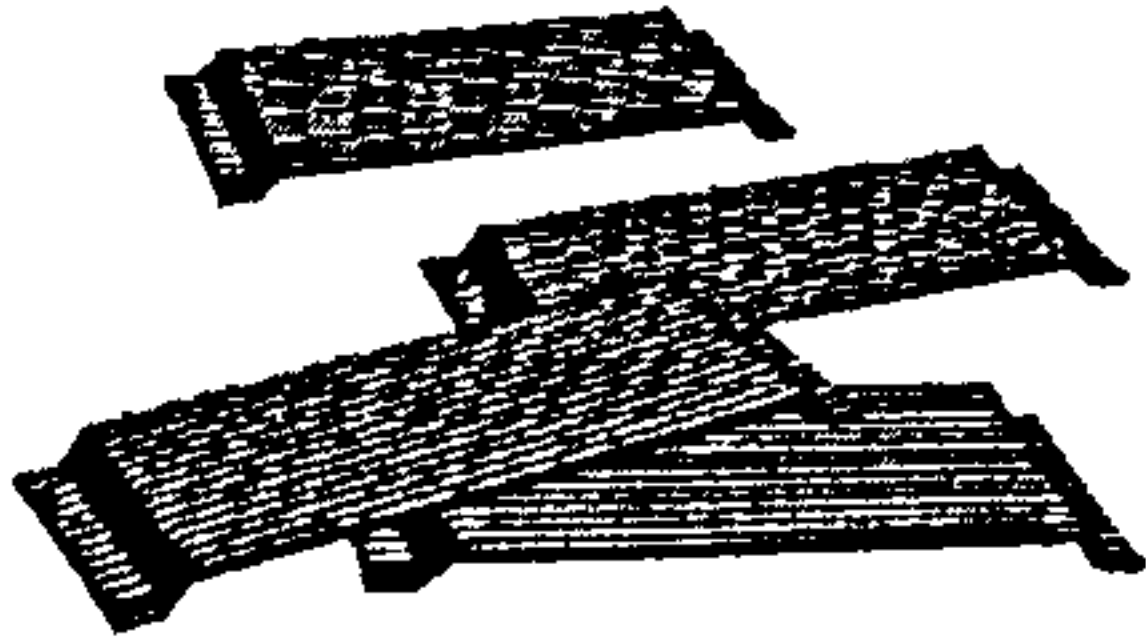
Values are indicative only. Modifications reserved. All details describe our products in general form only. For ordering and design only use official specifications and documents. N.V. Bekaert S.A. 2002

Dramix®



Description:

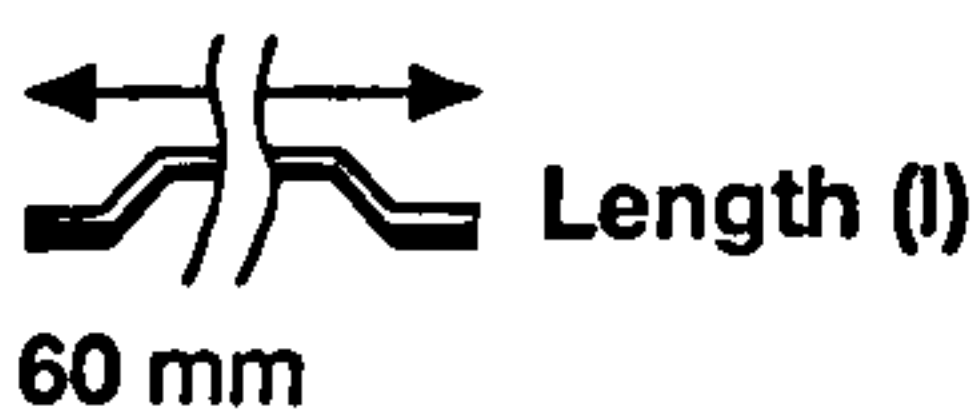
Dramix® fibres are filaments of wire, deformed and cut to lengths, for reinforcement of concrete, mortar and other composite materials. Dramix® RC-65/60-BN is a cold drawn wire fibre, with hooked ends, and glued in bundles.



Applications:

- slabs on vibrocompacted piles
- liquid tight floors
- industrial floors
- overlays
- piles
- suspended ground slabs
- segmental linings
- cellar walls
- pavements
- jointless floors
- jointless floors on vibrocompacted piles
- outdoor slabs
- foundation slabs

Geometry:



65 Performance class: 65
Aspect ratio (= l/d): 67

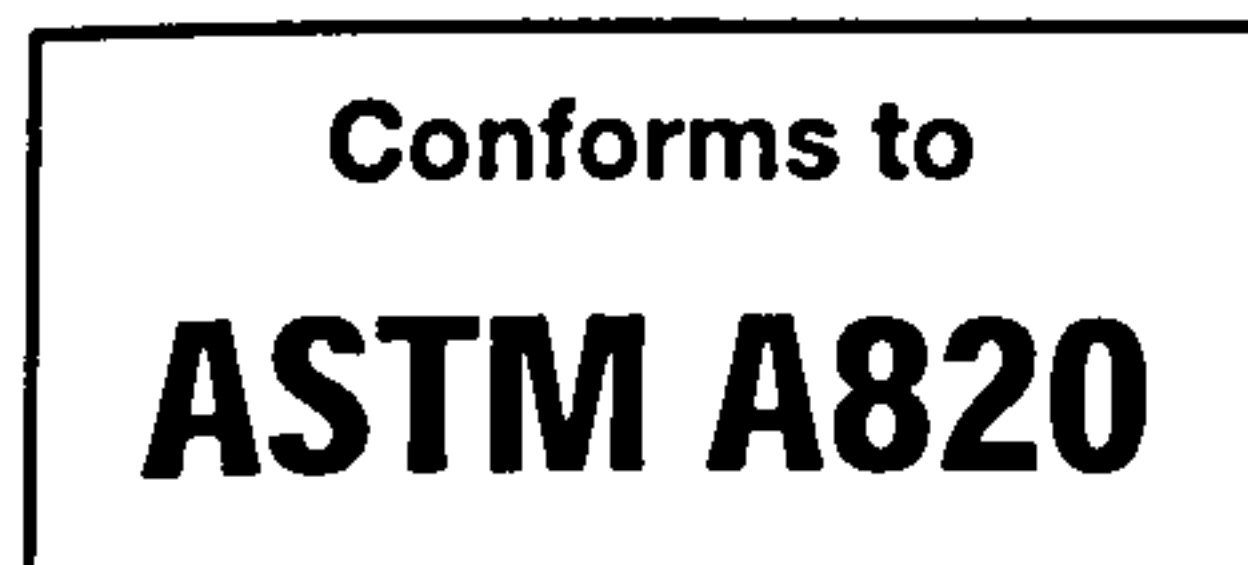
3200 fibres/kg

Tensile strength:

- on the wire: minimum 1000 N/mm²
- low carbon conforms to: - DIN 17 140-D9
- EN 10016-2 - C9D

Coating: None

Approvals:



Product



Product



Technical data:

For industrial floors, floors on vibrocompacted piles, jointless floors... ask for specialized documentation.

Recommendations - mixing

1. General

- ✓ preferably use a central batching plant mixer
- ✓ recommended maximum dosage:

Max. aggregate size (mm)	Dosage (kg/m ³)	
	pour	pump
8	110	80
16	70	55
32	60	45

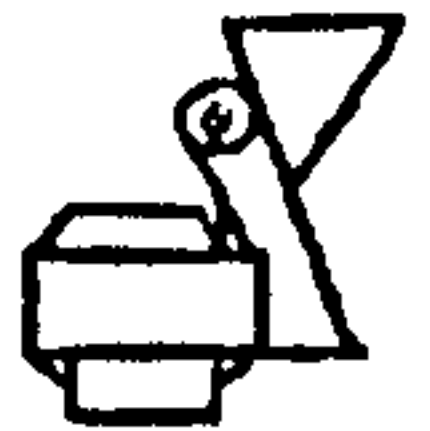
- ✓ a continuous grading is preferred
- ✓ mix until all glued fibres are separated into individual fibres. Fibres don't increase mixing time significantly.



if special cements or admixtures are used, a preliminary test is recommended

2. Fibre addition

2.1. In batching plant mixer



- ✓ never add fibres as first component in the mixer
- ✓ fibres can be introduced together with sand and aggregates, or can be added in freshly mixed concrete
- ✓ only for drummixer: unopened degradable bags can be thrown directly in the mixer

2.2. Truckmixer



- ✓ run mixer at drum speed: 12-18 rpm
- ✓ adjust slump to a min. of 12 cm (preferably with water reducing agents or high water reducing agents)
- ✓ add fibres with maximum speed of 60 kg/min
- ✓ unopened degradable bags can be added provided that drum speed is min. 12 rpm
- ✓ optional equipment: belt-hoist elevator
- ✓ after adding the fibres, continue mixing at highest speed for 4-5 min. (± 70 rotations)

2.3. Automatic dosing



- ✓ Fibres can be dosed from bulk at rates from 0 up to 3,5 kg/sec with a specially developed dosing equipment

Recommendations - storage



Protect the pallets against rain



Do not stack the pallets on top of each other

Delivered In



degradable bags of 20 kg on pallet 1200 kg



big bag 1100 kg

N.V. Bekaert S.A. - Bekaertstraat 2 - 8550 Zwevegem - Belgium
Tel. +32 (0) 56 / 76 69 86 - Fax +32 (0) 56 / 76 79 47
Internet: <http://www.bekaert.com/building>

Values are indicative only. Modifications reserved. All details describe our products in general form only. For ordering and design only use official specifications and documents. N.V. Bekaert S.A. 2002

APPENDIX B

Laboratory Test Data

Specimen Set	Identification code	Test No	Phase I - II		Phase II - III		Phase III - IV	
			Cycles	Diff. Dis. (mm)	Cycles	Diff. Dis. (mm)	Cycles	Diff. Dis. (mm)
Non-Reinforced	40/Non/0/V/0.66/4	1	25000	0.27				
		2	10000	0.32				
		Average	17500	0.295				
		1	2000	0.7	70000	1.1	72000	1.6
		2	10000	0.8	170000	1.2	185000	1.6
		Average	6000	0.75	120000	1.15	128500	1.6
Mortar	Mor/Non/30/V/0.66/4	1	0	0.8	500	0.8	1500	1.6
30kg/m3 Fibre		2	10000	0.3	15000	0.9	20000	1.6
		Average	5000	0.55	7750	0.85	10750	1.6
		1	100000	0.06				
		2	80000	0.1				
		Average	90000	0.08				
20kg/m3 Fibre	40/65-60/20/V/1.98/4	1	40000	0.095				
		2	30000	0.042				
		Average	35000	0.0685				
		1	20000	0.22				
		2	15000	0.055				
		Average	17500	0.1375				
	40/65-60/20/V/3.96/4	1	10000	0.125				
		Average	10000	0.125				
		1	2000	0.55	45000	1.2	50000	1.6
		2	2000	0.4	115000	1	113000	1.6
		Average	2000	0.475	80000	1.1	81500	1.6
30kg/m3 Fibre	40/65-60/30/V/1.98/4	1	40000	0.041				
		2	150000	0.09				
		Average	95000	0.0655				
		1	5000	0.23				
		2	20000	0.125				
		3	25000	0.15				
		Average	16666.67	0.17				
	40/65-60/30/V/4.62/4	1	15000	0.22				
		2	20000	0.25				
		Average	17500	0.235				

	40/65-60/30/V/5.94/4	1	2000	0.45	20000	0.9	30000	1.6
		2	2000	0.2	9000	0.7	10500	1.6
		Average	2000	0.325	14500	0.8	20250	1.6
40kg/m3 Fibre	40/65-60/40/V/1.98/4	1	150000	0.065				
		2	5000	0.065				
		Average	77500	0.065				
	40/65-60/40/V/3.3/4	1	30000	0.085				
		2	55000	0.15				
		Average	42500	0.1175				
	40/65-60/40/V/4.62/4	1	15000	0.14				
		2	18000	0.17				
		Average	16500	0.155				
	40/65-60/40/V/5.94/4	1	2000	0.1	210000	0.6	212000	1.6
		2	20000	0.1	240000	0.7		
		Average	11000	0.1	225000	0.65	106000	0.8
RC-80/60-BN	40/80-60/40/V/1.98/4	1	50000	0.04				
		2	25000	0.1				
		Average	37500	0.07				
	40/80-60/40/V/3.3/4	1	10000	0.045				
		2	50000	0.08				
		Average	30000	0.0625				
	40/80-60/40/V/4.62/4	1	15000	0.12				
		2	50000	0.08				
		3	20000	0.11				
		Average	35000	0.095				
RC-45/50-BN	40/45-50/40/V/1.98/4	1	25000	0.17				
		2	25000	0.08				
		Average	25000	0.125				
	40/45-50/40/V/3.3/4	1	40000	0.13				
		2	30000	0.16				
		3	5000	0.3	210000	0.65	245000	1.6
		Average	17500	0.23	210000	0.65	245000	1.6
	40/45-50/40/V/4.62/4	1	50000	0.21				
		2	5000	0.35	20000	0.6	35000	1.6
		3	25000	0.3				
		Average	15000	0.325	20000	0.6	35000	1.6

7mm Rebar	40/Trad/7N/1.98/4	1	40000	0.045					
		2	2000	0.03					
		Average	21000	0.0375					
	40/Trad/7N/3.3/4	1	50000	0.07					
		Average	50000	0.07					
	40/Trad/7N/4.62/4	1	10000	0.057					
		2	5000	0.035					
		Average	7500	0.046					
A142 Fabric	40/Mesh/7N/1.98/4	1	15000	0.04					
		2	25000	0.045					
		Average	20000	0.0425					
	40/Mesh/7N/3.3/4	1	15000	0.028					
		2	50000	0.041					
		Average	32500	0.0345					
	40/Mesh/7N/4.62/4	1	20000	0.095					
		2	2000	0.058					
		3	5000	0.041					
		Average	3500	0.0495					
2kN Load	40/65-60/30N/1.98/2	1	5000	0.03					
		2	5000	0.03					
		Average	5000	0.03					
	40/65-60/30N/3.3/2	1	10000	0.05					
		2	10000	0.05					
		Average	10000	0.05					
	40/65-60/30N/4.62/2	1	10000	0.05					
		2	50000	0.042					
		3	15000	0.05					
		Average	32500	0.046					
6kN Load	40/65-60/30N/0.66/6	1	45000	0.14					
		2	100000	0.18					
		Average	72500	0.16					
	40/65-60/30N/1.98/6	1	35000	0.17					
		2	5000	0.19		40000	0.3	80000	1.6
		3	3000	0.2		80500	0.65	97000	1.6
		Average	4000	0.195		60250	0.475	88500	1.6
20kg/m3 Fibre	40/65-60/20/Par/0.66/4	1	50000	0.078					

Parallel			2	8000	0.22								
			Average	29000	0.149								
		40/65-60/20/Par/1.98/4	1	15000	0.15								
			2	25000	0.3								
			Average	20000	0.225								
30kg/m3 Fibre		40/65-60/30/Par/0.66/4	1	25000	0.17								
Parallel			2	40000	0.16								
			Average	32500	0.165								
		40/65-60/30/Par/1.98/4	1	25000	0.15		30000	1	40100		1.6		
			2	15000	0.3		4000	0.6	6000		1.6		
			Average	20000	0.225		17000	0.8	23050		1.6		
40kg/m3 Fibre		40/65-60/40/Par/0.66/4	1	50000	0.18								
Parallel			2	5000	0.21								
			Average	27500	0.195								
		40/65-60/40/Par/1.98/4	1	20000	0.6		170000	1.4	197000		1.6		
			2	15000	0.3								
			Average	17500	0.45		170000	1.4	197000		1.6		